

UNIVERSITY OF KWAZULU-NATAL

**SYNTHESIS, CHARACTERISATION AND
BIOLOGICAL ACTIVITIES OF
HOMOISOFLAVONOIDS**

2012

KAALIN GOPAUL

**SYNTHESIS, CHARACTERISATION AND
BIOLOGICAL ACTIVITIES OF
HOMOISOFLAVONOIDS**

KAALIN GOPAUL

2012

A thesis submitted to the School of Chemistry and Physics, University of KwaZulu-Natal,
Westville, for the degree of Masters of Science.

As the candidate's supervisor, I have approved this thesis for submission.

Supervisor:

Signed: -----Name: ----- Date: -----

To my family...

ज्ञान शक्ति है.

“Knowledge is power”

DECLARATIONS

DECLARATION 1- PLAGIARISM

I, **KAALIN GOPAUL**, declare that the experimental work described in this dissertation was carried out at the School of Chemistry and Physics, University of KwaZulu-Natal, Westville campus under the supervision of Dr. N. A. Koorbanally, and that:

1. The research reported in this thesis is my original research, except where otherwise indicated.
2. This thesis has not been submitted for any degree or examination at any other university.
3. This thesis does not contain other persons' data, pictures, graphs or other information, unless specifically acknowledged as being sourced from other persons.
4. This thesis does not contain other persons' writing, unless specifically acknowledged as being sourced from other researchers. Where other written sources have been quoted, then:
 - a. Their words have been re-written but the general information attributed to them have been referenced
 - b. Where their exact words have been used, then their writing has been placed in italics and inside quotation marks, and referenced.
5. This thesis does not contain text, graphics or tables copied and pasted from the Internet, unless specifically acknowledged, and the source being detailed in the thesis and in the References sections.

Signed

DECLARATION 2- PUBLICATIONS

DETAILS OF CONTRIBUTION TO PUBLICATIONS that form part and/or include research presented in this thesis.

Publication 1

Kaalin Gopaul, Mahidansha Shaikh, Deresh Ramjugernath, Neil A. Koorbanally and Bernard Omondia, 3-(3-Methoxybenzylidene)chroman-4-one, Acta Crystallographica Section E, Accepted for publication: 4 March 2012

Publication 2

Kaalin Gopaul, Mahidansha M. Shaikh, Neil A. Koorbanally, Deresh Ramjugernath and Bernard Omondia, (*E*)-3-(4-Cyclohexyl-3-fluorobenzylidene)chroman-4-one, Acta Crystallographica Section E, Accepted for publication: 28 May 2012

Publication 3

Kaalin Gopaul, Neil Anthony Koorbanally, Mahidansha M. Shaikh, Hong Su and Deresh Ramjugernath, 3-(3,4-Dichlorobenzylidene)chroman-4-one, Acta Crystallographica Section E, Accepted for publication: 25 September 2012

From all the above publications, my role included carrying out the experimental work and contributing to the writing of the publications along with my supervisor. The other co-authors contribution was that of an editorial nature and checking on the scientific content and my correct interpretation. Based on their expertise, they have added minor parts to the manuscripts.

Signed:

ACKNOWLEDGEMENTS

- To my parents, Prem and Preetha Gopaul, and my brother, Breneil Gopaul, I am unconditionally grateful for your motivation and support. I would not be where I am without you.
- To my supervisor, Dr. N.A. Koorbanally, Thank you for the opportunity to work with you and for your guidance throughout this study and the long hours endured in writing and editing this dissertation. Your time and dedication are sincerely appreciated. I look forward to continuing my academic career under your supervision.
- To Dr M. Shaikh for imparting his practical knowledge to me on a daily basis, you made my labwork enjoyable.
- Dr. H.Y. Chenia, at the School of Biochemistry, Genetics and Microbiology, UKZN Westville for assisting me when carrying out the antibacterial testing.
- Dr B.O. Owaga and Dr. Hong Su for the collection and refinement of crystallographic data.
- To my labmates in the Natural Products Research Group for always being there to discuss any problem that I might have encountered through my studies.
- Mr. D. Jagjivan for assistance with NMR experiments.
- To my friends, Vashen Moodley, Shirveen Sewpersad, Michael Nivendran Pillay Rasmika Prithipal and Arisha Prithipal for sharing the fun times with me.
- To the technical and support staff of the School of Chemistry and Physics for being ever willing to assist me.
- The National Research Foundation (NRF) for financial support through a Scarce Skills Scholarship.

LIST OF ABBREVIATIONS

^1H NMR	proton nuclear magnetic resonance spectroscopy
^{13}C NMR	carbon-13 nuclear magnetic resonance spectroscopy
^{19}F NMR	fluorine-19 nuclear magnetic resonance spectroscopy
DEPT	distortionless enhancement by polarization transfer
COSY	correlated nuclear magnetic resonance spectroscopy
HSQC	heteronuclear single quantum coherence
HMBC	heteronuclear multiple bond coherence
NOESY	nuclear overhauser effect spectroscopy
CDCl_3	deuterated chloroform
DMSO	deuterated dimethyl sulfoxide
TMS	tetramethylsilane
EtOH	ethanol
PPA	polyphosphoric acid
TCA	trichloroacetic acid
EI-MS	electron impact mass spectrometry
min	minutes
hrs	hours
Hz	hertz
IR	infrared
UV	ultraviolet
m	multiplet
d	doublet
dd	double doublet
ddd	double double doublet
s	singlet
t	triplet
td	triplet of doublets
m.p.	melting point
$^{\circ}\text{C}$	degrees Celsius
TLC	thin layer chromatography
MIC	minimum inhibitory concentration
TET	tetracycline

AMP	ampicillin
TSA	trypticase soy agar
MH	Mueller-Hinton
AI	activity index
DPPH	2,2-diphenyl-1-picrylhydrazyl
FRAP	ferric reducing antioxidant power
ABTS	2,2'-azino-bis(3-ethylbenzothiazoline-6-sulfonic acid)
ORAC	oxygen radical absorbance capacity
INT	<i>p</i> -iodonitrotetrazolium
ORTEP	Oak Ridge Thermal Ellipsoid Plot

LIST OF TABLES

Table 1: Comparative prices of commercially available 4-chromanones.....	8
Table 2: ¹ H NMR data of compounds 3-10	67
Table 3: ¹ H NMR data of compounds 11-17	68
Table 4: ¹³ C NMR data of compounds 3-10	69
Table 5: ¹³ C NMR data of compounds 11-17	70
Table 6: The DPPH free radical scavenging activity of the homoisoflavonoids (13, 14, 15) and ascorbic acid.....	72
Table 7: The ferric reducing antioxidant power of the homoisoflavonoids (13-15) and ascorbic acid	73
Table 8: The strains of bacterial cultures tested against in the disc diffusion assay.....	75
Table 9: The zone diameters and activity indices of compounds 3-6 and 8-15 against bacterial strains: <i>Staphylococcus aureus</i> , <i>Staphylococcus saprophyticus</i> and <i>Staphylococcus</i> <i>scuiri</i>	76
Table 10: The zone diameters and activity indices of compounds 3-6 and 8-15 against bacterial strains: <i>Staphylococcus xylosus</i> , <i>Streptococcus agalactiae</i> , <i>Streptococcus</i> <i>pyogenes</i> and <i>Escherichia coli</i>	77

LIST OF FIGURES

Figure 1: The basic structure of a 3-benzylidene homoisoflavonoid.....	1
Figure 2: The chemical structures of eucomin (a) and eucomol (b)	2
Figure 3: The structural skeleton of an isoflavonoid (a) and a homoisoflavonoid (b)	2
Figure 4: The formation of the A and B ring of the chalcone which is further cyclised into the homoisoflavonoid	3
Figure 5: The <i>E</i> and <i>Z</i> -isomers of 3-benzylidene-4-chromanone	6
Figure 6: Homoisoflavonoids showing good antioxidant activity.....	15
Figure 7: 3-(Benzo[1,3]dioxol-5-ylmethylene)-7-hydroxychroman-4-one, a 3-benzylidene-4- chromanone with good antibacterial activity.....	15
Figure 8: The substituted 3-benzylidene-4-chromanones with good antibacterial activity against <i>Staphylococcus aureus</i> (ATCC 12600).....	16
Figure 9: The reduction of Fe ³⁺ to Fe ²⁺ in the presence of an antioxidant	18
Figure 10: The chromanone ring (2) showing protons H-2a, H-2b, H-3a and H-3b	26
Figure 11: Anisotropic effect causing H-5 occurring more downfield than H-7.....	32
Figure 12: The chemical structures of ascorbic acid and compound 15	46
Figure 13: ORTEP diagram of compound 4 drawn at the 50% probability level.....	59
Figure 14: ORTEP diagram of compound 5 drawn at the 50% probability level.....	59
Figure 15: ORTEP diagram of compound 6 drawn at the 50% probability level.....	60
Figure 16: ORTEP diagram of compound 9 drawn at the 50% probability level.....	62
Figure 17: ORTEP diagram of compound 14 drawn at the 50% probability level.....	64
Figure 18: ORTEP diagram of compound 16 drawn at the 50% probability level.....	65
Figure 19: ORTEP diagram of compound 17 drawn at the 50% probability level.....	66

LIST OF SCHEMES

Scheme 1: The biosynthetic formation of the chalcone precursor (Hahlbrock and Grisebach, 1975).....	4
Scheme 2: The biosynthetic pathway from 2,4,4'-trihydroxy-2'-methoxychalcone to its corresponding homoisoflavonoids (Dewick, 1975).....	5
Scheme 3: The proposed biosynthesis of scillascillin (Dewick, 1975)	6
Scheme 4: A retrosynthetic approach to 3-benzylidene-4-chromanone	7
Scheme 5: (a) The synthesis of 3-phenoxypropanoic acid (1) and 4-chromanone (2) (Siddaiah <i>et al.</i> , 2006); (b) The synthesis of 7-hydroxy-4-chromanone (Foroumadi <i>et al.</i> , 2007); (c) The synthesis of 7,8-dihydroxy-4-chromanone (Siddaiah <i>et al.</i> , 2007) ..	10
Scheme 6: The proposed reaction mechanism for the acid-catalysed preparation of 3-benzylidene-4-chromanone.....	11
Scheme 7: The proposed reaction mechanism for the base-catalysed preparation of 3-benzylidene-4-chromanone.....	12
Scheme 8: The reaction scheme for the preparation of 3-benzylidene-4-chromanone by the Baylis-Hillman reaction (Basavaiah and Bakthadoss, 1998).....	13
Scheme 9: The reaction of DPPH with a hydrogen radical (Shyam <i>et al.</i> , 2012)	17
Scheme 10: The reaction between ABTS and the antioxidant (Osman <i>et al.</i> , 2006)	18
Scheme 11: The synthetic scheme for the synthesis of 3-phenoxy propanoic acid (1), 4-chromanone (2) and homoisoflavonoids (3-17).....	23
Scheme 12: The proposed reaction mechanism for the synthesis of 3-phenoxypropanoic acid (1) and 4-chromanone (2)	24
Scheme 13: The proposed fragmentation pattern of 4-chromanone (2)	25
Scheme 14: The fragmentation pattern of (<i>E</i>)-3-(4'-methoxybenzylidene)chroman-4-one (4)	30
Scheme 15: Resonance structures of phenol showing electronic effects of the hydroxyl group and the build-up of electron density at the <i>ortho</i> and <i>para</i> positions, resulting in protons occurring more upfield.....	31
Scheme 16: Resonance structures of acetophenone showing electronic effects of the acyl group and the withdrawal of electron density from the <i>ortho</i> and <i>para</i> positions resulting in protons occurring more downfield.....	31
Scheme 17: The proposed mechanism for the antioxidant activity of (<i>E</i>)-3-(3',4'-dihydroxybenzylidene)chroman-4-one	47

Scheme 18: The preparation of 3-phenoxypropanoic acid (1).....	54
Scheme 19: The preparation of 4-chromanone (2)	55
Scheme 20: The preparation of homoisoflavonoids (3-17)	56

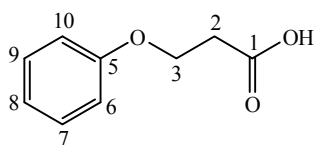
LIST OF GRAPHS

Graph 1: The scavenging ability of compounds 13 , 14 and 15 in comparison to ascorbic acid at various concentrations	45
Graph 2: The reducing power of compound 15 and ascorbic acid	48
Graph 3: The reducing power of compound 13 and compound 14	48
Graph 4: The zone of inhibition of compounds 3 (unsubstituted), 11 (3'-F), 12 (3',4'-diF), 13 (4'-OH), 14 (3'-OH) and 15 (3',4'-diOH) against <i>Staphylococcus aureus</i> (ATCC 43300).....	51

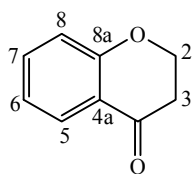
ABSTRACT

Fifteen homoisoflavonoids (**3-17**) were synthesised using the base-catalysed aldol condensation, thirteen of which were of the 3-benzylidene-4-chromanone type and the remaining two of the 3-benzyl-4-chromanone type. The substitution patterns of the homoisoflavonoids were varied by keeping the A-ring unsubstituted whilst changing the substituent's on the 3' and 4' positions of the B-ring. Methoxy, hydroxy, chloro, fluoro and nitro groups were inserted on the B-ring of the homoisoflavonoids. All homoisoflavonoids were characterised by NMR (1D and 2D), IR, UV spectroscopy and GC-MS. The crystal structures were obtained for seven of the homoisoflavonoids. The homoisoflavonoids (**3-17**) were tested for their antibacterial activity against ten gram-positive and six gram-negative bacterial strains using the method of disc diffusion. Five compounds showed moderate antibacterial activity whilst compound **14** showed good antibacterial activity against the gram positive bacteria. The hydroxylated compounds were tested for their antioxidant activity using the DPPH (2,2-diphenyl-1-picrylhydrazyl) radical scavenging method as well as the FRAP (ferric reducing antioxidant power) method. Compound **15** showed good antioxidant activity, comparable to that of ascorbic acid, due to the presence of a catechol system within the molecule.

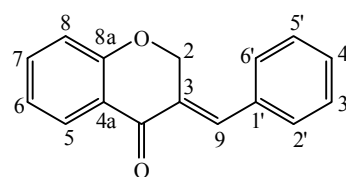
STRUCTURES OF COMPOUNDS SYNTHESISED



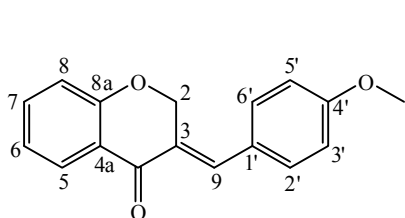
(1)



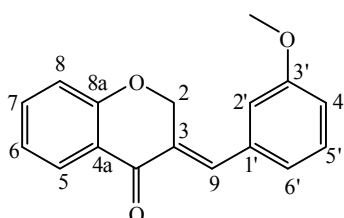
(2)



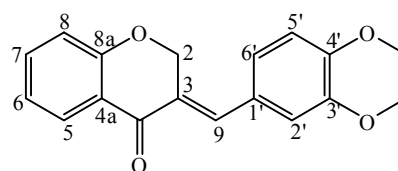
(3)



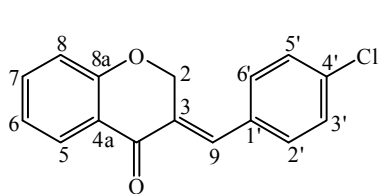
(4)



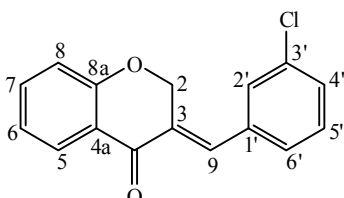
(5)



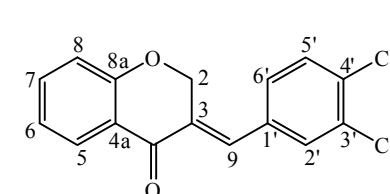
(6)



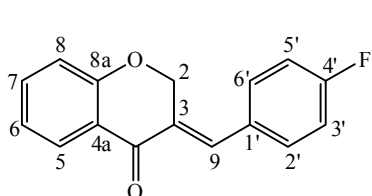
(7)



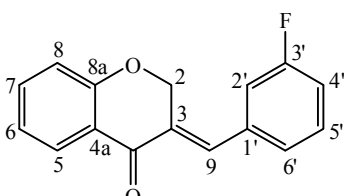
(8)



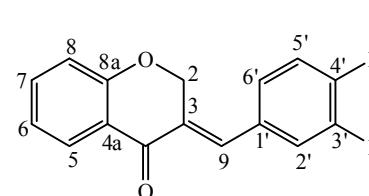
(9)



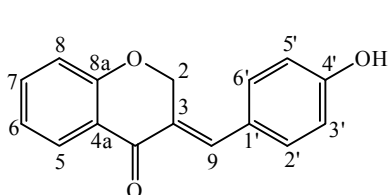
(10)



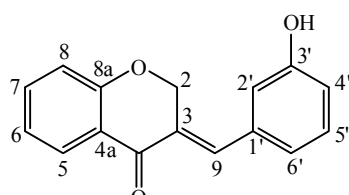
(11)



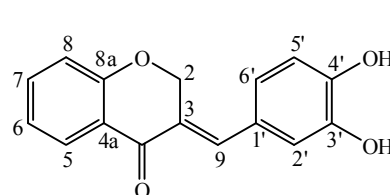
(12)



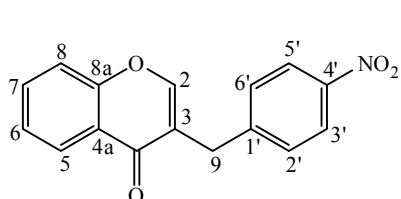
(13)



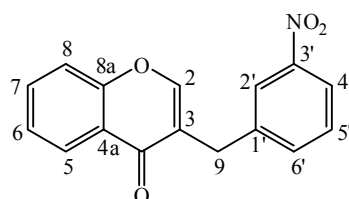
(14)



(15)



(16)



(17)

TABLE OF CONTENTS

Declaration 1- Plagiarism	v
Declaration 2- Publications.....	vi
Acknowledgements.....	vii
List of Abbreviations	viii
List of Tables	x
List of Figures.....	xi
List of Schemes.....	xii
List of Graphs	xiv
Abstract.....	xv
Structures of compounds synthesised	xvi
CHAPTER 1 INTRODUCTION	1
1.1 Classification, structure and biosynthesis of homoisoflavonoids	2
1.2 A review of the methods used to synthesise the 3-benzylidene-4 chromanones	7
1.2.1 Synthesis of the 4-chromanone (2) intermediate.....	9
1.2.2 Synthesis of the 3-benzylidene-4-chromanones from the 4-chromanone intermediate.....	10
1.2.3 Other methods used for the synthesis of 3-benzylidene-4-chromanones	12
1.3 Bioactivity of homoisoflavonoids.....	14
1.3.1 Antioxidant activities of substituted 3-benzylidene-4-chromanones	14
1.3.2 Antibacterial activities of substituted 3-benzylidene-4-chromanones.....	15
1.4 Methodology used for the bioassays.....	16
1.4.1 Methodology for the antioxidant assays.....	16
1.4.1.1 DPPH radical scavenging assay	17
1.4.1.2 Ferric reducing antioxidant power assay	17
1.4.1.3 ABTS assay	18
1.4.2 Methodology for the antibacterial assays	19
1.4.2.1 Kirby-Bauer disk-diffusion method.....	19
1.4.2.2 Bioautographic methods	19
1.4.2.3 Method of dilution.....	20
1.5 Hypothesis, aims and objectives	20
CHAPTER 2 RESULTS AND DISCUSSION	22

2.1	Synthesis and Characterisation	22
2.1.1	Synthesis and characterisation of the 4-chromanone (2) intermediate.....	23
2.1.2	Synthesis of the 3-benzylidene-4-chromanones	27
2.1.3	Structural elucidation of homoisoflavonoids (3-17).....	28
2.1.4	Structural elucidation of the <i>para</i> substituted derivatives (except 4'-fluoro)	33
2.1.5	Structural elucidation of the <i>meta</i> substituted derivatives (except 3'-fluoro).....	35
2.1.6	Structural elucidation of the 3',4'-disubstituted derivatives (except 3',4'-difluoro)...	37
2.1.7	Structural elucidation of the fluorine containing compounds (10, 11 and 12).....	39
2.1.8	Structural elucidation of the nitro containing compounds (16 and 17).....	41
2.2	Bioactivity of the synthesised homoisoflavonoids	44
2.2.1	Antioxidant activity of the synthesised homoisoflavonoids.....	44
2.2.1.1	DPPH radical scavenging assay	44
2.2.1.2	Ferric reducing antioxidant power assay	47
2.2.2	Antibacterial activity of the synthesised homoisoflavonoids	49
CHAPTER 3 EXPERIMENTAL		53
3.1	Chemistry.....	53
3.1.1	General experimental procedures	53
3.1.2	The synthesis of 3-phenoxypropanoic acid (1).....	54
3.1.3	The synthesis of 4-chromanone (2)	55
3.1.4	The base catalysed preparation of homoisoflavonoids (3-17).....	55
3.1.5	The physical and spectroscopic data of synthesised compounds (1-17)	56
3.2	Biochemistry.....	71
3.2.1	Antioxidant activity of the homoisoflavonoids synthesised.....	71
3.2.1.1	DPPH radical scavenging assay	71
3.2.1.2	Ferric reducing antioxidant power assay	72
3.2.2	Antibacterial activity of the homoisoflavonoids synthesised	73
3.2.2.1	Disc diffusion antimicrobial susceptibility testing	74
CHAPTER 4 CONCLUSION.....		78
REFERENCES		80

CHAPTER 1 INTRODUCTION

Homoisoflavonoids are a group of naturally occurring oxygen heterocyclic compounds which consist of either a chromane or chromanone system with a benzyl or benzylidene group at the 3-position (Figure 1) (Adinolfi *et al.*, 1986). They are referred to as homoisoflavonoids, homoisoflavanones or 3-benzyl-4-chromanones. The basic structure and nomenclature for the homoisoflavonoids are shown below (Figure 1).

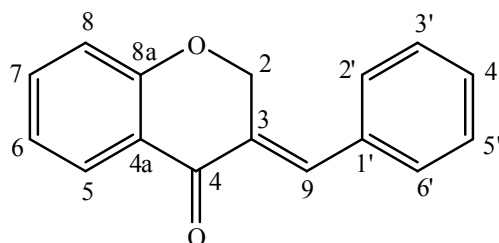


Figure 1: The basic structure of a 3-benzylidene homoisoflavonoid

Homoisoflavonoids belong more broadly to the flavonoids, and differ from another subclass, the isoflavonoids in that they have a C-16 rather than a C-15 skeleton (du Toit *et al.*, 2010). Whereas the isoflavonoids result from a phenyl shift from C-2 to C-3, the homoisoflavonoids have a varied biosynthetic pathway (Dewick, 1975), resulting in an extra carbon atom between the chromanone ring and the phenyl group, which distinguishes this subclass of isoflavonoids from the others (Dewick, 1975).

The first homoisoflavonoids, eucomin and eucomol, were isolated from *Eucomis bicolor* (Hyacinthaceae) in 1967 (Figure 2) (Böhler and Tamm, 1967). Since then, many homoisoflavonoids have been isolated from various plant families, but have remained to be a key chemotaxonomic marker amongst the Hyacinthaceae (Koorbanally *et al.*, 2006). Apart

from the Hyacinthaceae, they have also been isolated from the Fabaceae, Liliaceae, Dracaenaceae, Leguminosae and Convallariaceae plant families (Abegaz *et al.*, 2007). In recent studies, three new homoisoflavonoids which showed potent anti-inflammatory activity were isolated from *Ophiopogon japonicas* (Liliaceae) (Hung *et al.*, 2010).

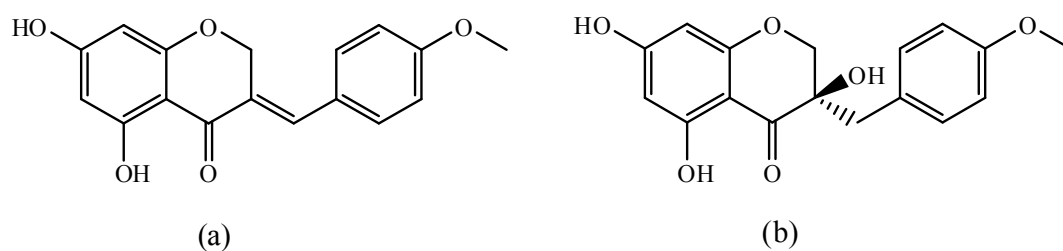


Figure 2: The chemical structures of eucomin (a) and eucomol (b)

1.1 Classification, structure and biosynthesis of homoisoflavonoids

Homoisoflavonoids contain a chromanone ring, which is a benzene ring fused with a tetrahydropyran ring, and a phenyl ring joined together by a carbon atom at C-3, which makes them different from both the flavonoids and the isoflavonoids (Figure 3). In nature, different substitution patterns occur on both the chromanone and phenyl moieties, leading to various permutations of hydroxylated, methoxylated and acetylated compounds as well as others such as the prenylated compounds.

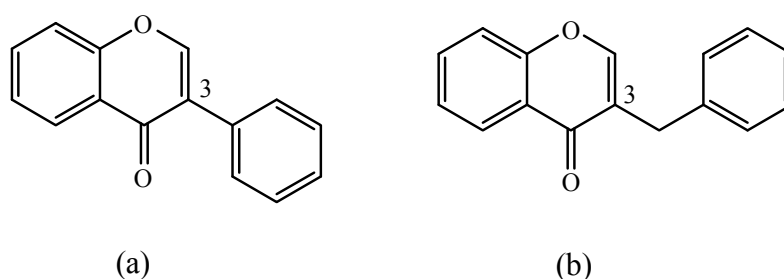


Figure 3: The structural skeleton of an isoflavonoid (a) and a homoisoflavonoid (b)

Homoisoflavonoids are biosynthesised from chalcone precursors. The mechanism and biosynthetic pathways by which homoisoflavonoids are formed were determined by labeling studies with phenylalanine, sodium acetate and methionine in *Eucomis comosum*, where labeled precursors were incorporated into the chalcone intermediates and further into the homoisoflavonoid (Dewick, 1975).

Phenolic compounds can be biosynthesised by two pathways: the shikimate pathway or the polyketide pathway. Homoisoflavonoids are of mixed biosynthetic origin, the A-ring is polyketide derived and the B-ring is shikimate derived (Figure 4) (Mann *et al.*, 1994).

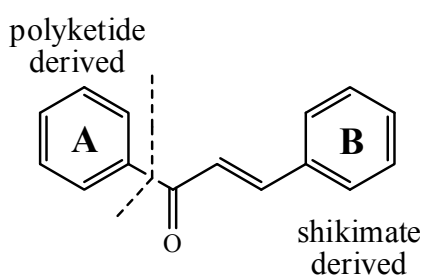
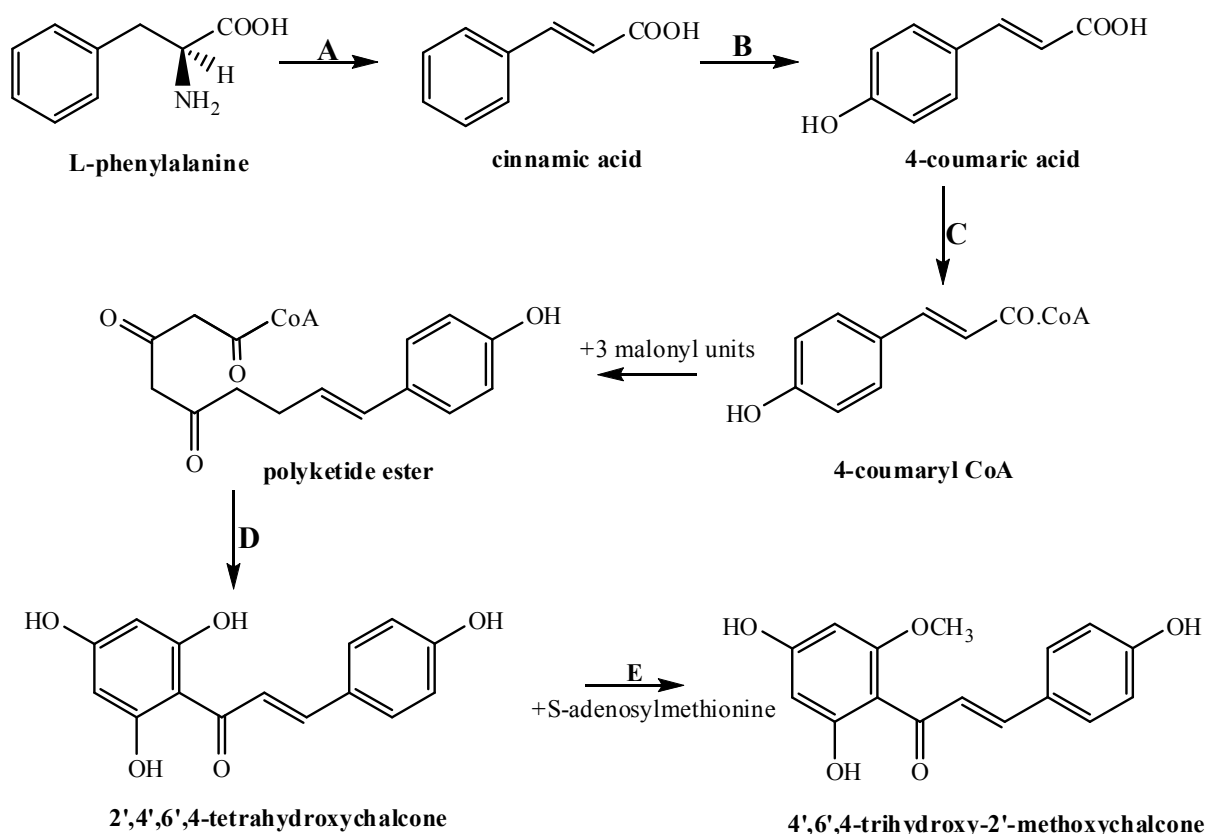


Figure 4: The formation of the A and B ring of the chalcone which is further cyclised into the homoisoflavonoid

The first step to the biosynthesis of homoisoflavonoids is the biosynthesis of the chalcone precursor (Figure 4). Chalcone biosynthesis (Scheme 1) starts with the deamination of L-phenylalanine to cinnamic acid and oxidized at the *para*-position to 4-coumaric acid, which is then converted to 4-coumaryl CoA (Bhandari *et al.*, 1992). This process is mediated by three enzymes, L-phenylalanine ammonia lyase, cinnamate-4-hydroxylase and coumarate-CoA-ligase. The 4-coumaryl CoA intermediate then combines with three molecules of malonyl CoA yielding the polyketide ester, which cyclises *via* a Claisen type condensation, producing the chalcone precursor, 2',4',6',4-tetrahydroxychalcone. This process is catalyzed by

chalcone synthase. Methionine is the source of the extra carbon atom, methylating the 2'-hydroxy group (Scheme 1-E), a key step in the biosynthesis of the homoisoflavonoids, since pyranone ring cyclisation involves this methoxyl group (Scheme 1).

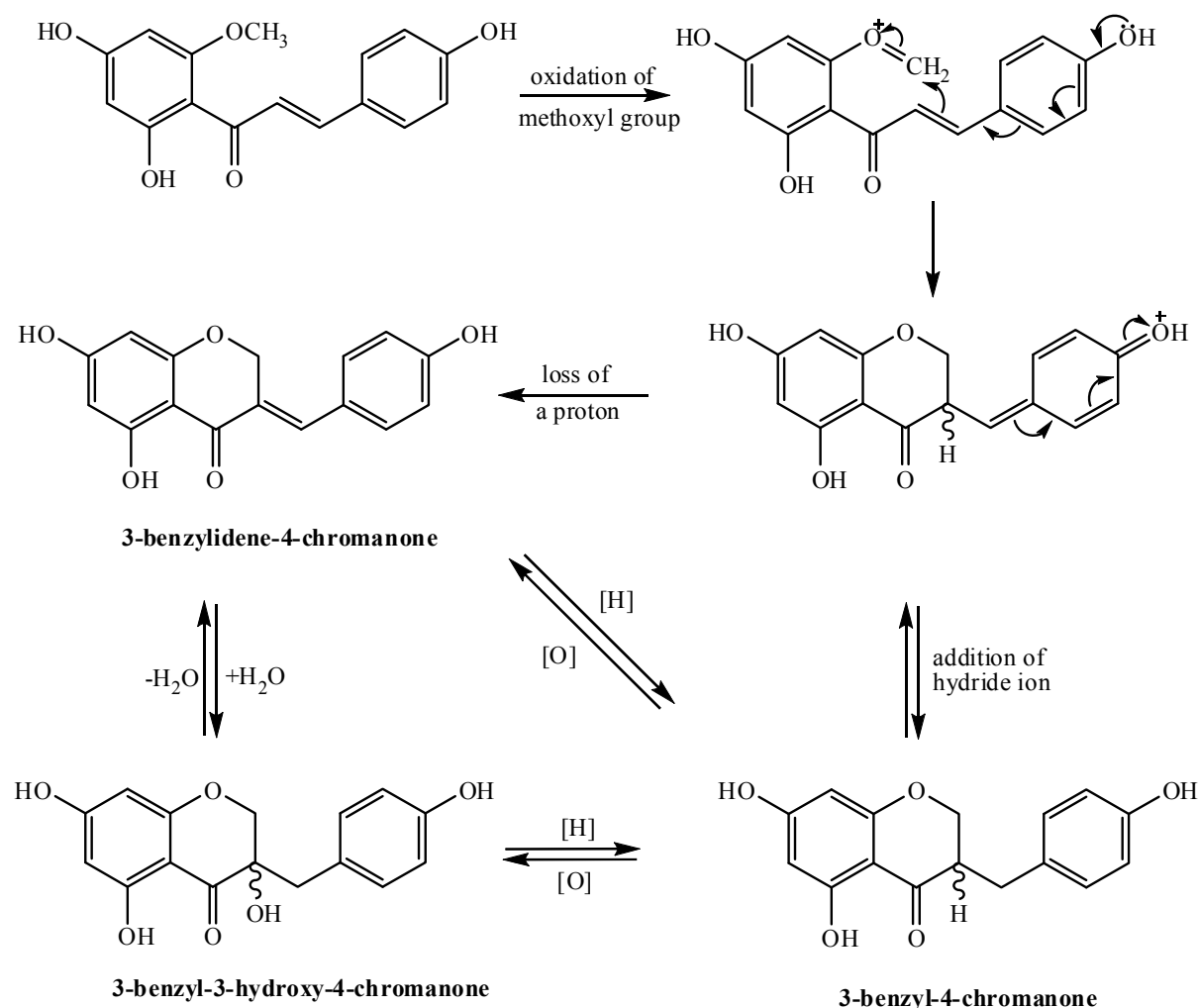


Enzymes: **A** - phenylalanine ammonia lyase **B** - cinnamate 4-hydroxylase
 C - 4-coumarate CoA ligase **D** - chalcone synthase
 E - methyl transferase

Scheme 1: The biosynthetic formation of the chalcone precursor (Hahlbrock and Grisebach, 1975)

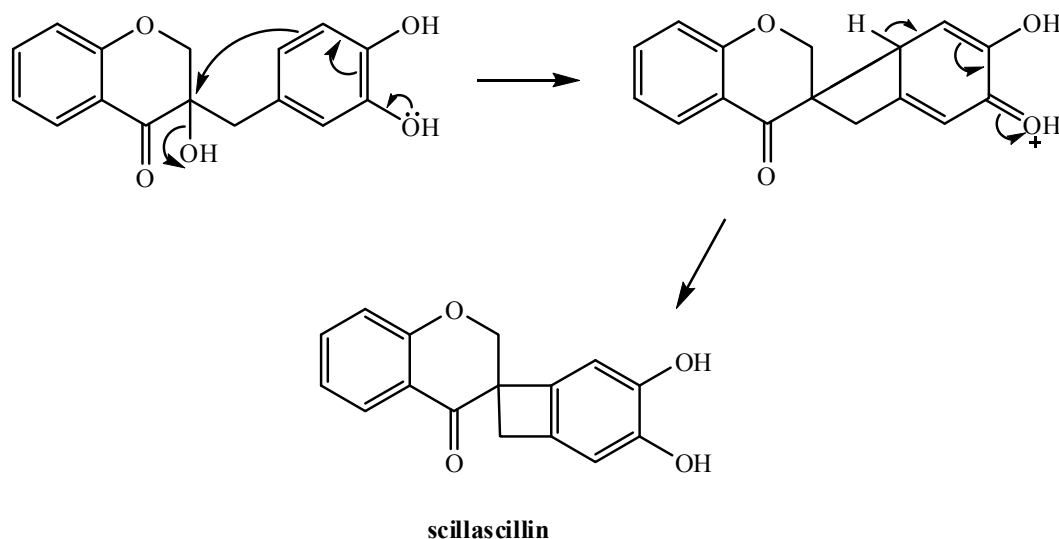
The biosynthesis of homoisoflavonoids from chalcones was proposed by Dewick (1975). The 2'-methoxy group is pivotal in this biosynthesis, which is oxidized by the loss of a proton. Subsequent cyclisation resulting from a flow of electrons from the lone pair on the 4'-hydroxy oxygen atom to the oxidized methoxy oxygen at the 2-position leads to the

formation of the three basic types of homoisoflavonoids, the methoxy carbon ending up as C-2 on the homoisoflavonoid skeleton. Addition of a hydride ion or loss of a proton results in either the 3-benzyl-4-chromanone or the 3-benzylidene-4-chromanones. Water added across the double bond of the 3-benzylidene-4-chromanones leads to the third type, the 3-benzyl-3-hydroxy-4-chromanones. The 3-benzyl-3-hydroxy-4-chromanone can also be formed by oxidation of 3-benzyl-4-chromanone at the 3-position. The mechanism for the formation of the homoisoflavonoids is illustrated in Scheme 2.



Scheme 2: The biosynthetic pathway from 2,4,4'-trihydroxy-2'-methoxychalcone to its corresponding homoisoflavonoids (Dewick, 1975)

The fourth type of homoisoflavonoid, the scillascillin type, is formed by the cyclisation of the 3-benzyl-3-hydroxy-4-chromanone, forming a strained but stable four-membered ring (Scheme 3) (Dewick, 1975).



Scheme 3: The proposed biosynthesis of scillascillin (Dewick, 1975)

Due to the presence of the double bond at the 3-position, 3-benzylidene-4-chromanones may undergo chemical conversion and exist as either the *trans* (*E*) or *cis* (*Z*) isomer (Kirkiacharian *et al.*, 1984) (Figure 5). In natural products, the *E* isomer is prevalent but can be converted to the *Z* isomer by light (Siddaiah *et al.*, 2006).

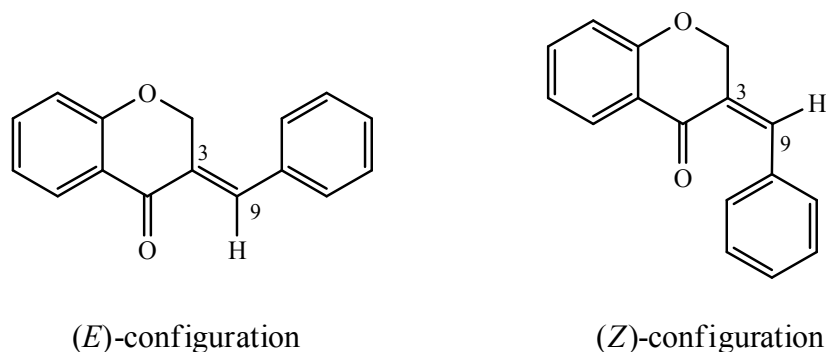
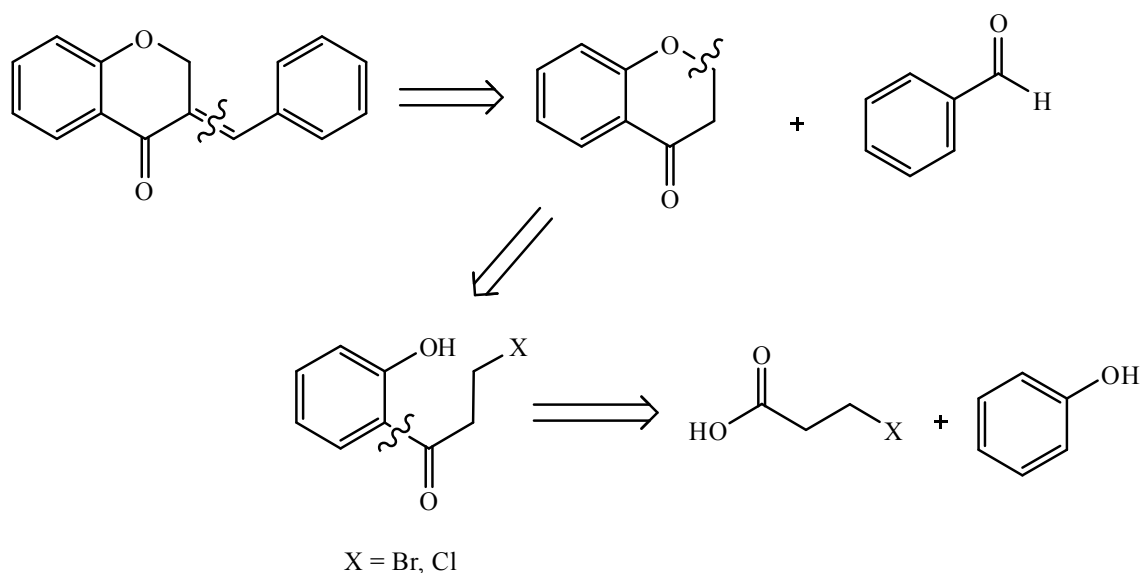


Figure 5: The *E* and *Z*-isomers of 3-benzylidene-4-chromanone

1.2 A review of the methods used to synthesise the 3-benzylidene-4-chromanones

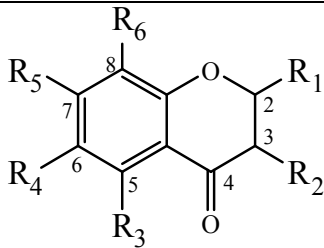
Homoisoflavonoids have been synthesised since the mid twentieth century (Farkas *et al.*, 1968). The first synthesis of homoisoflavonoids was completed just a year after these compounds were first isolated (Farkas *et al.*, 1968). A retrosynthetic analysis of these compounds results in aromatic aldehydes, phenols and carboxylic acid synthons. The carboxylic acid synthon has a halide functionality at the other end (Scheme 4).



Scheme 4: A retrosynthetic approach to 3-benzylidene-4-chromanone

The synthesis of 3-benzylidene-4-chromanones involves formation of the 4-chromanone (2), which is then condensed with aromatic aldehydes in the presence of an acid or base catalyst *via* the mechanisms in Scheme 6 and Scheme 7. However, various chromanones are commercially available and need not be synthesised as a first step. A survey on the Aldrich website indicates the availability of nine derivatives (Table 1) (www.sigmaaldrich.com/4-chromanone).

Table 1: Comparative prices of commercially available 4-chromanones

							
Compound Name	R ₁	R ₂	R ₃	R ₄	R ₅	R ₆	Price (ZAR)
4-chromanone	H	H	H	H	H	H	545.61/ 10 g
6-bromo-4-chromanone	H	H	H	Br	H	H	1377.61/ 0.25 g
6-chloro-4-chromanone	H	H	H	Cl	H	H	324.80/ 1 g
6-methyl-4-chromanone	H	H	H	CH ₃	H	H	1177.61/ 5 g
6-fluoro-4-chromanone	H	H	H	F	H	H	476.80/ 1 g
7-fluoro-4-chromanone	H	H	H	H	F	H	1264.01/ 1 g
6,7-dimethoxy-2,2-dimethyl-4-chromanone	diCH ₃	H	H	OCH ₃	OCH ₃	H	1072.01/ 1g
2,2-dimethyl-5,7,8-trimethoxy-4-chromanone	diCH ₃	H	OCH ₃	H	OCH ₃	OCH ₃	708.80/ 0.05 g
2,2-dimethyl-7-ethoxy-6-methoxy-4-chromanone	diCH ₃	H	H	OCH ₃	OCH ₃ CH ₂	H	708.80/ 0.1 g
7-acetoxy-3-acetyl-2-methyl-4-chromanone	CH ₃	CH ₃ CO	H	H	CH ₃ CO ₂	H	708.80/ 0.05 g

Several of the chromanone derivatives that are commercially available are relatively expensive, compared to the unsubstituted chromanone therefore derivatisation of the chromanone may be a better alternative to purchasing the derivatives.

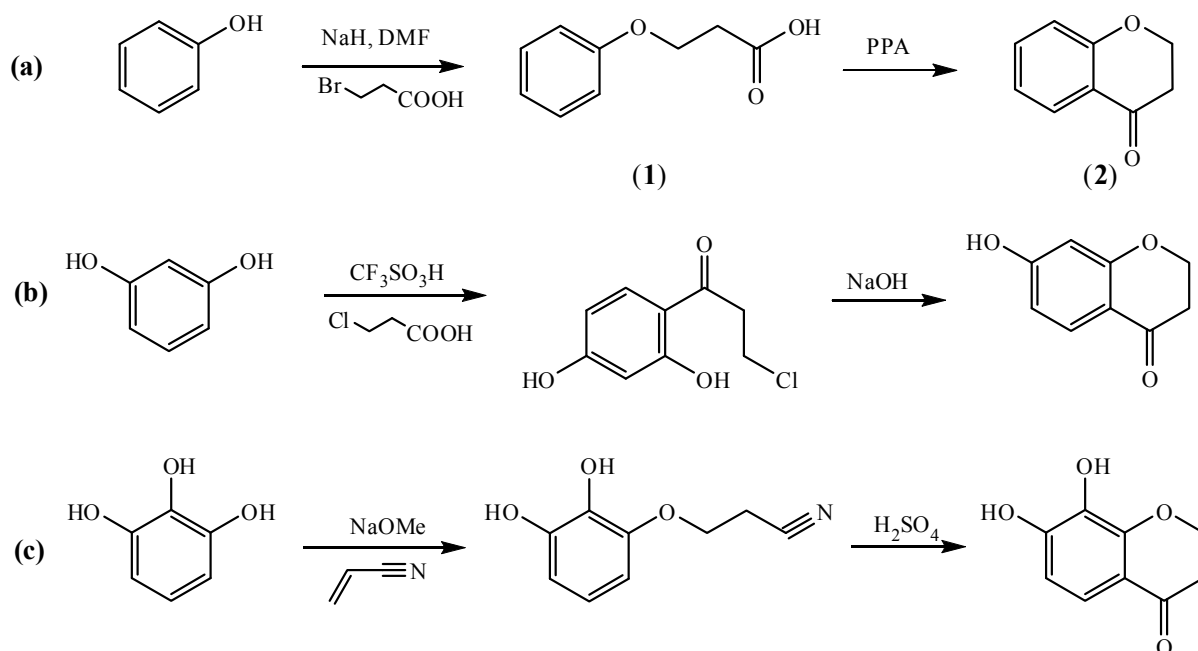
1.2.1 Synthesis of the 4-chromanone (2) intermediate

Even though the 4-chromanone intermediates are available, researchers in the field still synthesise the intermediate en route to the homoisoflavonoids. Different methods were employed for their synthesis (Scheme 5) (Siddaiah *et al.*, 2006; Foroumadi *et al.*, 2007; Siddaiah *et al.*, 2007; Shaikh *et al.*, 2011a).

They can be formed from the reaction of:

- (a) 3-bromo- or 3-chloropropanoic acids and phenols under basic conditions, producing a phenoxypropanoic acid which can be cyclised with polyphosphoric acid (Siddaiah *et al.*, 2006; Shaikh *et al.*, 2011a);
- (b) 3-bromo- or 3-chloropropanoic acids and phenols under acidic conditions, producing a benzophenone alkyl chloride which can be cyclised with sodium hydroxide (Foroumadi *et al.*, 2007);
- (c) acrylonitrile and phenols under basic conditions forming a phenoxynitrile which is followed by the cyclisation with sulfuric acid (Siddaiah *et al.*, 2007).

In all cases, an activated carbon is produced in the intermediate. In the case of the acid and nitrile intermediates, an acid is used as a catalyst for the cyclisation by activating the carboxyl or nitrile groups toward nucleophilic substitution and for the alkyl chloride, a base is needed for the abstraction of the proton of the hydroxyl group, which is then followed by nucleophilic substitution.



Scheme 5: (a) The synthesis of 3-phenoxypropanoic acid (**1**) and 4-chromanone (**2**) (Siddaiah *et al.*, 2006); (b) The synthesis of 7-hydroxy-4-chromanone (Foroumadi *et al.*, 2007); (c) The synthesis of 7,8-dihydroxy-4-chromanone (Siddaiah *et al.*, 2007)

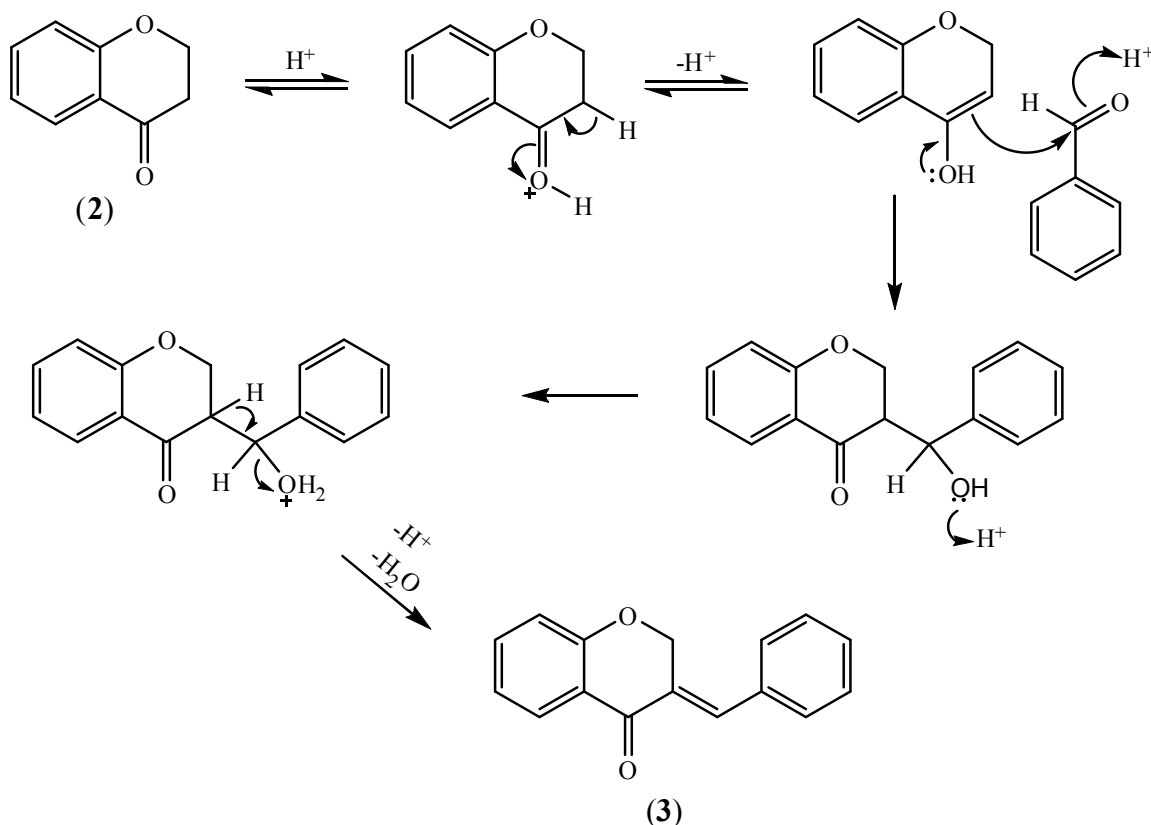
The method employed for the synthesis of chromanone depends on the functionalities on the A-ring of the molecule. Strong bases may not be used with more than one hydroxyl group on the A-ring, due to the unwanted complete deprotonation of the hydroxyl groups.

Methods **a**, **b** and **c** above has reasonable yields of 46%, 54% and 61% respectively (Siddaiah *et al.*, 2006; Foroumadi *et al.*, 2007; Siddaiah *et al.*, 2007).

1.2.2 Synthesis of the 3-benzylidene-4-chromanones from the 4-chromanone intermediate

Benzaldehydes are condensed onto the 3-position of the 4-chromanone intermediate using either acids or bases as a catalyst. Acid-catalysed condensation requires protic acids, such as phosphoric (Desideri *et al.*, 2011; Shaikh *et al.*, 2011a) and hydrochloric acid (Evans and

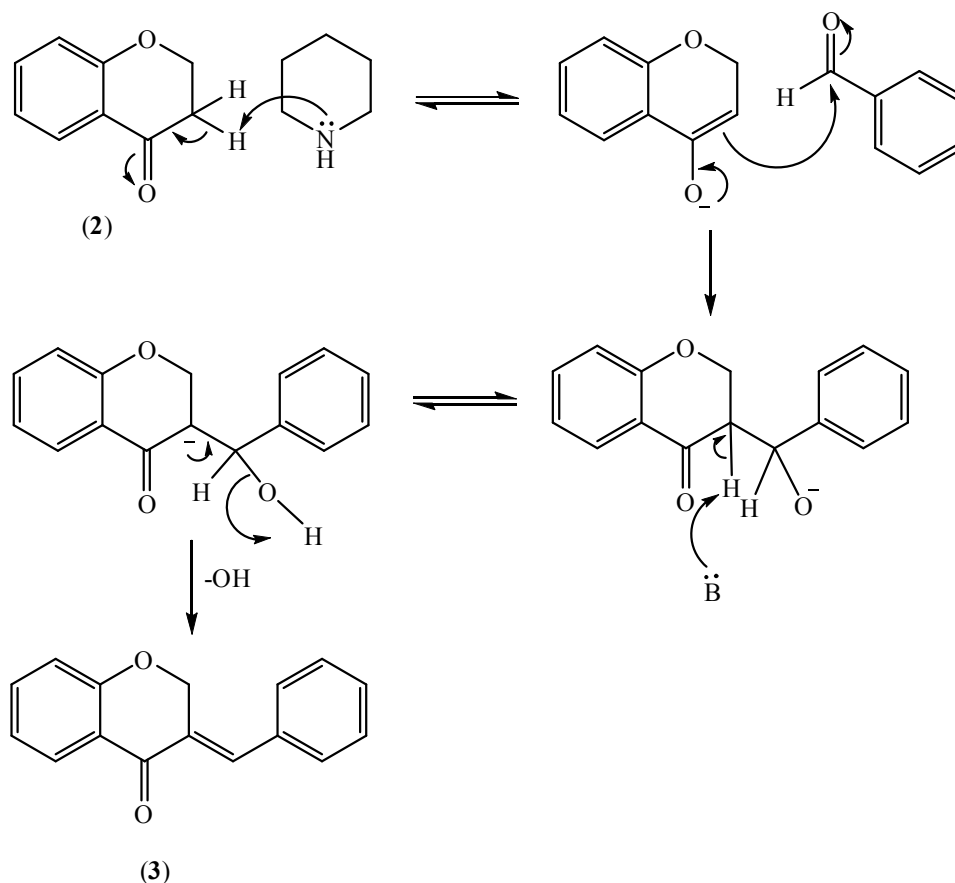
Lockhart, 1966; Foroumadi *et al.*, 2007; Cheng *et al.*, 2011; Desideri *et al.*, 2011), which protonate the carbonyl group of the 4-chromanone intermediate, promoting enol formation and also protonate the carbonyl group of the aldehyde, activating the carbonyl group, making it more electrophilic and more susceptible to nucleophilic attack (Scheme 6).



Scheme 6: The proposed reaction mechanism for the acid-catalysed preparation of 3-benzylidene-4-chromanone

Base-catalysed condensation involves the abstraction of the alpha proton by weak bases such as piperidine (Lévai and Schág, 1979; Perjési *et al.*, 2008; Shaikh *et al.*, 2011a; Jacquot *et al.*, 2012), which result in the enolate anion, a better nucleophile than the enol, thereby promoting the addition of the nucleophile to the aldehyde.

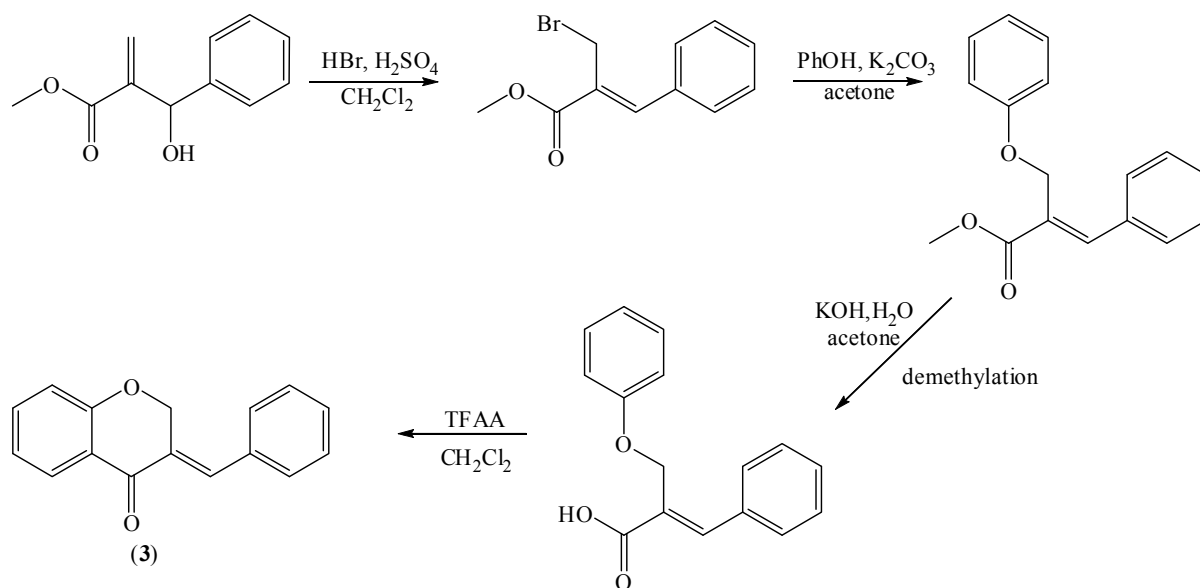
In the base-catalysed mechanism, the driving force for the elimination of water is the highly conjugated product that forms as a result of the elimination (Scheme 7). Other bases such as pyrrolidine have also been used (Shankar *et al.*, 2012).



Scheme 7: The proposed reaction mechanism for the base-catalysed preparation of 3-benzylidene-4-chromanone

1.2.3 Other methods used for the synthesis of 3-benzylidene-4-chromanones

Rather than synthesising the chromanone and then condensing it with an aldehyde to prepare the homoisflavonoid, Basavaiah and Bakthadoss (1998) applied the Baylis-Hillman reaction and started with the construction of the benzylidene moiety and then the chromanone ring system (Scheme 8). This method is better at synthesising homoisflavonoids with different substituents on the chromanone A-ring as different phenols can be used in the first step.



Scheme 8: The reaction scheme for the preparation of 3-benzylidene-4-chromanone by the Baylis-Hillman reaction (Basavaiah and Bakthadoss, 1998)

The synthesis of several types of homoisoflavonoids has been reported in the literature (Farkas *et al.*, 1968; Lévai and Schág, 1979; Basavaiah and Bakthadoss, 1998; Siddaiah *et al.*, 2006; Foroumadi *et al.*, 2007; Siddaiah *et al.*, 2007; Perjési *et al.*, 2008; Rao *et al.*, 2008; Zhang *et al.*, 2008; Das *et al.*, 2009; Cheng *et al.*, 2011; Desideri *et al.*, 2011; Shaikh *et al.*, 2011a; Jacquot *et al.*, 2012; Shankar *et al.*, 2012).

5,7-diacetoxy-3(4-methoxybenzal)-4-chromanone was synthesised by refluxing 5,7-dihydroxy-4-chromanone in acetic anhydride. Deacylation of 5,7-diacetoxy-3(4-methoxybenzal)-4-chromanone yielded eucomin (Farkas *et al.*, 1968). Other natural homoisoflavonoids, such as punctatin, were also synthesised by refluxing chromanone and an aldehyde in hot acetic anhydride (Farkas *et al.*, 1971), however this method was inefficient due to the long reaction times (Lévai, 2004).

1.3 Bioactivity of homoisoflavonoids

Homoisoflavonoids have been reported to have a wide range of biological activities (du Toit *et al.*, 2010). They have been found to exhibit antibacterial (Das *et al.*, 2009; Shankar *et al.*, 2012), antioxidant (Farkas *et al.*, 1968; Siddaiah *et al.*, 2006; Siddaiah *et al.*, 2007; Lin *et al.*, 2010), anti-inflammatory (Hung *et al.*, 2010; Shaikh *et al.*, 2011b), antifungal (Rao *et al.*, 2008), antiviral (Tait *et al.*, 2006), antimutagenic (Miadoková *et al.*, 2002), anticancer (Yan *et al.*, 2012) and antirhinovirus (Conti and Desideri, 2009) activity. Naturally occurring homoisoflavonoids serve as potent protein tyrosine kinase inhibitors (Lin *et al.*, 2008).

Since the homoisoflavonoids synthesised in this work were tested for their antioxidant and antibacterial activity, these activities are reviewed below.

1.3.1 Antioxidant activities of substituted 3-benzylidene-4-chromanones

Polyphenolic homoisoflavonoids such as 7-hydroxy-3-(3,4-dihydroxybenzylidene)chroman-4-one (sappanone A) and 7-hydroxy-3-(3,4,5-trihydroxybenzylidene)chroman-4-one (Figure 6) showed potent antioxidant activity, stronger than that of ascorbic acid, a commonly consumed antioxidant (Siddaiah *et al.*, 2006). This was attributed to the catechol like system within these molecules. This finding was also confirmed by Foroumadi *et al.* (2007) who studied a range of C1-C4 (methoxy through to n-butoxy). The 7-substituted alkyloxy benzylidene-4-chromanones showed the best antioxidant activity (Foroumadi *et al.*, 2007).

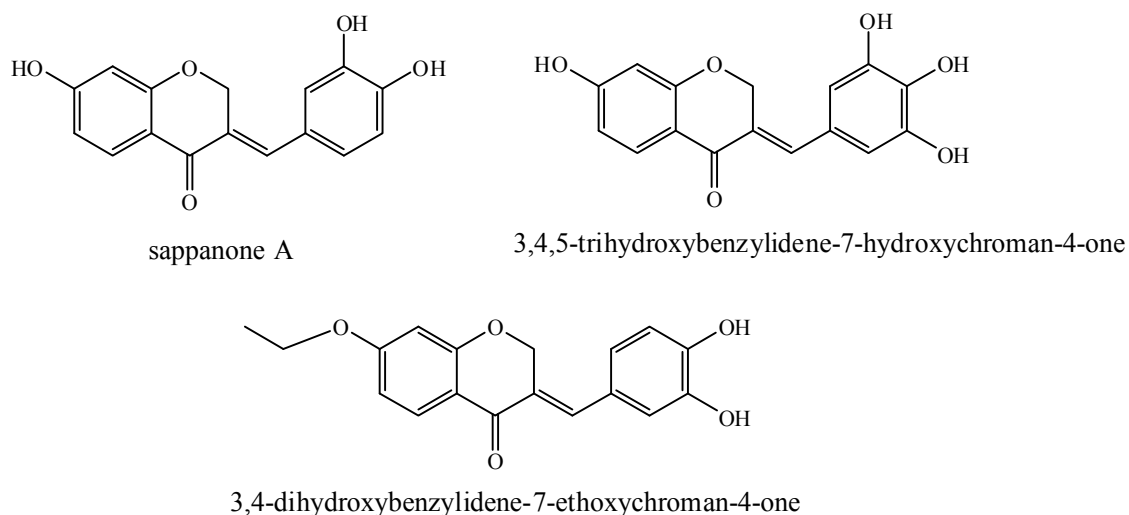


Figure 6: Homoisoflavonoids showing good antioxidant activity

1.3.2 Antibacterial activities of substituted 3-benzylidene-4-chromanones

Flavonoids have been shown to be active against many species of bacteria, both gram positive and gram negative strains (du Toit *et al.*, 2010). Das *et al.* (2009) tested a range of naturally occurring homoisoflavonoids and their derivatives against three gram positive (*Staphylococcus aureus*, *Bacillus subtilis*, *Bacillus sphaericus*) and three gram negative (*Klebsiella aerogenes*, *Chromobacterium violaceum*, *Pseudomonas aeruginosa*) bacterial strains. Of the compounds tested, the benzylidene-4-chromanone with a hydroxy group at C-7 and a 3',4'-methylenedioxy group showed good antibacterial activity against *Staphylococcus aureus* (gram positive), *Klebsiella aerogenes* and *Chromobacterium violaceum* (gram negative) (Figure 7) (Das *et al.*, 2009).

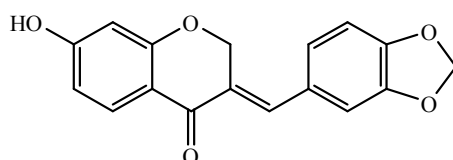


Figure 7: 3-(Benzo[1,3]dioxol-5-ylmethylene)-7-hydroxychroman-4-one, a 3-benzylidene-4-chromanone with good antibacterial activity

A series of thirteen naturally occurring homoisoflavonoids, of all structural types, was screened against *Staphylococcus aureus* (ATCC 12600) (du Toit *et al.*, 2007), where two homoisoflavonoids of the 3-benzylidene-4-chromanone type (Figure 8) oxygenated at the 5,7,4' and 5,7,8,4'-positions showed good antibacterial activity with minimum inhibitory concentrations (MIC) of 0.52 and 0.24 mM respectively.

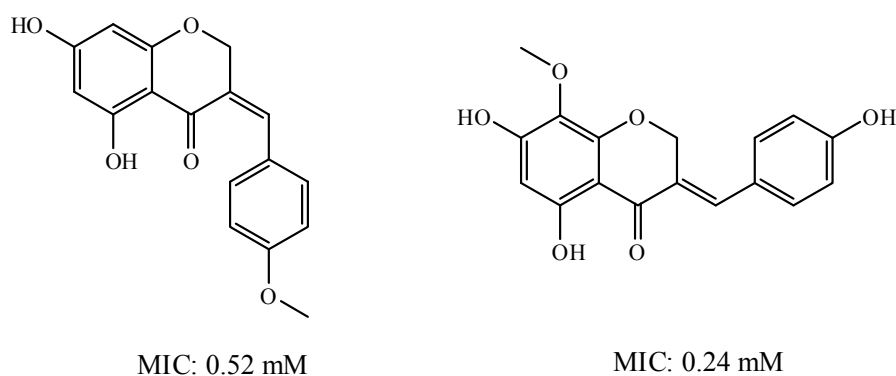


Figure 8: The substituted 3-benzylidene-4-chromanones with good antibacterial activity against *Staphylococcus aureus* (ATCC 12600)

1.4 Methodology used for the bioassays

Antioxidant assays are carried out using several different types of assays, a few of them being ABTS, DPPH, FRAP, and ORAC assays. The antibacterial assays include the Kirby-Bauer disk-diffusion method and the bioautographic method. Minimum inhibitory concentration may be determined using a microdilution method on a 96 well microtitre plate.

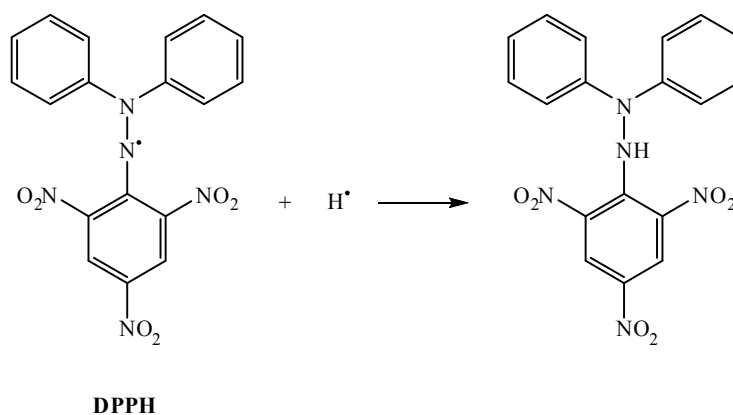
1.4.1 Methodology for the antioxidant assays

Several methods have been established to determine the antioxidant potential of compounds, each providing unique information on the way the compounds exhibit this antioxidant activity. The main methods included the 2,2-diphenyl-1-picrylhydrazyl (DPPH) radical

scavenging, ferric reducing antioxidant power (FRAP) and the 2,2'-azino-bis(3-ethylbenzothiazoline-6-sulfonic acid) ABTS method (Thaipong *et al.*, 2006).

1.4.1.1 DPPH radical scavenging assay

The DPPH radical scavenging method is the simplest of all those mentioned above and the most commonly used. DPPH is a stable free radical containing compound, which absorbs light at 517 nm. In the presence of a compound with antioxidant potential, the DPPH radical is reduced, by accepting an electron or a hydrogen radical, to form a stable diamagnetic molecule, resulting in a decrease in absorbance. Upon reduction, a colour change from purple to yellow is observed. The amount by which the absorbance decreases is a measure of the strength of the antioxidant. The structure of DPPH and the reaction that occurs between it and the antioxidant compound is illustrated below (Scheme 9) (Shyam *et al.*, 2012).



Scheme 9: The reaction of DPPH with a hydrogen radical (Shyam *et al.*, 2012)

1.4.1.2 Ferric reducing antioxidant power assay

The ferric reducing antioxidant power (FRAP) measures the ability of a compound to reduce Fe^{3+} to Fe^{2+} . Ferric chloride ($\text{Fe}^{3+}\text{Cl}_3^-$) (dark green in colour) is reduced in the presence of an antioxidant at a low pH, resulting in ferrous chloride ($\text{Fe}^{2+}\text{Cl}_2^-$), which is deep blue in

solution. The absorbance of the resulting solution, measured at 700 nm, is an indication of the strength of the antioxidant *i.e.* the more Fe^{3+} is reduced, the more blue the solution is and the higher the absorbance, indicating a higher activity of the antioxidant (Figure 9).

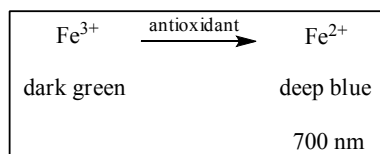
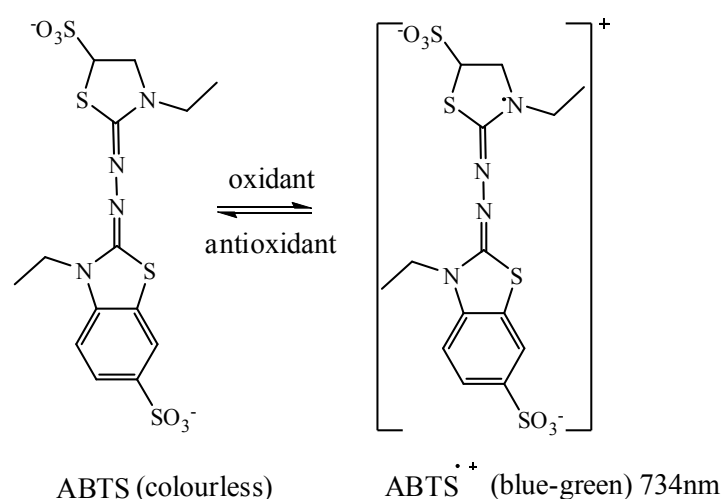


Figure 9: The reduction of Fe^{3+} to Fe^{2+} in the presence of an antioxidant

1.4.1.3 ABTS assay

The 2,2'-azino-bis(3-ethylbenzothiazoline-6-sulfonic acid) (ABTS) assay is a colorimetric assay which involves the conversion of the coloured ABTS radical to the colourless ABTS. Colourless neutral ABTS is oxidised creating the blue-green ABTS radical cation. In the presence of a compound with antioxidant potential, the ABTS radical cation reacts with the antioxidant and is neutralized. The measure of antioxidant capacity is measured spectrophotometrically at a wavelength of 734 nm. The decrease in the absorbance is an indication of how much the ABTS radical cation has been neutralised and hence the compounds' antioxidant potential (Scheme 10) (Erel, 2004; Osman *et al.*, 2006).



Scheme 10: The reaction between ABTS and the antioxidant (Osman *et al.*, 2006)

(Note the radical formation on the nitrogen in the top half of the molecule)

1.4.2 Methodology for the antibacterial assays

Antimicrobial activities may be determined in one of three general ways *i.e.* by dilution, diffusion or bioautographic methods. Diffusion and bioautographic methods are qualitative methods whereas dilution is a quantitative method. Compounds are screened initially using either the diffusion or bioautographic method to determine if the compound has antibacterial activity. Once this has been established, the minimum inhibitory concentration may be determined using the method of dilution.

1.4.2.1 Kirby-Bauer disk-diffusion method

The Kirby-Bauer disk-diffusion method, also known as the agar disc diffusion method, involves the inhibition of the growth of bacteria on a Müller-Hinton agar surface in the presence of an antibacterial agent. Petri dishes are filled with Müller-Hinton agar, onto which a bacterial strain is swabbed. Test compounds are impregnated onto filter discs and placed onto the agar surface. The plates are then incubated for bacterial growth. The test compound diffuses from the filter paper onto the agar. Depending on the activity of the compound, the bacterial growth surrounding the disc is inhibited. After incubation is complete, the zones of inhibition are measured, *i.e.* the area around the filter disc on which the bacterial growth was inhibited. The zones of inhibition are a clear indication whether a specific test compound shows antibacterial activity against bacterial strains.

1.4.2.2 Bioautographic methods

This method involves the inhibition of growth of bacterial strains on a silica based surface in the presence of an antibacterial agent. Test compounds are spotted onto thin layer chromatography (TLC) plates at various concentrations. The plates are then coated with a bacterial strain and incubated for bacterial growth. Test compounds diffuse inhibiting

bacterial growth. After incubation the plates are sprayed with an indicator solution of *p*-iodonitrotetrazolium (INT) violet. This indicator solution colours the plate where the bacteria is present, thereby clearly showing areas in which the bacterial growth was inhibited. Zones of inhibition are measured as an indication of the compounds antibacterial activity (Valgas *et al.*, 2007).

1.4.2.3 Method of dilution

The method of dilution is employed to determine the minimum inhibitory concentration of test compounds. A range of concentrations of the test compound are prepared. A 96-microwell plate is prepared by adding a standard amount of test compound, Müller-Hinton broth and bacterial standard into each well. The plate is then incubated for bacterial growth. A small volume of INT violet is then added to each well. In the wells which have a negative result, *i.e.* where the bacterial growth was not inhibited, the INT changes from yellow to purple. The results may be read spectrophotometrically or visually. The lowest concentration at which the INT remained yellow is the minimum inhibitory concentration (Valgas *et al.*, 2007).

1.5 Hypothesis, aims and objectives

Since naturally occurring homoisoflavonoids of the 3-benzylidene type have shown antibacterial and antioxidant activities (Siddaiah *et al.*, 2007; Das *et al.*, 2009), it was hypothesised that various derivatives with chemical modifications to the phenyl ring could produce enhanced activity in antibacterial and antioxidant assays. Investigations into various constituents on the phenyl ring of the homoisoflavonoids were explored to see which of the groups are essential for good biological activity.

The aim of the study was to synthesise and characterise a series of homoisoflavonoids with modified phenyl rings and to test them for their antibacterial and antioxidant activity. To this end, substitution on the B-ring of the homoisoflavonoids were varied with fluoro, chloro, nitro, hydroxy and methoxy groups in order to determine which substituents as well as their position on the phenyl ring will be the most biologically active. Mono- and di-substituted derivatives were prepared to see whether or not substitution at more than one position could also lead to enhanced activity.

The objective of the study is to find new target molecules for the development of more potent antibacterial and antioxidant drugs.

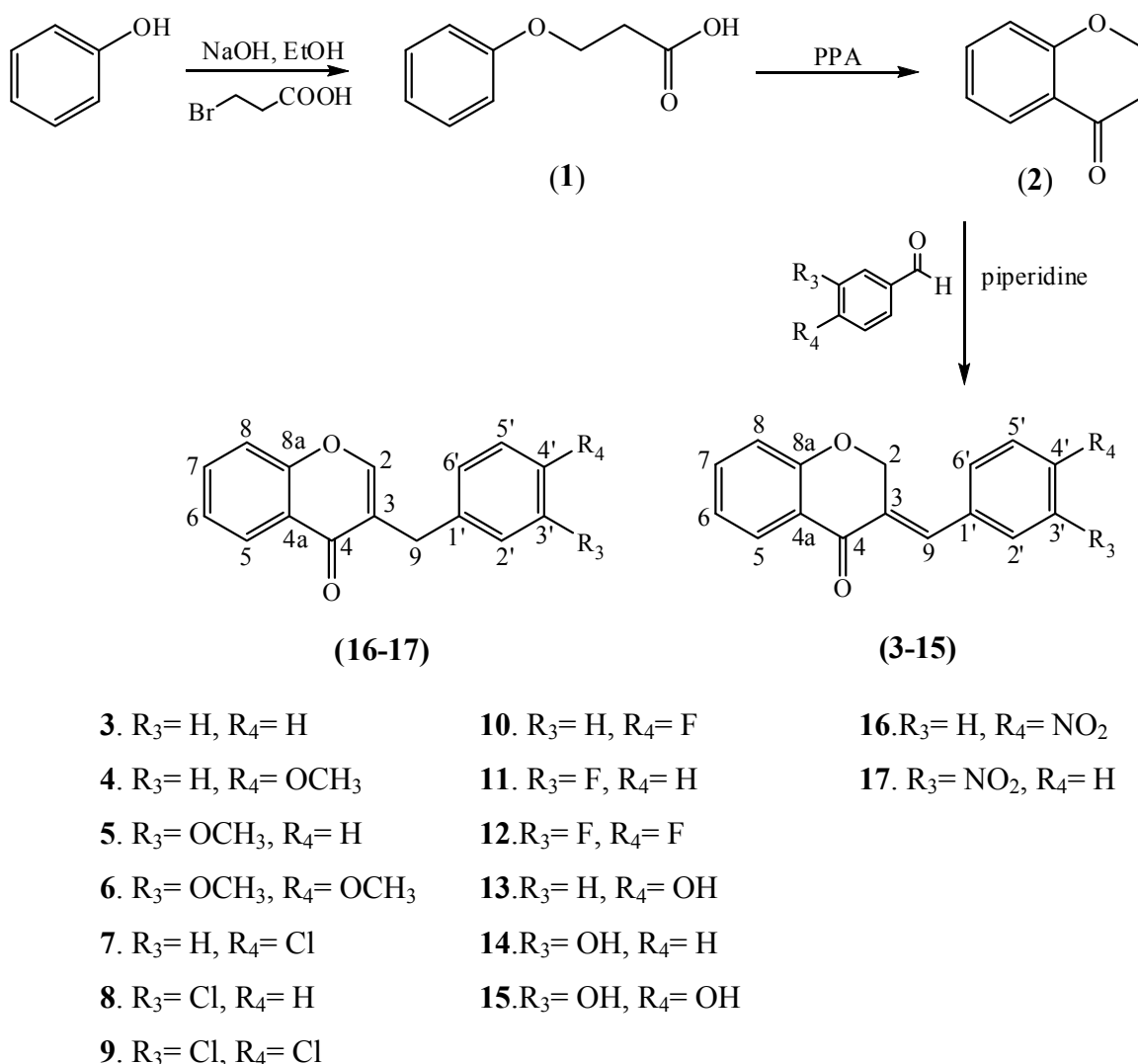
CHAPTER 2 RESULTS AND DISCUSSION

This chapter includes a discussion of the synthesis and characterisation of 3-benzylidene-4-chromanones as well as the antioxidant and antibacterial activities of the synthesised compounds. The methods used to synthesise the compounds are discussed together with mechanisms for the reactions. The characterisations of the compounds include a discussion of the NMR data along with other data such as mass spectrometry, IR and UV to validate the structures assigned to the synthesised products. The data for the antioxidant and antibacterial assays as well as the interpretation of it are also included in this chapter.

2.1 Synthesis and Characterisation

Thirteen 3-benzylidene-4-chromanones and two 3-benzyl-4-chromanones with different substitution patterns on the phenyl ring (B-ring) (Scheme 11) were synthesised in good yields of between 50 and 90% according to the modified procedure by Shaikh *et al.* (2011a). The target molecules were chosen to examine the effect that the fluorine, chlorine, methoxy, hydroxy and nitro groups have on different positions of the phenyl ring with regard to reactivity and biological activity. This would enable us to study the structure-activity relationship of the substituted benzylidene-4-chromanones with regard to antioxidant and antibacterial activity.

The synthesis of the homoisoflavonoids from phenol is a three step reaction process; the synthesis of 3-phenoxypropanoic acid (**1**) from phenol, the cyclisation of 3-phenoxypropanoic acid to 4-chromanone (**2**), and the condensation of 4-chromanone with the aromatic aldehyde to the homoisoflavonoid (**3-17**) (Scheme 11).

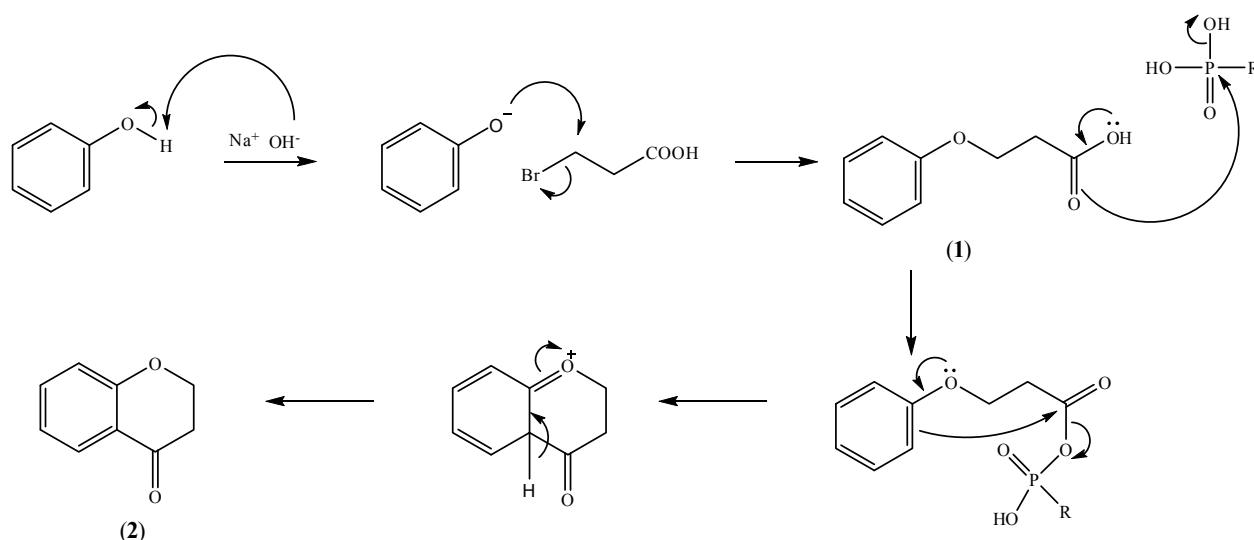


Scheme 11: The synthetic scheme for the synthesis of 3-phenoxy propanoic acid (1), 4-chromanone (2) and homoisoflavonoids (3-17)

2.1.1 Synthesis and characterisation of the 4-chromanone (2) intermediate

The 4-chromanone intermediate was synthesised in two steps (Scheme 11). The first step involves the reaction of phenol with bromopropanoic acid and a strong base (NaOH) to abstract the proton of the hydroxyl group on phenol. The resultant phenolate anion is stabilised by resonance structures. It then attacks the electrophilic carbon alpha to the bromine in probably a S_N2 type mechanism forming 3-phenoxypropanoic acid (1), which

cyclises upon addition of polyphosphoric acid (PPA). PPA forms a phosphate ester with the 3-phenoxypropanoic acid, which is followed by electrophilic substitution of the ester on the aromatic ring forming a pyran ring. Polyphosphoric acid is an oligomer of phosphoric acid and commonly used to activate the carboxyl group, making nucleophilic substitution possible (Clayden *et al.*, 2001). A proposed mechanism is given below (Scheme 12).



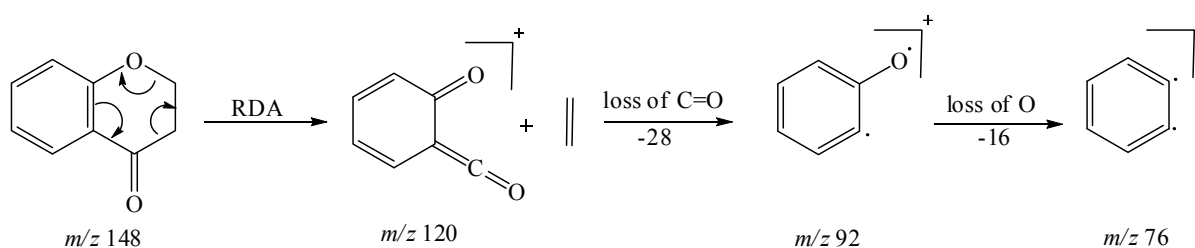
Scheme 12: The proposed reaction mechanism for the synthesis of 3-phenoxypropanoic acid (1) and 4-chromanone (2)

The reaction was carried out at ambient conditions for 30 min and then heated under reflux for 2 hrs. A yield of 52% was obtained from the reaction of 3-phenoxypropanoic acid with polyphosphoric acid to 4-chromanone, which compares well to the yields reported in the literature (Siddaiah *et al.*, 2006). On heating for longer durations, no improvement in the yield was observed. Purification of the target compound was necessary after the reaction occurred. This was carried out on silica gel using column chromatography.

The infrared spectrum of the first intermediate, 3-phenoxypropanoic acid (1), showed a sharp band at 1688 cm⁻¹ and a broad band at 2931cm⁻¹, indicating the presence of a carbonyl and

hydroxy group respectively. This serves as an indication for the formation of the acid. After the cyclisation of 3-phenoxypropanoic acid to 4-chromanone (**2**), the carbonyl band shifted from 1688 cm^{-1} to 1682 cm^{-1} . Other characteristic absorption bands observed in **2** were that of the aromatic ring, C=C stretching vibrations ($1599, 1476, 1453\text{ cm}^{-1}$) and the C-O stretching vibration at 1258 cm^{-1} .

The mass spectrum confirmed the presence of 4-chromanone (**2**) by displaying the molecular ion peak $[M^+]$ of 148 mass units. The base peak was observed at 120 mass units as a result of a retro Diels-Alder cleavage. Other intense peaks were seen at 92 and 64 mass units. The proposed fragmentation scheme of 4-chromanone is illustrated below (Scheme 13).



Scheme 13: The proposed fragmentation pattern of 4-chromanone (**2**)

The ^1H NMR spectrum of 3-phenoxypropanoic acid (**1**) is characterised by two methylene triplets (t) at δ_{H} 2.83 and δ_{H} 4.23 with coupling constants of $J = 6.24\text{ Hz}$, with the methylene proton resonance adjacent to the oxygen being more deshielded than that next to the acid group. The aromatic protons of H-6/10 appear at δ_{H} 6.89 and that of H-7/9 appear at δ_{H} 7.26. The H-6/10 resonance appears more upfield due to the electron donation by resonance from the oxygenated group. The H-8 proton resonance appears as a triplet, due to the coalescing of doublets with similar coupling constants, at δ_{H} 6.94 with $J = 7.42\text{ Hz}$. The ^{13}C NMR spectrum shows the two methylene carbon resonances at δ_{C} 34.49 and 63.05 and the aromatic carbon resonances between δ_{C} 114.65 to δ_{C} 129.50 with the aromatic C-O resonance at δ_{C}

158.39 and an additional carbonyl resonance at δ_C 176.93 for the carboxylic acid carbonyl group.

The ^1H NMR spectrum of the 4-chromamone (**2**) intermediate differs from the phenoxypropanoic acid intermediate in that the two H-2 and two H-3 resonances are now not equivalent. Due to chemical shift overlap of H-2a and H-2b and also H-3a and H-3b, the coupling pattern is no longer first order, but is now second order (Figure 10). H-2 and H-3 splitting patterns are therefore difficult to interpret and are reported as multiplets.

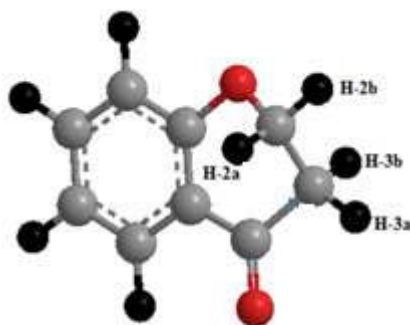


Figure 10: The chromanone ring (**2**) showing protons H-2a, H-2b, H-3a and H-3b

The aromatic resonances for H-5 and H-7 are seen to occur distinctly from the H-6/8 resonances. The H-6/8 resonances overlap, but can be distinguished with H-8 occurring as a doublet at δ_H 6.93 ($J = 8.44$ Hz) and H-6 as a triplet of doublets showing both *ortho* and *meta* coupling at δ_H 6.97 ($J = 7.84, 0.76$ Hz). The H-7 and H-5 protons are both *meta* to the oxygenated group at C-8a and are therefore more deshielded due to the electronic effects discussed below (Scheme 15). The H-7 resonance appears as a double double doublet (ddd) at δ_H 7.42 with $J = 8.64, 7.16$ and 1.64 Hz, showing *ortho* coupling with H-8 and H-6 and *meta* coupling with H-5. The H-5 resonance is the most deshielded due to the magnetic

anisotropic effect. The H-5 proton is in the deshielded part of the cone formed by the π -electrons of the carbonyl group and appears as a double doublet (dd) at δ_{H} 7.85 ($J = 7.84, 1.72$ Hz) (Figure 11). The ^{13}C NMR resonance of the carbonyl group appears at δ_{C} 191.80, indicating the conversion from the acid to the cyclised chromanone in that electron donation from the hydroxy group no longer occurs in the chromanone resulting in the carbonyl resonance being more deshielded and closer to that of a pure ketone resonance. The oxygenated aromatic C-O resonance occurs at δ_{C} 161.86 and the other aromatic carbon resonances occur between δ_{C} 117.88 and δ_{C} 135.96 (C-4a, C-5-8). The methylene group closest to the oxygen, C-2 occurs at δ_{C} 67.00 and that close to the carbonyl group appears at δ_{C} 37.78.

2.1.2 Synthesis of the 3-benzylidene-4-chromanones

The condensation of 4-chromanone with the aromatic aldehyde is achieved with piperidine as a base, which abstracts the most acidic proton at the alpha carbon (C-3) resulting in the formation of an anion, followed by an aldol addition to the aldehyde forming a β -hydroxy carbonyl compound. The extensive conjugation in the molecule drives the elimination of water from this intermediate without the addition of acid to form a highly conjugated molecule, the 3-benzylidene-4-chromanone (Scheme 7).

The reaction of 4-chromanone with various substituted benzaldehydes to give the homoisoflavonoids were carried out under reflux at 80-90 °C. Reaction temperatures were monitored and kept below 90 °C, due to exocyclic to endocyclic bond migration which may occur at ~ 150 °C (Jacquot *et al.*, 2012). Exocyclic to endocyclic bond migration, however

did occur at 80-90 °C with the electron withdrawing nitro groups resulting in the 3-benzyl homoisoflavonoid rather than the 3-benzylidene homoisoflavonoid (Valkonen *et al.*, 2012).

All homoisoflavonoids synthesised were obtained in good yields of between 50-80%. For the deactivating groups, chloro and fluoro substituents, higher yields were obtained for the *meta* substituted than the *para* substituted compounds. For the activating groups, the hydroxy and methoxy group, a higher yield was obtained for the *para* substituted product. In the case of all disubstituted benzaldehydes, the product yields were lower than that of the mono-substituted benzaldehydes. For the hydroxy substituents, separation of these compounds from the reaction mixture was problematic. In the extraction process with ethyl acetate, a clear distinction could not be made between the phases and although careful care was taken to recover the amount of ethyl acetate used, some of the product could have been sacrificed in this procedure. This may account for the lower yields with the hydroxy groups as opposed to the other substituents.

2.1.3 Structural elucidation of homoisoflavonoids (3-17)

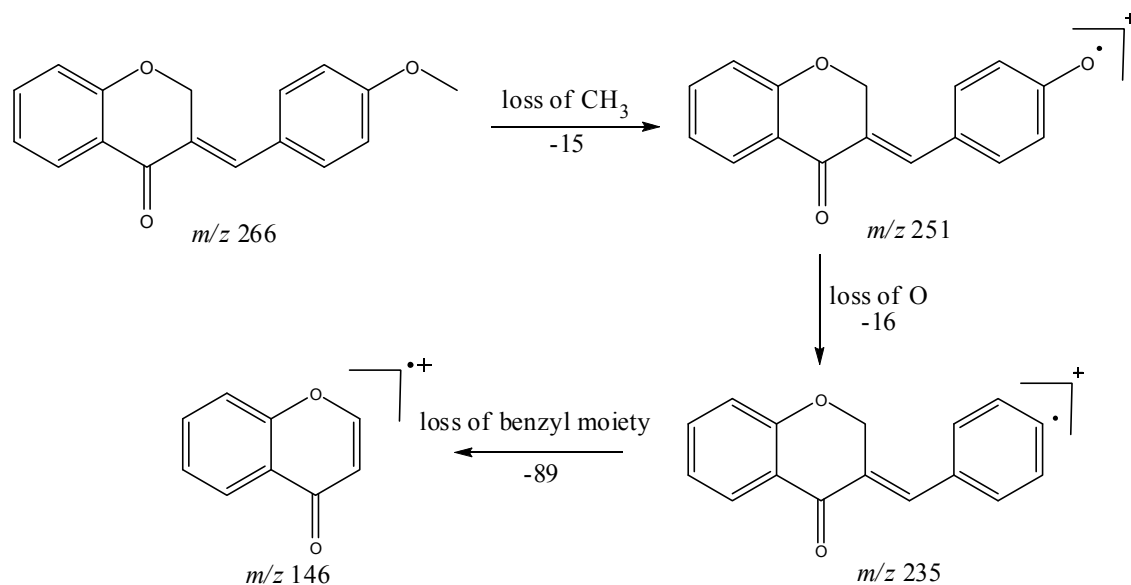
Infrared spectroscopy was used to confirm the presence of functional groups within the homoisoflavonoids synthesised. The infrared spectrum of **3** showed a sharp peak at 1665 cm^{-1} which is attributed to the carbonyl group (C=O, C-4). The low frequency of the absorption is indicative of the conjugation in the molecules resulting in greater single bond character and lower wavenumbers. The peaks at 1466 and 1450 cm^{-1} are as a result symmetrical stretching of the aromatic alkene (C=C) groups. The asymmetrical stretching peaks for the aromatic C=C bonds are observed at 1308 and 1267 cm^{-1} . The ether group (C-O-C) stretching frequency is observed at 1209 cm^{-1} .

The infrared spectrum of compounds **13**, **14** and **15** showed broad bands at 3093, 3255, 3117 cm^{-1} respectively, confirming the presence of a hydroxyl group. The compounds containing a nitro group, **16** and **17**, showed two strong bands for the stretching of the N-O bond at 1462 cm^{-1} (asymmetrical) and 1341 cm^{-1} (symmetrical) for **17**, and 1464 cm^{-1} (asymmetrical) and 1339 cm^{-1} (symmetrical) for **16**. For the mono-fluorinated compounds, a single band is observed at 1145 cm^{-1} for **10**, and at 1144 cm^{-1} for **11** which is characteristic of the C-F bond. The di-fluorinated compounds shows two strong bands at 1116 and 1145 cm^{-1} as a result of symmetric and asymmetric stretching.

Flavonoids are commonly identified by the existence of two characteristic bands in the UV spectrum. These two bands occur in the region of 300 to 550 nm, attributed to B-ring and 240 to 285 nm attributed to the A-ring (Heller and Tamm, 1981). For the homoisoflavonoids (**3-17**) synthesised, the same trend was observed with two bands occurring in the region of 280-300 nm and 340-360 nm indicating that this skeletal structure was also present in the synthesised compounds.

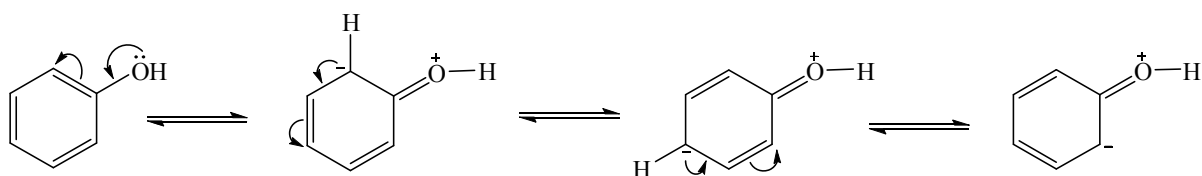
The mass spectra for the homoisoflavonoids are all similar in that they display the same type of fragmentation pattern. The differences in the mass spectra are associated with that of the phenyl ring, due to there being different substituents on the ring and hence fragment with different masses. The fragmentation pattern of the chromanone moiety of the homoisoflavonoid is illustrated in Scheme 13. The mass spectra of the chloro containing homoisoflavonoids (**7**, **8** and **9**) show peaks for both the chlorine isotopes (^{35}Cl and ^{37}Cl) with a peak height ratio of 3:1.

For **4**, the *para* methoxy derivative, the molecular ion peak $[M^+]$ is observed at 266 mass units which confirm the formation of the homoisoflavonoid. The proposed fragmentation pattern of the B-ring of the homoisoflavonoid is illustrated below (Scheme 14). Thereafter the chromanone moiety is fragmented as described above (Scheme 13).



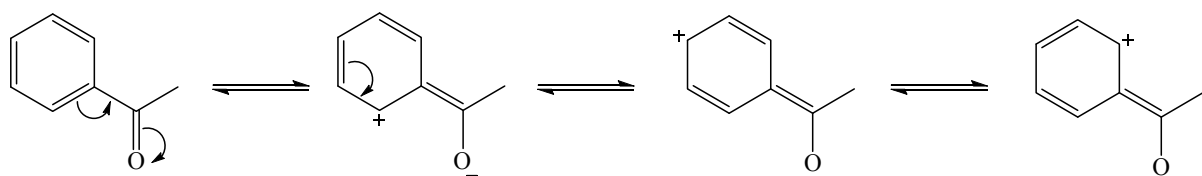
Scheme 14: The fragmentation pattern of (*E*)-3-(4'-methoxybenzylidene)chroman-4-one (**4**)

The proton NMR spectrum of compound **3** showed the characteristic resonances for the benzylidene proton (H-9) as a singlet (s) at δ_{H} 7.86 and the H-2 proton resonance, a two proton resonance occurring as a doublet (d) at δ_{H} 5.33 with a small coupling constant of $J = 1.32$ Hz due to the geminal coupling between the two H-2 protons. The oxygenated moiety and the carbonyl moiety attached to C-8a and C-4a respectively play a significant role in the chemical shift of the proton resonances on the chromanone ring. For example, in **3**, the H-6 and H-8 resonances are more upfield at δ_{H} 7.05 and δ_{H} 6.95 due to the electronic effects of the oxygenated moiety, similar to that occurring in a phenol substituted structure (Scheme 15).



Scheme 15: Resonance structures of phenol showing electronic effects of the hydroxyl group and the build-up of electron density at the *ortho* and *para* positions, resulting in protons occurring more upfield.

In the same manner, the H-5 and H-7 proton resonances are more downfield similar to that which occurs in an acetophenone substituted structure (Scheme 16).



Scheme 16: Resonance structures of acetophenone showing electronic effects of the acyl group and the withdrawal of electron density from the *ortho* and *para* positions resulting in protons occurring more downfield.

The H-5 resonance however is noticeably more downfield than H-7 due to an anisotropic effect (Figure 11), and occurs at δ_{H} 8.00 away from the other aromatic resonances. The H-7 resonance occurs at δ_{H} 7.47. The phenyl proton resonances in the absence of substituents on this ring occur typically in the aromatic region between δ_{H} 7.29 to 7.42.

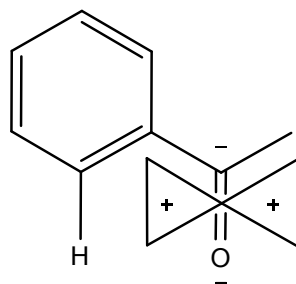


Figure 11: Anisotropic effect causing H-5 occurring more downfield than H-7

The splitting pattern of the protons on the chromanone ring in the absence of substituents shows a doublet of doublets for H-5 with $J = 7.86$ Hz, typical of *ortho* coupling and 1.10 Hz attributed to *meta* coupling with H-7. *Para* coupling was not observed in the ^1H NMR spectra. In the case of the H-8 proton resonance, only *ortho* coupling with $J = 8.32$ Hz was present and *meta* and *para* coupling could not be detected, but in the COSY spectrum H-8 was seen coupled to H-6. The H-6 proton resonance appeared as a triplet due to the coalescing of the double doublets that occurs because of similar coupling constants between H-6 and H-5 and H-6 and H-7 with $J = 7.50$ Hz. Although this should also be observed for H-7, this cannot be distinguished because of overlapping with the aromatic protons of the phenyl ring. In the case of the phenyl ring protons, the H-3'/5' resonance and the H-2'/6' resonances can both be distinguished as doublets with similar J values of 7.36 and 6.96 Hz respectively. There is a small difference between the coupling constants of coupled proton resonances, for example, the H-5 proton resonance has $J = 7.86$ Hz, but the triplet of H-6 has a J value of 7.50 Hz. We attribute this to the coalescing of resonances, where peaks overlap and also to the broadened resonances for some of the proton peaks. However, we confirmed the coupling of all the resonances with the aid of the COSY spectrum.

The ^{13}C NMR spectrum of compound **3** showed the presence of fourteen carbon resonances with two of the resonances being equivalent and therefore amounting to sixteen carbon

resonances, which confirms the presence of a homoisoflavonoid skeleton. The oxygenated aliphatic carbon resonance of C-2 occurs at δ_C 67.61 typical for C-2, with that of C-4, the carbonyl resonance occurring at δ_C 182.27 and the oxygenated aromatic carbon of C-8a occurring at δ_C 161.14 typical for these resonances in benzylidene homoisoflavonoids (Jacquot *et al.*, 2012). This was confirmed by the presence of HMBC correlations between C-4 and H-5, C-2 and H-9 and C-8a with H-2, H-5 and H-8.

The C-6, C-8 and C-4a are the most shielded of all the aromatic resonances due to the electronic effects explained above (Scheme 15 and Scheme 16). The remaining two aromatic carbon resonances on the chromanone ring, C-5 and C-7 occur at δ_C 127.96 and 135.89 respectively. The resonances of C-5 to C-8 were determined by their corresponding proton resonances in the HSQC spectrum. The equivalent phenyl carbon resonances of C-2'/6' occurs slightly more downfield at δ_C 129.99 compared to the C-3'/5' resonance of δ_C 128.74. This was confirmed by a HMBC correlation between C-2'/6' and H-9. The C-4' carbon resonance lies in between these two resonances at δ_C 129.48. The C-1' carbon resonance was assigned at δ_C 134.39 due to a HMBC correlation with H-3'/5'. The remaining olefinic carbon resonance of C-3 was assigned to δ_C 130.92 because of a HMBC correlation to H-2. The ^1H and ^{13}C NMR resonances compare well with that in the literature (Jacquot *et al.*, 2012).

2.1.4 Structural elucidation of the *para* substituted derivatives (except 4'-fluoro)

For the *para* substituted B-ring benzylidene homoisoflavonoids (**4**, **7** and **13**), excluding the *para* fluoro substituted compound (**10**), the ^1H NMR spectrum showed the *ortho* coupled proton resonances of H-2'/6' and H-3'/5' as doublets with coupling constants between 8.4 and

8.8 Hz for the three compounds. These are located at δ_{H} 7.26 and 6.96 for the methoxy derivative (**4**), δ_{H} 7.32 and 6.89 for the hydroxy derivative (**13**) and δ_{H} 7.22 and 7.40 for the chloro derivative (**7**) for the H-2'/6' and H-3'/5' resonances respectively. For compounds **4** and **13**, with an activating electron donating methoxy or hydroxy group at the *para* position, the H-3'/5' resonance is more shielded due to electron donation and build-up of electron density at these carbon atoms. In contrast, the *para* chloro derivative had the H-3'/5' proton resonances more deshielded. Even though the chloro group has lone pairs and is capable of electron donation toward the ring, the inductive effects of the deactivating chloro group is responsible for this effect. In the unsubstituted benzylidene homoisoflavonoid (**3**), the H-7 and H-3'/5' resonances overlapped at δ_{H} 7.47 but when a substituent was placed at the *para* position of this ring, causing the H-3'/5' resonance to be shifted, the H-7 resonance can now be clearly seen as a triplet of doublets (td) in the chloro (**7**) and hydroxy derivatives (**13**) with $J_{7,8}$ and $J_{6,7}$ being the same at approximately 7.7 Hz. In **4**, a double double doublet (ddd) was seen with $J_{7,8}$ being slightly larger than $J_{6,7}$. Both coupling constants were in the region of 8.0 Hz. The $J_{5,7}$ coupling constant was seen to be approximately 1.70 Hz. A singlet resonance for the methoxy group was seen at δ_{H} 3.83 in **4**.

For **4** and **13**, the C-4' resonance shifted more downfield in the region of C-8a at approximately δ_{C} 160 because of the oxygenated substituent at this position. In **7**, the *para* chloro derivative, C-4' occurred more in the region of C-7 and C-9 at δ_{C} 135.59 due to the chloro group being less electronegative than the oxygenated groups. The ^1H and ^{13}C NMR data of **4**, **7** and **13** compare well with that in the literature (Jacquot *et al.*, 2012; Valkonen *et al.*, 2012).

2.1.5 Structural elucidation of the *meta* substituted derivatives (except 3'-fluoro)

For the *meta* substituted compounds (**5**, **8** and **14**, excluding the fluorinated compound **11**), all the NMR spectra were similar with some subtle changes brought about by the different substituted groups. For **5**, the 3-(3'-methoxybenzylidene)chroman-4-one, the proton resonances for the aromatic ring and the chromanone ring are well resolved. The H-5 resonance appears as a double doublet at δ_{H} 8.00 ($J = 7.82, 1.46$ Hz), deshielded due to hydrogen bonding as described above (Figure 11), the H-9 resonance appears as a singlet at δ_{H} 7.82 and the H-7 and H-6 resonances occurred at δ_{H} 7.47 (td, $J = 7.72, 1.60$ Hz) and δ_{H} 7.05 (t, $J = 7.52$ Hz) respectively. The H-8 and H-4' resonances overlap at δ_{H} 6.94, however the doublet resonance of H-8 could be distinguished and its coupling constant was determined to be $J = 8.12$ Hz. The multiplicity of the H-4' resonance could not be determined due to overlap with H-8. Due to the *meta* substitution on the phenyl ring, the H-2' resonance should show *meta* coupling with either H-6' or H-4', but this was not observed. Rather, a broad singlet for this resonance was observed at δ_{H} 6.82, however coupling in the COSY spectrum was observed between this resonance and that of H-4' and the H-6' resonance which appears as a doublet at δ_{H} 6.87 ($J = 7.60$ Hz). The H-5' resonance appears as a triplet at δ_{H} 7.34 ($J = 7.92$ Hz). HMBC correlations between H-5 and the carbonyl resonance, C-4 at δ_{C} 182.23 and H-8 and C-4 confirm these assignments. The H-2 resonance appears at δ_{H} 5.33, which was confirmed by a HMBC correlation to C-4. The methoxy resonance was seen at δ_{H} 3.82 as an intense singlet resonance in the ^1H NMR spectrum.

All the protonated carbon resonances were identified from their corresponding proton resonances using the HSQC spectrum. There were five carbon resonances beside the carbonyl resonance, which were non-protonated. These occurred at δ_{C} 122.02, 131.15, 135.69, 159.69, and 161.18 and were identified using HMBC correlations. The C-8a

resonance was identified at δ_C 161.18 by a HMBC correlation to H-2 and the other oxygenated carbon resonance at δ_C 159.60 was then attributed to C-3'. This was corroborated by HMBC correlations between C-3' and both H-4' and H-5'. The resonance at δ_C 131.15 shows a correlation to H-2 and was therefore attributed to C-3, and the resonance at δ_C 135.69 shows a correlation to H-5' and was attributed to C-1'. The remaining resonance at δ_C 122.02 showed a correlation to H-6 and was therefore assigned to C-4a.

The ^1H NMR spectrum of **14**, the 3'-hydroxy derivative was very similar to **5**, but had the notable difference in that the H-4' resonance which overlapped with H-8 in **5**, was now seen overlapping with the H-6' resonance and could be seen as a two proton doublet resonance for H-4'/6' at δ_H 6.86 with $J = 8.08$ Hz. This allowed the H-8 resonance to be clearly seen as a doublet at δ_H 7.06 with $J = 8.28$ Hz. The rest of the resonances have similar splitting patterns and chemical shifts to **5**. There was an added hydroxyl proton resonance at δ_H 9.71 for **14**. The carbon resonances in both **5** and **14** were similar. In **14**, the resonances for C-4' and C-6' could not be unequivocally assigned from their HMBC correlations and we have based their assignments on those made for **5**.

In the *meta* chloro derivative **8**, all the proton resonances for the chromanone ring, H-2 and H-5 to H-9 were all similar to **5**. Changes were observed for the H-2', and H-4' to H-6' resonances due to a now weakly deactivating group. The H-2' resonance shifted more downfield from δ_H 6.82 in **5** to δ_H 7.27 in **8**, probably by the electron withdrawal inductive effects of the chloro group. The same can be seen for the H-4' and H-6' resonances which now shifted more downfield to δ_H 7.37 and occur as overlapping resonances. It is observed that the H-5' resonance for the chloro compound is shifted slightly more upfield from 7.34 in

5 to 7.17 in **8**, probably due to a greater resonance effect by the chloro group, donating more electron density to the *meta* position.

In the ^{13}C NMR spectrum of **8**, there was a noticeable shift of the C-2', C-3', C-4' and C-6' resonances. The C-2', C-4' and C-6' resonances were all shifted more downfield to δ_{C} 130.00, 129.42 and 129.62 in **8**, from 115.42, 115.06 and 122.28 in **5**. The C-3' resonance shifted more upfield to δ_{C} 134.76 in **8**, from 159.69 in **5**, due to the weaker electronegativity of the chloro group as opposed to oxygen, resulting in less electron withdrawal by induction from the chloro group.

2.1.6 Structural elucidation of the 3',4'-disubstituted derivatives (except 3',4'-difluoro)

The proton NMR resonances for the chromanone ring (including that of H-9) of compounds **6**, **9** and **15** were similar to that described for **5**, **8** and **14** above with regard to chemical shift and splitting patterns. The carbon resonances of C-2 to C-9 including C-4a and C-8a of the chromanone moiety were also similar to **5**, **8** and **14**.

With regard to the phenyl group, the 3',4'-substitution in **15** resulted in H-2', H-5' and H-6' having the expected splitting patterns of doublets for H-2' and H-5' and a double doublet for H-6' at δ_{H} 6.81 ($J = 2.04$ Hz), δ_{H} 6.79 ($J = 9.16$ Hz) and 6.73 ($J = 9.14, 1.88$ Hz) respectively. Their corresponding carbon resonances occurred at δ_{C} 117.76 (C-2'), 115.85 (C-5') and 123.47 (C-6'). These assignments were confirmed by HMBC correlations between H-9 and C-2' and C-6'. The two resonances at δ_{C} 145.38 and 147.87 were attributed to C-3' and C-4' respectively. They were assigned as such because of a HMBC correlation between C-4' and all the protons on the phenyl ring, H-2', H-5' and H-6', whereas C-3' showed a HMBC correlation to H-2' and H-5' only. The extra HMBC correlation between C-4' and H-6'

allowed the unambiguous assignment of these two carbon resonances (C-3' and C-4'). The C-1' carbon resonance was identified at δ_C 125.18 due to a HMBC correlation between this carbon resonance and H-2', H-6' and H-5'.

For the dimethoxy compound **6**, the resonances in the ^1H NMR spectrum are slightly different to that of **15** due to solvent effects, **15** being acquired in deuterated DMSO and **6** being acquired in deuterated CDCl_3 . This resulted in H-5' and H-6' overlapping at δ_H 6.88-6.90 and H-2' being a doublet at δ_H 6.83 ($J = 1.72$ Hz). The C-5' and C-6' resonances were difficult to identify using the HSQC spectrum because of the overlap of H-5' and H-6', but in comparison to **15** they were made at δ_C 123.64 (C-6') and δ_C 111.06 (C-5'). This was confirmed by a HMBC correlation between H-9 and C-6'. The H-2' resonance occurred as a doublet at δ_H 6.83 ($J = 1.72$ Hz) with a corresponding carbon resonance at δ_C 113.31. Two methoxy proton resonances can be seen in the ^1H NMR spectrum at δ_H 3.89 and 3.91 as two intense singlets, both corresponding to the overlapping carbon resonance at δ_C 55.99. The aromatic C-O resonances occurred at δ_C 148.99 and 150.41 as for **15** above.

In the disubstituted chloro compound **9**, the proton resonances for H-2', H-5' and H-6' all kept their splitting patterns as that for above, but all these resonances shifted more downfield in comparison to **6** and **15**. The H-5' resonance now occurred as a doublet at δ_H 7.50 ($J = 8.40$ Hz), H-2' as a doublet at δ_H 7.38 ($J = 1.92$ Hz) and H-6' as a double doublet at δ_H 7.12 ($J = 8.28, 1.96$ Hz). This shift downfield was probably due to the greater inductive effect of chlorine versus its electron donating effect. In **6** and **15**, the oxygenated groups probably had a greater electron donating effect than an inductive effect. This is consistent with the chloro group being deactivating and the hydroxy and methoxy groups being activating. Due to the chloro substitution at C-3' and C-4', these resonances shifted more upfield to δ_C 133.70 and

134.28. Similar to the proton resonances, the corresponding carbon resonances, C-2', C-5' and C-6' shifted more downfield to δ_C 131.41, 130.79 and 128.94 respectively.

2.1.7 Structural elucidation of the fluorine containing compounds (10, 11 and 12)

As above, the proton and carbon resonances for the chromanone ring did not change and therefore a discussion for this part of the molecule will not be repeated. The only changes that occurred were in that of the phenyl ring. In compound **10**, the *para*-fluorinated compound, the H-2'/6' and H-3'/5' proton resonances, which appeared as a pair of doublets in **7** (the *para*-chlorinated compound) at δ_H 7.22 and 7.40 now appeared as a doublet of doublets with $J = 8.60$ and 5.40 Hz at δ_H 7.28 (H-2'/6'), and a triplet with $J = 8.62$ Hz at δ_H 7.13 (H-3'/5'). The H-3'/5' resonance was most affected by the substitution with fluorine in terms of chemical shift, resulting in the resonance being shifted from δ_H 7.40 in **7** to δ_H 7.13 in **10**. The H-2'/6' resonance did not shift notably from δ_H 7.22 to δ_H 7.28. However, the splitting patterns of the two resonances in the fluoro compound were markedly different to that of the chloro compound. The H-2'/6' resonance was split into a double doublet by the fluorine with $J_{HF} = 5.40$ Hz and the proton *ortho* to it with $J = 8.60$ Hz. The H-3'/5' resonance being closer to the fluorine substituent experienced the same coupling constant for both J_{HF} and the *ortho* coupled protons $J_{H-2'/6', H-3'/5'}$ with $J = 8.62$ Hz. These resonances were distinguished by the H-2'/6' resonance showing a HMBC correlation with C-9 at δ_C 136.27 and the C-3'/5' resonance a HMBC correlation to C-1' at δ_C 130.52.

In the ^{13}C NMR spectrum, all the carbon resonances of the phenyl ring were seen coupled to fluorine and appeared as doublets. The *ipso* carbon (C-4') directly bonded to the fluorine atom appeared at δ_C 163.21 and had a coupling constant of $J = 250.87$ Hz. Care must be

taken when making these assignments so as not to confuse this resonance for two separate carbon resonances. This resonance was confirmed by correlations to both the H-2'/6' and H-3'/5'. Also present in the ^{13}C NMR spectrum were resonances at δ_{C} 115.98 as a doublet with $J = 21.59$ Hz, typical of *ortho* coupled carbon resonances and δ_{C} 131.97 ($J = 8.55$ Hz) typical for *meta* coupling and were assigned to C-3'/5' and C-2'/6' respectively. The C-2'/6' carbon resonance was coupled to H-9 in the HMBC spectrum as expected. The remaining doublet at δ_{C} 130.52 ($J = 2.97$ Hz) was assigned to C-1' and the fact that this was a doublet was used to distinguish between the C-1' and C-3 carbon resonances which were located in the same region of the ^{13}C NMR spectrum.

In compound **11**, the 3'-fluoro derivative, the fluorine couples to the H-2', H-4' and H-5' protons. Both the H-4' and H-5' proton resonances appear as triplets of doublets, however they can be distinguished by their coupling constants. The H-4' resonance at δ_{H} 7.09 experiences J_{HF} and J_{HH} coupling with similar coupling constants, hence the triplet with $J = 8.44$ Hz and the *meta* coupling ($J = 2.40$ Hz) results in the triplet being further split into a triplet of doublets. The H-5' resonance at δ_{H} 7.39 shows a larger second coupling ($J = 5.96$ Hz) since this is due to the H-F coupling, the triplet ($J = 8.00$ Hz) being due to the coupling between the two protons *ortho* to it, H-4' and H-6'. The H-2' proton resonance, *ortho* to the fluorine atom, appears as a doublet with $J = 9.52$ Hz at δ_{H} 6.98. Similar to **10**, all the carbon resonances of the phenyl ring were doublets displaying *ipso* (δ_{C} 162.70, $J = 245.90$ Hz, C-3'), *ortho* (δ_{C} 116.35, $J = 15.56$ Hz, C-4'; δ_{C} 116.57, $J = 16.28$ Hz, C-2'), *meta* (δ_{C} 130.31, $J = 8.24$ Hz, C-5', δ_{C} 136.40, $J = 7.80$, C-1'), and *para* (δ_{C} 125.66, $J = 2.92$ Hz, C-6') coupling. Since the C-9 carbon atom is now only four bonds away from fluorine, this carbon resonance is also coupled by fluorine with a coupling constant of $J = 2.27$ Hz. HMBC correlations

between C-9 and H-2' and H-6' as well as between C-1' and H-5' are also present confirming the assignments of these carbon resonances.

In the ^1H NMR spectrum of **12**, the 3',4'-difluoro derivative, the H-5' *ortho* coupled proton appears as a triplet of doublets at δ_{H} 7.22 ($J= 9.88$ and 8.28 Hz), the triplet being due to the same coupling constant between H-5' and the *ortho* fluorine and H-5' and H-6', which was split further into a triplet of doublets by the other *meta* fluorine atom. The H-2' resonance was split into a ddd because of coupling to both the *ortho* ($J = 10.08$ Hz) and *meta* ($J = 7.52$ Hz) fluorine atoms as well as the *meta* proton ($J = 2.04$ Hz, H-6'). The H-6' proton resonance overlaps with the multiplet of resonances at δ_{H} 7.04. HMBC correlations between H-2', H-6' and C-9 as well as C-1' and H-5' confirm the assignments of these resonances.

The carbon resonances of the phenyl moiety are once again all split by the fluorine atoms. However in this instance, double doublets are experienced by all but the *ortho* coupled C-2' and C-5' resonances which appear as doublets at δ_{C} 118.74 ($J = 17.66$ Hz) and δ_{C} 117.85 ($J = 17.69$ Hz). This is due to there being two fluorine atoms present on the phenyl ring. The other four resonances are present at δ_{C} 150.25 ($J = 248.55$ and 12.80 Hz, C-3'), δ_{C} 150.78 ($J = 261.53$ and 12.86 Hz, C-4'), δ_{C} 131.40 ($J = 5.98$ and 3.80 Hz, C-1') and δ_{C} 126.48 ($J = 6.25$ and 3.47 Hz, C-6'). HMBC correlations are also seen for H-9 with C-2' and C-6' confirming the assignment of these carbon resonances.

2.1.8 Structural elucidation of the nitro containing compounds (**16** and **17**)

In comparison to the other compounds previously described, there were changes to the chromanone ring proton resonances in the nitro derivatives **16** and **17** indicating that some kind of conversion must have taken place. Of particular importance was the HMBC

correlation between the proton resonance at δ_{H} 7.45 ($J = 8.48$ Hz), attributed to the H-2'/6' resonance and the methylene carbon resonance at δ_{C} 31.89 in **16**. This was not encountered for the other molecules. This now meant that the methylene group, which occurred at C-2 in the other molecules, was now present at C-9 in **16**. This change was accompanied by a change in chemical shift of the methylene carbon resonance from approximately δ_{C} 67 to δ_{C} 31.89 in **16**, which also indicated that the methylene carbon was no longer situated next to the oxygen atom. There was however no change in the olefinic methine resonance at δ_{H} 7.79 when compared to the other compounds, but the C-2 resonance was now more deshielded at δ_{C} 153.14 in comparison to the C-9 resonance in the other compounds. This was due to being situated close to the oxygen atom on the chromanone ring. This meant that an *exo-endo* bond migration had occurred in **16** and **17** due to the highly electron withdrawing nitro group. This was reported to occur previously (Valkonen *et al.*, 2012).

For the H-5 to H-8 proton resonances in **16**, all the resonances were shifted downfield in comparison to the 4-chloro derivative **7**, between 0.15 to 0.50 Hz. However, these resonances retained their splitting patterns, being present as a doublet of doublets at δ_{H} 8.18 ($J = 7.98, 0.66$ Hz, H-5), δ_{H} 7.65, a triplet of doublets ($J = 8.32, 1.10$ Hz, H-7), δ_{H} 7.41, a doublet ($J = 8.60$ Hz, H-8) and δ_{H} 7.38 as a triplet ($J = 7.54$ Hz, H-6). For the carbon resonances in **16** there is not much difference in chemical shift of the carbon resonances C-4a through to C-8a with the largest shift being experienced by C-8a, which is only a 5 ppm shift upfield from δ_{C} 161 in **7** to δ_{C} 156 in **16**. A 5 ppm shift was also experienced by the carbonyl carbon resonance from δ_{C} 182 in **7** to δ_{C} 177 in **16**.

In the phenyl ring of **16**, due to the electron withdrawing nitro group, a downfield shift was experienced by both the H-3'/5' and H-2'/6' resonances by 0.72 Hz and 0.23 Hz respectively,

H-3'/5' now occurring at δ_{H} 8.12 ($J = 8.56$ Hz) and H-2'/6' at δ_{H} 7.45 ($J = 8.48$ Hz) in comparison to the *para*-chloro compound **7**. In comparison to **7**, the carbon resonances of the phenyl ring C-1' through to C-6' were all shifted upfield by approximately 2 to 11 ppm in **16** at δ_{C} 123.06 (C-1'), 129.65 (C-2'/6'), 123.79 (C-3'/5') and 146.76 (C-4'). In **7**, there was conjugation between the phenyl ring with the C-3 (9) double bond, delocalising the electrons amongst more carbon atoms, hence the more downfield chemical shift. In **16**, due to the double bond migrating to the Δ^2 position, this delocalisation does not occur and the electrons are localised to the phenyl group, hence more upfield chemical shifts are experienced.

In **17**, there are now four separate resonances for the phenyl group protons as opposed to only two in **16**. This was due to the nitro group now being at the 3' position. The H-2' resonance occurred as a broad singlet at δ_{H} 8.13, the H-4' and H-6' proton resonances occurred as doublets at δ_{H} 8.06 ($J = 8.16$ Hz) and δ_{H} 7.69 ($J = 7.68$ Hz) and the H-5' resonance occurred at δ_{H} 7.45 as a triplet with J being 8.16 Hz. The other proton resonances of **17**, the chromanone proton resonances as well as H-2 and H-9 were the same as that for **16** as were the carbon resonances of C-2 to C-9. There were however changes in chemical shifts for the carbon resonances on the phenyl ring. The C-3' carbon to which the nitro group was attached had a resonance of δ_{C} 148.41 and the carbon resonances *meta* to the nitro group, C-1' and C-5' resonated at δ_{C} 141.02 and δ_{C} 129.42 respectively, while the *ortho* positioned carbon atoms (C-2' and C-4') resonated at δ_{C} 123.52 and δ_{C} 121.71. This is consistent with the *ortho* and *para* carbon resonances being more shielded and the *meta* resonances being more deshielded due to electron withdrawal by resonance by the nitro group.

2.2 Bioactivity of the synthesised homoisoflavonoids

The synthesised homoisoflavonoids were subjected to antibacterial tests using the disc diffusion assay, and antioxidant testing by the DPPH radical scavenging and the ferric reducing antioxidant power assay. The results are reported and discussed in relation to the chemical structures of the homoisoflavonoids.

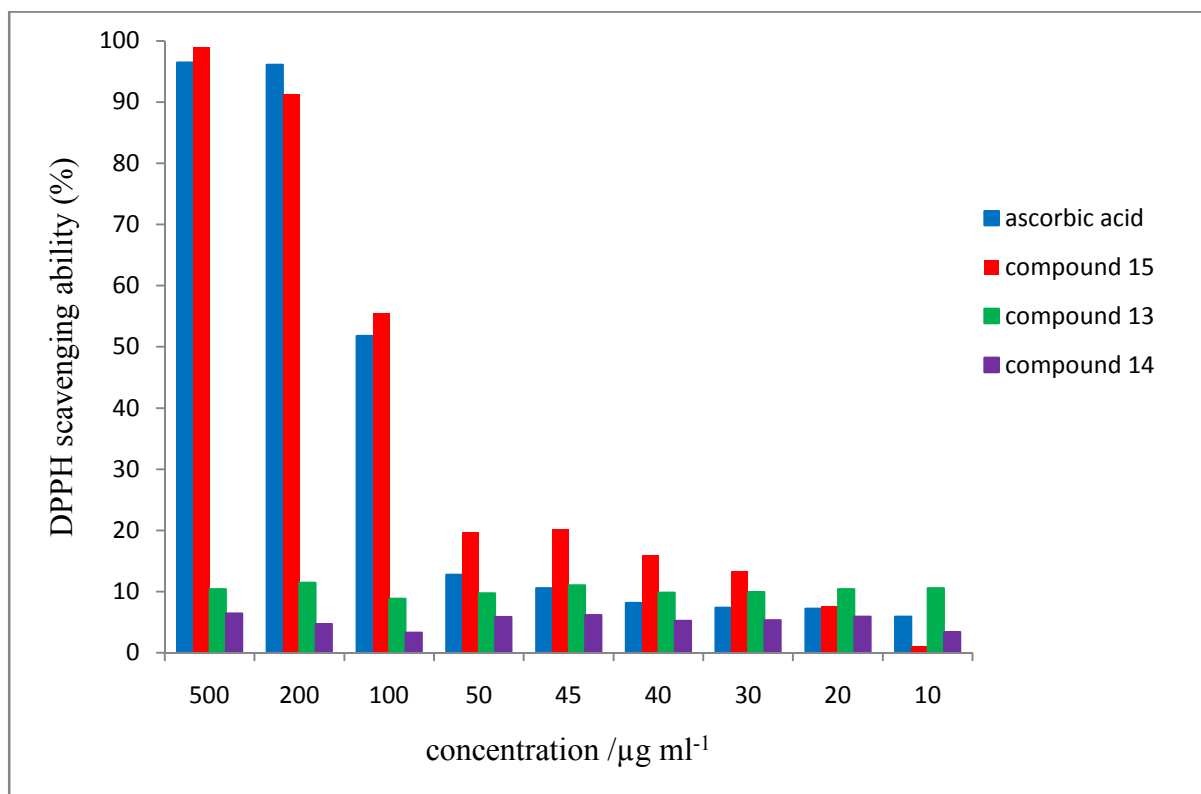
2.2.1 Antioxidant activity of the synthesised homoisoflavonoids

The three hydroxylated homoisoflavonoids (**13-15**) were tested for their antioxidant activity by the DPPH radical scavenging assay and the FRAP assay as hydroxylated flavonoids are commonly known to be antioxidants. Ascorbic acid, a common antioxidant, served as the positive control for these experiments. A sample, containing all required reagents except for the antioxidant was used as a blank.

2.2.1.1 DPPH radical scavenging assay

The principles for this assay are discussed in chapter 1 (1.4.1.1), and the methodology described in chapter 3 (3.2.1.1).

Polyhydroxylated compounds are known to have good antioxidant activity. Compounds **13**, **14** and **15** are hydroxylated compounds and were therefore tested for their antioxidant activity. As expected, compound **15**, which has two hydroxy groups at the 3' and 4' positions, showed strong antioxidant activity, comparable to that of ascorbic acid, and compounds **13** (the 4'-hydroxy) and **14** (the 3'-hydroxy) which have one hydroxy group showed weak antioxidant activity.



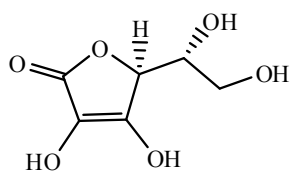
Graph 1: The scavenging ability of compounds **13**, **14** and **15** in comparison to ascorbic acid at various concentrations

Graph 1 shows the percentage scavenging activity (donation of hydrogen to the DPPH radical) of the tested compounds at different concentrations in comparison to ascorbic acid. At 30-50 $\mu\text{g/mL}$, the scavenging ability of compound **15** is much higher than that of ascorbic acid, indicating its ability to act as a scavenger at low concentrations. At 500 $\mu\text{g/mL}$, compound **15** shows 99% scavenging activity, higher than that of ascorbic acid which showed 96% scavenging activity at the same concentration.

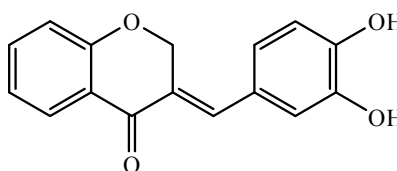
Compound **13** shows a higher scavenging ability than compound **14** indicating that it is preferable for antioxidants to have a hydroxy group on the 4'-position than the 3'-position. This may be as a result of the stability of the quinone resonance structures that form for the *para* substituted product (**13**) when a hydrogen atom is transferred to a radical, making it

more stable than the radical that results when the *meta* product (**14**) transfers its hydrogen atom.

When comparing the chemical structure of ascorbic acid to that of compound **15**, it can be seen that ascorbic acid is polyhydroxylated and that a catechol moiety is present in **15**. The similarity in the two structures is having two hydroxy groups adjacent to each other as in catechol (Figure 12).



Ascorbic acid

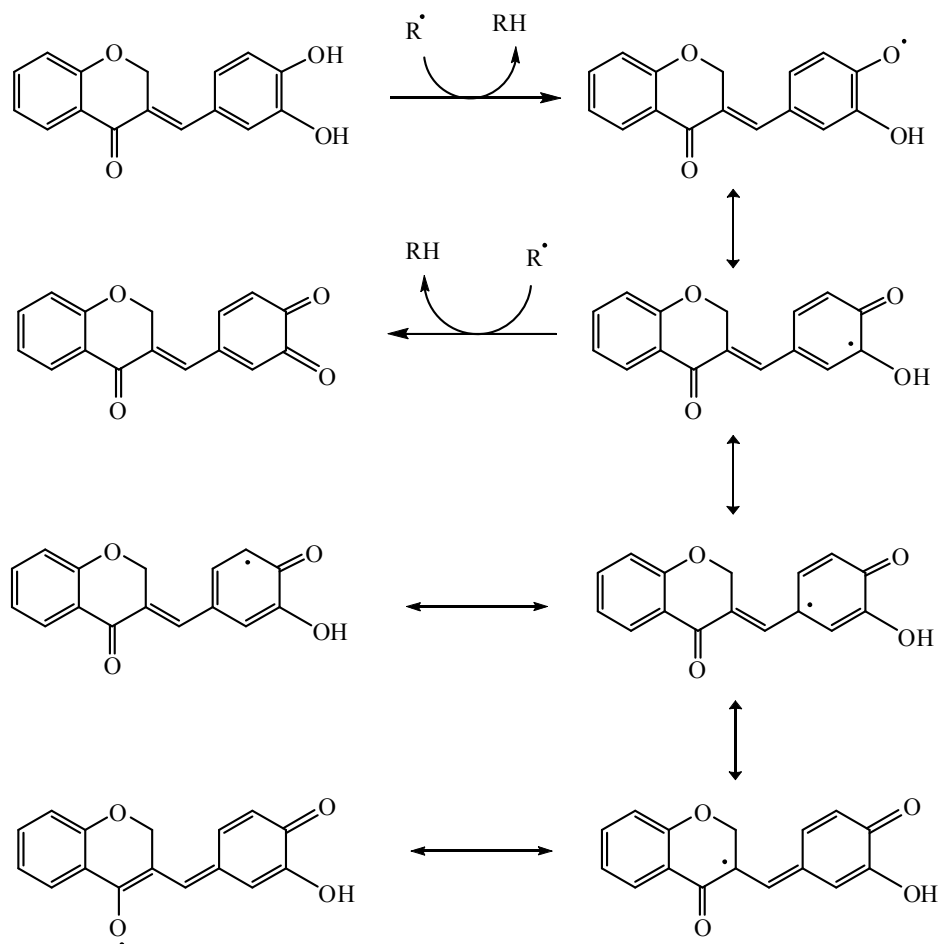


(*E*)-3-(3',4'-dihydroxybenzylidene)chroman-4-one

Figure 12: The chemical structures of ascorbic acid and compound **15**

Ascorbic acid is a known antioxidant which is a polyhydroxylated compound. The weak O–H bond present in phenolic compounds is responsible for their radical scavenging activity as this bond can easily be cleaved homolytically and the hydrogen atom transferred to a radical species. Other hydrogen atoms, such as those bonded to the aromatic ring and a methyl group are bonded to a carbon atom and are not easily scavengable since the C–H bond is much stronger and hence compounds containing these groups only are not good antioxidants. Compound **15**, which has two hydroxy groups, shows results comparable to that of ascorbic acid. By further derivatising compound **15**, for example substituting hydroxy groups on the A-ring in a catechol like manner may enhance its antioxidant activity. A proposed mechanism by which compound **15** is thought to scavenge radicals is illustrated below (Scheme 17). From this mechanism, it can be seen that the many resonance structures stabilise the resultant radical homoisoflavonoid that results when a hydrogen atom is

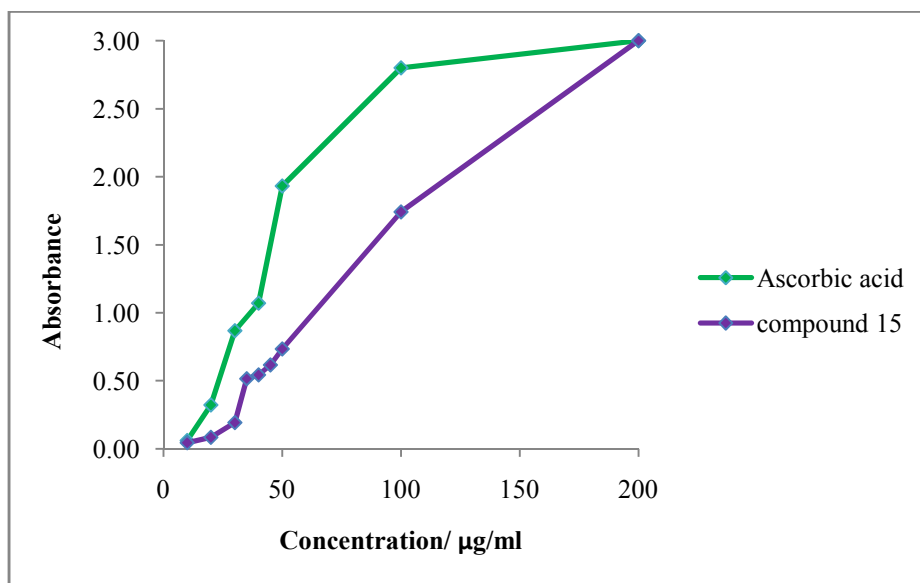
transferred to a radical species and that the diketone structure is also a stable structure resulting in the excellent antioxidant activity shown by this compound.



Scheme 17: The proposed mechanism for the antioxidant activity of (*E*)-3-(3',4'-dihydroxybenzylidene)chroman-4-one

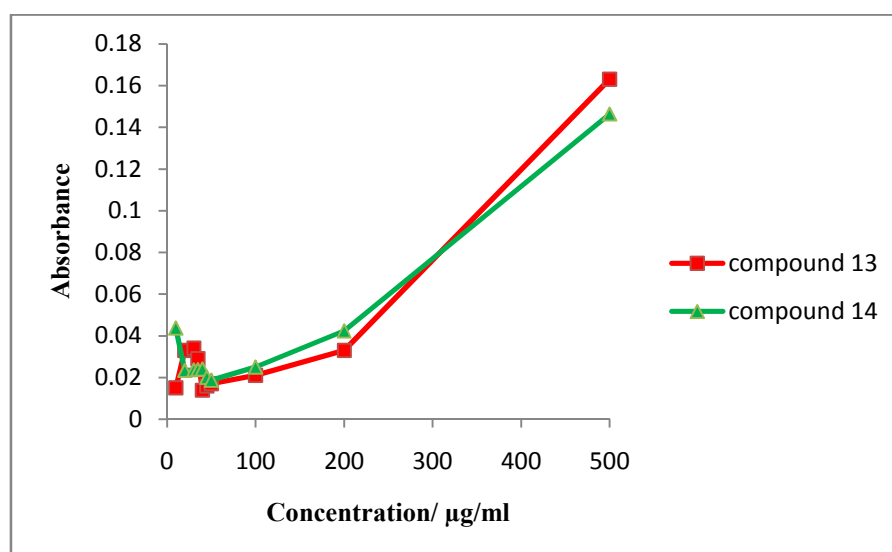
2.2.1.2 Ferric reducing antioxidant power assay

The results of the FRAP assay confirm the conclusions made from the DPPH radical scavenging assay in that compound **15** compares well to ascorbic acid and that compound **13** and **14** are weak antioxidants. The methodology and experimental data are reported in chapter 3 (3.2.1.2).



Graph 2: The reducing power of compound **15** and ascorbic acid

Graph 2 shows the concentration against absorbance curves for compound **15** in comparison to ascorbic acid in the FRAP assay. The results of this assay differs from that of the DPPH assay in that it shows that compound **15** is a slightly weaker antioxidant than ascorbic acid at all concentrations. The trend observed is that as the concentration increases, the reducing power (transformation of Fe^{3+} to Fe^{2+}) increases.



Graph 3: The reducing power of compound **13** and compound **14**

Graph 3 shows, by the low absorbance values as compared to those in graph 2 for ascorbic acid and **15** that compounds **13** and **14** are weak antioxidants at low concentrations. At concentrations higher than 200 µg/mL, a sharp increase in its antioxidant activity is observed but its activity is still nowhere near that of **15** and ascorbic acid. The *para* hydroxy derivative (**13**) shows slightly better antioxidant activity than the *meta* hydroxy derivative (**14**), which is consistent with the results from the DPPH assay. The reducing power of the tested compounds in decreasing order was found to be: ascorbic acid > compound **15** > compound **13** > compound **14**.

2.2.2 Antibacterial activity of the synthesised homoisoflavonoids

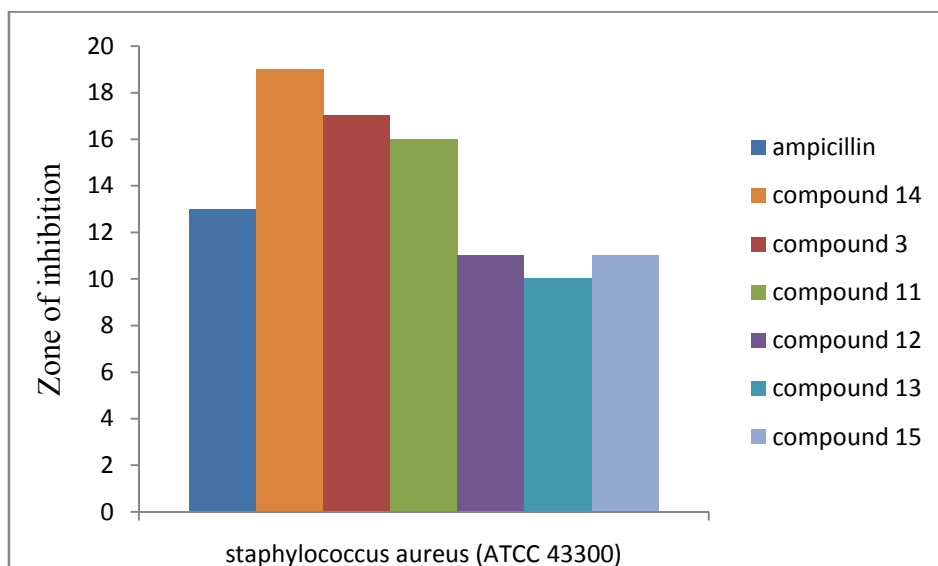
The antibacterial activities of the homoisoflavonoids synthesised were tested against ten gram positive and six gram negative bacterial strains using the Kirby-Bauer disk-diffusion method.

In general, the homoisoflavonoids tested were more active against the gram positive than the gram negative bacteria. No antibacterial activity was shown against the following gram negative strains of bacteria: *Salmonella arizonae* (ATCC 13314), *Escherichia coli* (ATCC 35219), *Pseudomonas aeruginosa* (ATCC 27853 and ATCC 35037), and *Klebsiella pneumoniae* (ATCC 70063). This is because gram negative bacteria have an extra membrane, known as the outer membrane which is made up of lipopolysaccharides and protein, which is difficult to diffuse or penetrate through. Therefore gram negative bacteria are more difficult to destroy. Since the homoisoflavonoids show good antibacterial activity against gram positive bacteria, they may be tested for antituberculosis activity and against nosocomial pathogens.

These homoisoflavonoids show the best inhibitory activity against the bacterial strain, *Staphylococcus aureus*, therefore two strains of *Staphylococcus aureus* were used in the antibacterial tests, *Staphylococcus aureus* (ATCC 29212) and *Staphylococcus aureus* (ATCC 43300).

The *para* substituted derivatives showed weaker activity than the *meta* substituted derivatives except for the *para* fluoro derivative against *Staphylococcus saprophyticus* (ATCC 35552). The *para* methoxy (**4**), chloro (**7**) and nitro (**16**) derivatives showed no activity against the bacterial strains tested.

Compound **14**, the *meta* substituted hydroxylated homoisoflavonoid, showed the broadest range of antibacterial activity. It was the only homoisoflavonoid to show mild activity against the gram negative strain, *Escherichia coli* (ATCC 29522). Compound **14** was strongly active against *Staphylococcus aureus* (ATCC 29212 and ATCC 43300) and was moderately active against *Staphylococcus saprophyticus* (ATCC 35552), *Staphylococcus scuiiri* (ATCC 29062), *Staphylococcus xylosus* (ATCC 35033) and *Streptococcus pyogenes* (ATCC 19615).



Graph 4: The zone of inhibition of compounds **3** (unsubstituted), **11** (3'-F), **12** (3',4'-diF), **13** (4'-OH), **14** (3'-OH) and **15** (3',4'-diOH) against *Staphylococcus aureus* (ATCC 43300)

With respect to *Staphylococcus aureus* (ATCC 43300), compounds **3**, **11** and **14**, the unsubstituted, the 3'-fluoro and the 3'-hydroxy homoisoflavonoids respectively showed better activity than the common antibiotic ampicillin, with activity indexes of 1.31, 1.23 and 1.46 respectively (Graph 4). Compound **3**, the unsubstituted homoisoflavonoid, has an activity index of 1.31, which is decreased when substituents are introduced onto the B-ring of the homoisoflavonoid, except for when a hydroxyl group is introduced at the 3'-position of the B-ring. The *meta* hydroxy substituent enhances its antibacterial activity, increasing the activity index from 1.31 to 1.46 for ampicillin and 0.52 to 0.58 for tetracycline. The activity of the 3'-fluoro derivative **11**, is only slightly decreased by the introduction of fluorine at the 3'-position and therefore the positive effects of having a fluorine atom in the molecule for the development of an antibacterial agent such as increased lipophilicity makes it an interesting subject for further research.

By comparing the activity indices of the fluorinated compounds **10**, **11** and **12** against *Staphylococcus aureus* (ATCC 43300), it can be seen that the most favourable substitution pattern for antibacterial activity is the *meta* substitution with activity indices of 1.23 (AMP) and 0.48 (TET). The *para* substituted fluoro derivative showed no activity. The disubstituted fluorinated derivative, **12**, showed a decrease in activity when compared to the *meta* fluoro derivative. By introducing an additional fluorine atom on the 4'-position of the *meta* substituted derivative, the activity is decreased from 1.23 to 0.85. This may be due to the mechanism by which the antibacterial agent works. Substitution at the 4'-position may inhibit binding to the active site of enzymes required for normal functional of the bacterial species. This explains why the activity decreases when the homoisoflavonoid is disubstituted. In contrast, substitution at the 3'-position with a molecule or group capable of hydrogen bonding, such as fluorine (**11**) or the hydroxy group (**14**) may be perfect for binding to enzymes responsible for the functioning of bacterial cells. Once bound to these enzymes, they may alter their function and hence lead either to cell death of the bacterial species or inhibit replication of the bacterial species.

Staphylococcus aureus (ATCC 43300) is resistant to both methicillin and oxacillin (<http://www.straininfo.net/strains/54914/>). Such strains of bacteria are referred to as methicillin resistant *Staphylococcus aureus* (MRSA). Compound **14** may therefore serve as a useful antibacterial agent against *Staphylococcus aureus* (ATCC 43300). MRSA is one of the most dangerous bacterial infections that occur in the commercial health care sector (hospitals), as these bacterial infections cannot be easily destroyed. As compound **14**, shows good antibacterial activity against *Staphylococcus aureus* (ATCC 43300), it may be applied to combat such infections. Derivatisation of compound **14**, by varying the substitution on the A-ring can be conducted in order to develop better antibacterial agents.

CHAPTER 3 EXPERIMENTAL

This chapter includes the experimental techniques employed to synthesise and characterise the thirteen benzylidene and two benzyl homoisoflavonoids. Characteristic data, such as the ^1H and ^{13}C NMR, UV, IR and MS data are reported in the chapter. New crystal structures for seven of the homoisoflavonoids were obtained. The methodology used to determine the antioxidant and antibacterial activities of the test compounds are also included here.

3.1 Chemistry

The experimental procedure for the synthesis of the intermediates 3-phenoxypropanoic acid (**1**) and 4-chromanone (**2**) as well as the homoisoflavonoids (**3-17**) are included here. The instrument details and parameters used for the characterisation techniques employed are also reported.

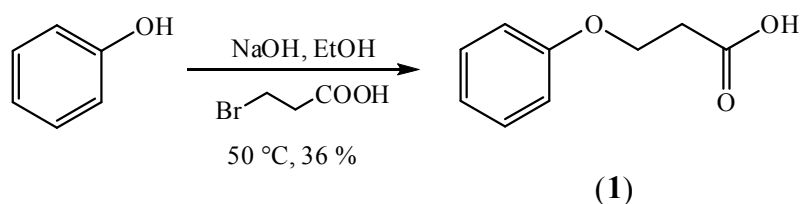
3.1.1 General experimental procedures

The reagents and chemicals used in this study were purchased from Sigma Aldrich *via* Capital Lab, South Africa and were reagent grade. All organic solvents were redistilled and dried according to standard procedures. The melting points were recorded on an Ernst Leitz Wetziar micro-hot stage melting point apparatus. IR spectra were recorded on a Perkin Elmer Spectrum 100 FTIR spectrometer with universal ATR sampling accessory. UV spectra were obtained on a Varian Cary UV-VIS Spectrophotometer in dichloromethane (**1-12**, **16-17**) and methanol (**13-15**). For GC-MS analyses, the samples were analysed on an Agilent GC-MSD apparatus equipped with DB-5SIL MS (30 m x 0.25 mm i.d., 0.25 μm film thickness) fused-silica capillary column. Helium (at 2 mL/min) was used as a carrier gas. The MS was operated in the EI mode at 70 eV. The NMR spectra were recorded using a

Bruker Avance ^{III} (400 MHz) spectrometer at room temperature (25 °C). The chemical shifts (δ) were referenced against an internal standard, tetramethylsilane (TMS) for ¹H and ¹³C and trifluorotoluene for ¹⁹F NMR. Solution NMR was performed in deuterated solvents, CDCl₃ (**1-12, 16-17**) and DMSO (**13-15**).

3.1.2 The synthesis of 3-phenoxypropanoic acid (**1**)

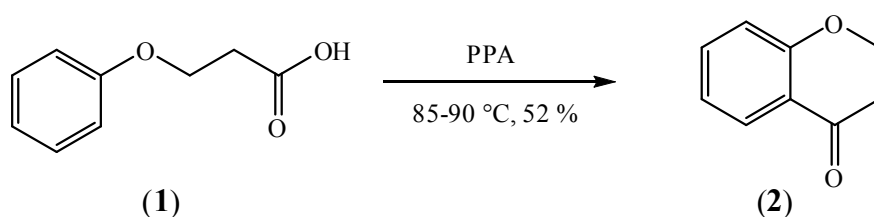
To a 100 mL round bottom flask, a solution of phenol (5.27 g, 56 mmol) in EtOH (30.00 mL) and a solution of NaOH (3.401 g, 85 mmol) in deionized water was added under cool conditions (10-15 °C) and stirred for 45 min for the deprotonation of phenol. A solution of 3-bromopropionic acid (10.57 g, 69 mmol) in EtOH (30.00 mL) was then added using a dropping funnel at 0 °C and the reaction mixture stirred for 12 hrs at 50 °C under reflux. The reaction mixture was cooled and acidified with 10% HCl and extracted with ethyl acetate (3 × 50 mL). The ethyl acetate layers were combined, washed with brine (1 × 20 mL), water (2 × 10 mL) and dried over anhydrous magnesium sulfate. The residue obtained after evaporation of the solvent was purified by column chromatography using silica gel with 10% ethyl acetate in hexane as the mobile phase. Compound **1** has an R_f of 0.36 in an ethyl acetate: hexane (20:80) solvent system (Scheme 18) (3.35g, 36%).



Scheme 18: The preparation of 3-phenoxypropanoic acid (**1**)

3.1.3 The synthesis of 4-chromanone (2)

In a 250 mL round bottom flask, a mixture of 3-phenoxypropanoic acid (4.51 g, 27 mmol) and polyphosphoric acid (13.52 g, 40 mmol) was stirred at 85-90 °C under reflux for 2 hrs (solvent free reaction). The viscous reaction mixture was poured onto crushed ice and extracted with diethyl ether (3 × 30 mL). The extract was washed with NaOH (30 mL), water (50 mL) and dried over magnesium sulfate. The residue obtained after evaporation of the solvent was purified by column chromatography using silica gel with 5% ethyl acetate in hexane as the mobile phase. Compound **2** has an R_f of 0.53 in an ethyl acetate: hexane (20:80) solvent system (Scheme 19) (2.08 g, 52%).

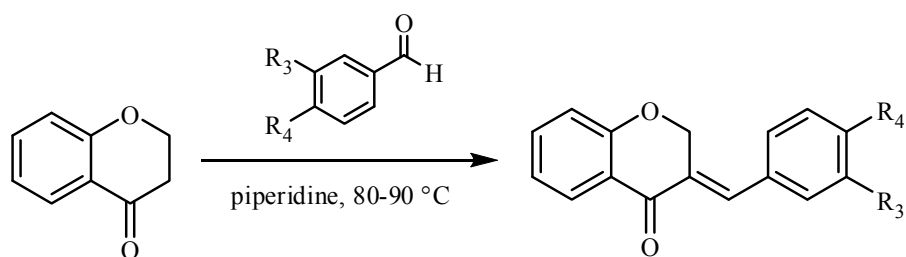


Scheme 19: The preparation of 4-chromanone (2)

3.1.4 The base catalysed preparation of homoisoflavonoids (3-17)

In a 50 mL round bottom flask, a mixture of 4-chromanone (68 mmol), the desired substituted benzaldehyde (81 mmol) and 10–15 drops of piperidine was stirred at 80-90 °C under reflux for 12-36 hrs (Scheme 20). Typically masses between 1.01 g and 1.21 g of 4-chromanone were used. The reaction mixture was monitored for completion by thin layer chromatography. Upon completion, the reaction mixture was cooled, diluted with water and neutralized using 10% HCl. For compounds **16** and **17**, 10 mL of ethyl acetate was added to the viscous solution and the homoisoflavonoids precipitated out upon addition of hexane. The powdered product was filtered, washed with hexane and dried under vacuum.

For the other compounds, the reaction mixture was extracted with ethyl acetate (3 × 30 mL). The ethyl acetate layers were combined, washed with brine (20 mL), water (2 × 10 mL), dried over anhydrous magnesium sulfate and the solvent evaporated. On slow evaporation, crystals of compound **6** were obtained. In this case, the supernatant liquid was decanted. The crystals were then filtered and dried under vacuum. The remaining compounds were subjected to column chromatography on silica gel using various ethyl acetate: hexane mixtures as the mobile phase depending on the polarity of the compound. A 2 cm diameter column was used and 50 mL fractions were collected until the compound was eluted from the column. Upon slow evaporation of the solvent, crystals of the homoisoflavonoids were obtained. The crystals were then filtered and dried under vacuum.

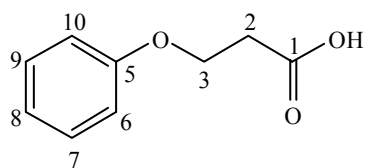


Scheme 20: The preparation of homoisoflavonoids (**3-17**)

3.1.5 The physical and spectroscopic data of synthesised compounds (1-17)

The chemical formula, molecular mass, physical description, melting points and yields of the synthesised compounds are listed below. Spectroscopic data including the UV, IR, MS and NMR data are listed. The ¹H and ¹³C NMR data of **3-17** are contained in Table 2, 3, 4 and 5.

3-phenoxypropanoic acid (1)



$C_9H_{10}O_3$ (166.17 g mol⁻¹);

Cream powder,

m.p.: 98-100 °C, yield: 36%

R_f: 0.36 (hexane: ethyl acetate, 80:20)

UV λ_{max} (nm) (log ε): 270 (2.68), 277 (2.60)

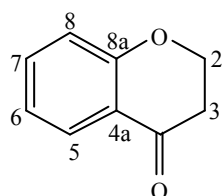
IR ν_{max} (cm⁻¹): 2931 (O-H), 1688 (C=O), 1596, 1493 (C=C), 1231 (C-O)

EI MS *m/z* (%): 166 (38) [M⁺], 94 (100), 77 (15), 66 (15), 65 (15), 55 (8), 51 (9)

¹H NMR (400 MHz, CDCl₃) δ: 2.83 (2H, t, *J* = 6.24 Hz, H-2), 4.23 (2H, t, *J* = 6.24 Hz, H-3), 6.89 (2H, d, *J* = 8.04 Hz, H-6/10), 6.94 (1H, t, *J* = 7.42 Hz, H-8), 7.26 (2H, dd, *J* = 8.44, 7.48 Hz, H-7/9)

¹³C NMR (100 MHz, CDCl₃) δ: 34.49 (C-2), 63.05 (C-3), 114.65 (C-6/10), 121.17 (C-8), 129.50 (C-7/9), 158.39 (C-5), 176.93 (C-1)

4-chromanone (2)



$C_9H_8O_2$ (148.16 g mol⁻¹);

White solid,

m.p.: 39-40 °C, yield: 52%

R_f: 0.53 (hexane: ethyl acetate, 80:20)

UV λ_{max} (nm) (log ε): 249 (3.91), 318 (3.53)

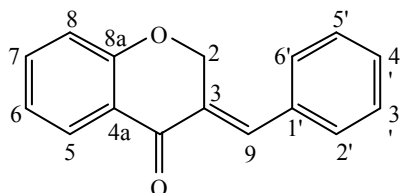
IR ν_{max} (cm⁻¹): 1682 (C=O), 1599, 1476, 1453 (C=C), 1258 (C-O)

EI MS *m/z* (%): 148 (89) [M⁺], 120 (100), 92 (77), 64 (18), 63 (17)

¹H NMR (400 MHz, CDCl₃) δ: 2.76 (1H, m, H-3a), 2.78 (1H, m, H-3b), 4.49 (1H, m, H-2b), 4.50 (1H, m, H-2a), 6.93 (1H, d, *J* = 8.44 Hz, H-8), 6.97 (1H, td, *J* = 7.84, 0.76 Hz, H-6), 7.42 (1H, ddd, *J* = 8.64, 7.16, 1.64 Hz, H-7), 7.85 (1H, dd, *J* = 7.84, 1.72 Hz, H-5).

^{13}C NMR (100 MHz, CDCl_3) δ : 37.78 (C-3), 67.00 (C-2), 117.89 (C-6/4a), 121.36 (C-8), 127.12 (C-5), 135.96 (C-7), 161.86 (C-8a), 191.79 (C-4)

(E)-3-benzylidene-chroman-4-one (3)



$\text{C}_{16}\text{H}_{12}\text{O}_2$ (236.27 g mol^{-1});

Colourless crystalline solid,

m.p.: 108-110 $^\circ\text{C}$, yield: 77%

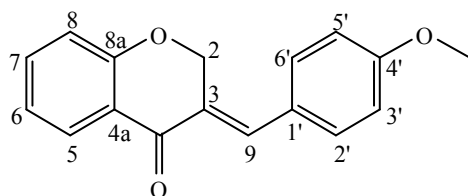
R_f : 0.69 (hexane: ethyl acetate, 80:20)

UV λ_{max} (nm) (log ϵ): 299 (4.13), 344 (3.91)

IR ν_{max} (cm^{-1}): 1665 (C=O), 1601, 1466, 1450 (C=C), 1209 (C-O)

EI MS m/z (%): 236 (100) [M^+], 235 (99), 207 (20), 178 (8), 131 (13), 121 (65), 115 (88), 92 (22), 79 (8), 63 (16)

(E)-3-(4'-methoxybenzylidene)chroman-4-one (4)



$\text{C}_{17}\text{H}_{14}\text{O}_3$ (266.29 g mol^{-1});

Pale yellow crystalline solid,

m.p.: 135-137 $^\circ\text{C}$, yield: 75%

R_f : 0.56 (hexane: ethyl acetate, 80:20)

UV λ_{max} (nm) (log ϵ): 247 (4.34), 351 (4.33)

IR ν_{max} (cm^{-1}): 1663 (C=O), 1595, 1509, 1463 (C=C), 1210 (C-O)

EI MS m/z (%): 266 (100) [M^+], 265 (51), 251 (20), 237 (14), 235 (14), 223 (8), 207 (14), 165 (5), 146 (32), 145 (19), 131 (26), 121 (64), 103 (29), 92 (12), 77 (18), 63 (9)

Crystal structure:

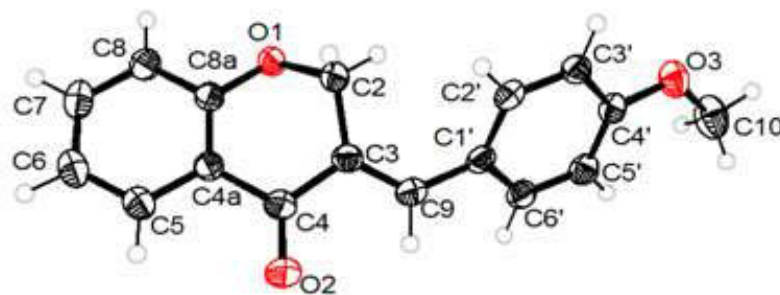
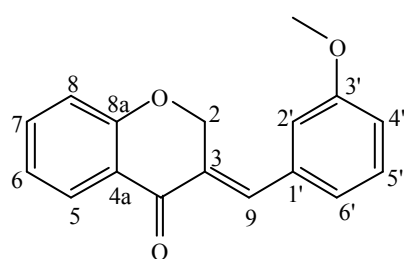


Figure 13: ORTEP diagram of compound 4 drawn at the 50% probability level

(E)-3-(3'-methoxybenzylidene)chroman-4-one (5)



$C_{17}H_{14}O_3$ (266.29 g mol⁻¹);

Pale yellow crystalline solid,

m.p.: 85-86 °C, yield: 72%

R_f: 0.63 (hexane: ethyl acetate, 80:20)

UV λ_{max} (nm) (log ε): 267 (4.06), 298 (4.04), 342 (3.99)

IR ν_{max} (cm⁻¹): 1667 (C=O), 1598, 1460 (C=C), 1264 (C-O)

EI MS *m/z* (%): 266 (95) [M⁺], 265 (42), 251 (11), 235 (30), 146 (17), 145 (13), 131 (14),

121 (100), 115 (17), 103 (23), 92 (12), 77 (17), 63 (10)

Crystal structure:

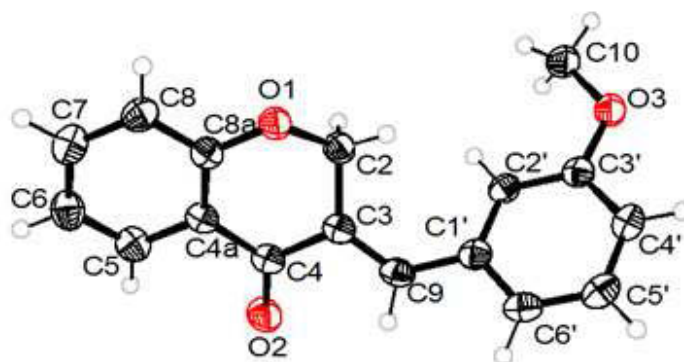
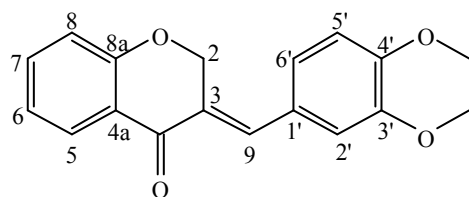


Figure 14: ORTEP diagram of compound 5 drawn at the 50% probability level

(E)-3-(3',4'-dimethoxybenzylidene)chroman-4-one (6)



$C_{18}H_{16}O_4$ (296.32 g mol⁻¹);

Pale yellow crystalline solid,

m.p.: 128-129 °C, yield: 61%

R_f: 0.34 (hexane: ethyl acetate, 80:20)

UV λ_{max} (nm) (log ε): 266 (4.22), 366 (4.28)

IR ν_{max} (cm⁻¹): 1661 (C=O), 1585, 1510, 1480 (C=C), 1241 (C-O)

EI MS *m/z* (%): 296 (100) [M⁺], 295 (24), 281 (23), 265 (29), 221 (10), 176 (22), 161 (20), 131 (10), 121 (99), 92 (14), 77 (12), 63 (11)

Crystal structure:

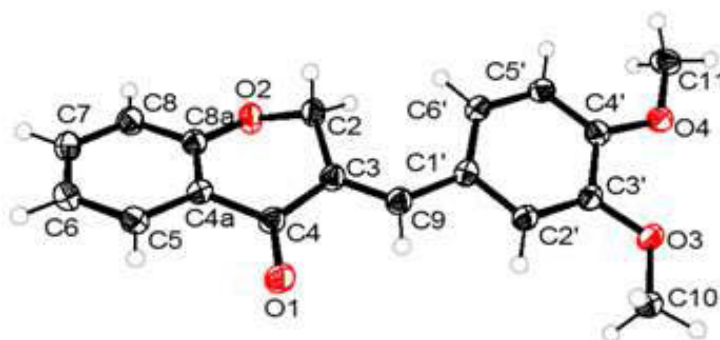
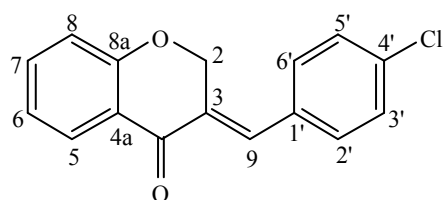


Figure 15: ORTEP diagram of compound **6** drawn at the 50% probability level

(E)-3-(4'-chlorobenzylidene)chroman-4-one (7)



$C_{16}H_{11}ClO_2$ (270.71 g mol⁻¹);

White needle-like crystals,

m.p.: 173 °C, yield: 67%

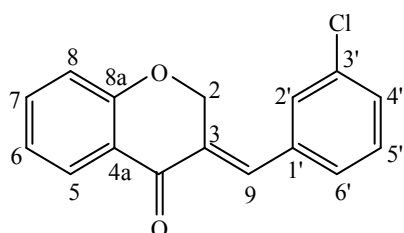
R_f: 0.69 (hexane: ethyl acetate, 80:20)

UV λ_{max} (nm) (log ε): 302 (4.20), 345 (3.88)

IR ν_{max} (cm⁻¹): 1670 (C=O), 1603, 1475 (C=C), 1217 (C-O), 748 (C-Cl)

EI MS m/z (%): 270 (100) [M^+], 269 (55), 241 (14), 235 (29), 207 (13), 179 (11), 178 (15), 150 (19), 149 (21), 134 (14), 131 (14), 121 (71), 120 (17), 117 (20), 115 (77), 92 (29), 89 (14), 76 (11), 63 (19)

(E)-3-(3'-chlorobenzylidene)chroman-4-one(8)



$C_{16}H_{11}ClO_2$ (270.71 g mol⁻¹);

White needle-like crystals,

m.p.: 123-124 °C, yield: 71%

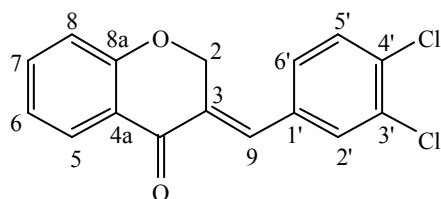
R_f: 0.56 (hexane: ethyl acetate, 80:20)

UV λ_{max} (nm) (log ϵ): 291 (4.17), 345 (3.71)

IR ν_{max} (cm⁻¹): 1671 (C=O), 1604, 1464 (C=C), 1218 (C-O), 750 (C-Cl)

EI MS m/z (%): 270 (100) [M^+], 269 (54), 241 (11), 235 (41), 207 (10), 178 (15), 149 (20), 131 (17), 121 (81), 120 (25), 117 (28), 115 (59), 92 (36), 76 (11), 63 (19)

(E)-3-(3',4'-dichlorobenzylidene)chroman-4-one (9)



$C_{16}H_{10}Cl_2O_2$ (305.16 g mol⁻¹);

White needle-like crystals,

m.p.: 165-167 °C, yield: 59%

R_f: 0.66 (hexane: ethyl acetate, 80:20)

UV λ_{max} (nm) (log ϵ): 297 (3.96), 346 (3.53)

IR ν_{max} (cm⁻¹): 1668 (C=O), 1604, 1464 (C=C), 1218 (C-O), 832, 746 (C-Cl)

EI MS m/z (%): 306 (57), 304 (90) [M^+], 275 (12), 269 (23), 234 (11), 205 (8), 183 (15), 178 (13), 151 (23), 149 (65), 134 (41), 121 (100), 120 (38), 114 (15), 113 (15), 93 (11), 92 (51), 76 (14), 64 (20), 63 (24)

Crystal structure:

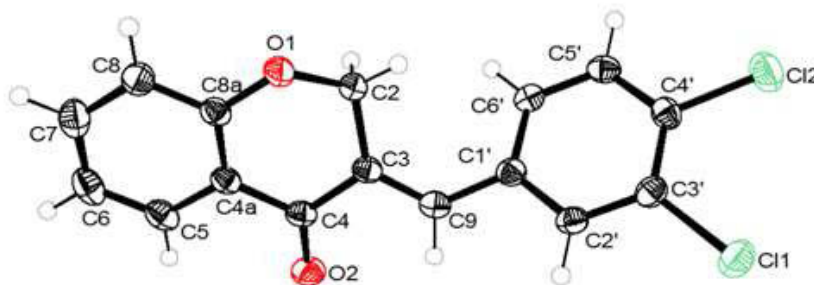
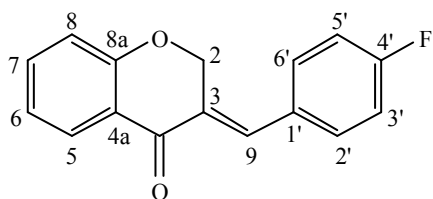


Figure 16: ORTEP diagram of compound **9** drawn at the 50% probability level

(*E*)-3-(4'-fluorobenzylidene)chroman-4-one (10)



$C_{16}H_{11}FO_2$ (254.26 $g\ mol^{-1}$);

Pale yellow needle-like crystals,

m.p.: 152-153 °C, yield: 59%

R_f : 0.63 (hexane: ethyl acetate, 80:20)

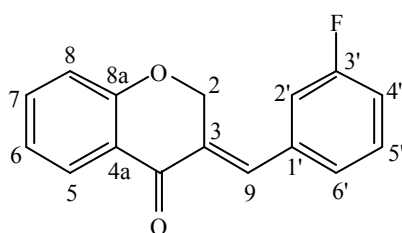
UV λ_{max} (nm) (log ϵ): 301 (3.97), 344 (3.63)

IR ν_{max} (cm^{-1}): 1671 (C=O), 1597, 1477 (C=C), 1217 (C-O), 1145 (C-F)

EI MS m/z (%): 254 (100) [M^+], 253 (53), 237 (5), 225 (22), 207 (6), 196 (5), 134 (41), 133 (87), 131 (14), 121 (55), 120 (17), 107 (8), 92 (25), 63 (11)

^{19}F NMR (376.5 MHz, $CDCl_3$) δ : -110.16

(*E*)-3-(3'-fluorobenzylidene)chroman-4-one(11)



$C_{16}H_{11}FO_2$ (254.26 $g\ mol^{-1}$);

Pale yellow needle-like crystals,

m.p.: 95-96 °C, yield: 61%

R_f: 0.66 (hexane: ethyl acetate, 80:20)

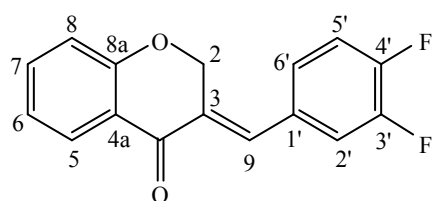
UV λ_{max} (nm) (log ε): 291 (3.99), 346 (3.55)

IR ν_{max} (cm⁻¹): 1666 (C=O), 1598, 1477 (C=C), 1213 (C-O), 1144 (C-F)

EI MS *m/z* (%): 254 (100) [M⁺], 253 (55), 237 (5), 225 (17), 134 (23), 133 (62), 121 (55), 120 (20), 92 (26), 63 (14)

¹⁹F NMR (376.5 MHz, CDCl₃) δ: 112.15

(*E*)-3-(3',4'-difluorobenzylidene)chroman-4-one (12)



C₁₆H₁₀F₂O₂ (272.25 g mol⁻¹);

Pale yellow needle-like crystals,

m.p.: 138-139 °C, yield: 50%

R_f: 0.69 (hexane: ethyl acetate, 80:20)

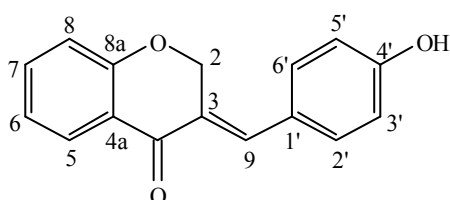
UV λ_{max} (nm) (log ε): 267 (3.96), 387 (4.05)

IR ν_{max} (cm⁻¹): 1672 (C=O), 1603, 1477 (C=C), 1217 (C-O), 1116, 1145 (C-F)

EI MS *m/z* (%): 272 (100) [M⁺], 271 (29), 243 (19), 152 (19), 151 (62), 134 (10), 131 (16), 121 (46), 120 (27), 92 (34), 63 (11)

¹⁹F NMR (376.5 MHz, CDCl₃) δ: -136.2 (d, *J* = 21.65 Hz), -134.83 (d, *J* = 21.46 Hz)

(*E*)-3-(4'-hydroxybenzylidene)chroman-4-one (13)



C₁₆H₁₂O₃ (252.26 g mol⁻¹);

Yellow powder,

m.p.: 222-224 °C, yield: 54%

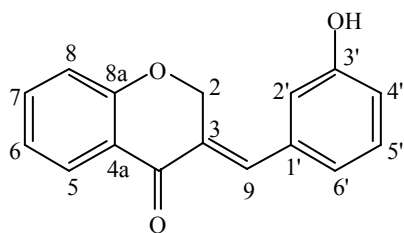
R_f: 0.22 (hexane: ethyl acetate, 80:20)

UV λ_{max} (nm) (log ε): 331 (3.98), 359 (3.97)

IR ν_{\max} (cm^{-1}): 3093 (O-H), 1651 (C=O), 1608, 1557, 1509 (C=C), 1291, 1209 (C-O)

EI MS m/z (%): 252 (100) [M^+], 251 (28), 235 (13), 223 (9), 207 (13), 132 (11), 131 (23), 121 (82), 77 (15), 63 (6)

(E)-3-(3'-hydroxybenzylidene)chroman-4-one (14)



$\text{C}_{16}\text{H}_{12}\text{O}_3$ (252.26 g mol^{-1});

Pale yellow powder,

m.p.: 199-200 $^{\circ}\text{C}$, yield: 51%

R_f : 0.31 (hexane: ethyl acetate, 80:20)

UV λ_{\max} (nm) ($\log \epsilon$): 267 (4.20), 340 (4.04)

IR ν_{\max} (cm^{-1}): 3255 (O-H), 1668 (C=O), 1593, 1461 (C=C), 1220 (C-O)

EI MS m/z (%): 252 (100) [M^+], 251 (23), 235 (14), 234 (17), 223 (8), 206 (22), 205 (12), 131 (18), 121 (83), 92 (8), 77 (16)

Crystal structure:

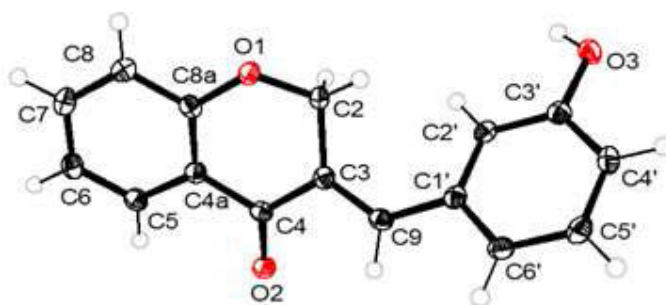
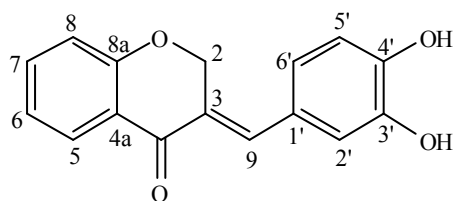


Figure 17: ORTEP diagram of compound **14** drawn at the 50% probability level

(E)-3-(3',4'-dihydroxybenzylidene)chroman-4-one (15)



$C_{16}H_{12}O_4$ (268.26 g mol⁻¹);

Yellow powder,

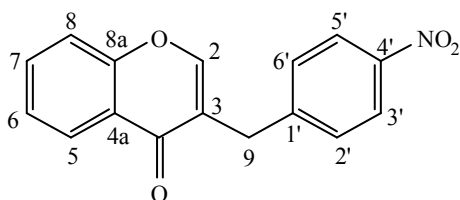
m.p.: 230-231 °C, yield: 45%

R_f: 0.16 (hexane: ethyl acetate, 80:20)

UV λ_{max} (nm) (log ε): 268 (3.62), 374 (3.68)

IR ν_{max} (cm⁻¹): 3453, 3117 (O-H), 1649 (C=O), 1601, 1558, 1531 (C=C), 1286, 1187 (C-O)

3-(4-nitrobenzyl)-4H-chromen-4-one (16)



$C_{16}H_{11}NO_4$ (281.26 g mol⁻¹);

White powder,

m.p.: 179-180 °C, yield: 80%

R_f: 0.34 (hexane: ethyl acetate, 80:20)

UV λ_{max} (nm) (log ε): 265 (4.07), 295 (4.15)

IR ν_{max} (cm⁻¹): 1624 (C=O), 1603, 1464 (C=C), 1145 (C-O), 1505, 1339 (N-O)

EI MS *m/z* (%): 281 (100) [M⁺], 264 (24), 235 (14), 234 (35), 205 (14), 178 (26), 121 (65),

120 (19), 117 (19), 115 (31), 92 (22), 77 (18), 63 (18)

Crystal structure:

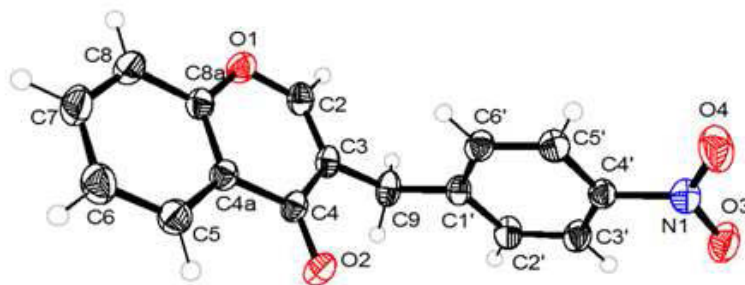
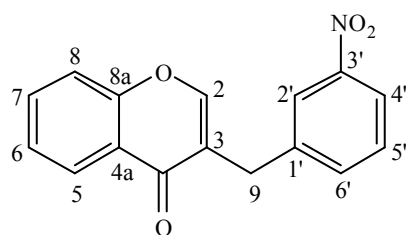


Figure 18: ORTEP diagram of compound **16** drawn at the 50% probability level

3-(3-nitrobenzyl)-4H-chromen-4-one (17)



$C_{16}H_{11}NO_4$ (281.26 $g\ mol^{-1}$);

Cream powder,

m.p.: 129-130 °C, yield: 72%

R_f : 0.38 (hexane: ethyl acetate, 80:20)

UV λ_{max} (nm) (log ϵ): 296 (3.96)

IR ν_{max} (cm^{-1}): 1623 (C=O), 1605, 1464 (C=C), 1142 (C-O), 1523, 1341 (N-O)

EI MS m/z (%): 281 (100) [M^+], 264 (83), 234 (89), 205 (26), 178 (18), 117 (17), 115 (18),

92 (11), 89 (9), 77 (8), 76 (10), 63 (10)

Crystal structure:

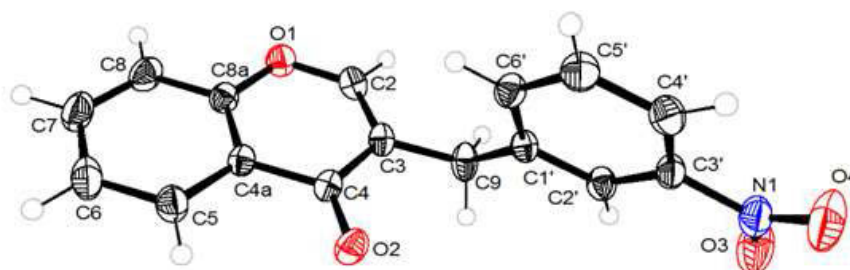


Figure 19: ORTEP diagram of compound 17 drawn at the 50% probability level

Table 2: ¹H NMR data of compounds **3-10**

	Homoisoflavonoids							
Pos.	3	4	5	6	7	8	9	10
2	5.33 (d, <i>J</i> = 1.32 Hz)	5.35 (d, <i>J</i> = 1.72 Hz)	5.33 (d, <i>J</i> = 1.68 Hz)	5.37 (d, <i>J</i> = 1.84 Hz)	5.29 (d, <i>J</i> = 1.84 Hz)	5.29 (d, <i>J</i> = 1.80 Hz)	5.27 (d, <i>J</i> = 1.88 Hz)	5.31 (d, <i>J</i> = 1.84 Hz)
5	8.00 (dd, <i>J</i> = 7.86, 1.10 Hz)	8.00 (dd, <i>J</i> = 7.84, 1.70 Hz)	8.00 (dd, <i>J</i> = 7.82, 1.46 Hz)	8.00 (dd, <i>J</i> = 7.86, 1.71 Hz)	8.00 (dd, <i>J</i> = 7.90, 1.58 Hz)	8.00 (dd, <i>J</i> = 7.88, 1.68 Hz)	8.00 (dd, <i>J</i> = 7.88, 1.64 Hz)	8.00 (dd, <i>J</i> = 7.86, 1.70 Hz)
6	7.05 (t, <i>J</i> = 7.50 Hz)	7.05 (td, <i>J</i> = 7.51, 0.78 Hz)	7.05 (t, <i>J</i> = 7.52 Hz)	7.04 (td, <i>J</i> = 7.52, 0.84 Hz)	7.06 (t, <i>J</i> = 7.38 Hz)	7.07 (td, <i>J</i> = 7.51, 0.82 Hz)	7.07 (td, <i>J</i> = 7.52, 0.68 Hz)	7.06 (td, <i>J</i> = 7.52, 0.76 Hz)
7	7.47 (m)	7.45 (ddd, <i>J</i> = 8.56, 7.29, 1.66 Hz)	7.47 (td, <i>J</i> = 7.72, 1.60 Hz)	7.44 (ddd, <i>J</i> = 8.58, 7.18, 1.64 Hz)	7.47 (td, <i>J</i> = 7.76, 1.60 Hz)	7.48 (ddd, <i>J</i> = 8.68, 7.50, 1.84 Hz)	7.49 (ddd, <i>J</i> = 8.72, 7.48, 1.72 Hz)	7.48 (ddd, <i>J</i> = 7.76, 6.52, 1.78 Hz)
8	6.95 (d, <i>J</i> = 8.32 Hz)	6.93 (d, <i>J</i> = 8.04 Hz)	6.94 (d, <i>J</i> = 8.12 Hz)	6.93 (d, <i>J</i> = 7.88 Hz)	6.95 (d, <i>J</i> = 8.20 Hz)	6.95 (d, <i>J</i> = 8.56 Hz)	6.96 (d, <i>J</i> = 8.28 Hz)	6.96 (d, <i>J</i> = 8.04 Hz)
9	7.86 (s)	7.81 (s)	7.82 (s)	7.80 (s)	7.78 (s)	7.77 (s)	7.72 (s)	7.81 (s)
2'	7.29 (d, <i>J</i> = 6.96 Hz)	7.26 (d, <i>J</i> = 8.68 Hz)	6.82 (s)	6.83 (d, <i>J</i> = 1.72 Hz)	7.22 (d, <i>J</i> = 8.44 Hz)	7.27 (s)	7.38 (d, <i>J</i> = 1.92 Hz)	7.28 (dd, <i>J</i> = 8.60, 5.40 Hz)
3'	7.42 (d, <i>J</i> = 7.36 Hz)	6.96 (d, <i>J</i> = 8.76 Hz)	-	-	7.40 (d, <i>J</i> = 8.40 Hz)	-	-	7.13 (t, <i>J</i> = 8.62 Hz)
4'	7.40 (m)	-	6.93 (m)	-	-	7.37 (d, <i>J</i> = 5.20 Hz)	-	-
5'	7.42 (d, <i>J</i> = 7.36 Hz)	6.96 (d, <i>J</i> = 8.76 Hz)	7.34 (t, <i>J</i> = 7.92 Hz)	6.90 (d, <i>J</i> = 8.36 Hz)	7.40 (d, <i>J</i> = 8.40 Hz)	7.17 (ddd, <i>J</i> = 5.20, 4.64 Hz)	7.50 (d, <i>J</i> = 8.40 Hz)	7.13 (t, <i>J</i> = 8.62 Hz)
6'	7.29 (d, <i>J</i> = 6.96 Hz)	7.26 (d, <i>J</i> = 8.68 Hz)	6.87 (d, <i>J</i> = 7.60 Hz)	6.88 (dd, <i>J</i> = 8.62, 1.80 Hz)	7.22 (d, <i>J</i> = 8.44 Hz)	7.37 (d, <i>J</i> = 5.20 Hz)	7.12 (dd, <i>J</i> = 8.28, 1.96 Hz)	7.28 (dd, <i>J</i> = 8.60, 5.40 Hz)
OCH₃	-	3.83 (s)	3.82 (s)	3.89 (s)	-	-	-	-
OCH₃	-	-	-	3.91 (s)	-	-	-	-

Table 3: ¹H NMR data of compounds **11-17**

Pos.	Homoisoflavonoids						
	11	12	13	14	15	16	17
2	5.29 (d, <i>J</i> = 1.88 Hz)	5.28 (d, <i>J</i> = 1.84 Hz)	5.41 (s)	5.40 (d, <i>J</i> = 1.36 Hz)	5.35 (d, <i>J</i> = 1.68 Hz)	7.79 (s)	7.82 (s)
5	7.99 (dd, <i>J</i> = 7.90, 1.66 Hz)	7.99 (dd, <i>J</i> = 7.86, 1.70 Hz)	7.86 (d, <i>J</i> = 7.80 Hz)	7.88 (dd, <i>J</i> = 7.88, 1.32 Hz)	7.79 (dd, <i>J</i> = 7.84, 1.60 Hz)	8.18 (dd, <i>J</i> = 7.98, 0.66 Hz)	8.18 (dd, <i>J</i> = 8.00, 1.36 Hz)
6	7.04 (t, <i>J</i> = 7.80 Hz)	7.06 (t, <i>J</i> = 7.44 Hz)	7.08 (t, <i>J</i> = 7.50 Hz)	7.13 (td, <i>J</i> = 7.50, 0.68 Hz)	7.05 (t, <i>J</i> = 7.50 Hz)	7.38 (t, <i>J</i> = 7.54 Hz)	7.38 (t, <i>J</i> = 7.52 Hz)
7	7.48 (ddd, <i>J</i> = 7.75, 6.41, 1.66 Hz)	7.48 (ddd, <i>J</i> = 7.78, 6.58, 1.80 Hz)	7.54 (td, <i>J</i> = 7.65, 1.18 Hz)	7.60 (td, <i>J</i> = 7.73, 1.50 Hz)	7.49 (ddd, <i>J</i> = 7.78, 6.46, 1.64 Hz)	7.65 (td, <i>J</i> = 8.32, 1.10 Hz)	7.60 (ddd, <i>J</i> = 7.80, 6.68, 1.52 Hz)
8	6.95 (d, <i>J</i> = 8.44 Hz)	6.96 (d, <i>J</i> = 8.44 Hz)	7.00 (d, <i>J</i> = 8.28 Hz)	7.06 (d, <i>J</i> = 8.28 Hz)	6.98 (d, <i>J</i> = 8.00 Hz)	7.41 (d, <i>J</i> = 8.60 Hz)	7.43 (d, <i>J</i> = 8.32 Hz)
9	7.78 (s)	7.73 (s)	7.68 (s)	7.66 (s)	7.54 (s)	3.87 (s)	3.88 (s)
2'	6.98 (d, <i>J</i> = 9.52 Hz)	7.12 (ddd, <i>J</i> = 10.08, 7.52, 2.04 Hz)	7.32 (d, <i>J</i> = 8.48 Hz)	6.82 (s)	6.81 (d, <i>J</i> = 2.04 Hz)	7.45 (d, <i>J</i> = 8.48 Hz)	8.13 (s)
3'	-	-	6.89 (d, <i>J</i> = 8.48 Hz)	-	-	8.12 (d, <i>J</i> = 8.56 Hz)	-
4'	7.09 (td, <i>J</i> = 8.44, 2.40 Hz)	-	-	6.86 (d, <i>J</i> = 8.08 Hz)	-	-	8.06 (d, <i>J</i> = 8.16 Hz)
5'	7.39 (td, <i>J</i> = 8.00, 5.96 Hz)	7.22 (td, <i>J</i> = 9.88, 8.28 Hz)	6.89 (d, <i>J</i> = 8.48 Hz)	7.30 (t, <i>J</i> = 7.86 Hz)	6.79 (d, <i>J</i> = 9.16 Hz)	8.12 (d, <i>J</i> = 8.56 Hz)	7.45 (t, <i>J</i> = 8.16 Hz)
6'	7.06 (d, <i>J</i> = 7.12 Hz)	7.04 (m)	7.32 (d, <i>J</i> = 8.48 Hz)	6.86 (d, <i>J</i> = 8.08 Hz)	6.73 (dd, <i>J</i> = 9.14, 1.88 Hz)	7.45 (d, <i>J</i> = 8.48 Hz)	7.69 (d, <i>J</i> = 7.68 Hz)
OH	-	-	-	9.71 (s)	-	-	-

Table 4: ^{13}C NMR data of compounds **3-10**

Pos.	Homoisoflavonoids							
	3	4	5	6	7	8	9	10
2	67.61	67.79	67.66	67.79	67.44	67.39	67.27	67.48
3	130.92	128.90	131.15	129.19	131.40	132.10	132.44	130.77
4	182.27	182.21	182.23	182.07	181.97	181.94	181.71	182.10
4a	122.03	122.13	122.02	122.10	121.91	121.87	121.79	121.95
5	127.96	127.89	127.96	127.89	127.97	127.94	128.00	127.96
6	121.93	121.84	121.93	121.88	122.04	122.07	122.16	122.00
7	135.89	135.67	135.89	135.71	136.02	136.09	136.19	135.96
8	117.92	117.82	117.93	117.82	117.94	117.99	118.00	117.92
8a	161.14	160.98	161.18	160.95	161.09	161.17	161.13	161.08
9	137.52	137.34	137.40	137.49	136.02	135.72	134.55	136.27
1'	134.39	127.03	135.69	127.28	132.79	136.11	133.15	130.52
2'	129.99	132.06	115.42	113.31	131.19	130.00	131.41	131.97 (d, $J = 8.55$ Hz)
3'	128.74	114.28	159.69	148.99	129.06	134.76	133.70	115.98 (d, $J = 21.59$ Hz)
4'	129.48	160.73	115.06	150.41	135.59	129.42	134.28	163.21 (d, $J = 250.87$ Hz)
5'	128.74	114.28	129.76	123.64	129.06	127.99	130.79	115.98 (d, $J = 21.59$ Hz)
6'	129.99	132.06	122.28	111.06	131.19	129.62	128.94	131.97 (d, $J = 8.55$ Hz)
OCH ₃	-	55.42	55.36	55.99	-	-	-	67.48

Table 5: ¹³C NMR data of compounds **11-17**

	Homoisoflavonoids						
Pos.	11	12	13	14	15	16	17
2	67.42	67.27	67.53	67.34	67.53	153.14	153.09
3	131.96	131.80	127.53	130.57	127.38	123.06	123.16
4	181.93	181.79	180.95	181.17	180.99	177.18	177.21
4a	121.88	121.81	121.61	121.45	121.62	123.83	123.86
5	127.97	127.98	127.14	127.23	127.12	125.92	125.93
6	122.04	122.12	121.76	121.95	121.82	125.32	125.28
7	136.06	136.13	135.79	136.20	135.86	133.84	133.80
8	117.97	117.98	117.73	117.90	117.73	118.15	118.15
8a	161.16	161.09	160.39	160.61	160.37	156.52	156.55
9	135.88 (d, $J = 2.27$ Hz)	134.94	136.90	136.73	137.27	31.89	31.73
1'	136.40 (d, $J = 7.80$ Hz)	131.40 (dd, $J = 5.98, 3.80$ Hz)	124.78	134.94	125.18	123.06	141.02
2'	116.57 (d, $J = 16.28$ Hz)	118.74 (d, $J = 17.66$ Hz)	132.74	116.68	117.76	129.65	123.52
3'	162.70 (d, $J = 245.90$ Hz)	150.25 (dd, $J = 248.55, 12.80$ Hz)	115.78	157.49	147.87	123.79	148.41
4'	116.35 (d, $J = 15.56$ Hz)	150.78 (dd, $J = 261.53, 12.86$ Hz)	159.30	116.87	145.38	146.76	121.71
5'	130.31 (d, $J = 8.24$ Hz)	117.85 (d, $J = 17.69$ Hz)	115.78	129.84	115.85	123.79	129.42
6'	125.66 (d, $J = 2.92$ Hz)	126.48 (dd, $J = 6.25, 3.47$ Hz)	132.74	121.08	123.47	129.65	135.29

3.2 Biochemistry

The experimental techniques employed to determine the antioxidant and antibacterial activities of the homoisoflavonoids are stated below as well as the experimental data.

3.2.1 Antioxidant activity of the homoisoflavonoids synthesised

The antioxidant activities of the homoisoflavonoids were determined using two common simple methods, *i.e.* the DPPH radical scavenging assay and the ferric reducing antioxidant power assay.

3.2.1.1 DPPH radical scavenging assay

The DPPH scavenging activity of homoisoflavonoids was determined according to the modified method by (Murthy *et al.*, 2012). The free radical scavenging activity was determined spectrophotometrically using a stable free radical, 1,1-diphenyl-2-picrylhydrazyl (DPPH). Stock solutions of each compound were prepared by dissolving 10 mg of the compound in 10 mL of methanol (1000 µg/mL). The stock solutions were used to prepare a series of eight concentrations (500, 200, 100, 50, 40, 30, 20, 10 µg/mL). A solution of DPPH was prepared by dissolving 1.97 mg of DPPH in 50 mL of methanol (0.1 mM) and protected from light by covering the volumetric flask with aluminum foil. An aliquot of each dilution of the compound (150 µl) was mixed with methanolic solution of DPPH (2850 µl) in glass test tubes. The mixtures were shaken vigorously and set in a dark cupboard at ambient temperature for 30 min. The absorbance was measured at 517 nm against methanol as a blank. All measurements were done in triplicate and the average absorbance was used. The percent scavenging activity of the compounds were calculated using the following formula:

$$\text{Scavenging activity (\%)} = 100 \times \frac{Abs_{control} - Abs_{compound}}{Abs_{control}}$$

The calculated scavenging activities are displayed below in Table 6.

Table 6: The DPPH free radical scavenging activity of the homoisoflavonoids (**13, 14, 15**) and ascorbic acid

	Scavenging activity (%)			
	Compound 13	Compound 14	Compound 15	Ascorbic acid
10 µg/mL	10.57	3.38	1.01	5.88
20 µg/mL	10.37	5.90	7.60	7.22
30 µg/mL	9.93	5.32	13.25	7.36
40 µg/mL	9.83	5.22	15.89	8.13
45 µg/mL	11.03	6.14	20.13	10.56
50 µg/mL	9.70	5.85	19.60	12.76
100 µg/mL	8.83	3.28	55.52	51.77
200 µg/mL	11.43	4.68	91.29	96.12
500 µg/mL	10.40	6.42	99.00	96.46

3.2.1.2 Ferric reducing antioxidant power assay

A series of methanolic standard solutions of varying concentrations (500, 200, 150, 100, 50, 40, 30, 20, 10 µg/mL) were prepared from a 1000 µg/mL stock solution. A 2.5 mL volume of the different concentrations were mixed with 2.5 mL phosphate buffer solution (0.1 M, pH = 6.6) and 2.5 mL of aqueous potassium hexacyanoferrate [K₃Fe(CN)₆] solution (1%) in test tubes. After 20 min of incubation at 50 °C in a water bath, a volume of 2.5 mL of 10% trichloroacetic acid (TCA) was added to the mixture and mixed thoroughly. A volume of 2.5

mL from the mixture was added to 2.5 mL of distilled water and 0.5 mL of FeCl₃ (0.1% solution). The resulting mixture was mixed thoroughly and allowed to stand for 10 min after which the absorbance was taken at 700 nm using a UV-Vis spectrophotometer. Ascorbic acid was used as a positive control. All measurements were taken in triplicate and the average absorbance is displayed below (Table 7).

Table 7: The ferric reducing antioxidant power of the homoisoflavonoids (**13-15**) and ascorbic acid

	Absorbance			
	Compound 13	Compound 14	Compound 15	Ascorbic acid
10 µg/mL	0.015	0.044	0.045	0.062
20 µg/mL	0.033	0.023	0.085	0.323
30 µg/mL	0.034	0.024	0.193	0.867
35 µg/mL	0.029	0.024	0.157	0.957
40 µg/mL	0.014	0.024	0.544	1.071
45 µg/mL	0.016	0.020	0.617	1.566
50 µg/mL	0.017	0.019	0.735	1.932
100 µg/mL	0.021	0.025	1.741	2.799
200 µg/mL	0.033	0.042	3.000	3.000
500 µg/mL	0.163	0.146	-	-

3.2.2 Antibacterial activity of the homoisoflavonoids synthesised

The fifteen synthesised homoisoflavonoids were screened for their antibacterial activity using the disc diffusion method. The principles of the technique are explained in Chapter 1 (1.4.2.1).

3.2.2.1 Disc diffusion antimicrobial susceptibility testing

The antibacterial activities of the synthesised homoisoflavonoids were determined using the Kirby-Bauer disk-diffusion method. The homoisoflavonoids synthesised were tested against ten gram positive and six gram negative bacteria (Table 8). Stock solutions (5 mg/mL) of each homoisoflavonoid were prepared by dissolving compounds in 1 mL of DMSO. Blank discs (5 mm; MAST, UK) were impregnated with 50, 100 and 200 µg/mL of each homoisoflavonoid and allowed to dry. Bacterial isolates were grown overnight on TSA agar plates and the turbidity of cell suspensions were adjusted equivalent to that of a 0.5 McFarland standard. These were used to inoculate Mueller-Hinton (MH) agar plates by streaking swabs over the entire agar surface followed by the application of the respective homoisoflavonoid discs. Plates were then incubated for 21 hrs at 30 °C. Testing was done in duplicate and tetracycline (TET) and ampicillin (AMP) discs were used as standard antimicrobial agent controls. The negative control was 5 µl of DMSO (100%). Zone diameters were measured physically and averaged. Activity indices of each compound were calculated by comparing zones of inhibition obtained with each of the compounds with those obtained with the standard antimicrobial agents, tetracycline and ampicillin. The following equation was used:

$$\text{Activity index (AI)} = \frac{\text{Inhibition diameter (mm) with test compound}}{\text{Inhibition diameter (mm) with standard antimicrobial agent}}$$

Table 8: The strains of bacterial cultures tested against in the disc diffusion assay

Gram positive bacteria	Gram negative bacteria
<i>Bacillus subtilis</i> (ATCC 6633)	<i>Escherichia coli</i> (ATCC 29522)
<i>Enterobacter aerogenes</i> (ATCC 13048)	<i>Escherichia coli</i> (ATCC 35219)
<i>Enterococcus faecalis</i> (ATCC 5129)	<i>Klebsiella pneumoniae</i> (ATCC 70063)
<i>Staphylococcus aureus</i> (ATCC 29212)	<i>Pseudomonas aeruginosa</i> (ATCC 27853)
<i>Staphylococcus aureus</i> (ATCC 43300)	<i>Pseudomonas aeruginosa</i> (ATCC 35037)
<i>Staphylococcus saprophyticus</i> (ATCC 35552)	<i>Salmonella arizonae</i> (ATCC 13314)
<i>Staphylococcus scuri</i> (ATCC 29062)	
<i>Staphylococcus xylosus</i> (ATCC 35033)	
<i>Streptococcus agalactiae</i> (ATCC 13813)	
<i>Streptococcus pyogenes</i> (ATCC 19615)	

The zone diameters obtained for the three concentrations of each homoisoflavonoid are displayed below (Table 9 and Table 10). The activity indexes were calculated for each compound at the highest concentration (200 µg/mL) and are displayed in Table 9 and Table 10. Compounds **4**, **7**, **16** and **17** showed no antibacterial activity and are therefore omitted from the tables. The homoisoflavonoids were tested but showed no activity against the following bacterial strains, which are also omitted from the data tables: *Salmonella arizonae* (ATCC 13314), *Escherichia coli* (ATCC 35219), *Pseudomonas aeruginosa* (ATCC 27853 and ATCC 35037), and *Klebsiella pneumoniae* (ATCC 70063).

Table 9: The zone diameters and activity indices of compounds **3-6** and **8-15** against bacterial strains: *Staphylococcus aureus*, *Staphylococcus saprophyticus* and *Staphylococcus scuri*

Bacteria Cultures																				
<i>Staphylococcus aureus</i> (ATCC 29212)						<i>Staphylococcus aureus</i> (ATCC 43300)					<i>Staphylococcus saprophyticus</i> (ATCC 35552)				<i>Staphylococcus scuri</i> (ATCC 29062)					
Concentration/ µg/mL and Activity index at 200 µg/mL																				
	50	100	200	Activity index		50	100	200	Activity index		50	100	200	Activity index		50	100	200	Activity index	
				TET	AMP				TET	AMP				TET	AMP				TET	AMP
3	12	12	21	0.67	0.84	11	15	17	0.52	1.31	-	-	9	0.30	0.24	-	-	8	0.32	0.23
4	-	-	-	-	-	-	-	-	-	-	-	-	-	-	-	-	-	-	-	-
5	9	10	12	0.39	0.48	7	10	11	0.33	0.85	-	-	7	0.23	0.19	-	-	7	0.28	0.20
6	-	8	10	0.32	0.40	-	-	9	0.27	0.69	-	-	-	-	-	-	-	-	-	-
8	-	-	8	0.26	-	-	9	10	0.30	0.77	-	-	-	-	-	-	-	7	0.28	0.20
9	9	10	12	0.39	0.32	-	-	-	-	-	-	-	-	-	-	-	-	-	-	-
10	-	-	-	-	-	-	-	-	-	-	-	7	10	0.33	0.27	-	-	-	-	-
11	9	12	15	0.48	0.60	10	14	16	0.48	1.23	-	-	9	0.30	0.24	-	-	8	0.32	0.23
12	-	7	7.5	0.23	0.30	-	7	11	0.33	0.85	-	-	7	0.23	0.19	-	-	-	-	-
13	9	10	12	0.39	0.48	-	8	10	0.30	0.77	-	-	9	0.30	0.24	-	-	-	-	-
14	17	19	22	0.71	0.88	14	16	19	0.58	1.46	10	12	14	0.47	0.38	10	12	13	0.52	0.37
15	10	12	13	0.42	0.52	7	8	11	0.33	0.85	7	8	10	0.33	0.27	-	-	8	0.32	0.23
Tetracycline (TET)				31		33					30				25					
Ampicillin (AMP)				25		13					37				35					
DMSO				-		-					-				-					

Table 10: The zone diameters and activity indices of compounds **3-6** and **8-15** against bacterial strains: *Staphylococcus xylosus*, *Streptococcus agalactiae*, *Streptococcus pyogenes* and *Escherichia coli*

Bacteria Cultures																				
<i>Staphylococcus xylosus</i> (ATCC 35033)						<i>Streptococcus agalactiae</i> (ATCC 13813)					<i>Streptococcus pyogenes</i> (ATCC 19615)				<i>Escherichia coli</i> (ATCC 29522)					
Concentration/ µg/mL and Activity index at 200/ µg/mL																				
	50	100	200	Activity index		50	100	200	Activity index		50	100	200	Activity index		50	100	200	Activity index	
				TET	AMP				TET	AMP				TET	AMP				TET	AMP
3	-	8	10	0.36	0.31	-	-	-	-	-	-	-	-	-	-	-	-	-	-	-
4	-	-	-	-	-	-	-	-	-	-	-	-	-	-	-	-	-	-	-	-
5	-	7	9	0.32	0.28	-	-	-	-	-	-	9	0.27	0.24	-	-	-	-	-	-
6	-	-	8	0.29	0.25	-	-	-	-	-	-	-	-	-	-	-	-	-	-	-
8	-	-	7	0.25	0.22	-	-	-	-	-	-	7	0.21	0.19	-	-	-	-	-	-
9	-	-	8	0.29	0.25	-	-	-	-	-	-	9	0.27	0.24	-	-	-	-	-	-
10	-	-	-	-	-	-	-	-	-	-	-	-	-	-	-	-	-	-	-	-
11	8	9	10	0.36	0.31	-	-	-	-	-	-	9	10	0.30	0.27	-	-	-	-	-
12	-	-	-	-	-	-	-	-	-	-	-	-	-	-	-	-	-	-	-	-
13	-	-	8	0.29	0.25	-	-	-	-	-	9	10	14	0.42	0.38	-	-	-	-	-
14	13	15	16	0.57	0.50	-	-	7	0.29	-	11	15	16	0.48	0.43	-	-	7	0.29	0.33
15	-	-	8	0.29	0.25	-	-	-	-	-	-	7	10	0.30	0.27	-	-	-	-	-
Tetracycline (TET)				28		24					33				24					
Ampicillin (AMP)				32		-					37				21					
DMSO				-		-					-				-					

CHAPTER 4 CONCLUSION

A series of fifteen homoisoflavonoids, three of the 3-benzylidene and two of the 3-benzyl type, were synthesised in a three step reaction. The solvent free base-catalysed aldol condensation of 4-chromanone and substituted benzaldehydes in the presence of piperidine resulted in the formation of the homoisoflavonoids in good yields of between 50 and 90%. Substitution of the phenyl ring was varied at the 3'-position, 4'-position and 3',4'-positions with methoxy, hydroxy, chloro, fluoro and nitro groups. Compounds containing the electron withdrawing nitro groups resulted in the formation of the 3-benzyl-4-chromanone rather than the desired 3-benzylidene-4-chromanone. The synthesised compounds were fully characterised by ^1H , ^{13}C and ^{19}F NMR, IR and UV spectroscopy and EI-MS. Crystal structures of seven homoisoflavonoids were also obtained and reported for the first time in this work.

The antioxidant testing of the homoisoflavonoids, using the DPPH radical scavenging assay and the ferric reducing antioxidant power assay, showed that the polyhydroxylated compounds have good antioxidant activity due to the fact that the hydrogen on an O-H group is scavengable. Compound **15**, a disubstituted hydroxyl compound, showed good antioxidant activity comparable to that of ascorbic acid. This was attributed to the fact compound **15** has a catechol moiety. Mono-substituted hydroxy containing homoisoflavonoids (**13** and **14**) showed weak antioxidant activity compared to compound **15**. Further derivatisation of compound **15**, by substituting a catechol moiety on the A-ring of the homoisoflavonoid, may result in increased antioxidant activity. Compound **15** is therefore an interesting target molecule to derivatise in the pursuit of good antioxidants.

The synthesised homoisoflavonoids were also subjected to antibacterial testing which showed that homoisoflavonoids are more active against gram positive than gram negative bacteria. The synthesised homoisoflavonoids showed good antibacterial activity against a methicillin resistant strain of bacteria, *Staphylococcus aureus* (ATCC 43300). Compounds **3**, **11** and **14** showed better antibacterial activity than the common antibiotic ampicillin. Compound **14**, the *meta* hydroxy homoisoflavonoid, showed the highest activity index of 1.46. Derivatisation of compound **14** with respect to the A-ring can be conducted and a structure-activity relationship determined.

REFERENCES

- Abegaz, B. M., Mutanyatta-Comar, J., Nindi, M., 2007. Naturally occurring homoisoflavonoids: Phytochemistry, biological activities and synthesis. *Natural Product Communications* 2, 475-498.
- Adinolfi, M., Lanzetta, R., Laonigro, G., Parrilli, M., Breitmaier, E., 1986. ^1H and ^{13}C chemical shift assignments of homoisoflavanones. *Magnetic Resonance in Chemistry* 24, 663-666.
- Basavaiah, D., Bakthadoss, M., 1998. A new protocol for the syntheses of (E)-3-benzylidenechroman-4-ones: a simple synthesis of the methyl ether of bonducellin. *Chemical Communications* 16, 1639-1640 .
- Bhandari, P., Crombie, L., Daniels, P., Holden, I., Van Bruggen, N., Whiting, D. A., 1992. Biosynthesis of the A/B/C/D-ring system of the rotenoid amorphigenin by *Amorpha fruticosa* seedlings. *Journal of the Chemical Society, Perkin Transactions* 1, 839-849.
- Böhler, P., Tamm, C., 1967. The homo-isoflavones, a new class of natural product. Isolation and structure of eucomin and eucomol. *Tetrahedron Letters* 8, 3479-3483.
- Cheng, X.-M., Huang, Z.-T., Zheng, Q.-Y., 2011. Topochemical photodimerization of (E)-3-benzylidene-4-chromanone derivatives from β -type structures directed by halogen groups. *Tetrahedron* 67.
- Clayden, J., Greeves, N., Warren, S., Wothers, P., 2001. *Organic Chemistry*. Oxford Univeristy Press, United States.
- Conti, C., Desideri, N., 2009. Synthesis and antirhinovirus activity of new 3-benzyl chromene and chroman derivatives. *Bioorganic & Medicinal Chemistry* 17, 3720-3727.

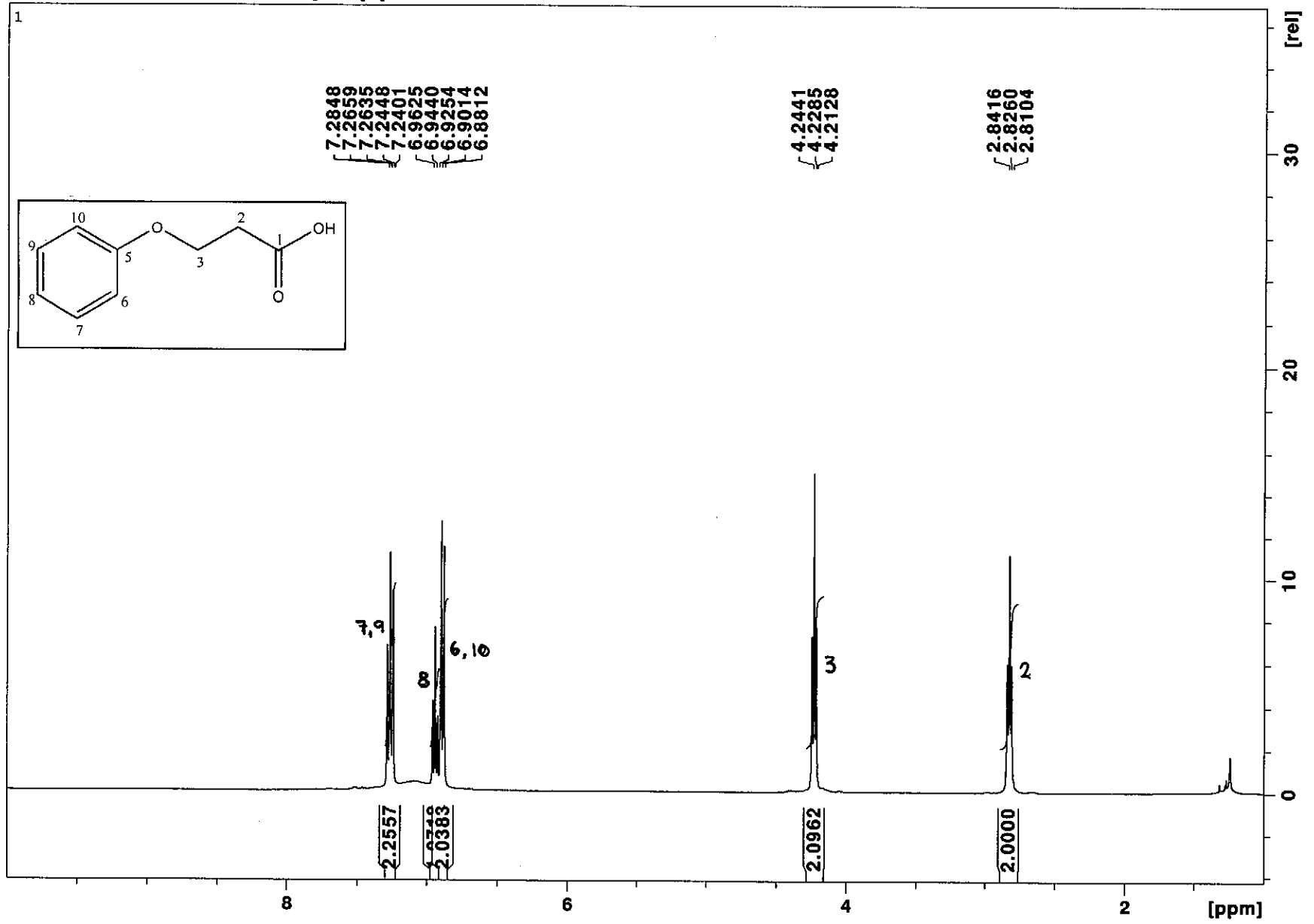
- Das, B., Thirupathi, P., Ravikanth, B., Kumar, R. A., Sarma, A. V. S., Basha, S. J., 2009. Isolation, Synthesis, and Bioactivity of Homoisoflavonoids from *Caesalpinia pulcherrima*. *Chemical Pharmaceutical Bulletin*. 57, 1139-1141.
- Desideri, N., Bolasco, A., Fioravanti, R., Proietti Monaco, L., Orallo, F., Yáñez, M., Ortuso, F., Alcaro, S., 2011. Homoisoflavonoids: Natural scaffolds with potent and selective monoamine oxidase-B inhibition properties. *Journal of Medicinal Chemistry* 54, 2155-2164.
- Dewick, P. M., 1975. Biosynthesis of the 3-Benzylchroman-4-one Eucomin in *Eucomis bicolor*. *Phytochemistry* 14, 983-988.
- du Toit, K., Drewes, S. E., Bodenstein, J., 2010. The chemical structures, plant origins, ethnobotany and biological activities of homoisoflavanones. *Natural Product Research* 24, 457-490.
- du Toit, K., Elgorashi, E. E., Malan, S. F., Mulholland, D. A., Drewes, S. E., Van Staden, J., 2007. Antibacterial activity and QSAR of homoisoflavanones isolated from six Hyacinthaceae species. *South African Journal of Botany* 73, 236-241.
- Erel, O., 2004. A novel automated direct measurement method for total antioxidant capacity using a new generation, more stable ABTS radical cation. *Clinical Biochemistry* 37, 277-285.
- Evans, D., Lockhart, I. M., 1966. Reaction of aromatic aldehydes and nitroso-compounds with 4-chromanones. *Journal of the Chemical Society C: Organic*, 711-712.
- Farkas, L., Gottsegen, A., Nógrádi, M., 1968. The synthesis of eucomin and (±)-eucomol. *Tetrahedron Letters* 38, 4099-4100.
- Farkas, L., Gottsegen, Á., Nógrádi, M., Strelisky, J., 1971. Synthesis of homoisoflavanones—II : Constituents of *Eucomis autumnalis* and *E. Punctata*. *Tetrahedron* 27, 5049-5054.

- Foroumadi, A., Samzadeh-Kermani, A., Emami, S., Dehghan, G., Sorkhi, M., Arabsorkhi, F., Heidari, M. R., Abdollahi, M., Shafiee, A., 2007. Synthesis and antioxidant properties of substituted 3-benzylidene-7-alkoxychroman-4-ones. *Bioorganic & Medicinal Chemistry Letters* 17, 6764-6769.
- Hahlbrock, K., Grisebach, H., 1975. *Biosynthesis of Flavonoids :The Flavonoids*. Chapman and Hall London.
- Heller, W., Tamm, C., 1981. Homoisoflavanones and biogenetically related compounds. *Fortschritte der Chemie organischer Naturstoffe*, 40, 105-152.
- Hung, T. M., Thu, C. V., Dat, N. T., Ryoo, S.-W., Lee, J. H., Kim, J. C., Na, M., Jung, H.-J., Bae, K., Min, B. S., 2010. *Bioorganic & Medicinal Chemistry Letters* 20, 2412-2416.
- Jacquot, Y., Byrne, C., Xicluna, A., Leclercq, G., 2012. Synthesis, structure, and estrogenic activity of 2- and 3-substituted 2,3-dihydro-4H-1-benzopyran-4-ones. *Medical Chemistry Research* 22, 681-691.
- Kirkiacharian, B. S., Gomis, M., Tongo, H. G., Mahuteau, J., Brion, J. D., 1984. *Organic Magnetic Resonance*. 22, 106.
- Koorbanally, C., Crouch, N. R., Mulholland, D. A., 2006. The phytochemistry and ethnobotany of the southern African genus *Eucomis* (Hyacinthaceae: Hyacinthoideae). *Phytochemistry: Advances in Research* 2, 69-85.
- Lévai, A., 2004. Synthesis of exocyclic α,β -unsaturated ketones. *ARKIVOC* vii, 15-33.
- Lévai, A., Schág, B., 1979. Synthesis of 3-Benzylidenechroman-4-one and -1-thiochroman-4-ones. *Pharmazie* 34, 749.
- Lin, L.-G., Xie, H., Li, H.-L., Tong, L.-J., Tang, C.-P., Ke, C.-Q., Liu, Q.-F., Lin, L.-P., Geng, M.-Y., Jiang, H., Zhao, W.-M., Ding, J., Ye, Y., 2008. Naturally Occurring Homoisoflavanoids Function as Potent Protein Tyrosine Kinase Inhibitors by c-Src-Based High-Throughput Screening. *Journal of Medicinal Chemistry* 51, 4419-4429.

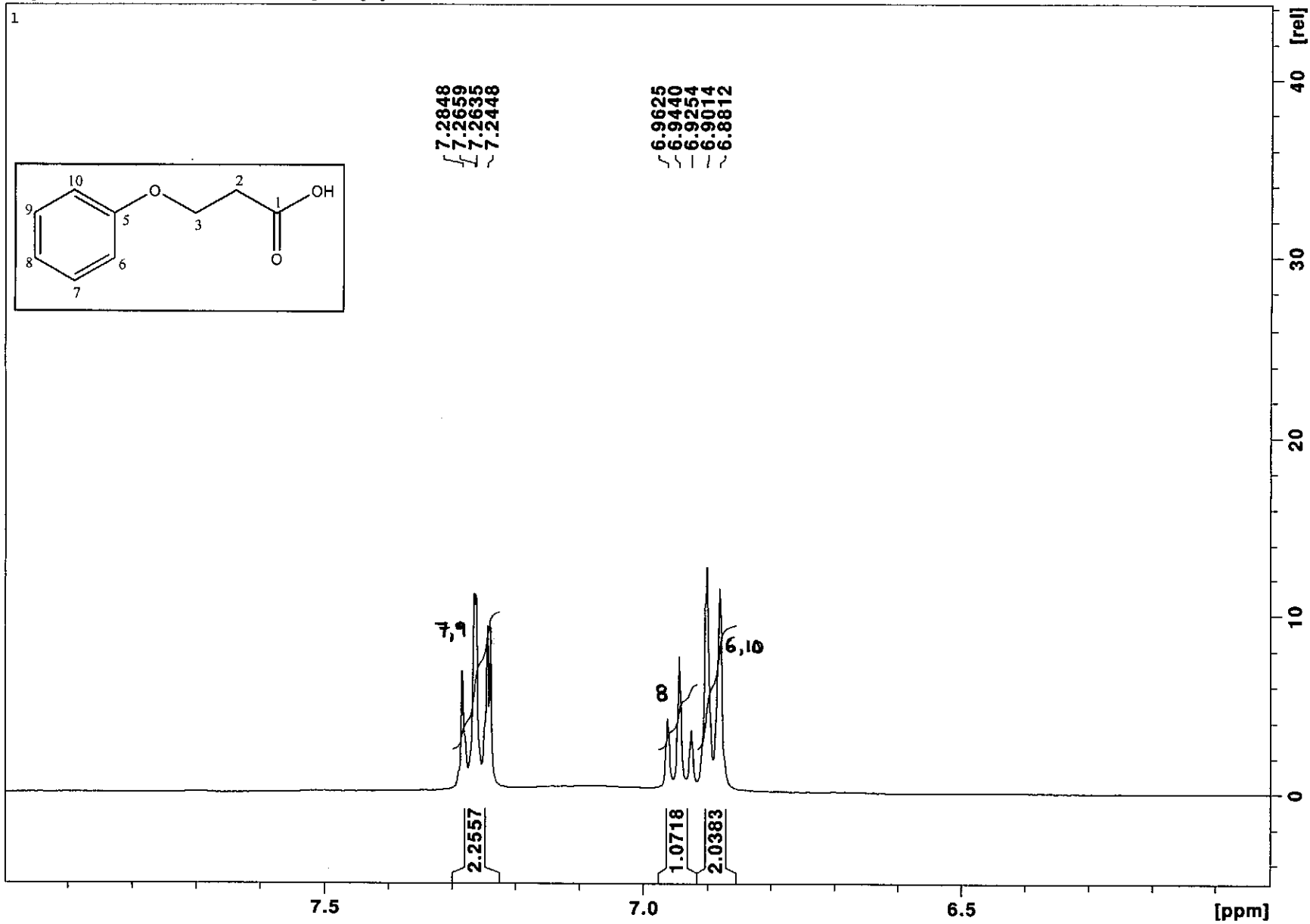
- Lin, Y., Zhu, D., Qi, J., Qin, M., Yu, B., 2010. Characterization of homoisoflavonoids in different cultivation regions of *Ophiopogon japonicus* and related antioxidant activity. *Journal of Pharmaceutical and Biomedical Analysis* 52, 757-762.
- Mann, J., Davidson, R. S., Hobbs, J. B., Banthorpe, D. V., Harborne, J. B., 1994. *Natural Products: Their Chemistry and Biological Significance*. Longman Scientific & Technical.
- Miadoková, E., Mašterová, I., Vlčková, V., Dúhová, V., Tóth, J., 2002. Antimutagenic potential of homoisoflavonoids from *Muscari racemosum*. *Journal of Ethnopharmacology* 81, 381-386.
- Murthy, P. S., Manjunatha, M. R., Sulochannama, G., Naidu, M. M., 2012. Extraction, Characterization and Bioactivity of Coffee Anthocyanins. *European Journal of Biological Sciences* 4, 13-19.
- Osman, A. M., Wong, K. K. Y., Fernyhough, A., 2006. ABTS radical-driven oxidation of polyphenols: Isolation and structural elucidation of covalent adducts. *Biochemical and Biophysical Research Communications* 346, 321-329.
- Perjési, P., Das, U., De Clercq, E., Balzarini, J., Kawase, M., Sakagami, H., Stables, J. P., Lorand, T., Rozmer, Z., Dimmock, J. R., 2008. Design, synthesis and antiproliferative activity of some 3-benzylidene-2,3-dihydro-1-benzopyran-4-ones which display selective toxicity for malignant cells. *European Journal of Medicinal Chemistry* 43, 839-845.
- Rao, V. M., Damu, G. L. V., Sudhakar, D., Siddaiah, V., Rao, C. V., 2008. New efficient synthesis and bioactivity of homoisoflavonoids. *ARKIVOC* xi 285-294.
- Shaikh, M., Petzold, K., Kruger, H., Toit, K. d., 2011a. Synthesis and NMR elucidation of homoisoflavanone analogues. *Structural Chemistry* 22, 161-166.

- Shaikh, M. M., Kruger, H. G., Bodenstein, J., Smith, P., du Toit, K., 2011b. Anti-inflammatory activities of selected synthetic homoisoflavanones. *Natural Product Research* 26, 1473-1482.
- Shankar, T., Gandhidasan, R., Venkataraman, S., 2012. Synthesis and characterization and antiinflammatory and antibacterial evaluation of 3-Arylidene-7-methoxychroman-4-ones. *Indian Journal of Chemistry-Section B*, 1202-1207
- Shyam, K. R., K, M., Kumar, G. M., 2012. Preparation, Characterization and Antioxidant Activities of Gallic Acid-Phospholipids Complex. *International Journal of Research in Pharmacy and Science* 2, 138-148.
- Siddaiah, V., Maheswara, M., Venkata Rao, C., Venkateswarlu, S., Subbaraju, G. V., 2007. Synthesis, structural revision, and antioxidant activities of antimutagenic homoisoflavonoids from *Hoffmanosseggia intricata*. *Bioorganic & Medicinal Chemistry Letters* 17, 1288-1290.
- Siddaiah, V., Rao, C. V., Venkateswarlu, S., Krishnaraju, A. V., Subbaraju, G. V., 2006. Synthesis, stereochemical assignments, and biological activities of homoisoflavonoids. *Bioorganic & Medicinal Chemistry* 14, 2545-2551.
- Tait, S., Salvati, A. L., Desideri, N., Fiore, L., 2006. Antiviral activity of substituted homoisoflavonoids on enteroviruses. *Antiviral Research* 72, 252-255.
- Thaipong, K., Boonprakob, U., Crosby, K., Cisneros-Zevallos, L., Hawkins Byrne, D., 2006. Comparison of ABTS, DPPH, FRAP, and ORAC assays for estimating antioxidant activity from guava fruit extracts. *Journal of Food Composition and Analysis* 19, 669-675.
- Valgas, C., Souza, S. M. d., Smânia, E. F. A., Jr, A. S., 2007. Screening methods to determine antibacterial activity of natural products, *Brazilian Journal of Microbiology* 38, 369-380.

- Valkonen, A., Laihia, K., Kolehmainen, E., Kauppinen, R., Perjési, P., 2012. Structural studies of seven homoisoflavonoids, six thiohomoisoflavonoids, and four structurally related compounds. *Structural Chemistry* 23, 209-217.
- Yan, J., Sun, L.-R., Zhou, Z.-Y., Chen, Y.-C., Zhang, W.-M., Dai, H.-F., Tan, J.-W., 2012. Homoisoflavonoids from the medicinal plant *Portulaca oleracea*. *Phytochemistry* 80, 37-41.
- Zhang, L., Zhang, W.-G., Kang, J., Bao, K., Dai, Y., Yao, X.-S., 2008. Synthesis of (\pm) homoisoflavanone and corresponding homoisoflavane. *Journal of Asian Natural Products Research* 10, 909-913.

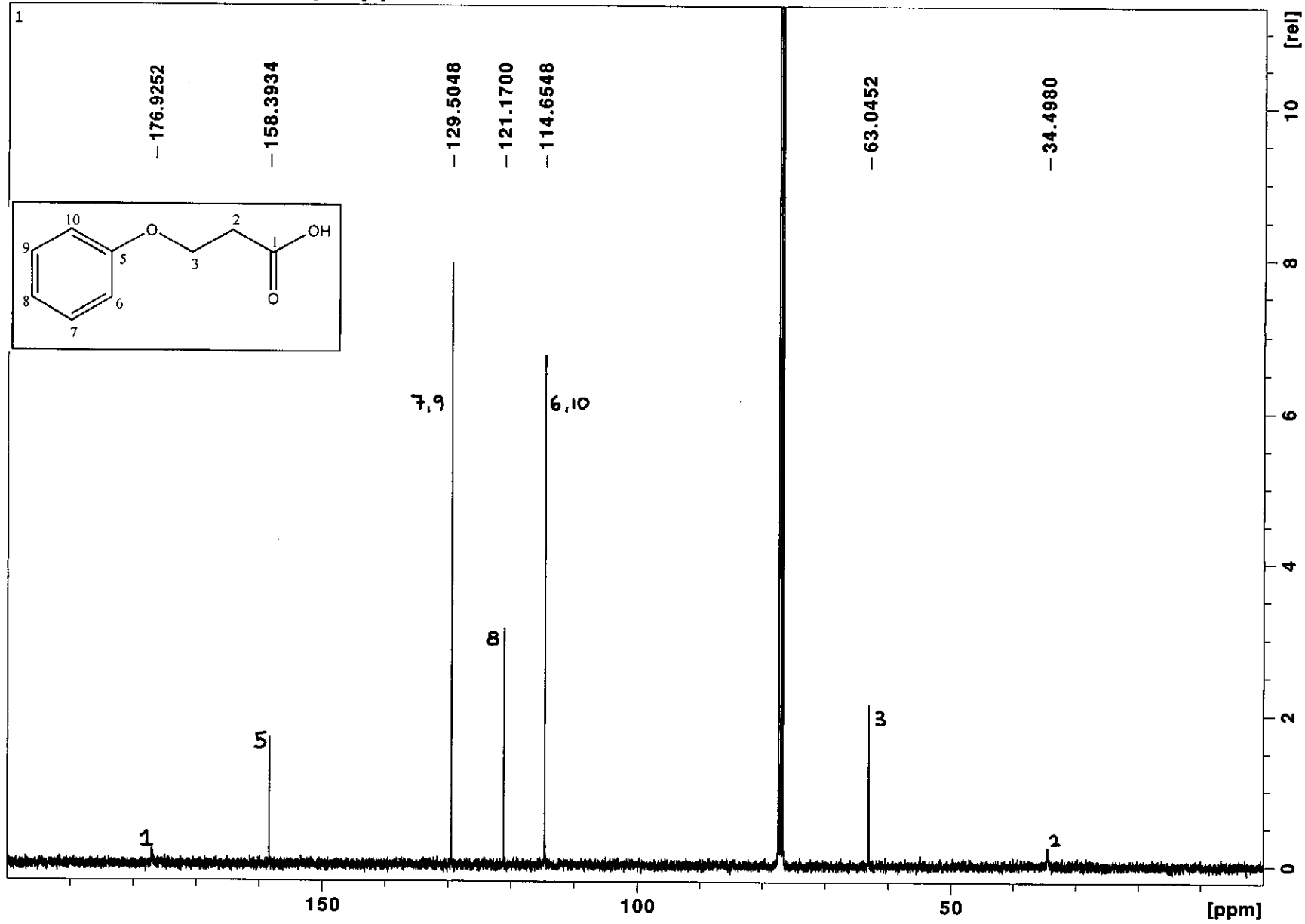


¹H NMR spectrum of compound 1



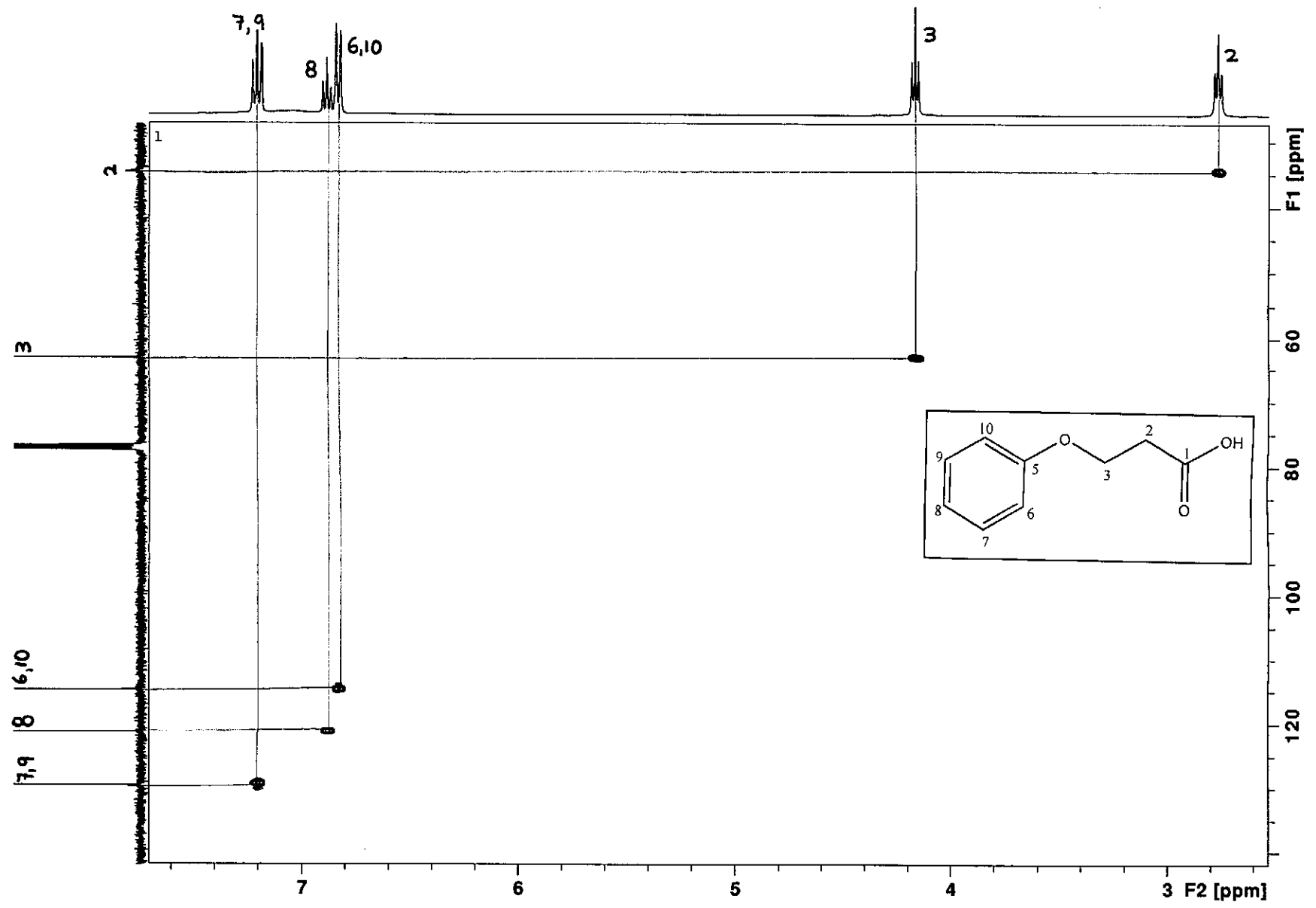
¹H NMR spectrum of compound 1 (expanded)

Aug02-2011-NK-kaalin 11 1 /opt/topspin NK



¹³C NMR spectrum of compound 1

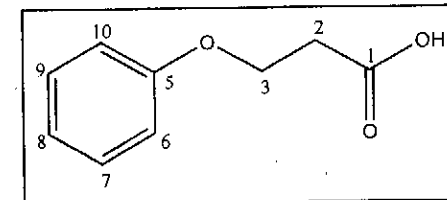
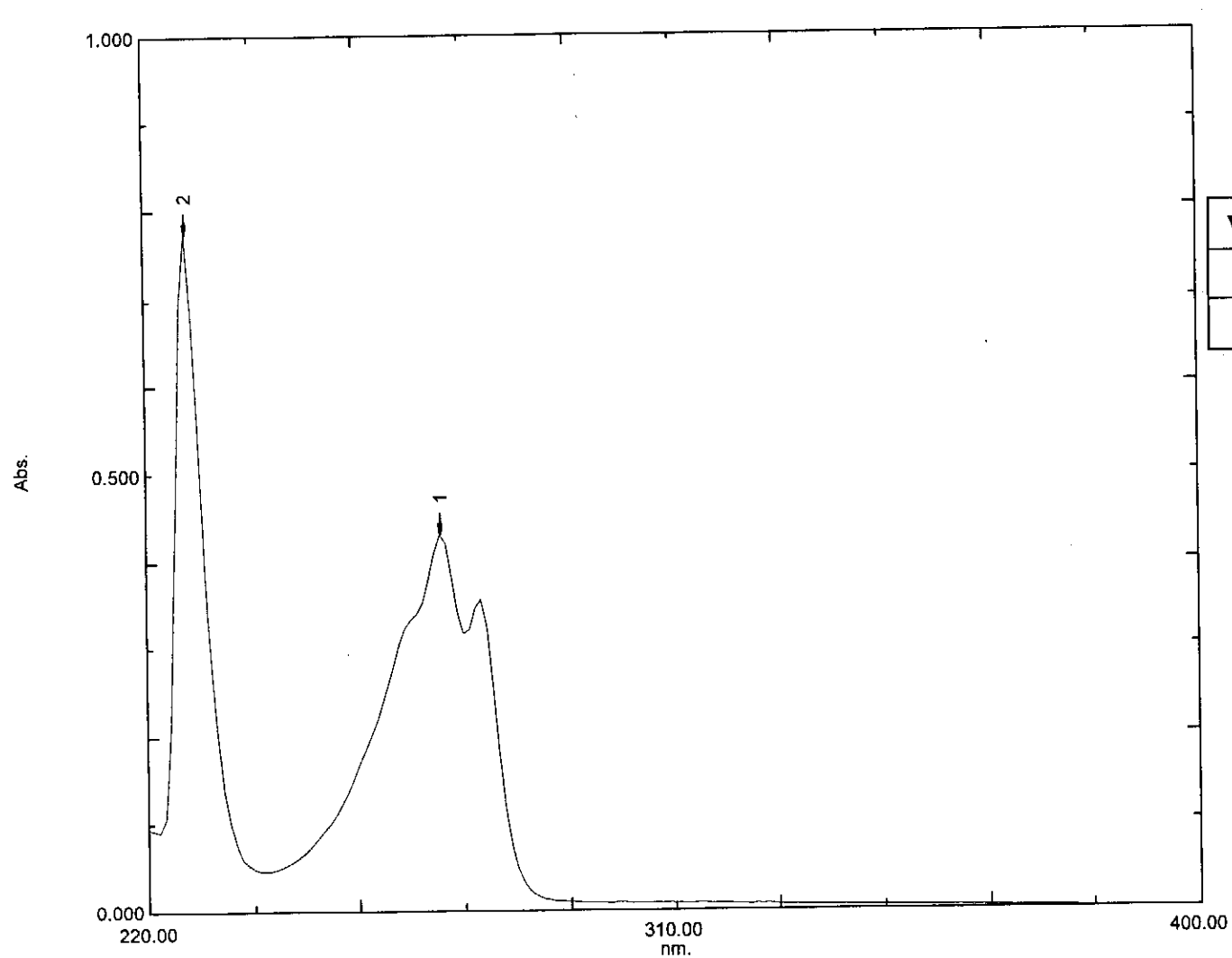
Aug02-2011-NK-kaalin 13 1 /opt/topspin NK



HSQC spectrum of compound 1

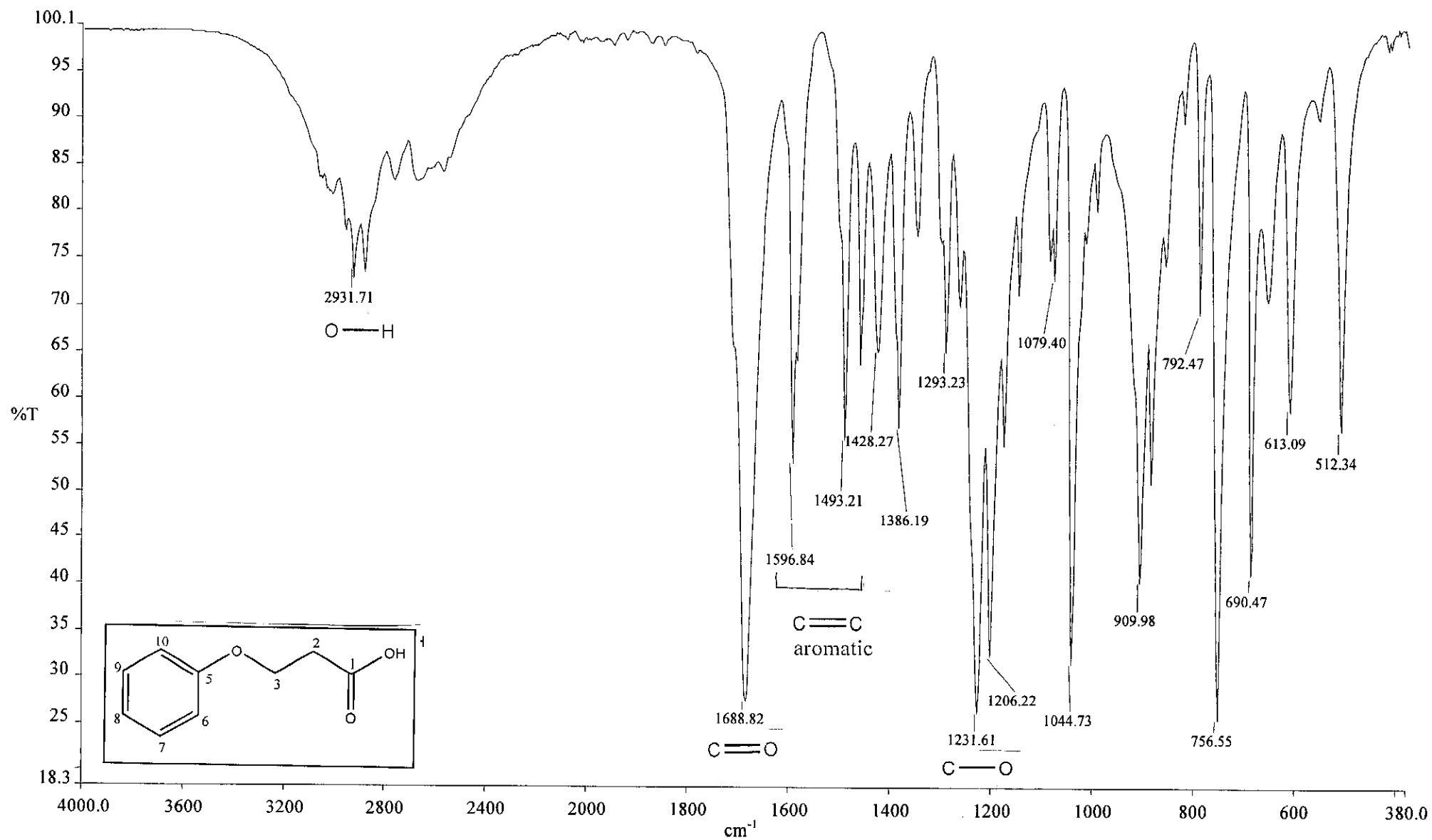
Overlay Spectrum Graph Report

15/05/2012 12:07:07 PM



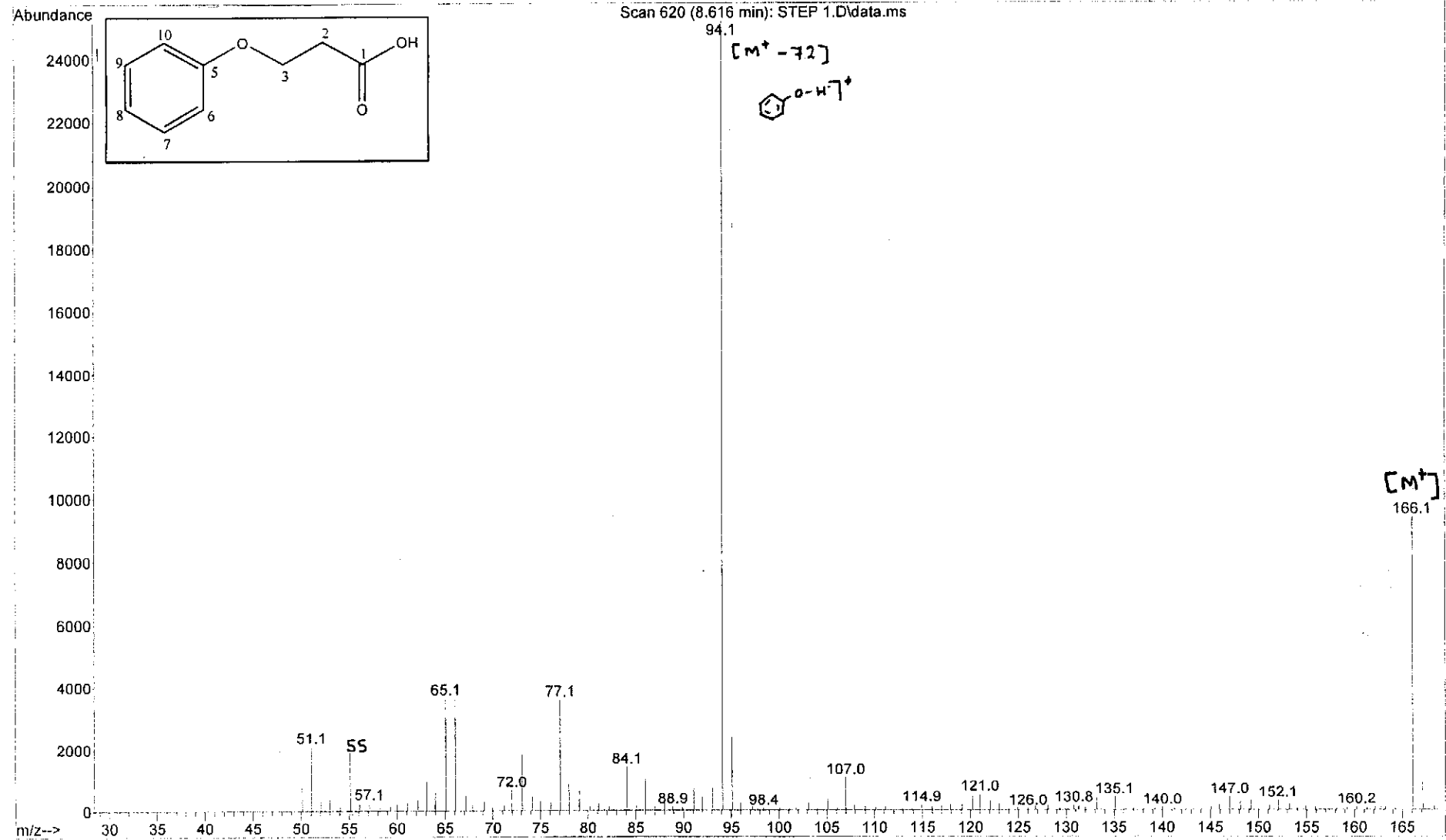
Wavelength/ nm	Absorbance	Log ϵ
270	0.431	2.68
277	0.355	2.60

UV-Vis spectrum of compound 1

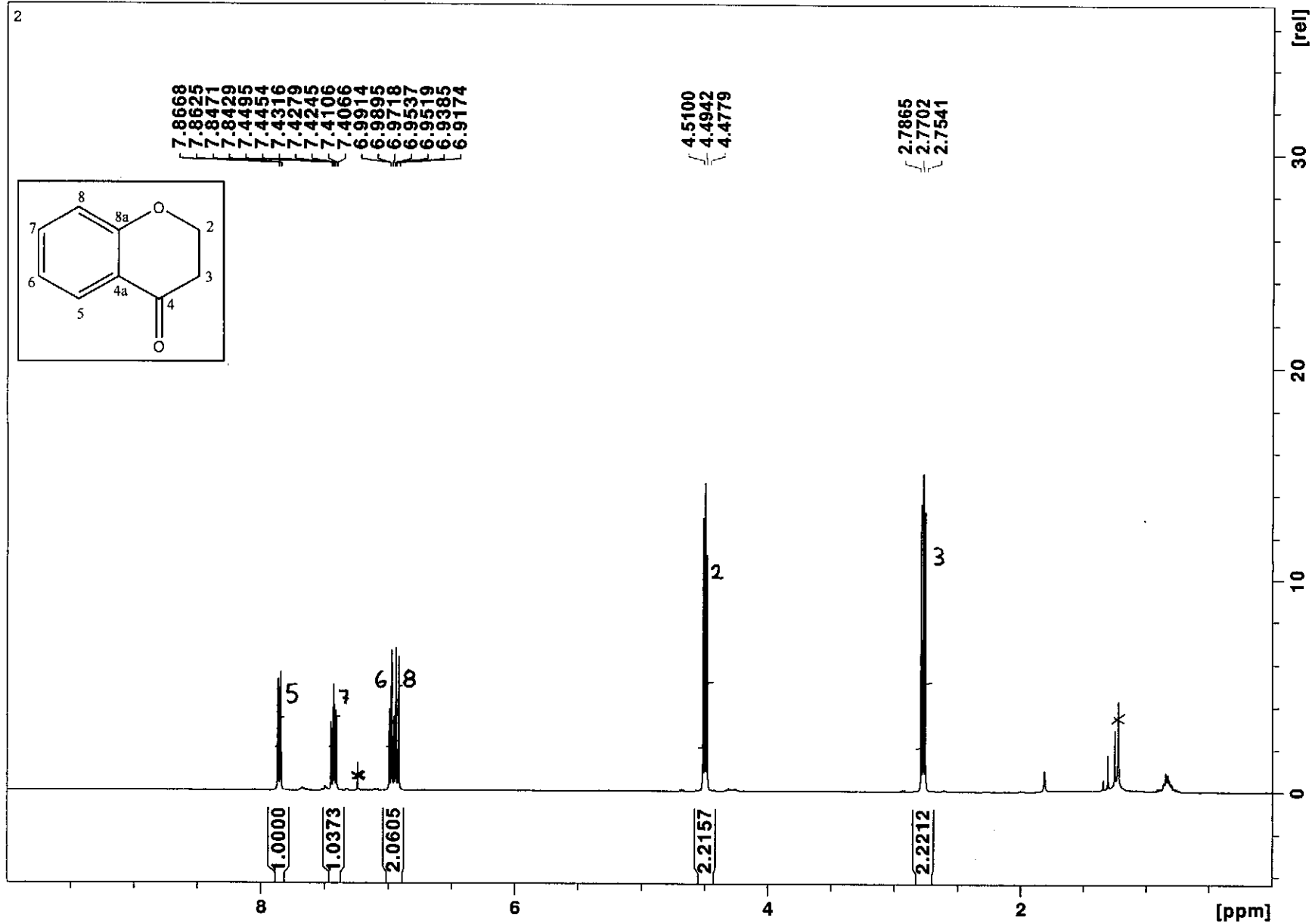


Infrared spectrum of compound 1

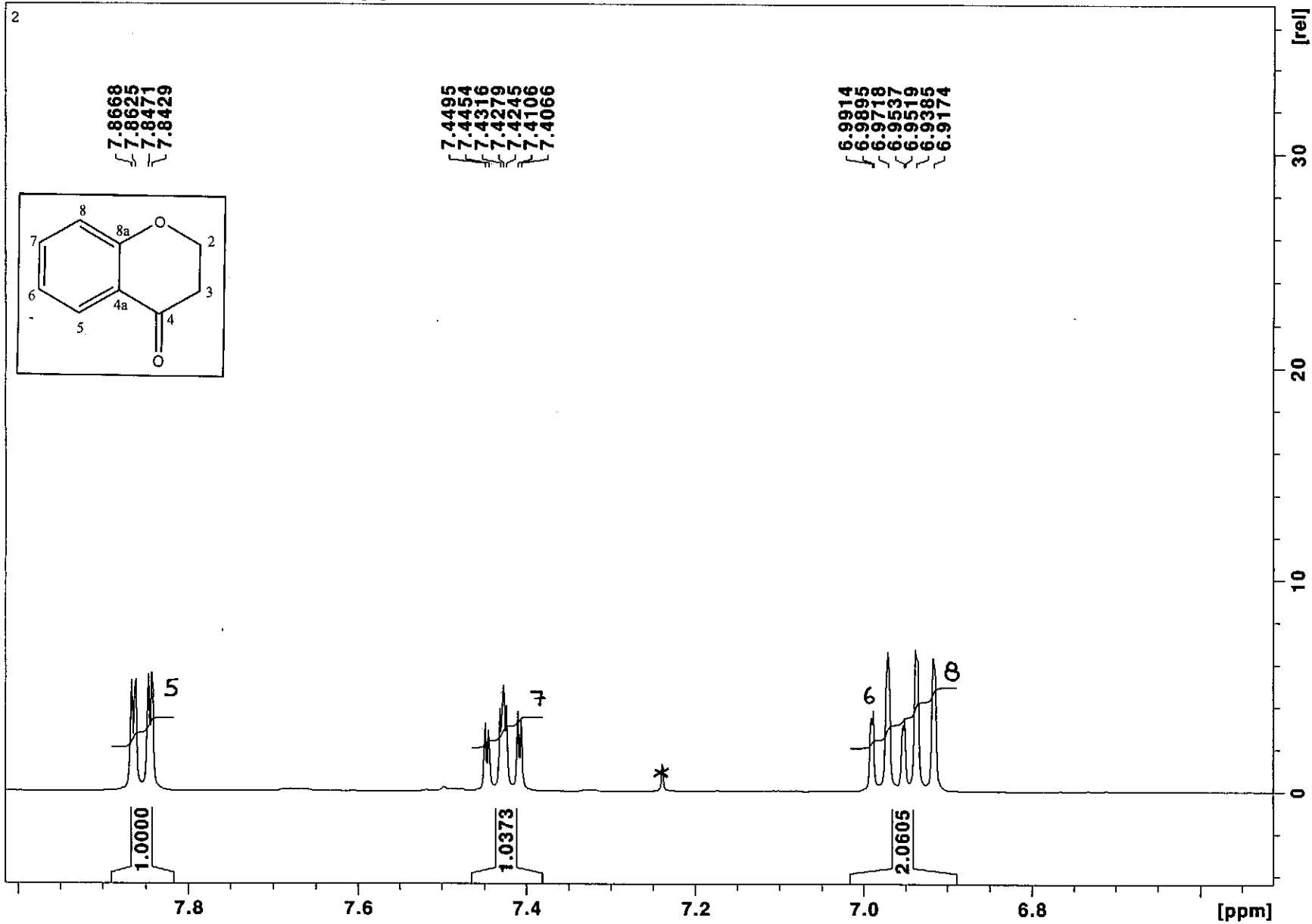
File :C:\msdchem\1\data\kaalin\STEP 1.D
Operator :
Acquired : 13 Jan 2012 16:15 using AcqMethod NATPRODUCTS MANUAL INJ.M
Instrument : 5973N
Sample Name:
Misc Info :
Vial Number: 1



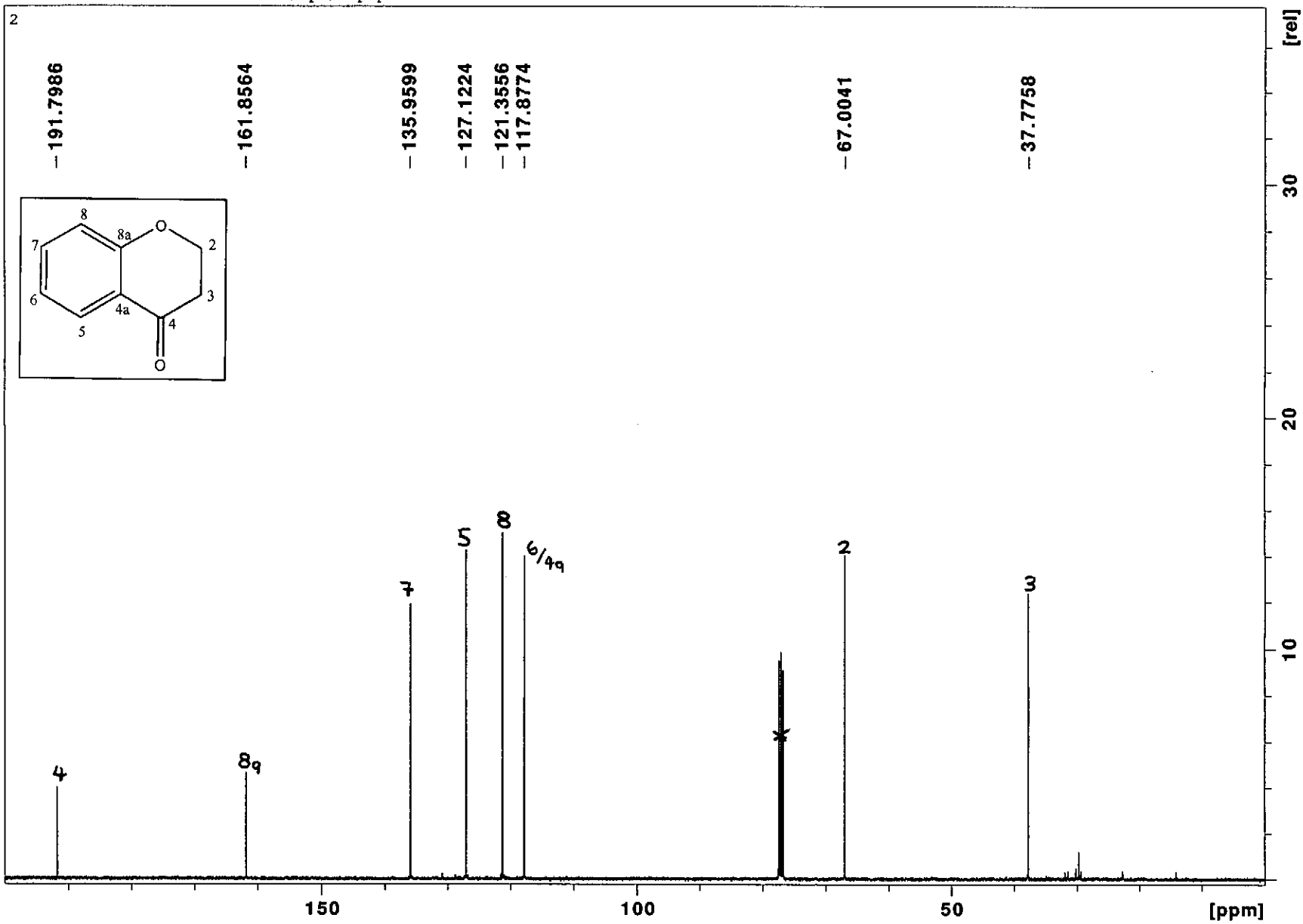
Mass spectrum of compound 1



¹H NMR spectrum of compound 2



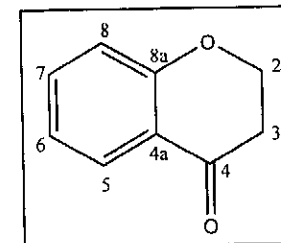
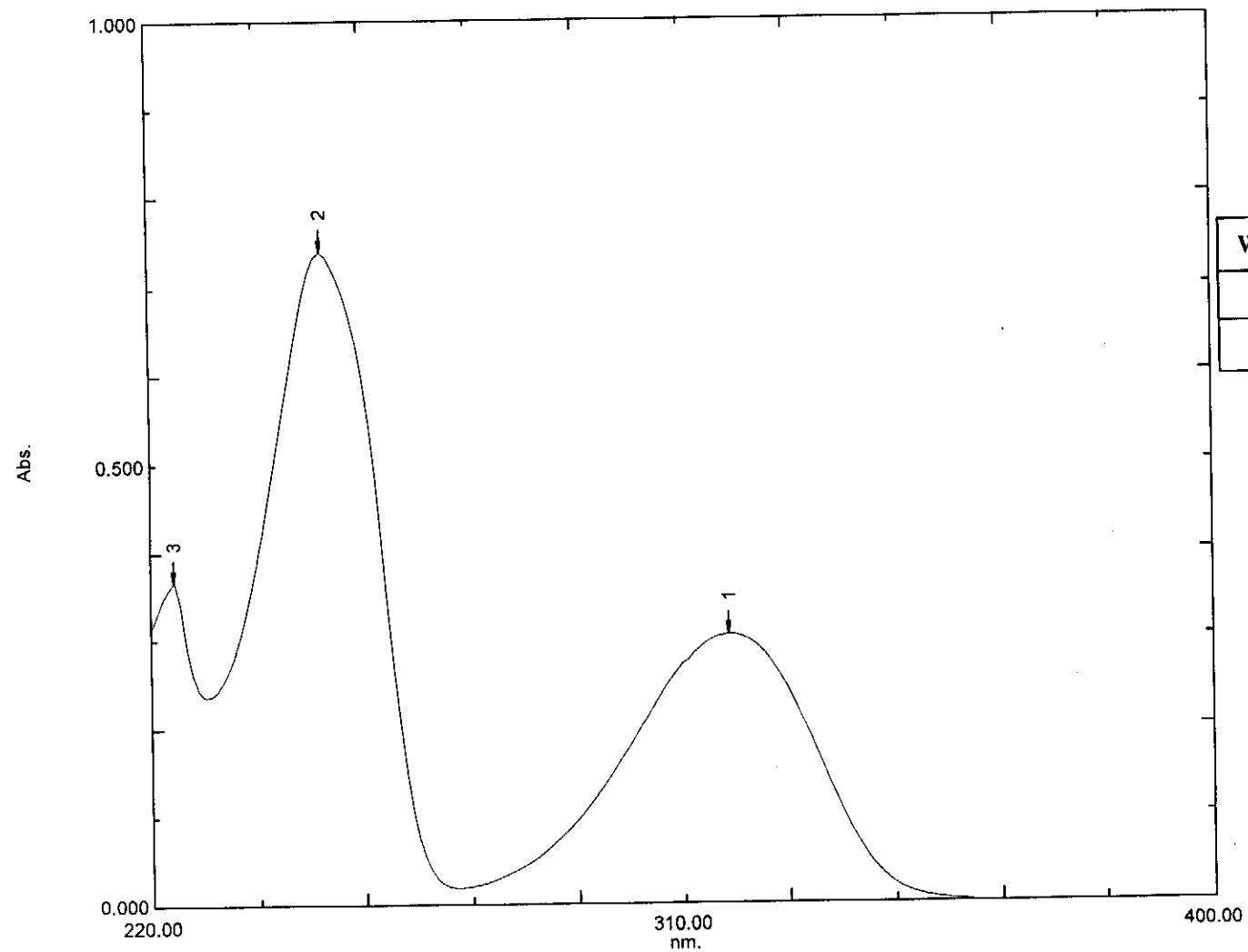
¹H NMR spectrum of compound 2 (expanded)



¹³C NMR spectrum of compound 2

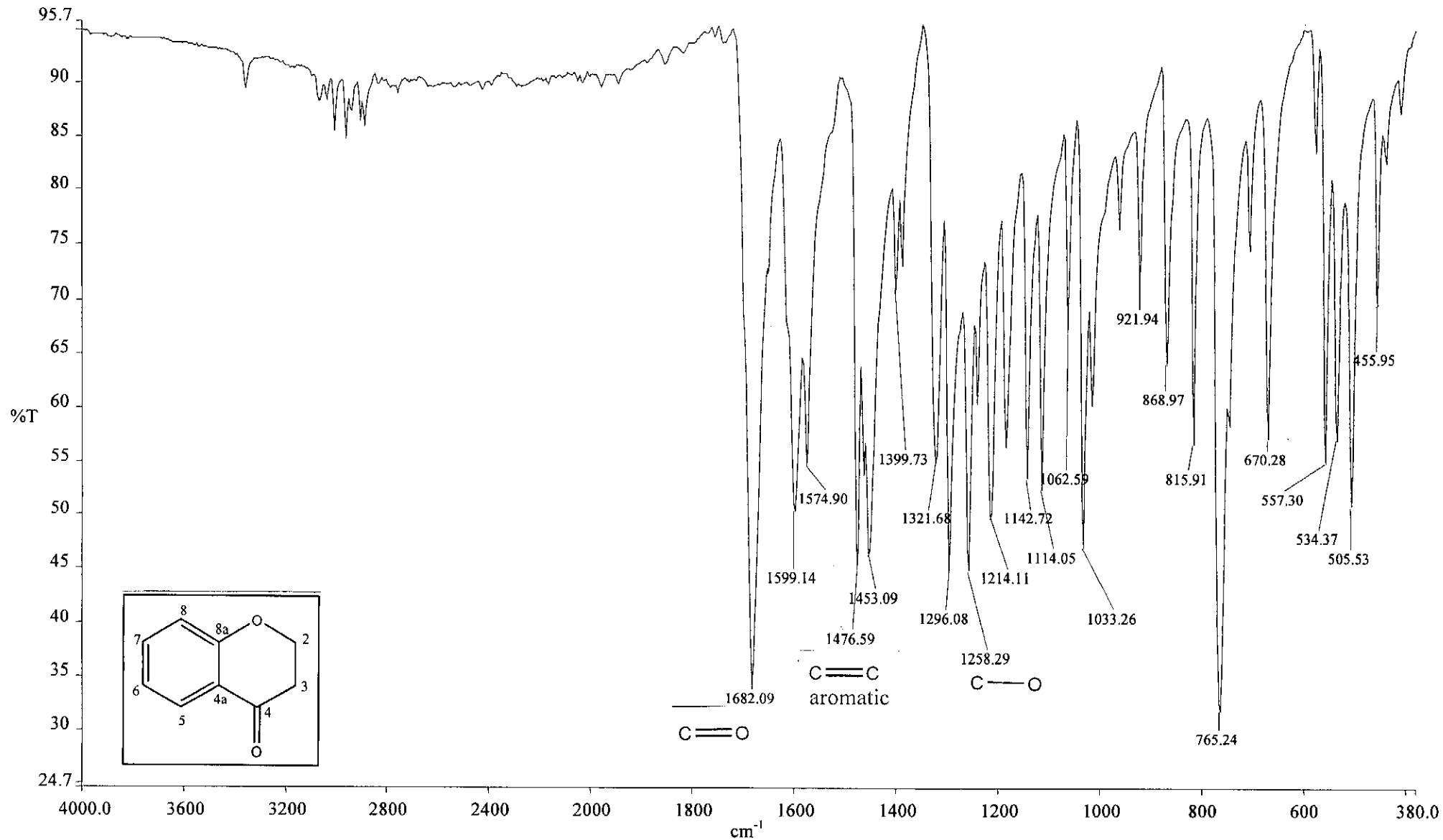
Overlay Spectrum Graph Report

15/05/2012 12:08:49 PM



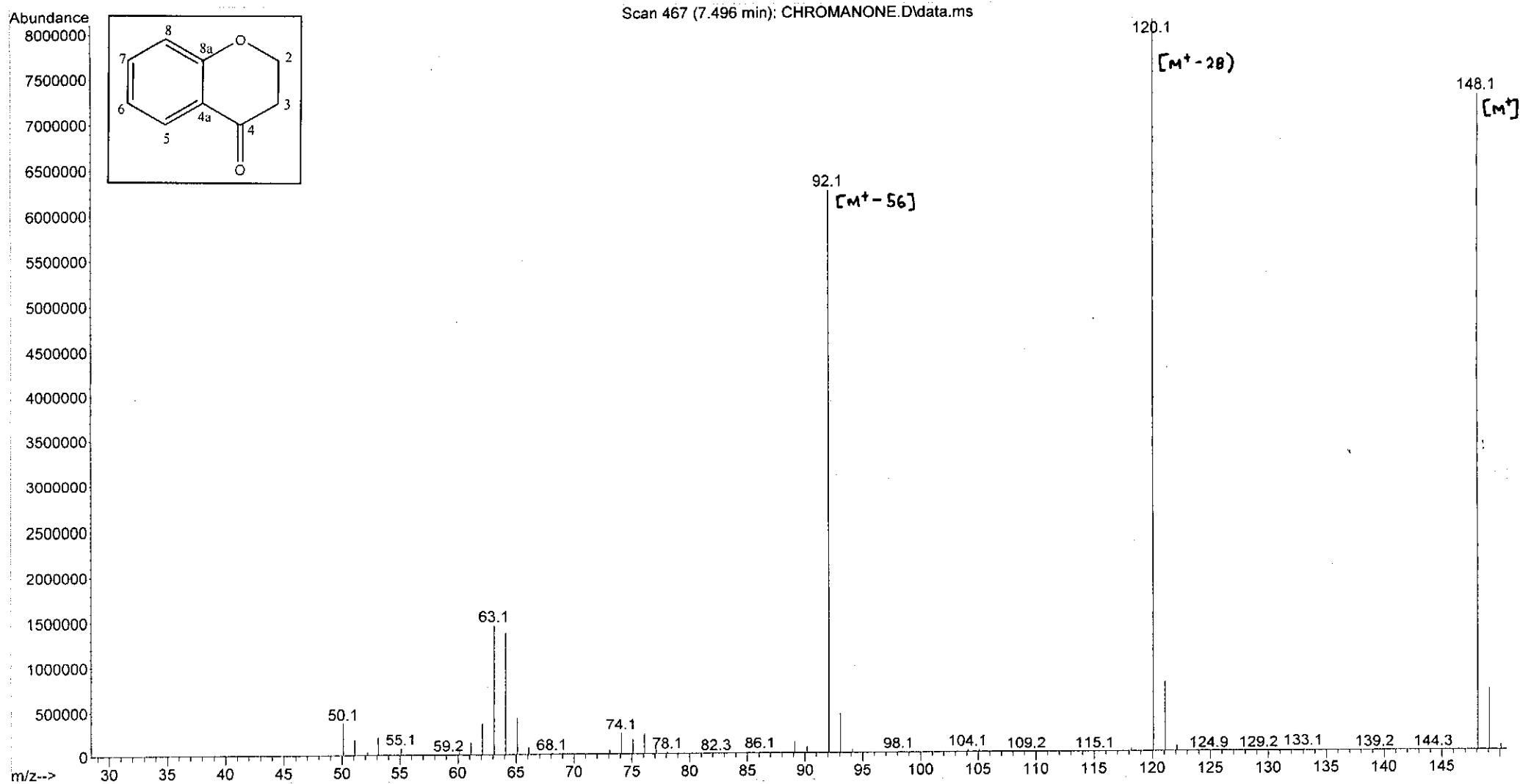
Wavelength/ nm	Absorbance	Log ϵ
249	0.740	3.91
318	0.304	3.53

UV-Vis spectrum of compound 2



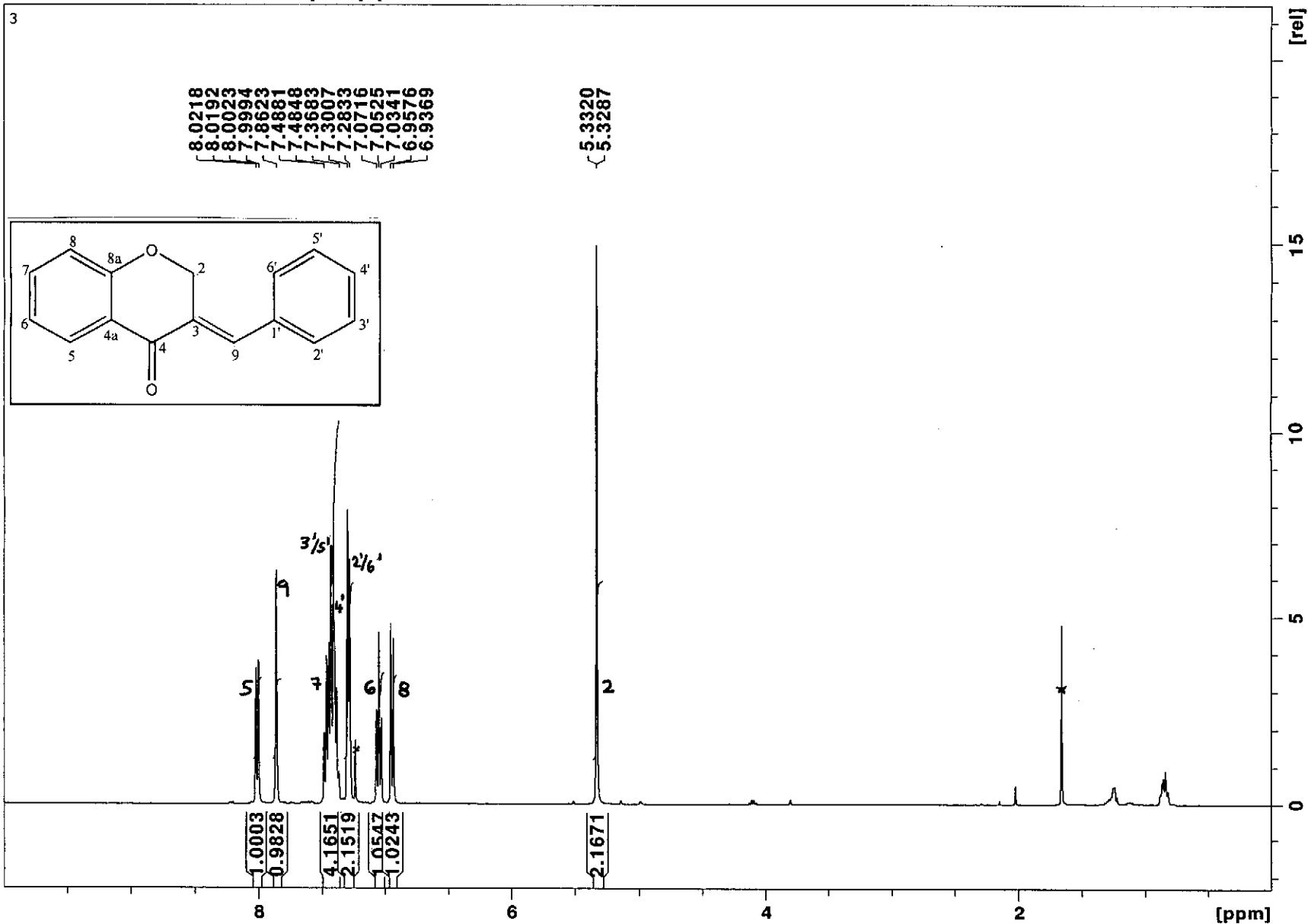
Infrared spectrum of compound 2

File : C:\msdchem\1\data\kaalin\CHROMANONE.D
Operator :
Acquired : 13 Jan 2012 13:23 using AcqMethod NATPRODUCTS MANUAL INJ.M
Instrument : 5973N
Sample Name :
Misc Info :
Vial Number: 1

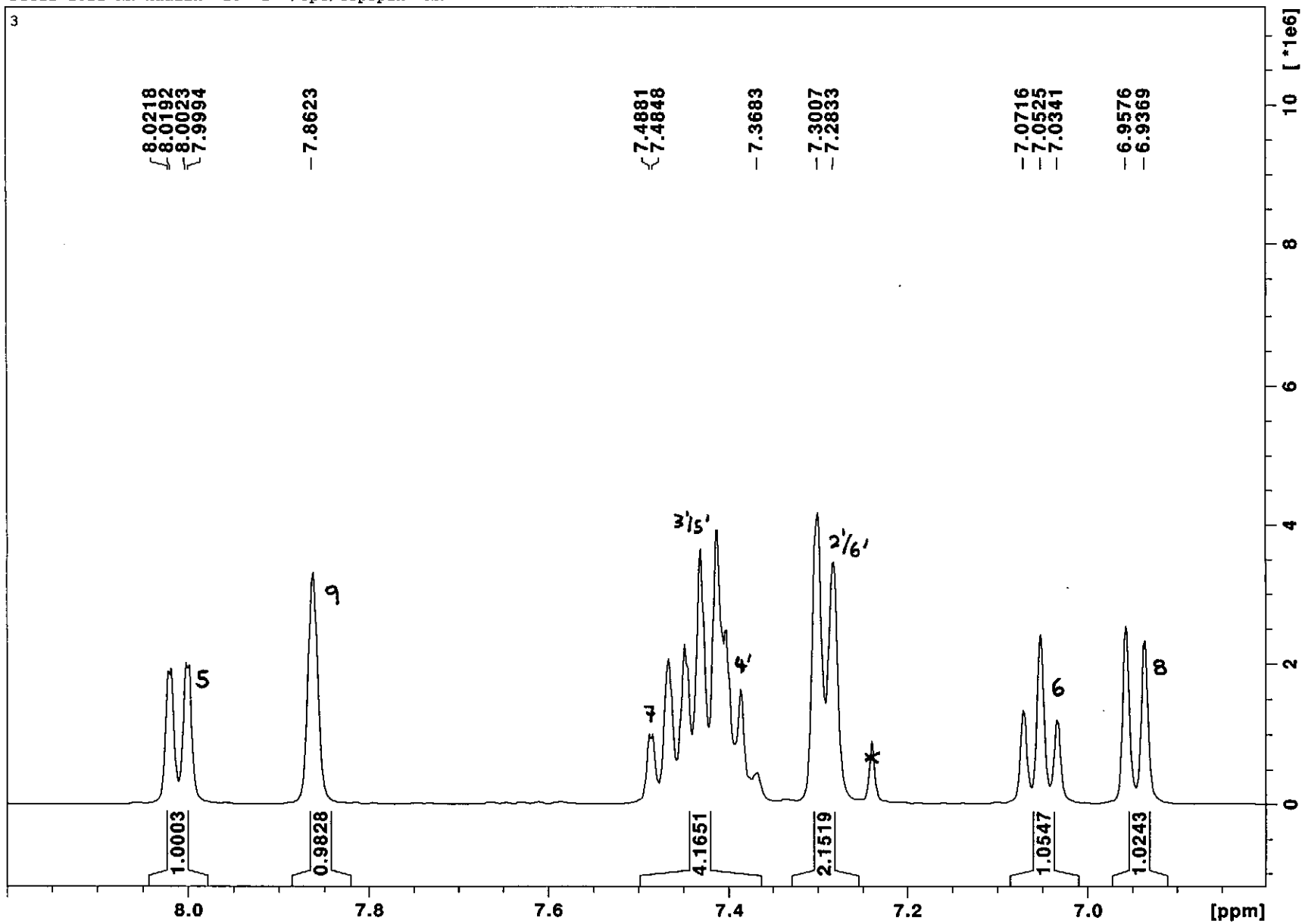


Mass spectrum of compound 2

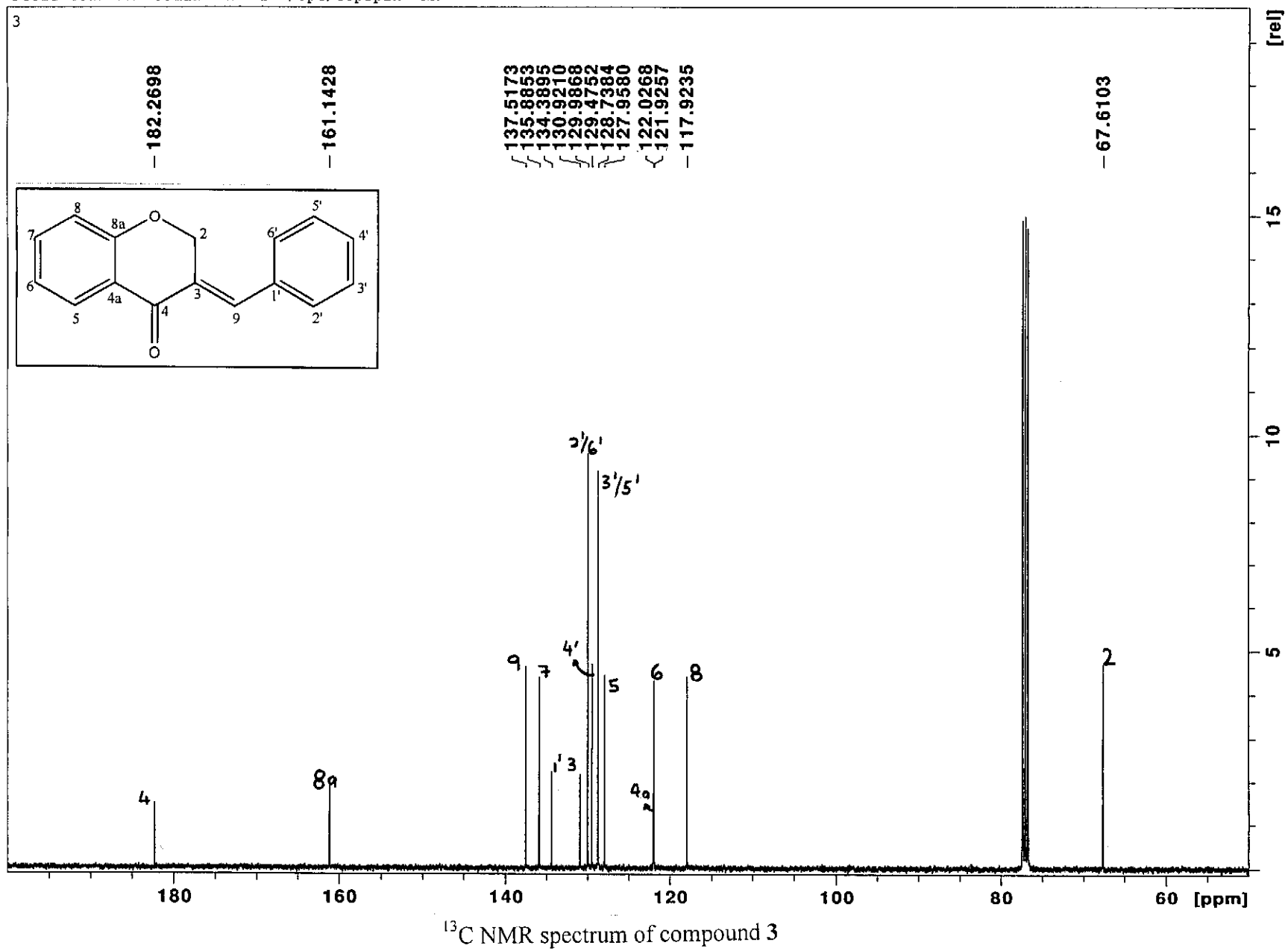
Dec12-2011-NK-kaalin 10 1 /opt/topspin NK



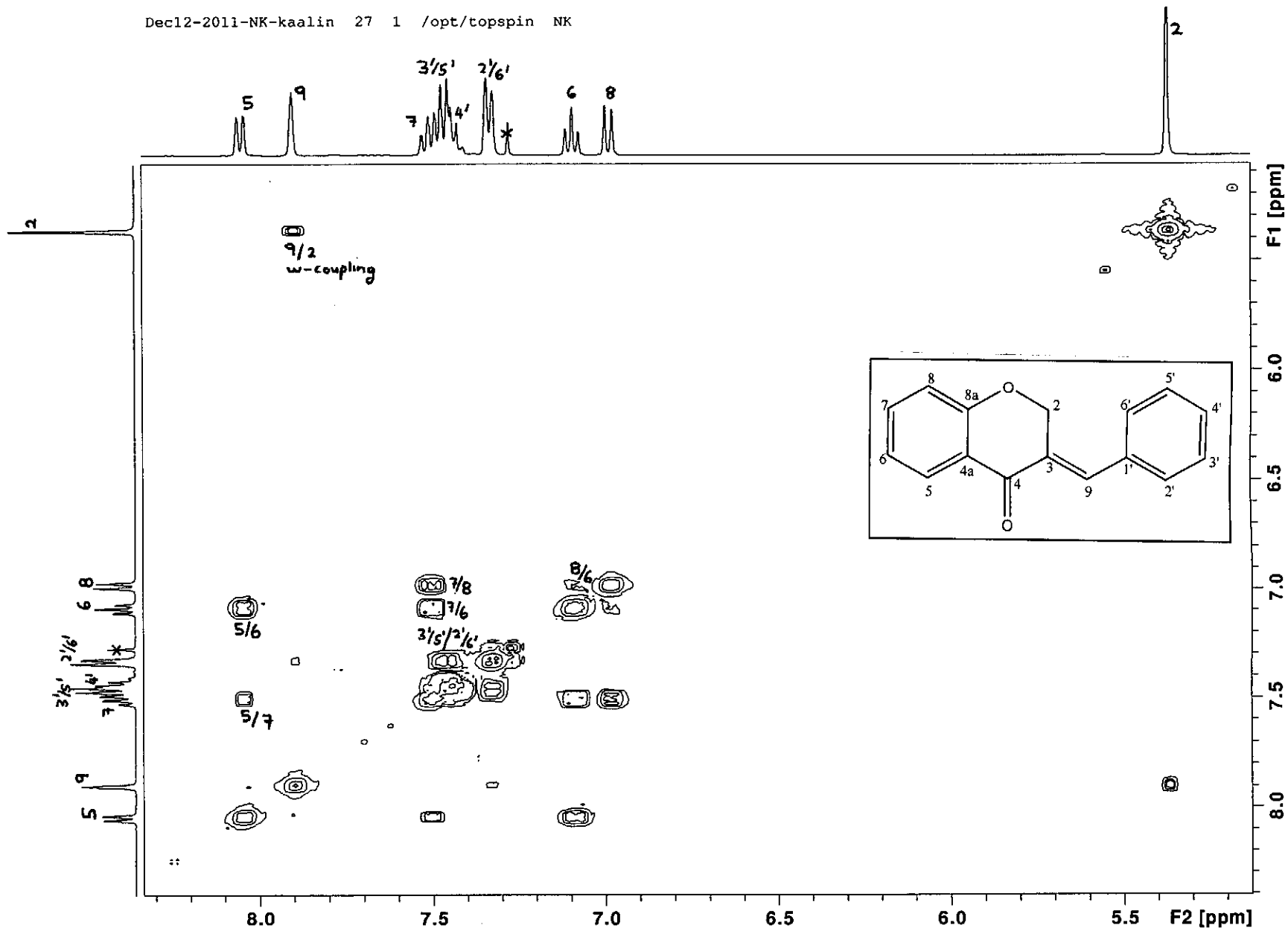
¹H NMR spectrum of compound 3



^1H NMR spectrum of compound 3 (expanded)

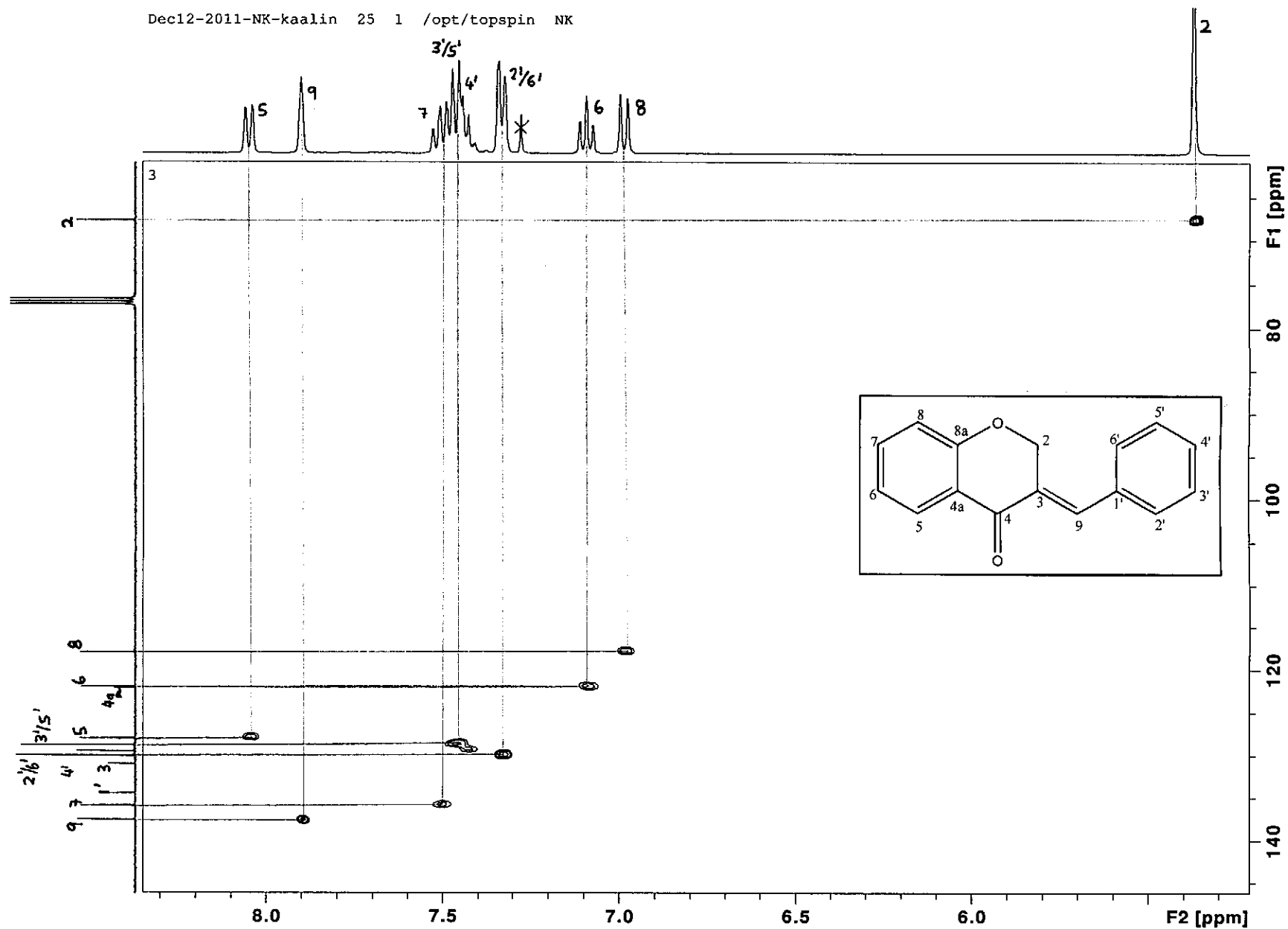


Dec12-2011-NK-kaalin 27 1 /opt/topspin NK



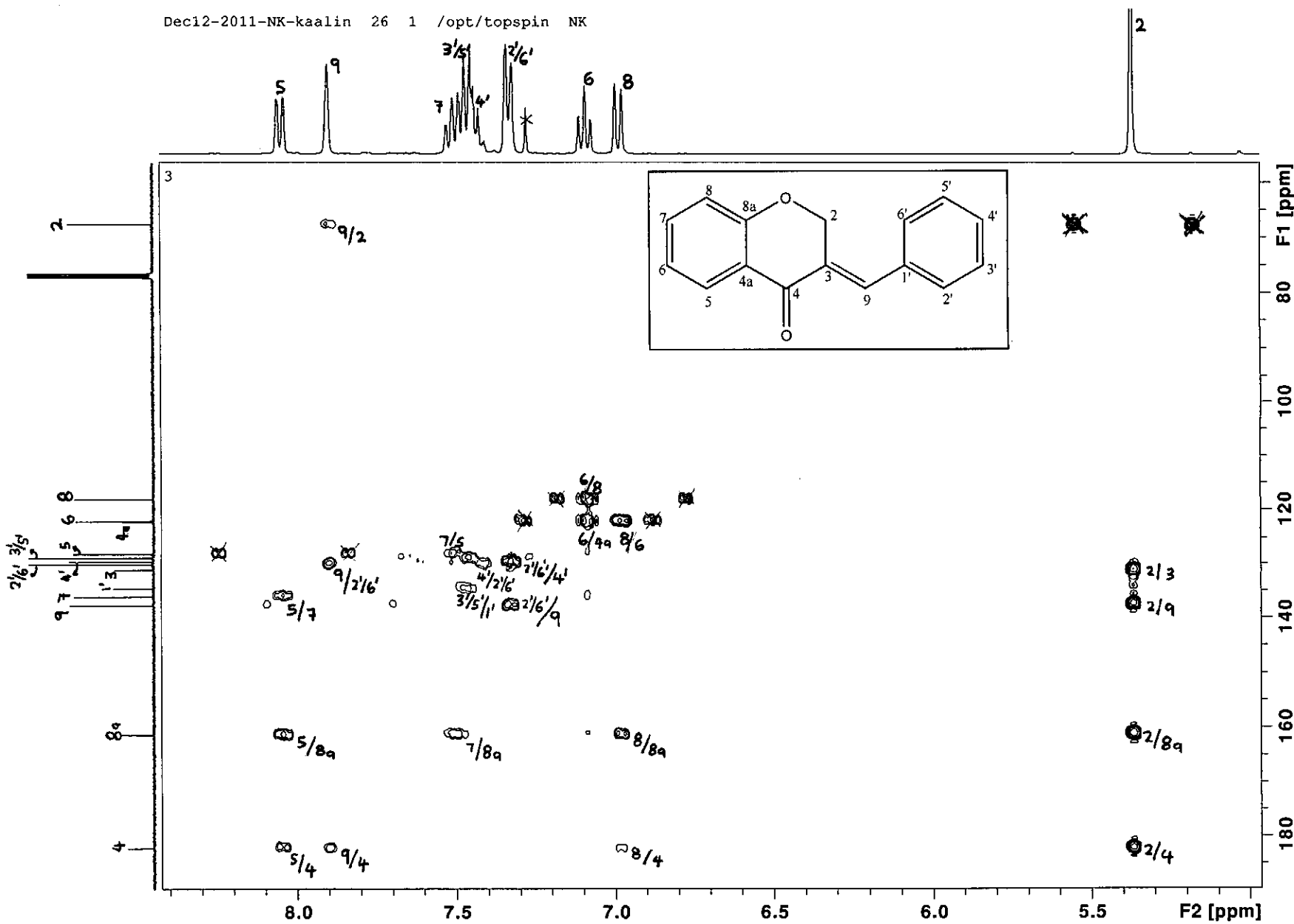
COSY spectrum of compound 3

Dec12-2011-NK-kaalin 25 1 /opt/topspin NK

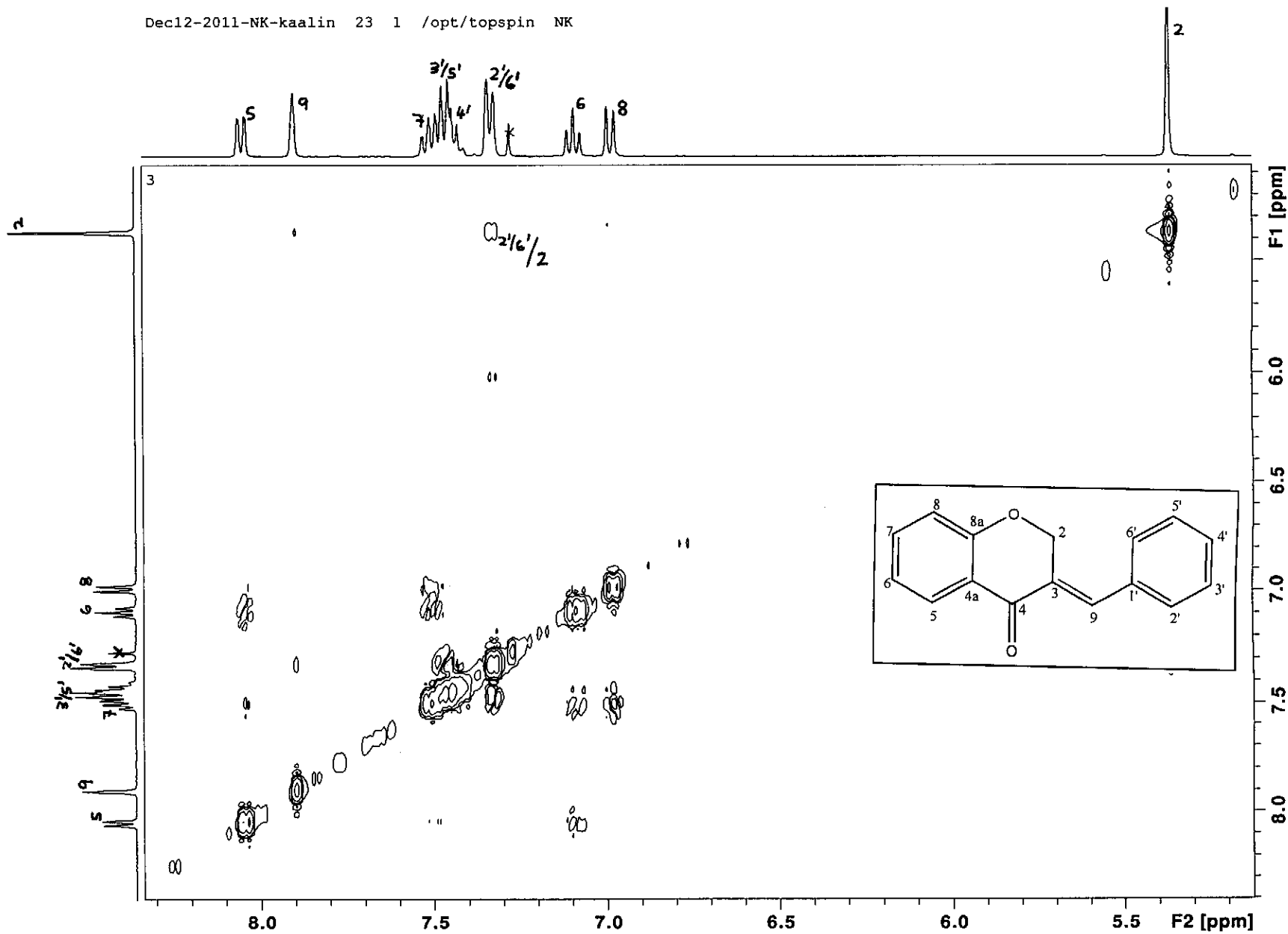


HSQC spectrum of compound 3

Dec12-2011-NK-kaalin 26 1 /opt/topspin NK



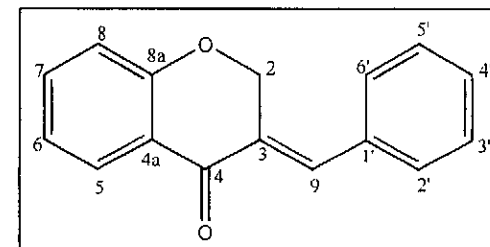
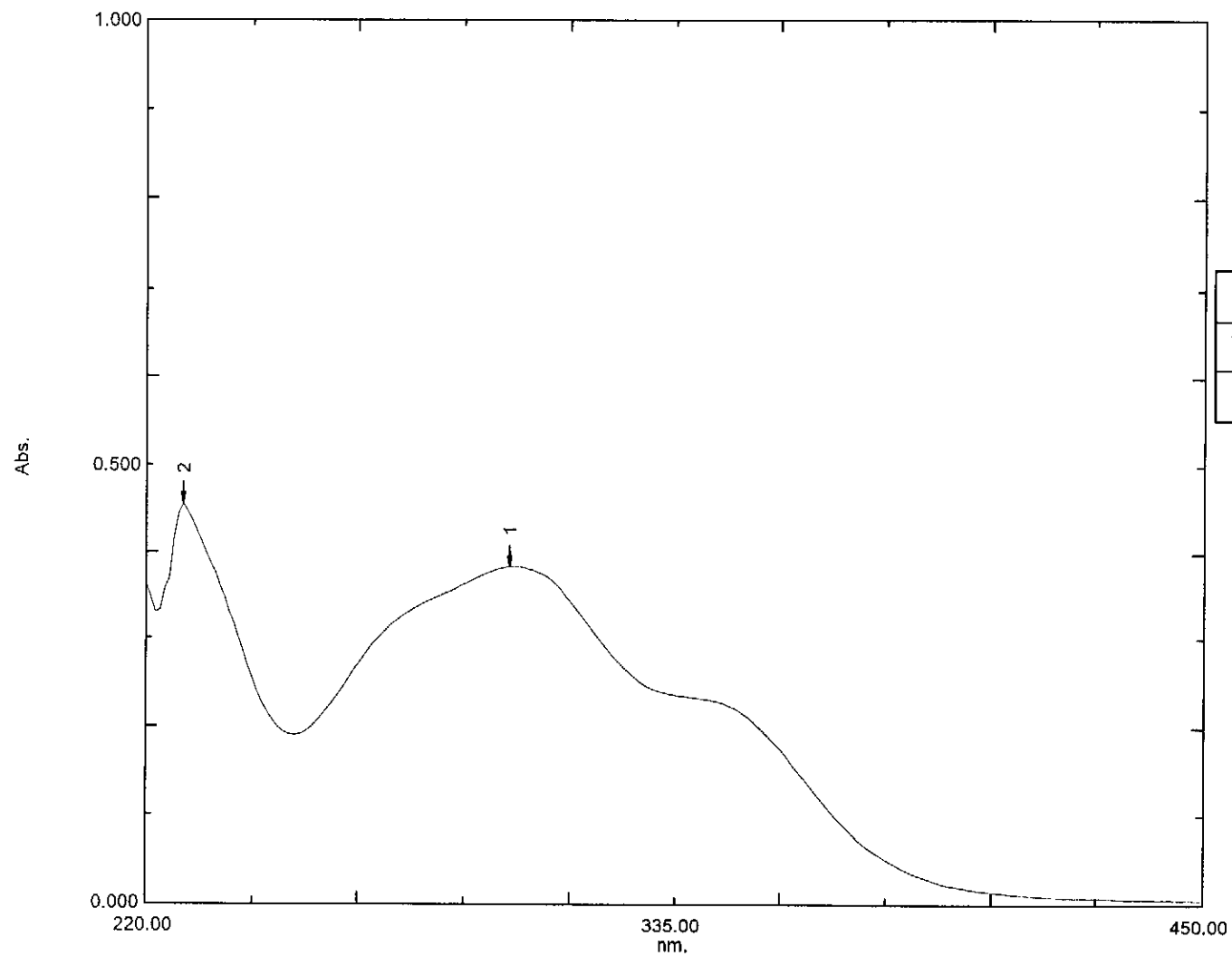
Dec12-2011-NK-kaalin 23 1 /opt/topspin NK



NOESY spectrum of compound 3

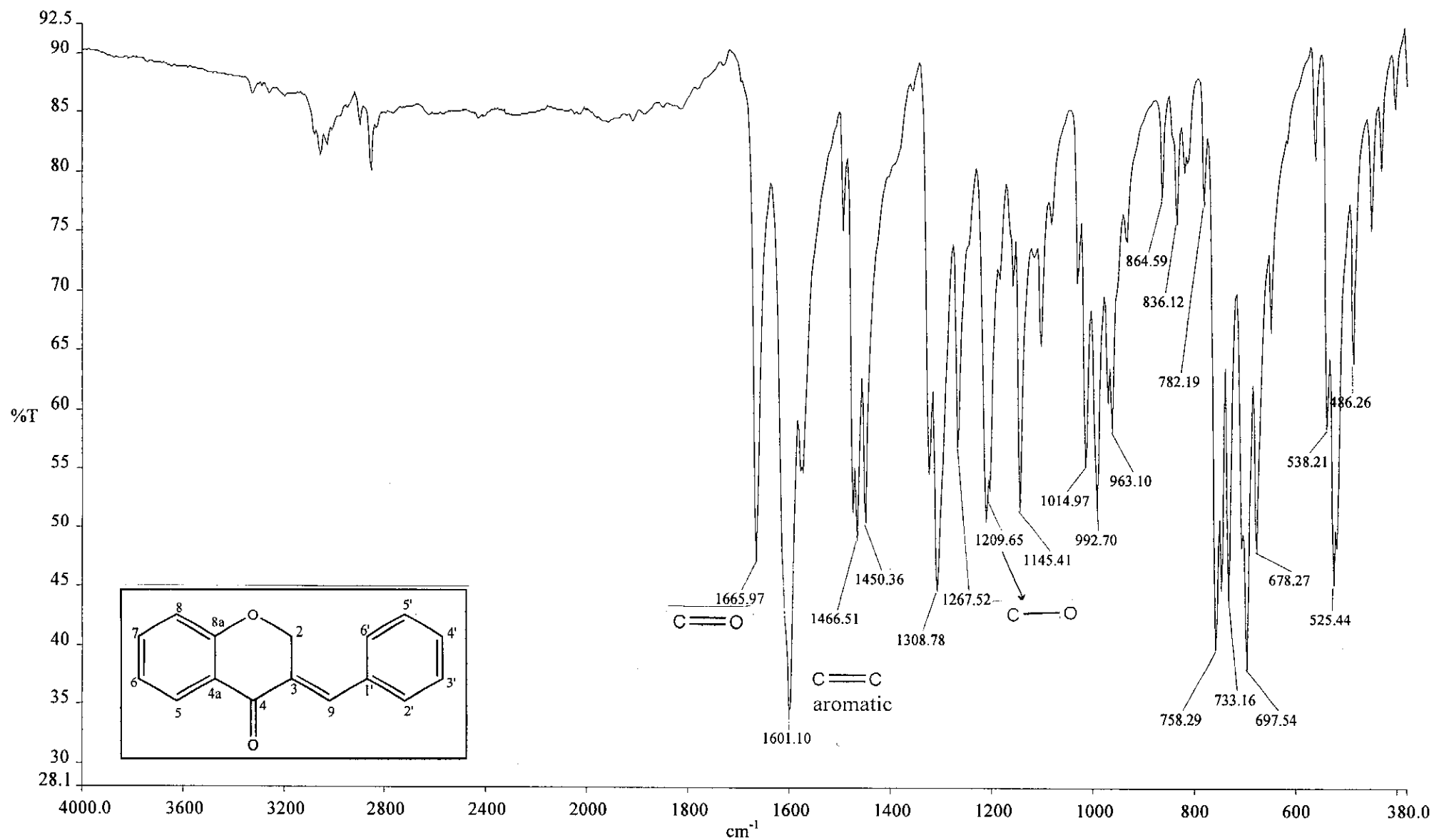
Overlay Spectrum Graph Report

15/05/2012 12:50:50 PM



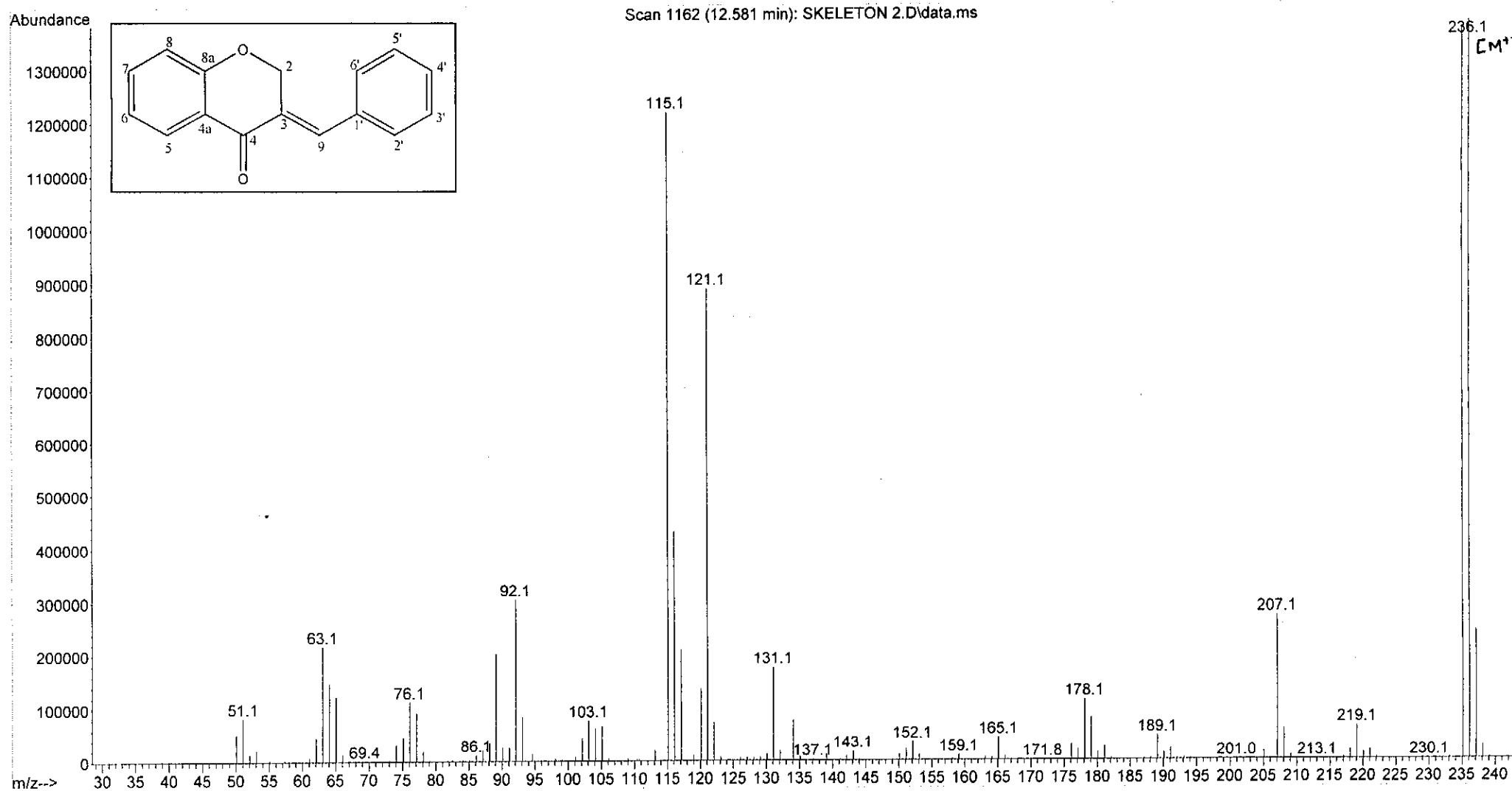
Wavelength/ nm	Absorbance	Log ϵ
299	0.383	4.13
344	0.229	3.91

UV-Vis spectrum of compound 3

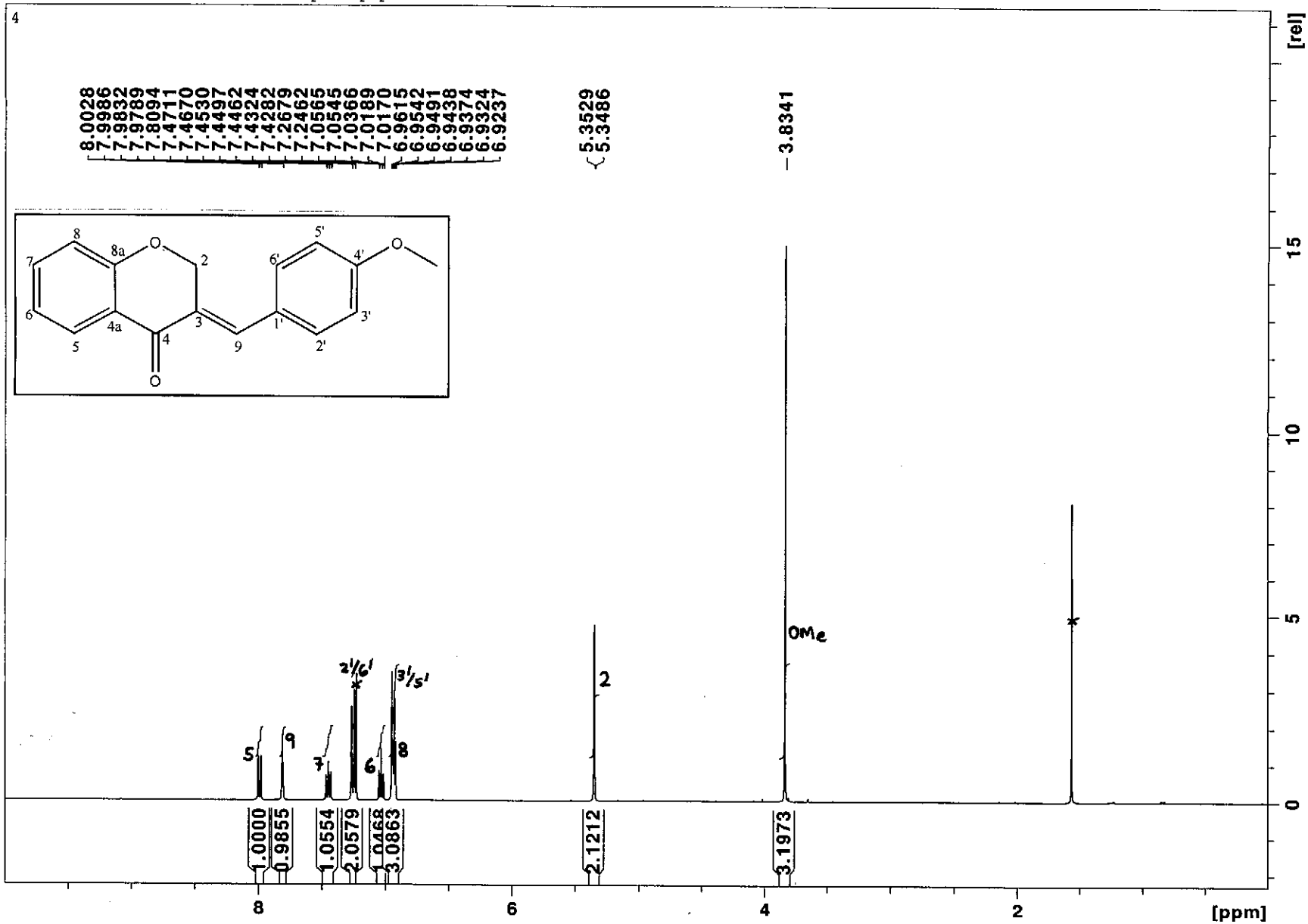


Infrared spectrum of compound 3

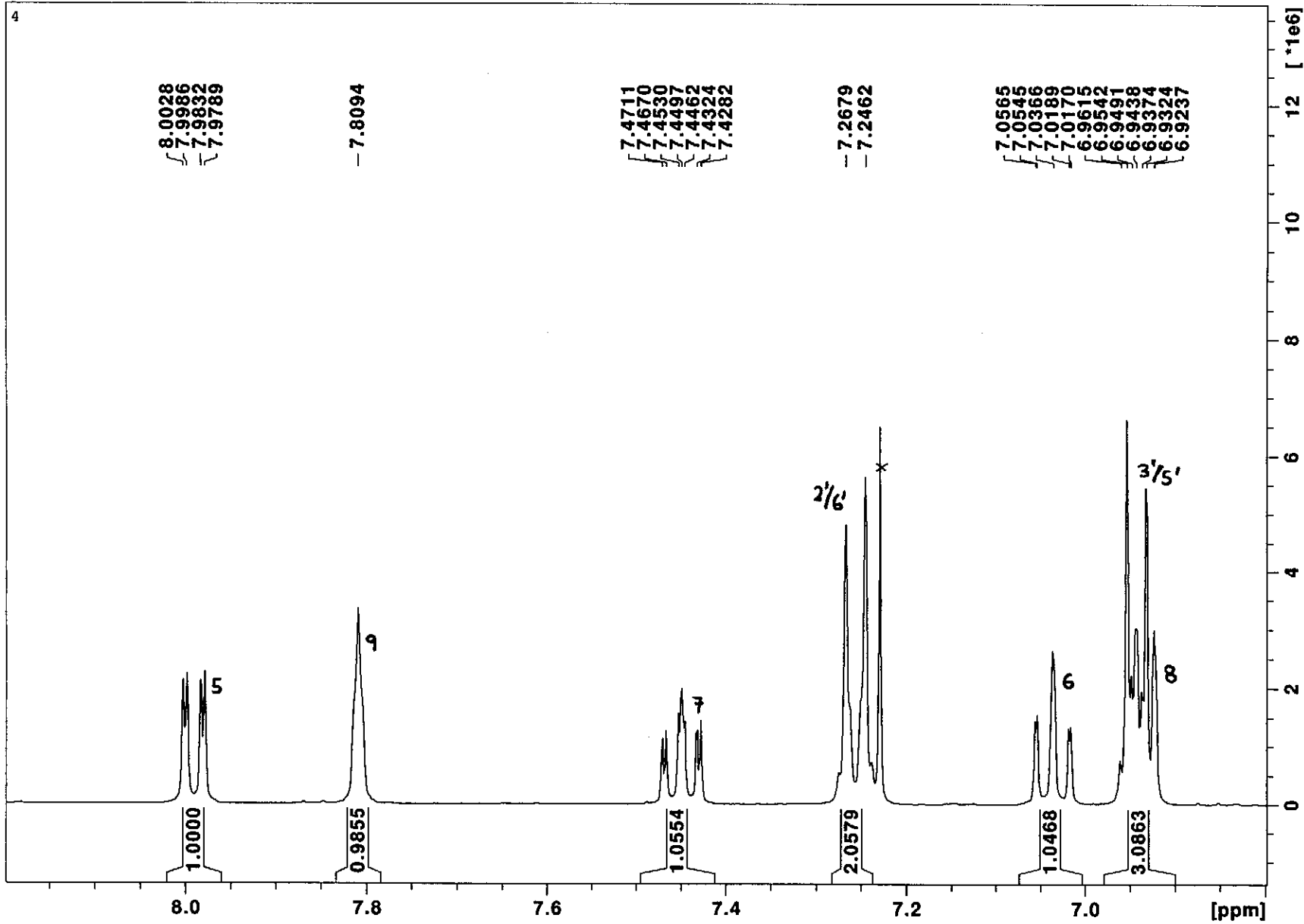
File :C:\msdchem\1\data\kaalin\SKELETON 2.D
Operator :
Acquired : 12 Jan 2012 12:40 using AcqMethod NATPRODUCTS MANUAL INJ.M
Instrument : 5973N
Sample Name:
Misc Info :
Vial Number: 1



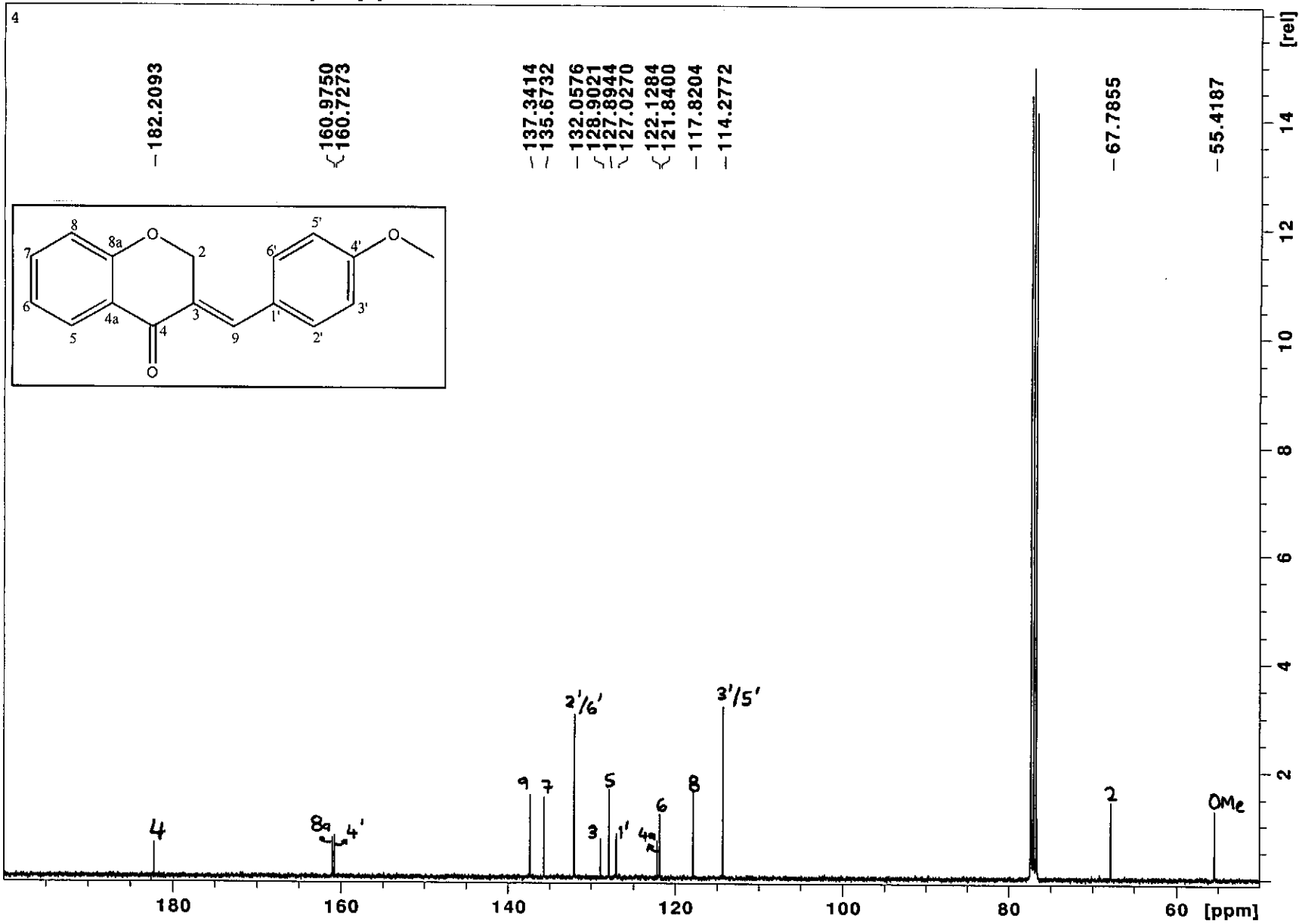
Mass spectrum of compound 3



¹H NMR spectrum of compound 4

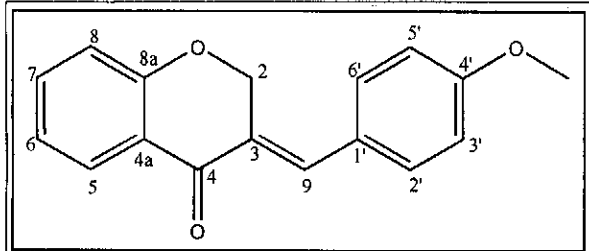


¹H NMR spectrum of compound 4 (expanded)

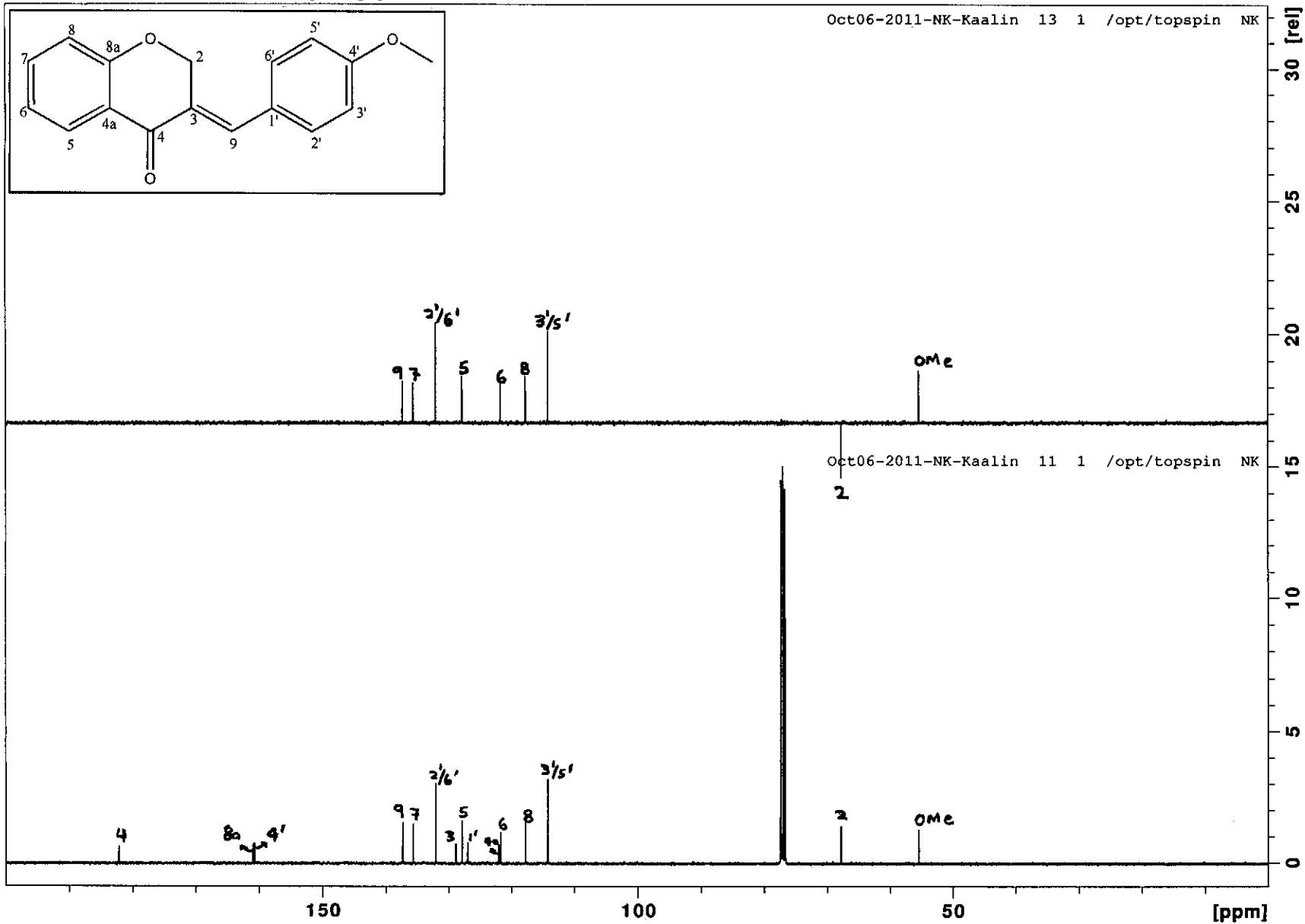


¹³C NMR spectrum of compound 4

Oct06-2011-NK-Kaalin 11 1 /opt/topspin NK

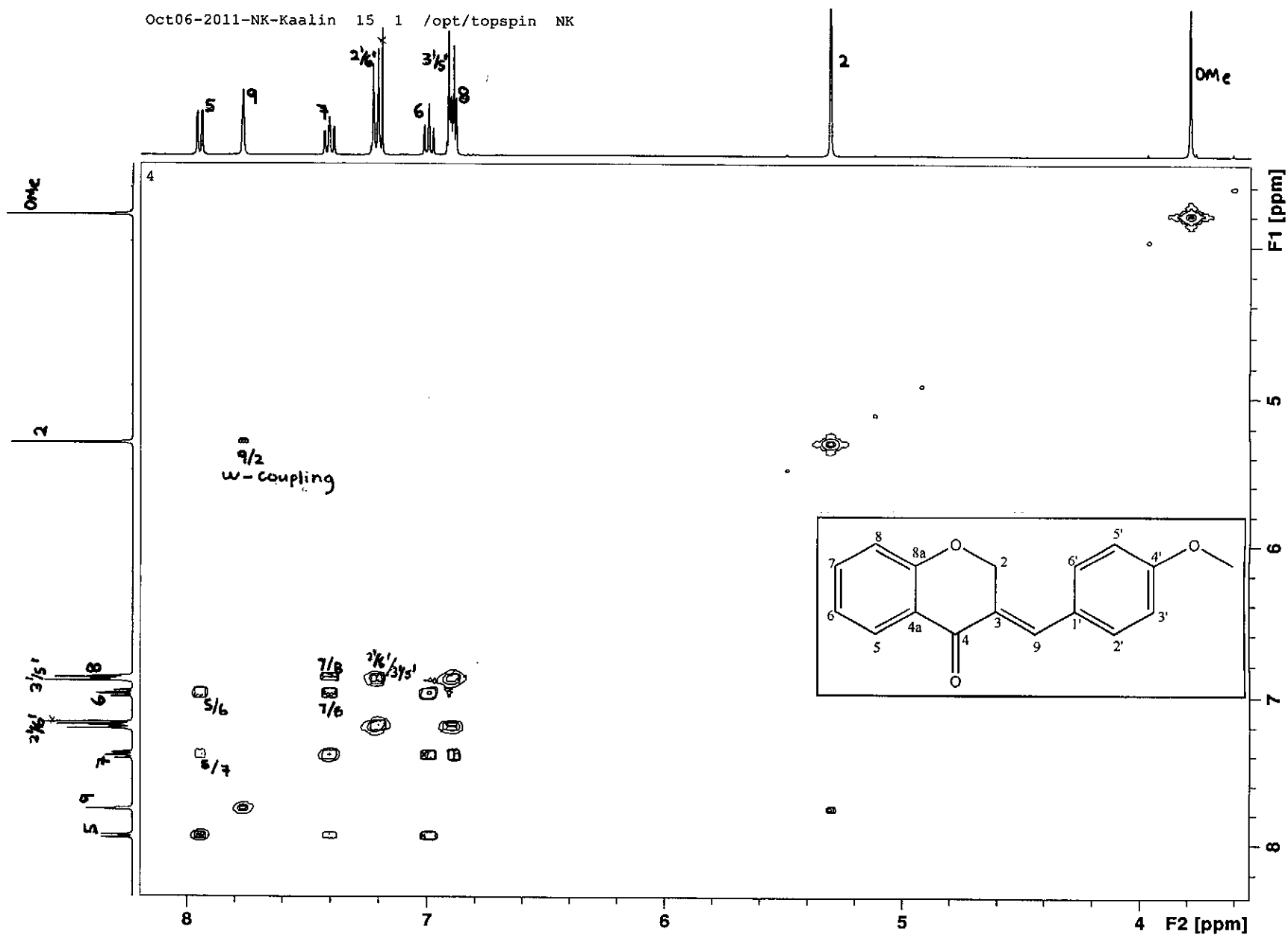


Oct06-2011-NK-Kaalin 13 1 /opt/topspin NK



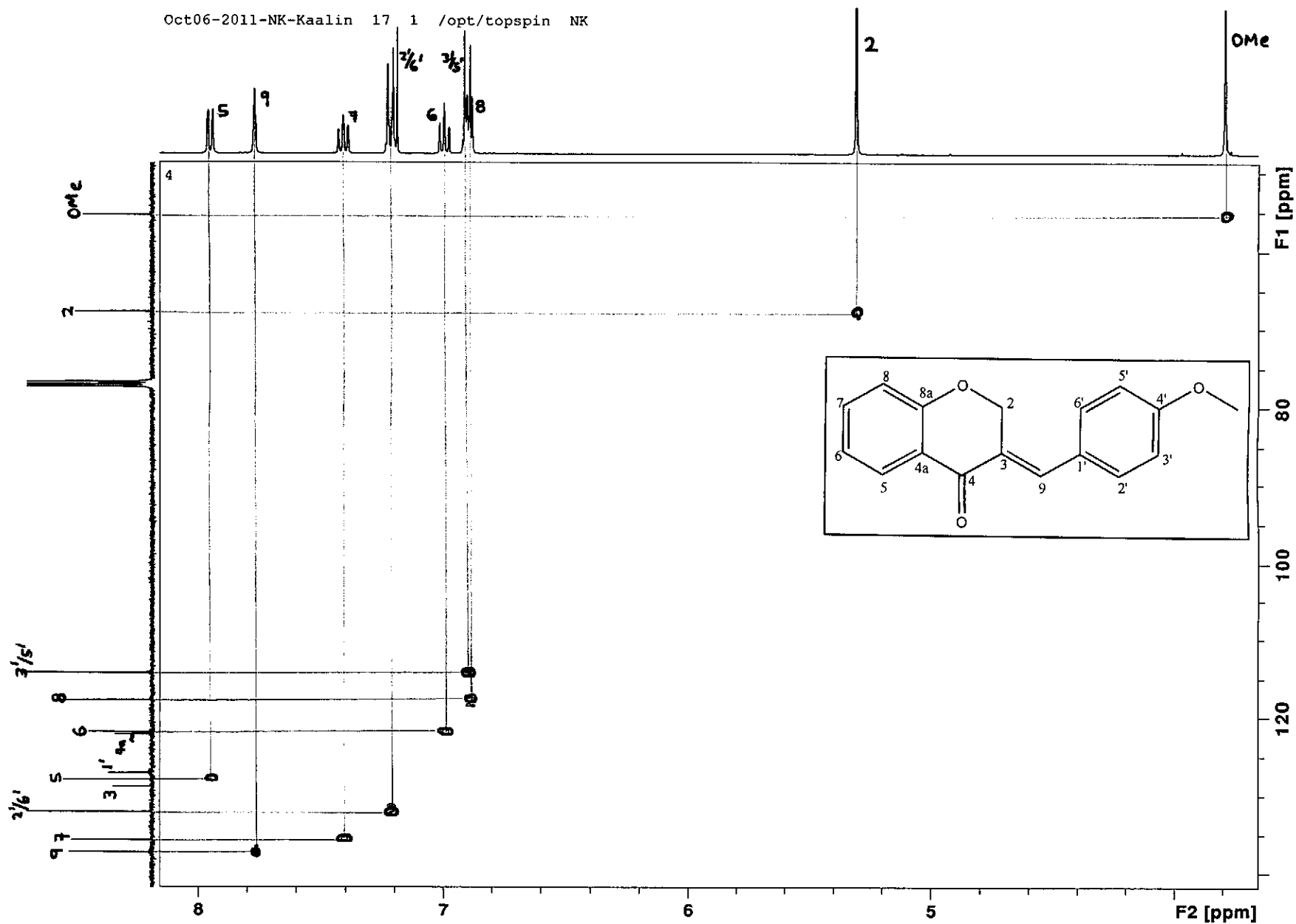
DEPT 135 spectrum of compound 4

Oct06-2011-NK-Kaalin 15 1 /opt/topspin NK



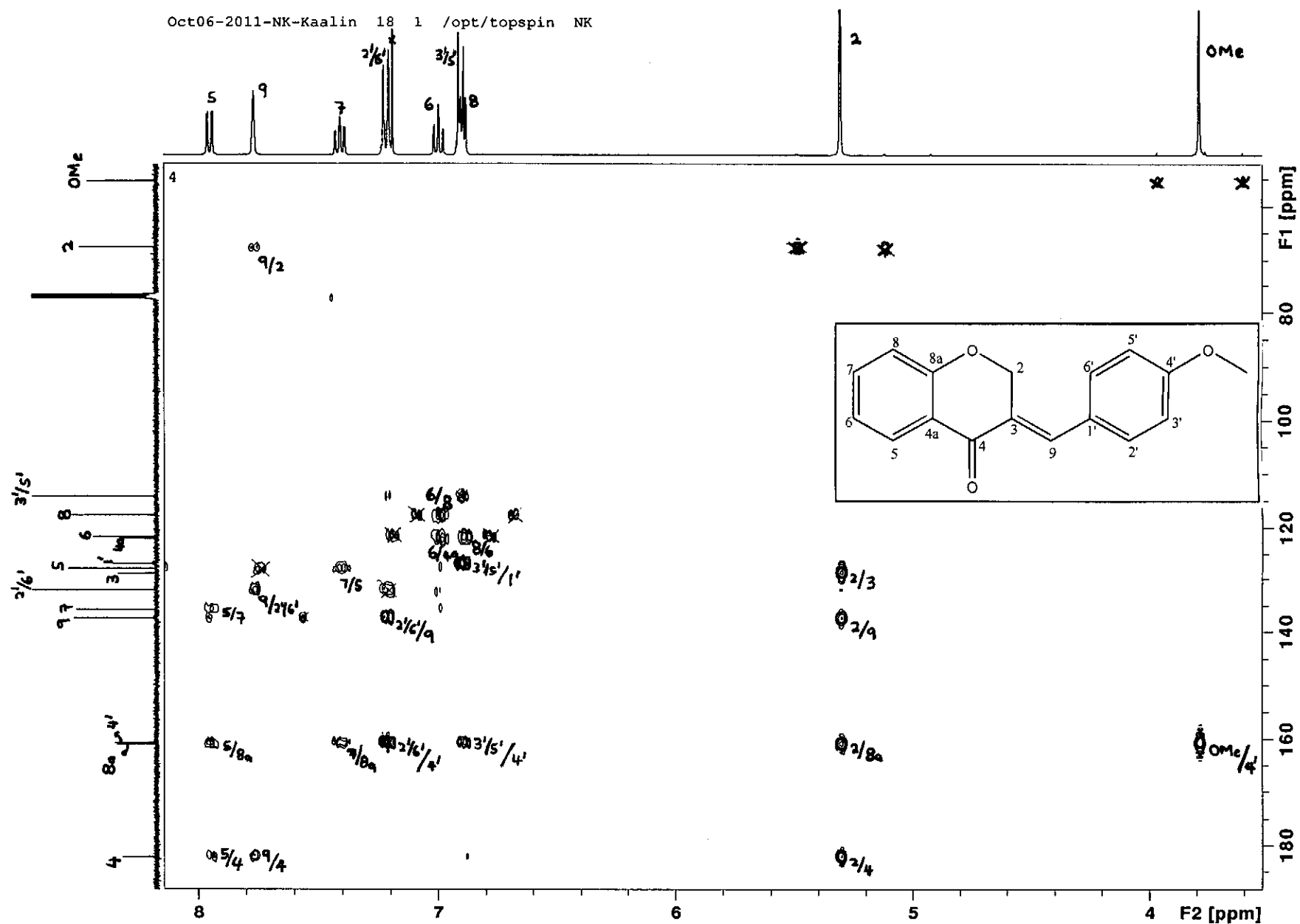
COSY spectrum of compound 4

Oct06-2011-NK-Kaalin 17 1 /opt/topspin NK



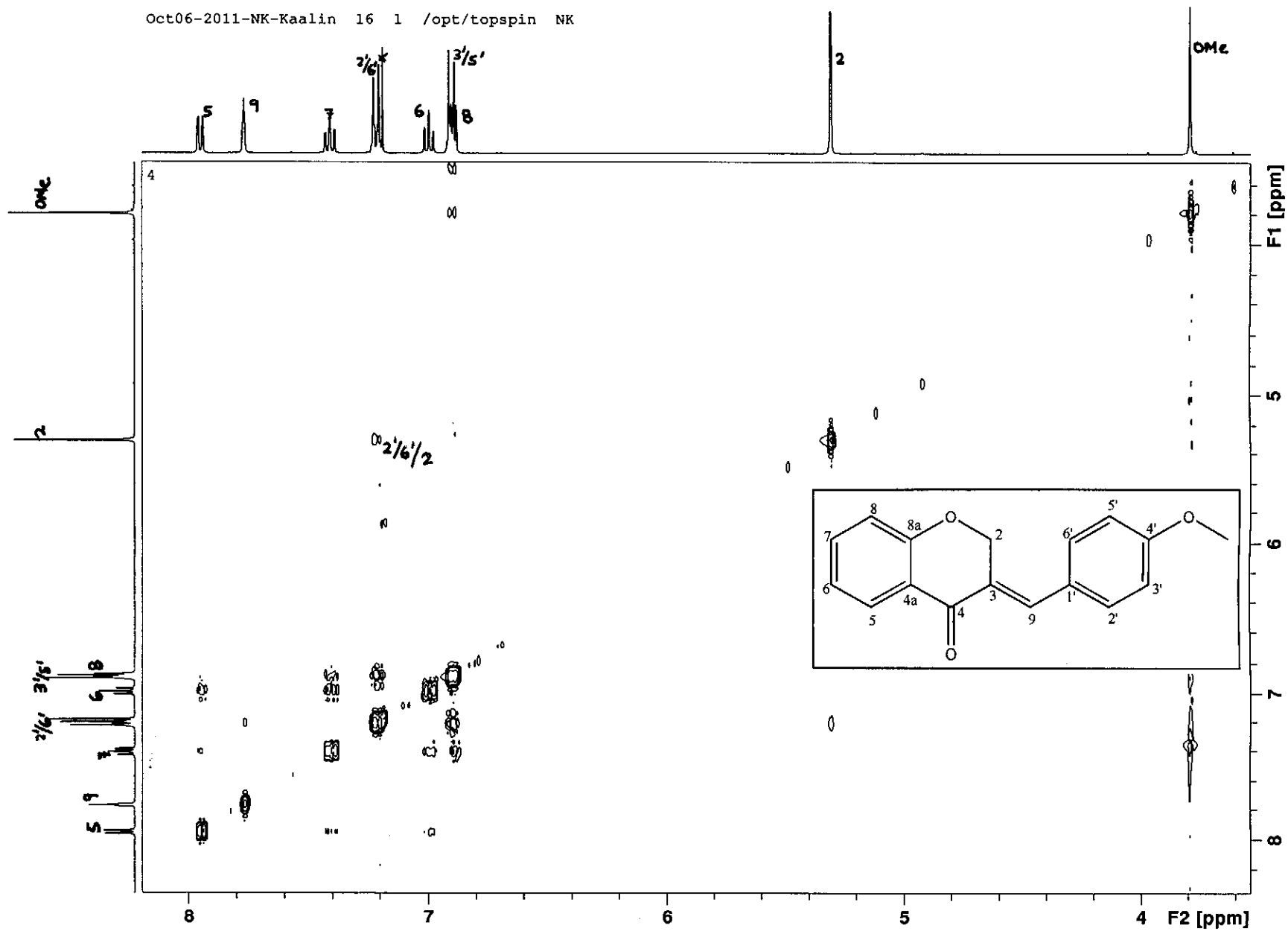
HSQC spectrum of compound 4

Oct06-2011-NK-Kaalin 18 1 /opt/topspin NK



HMBC spectrum of compound 4

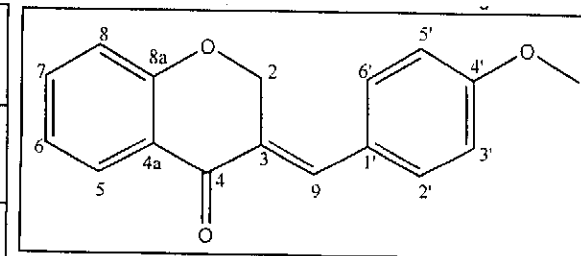
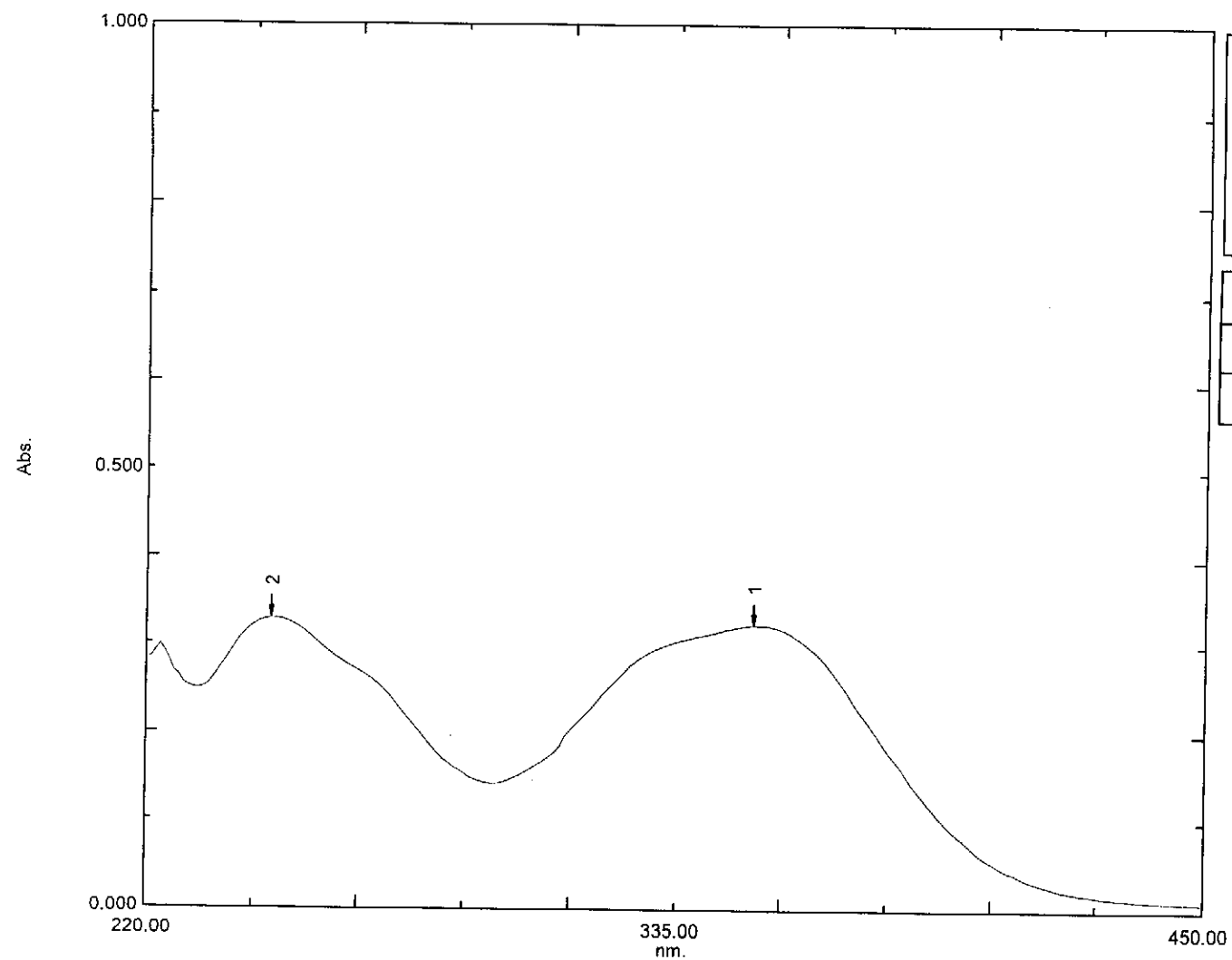
Oct06-2011-NK-Kaalin 16 1 /opt/topspin NK



NOESY spectrum of compound 4

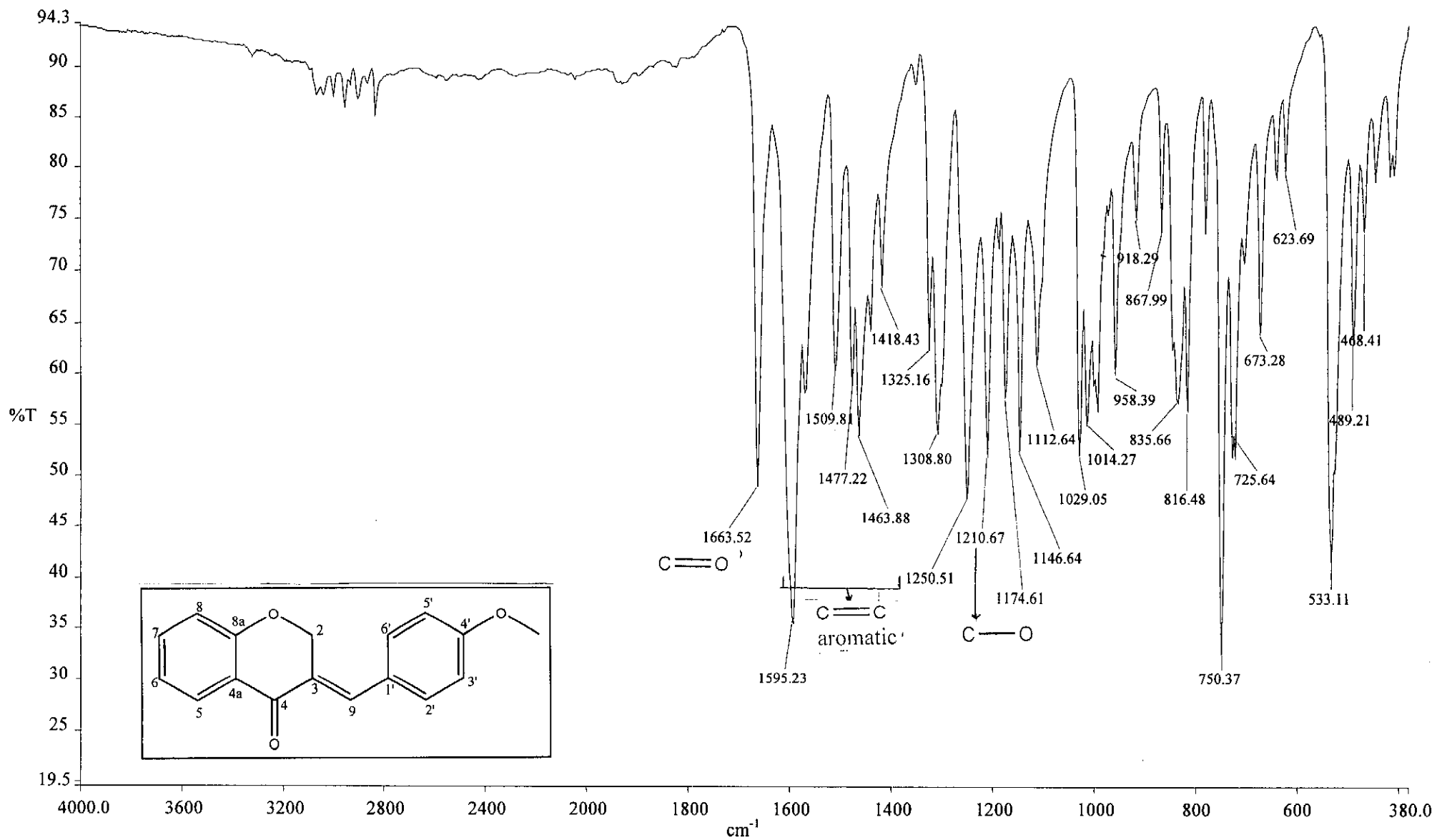
Overlay Spectrum Graph Report

15/05/2012 12:51:41 PM



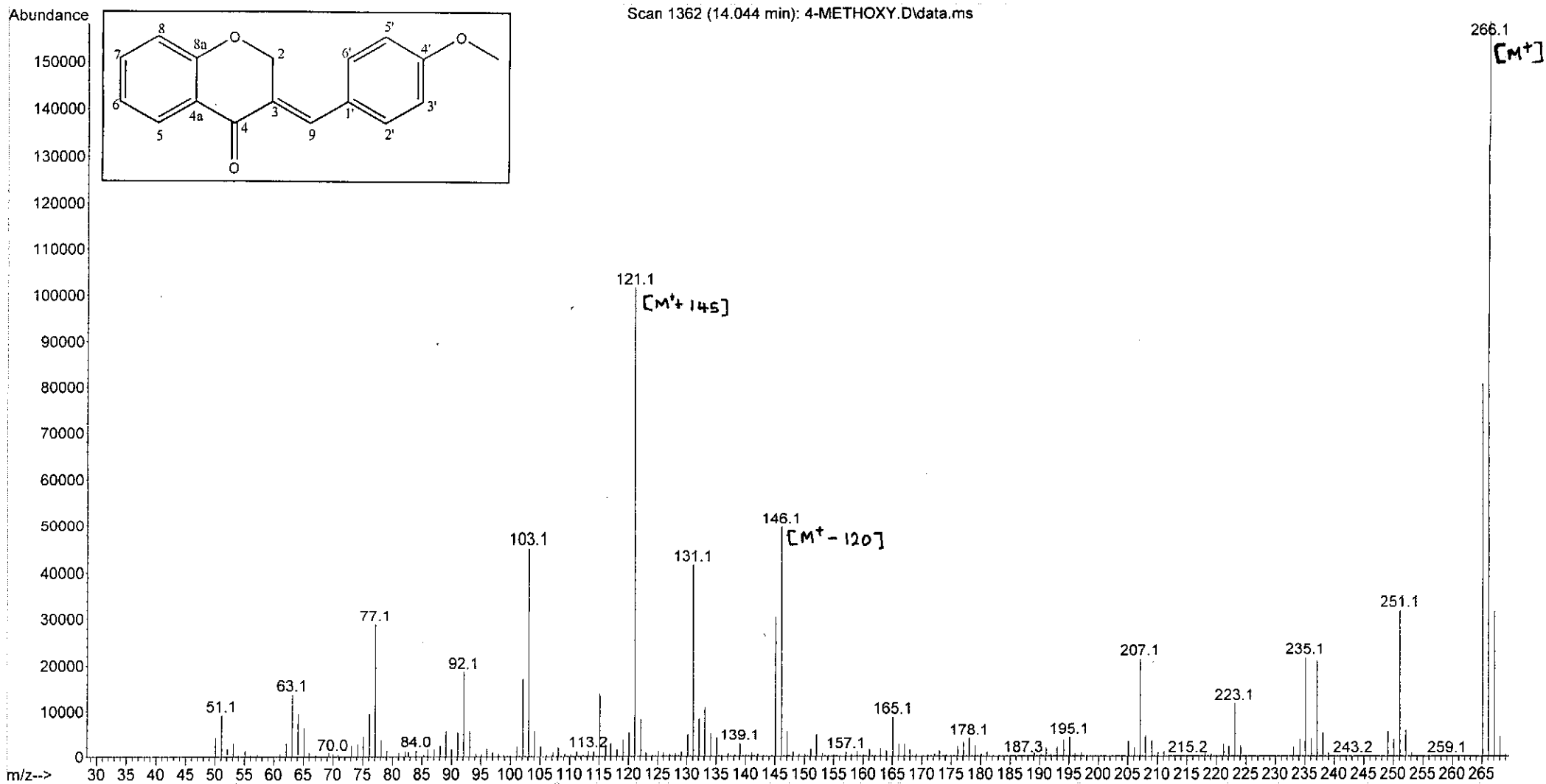
Wavelength/ nm	Absorbance	Log ϵ
247	0.329	4.34
351	0.323	4.33

UV-Vis spectrum of compound 4

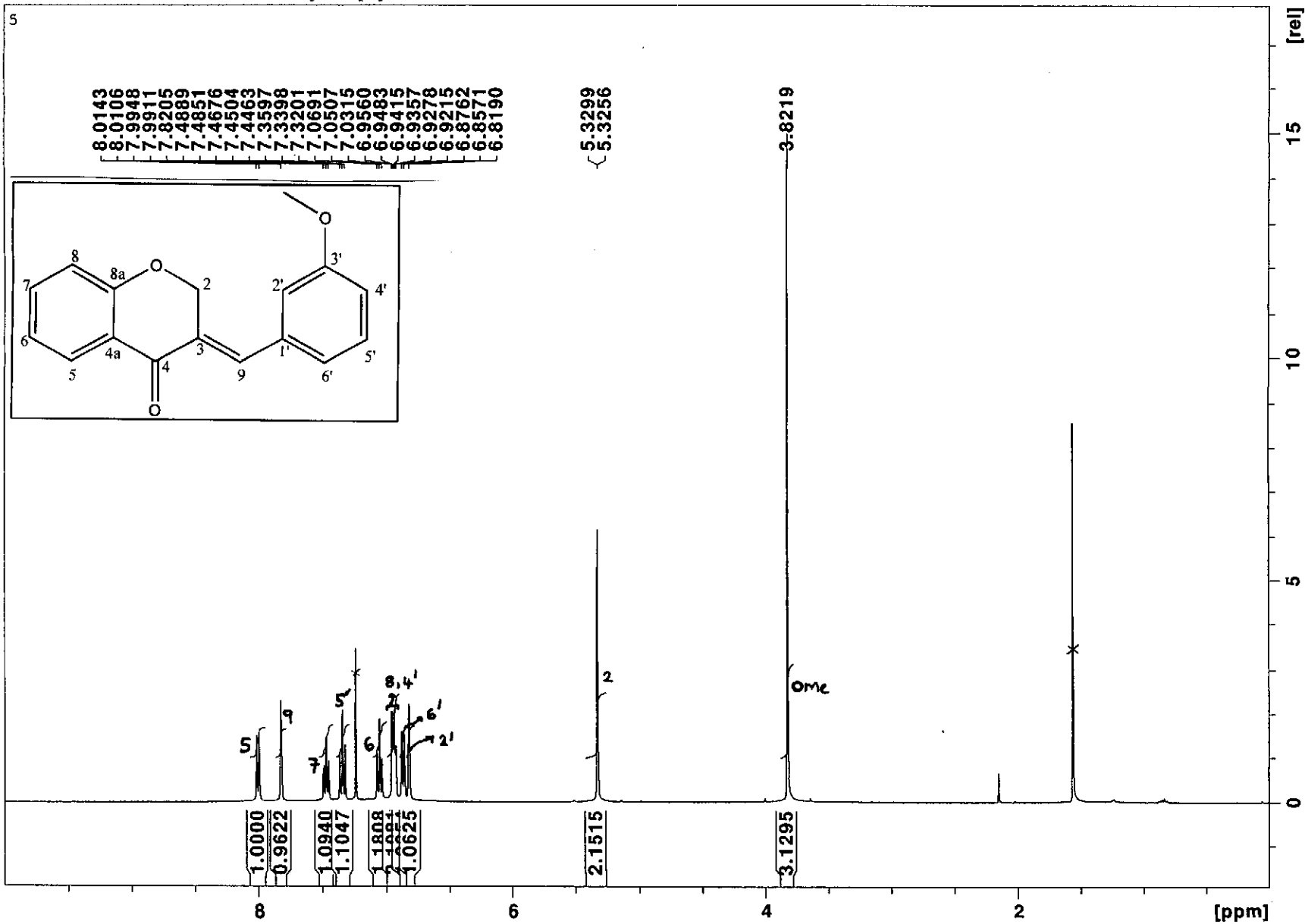


Infrared spectrum of compound 4

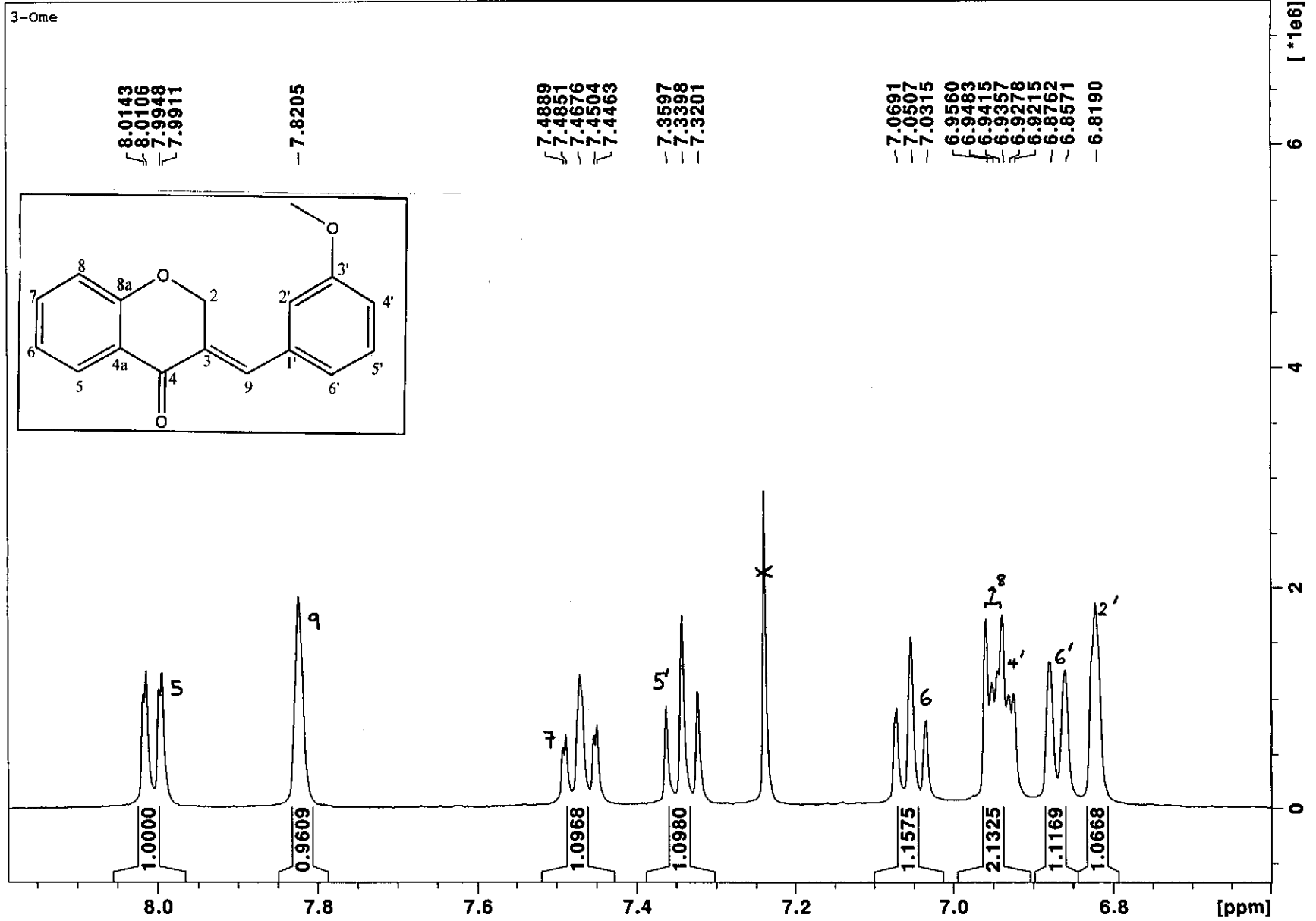
File : C:\msdchem\1\data\kaalin\4-METHOXY.D
Operator :
Acquired : 12 Jan 2012 13:09 using AcqMethod NATPRODUCTS MANUAL INJ.M
Instrument : 5973N
Sample Name:
Misc Info :
Vial Number: 1



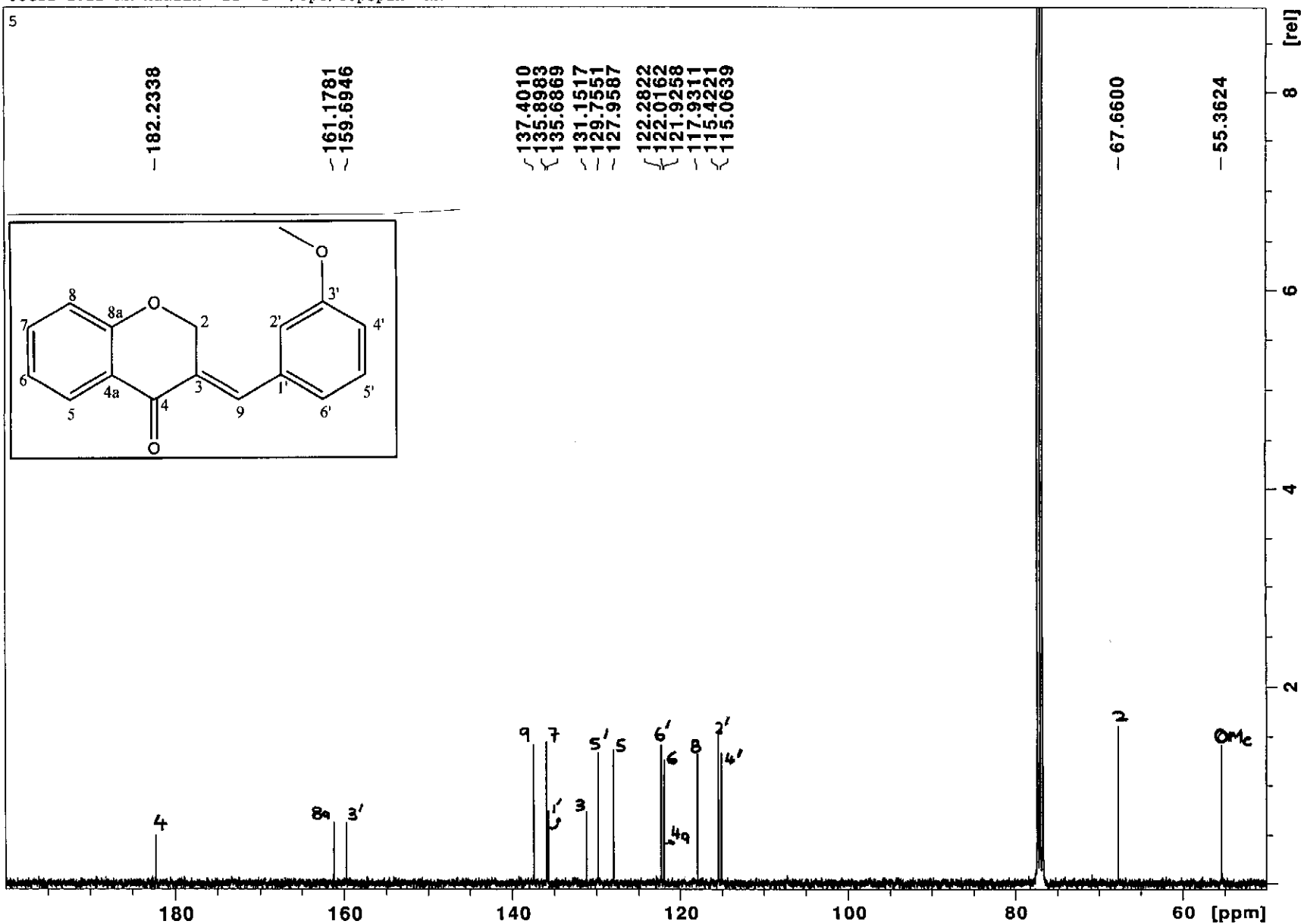
Mass spectrum of compound 4



¹H NMR spectrum of compound 5

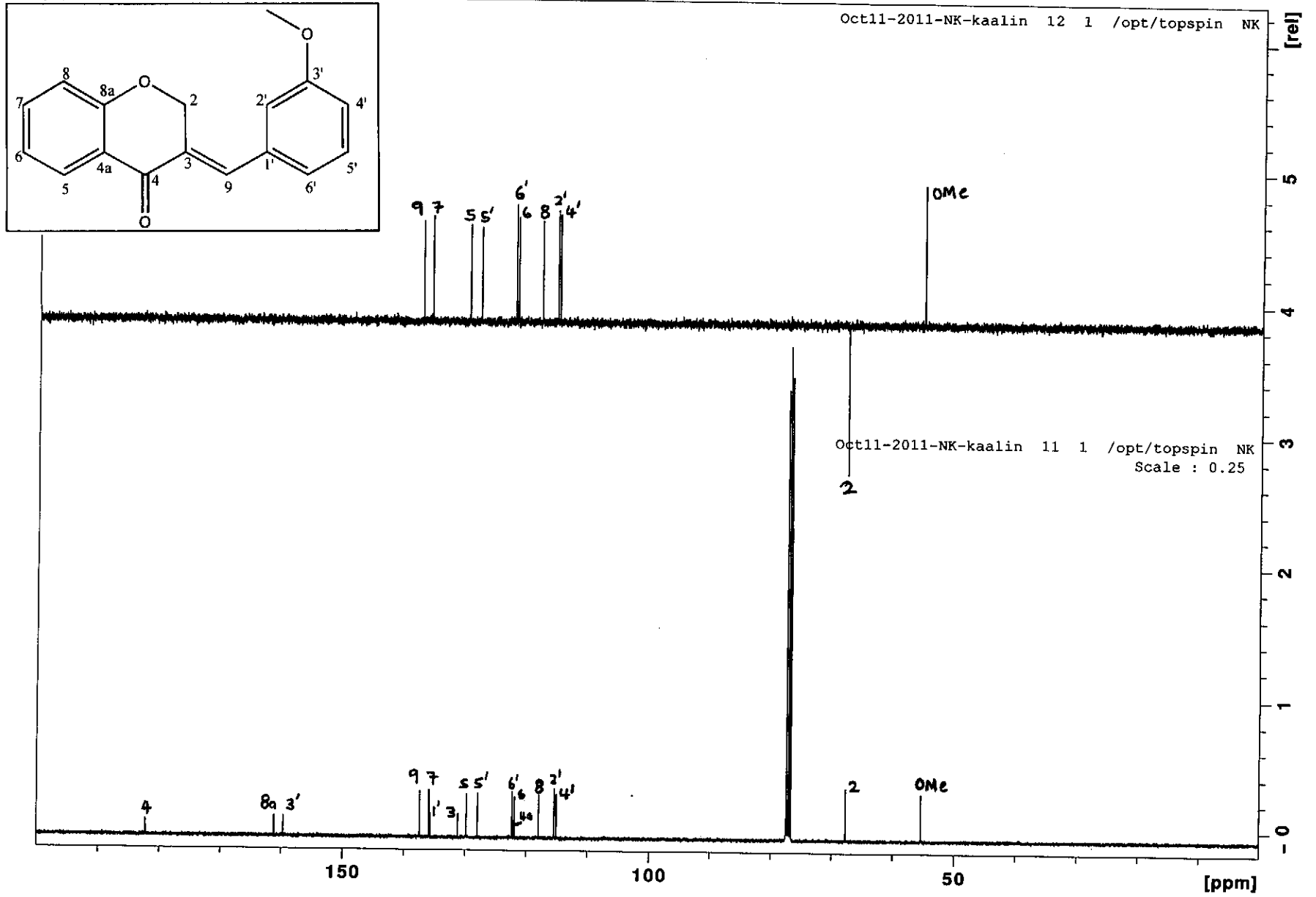


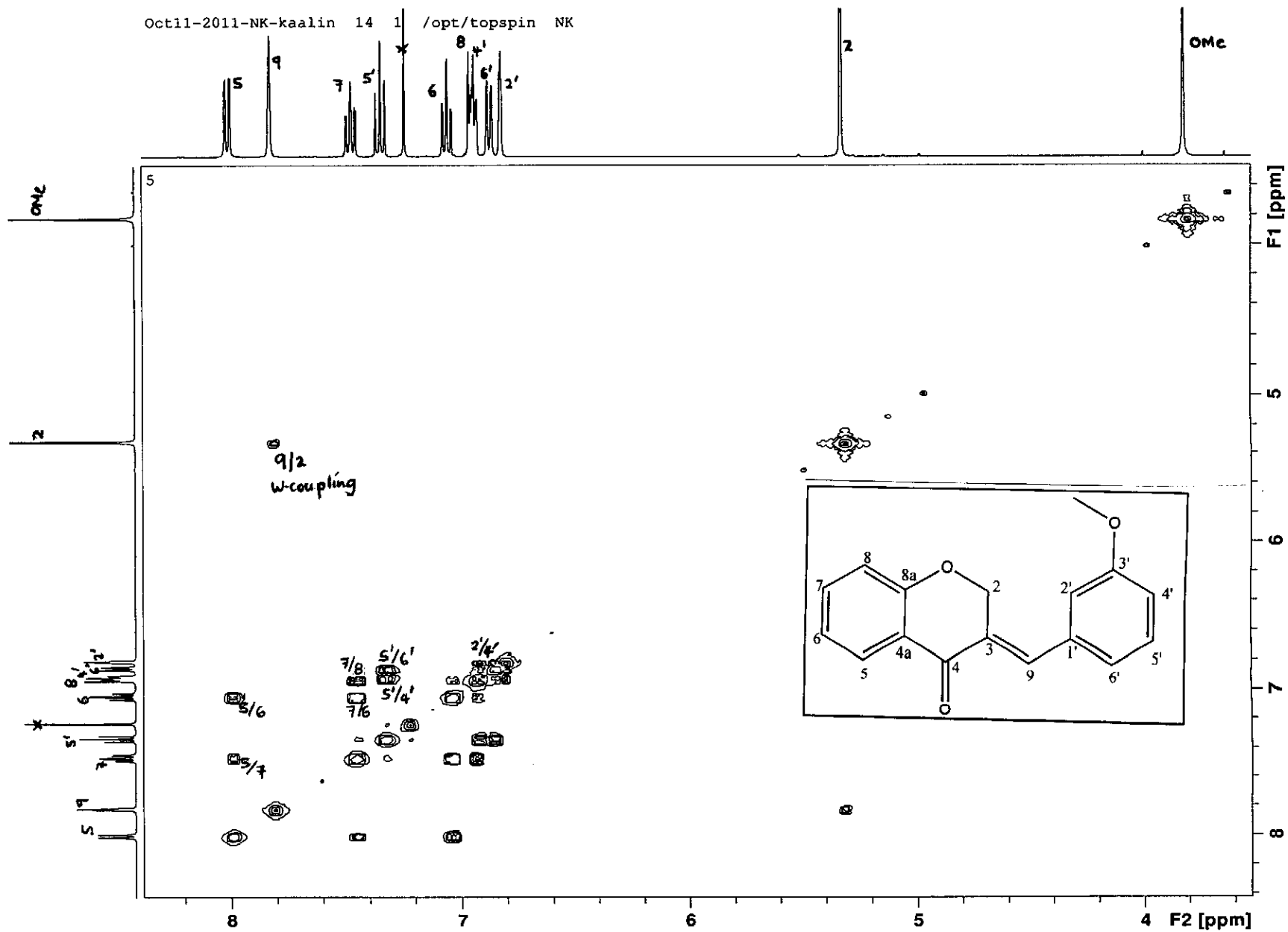
¹H NMR spectrum of compound 5 (expanded)



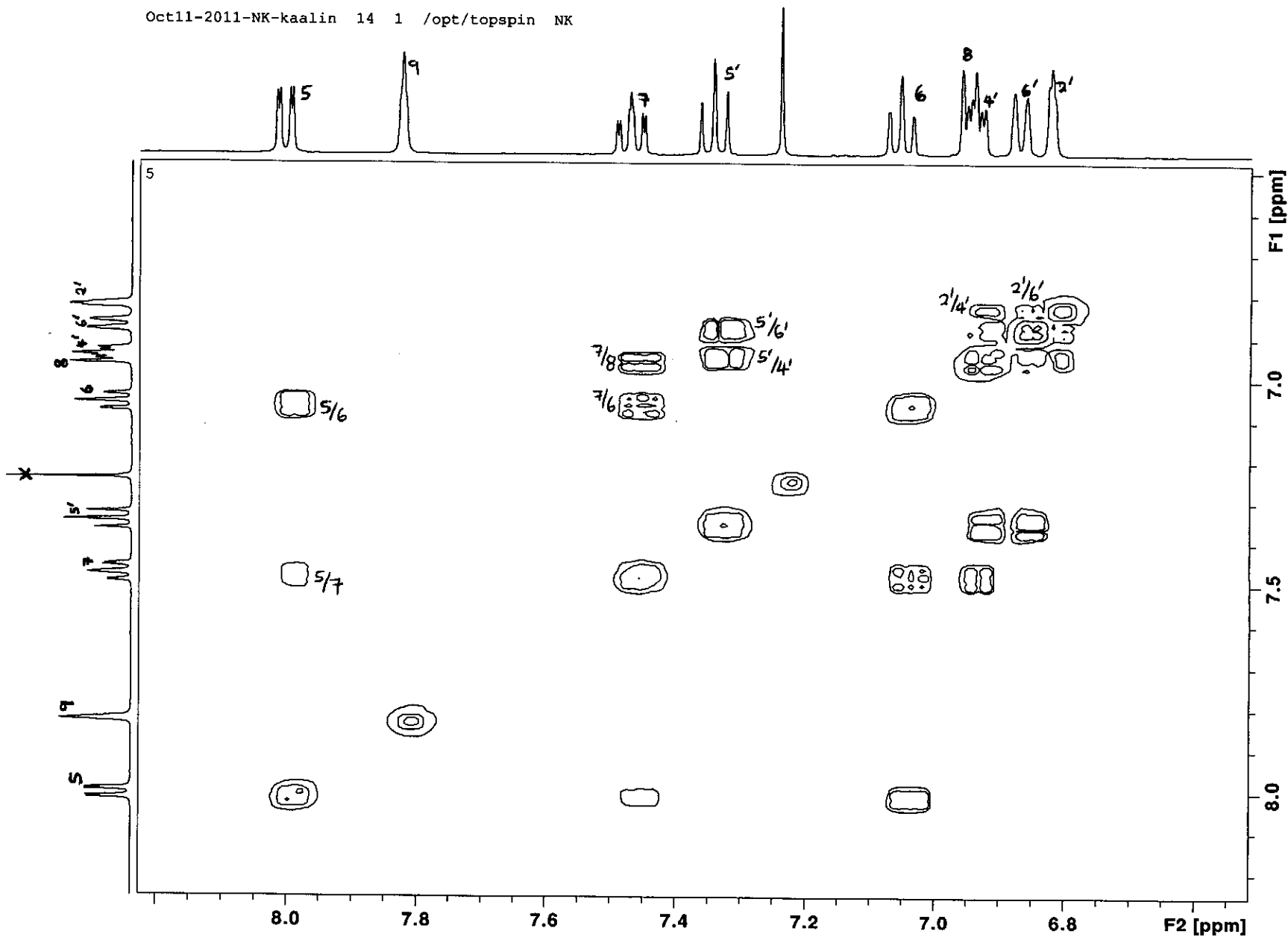
¹³C NMR spectrum of compound 5

Oct11-2011-NK-kaalin 11 1 /opt/topspin NK

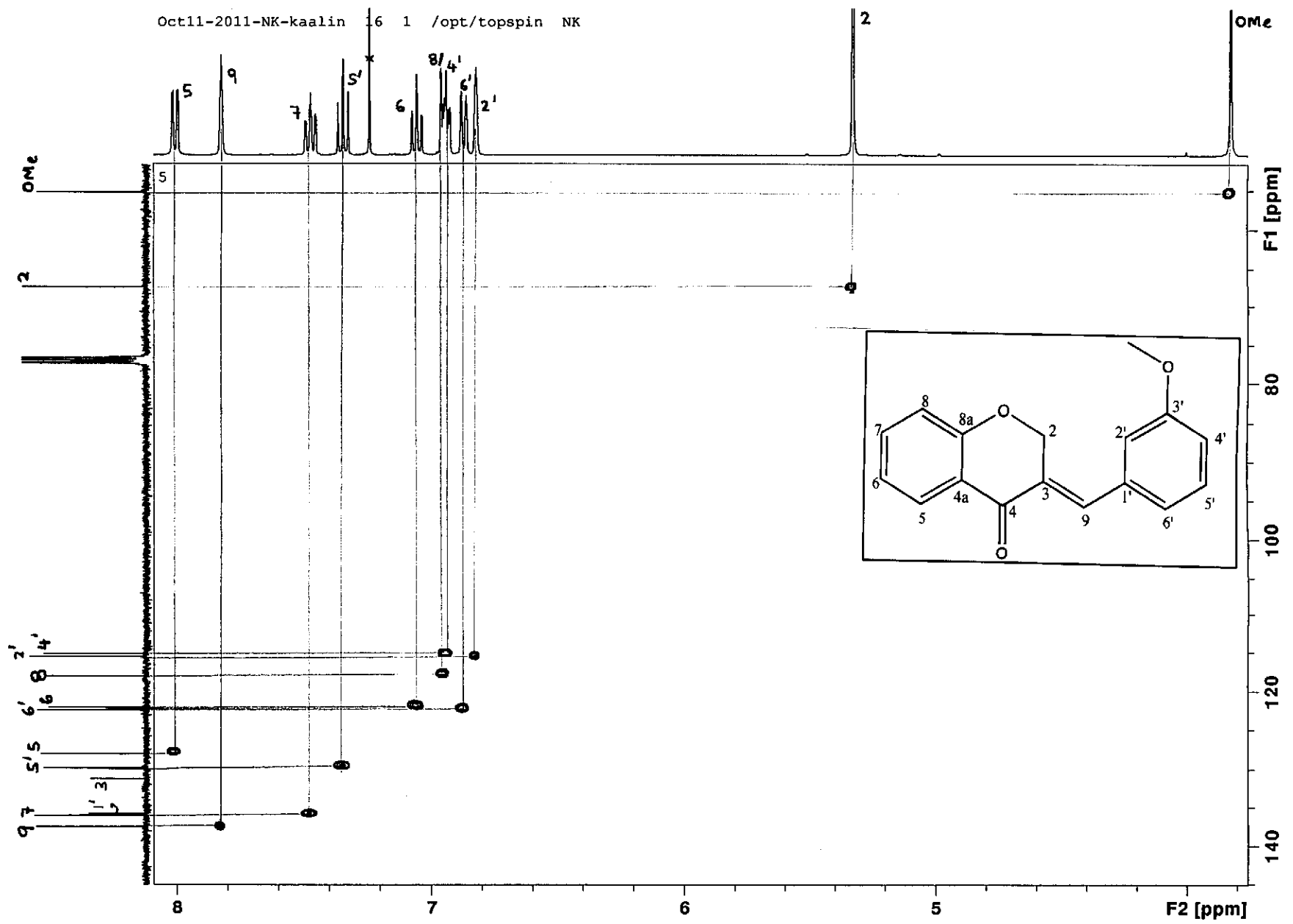




COSY spectrum of compound 5

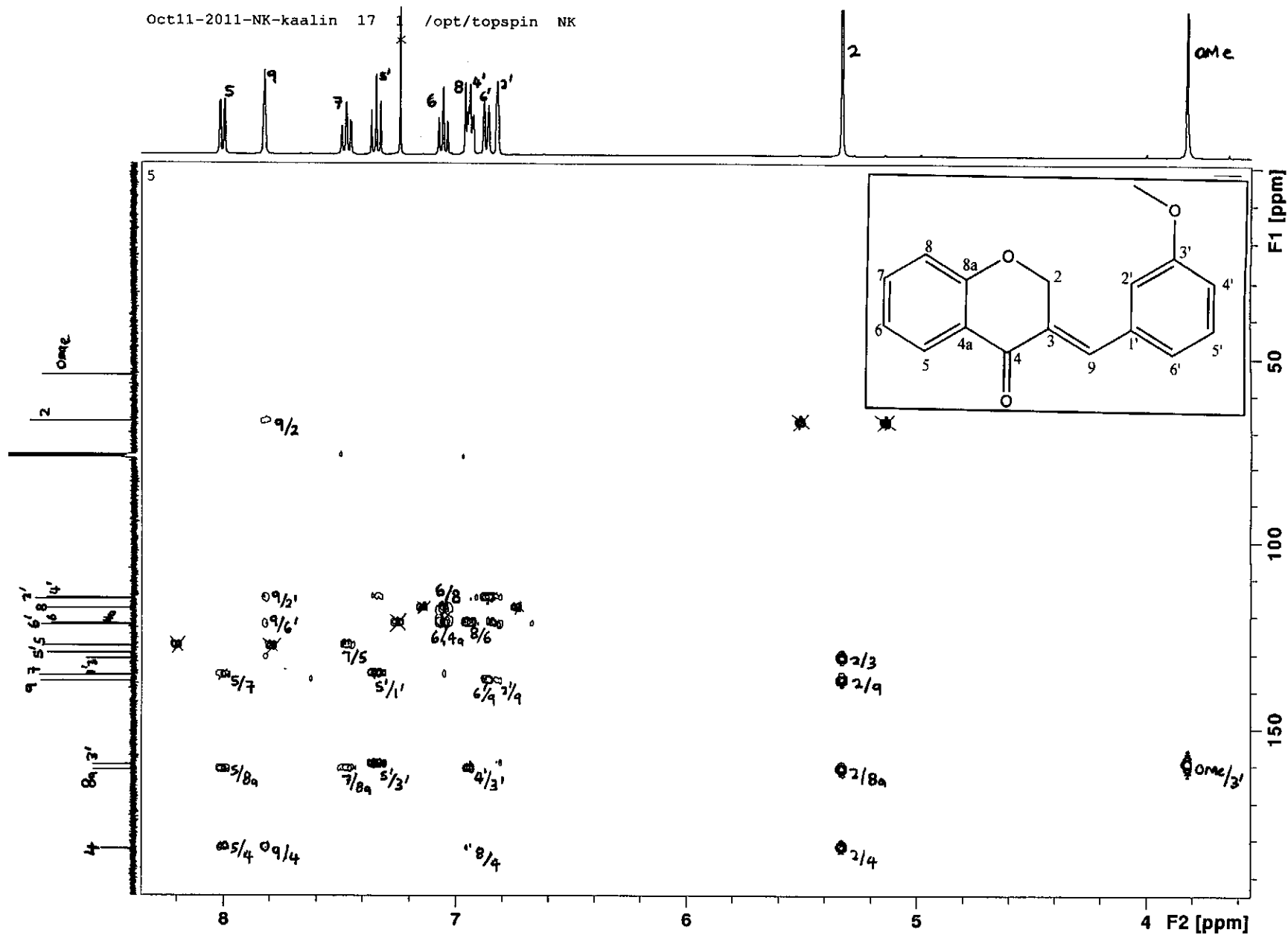


COSY spectrum of compound 5 (expanded)



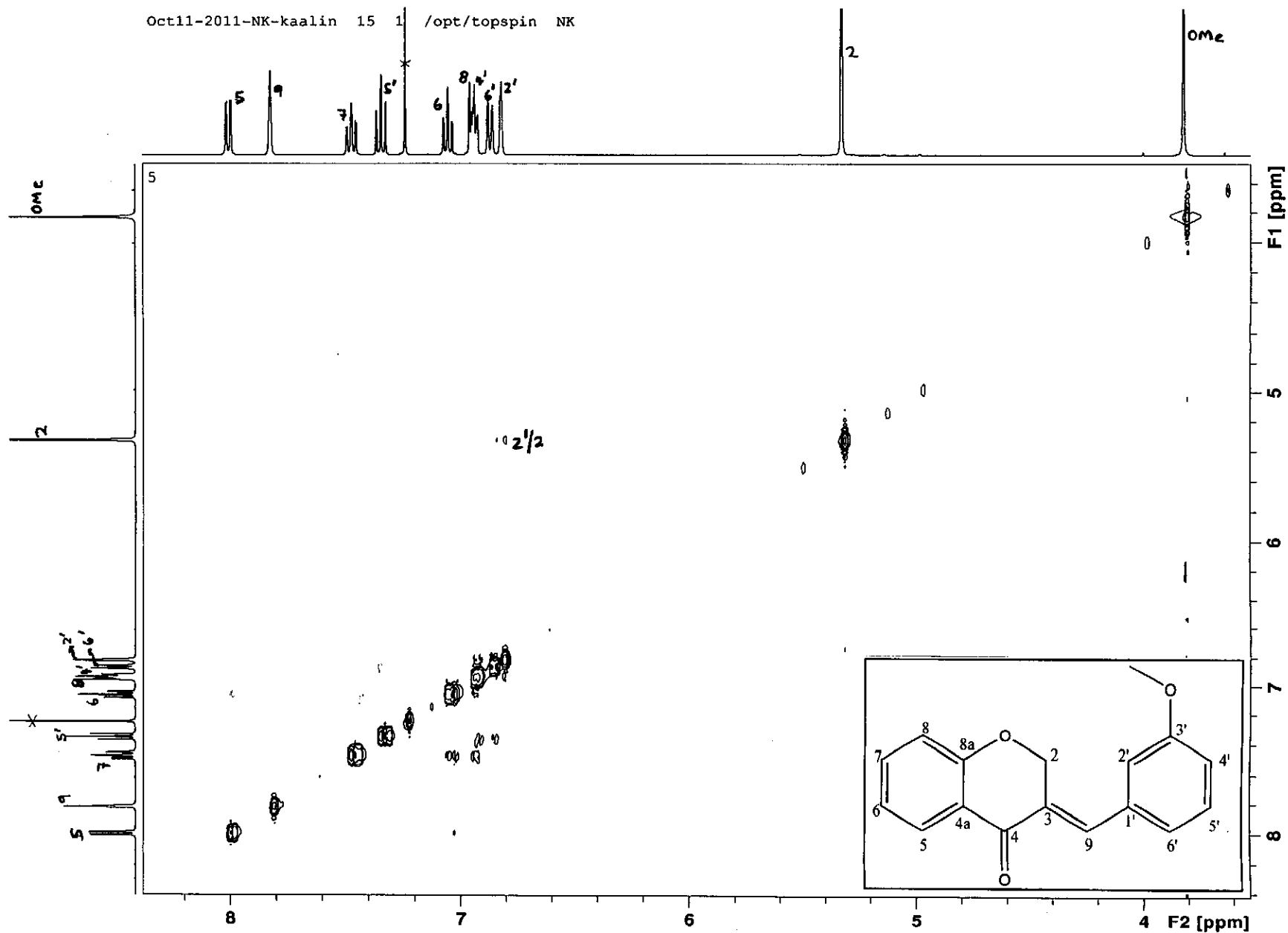
HSQC spectrum of compound 5

Oct11-2011-NK-kaalin 17 /opt/topspin NK



HMBC spectrum of compound 5

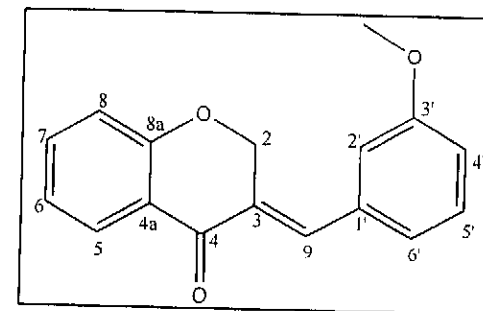
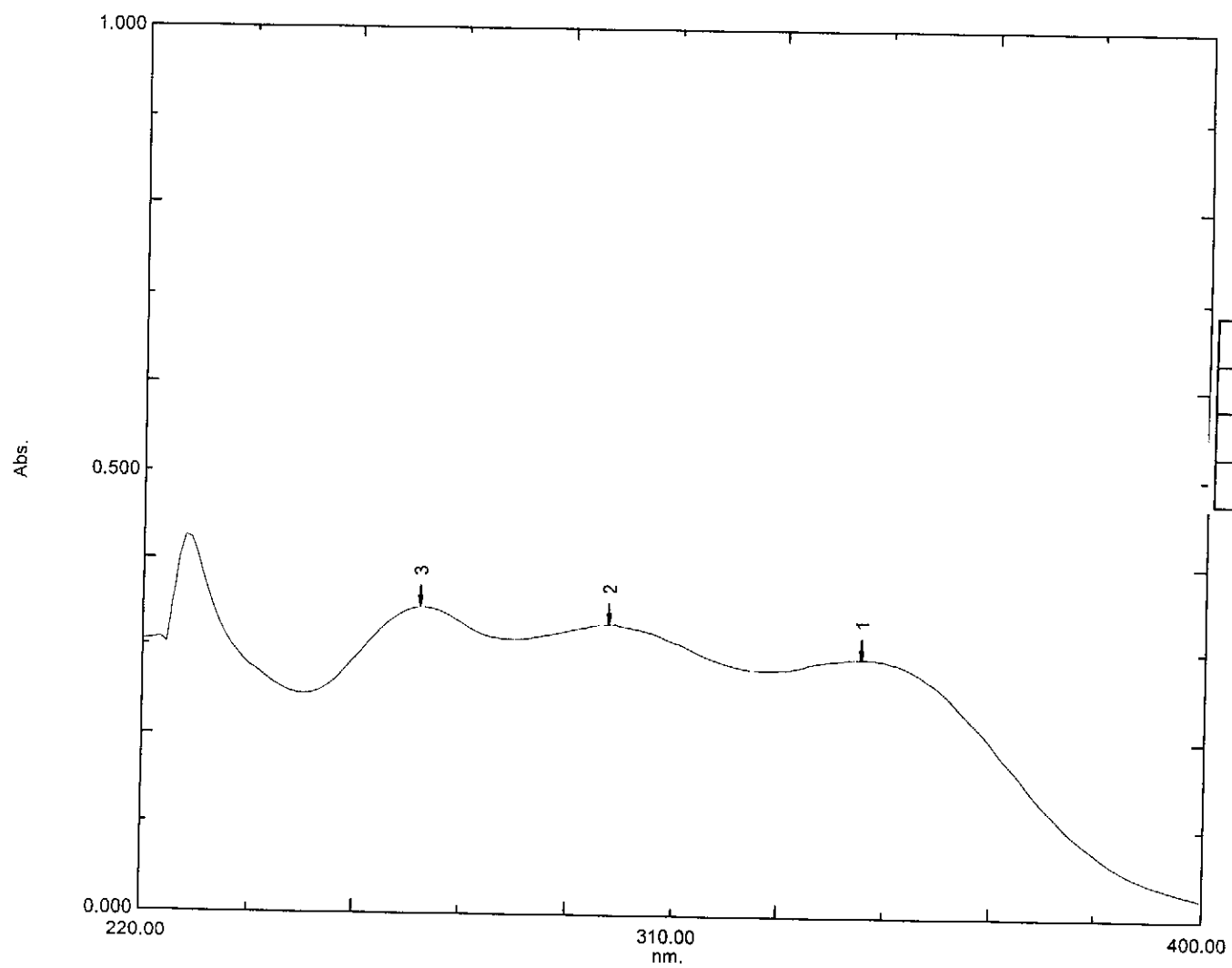
Oct11-2011-NK-kaalin 15 1 /opt/topspin NK



NOESY spectrum of compound 5

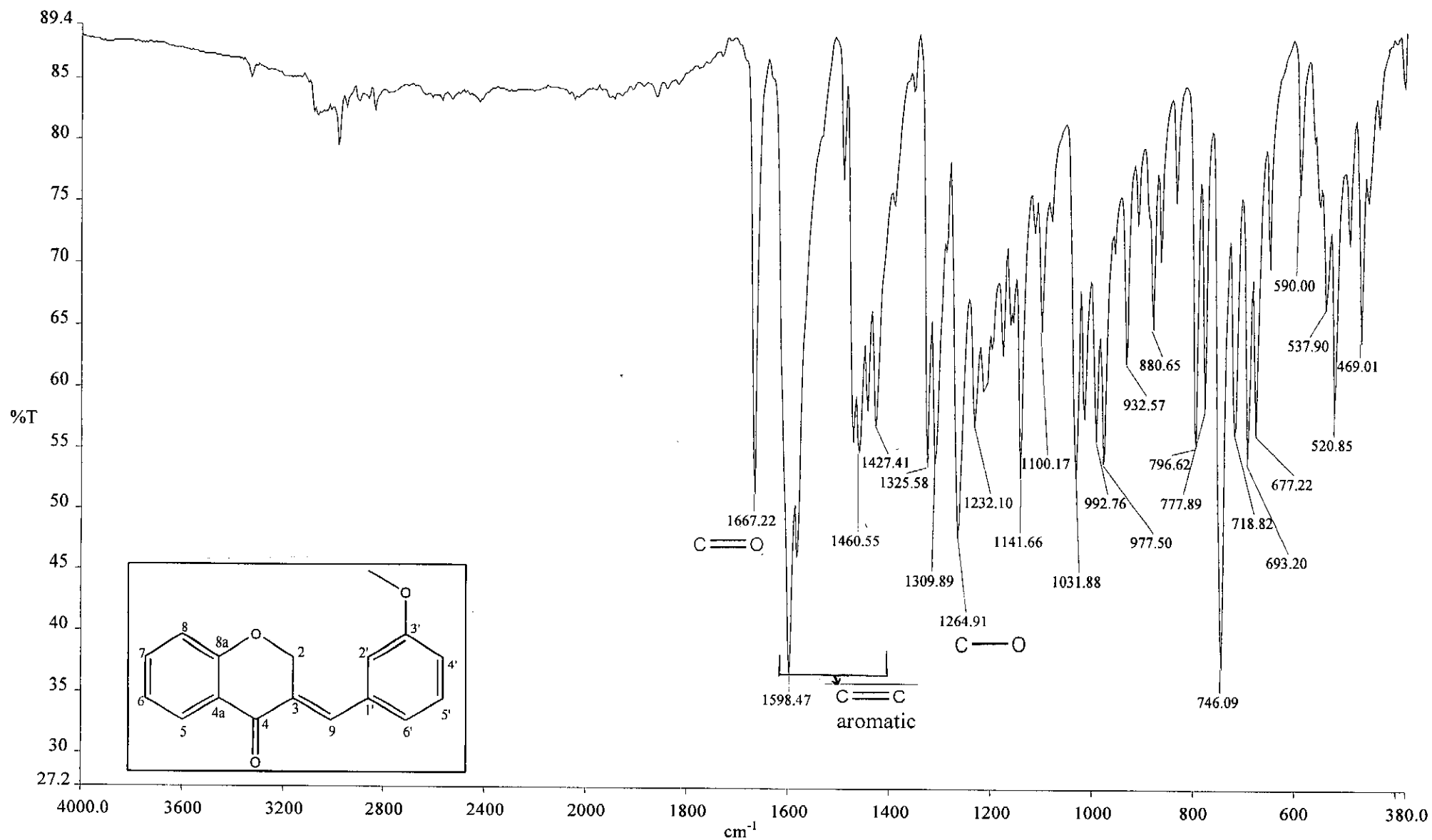
Overlay Spectrum Graph Report

15/05/2012 12:54:28 PM



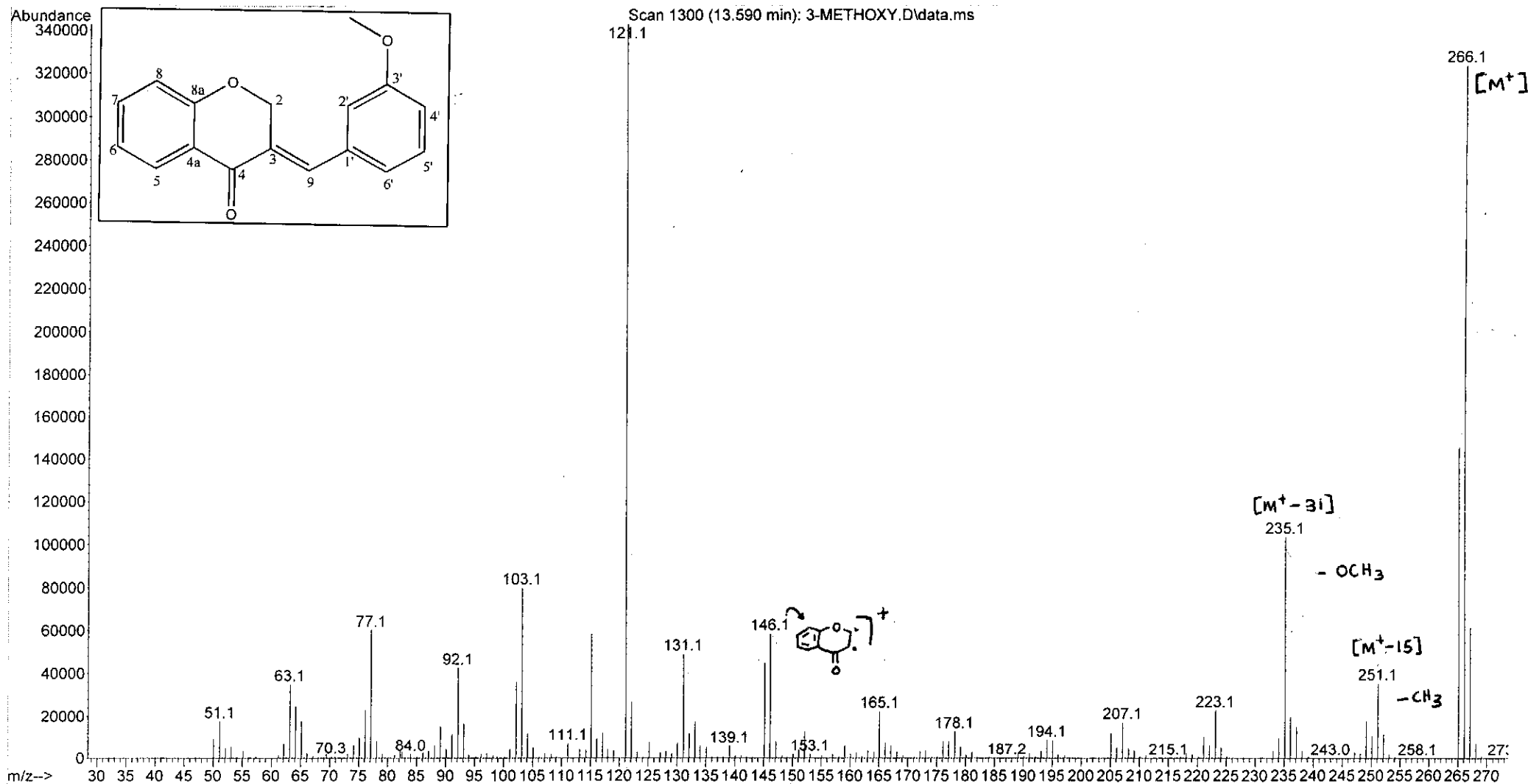
Wavelength/ nm	Absorbance	Log ϵ
267	0.345	4.06
298	0.327	4.04
342	0.291	3.99

UV-Vis spectrum of compound 5

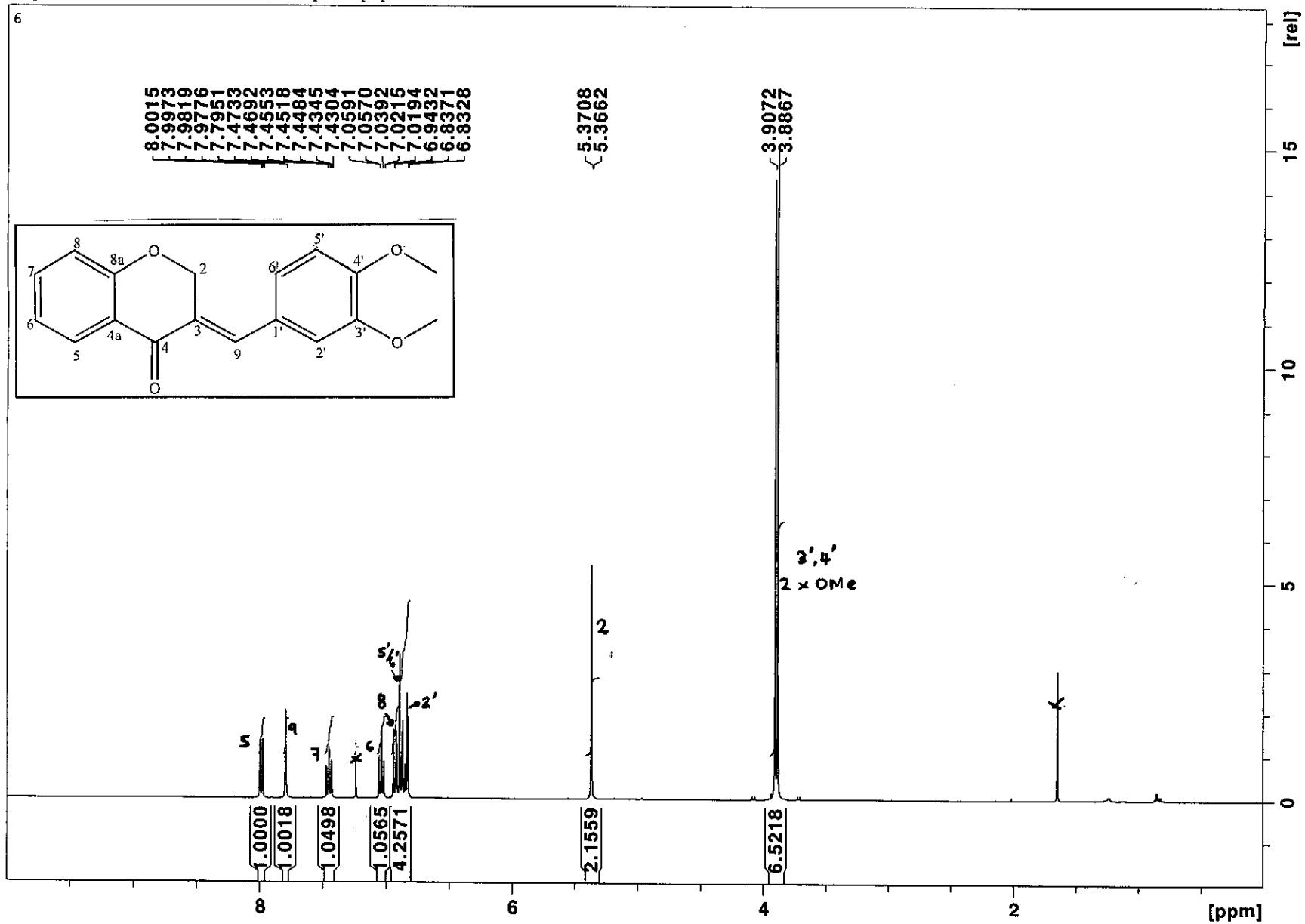


Infrared spectrum of compound 5

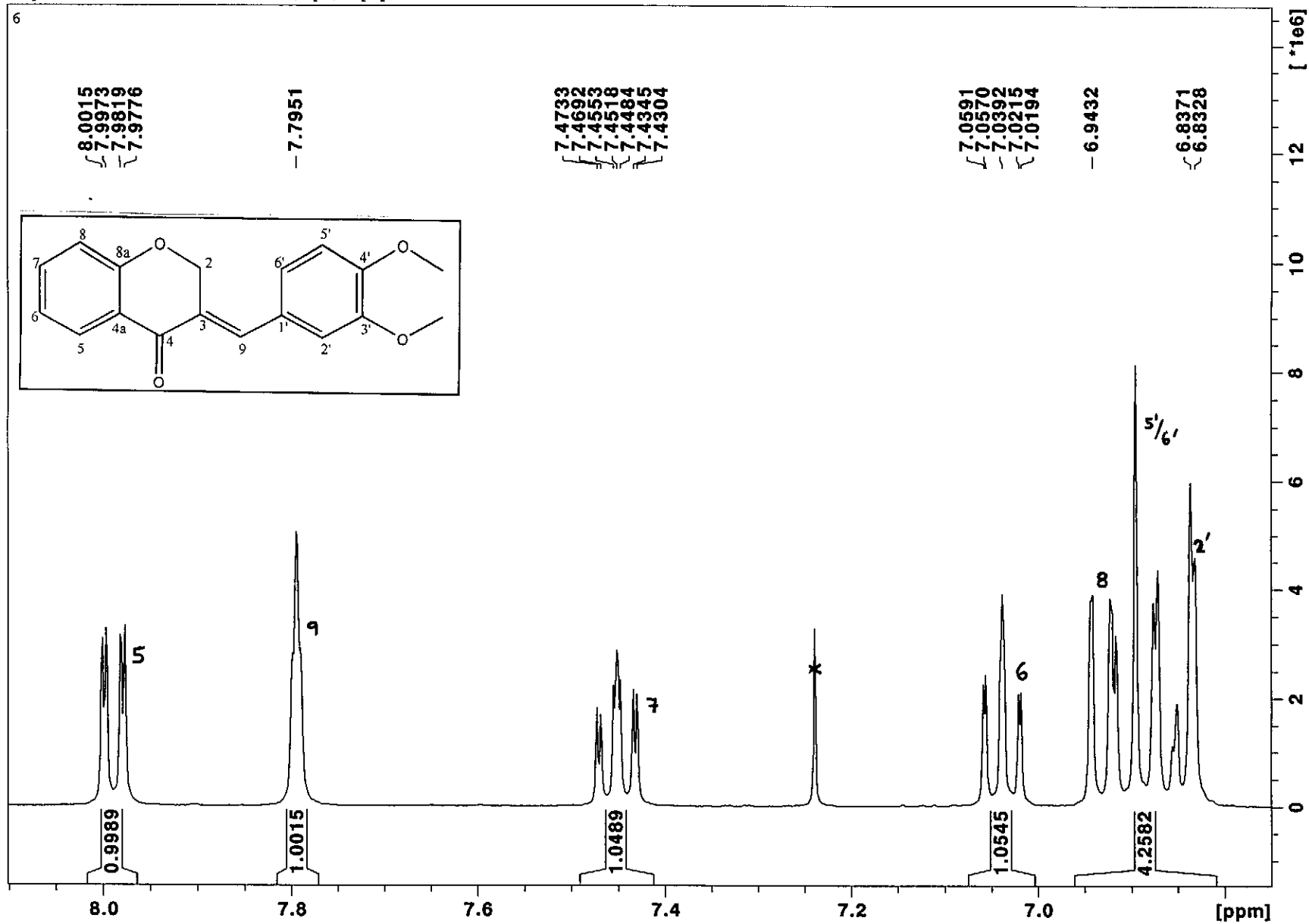
File :C:\msdchem\1\data\kaalin\3-METHOXY.D
 Operator :
 Acquired : 12 Jan 2012 13:41 using AcqMethod NATPRODUCTS MANUAL INJ.M
 Instrument : 5973N
 Sample Name:
 Misc Info :
 Vial Number: 1



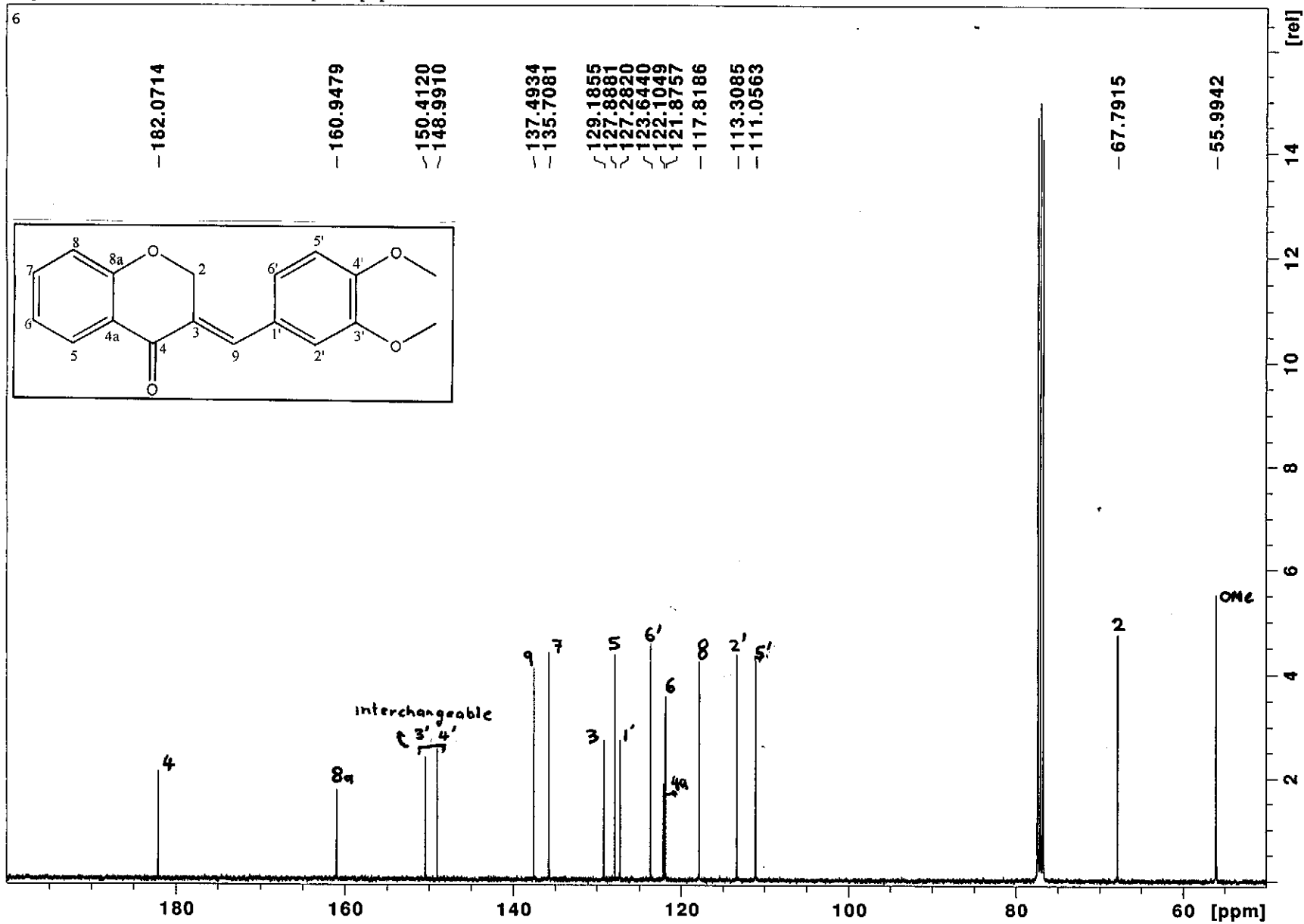
Mass spectrum of compound 5



¹H NMR spectrum of compound 6

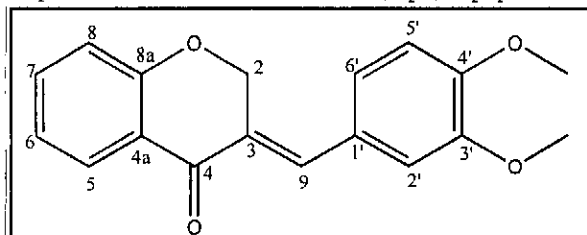


¹H NMR spectrum of compound 6 (expanded)

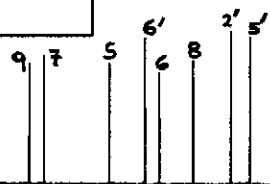


¹³C NMR spectrum of compound 6

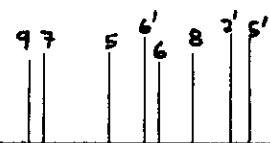
Sep30-2011-NK-KAALIN 11 1 /opt/topspin NK



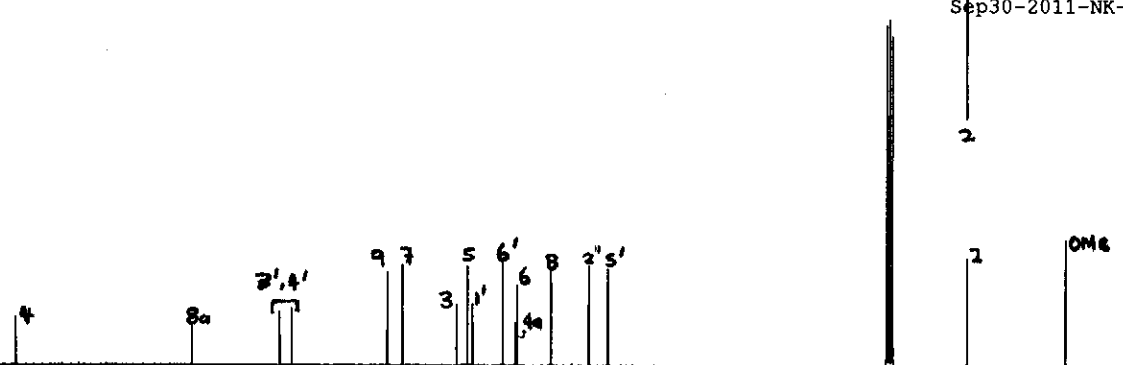
Sep30-2011-NK-KAALIN 14 1 /opt/topspin NK



Sep30-2011-NK-KAALIN 15 1 /opt/topspin NK



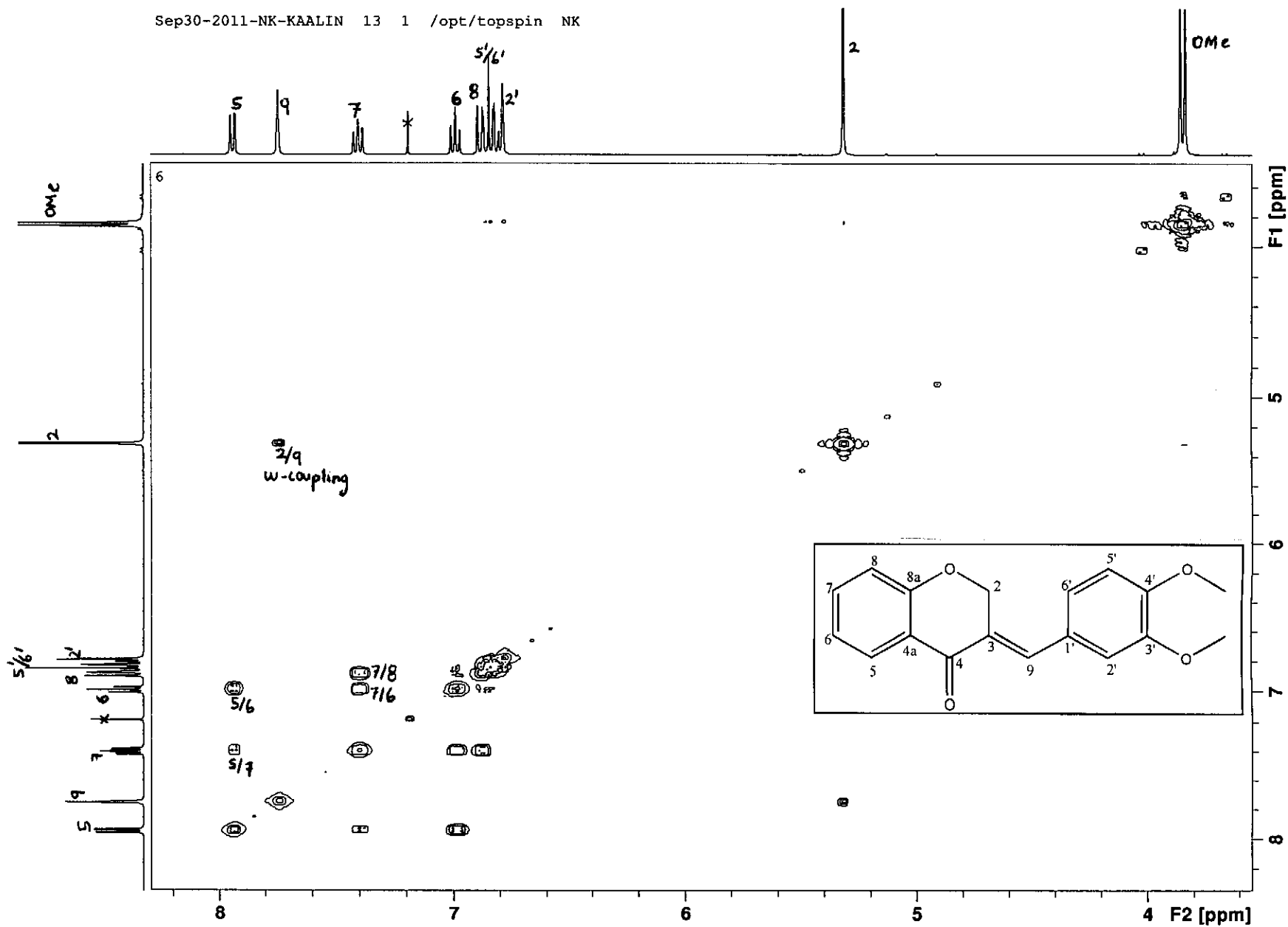
Sep30-2011-NK-KAALIN 11 1 /opt/topspin NK



150 100 50 [ppm]

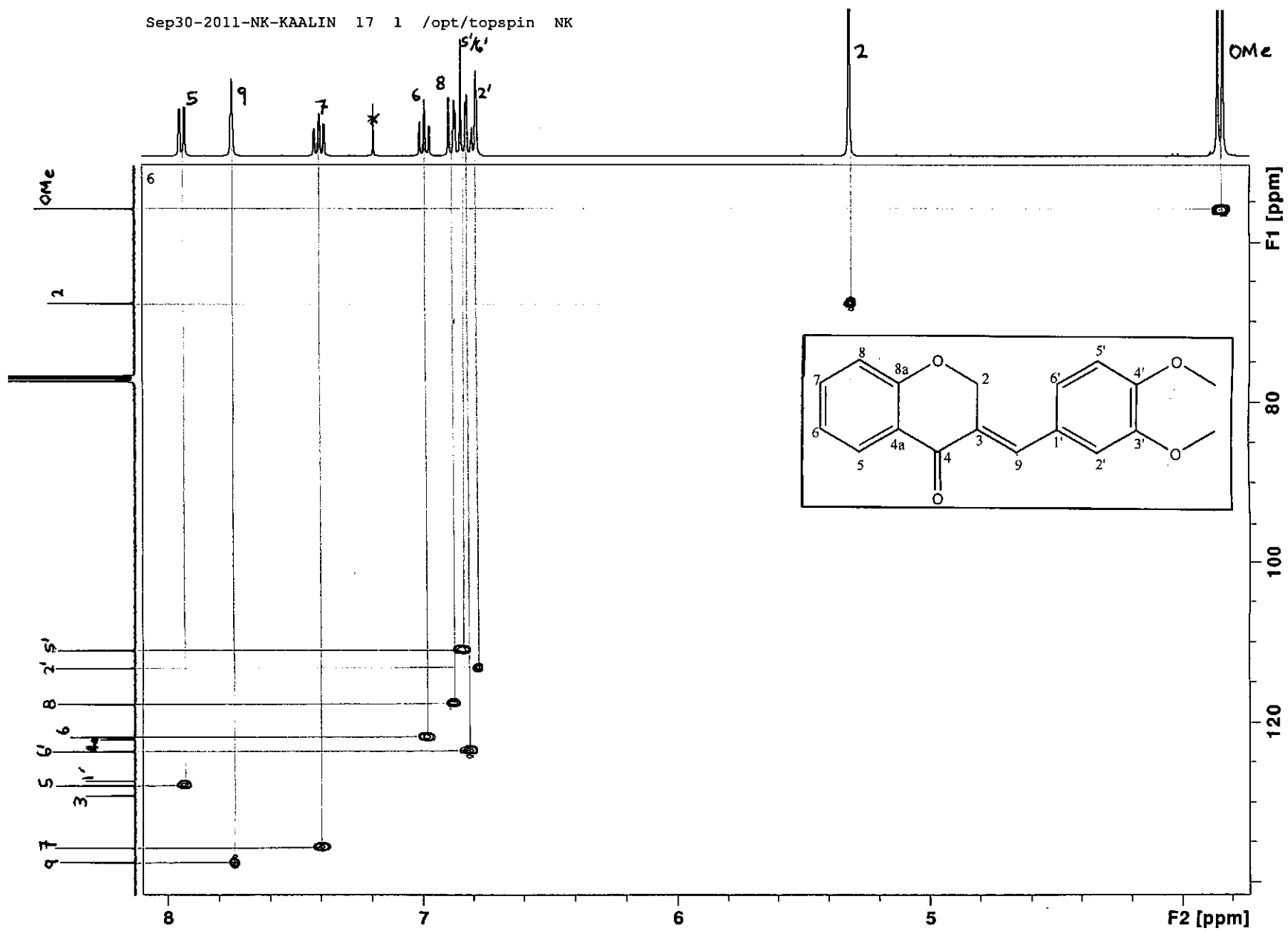
DEPT spectrum of compound 6

Sep30-2011-NK-KAALIN 13 1 /opt/topspin NK



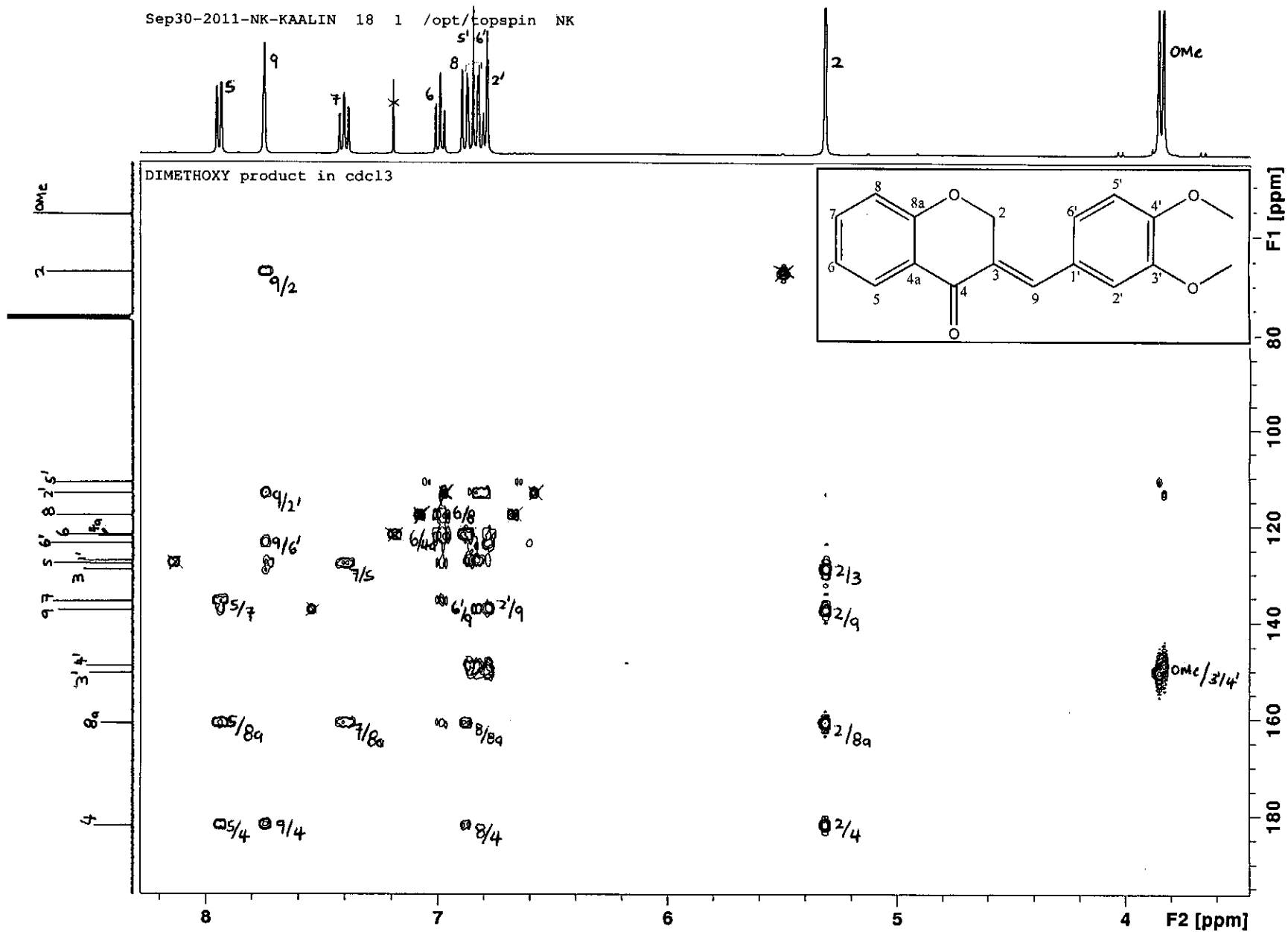
COSY spectrum of compound 6

Sep30-2011-NK-KAALIN 17 1 /opt/topspin NK



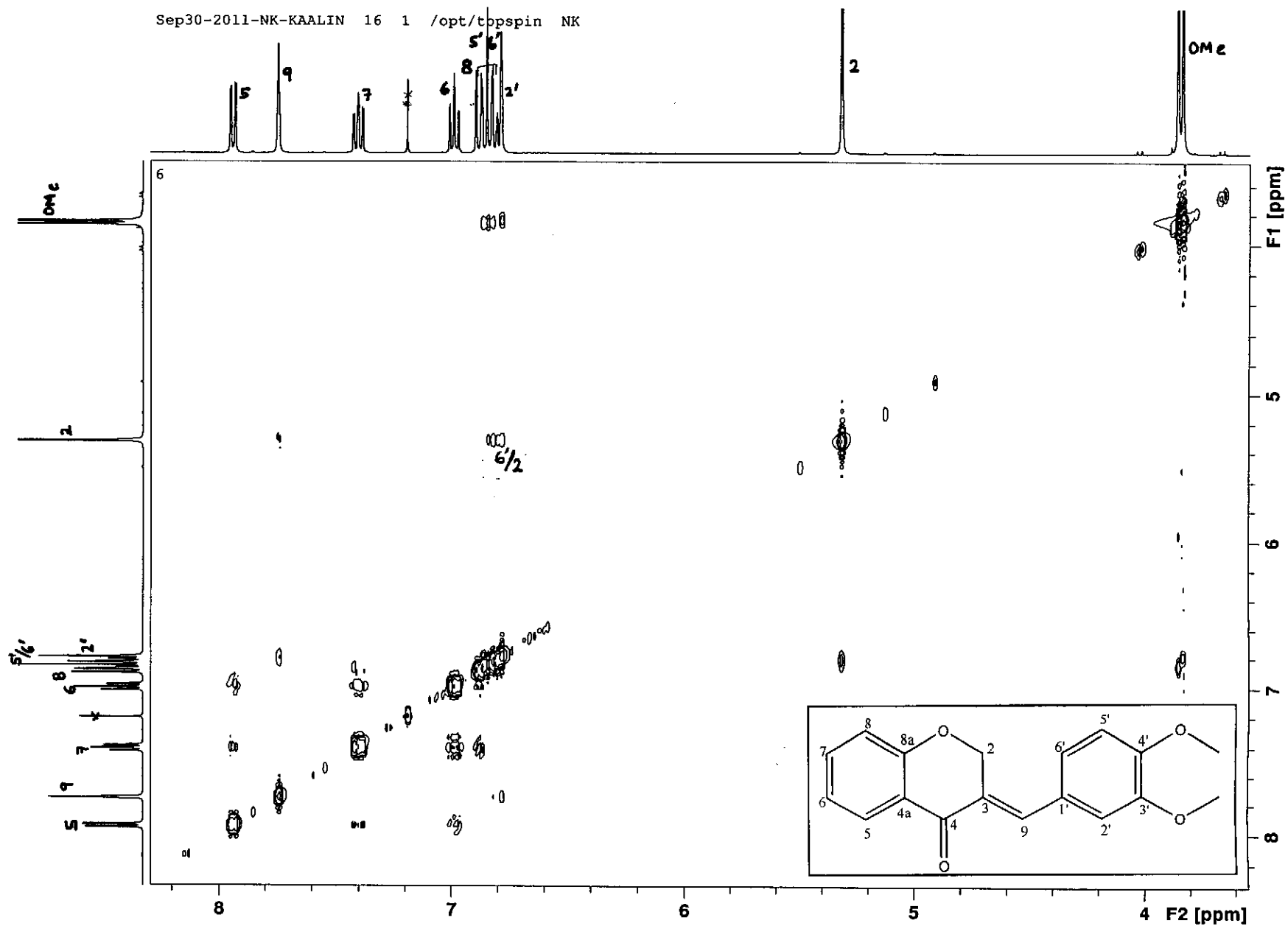
HSQC spectrum of compound 6

Sep30-2011-NK-KAALIN 18 1 /opt/topspin NK



HMBC spectrum of compound 6

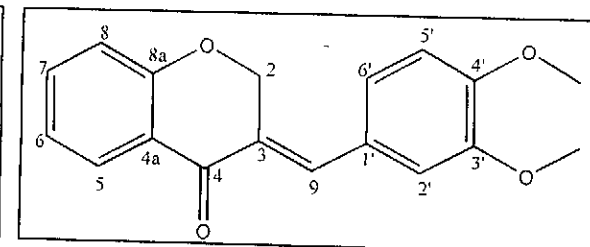
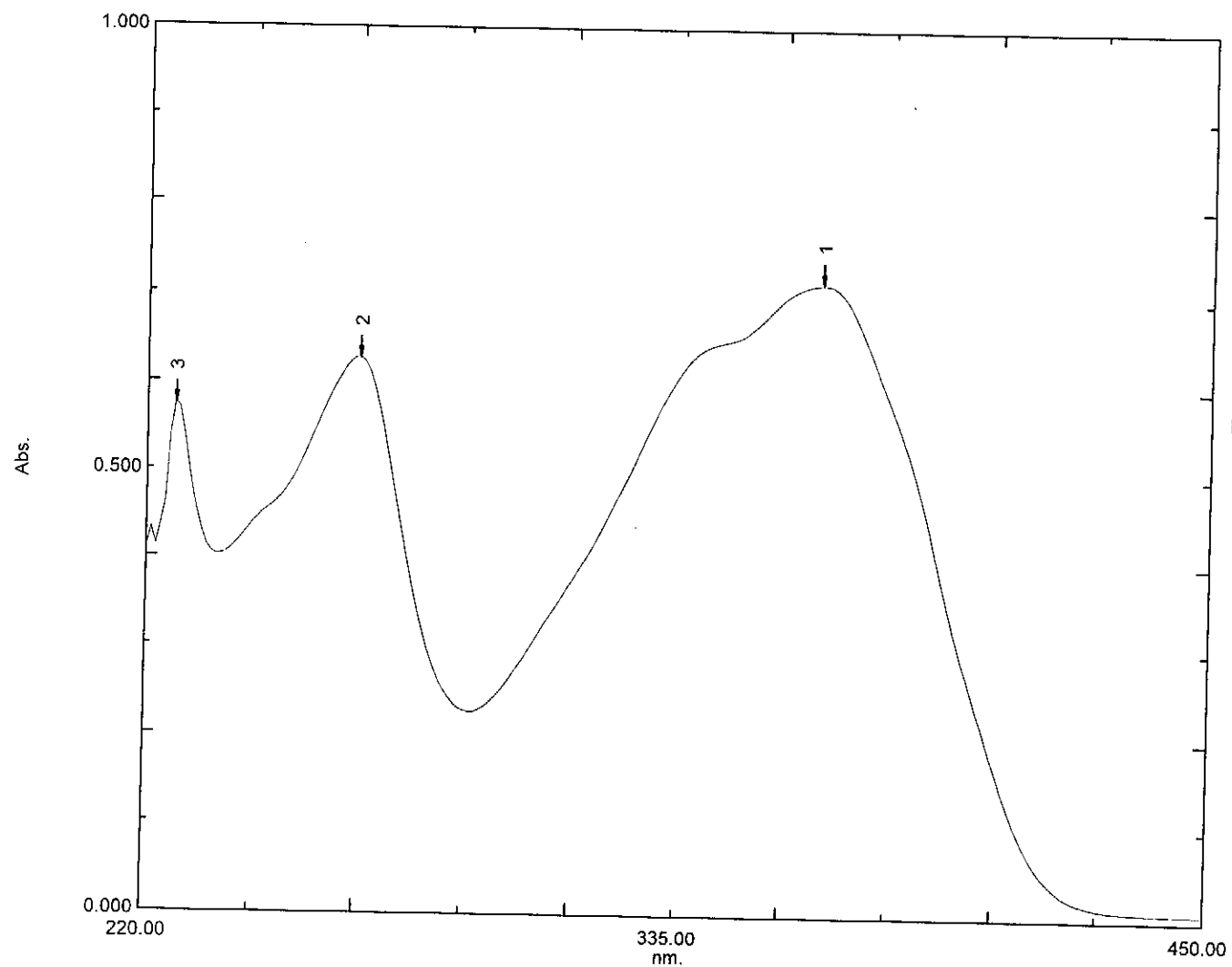
Sep30-2011-NK-KAALIN 16 1 /opt/tbpcspin NK



NOESY spectrum of compound 6

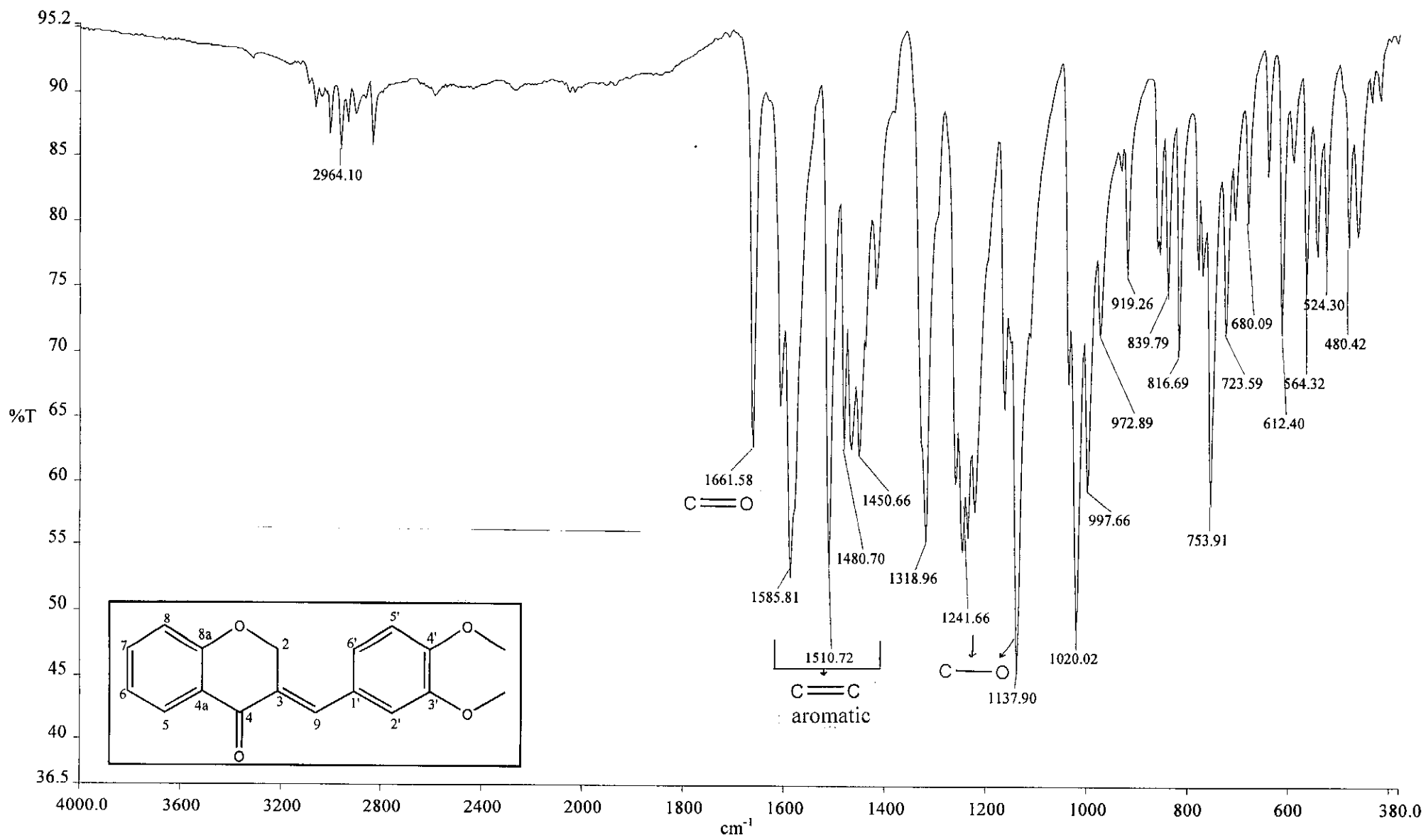
Overlay Spectrum Graph Report

15/05/2012 12:57:02 PM



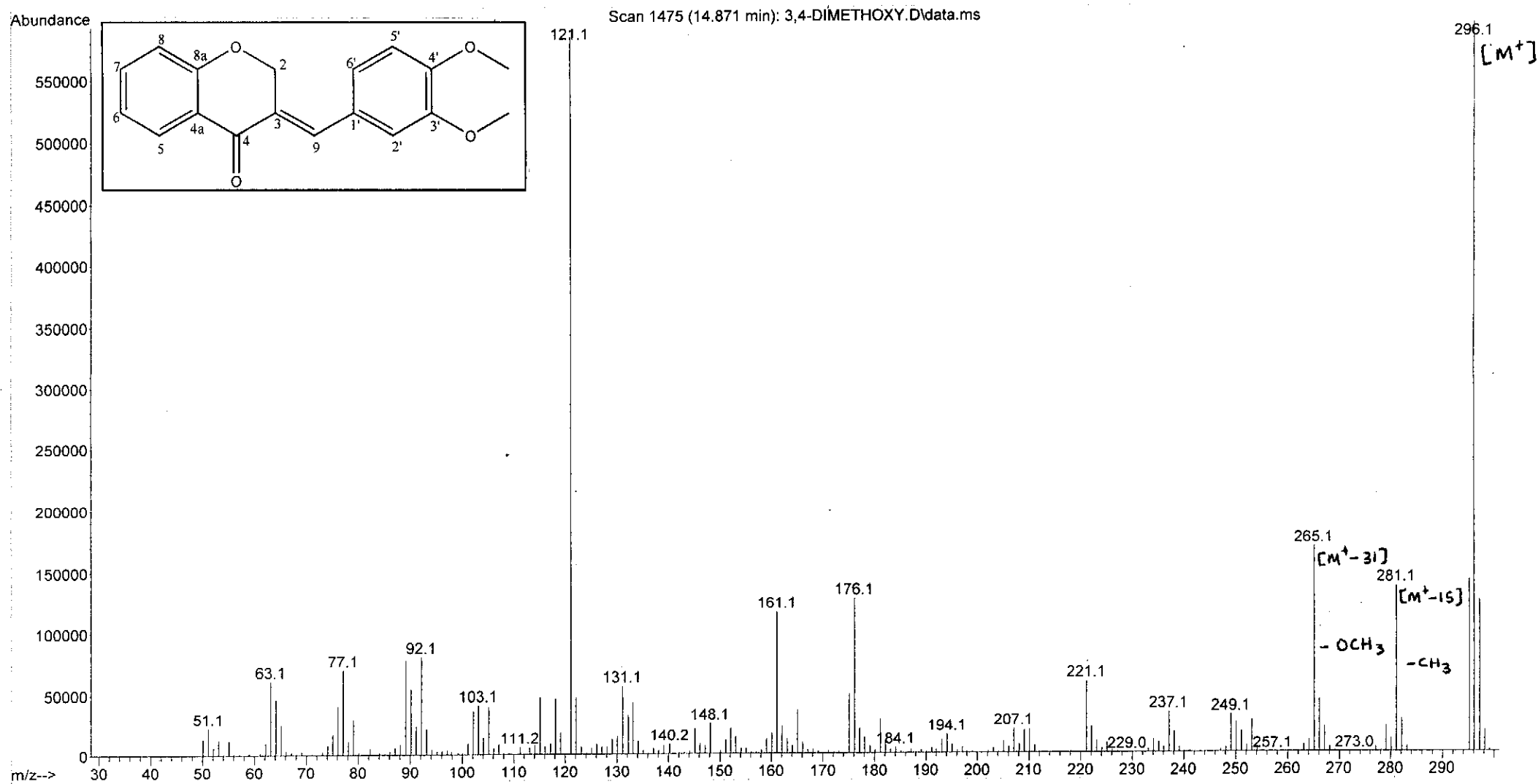
Wavelength/ nm	Absorbance	Log ϵ
266	0.629	4.22
366	0.715	4.28

UV-Vis spectrum of compound 6



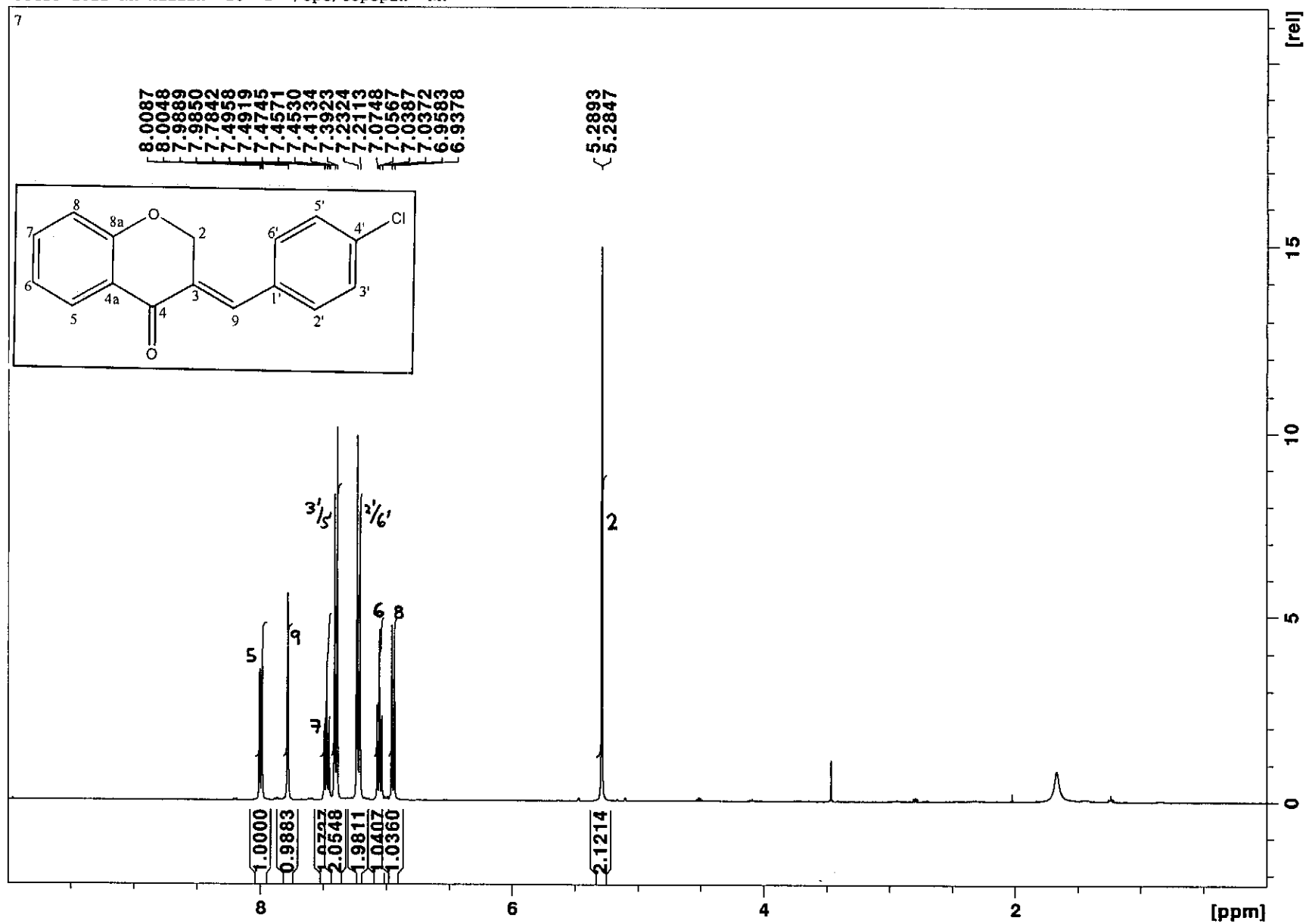
Infrared spectrum of compound 6

File :C:\msdchem\1\data\kaalin\3,4-DIMETHOXY.D
Operator :
Acquired : 12 Jan 2012 14:14 using AcqMethod NATPRODUCTS MANUAL INJ.M
Instrument : 5973N
Sample Name:
Misc Info :
Vial Number: 1

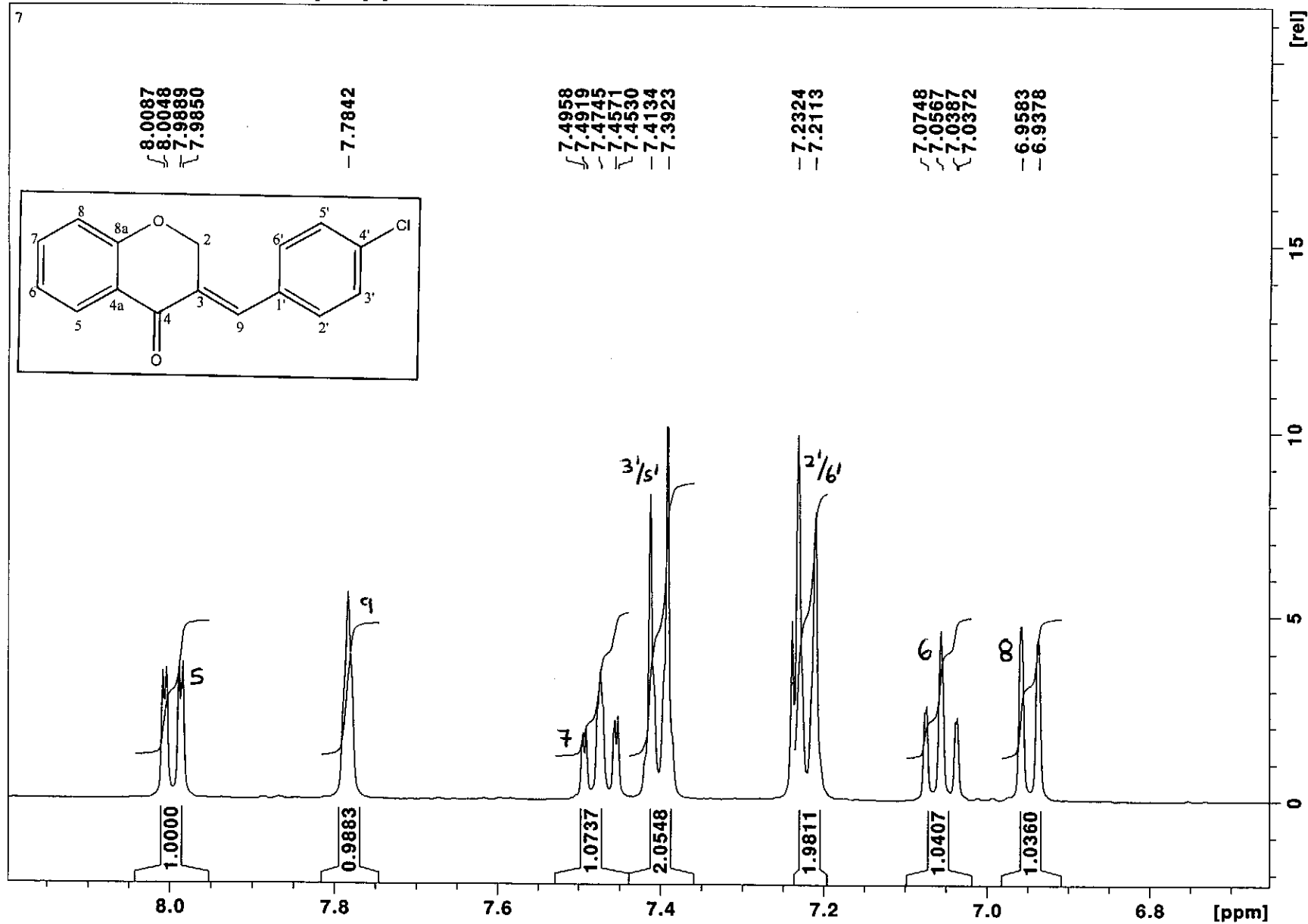


Mass spectrum of compound 6

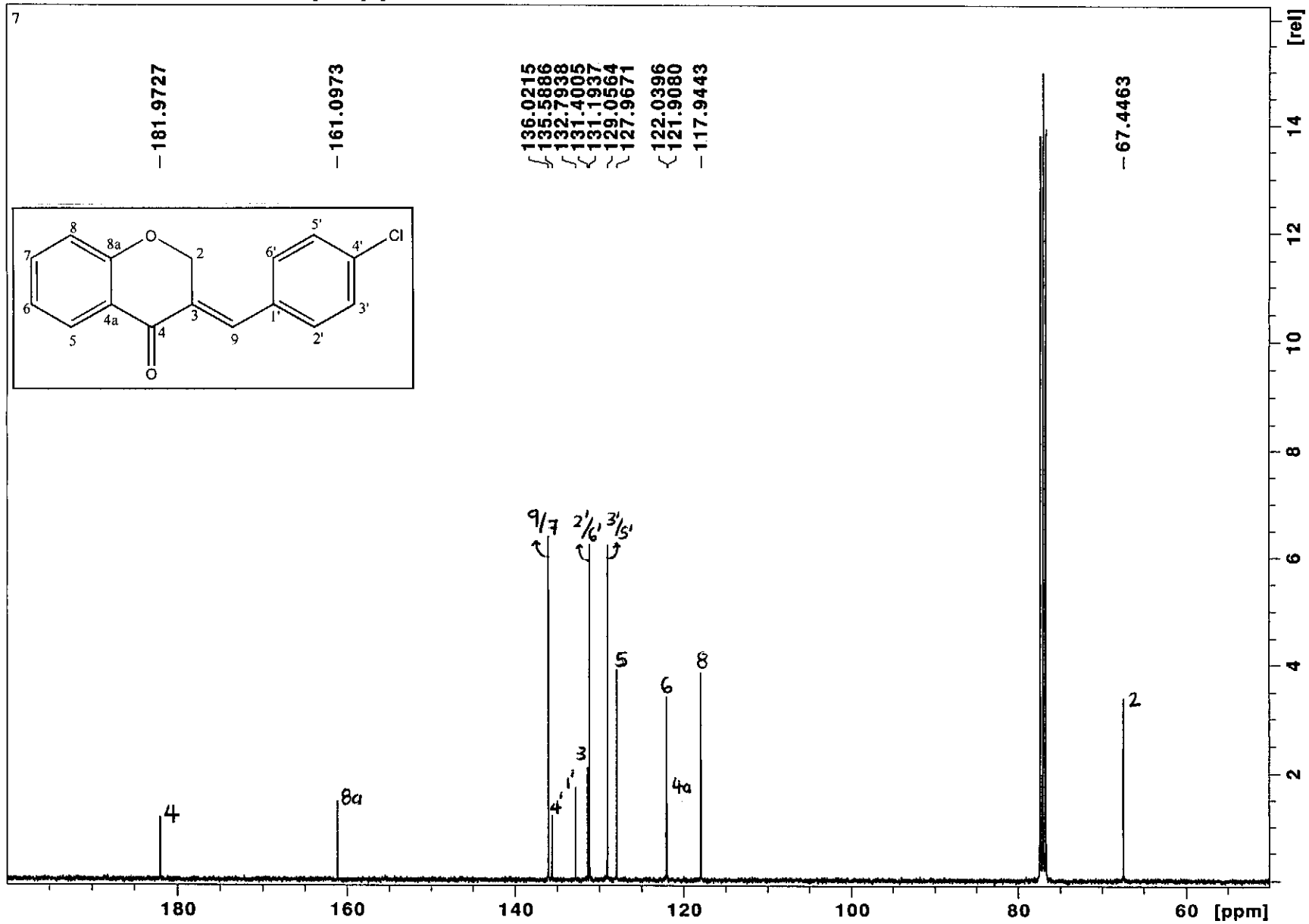
Oct15-2011-NK-kaalin 10 1 /opt/topspin NK



¹H NMR spectrum of compound 7

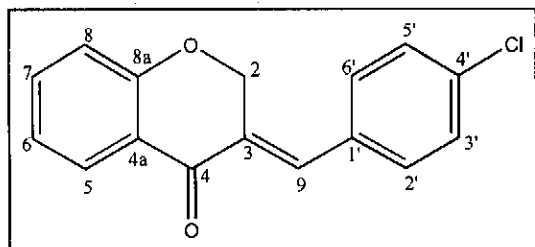


¹H NMR spectrum of compound 7 (expanded)

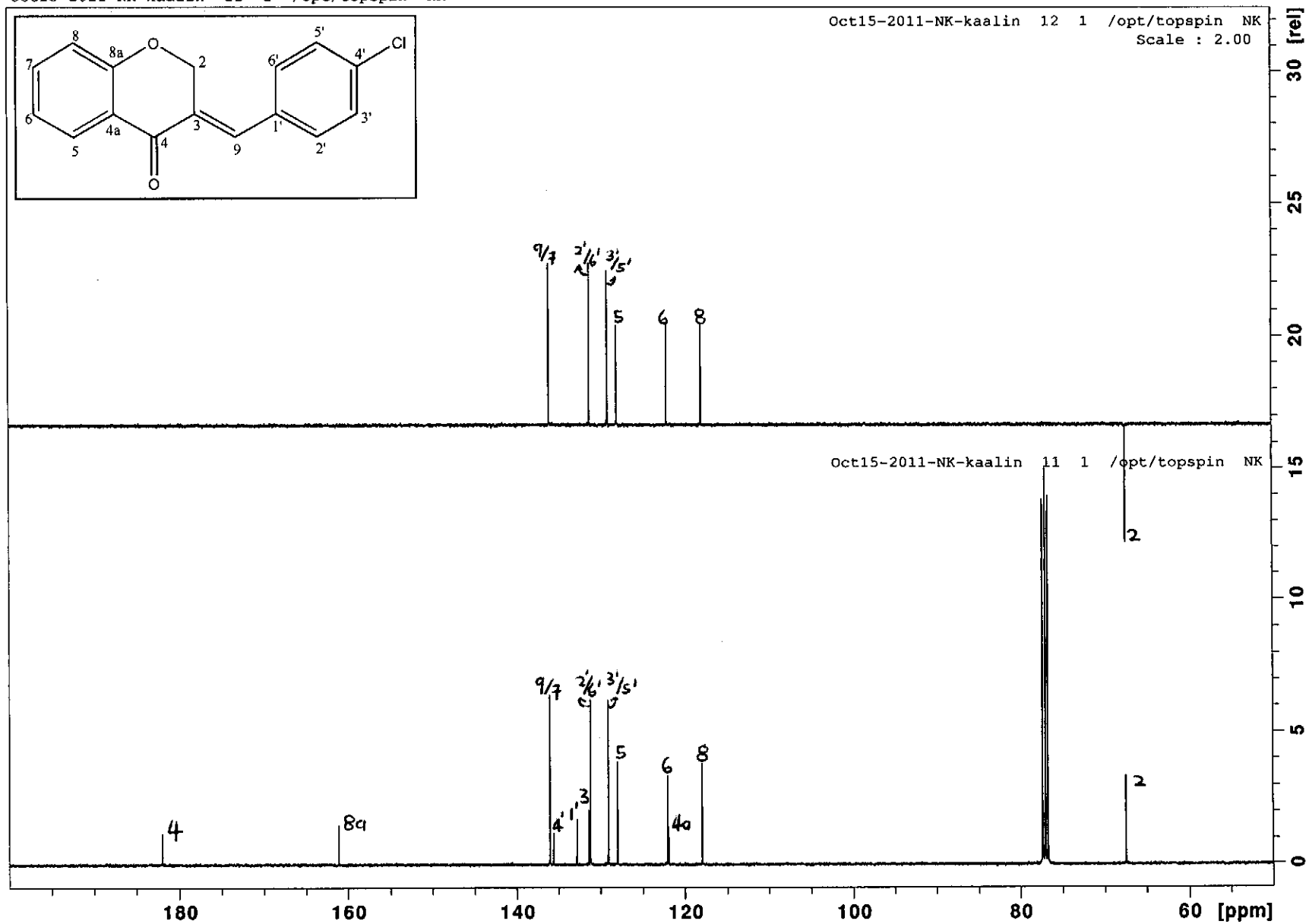


^{13}C NMR spectrum of compound 7

Oct15-2011-NK-kaalin 11 1 /opt/topspin NK

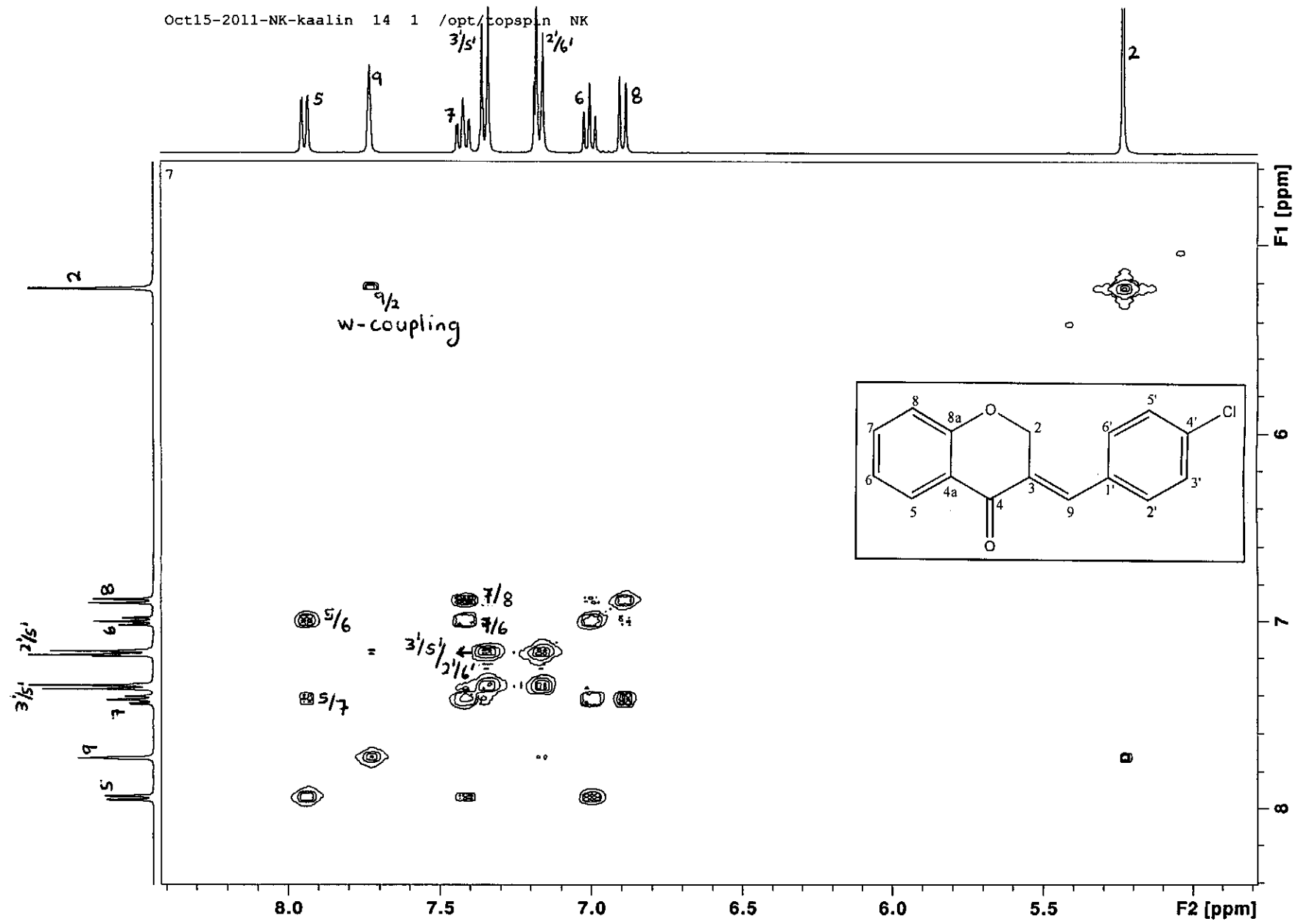


Oct15-2011-NK-kaalin 12 1 /opt/topspin NK
Scale : 2.00

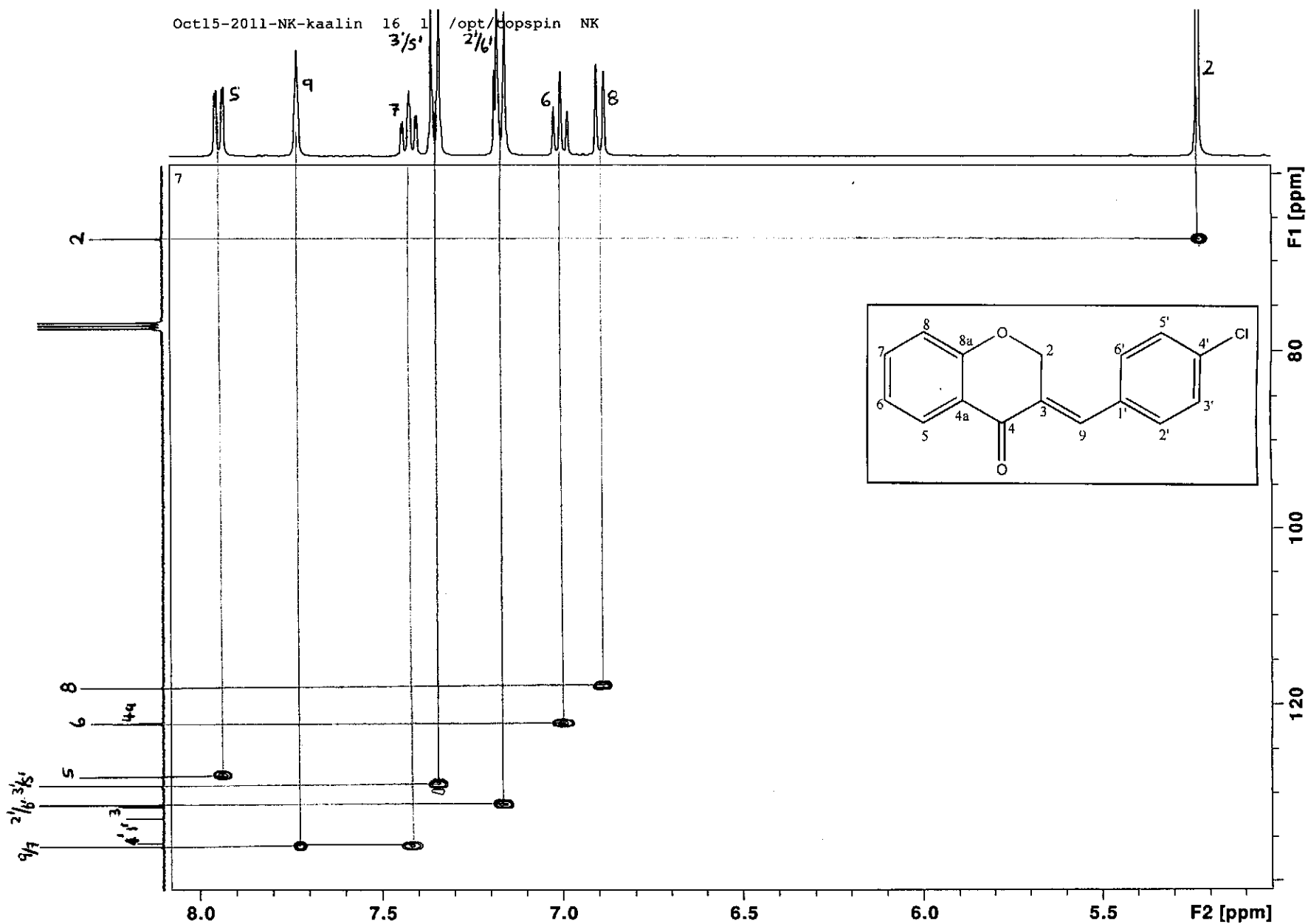


DEPT 135 spectrum of compound 7

Oct15-2011-NK-kaalin 14 1 /opt/topspin NK

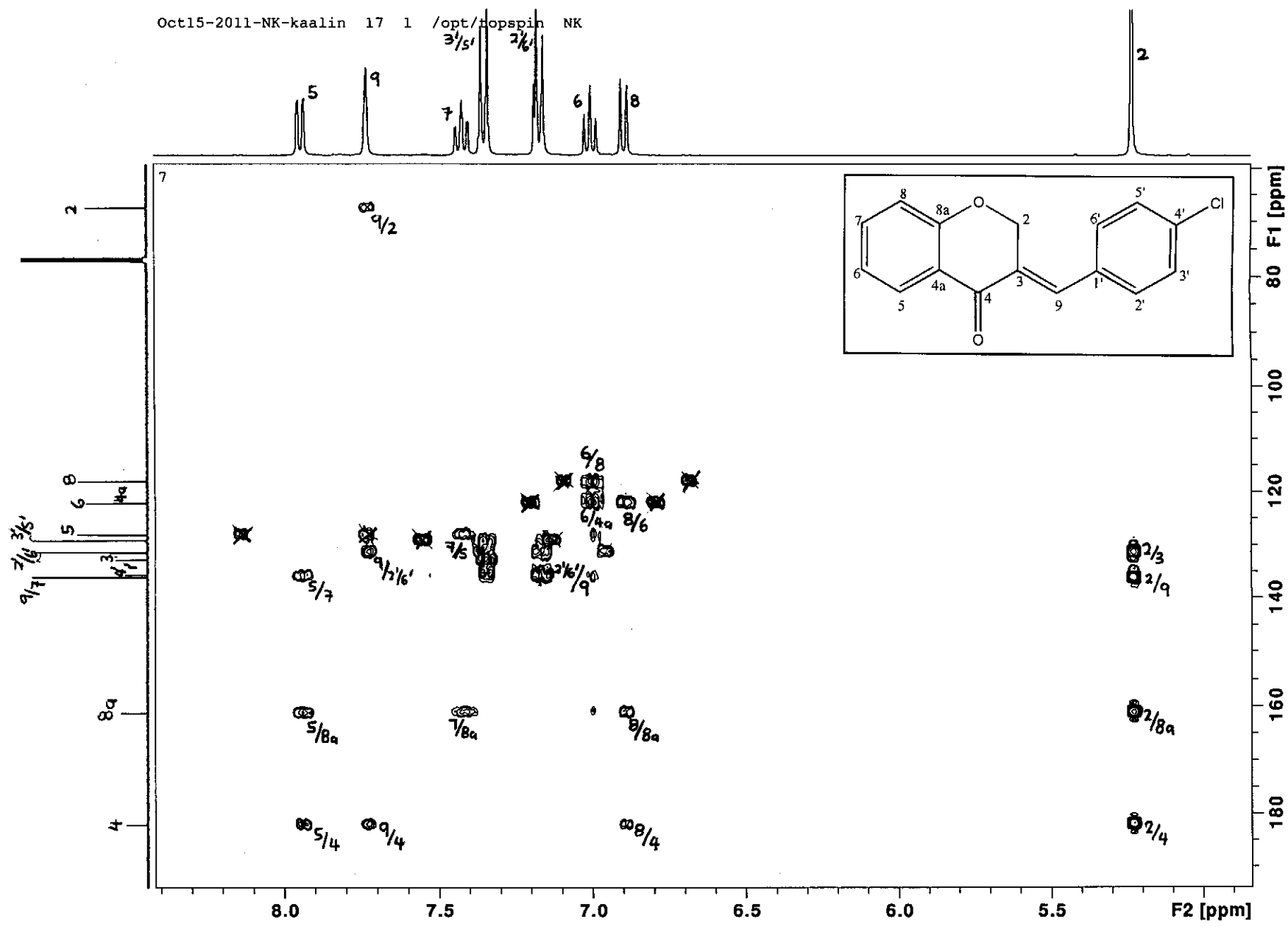


COSY spectrum of compound 7



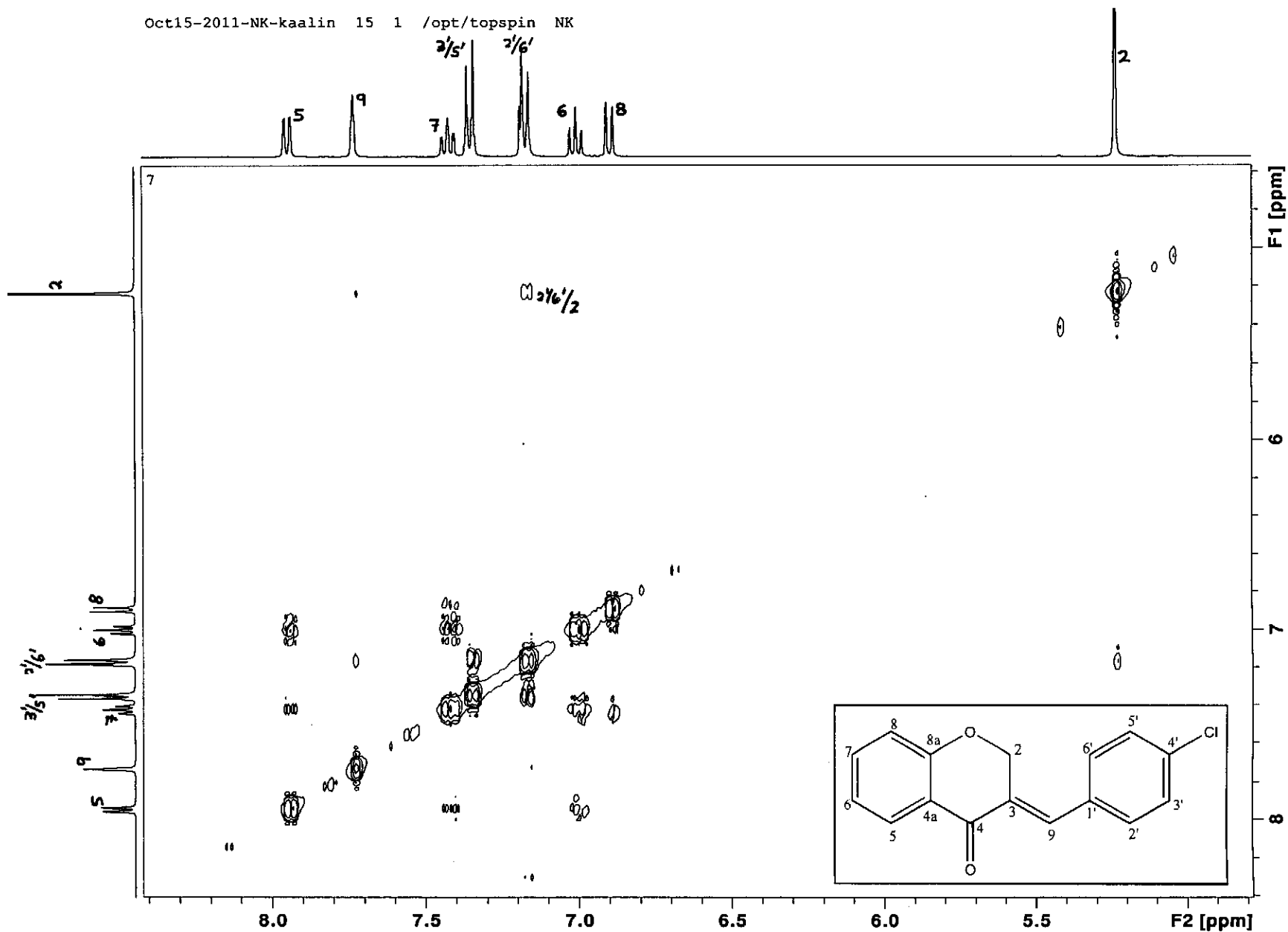
HSQC spectrum of compound 7

Oct15-2011-NK-kaalin 17 1 /opt/popspin NK



HMBC spectrum of compound 7

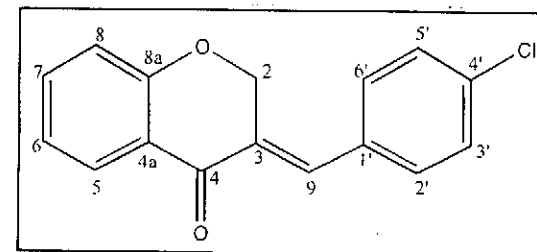
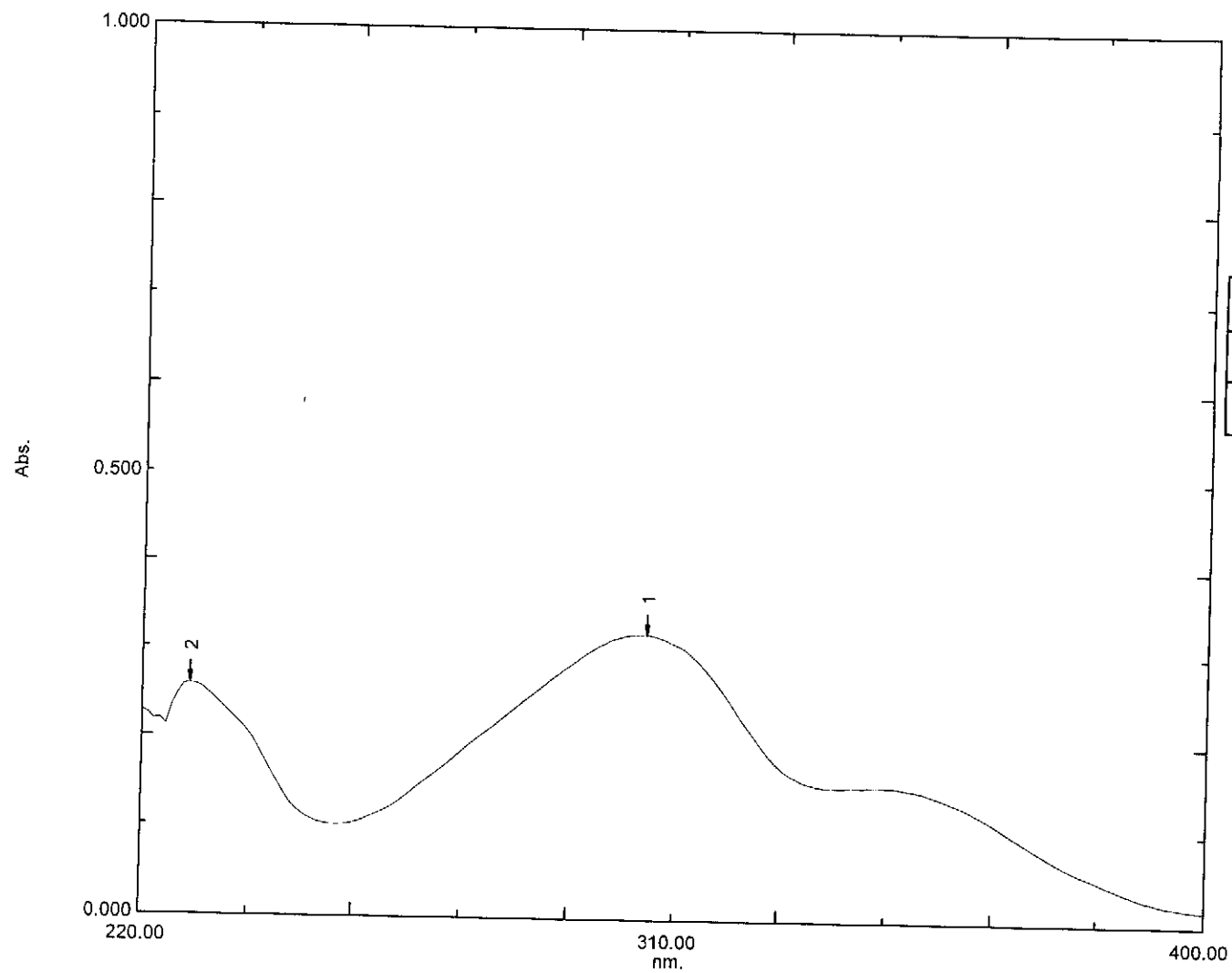
Oct15-2011-NK-kaalin 15 1 /opt/topspin NK



NOESY spectrum of compound 7

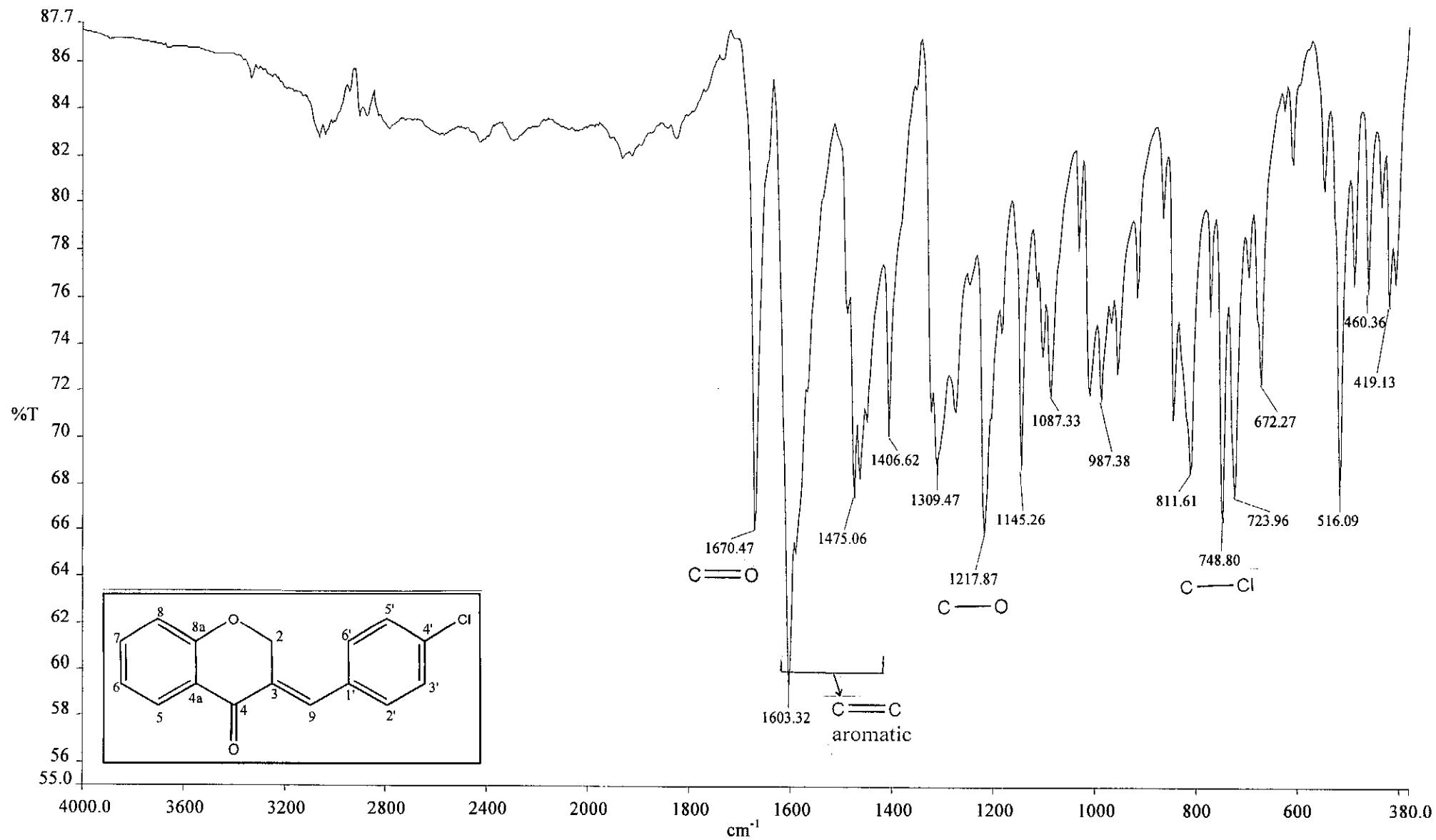
Overlay Spectrum Graph Report

15/05/2012 12:58:04 PM



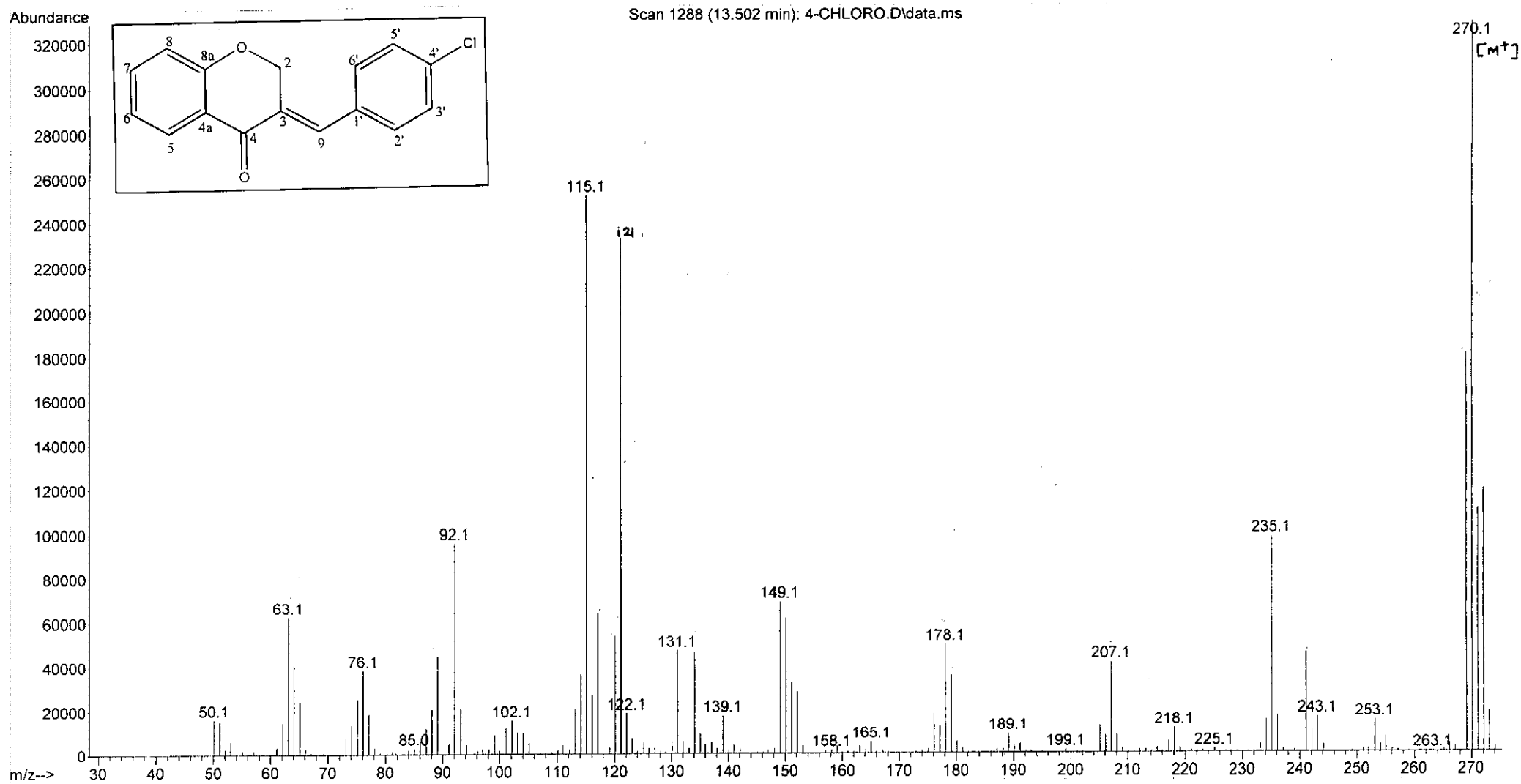
Wavelength/ nm	Absorbance	Log ϵ
302	0.320	4.20
345	0.152	3.88

UV-Vis spectrum of compound 7

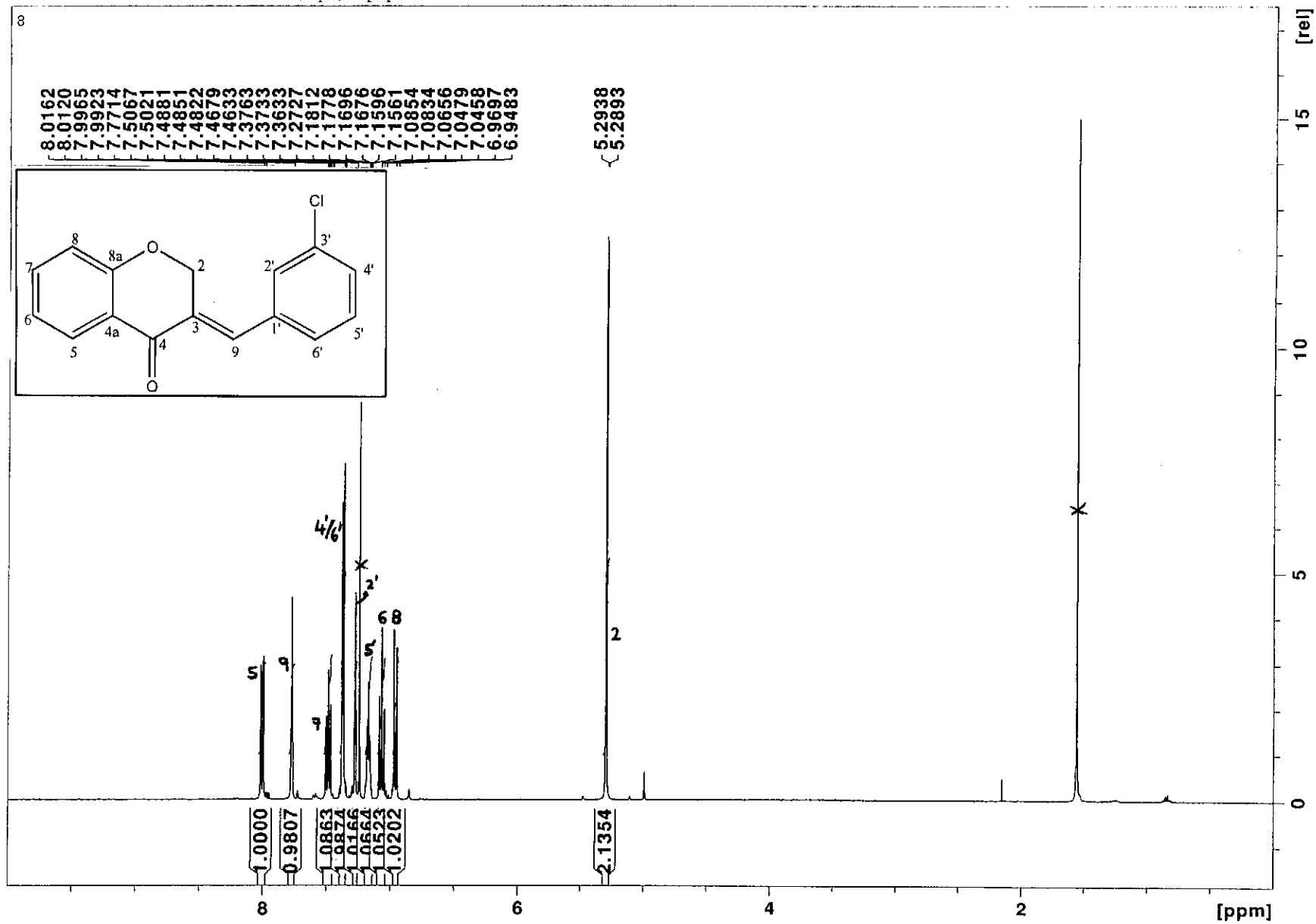


Infrared spectrum of compound 7

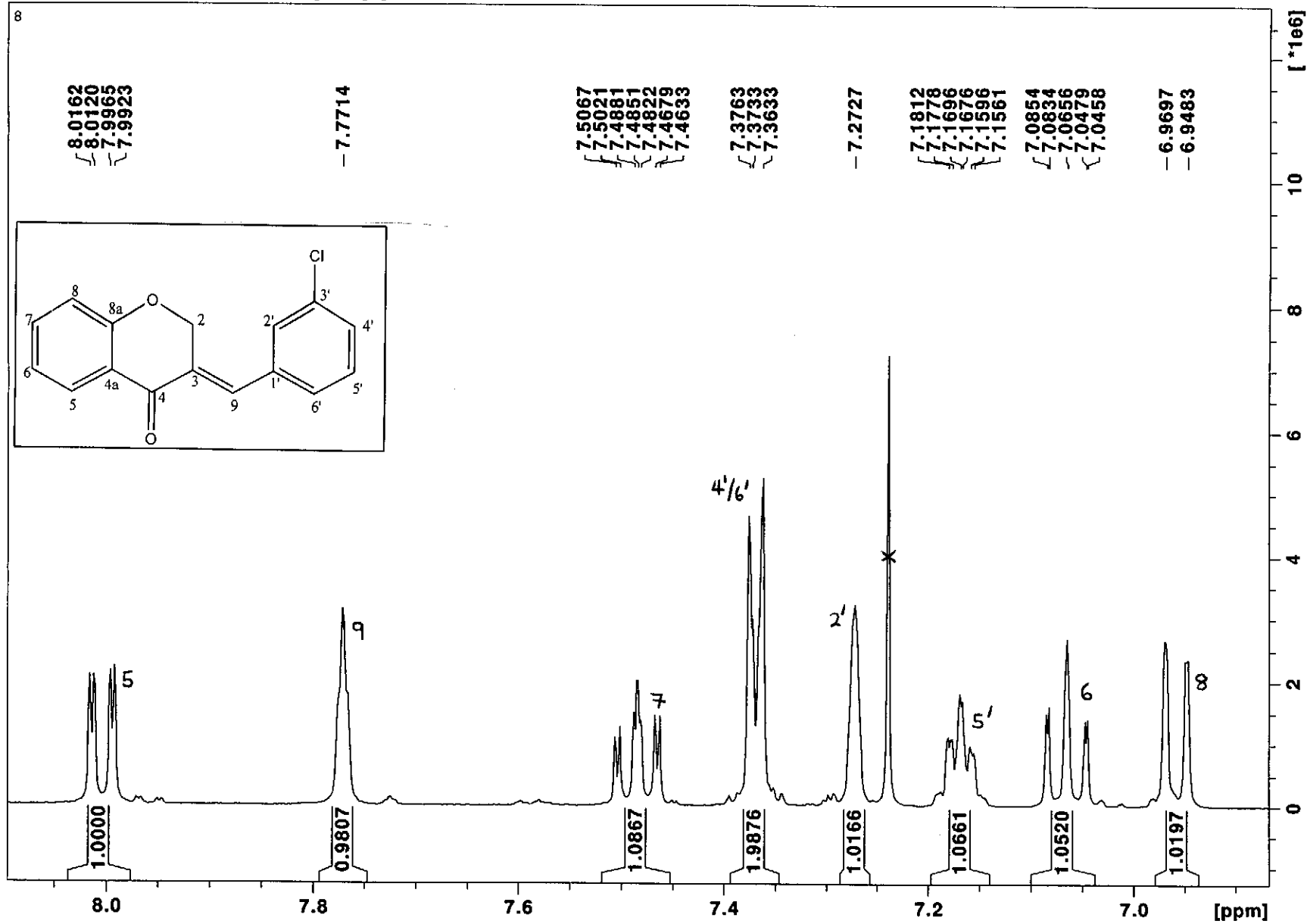
File :C:\msdchem\1\data\kaalin\4-CHLORO.D
Operator :
Acquired : 12 Jan 2012 15:25 using AcqMethod NATPRODUCTS MANUAL INJ.M
Instrument : 5973N
Sample Name:
Misc Info :
Vial Number: 1



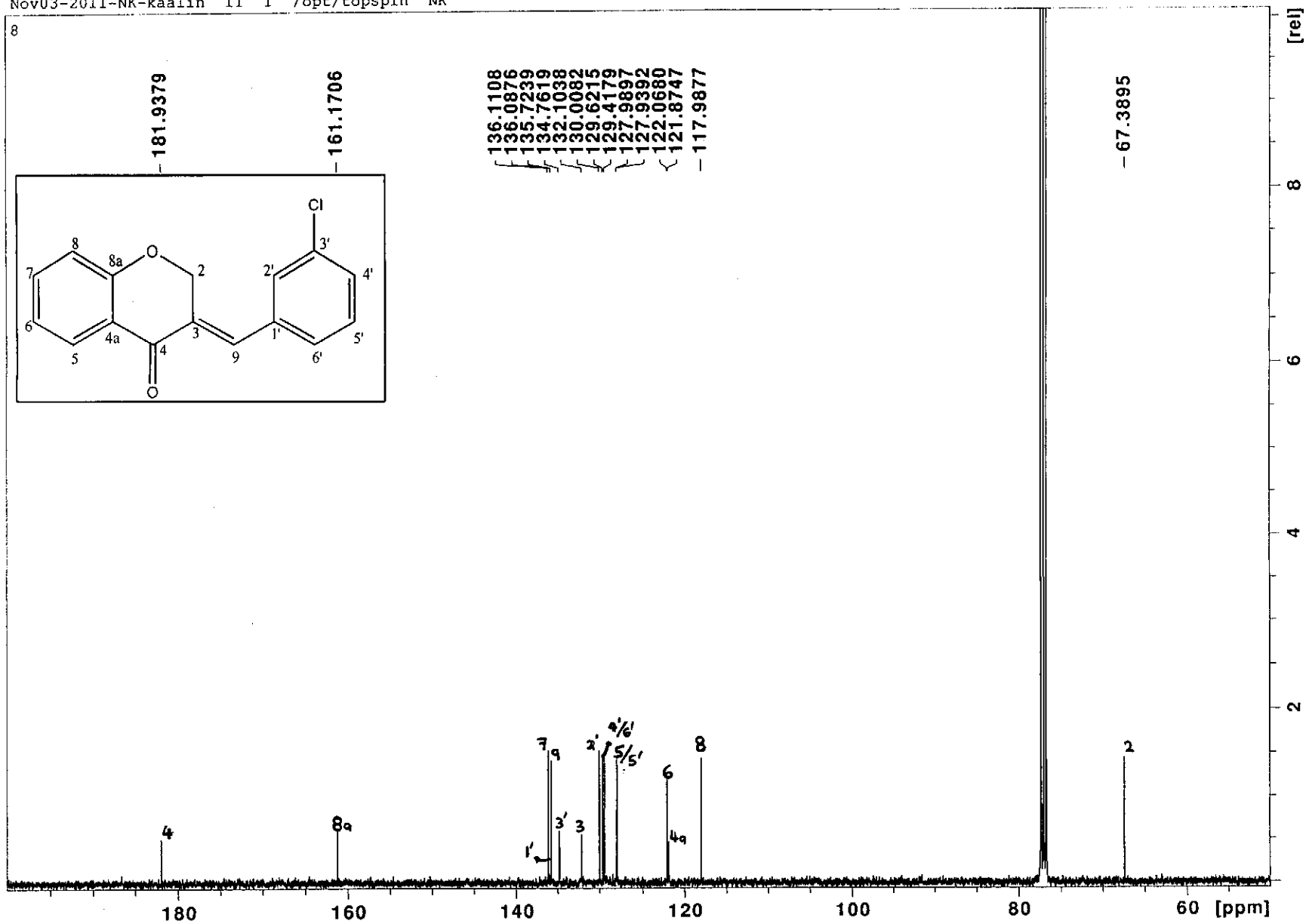
Nov03-2011-NK-kaalin 10 1 /opt/topspin NK



^1H NMR spectrum of compound 8

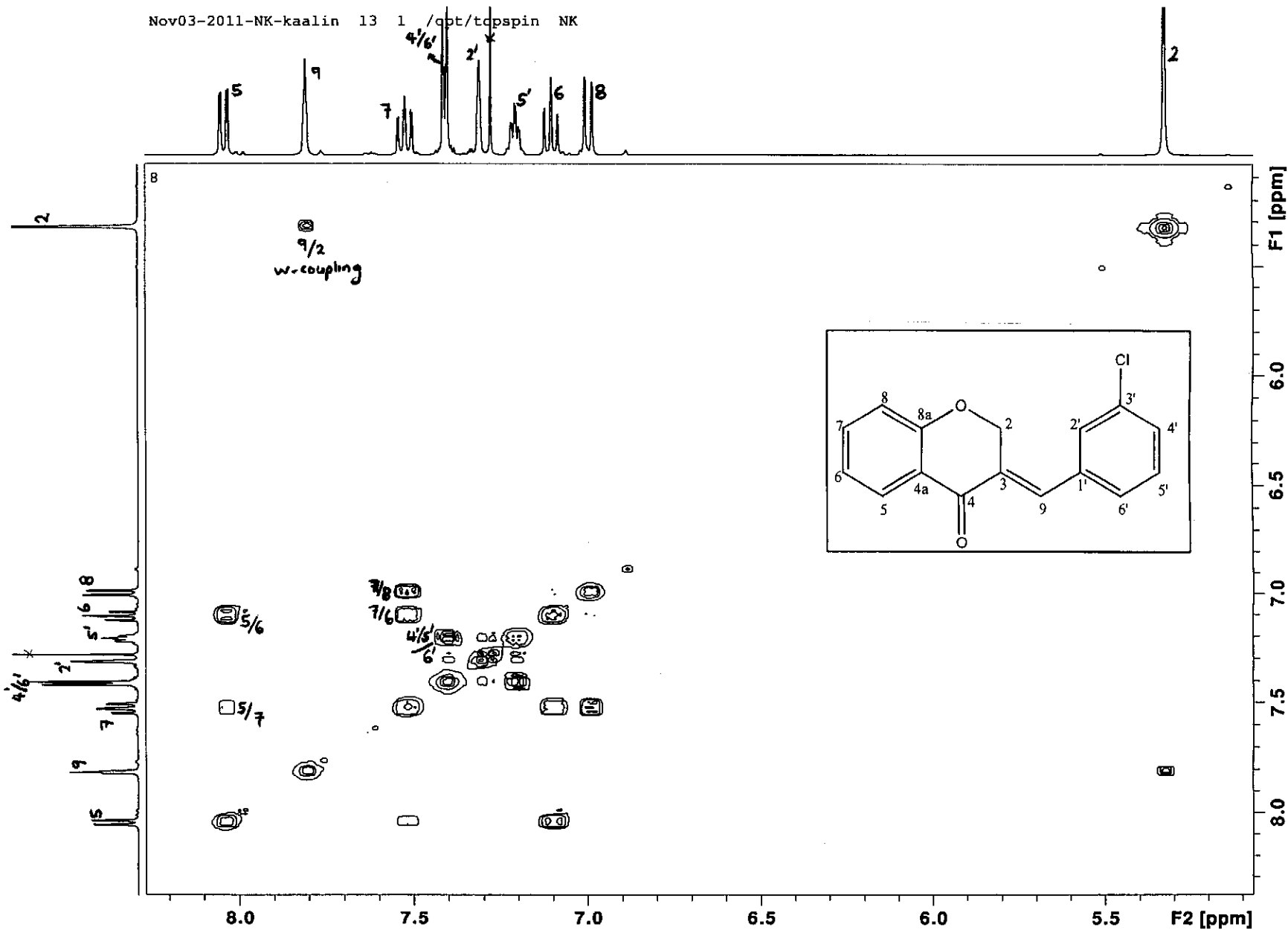


¹H NMR spectrum of compound 8 (expanded)



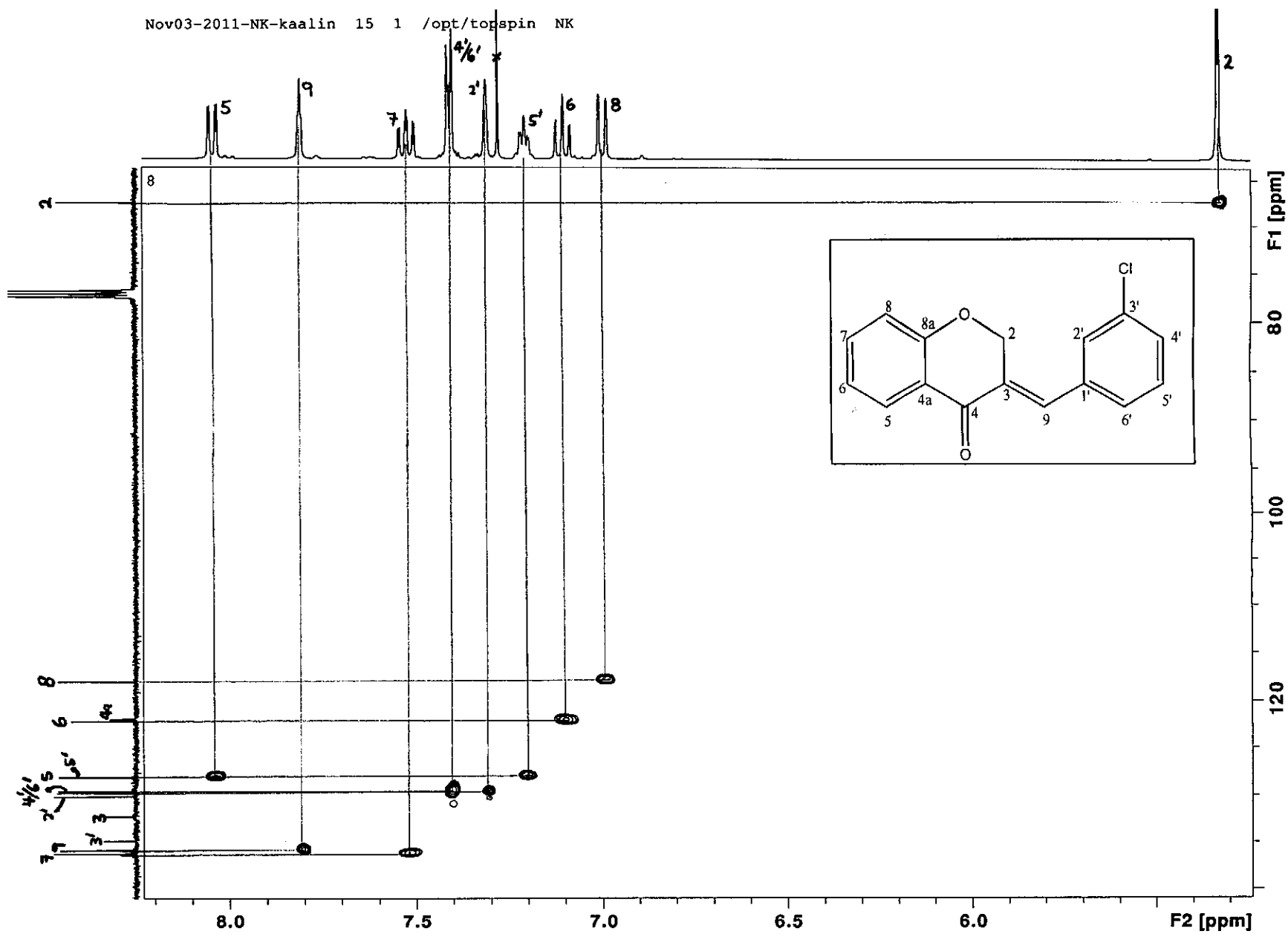
¹³C NMR spectrum of compound 8

Nov03-2011-NK-kaalin 13 1 /qbt/tcspspin NK



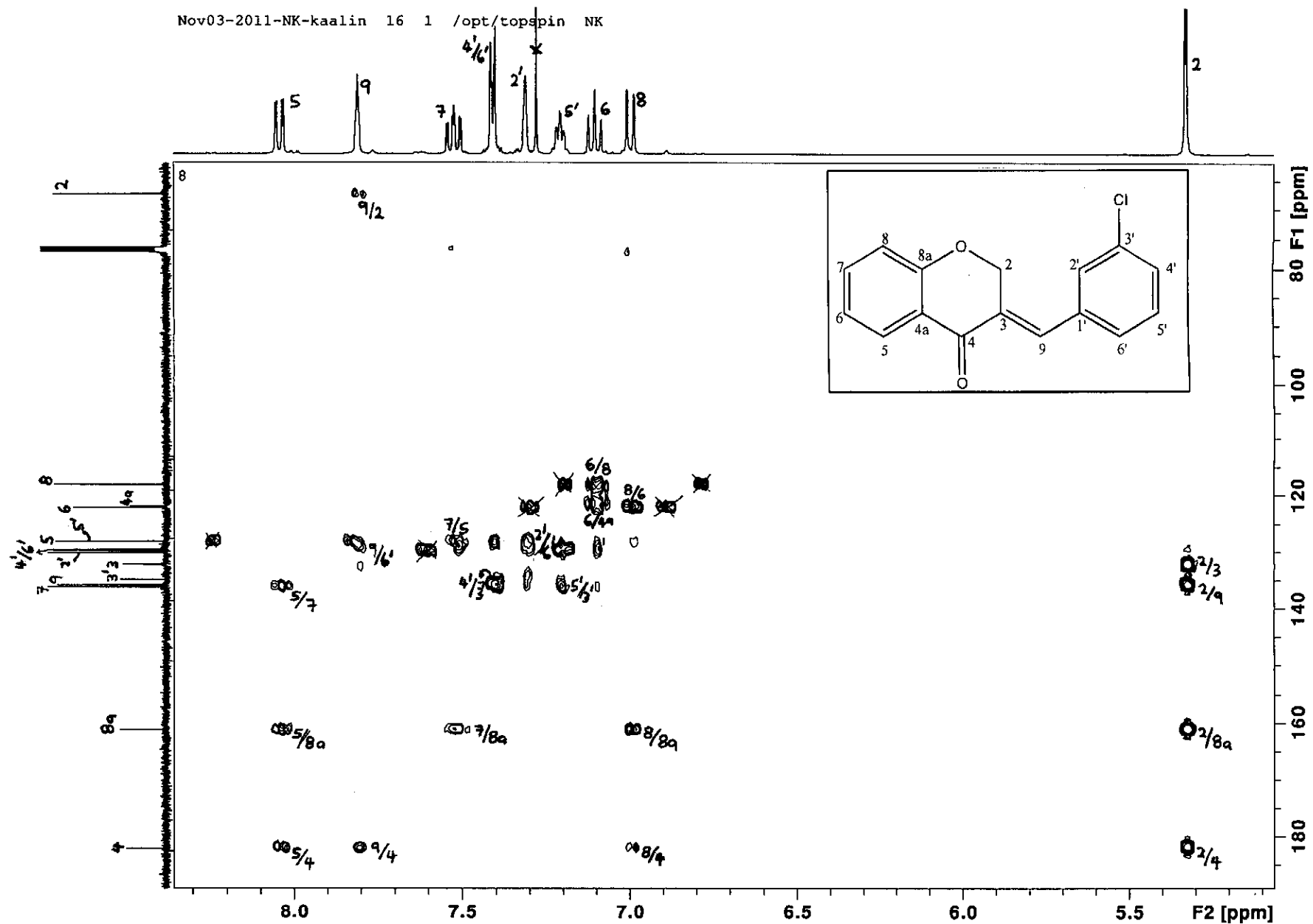
COSY spectrum of compound 8

Nov03-2011-NK-kaalin 15 1 /opt/topspin NK



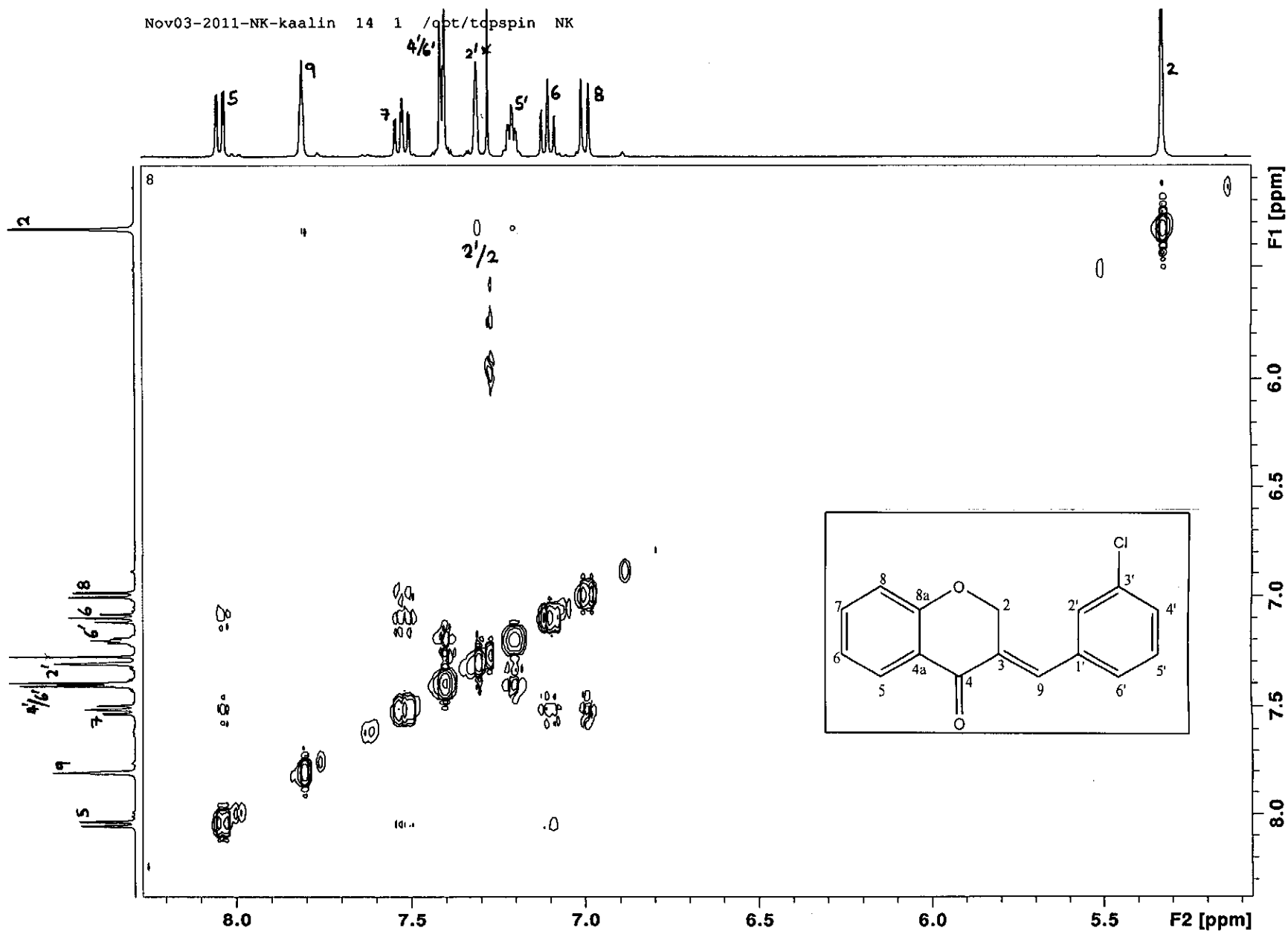
HSQC spectrum of compound 8

Nov03-2011-NK-kaalin 16 1 /opt/topspin NK



HMBC spectrum of compound 8

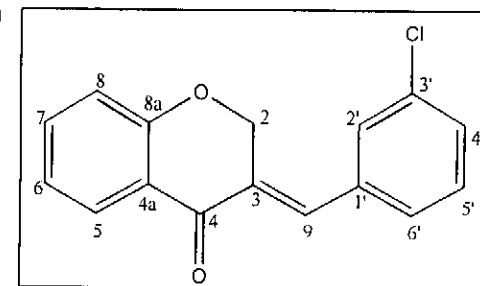
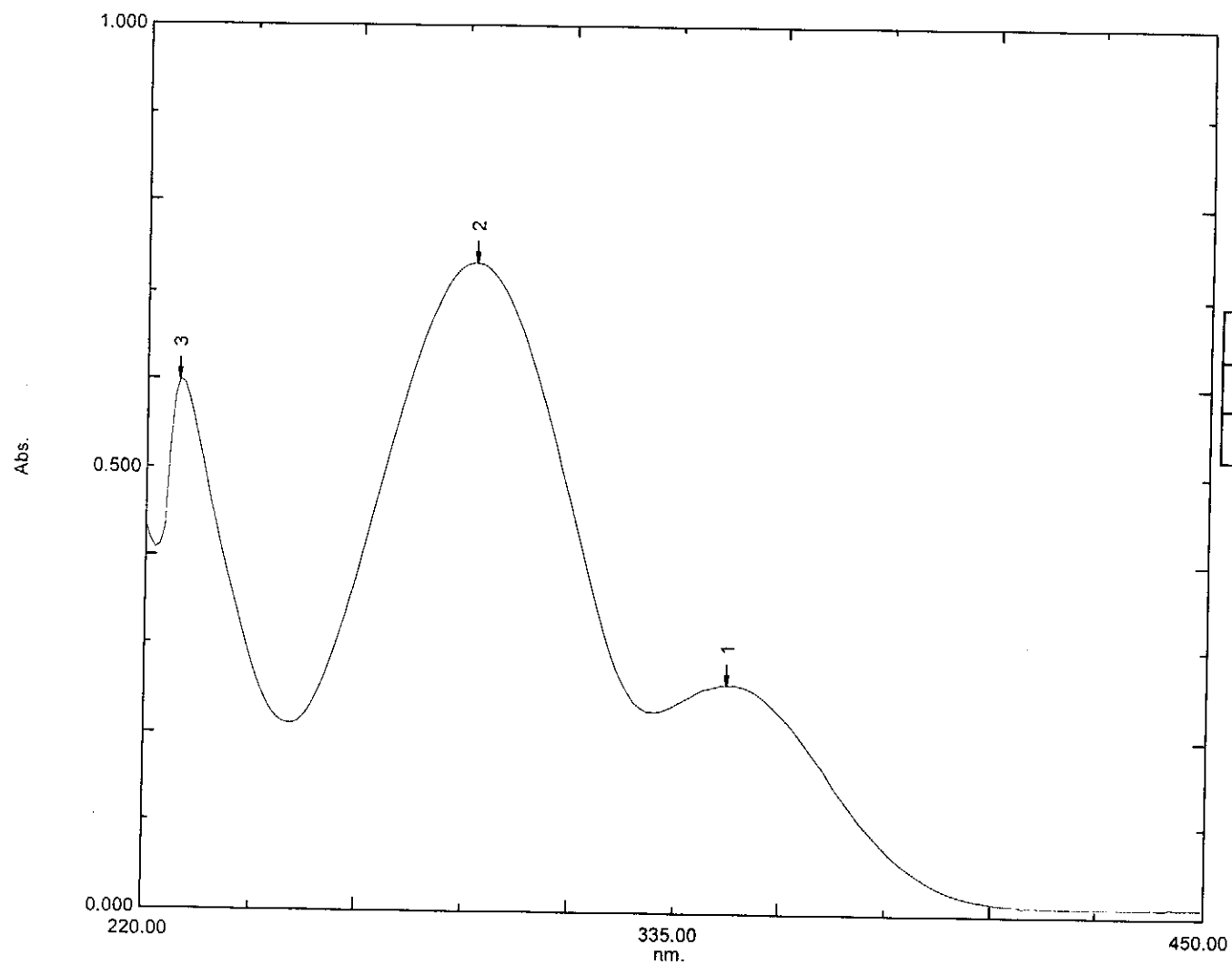
Nov03-2011-NK-kaalin 14 1 /opt/tcpspin NK



NOESY spectrum of compound 8

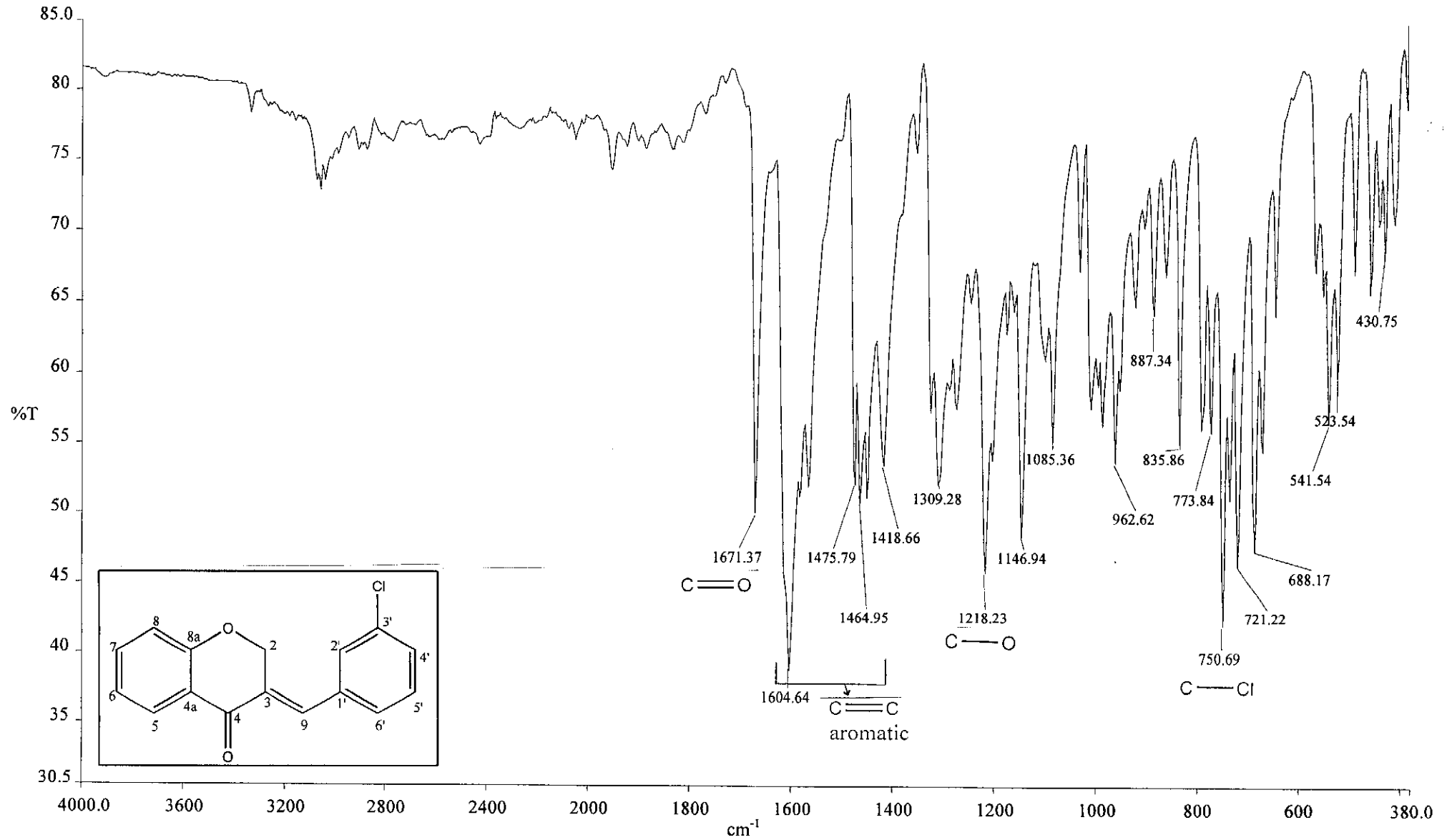
Overlay Spectrum Graph Report

15/05/2012 12:59:24 PM



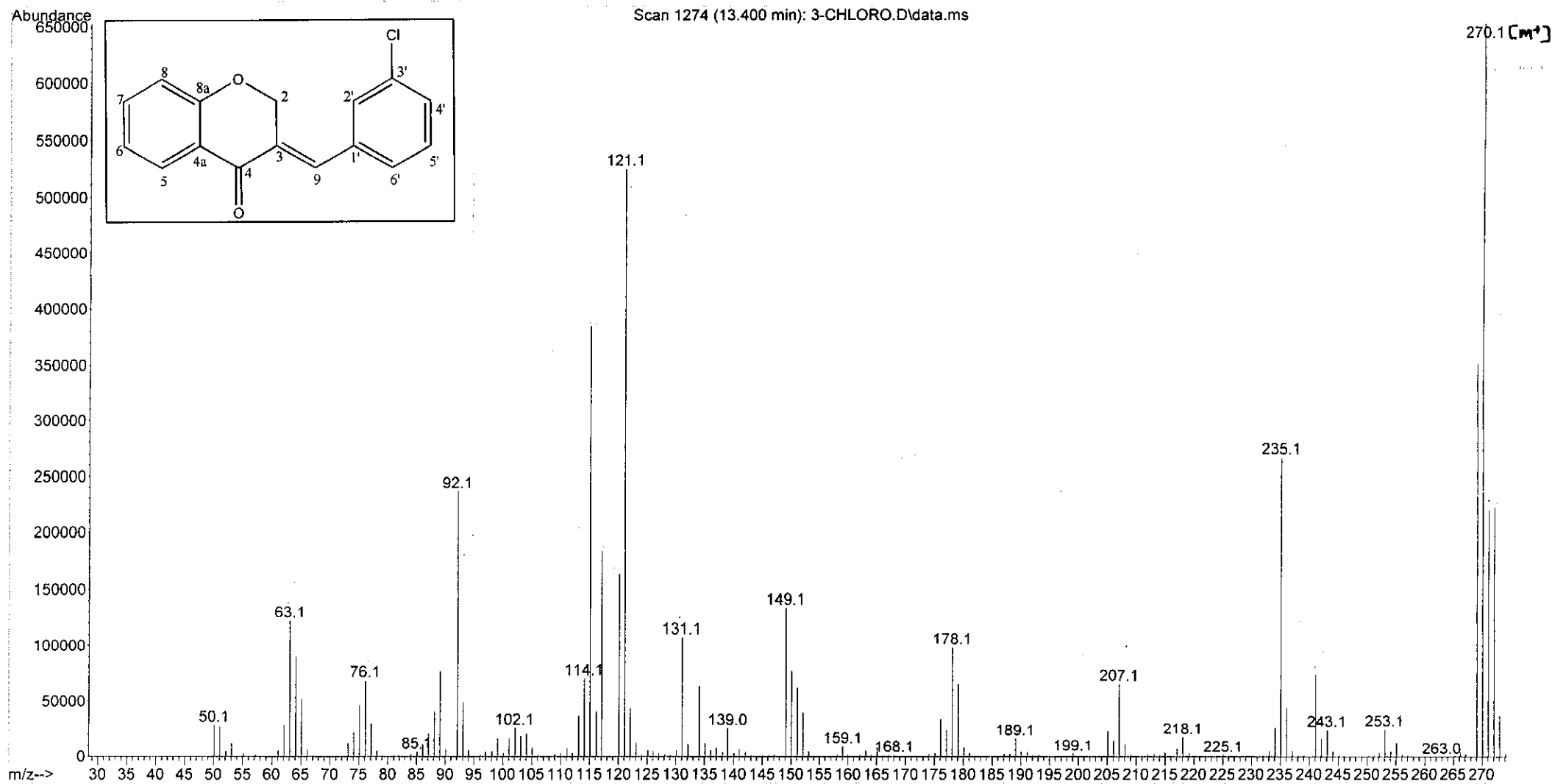
Wavelength/ nm	Absorbance	Log ϵ
291	0.734	4.17
345	0.259	3.71

UV-Vis spectrum of compound 8

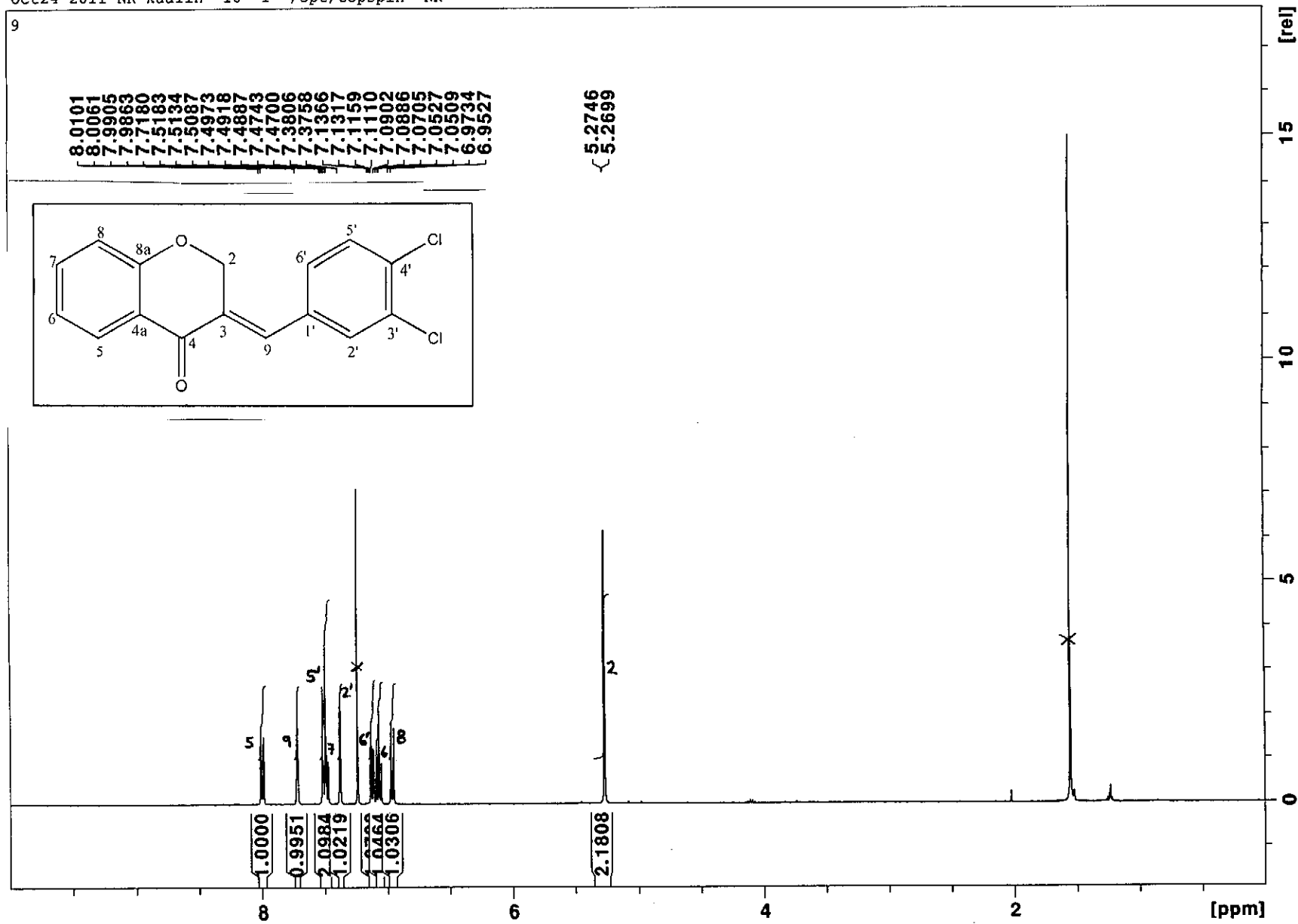


Infrared spectrum of compound 8

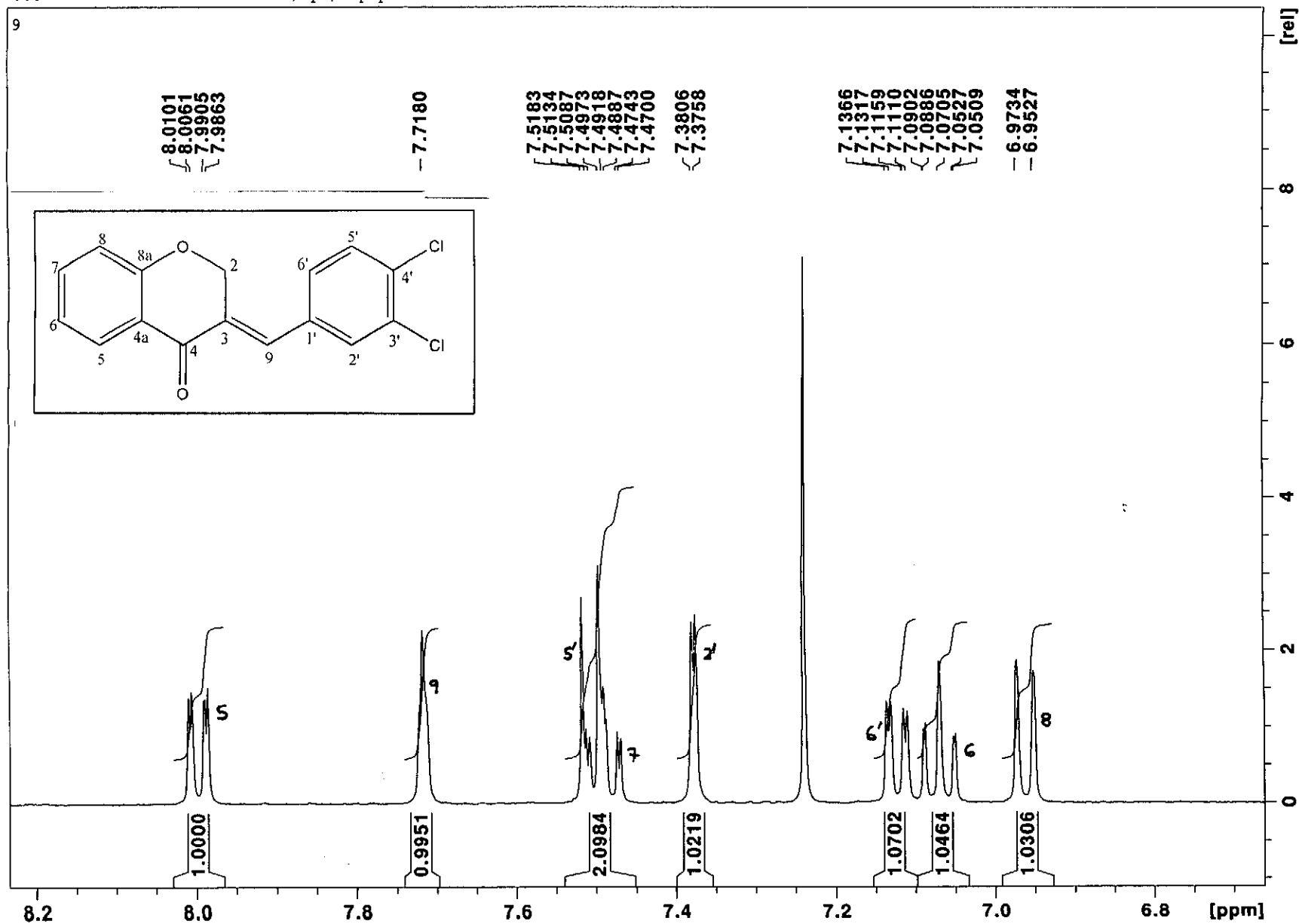
File :C:\msdchem\1\data\kaalin\3-CHLORO.D
Operator :
Acquired : 12 Jan 2012 16:37 using AcqMethod NATPRODUCTS MANUAL INJ.M
Instrument : 5973N
Sample Name:
Misc Info :
Vial Number: 1



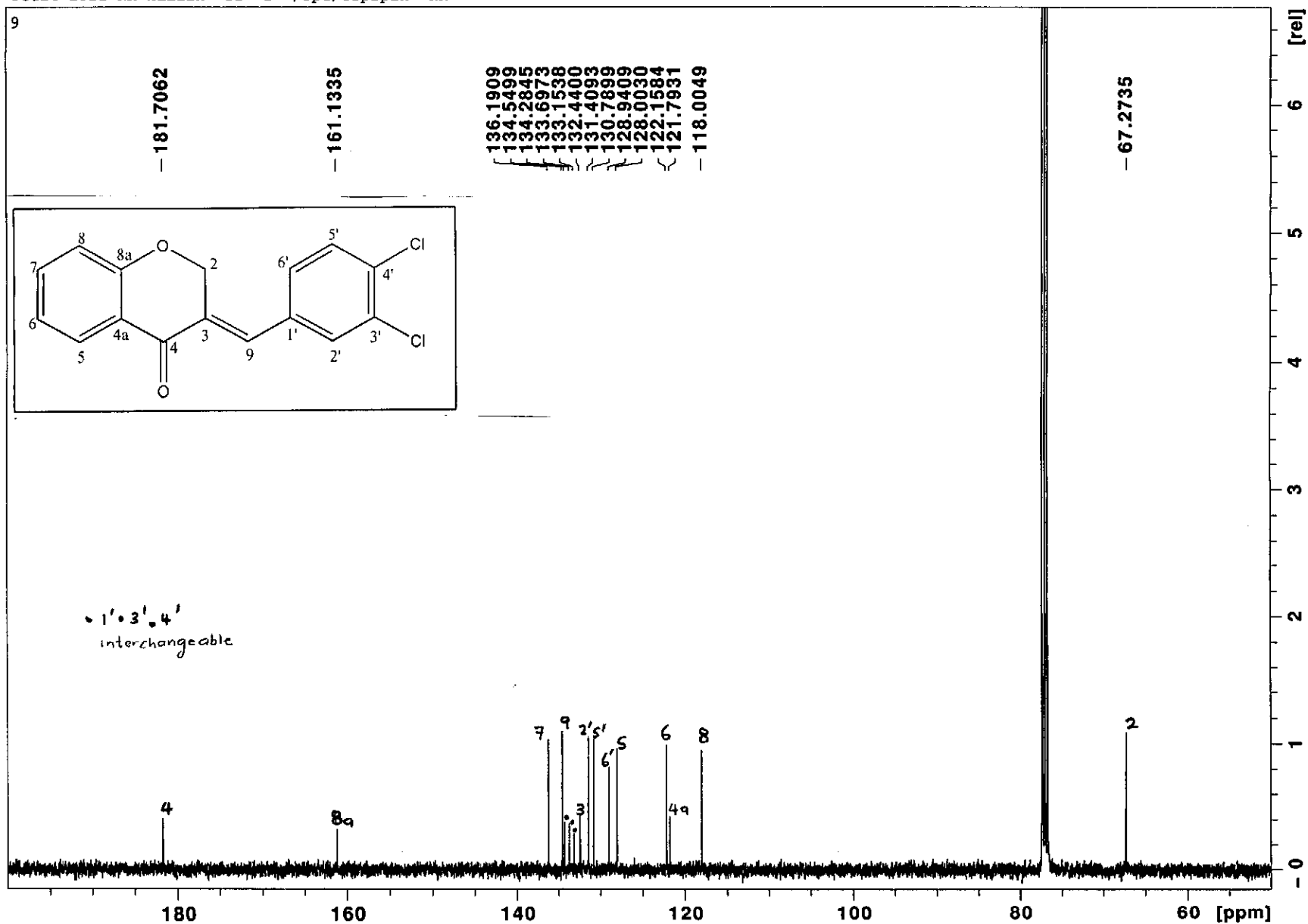
Oct24-2011-NK-kaalin 10 1 /opt/topspin NK



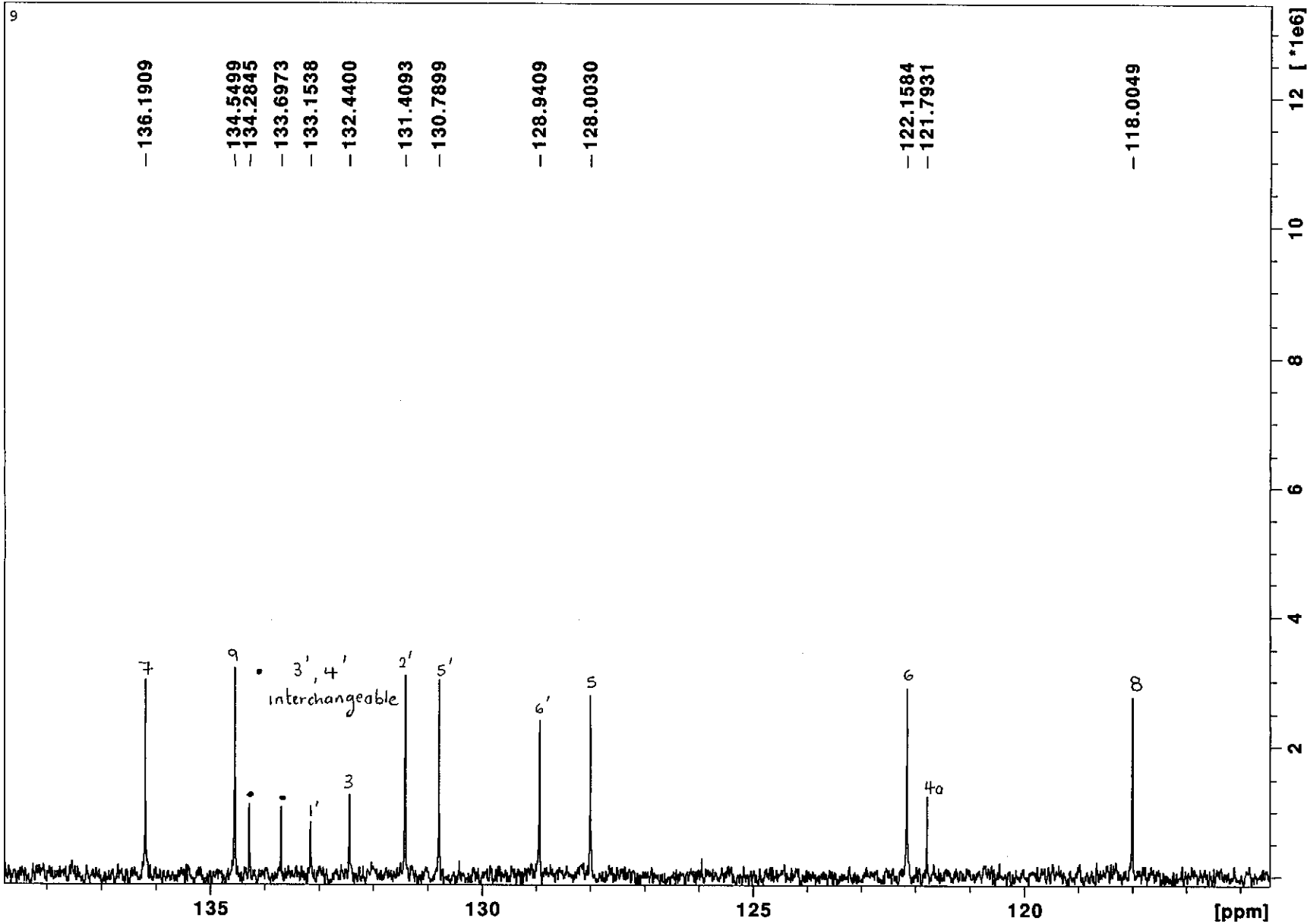
¹H NMR spectrum of compound 9



¹H NMR spectrum of compound 9 (expanded)

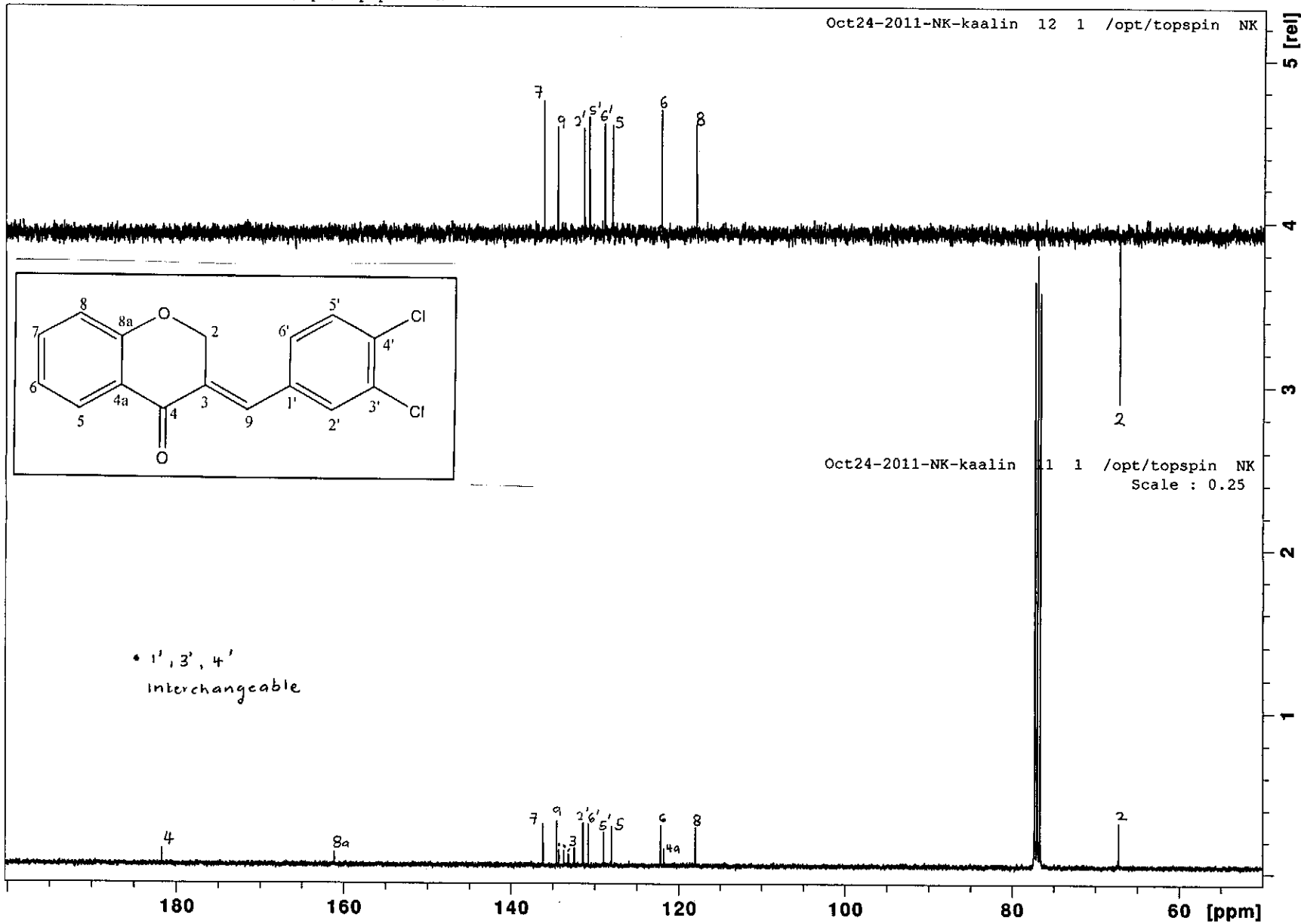


¹³C NMR spectrum of compound 9



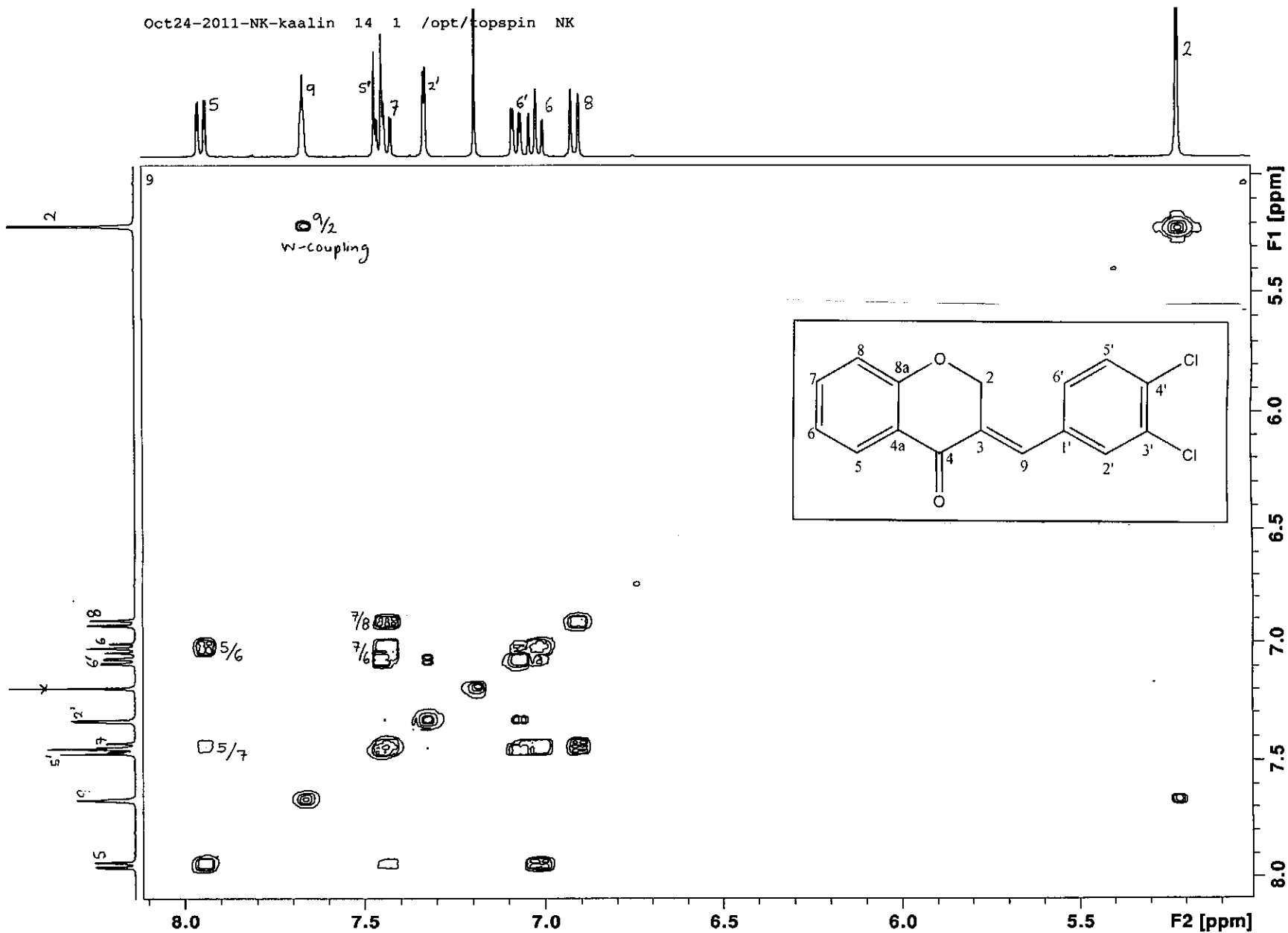
Oct24-2011-NK-kaalin 11 1 /opt/topspin NK

Oct24-2011-NK-kaalin 12 1 /opt/topspin NK



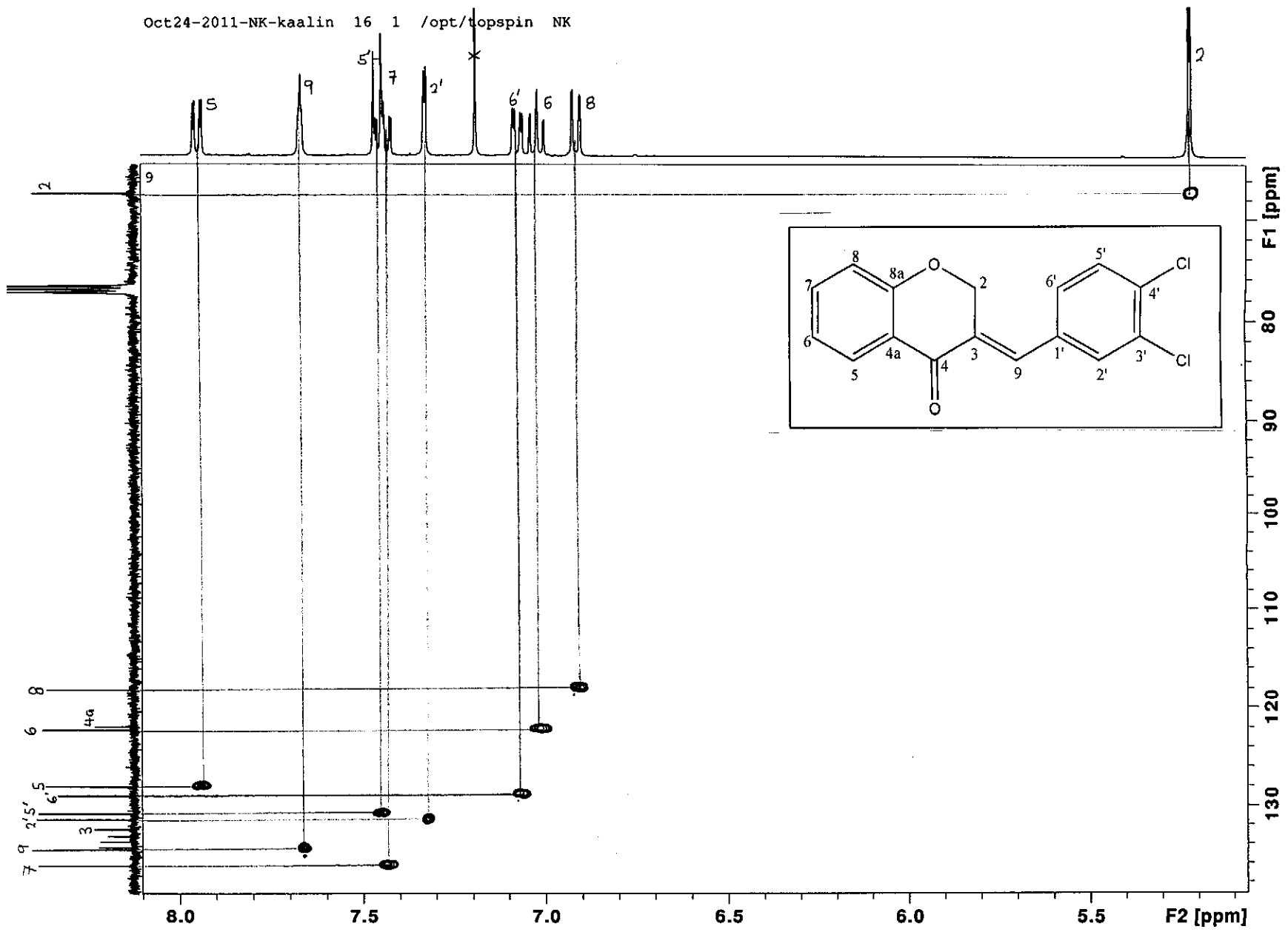
DEPT 135 spectrum of compound 9

Oct24-2011-NK-kaalin 14 1 /opt/topspin NK



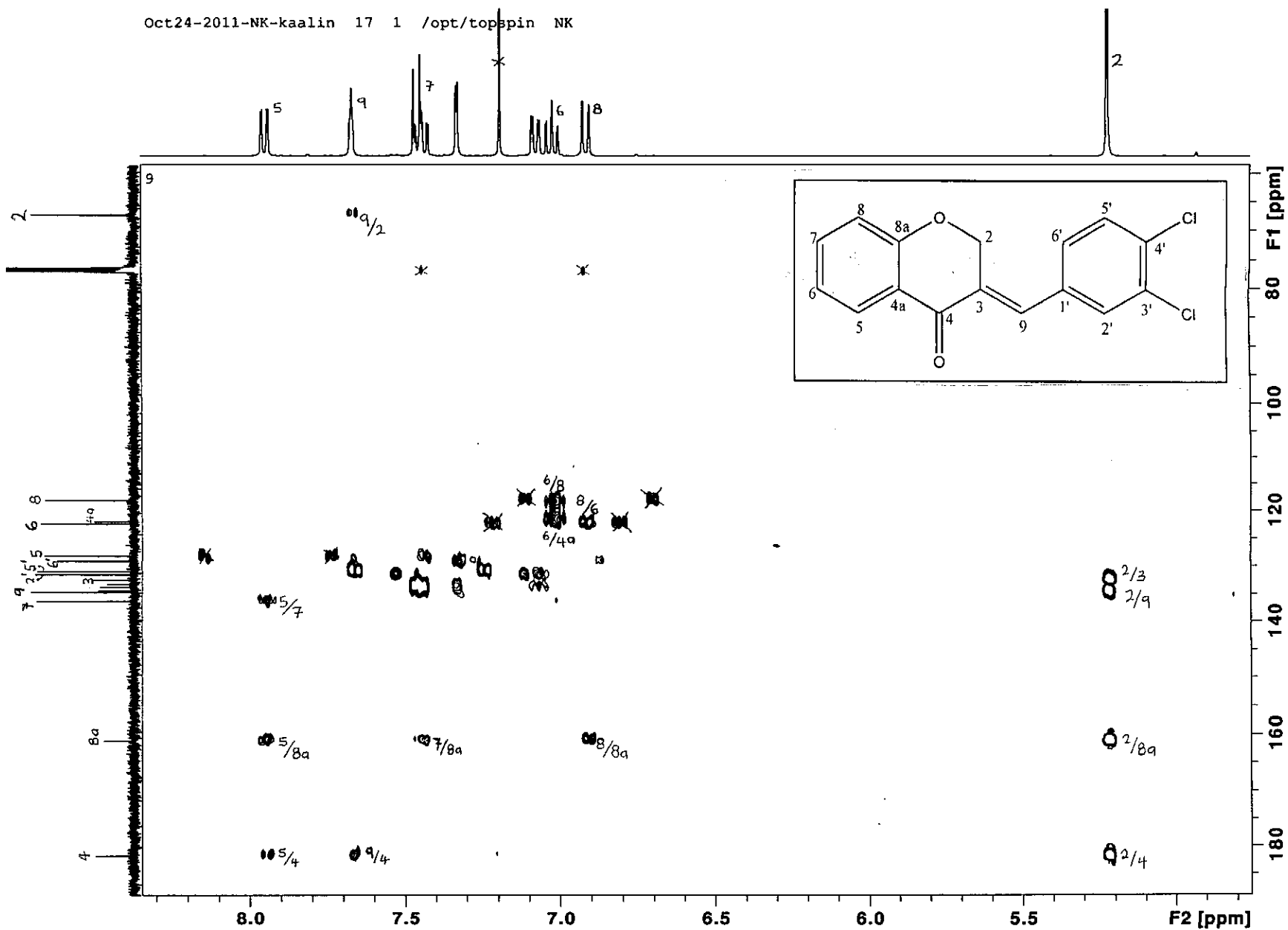
COSY spectrum of compound 9

Oct24-2011-NK-kaalin 16 1 /opt/topspin NK



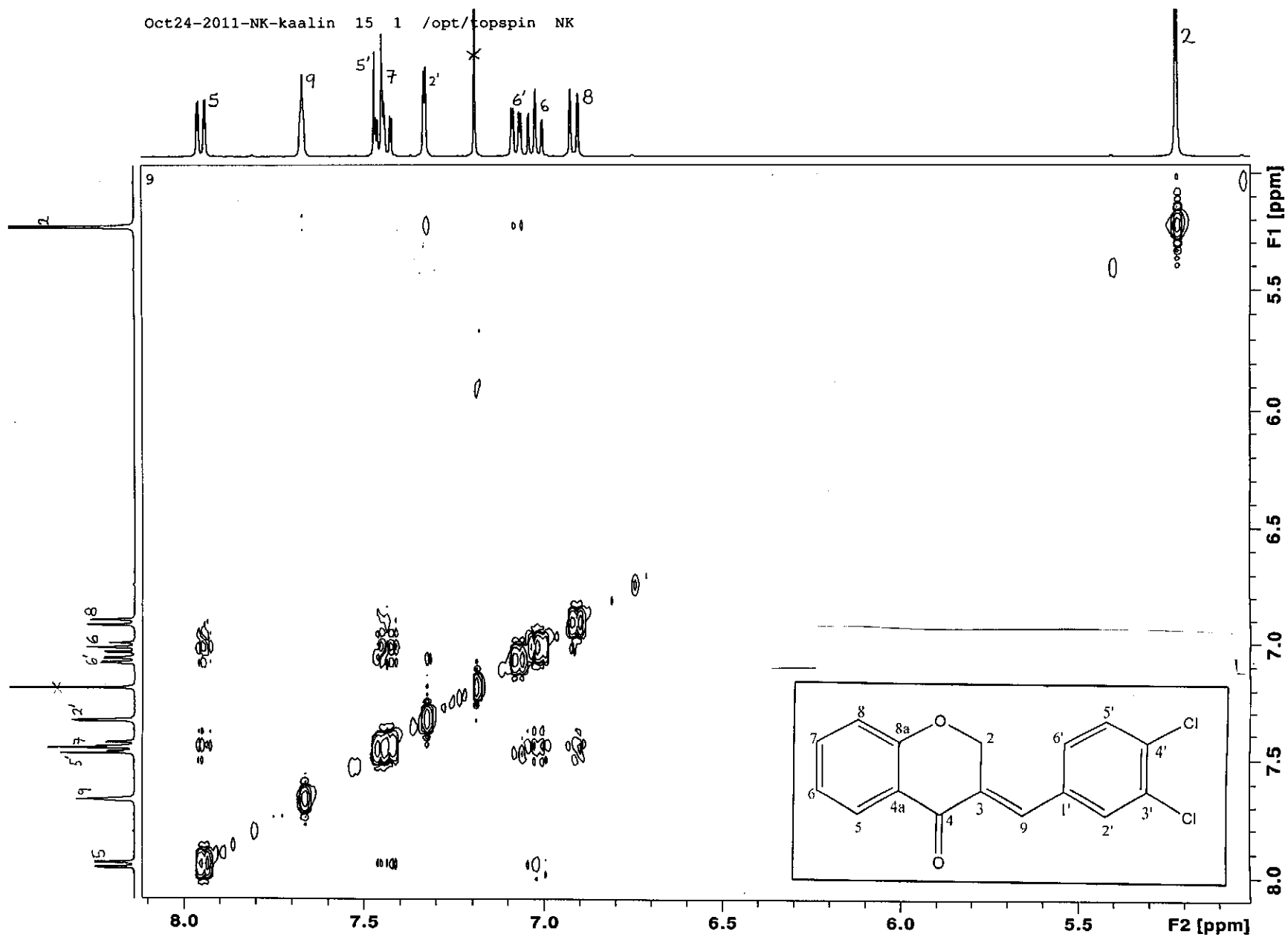
HSQC spectrum of compound 9

Oct24-2011-NK-kaalin 17 1 /opt/topspin NK



HMBC spectrum of compound 9

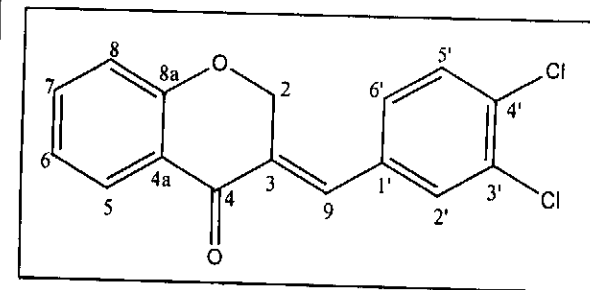
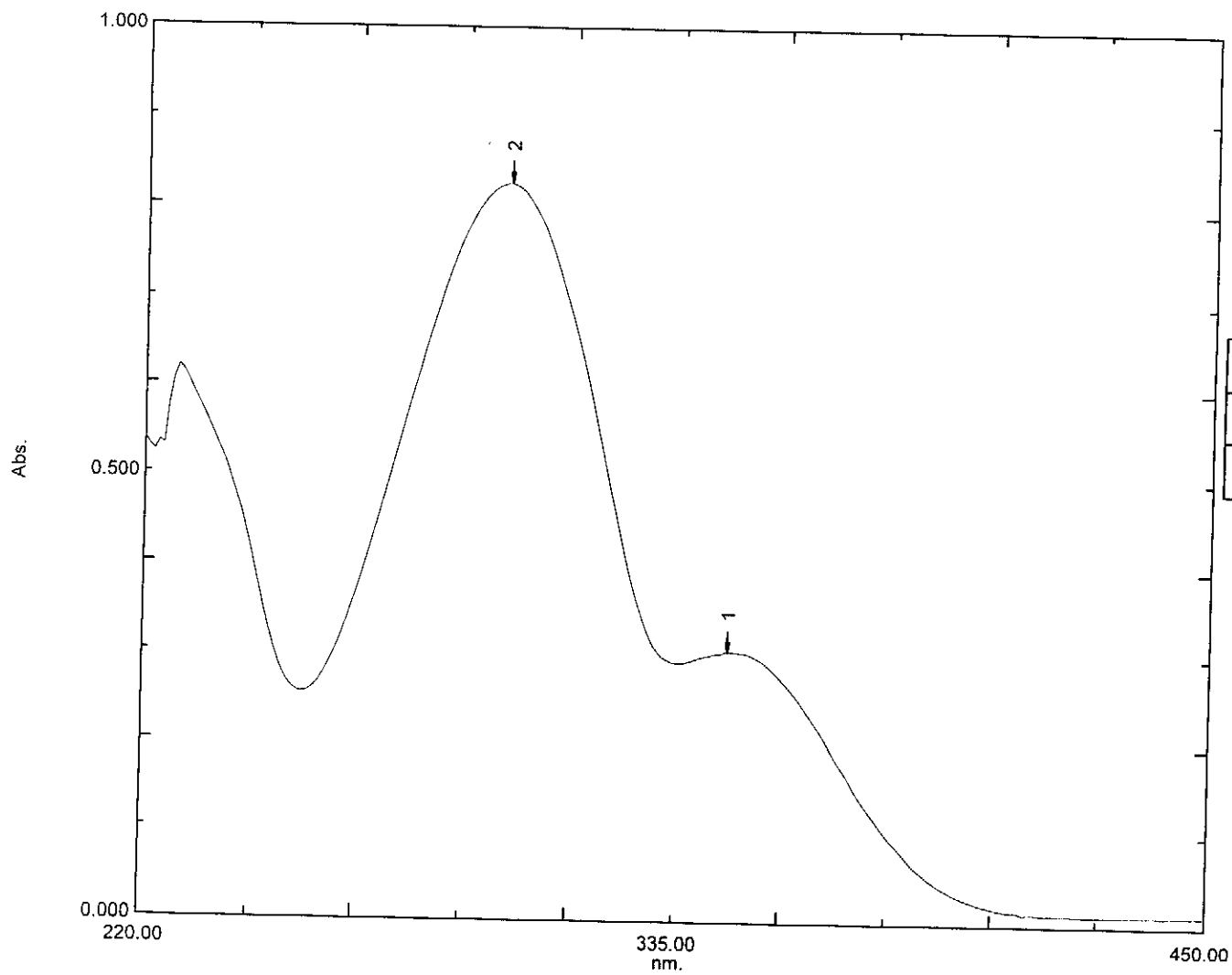
Oct24-2011-NK-kaalin 15 1 /opt/topspin NK



NOESY spectrum of compound 9

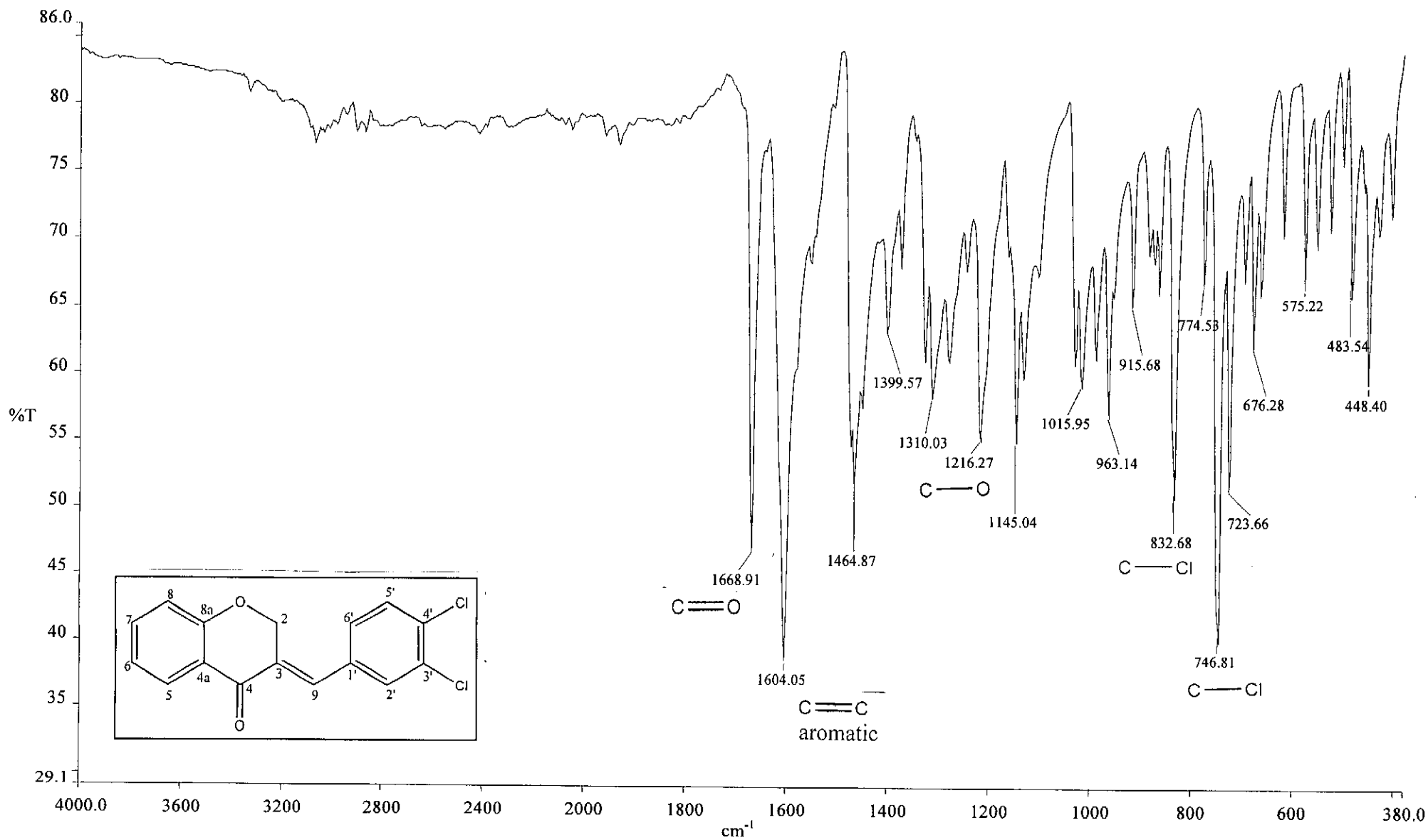
Overlay Spectrum Graph Report

15/05/2012 01:00:33 PM



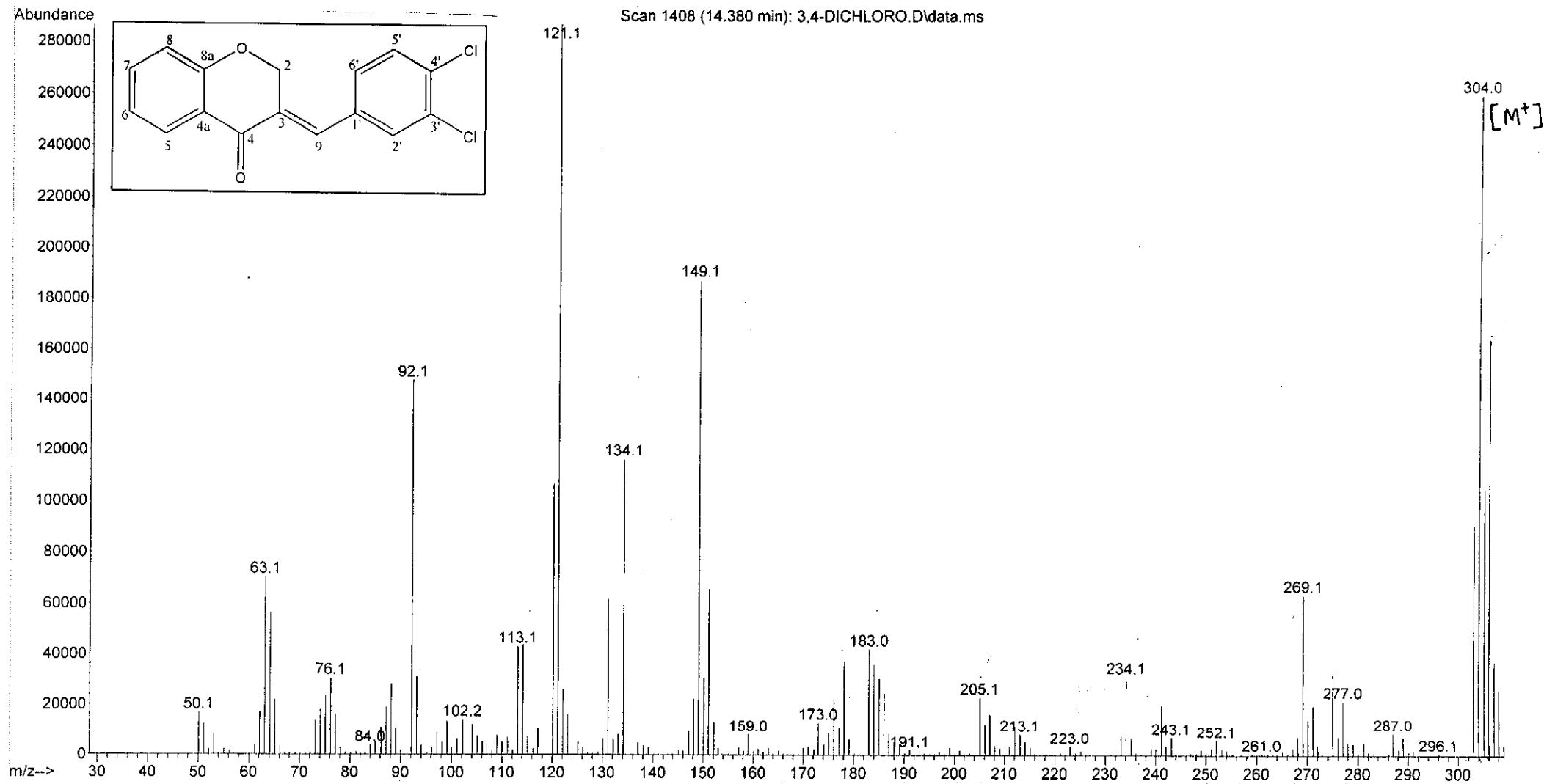
Wavelength/ nm	Absorbance	Log ϵ
297	0.825	3.96
346	0.305	3.53

UV-Vis spectrum of compound 9

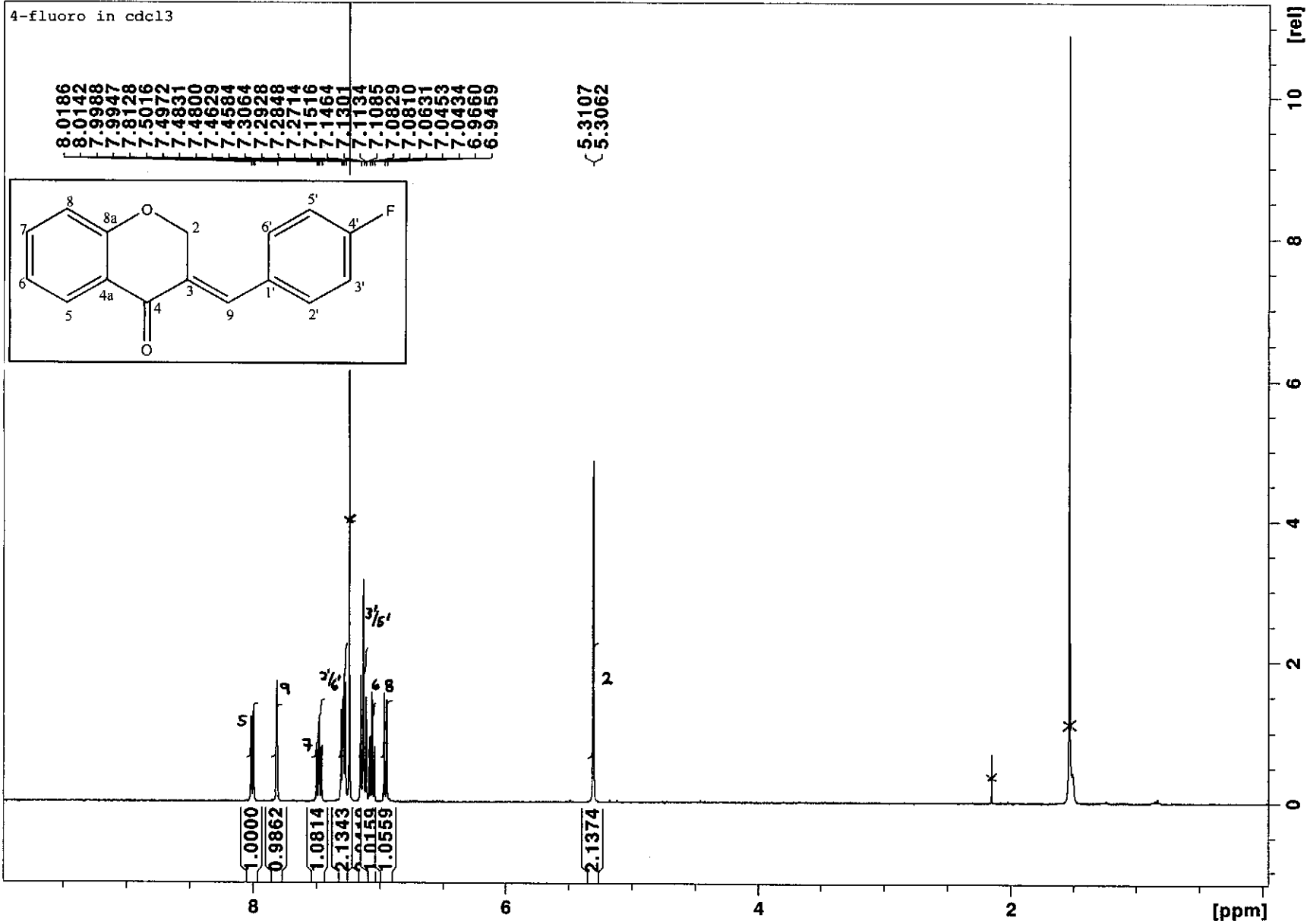


Infrared spectrum of compound 9

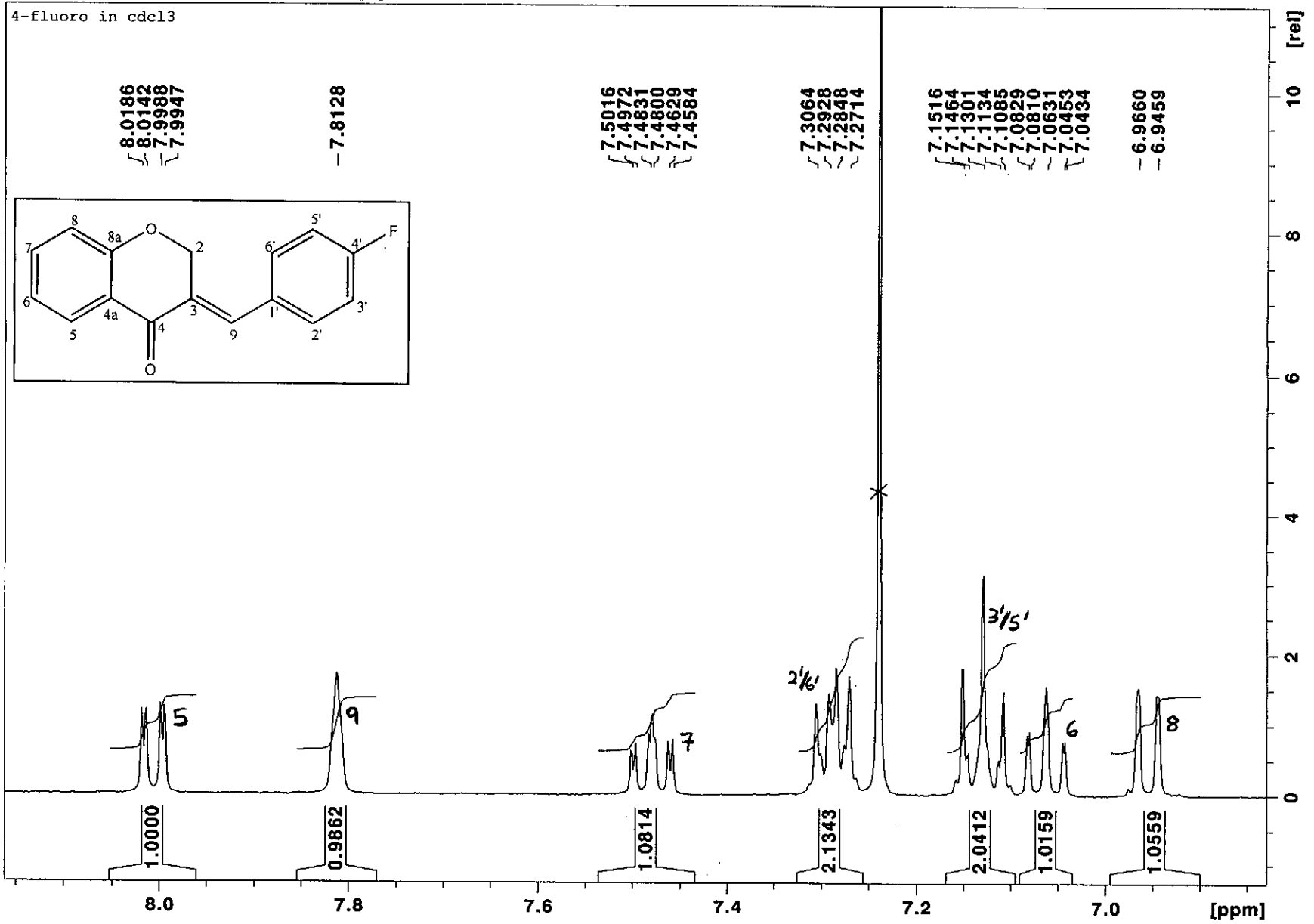
File :C:\msdchem\1\data\kaalin\3,4-DICHLORO.D
Operator :
Acquired : 12 Jan 2012 17:59 using AcqMethod NATPRODUCTS MANUAL INJ.M
Instrument : 5973N
Sample Name:
Misc Info :
Vial Number: 1



Oct31-2011-NK-kaalin 10 1 /opt/topspin NK



¹H NMR spectrum of compound 10



¹H NMR spectrum of compound 10 (expanded)

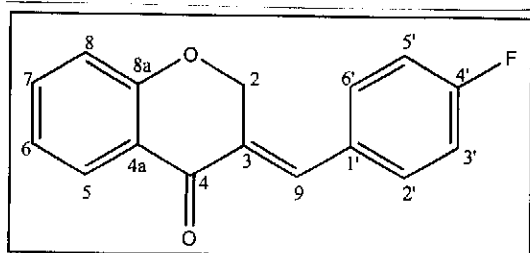
4-fluoro in cdcl3

- 182.1012

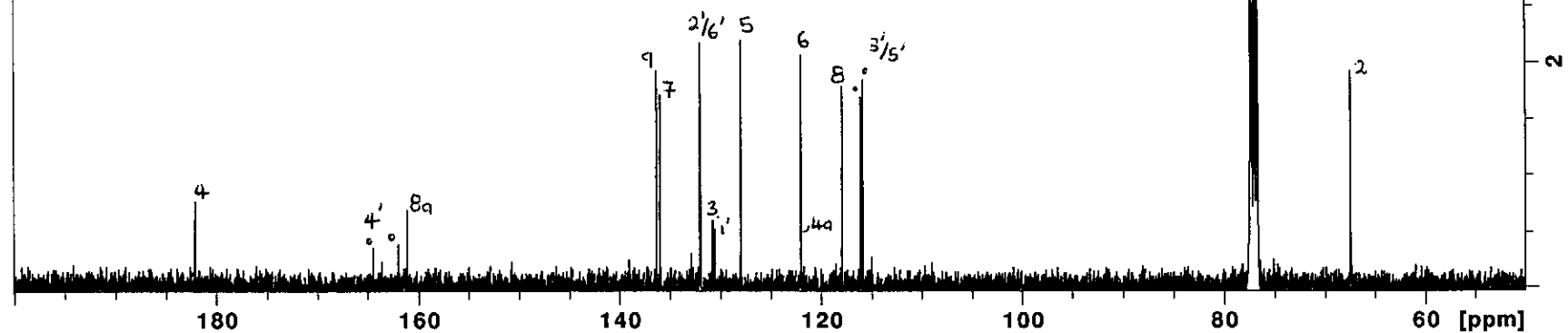
- 164.4679
- 161.9592
- 161.0762

136.2713
135.9597
132.0132
131.9277
130.7654
130.5529
130.5190
127.9602
122.0058
121.9543
117.9244
116.0891
115.8732

- 67.4755

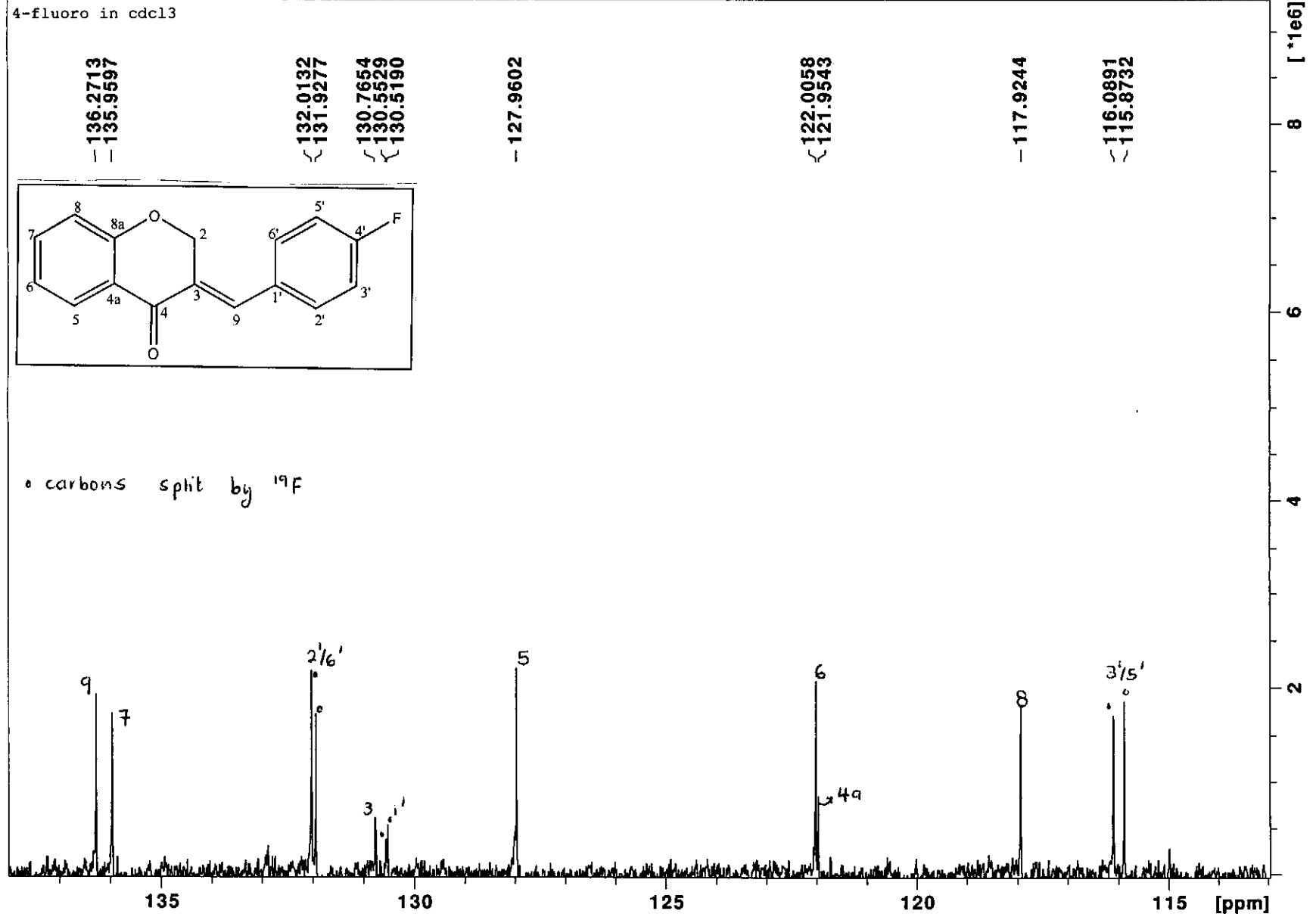


• carbons split by ^{19}F



^{13}C NMR spectrum of compound 10

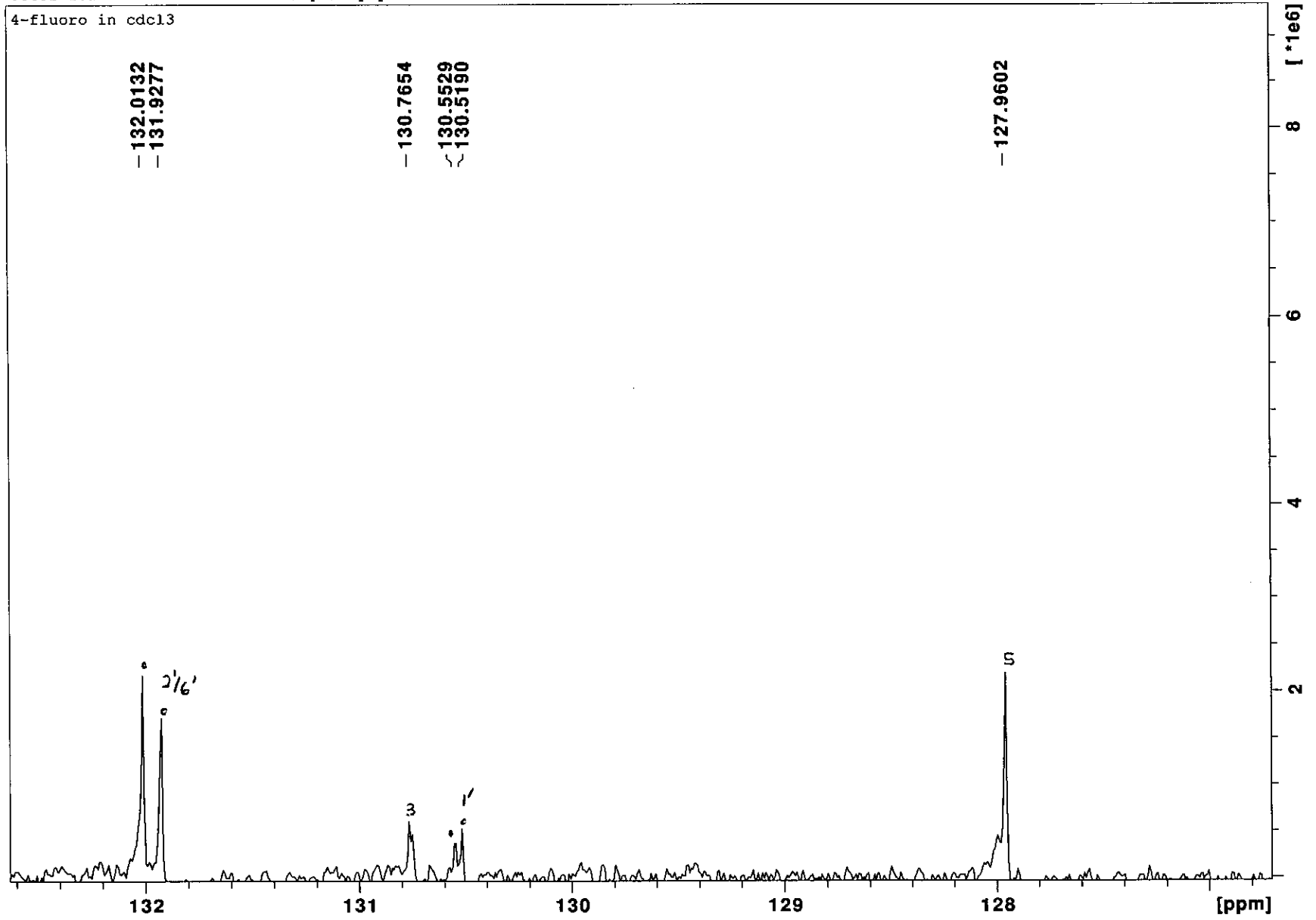
Oct31-2011-NK-kaalin 1i 1 /opt/topspin NK



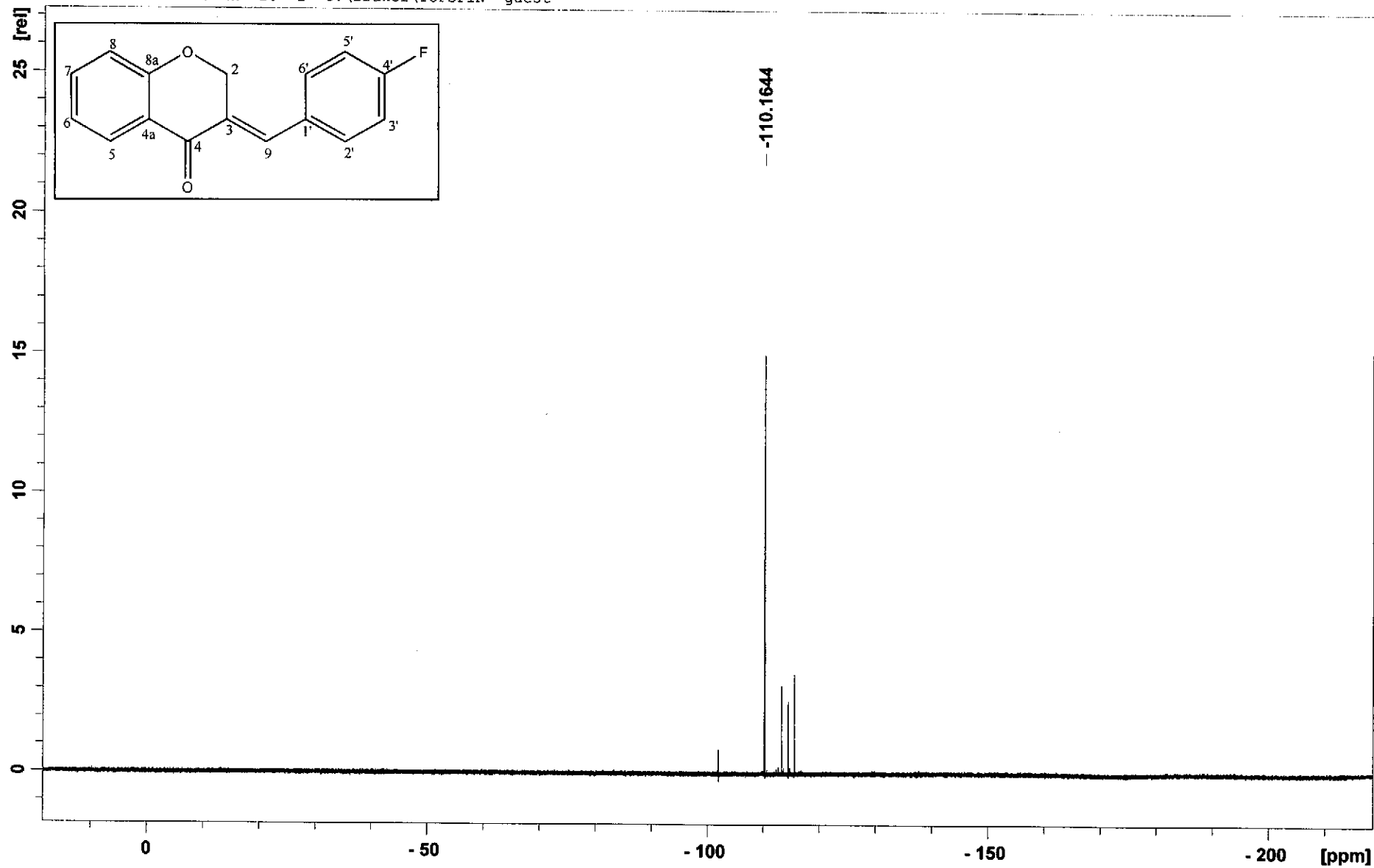
¹³C NMR spectrum of compound 10 (expanded)

Oct31-2011-NK-kaalin 11 1 /opt/topspin NK

4-fluoro in cdcl3

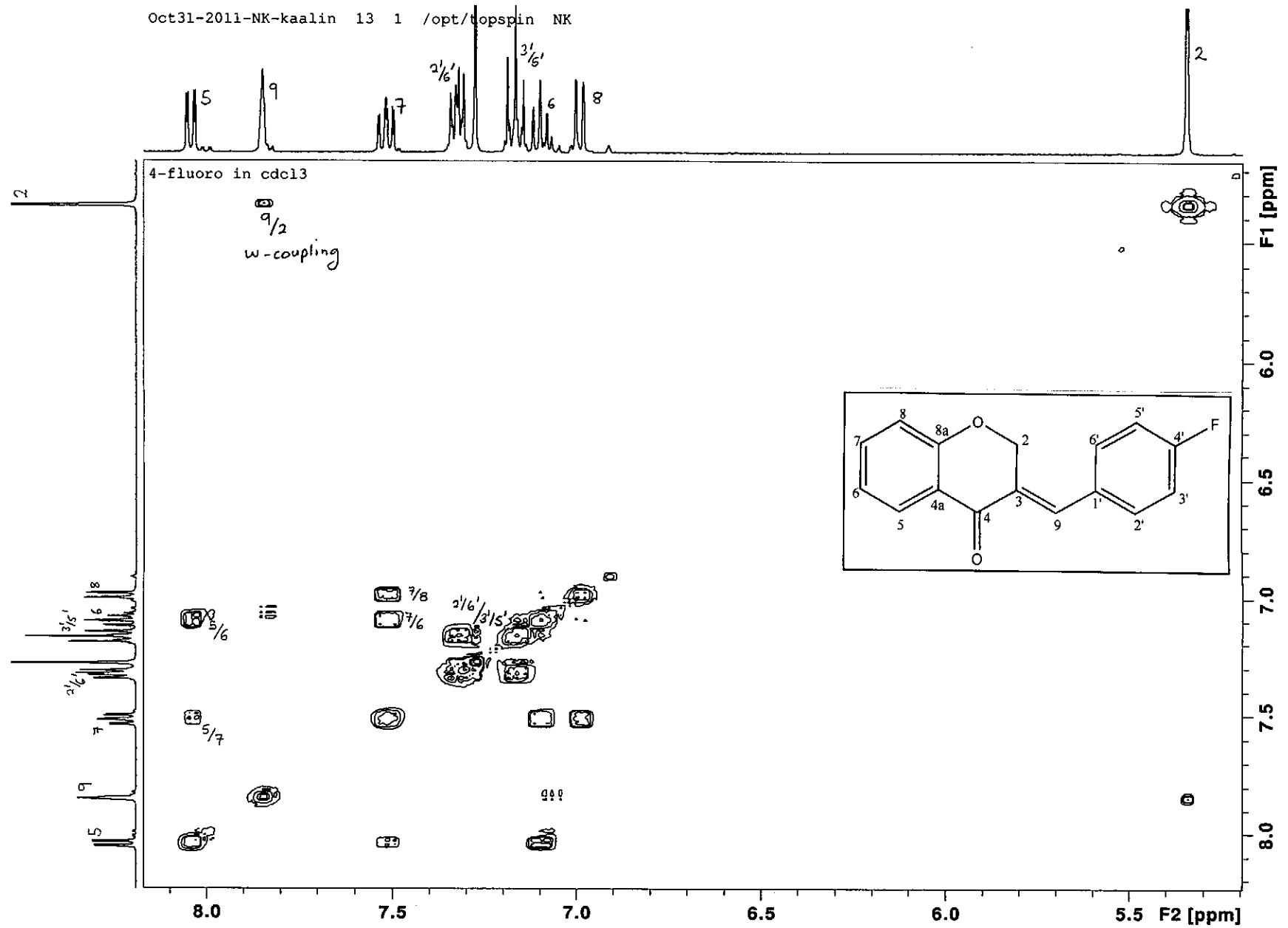


Feb08-2012-NK-kaalin 20 1 C:\Bruker\TOPSPIN guest



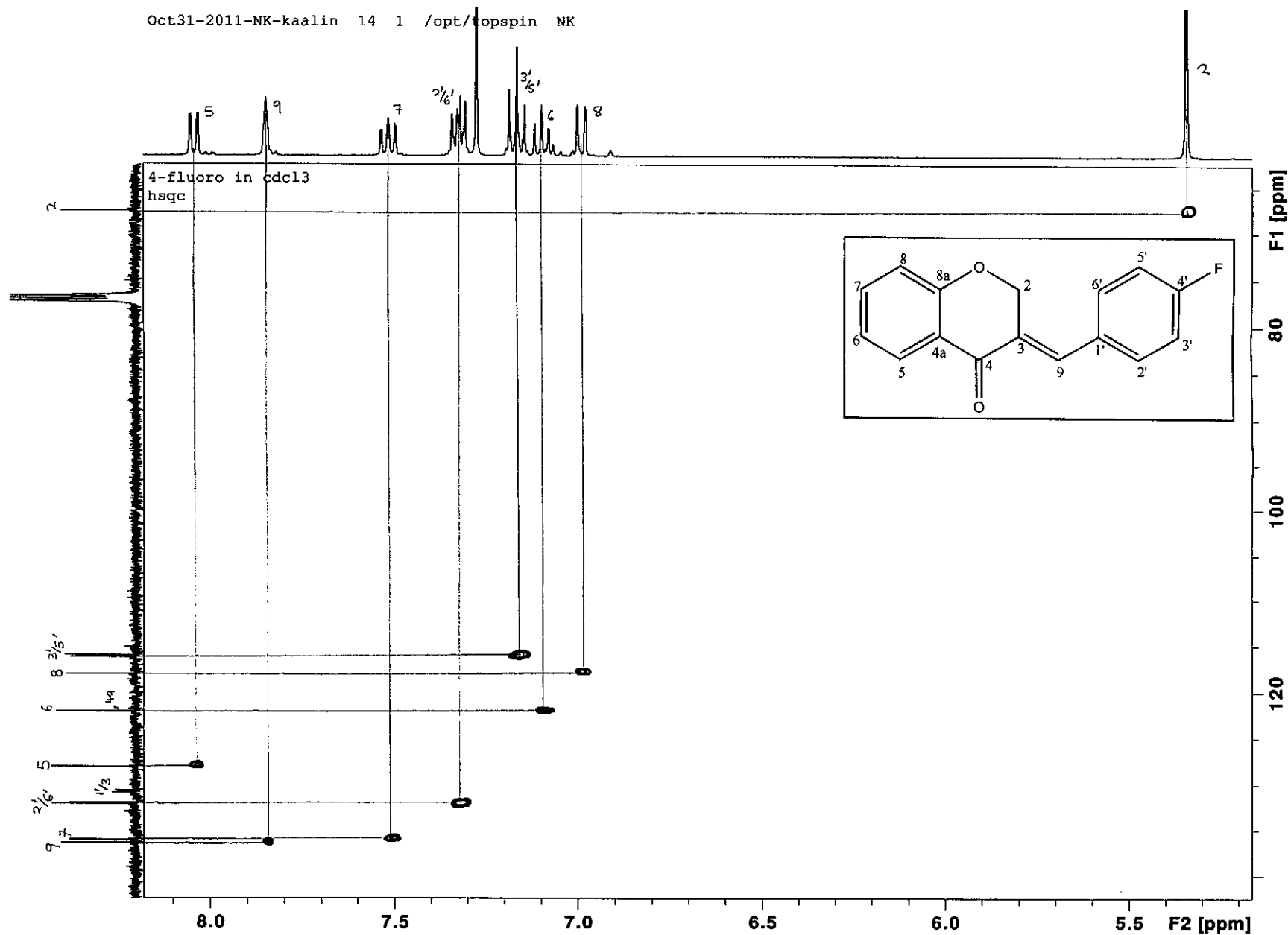
^{19}F NMR spectrum of compound 10

Oct31-2011-NK-kaalin 13 1 /opt/topspin NK



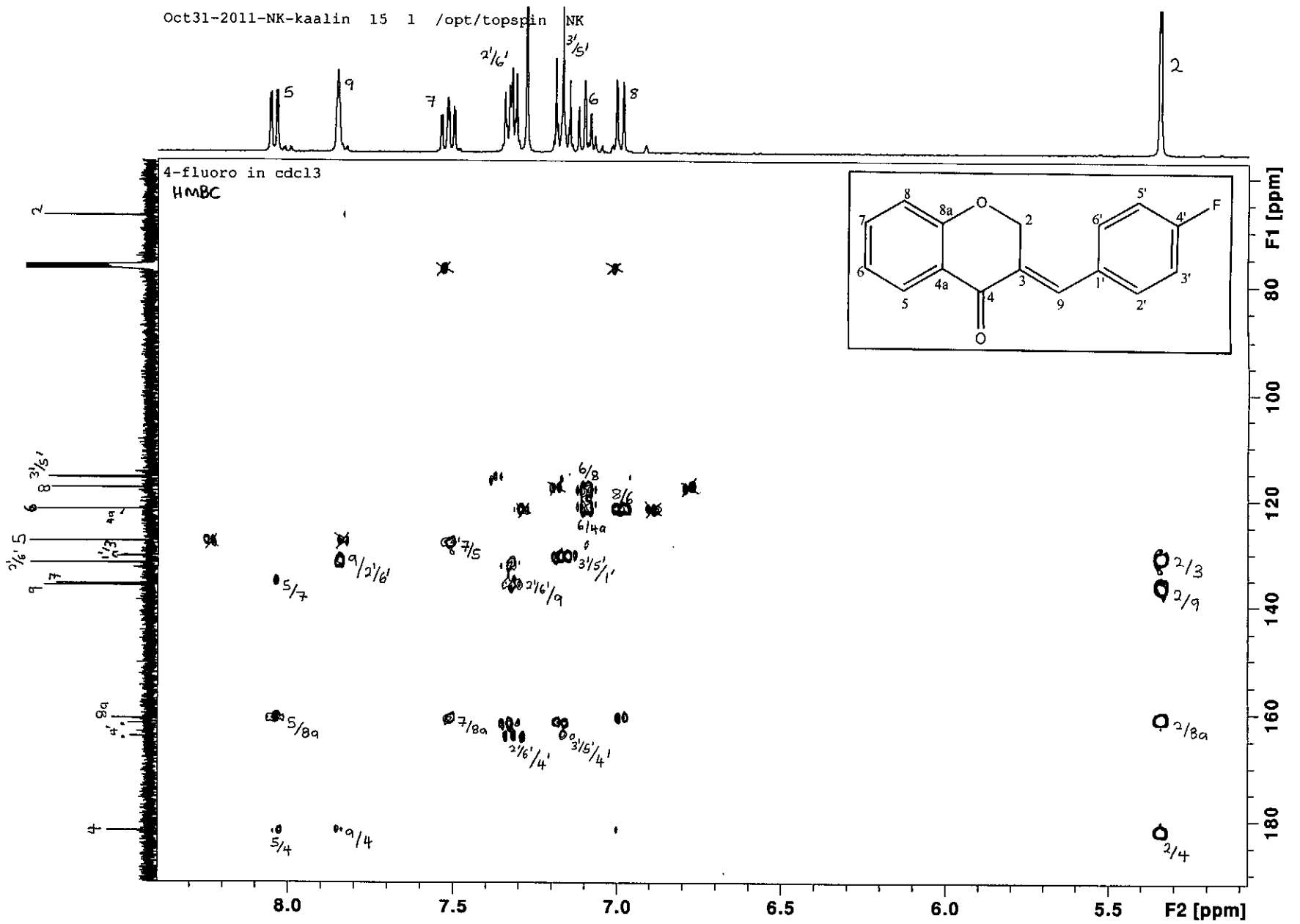
COSY spectrum of compound 10

Oct31-2011-NK-kaalin 14 1 /opt/topspin NK



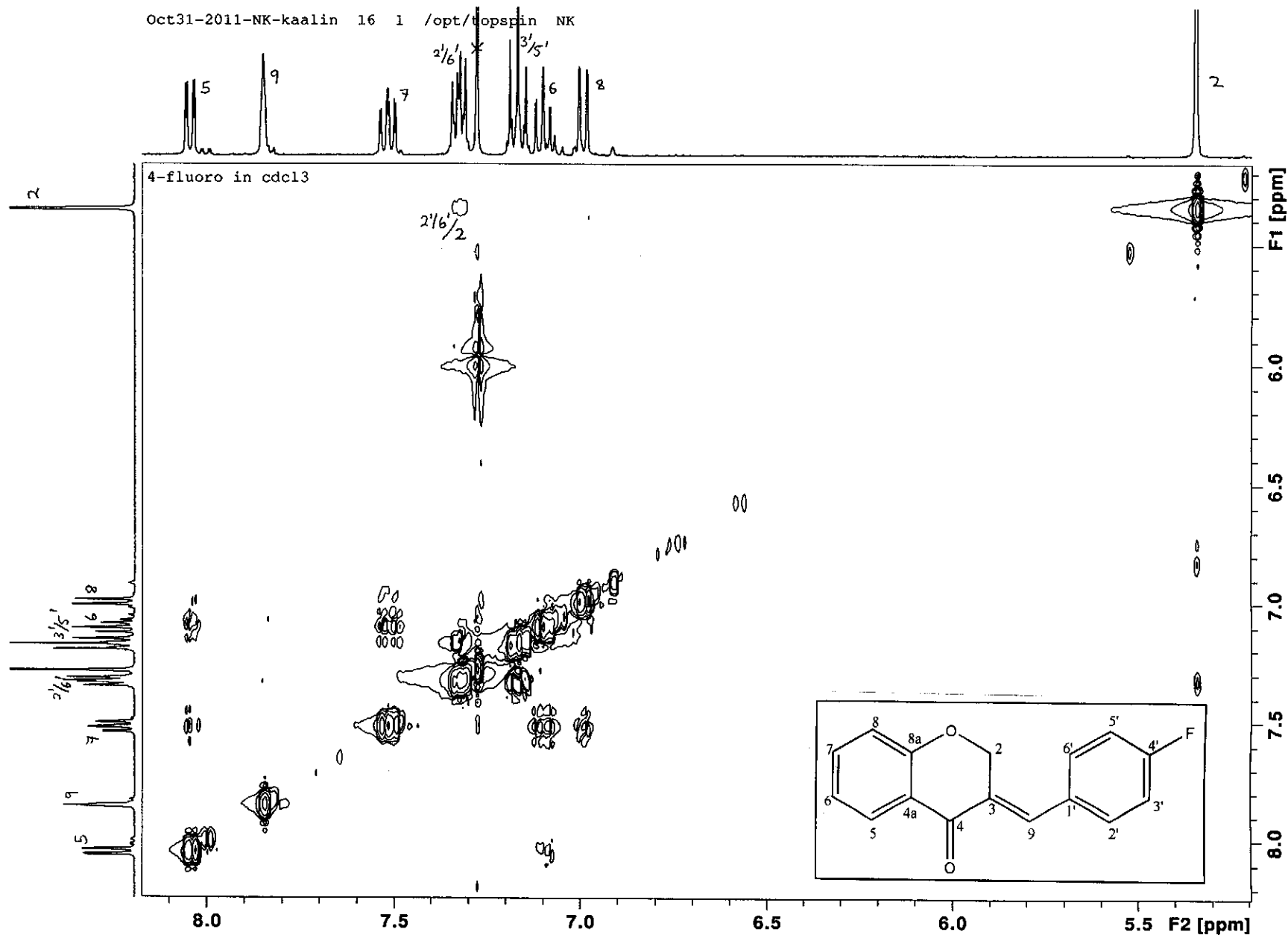
HSQC spectrum of compound 10

Oct31-2011-NK-kaalin 15 1 /opt/topspin NK



HMBC spectrum of compound 10

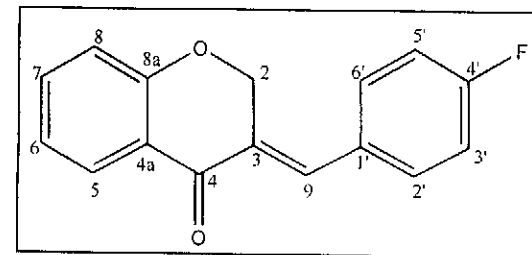
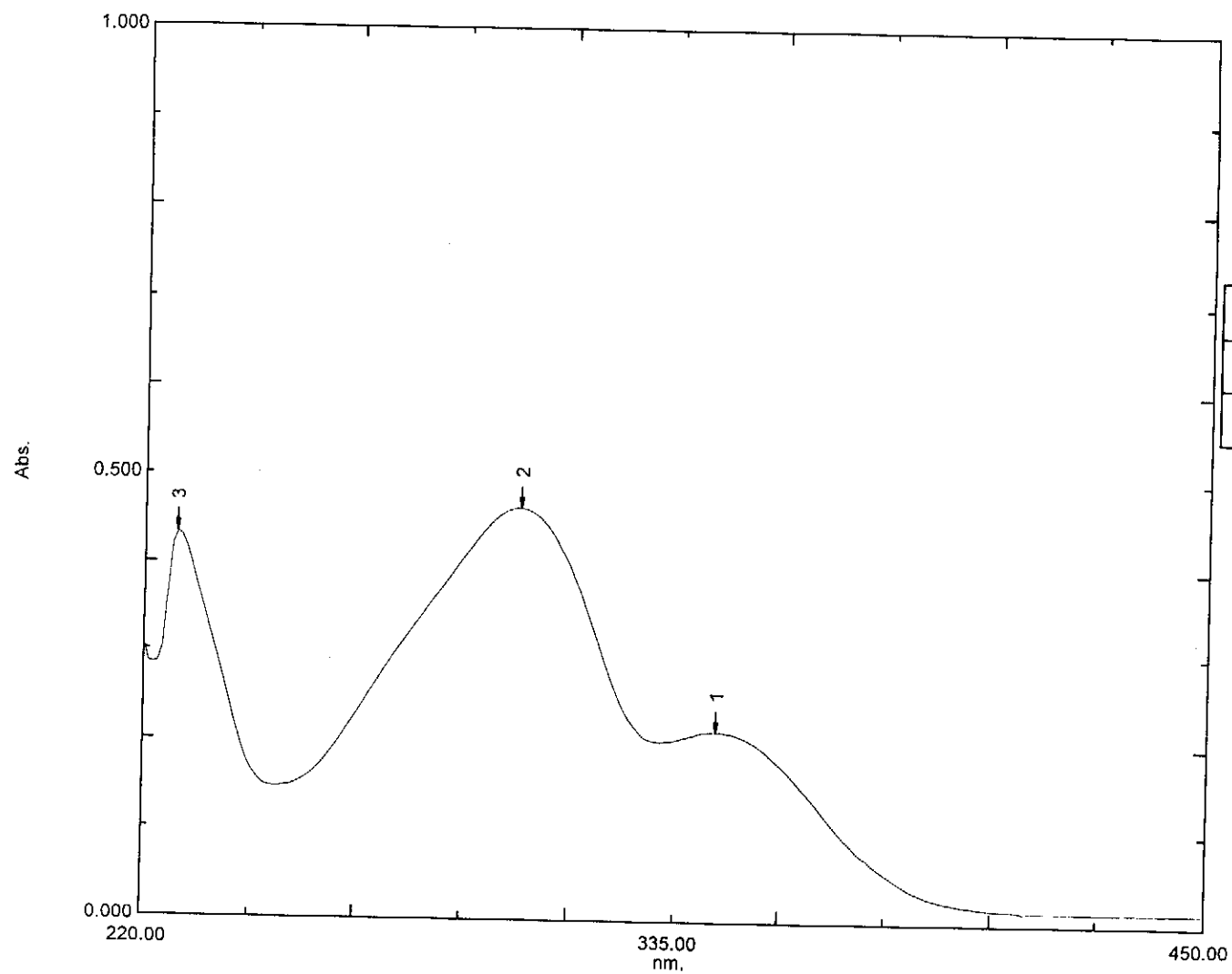
Oct31-2011-NK-kaalin 16 1 /opt/topspin NK



NOESY spectrum of compound 10

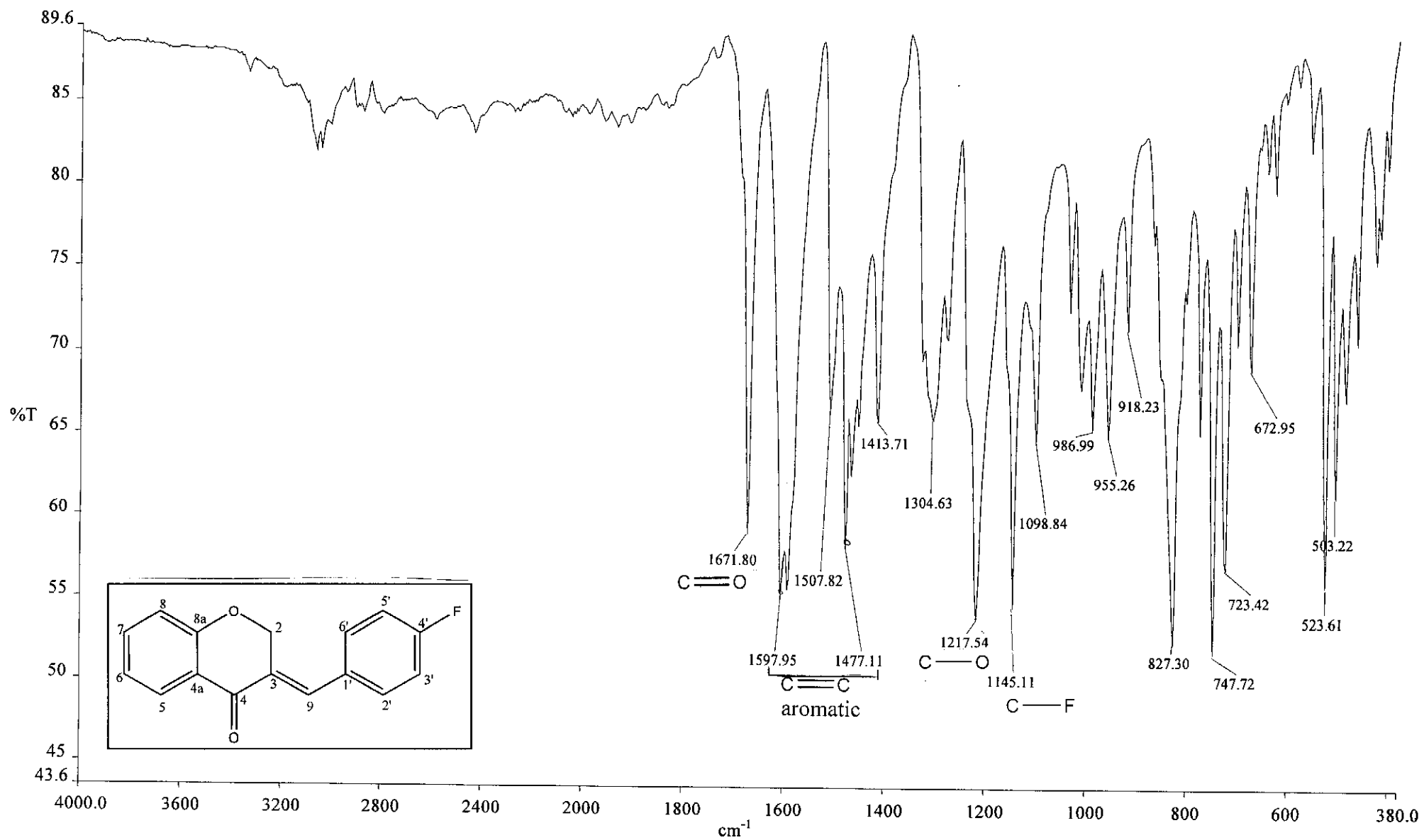
Overlay Spectrum Graph Report

15/05/2012 01:01:28 PM



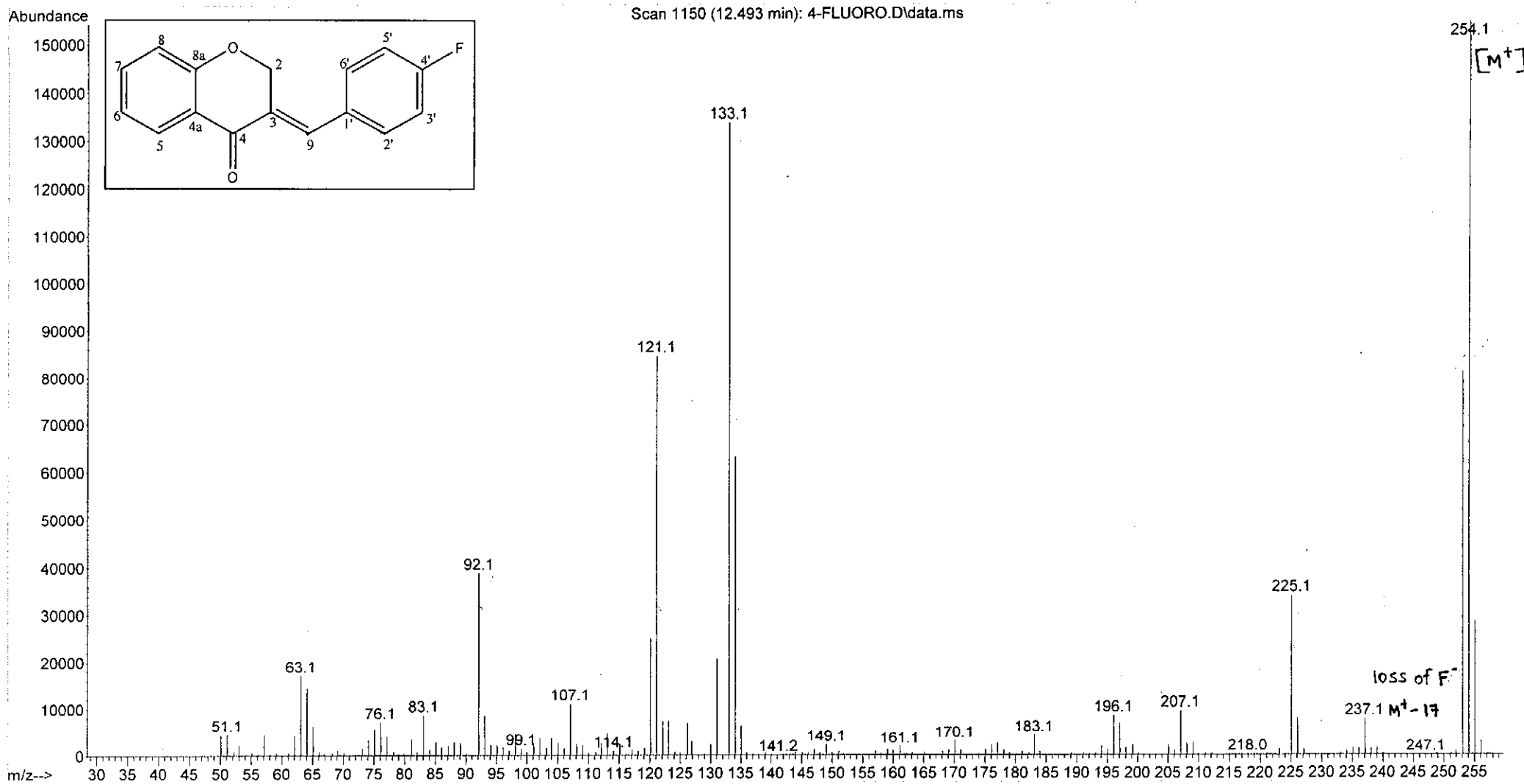
Wavelength/ nm	Absorbance	Log ϵ
301	0.464	3.97
344	0.213	3.63

UV-Vis spectrum of compound 10

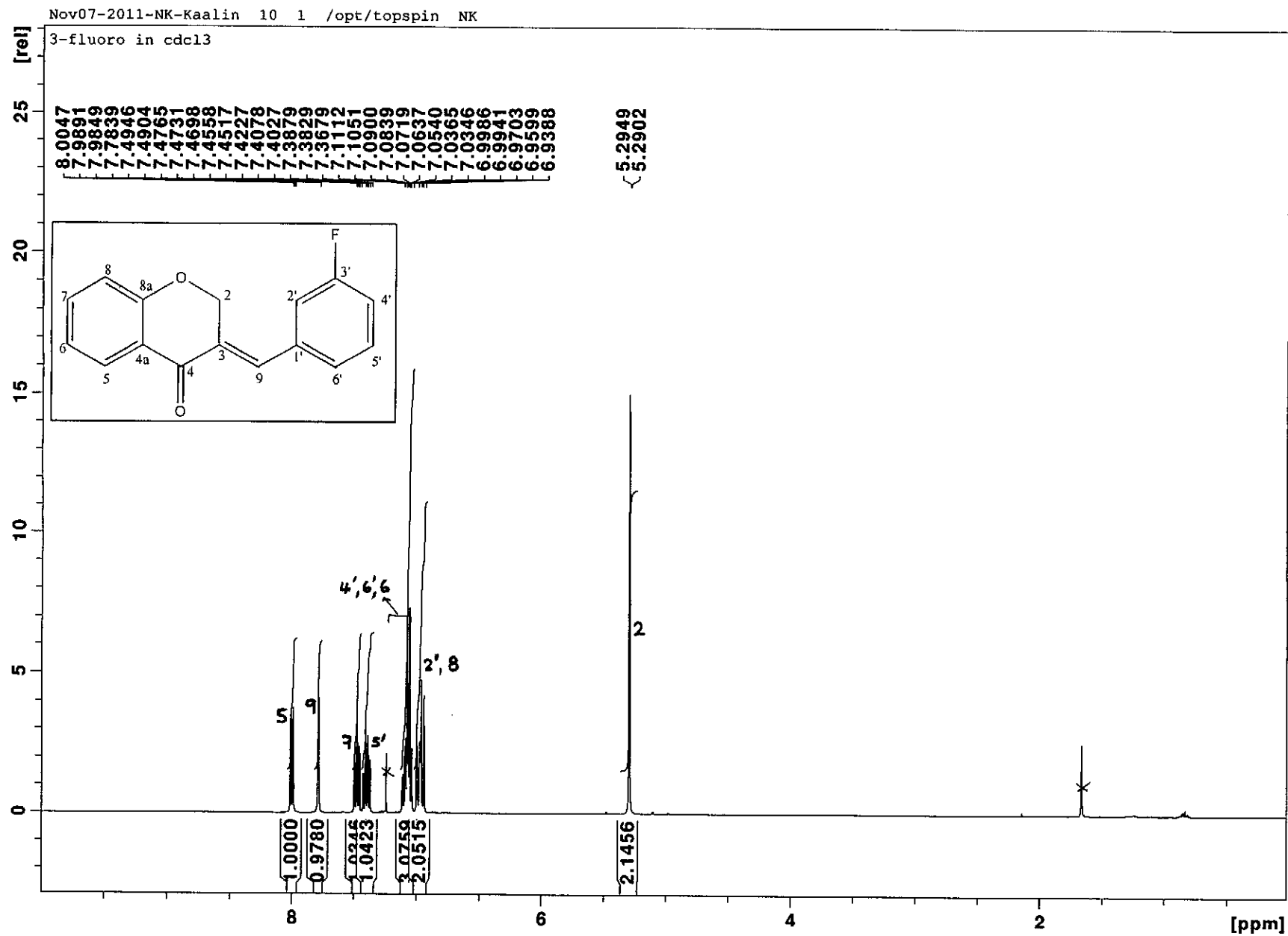


Infrared spectrum of compound 10

File : C:\msdchem\1\data\kaalin\4-FLUORO.D
Operator :
Acquired : 12 Jan 2012 18:44 using AcqMethod NATPRODUCTS MANUAL INJ.M
Instrument : 5973N
Sample Name:
Misc Info :
Vial Number: 1

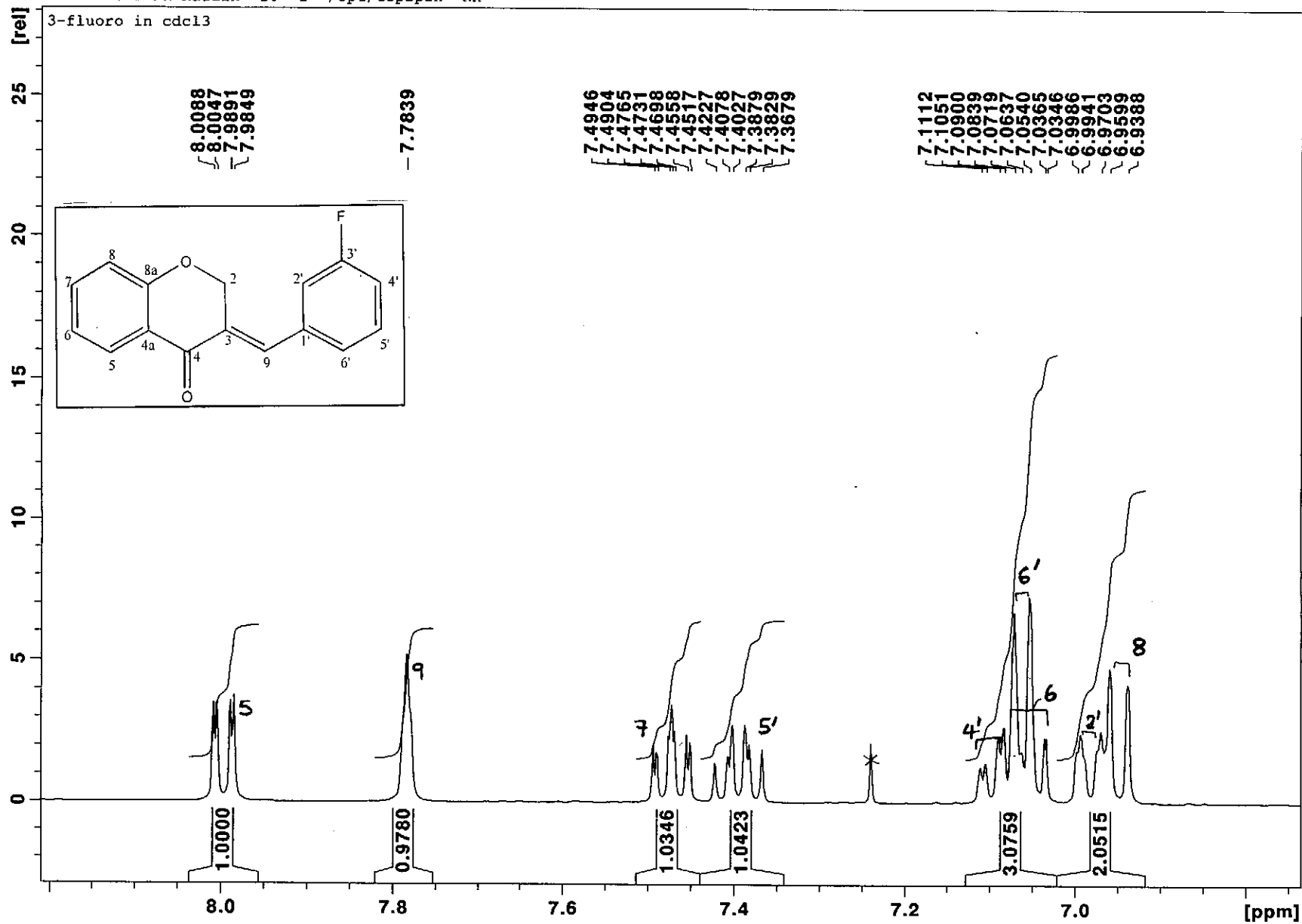


Mass spectrum of compound 10

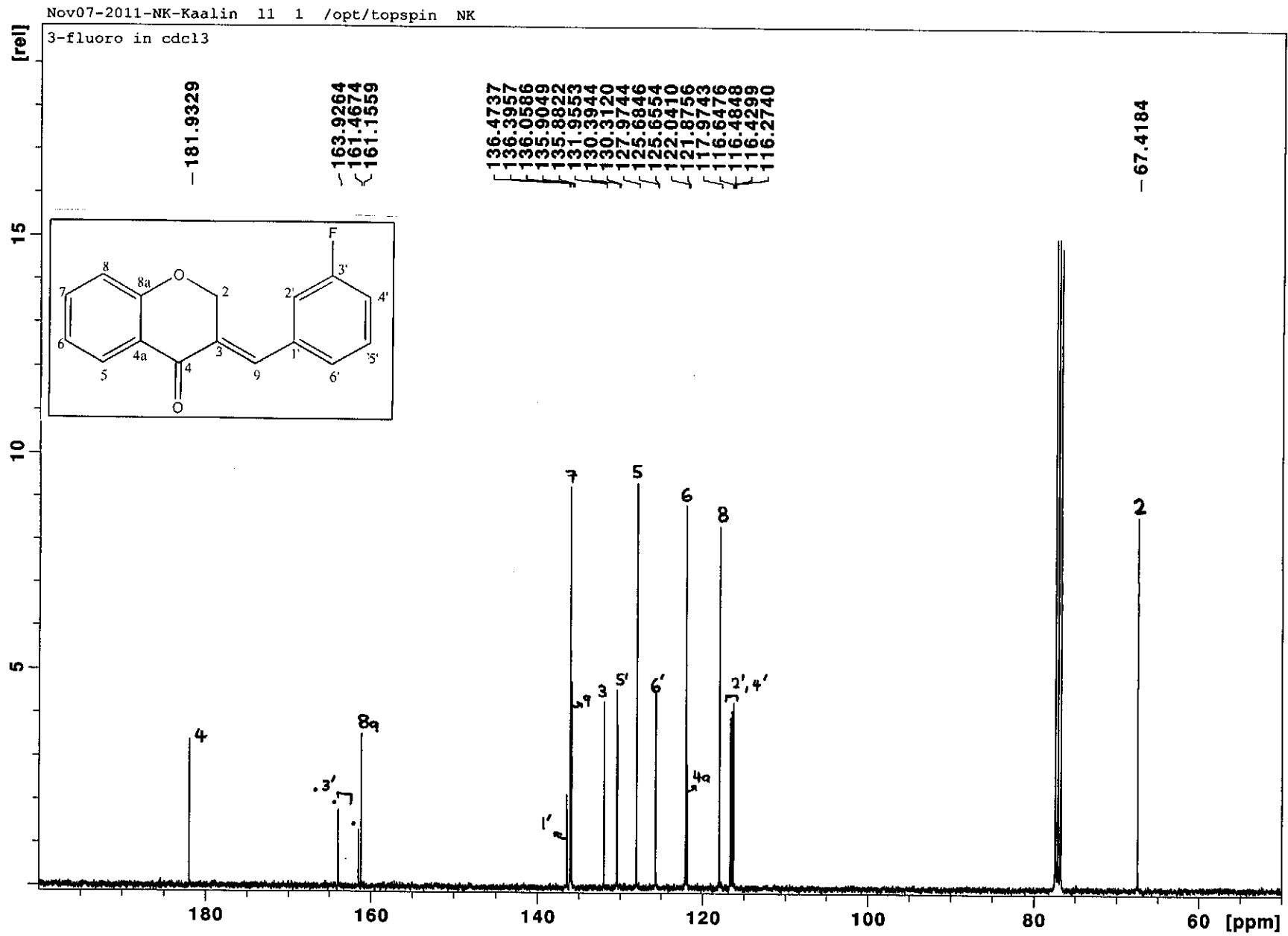


¹H NMR spectrum of compound 11

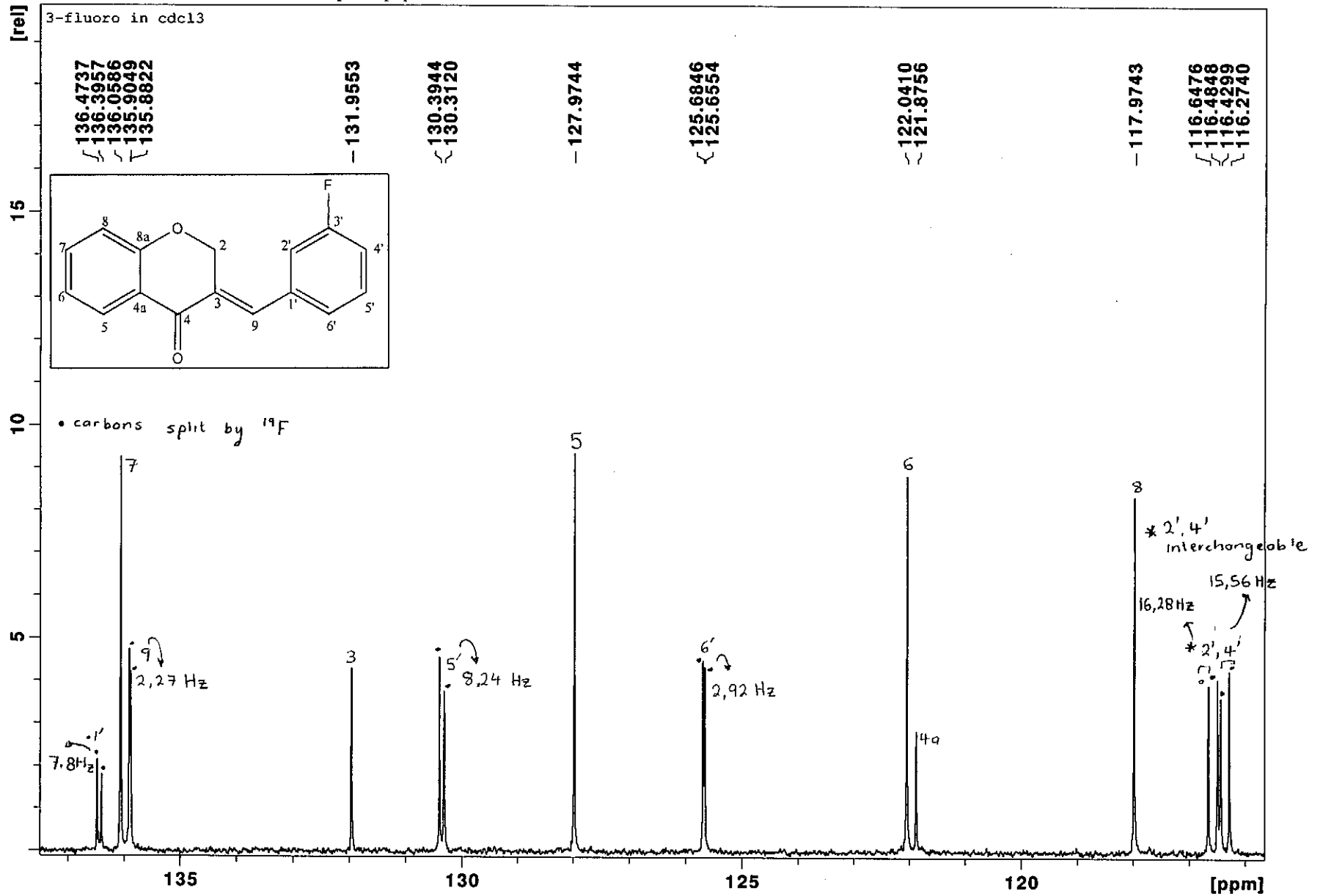
Nov07-2011-NK-Kaalin 10 1 /opt/topspin NK



¹H NMR spectrum of compound 11 (expanded)

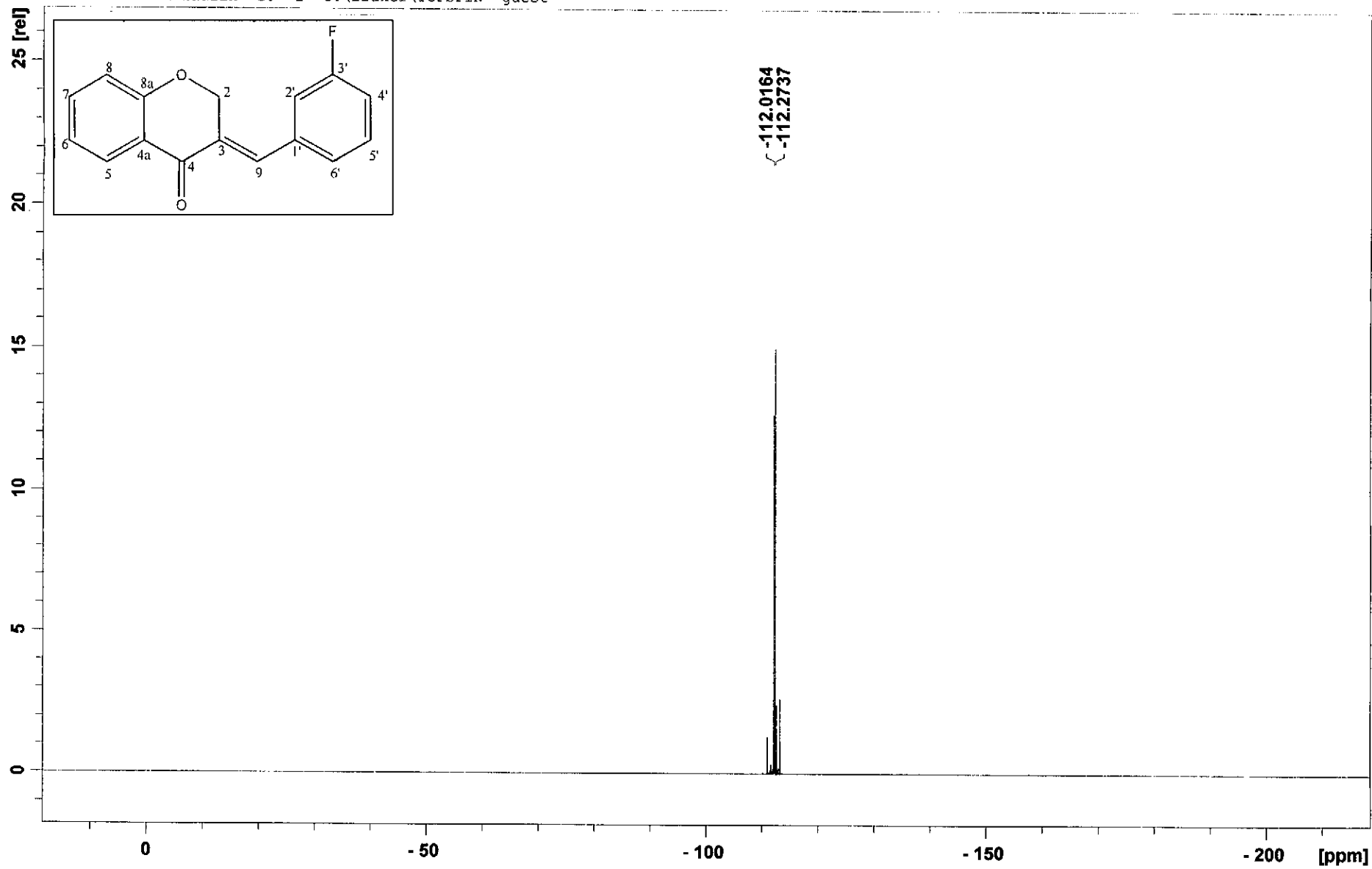


¹³C NMR spectrum of compound 11



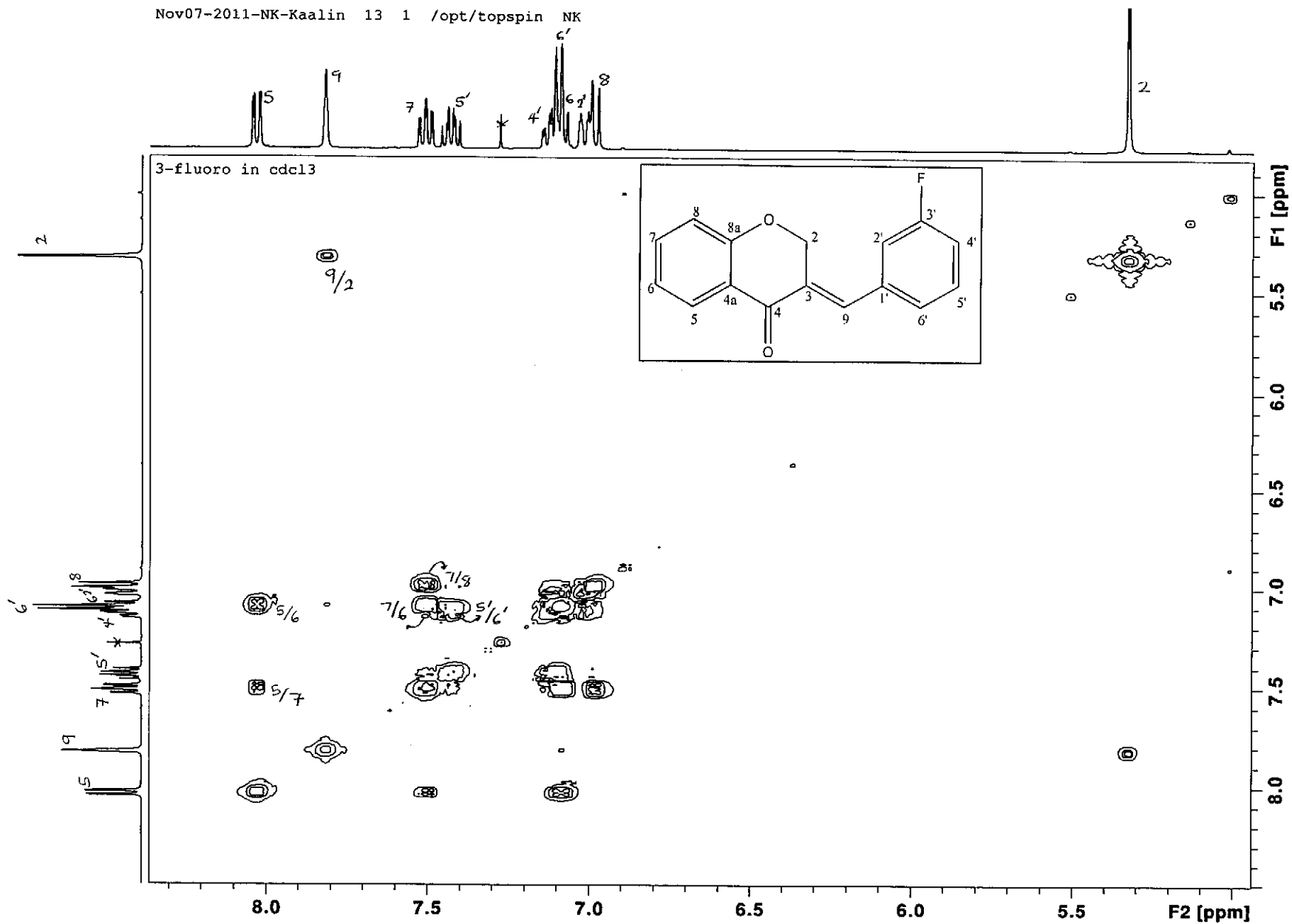
^{13}C NMR spectrum of compound 11 (expanded)

Feb08-2012-NK-kaalin 10 1 C:\Bruker\TOPSPIN guest



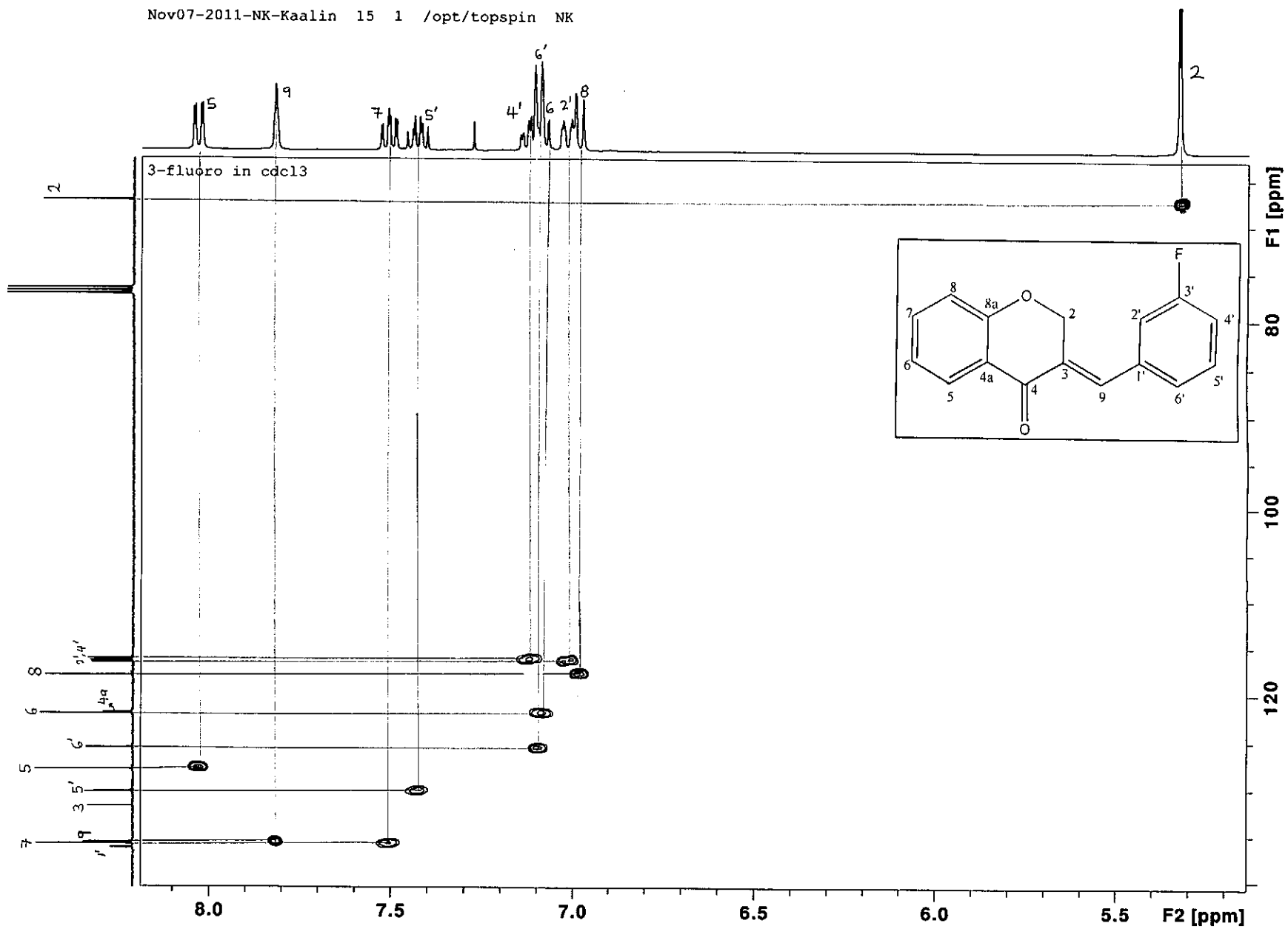
^{19}F NMR spectrum of compound 11

Nov07-2011-NK-Kaalin 13 1 /opt/topspin NK



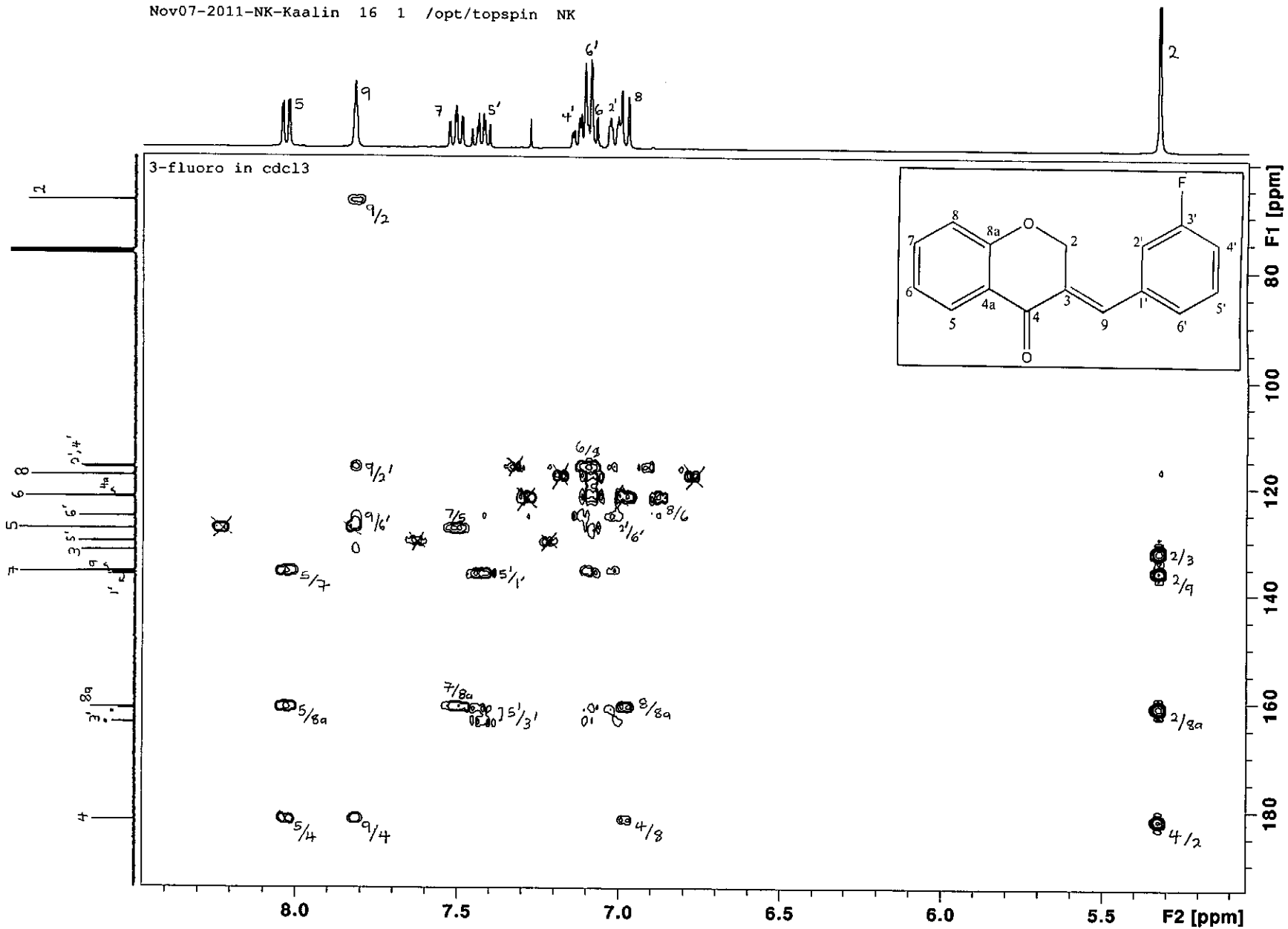
COSY spectrum of compound 11

Nov07-2011-NK-Kaalin 15 1 /opt/topspin NK



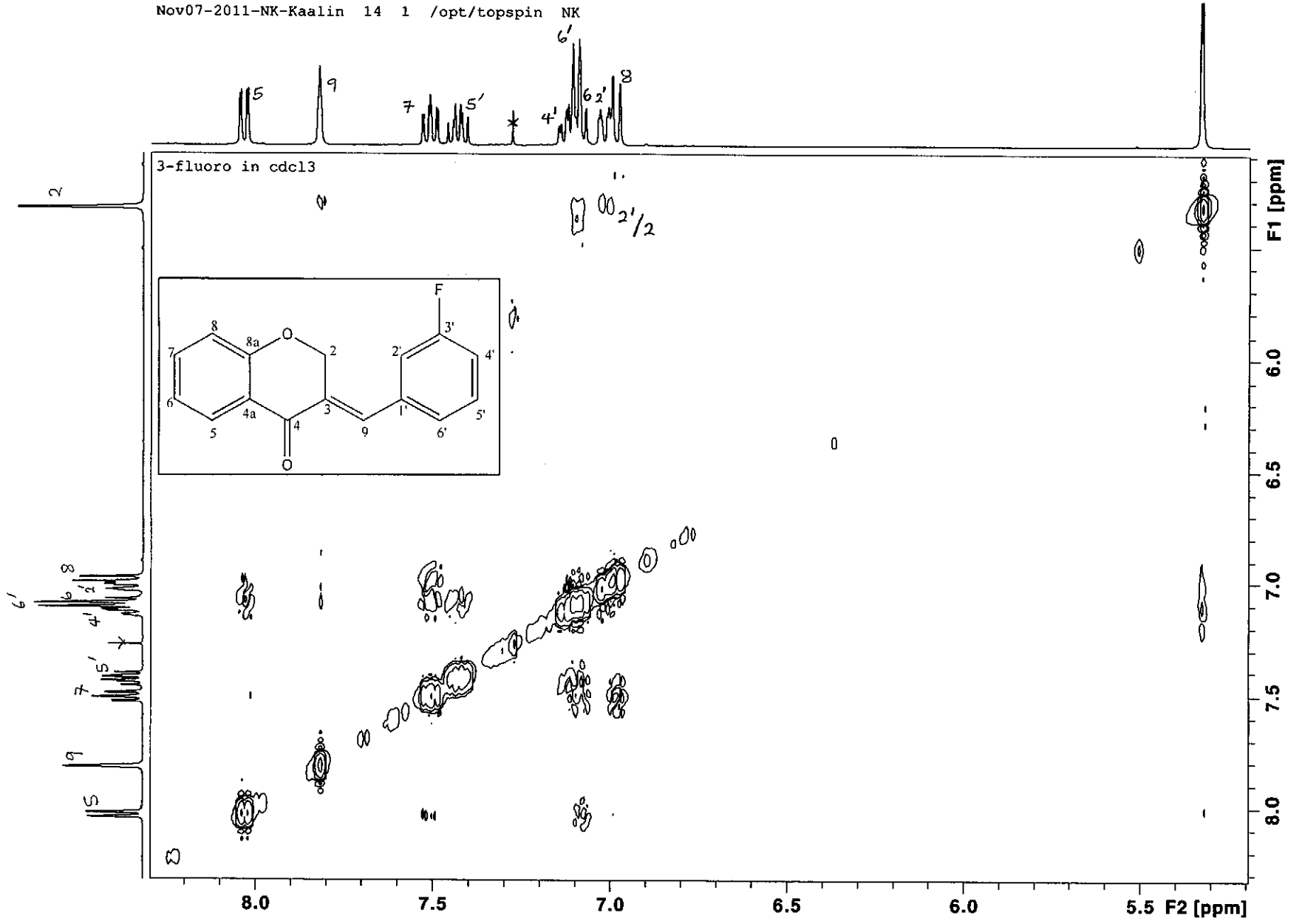
HSQC spectrum of compound 11

Nov07-2011-NK-Kaalin 16 1 /opt/topspin NK



HMBC spectrum of compound 11

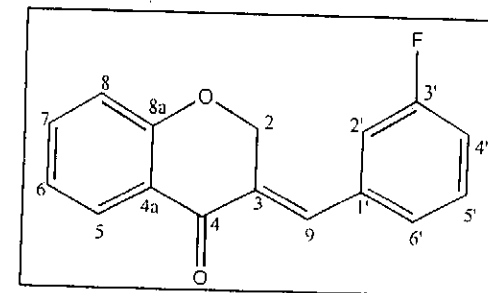
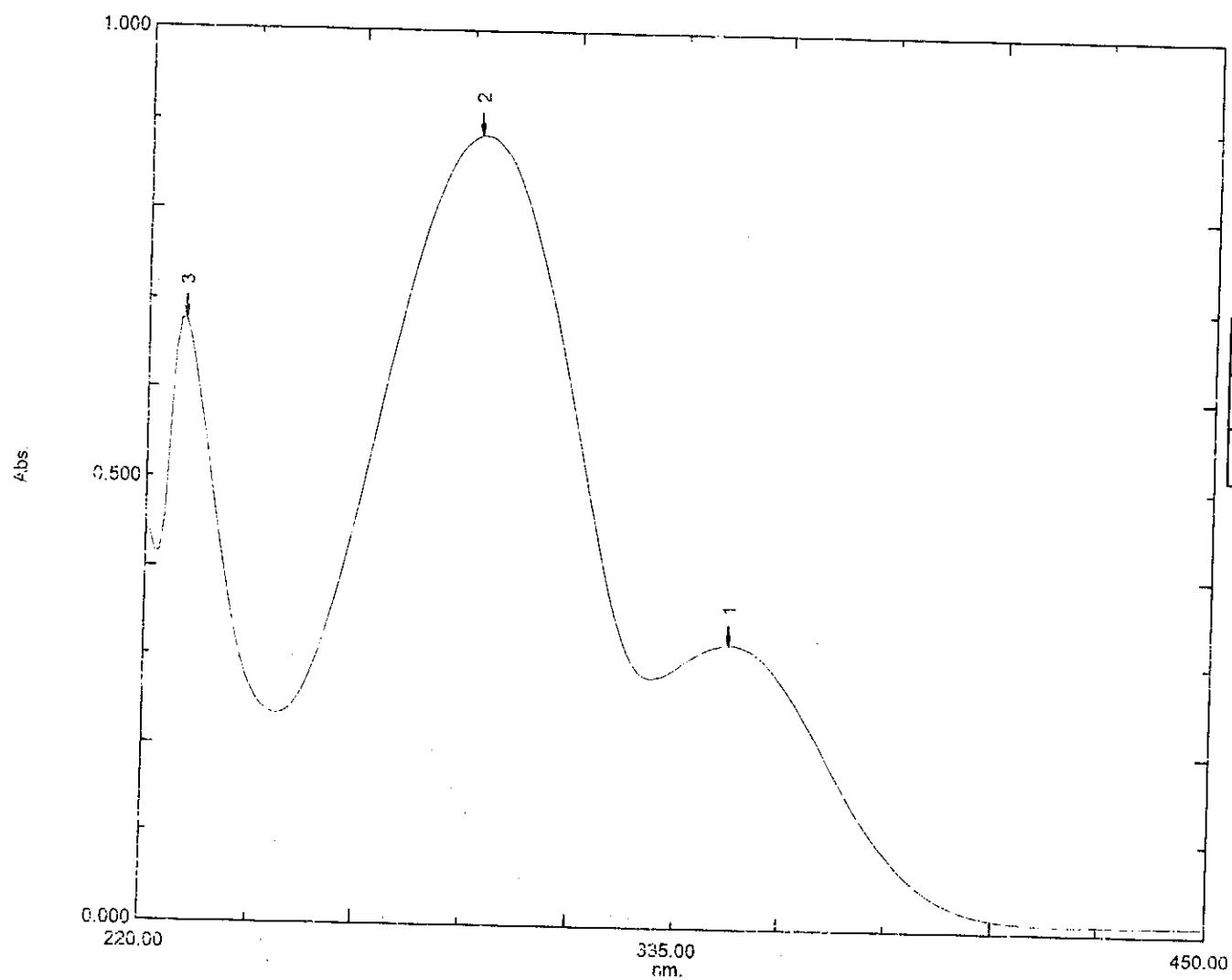
Nov07-2011-NK-Kaalin 14 1 /opt/topspin NK



NOESY spectrum of compound 11

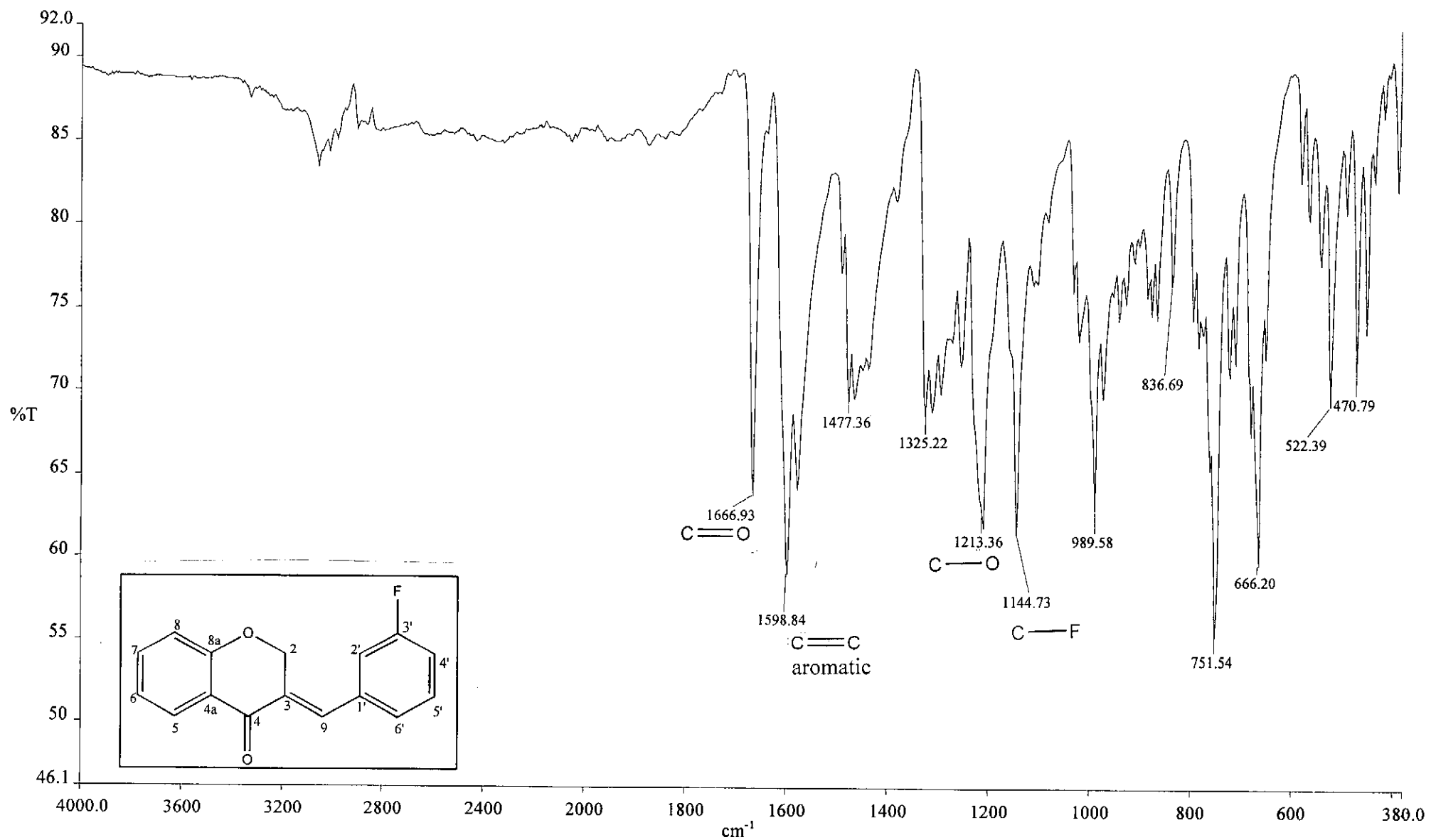
Overlay Spectrum Graph Report

15/05/2012 01:02:16 PM



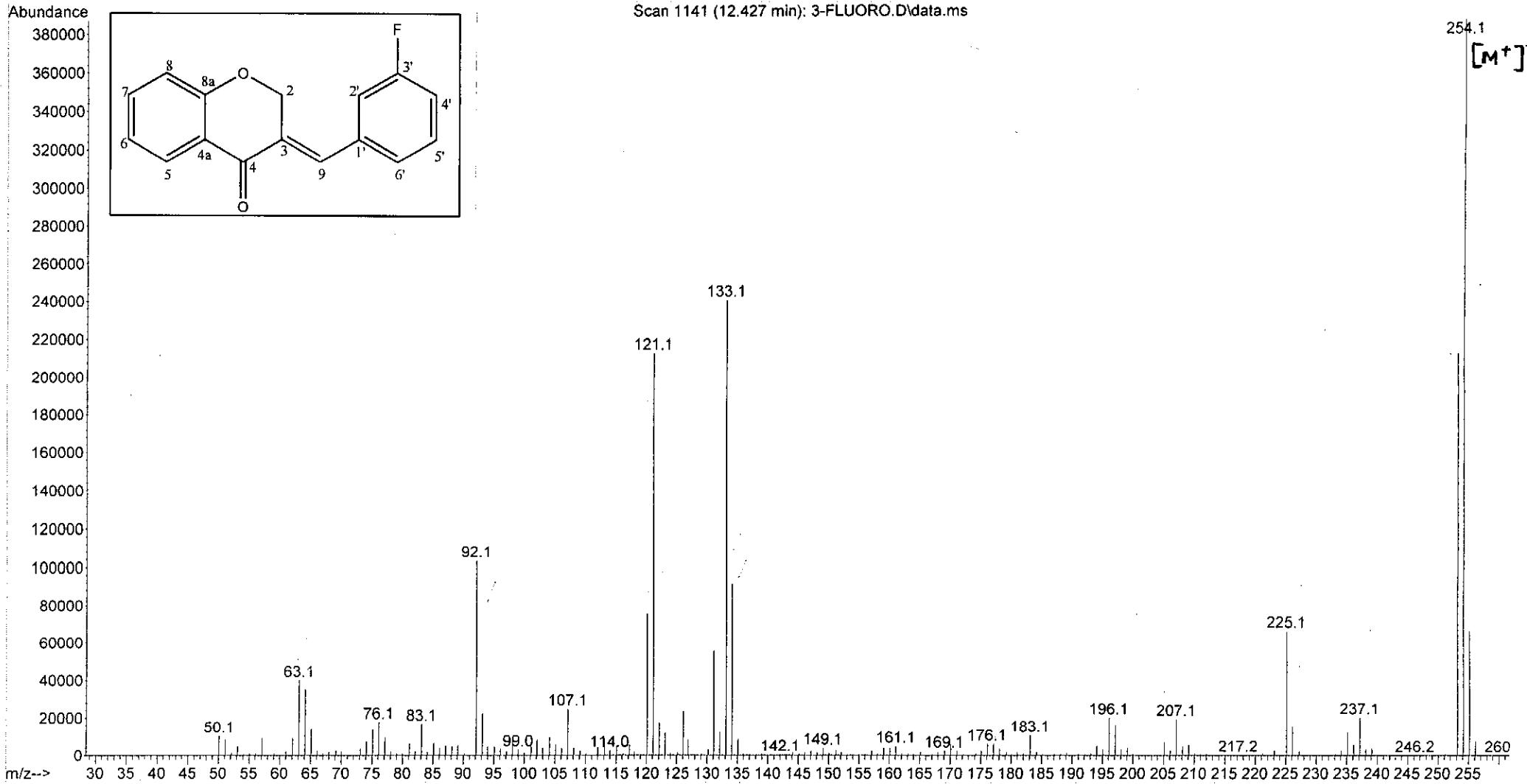
Wavelength/ nm	Absorbance	Log ϵ
291	0.885	3.99
346	0.319	3.55

UV-Vis spectrum of compound 11

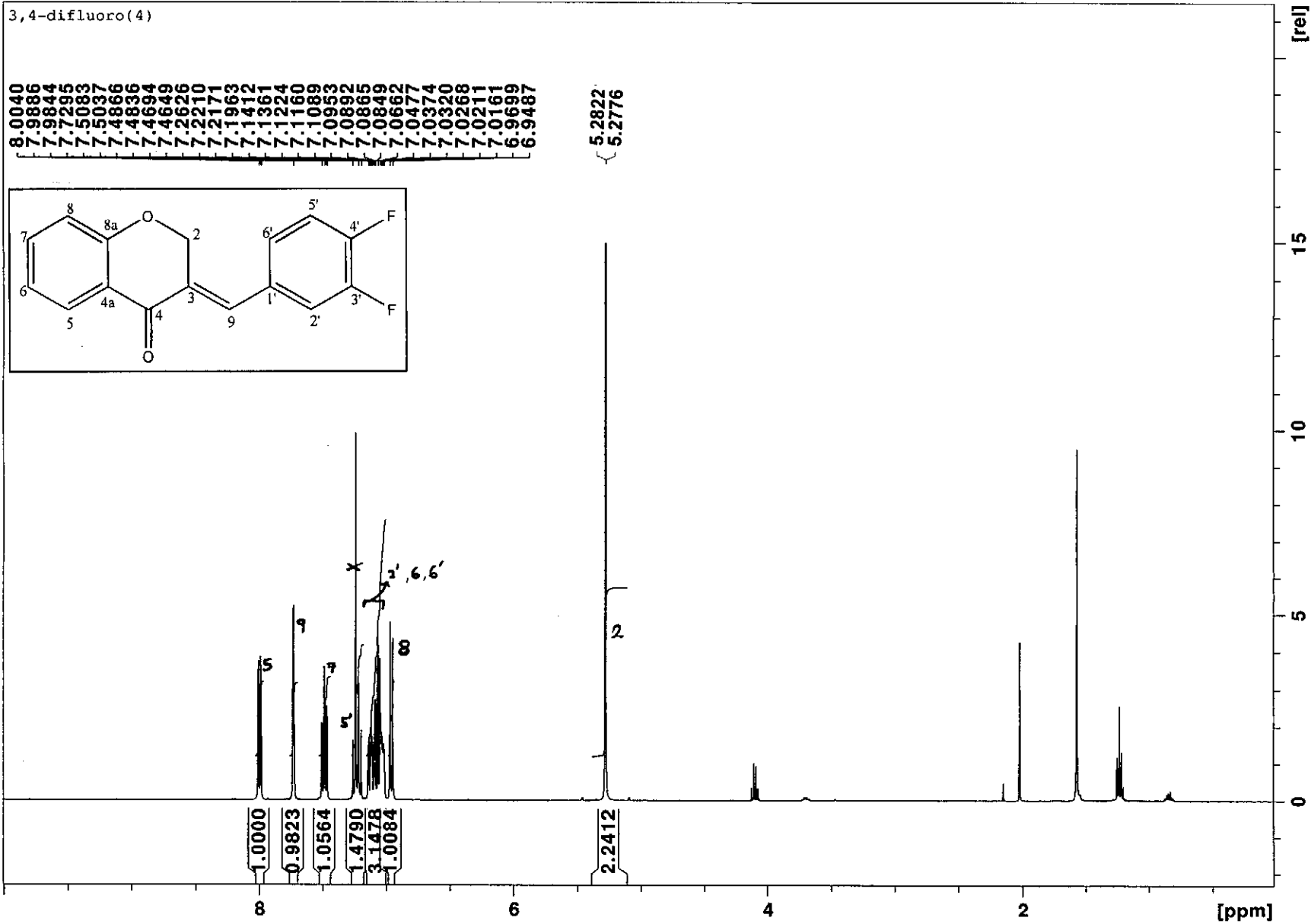


Infrared spectrum of compound 11

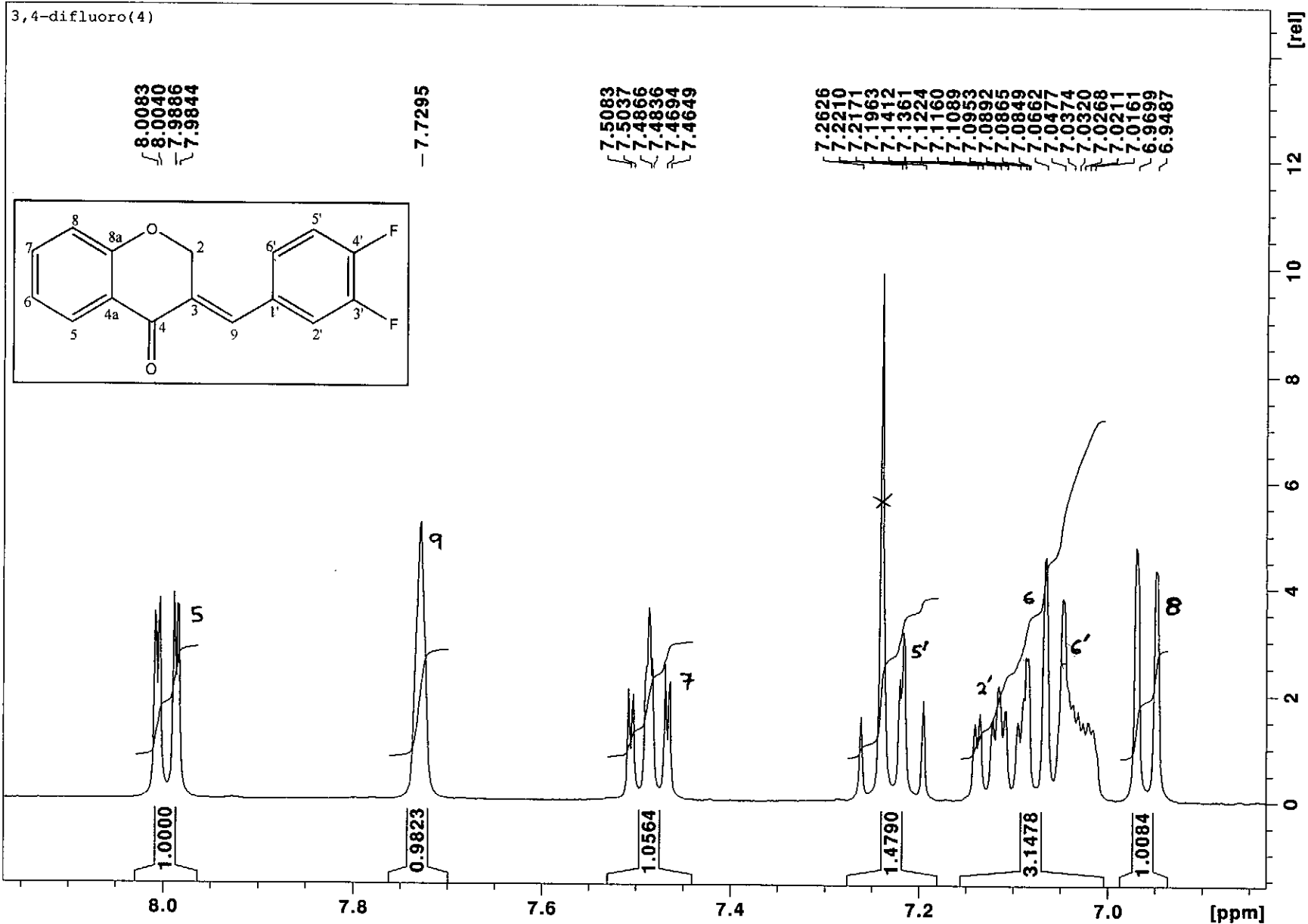
File : C:\msdchem\1\data\kaalin\3-FLUORO.D
Operator :
Acquired : 13 Jan 2012 10:20 using AcqMethod NATPRODUCTS MANUAL INJ.M
Instrument : 5973N
Sample Name:
Misc Info :
Vial Number: 1



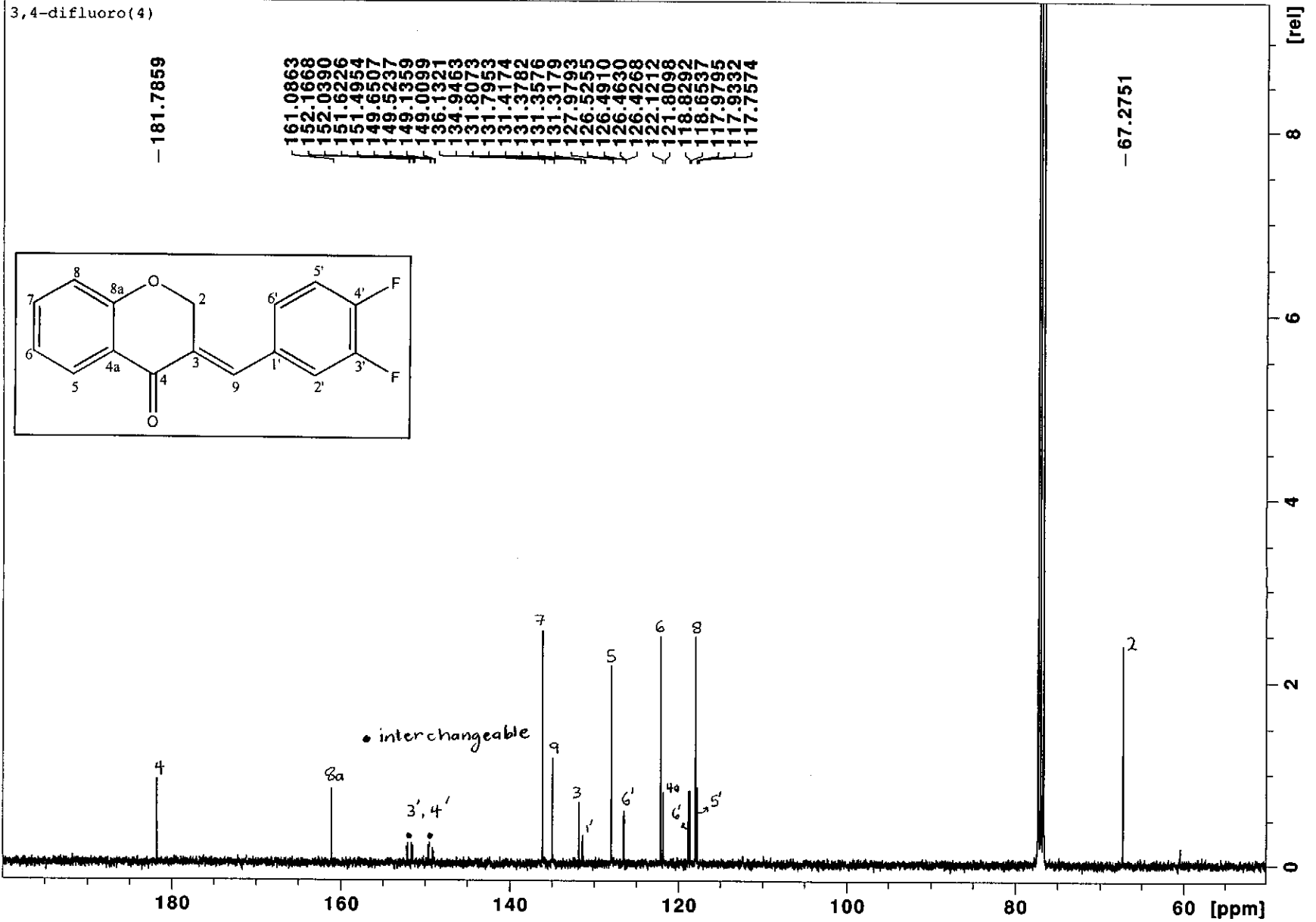
Nov15-2011-NK-Kaalin 10 1 /opt/topspin NK



¹H NMR spectrum of compound 12



¹H NMR spectrum of compound 12 (expanded)



¹³C NMR spectrum of compound 12

3,4-difluoro(4)

152.1668
152.0390
151.6226
151.4954
149.6507
149.5237
149.1359
149.0099

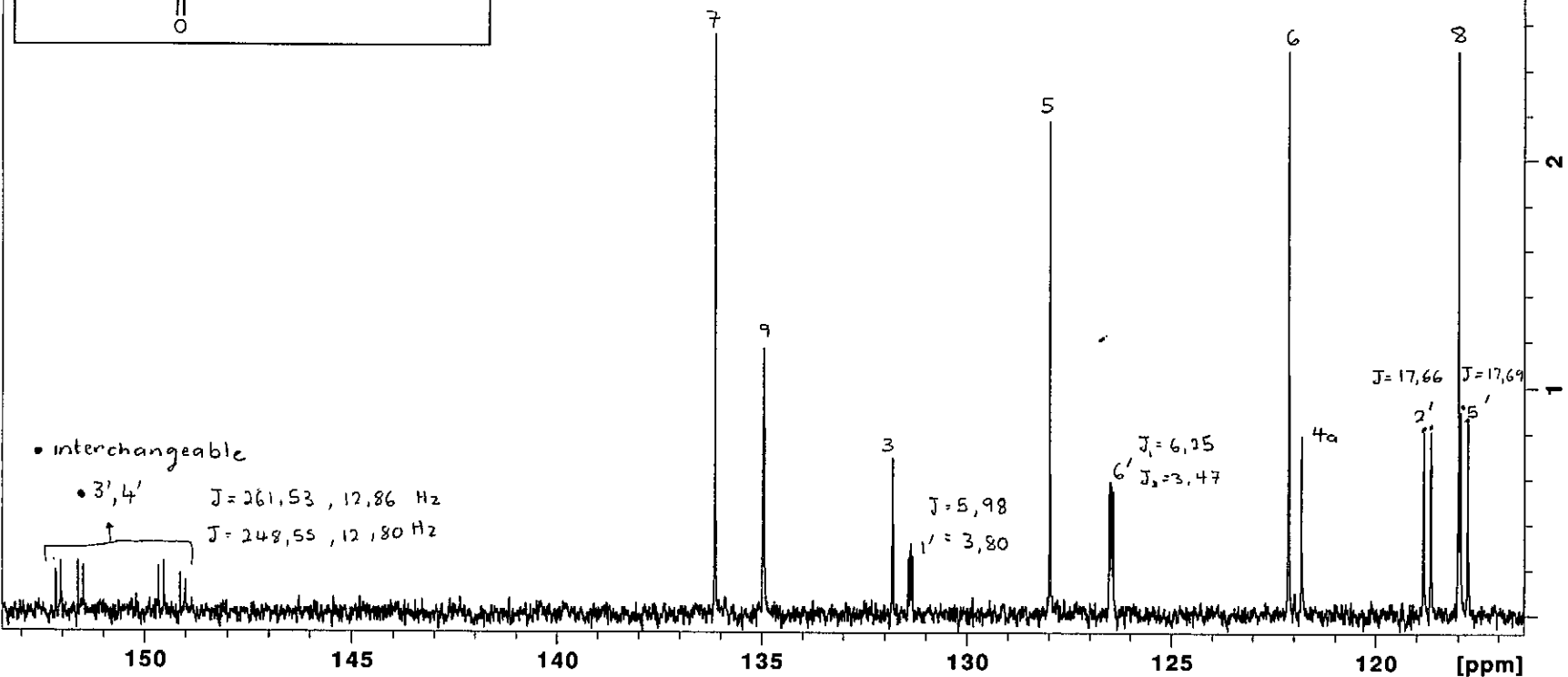
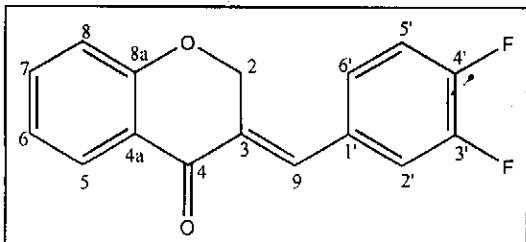
136.1321
134.9463

131.8073
131.7953
131.4174
131.3782
131.3576
131.3179

127.9793
126.5255
126.4910
126.4630
126.4268

122.1212
121.8098

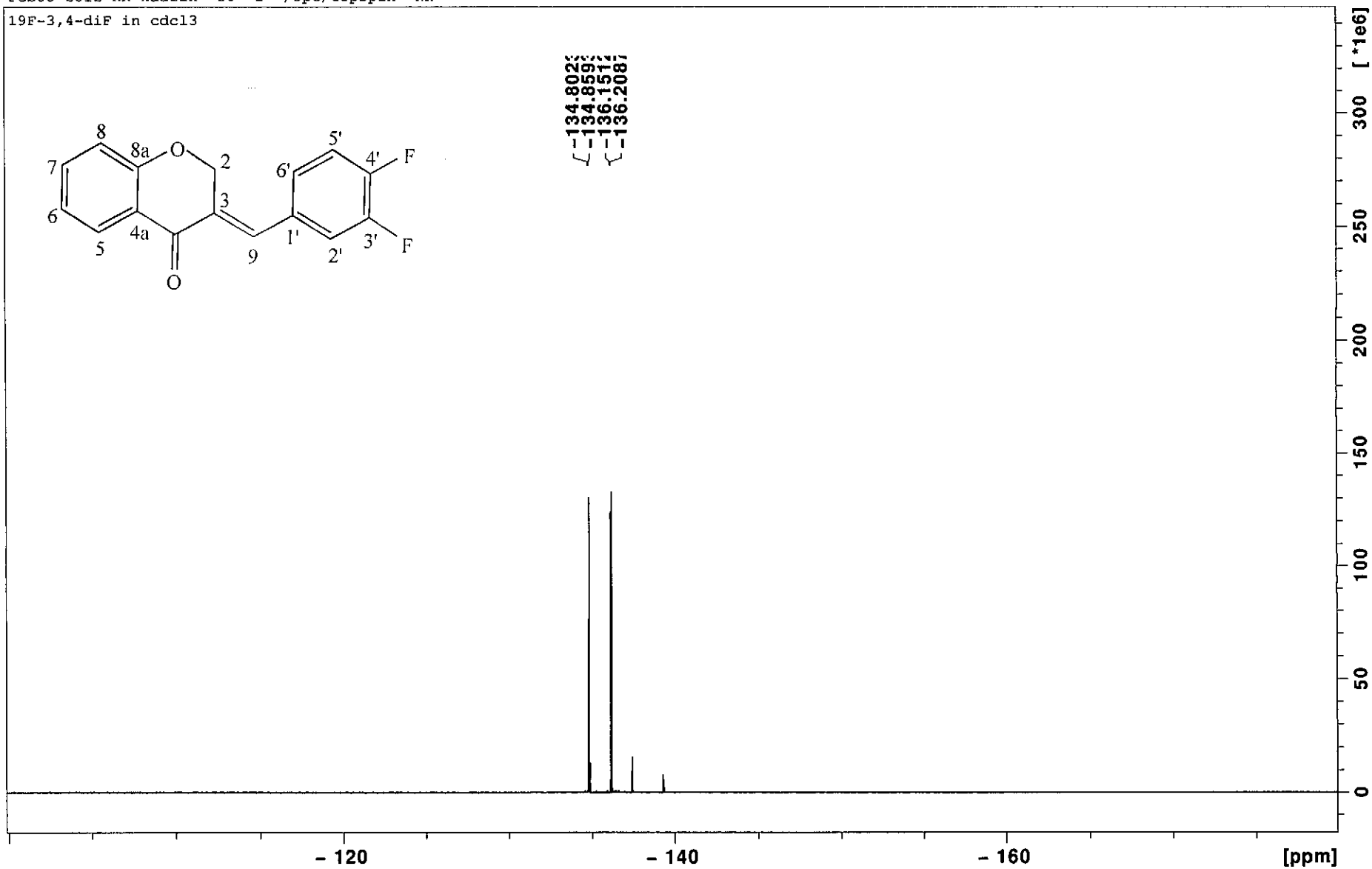
118.8292
118.6537
117.9795
117.9332
117.7574



¹³C NMR spectrum of compound 12 (expanded)

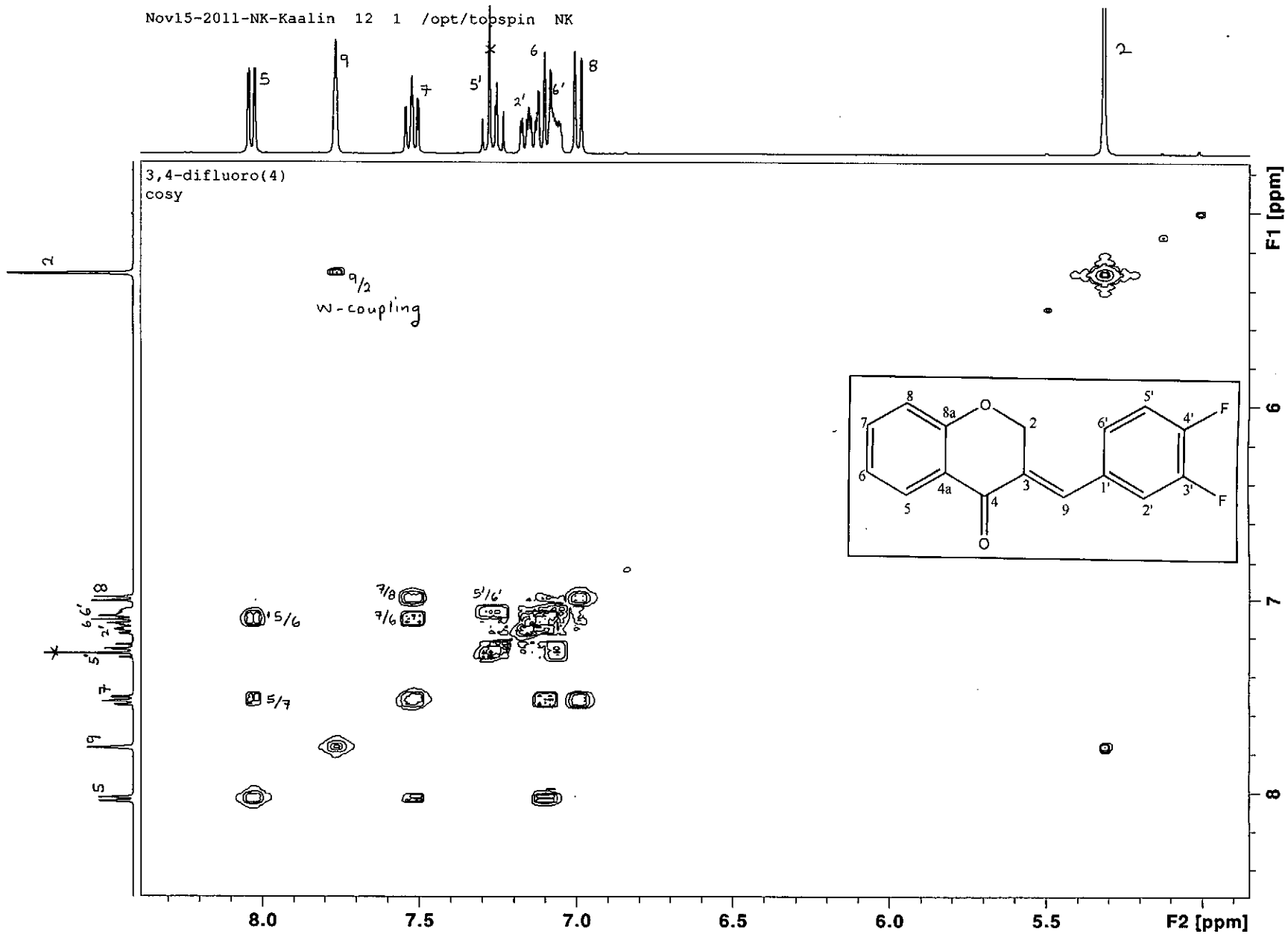
Feb08-2012-NK-kaalin 30 1 /opt/topspin NK

¹⁹F-3,4-diF in cdcl3

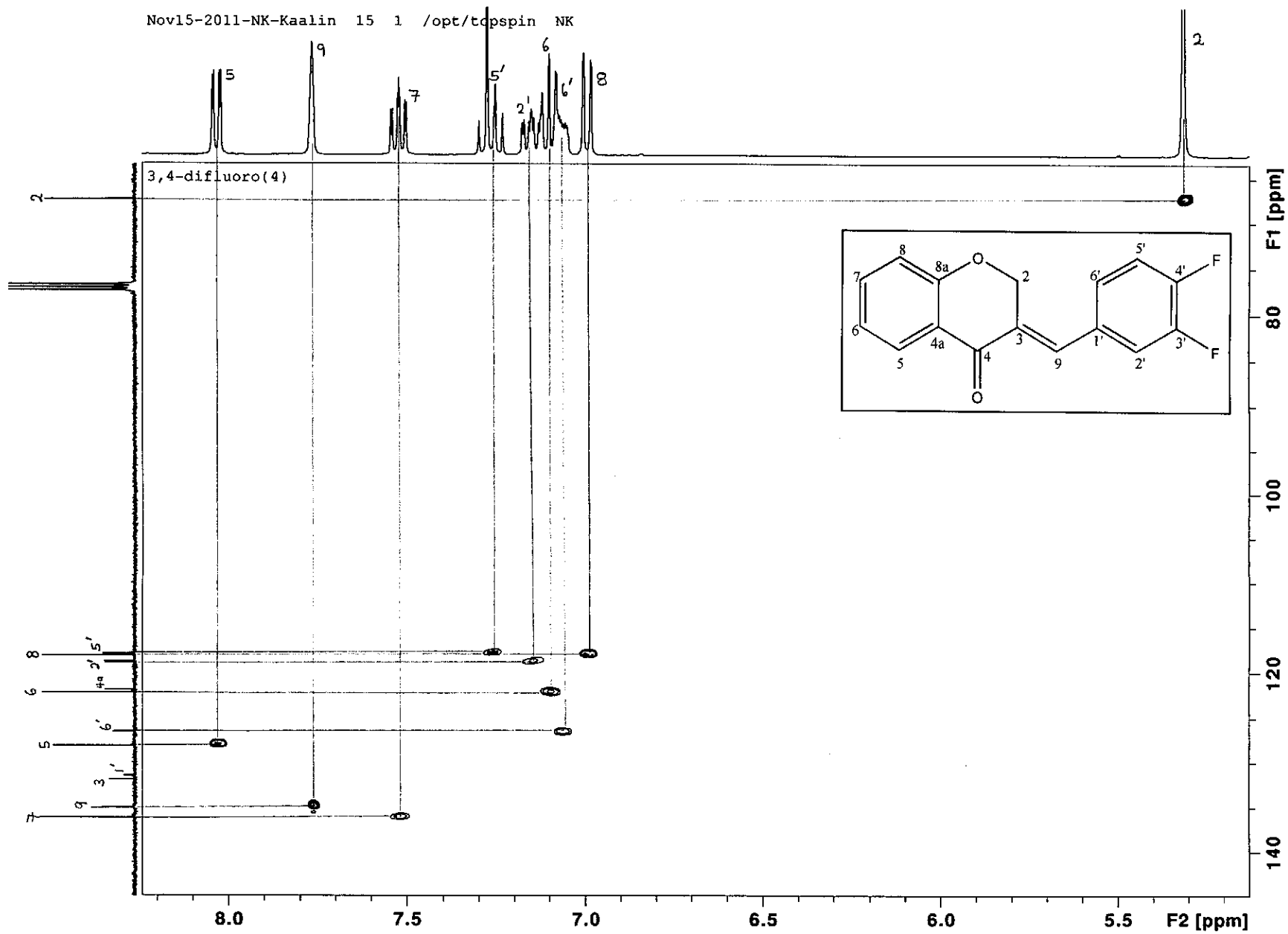


¹⁹F NMR spectrum of compound 12

Nov15-2011-NK-Kaalin 12 1 /opt/topspin NK

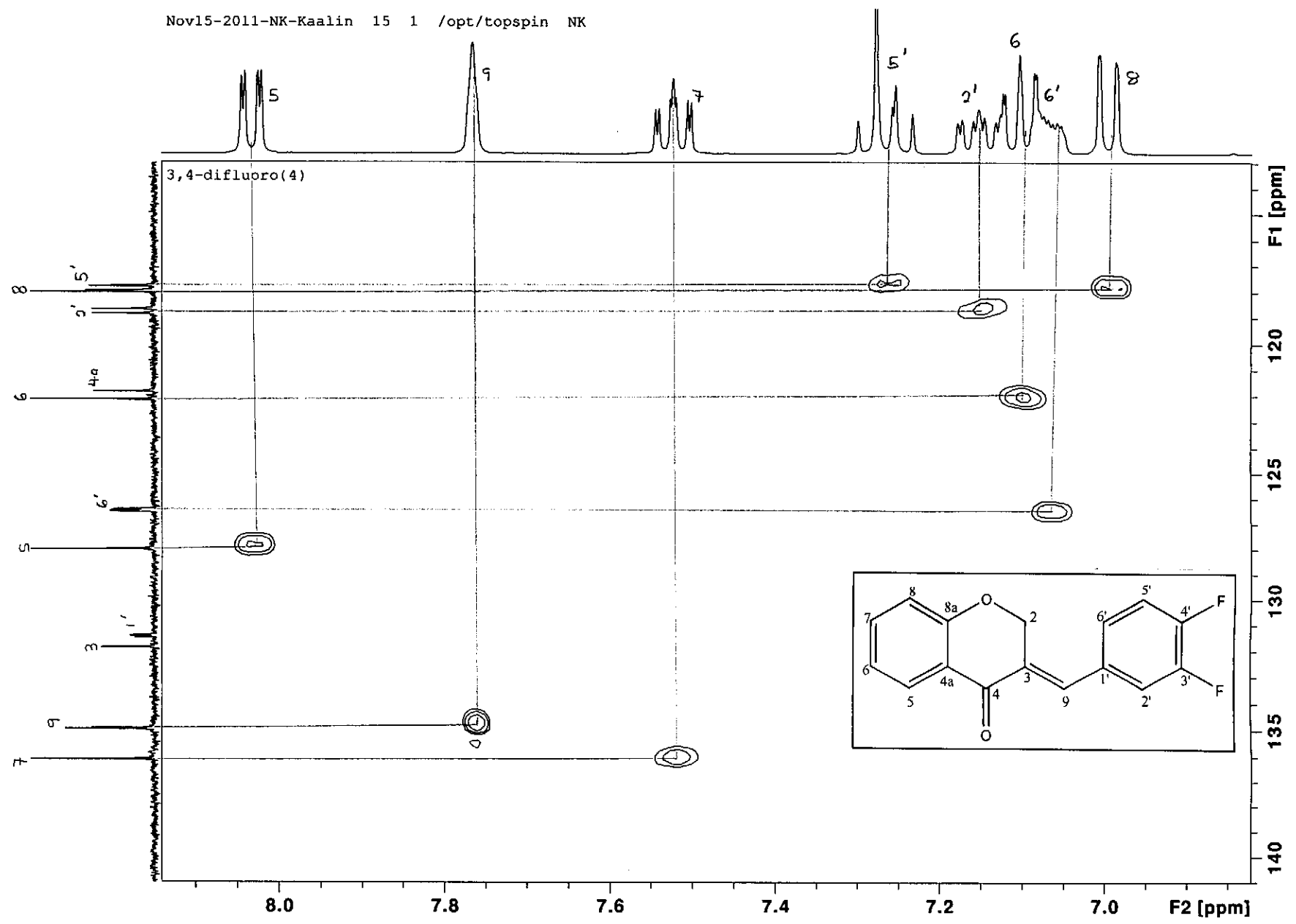


COSY spectrum of compound 12

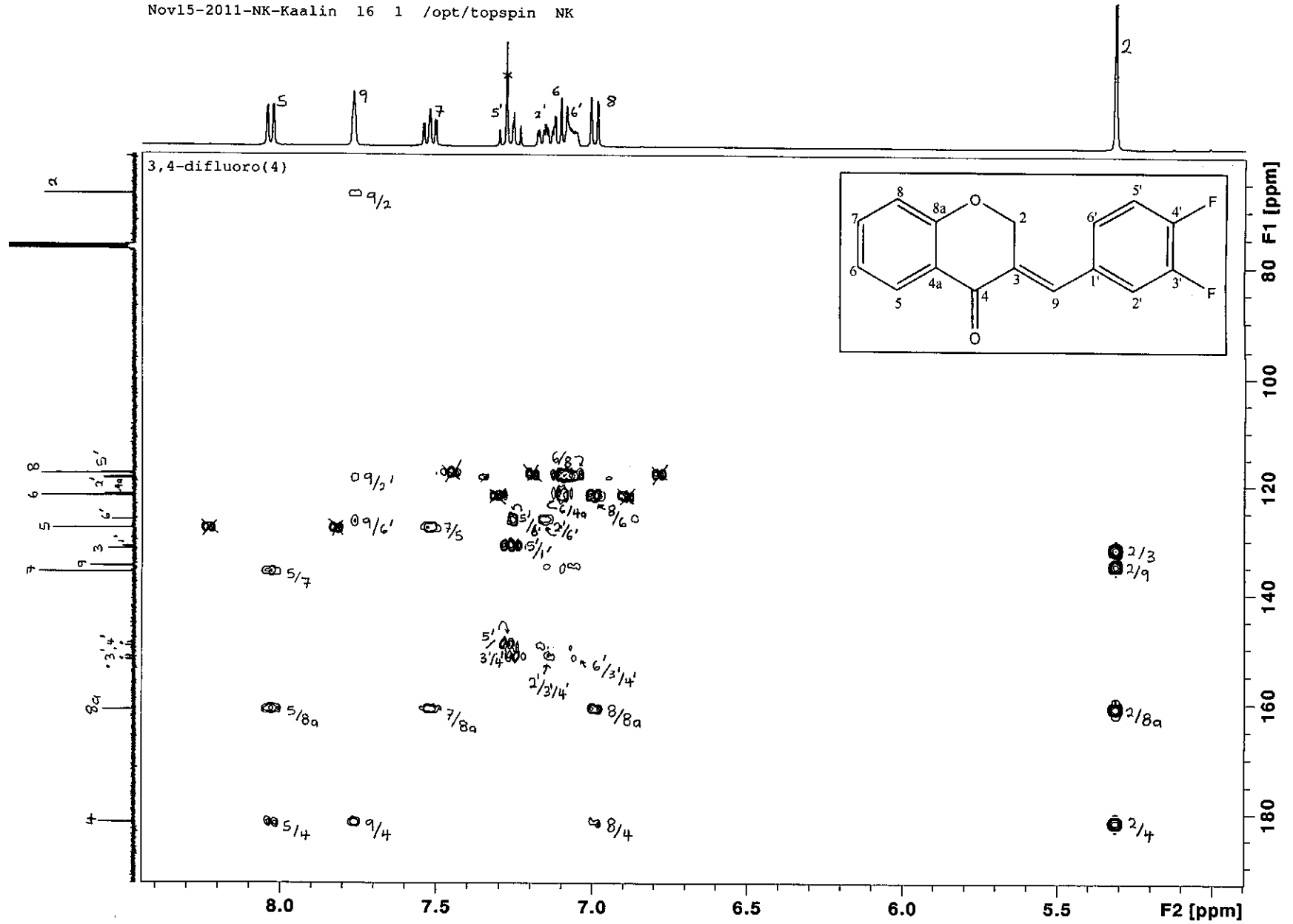


HSQC spectrum of compound 12

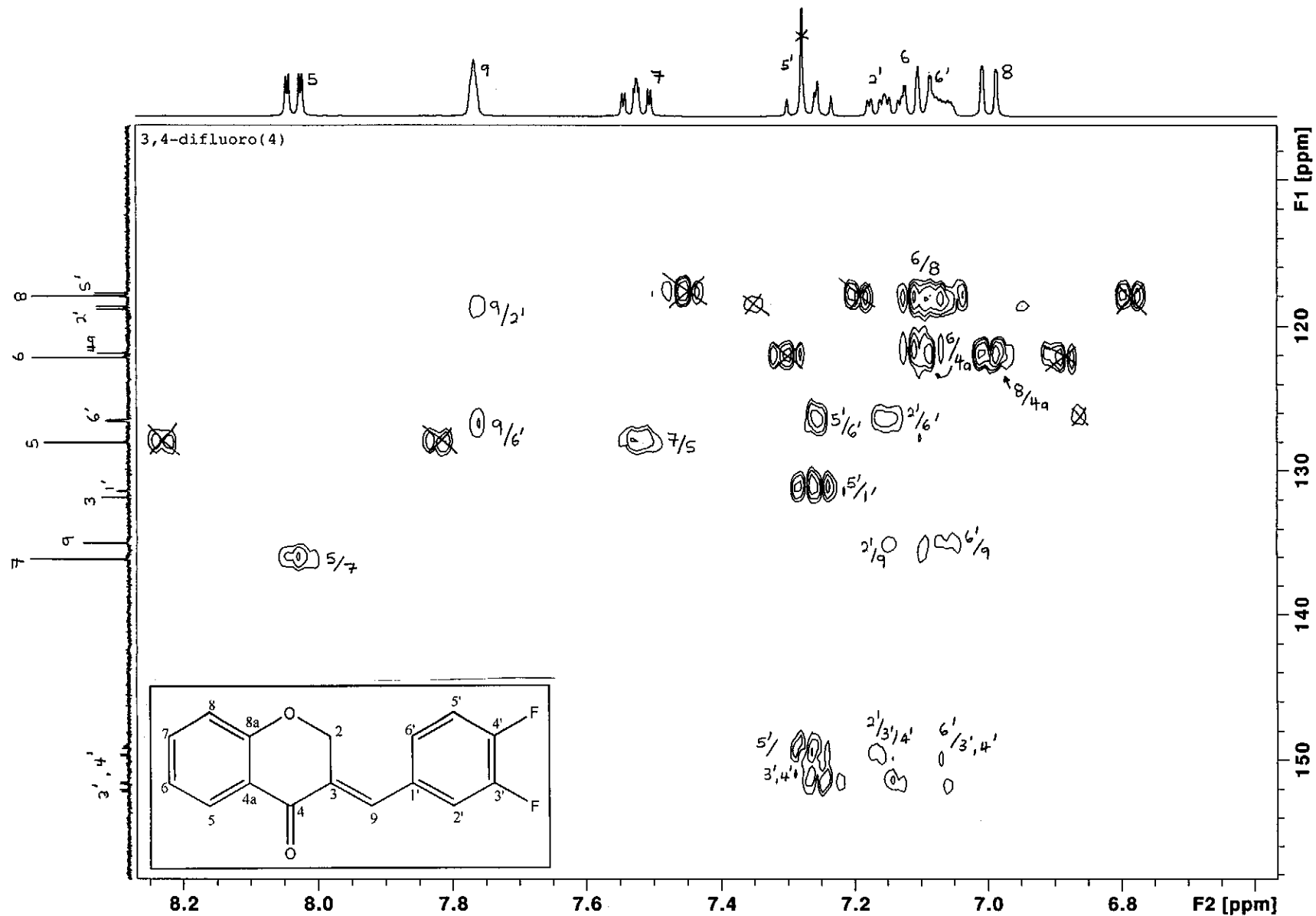
Nov15-2011-NK-Kaalin 15 1 /opt/topspin NK



HSQC spectrum of compound 12 (expanded)

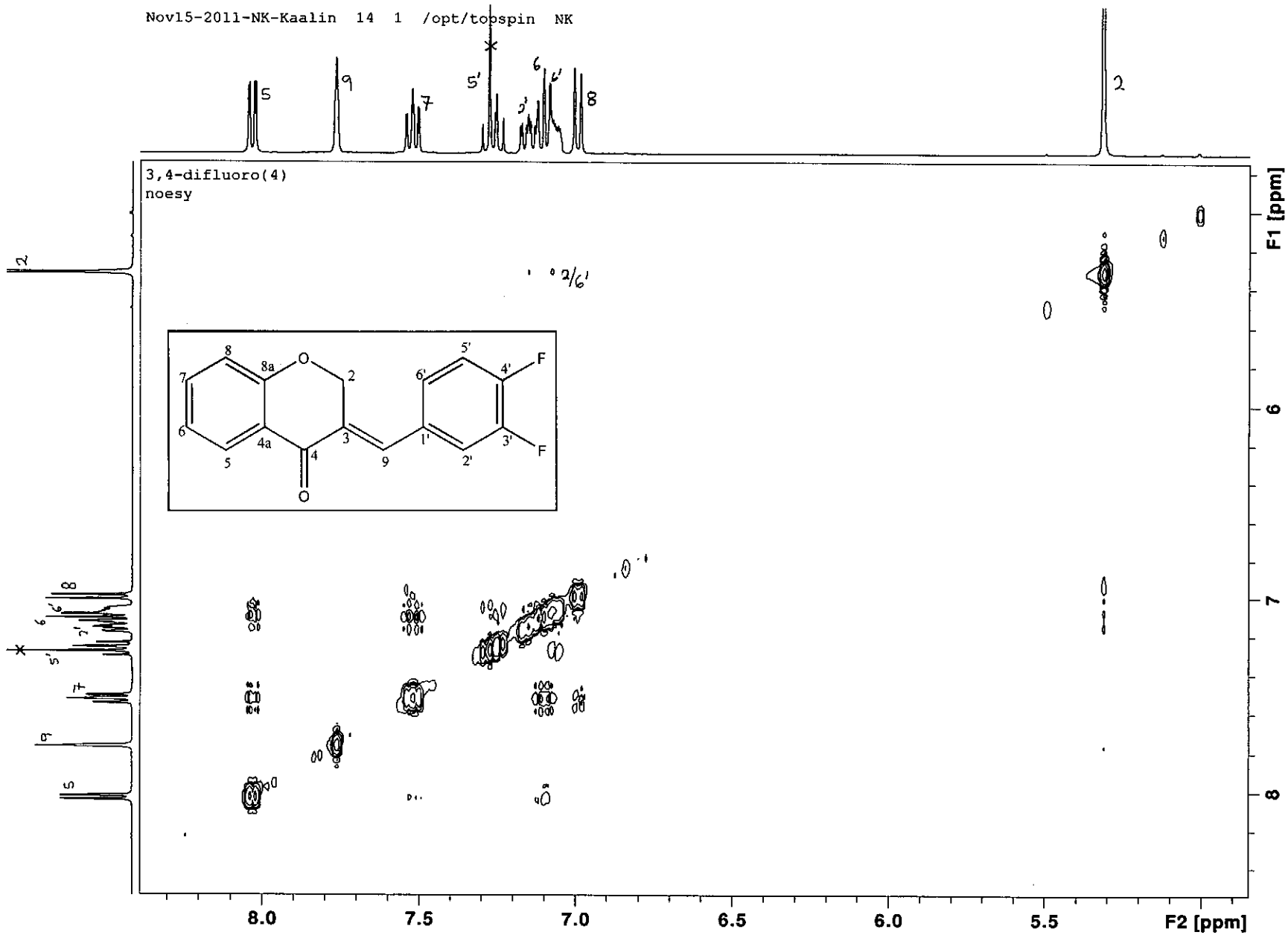


HMBC spectrum of compound 12



HMBC spectrum of compound 12 (expanded)

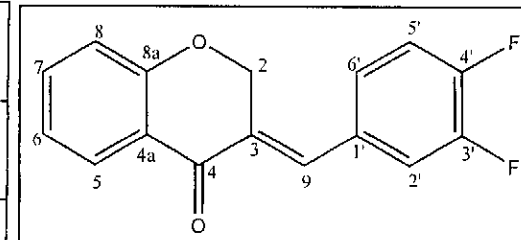
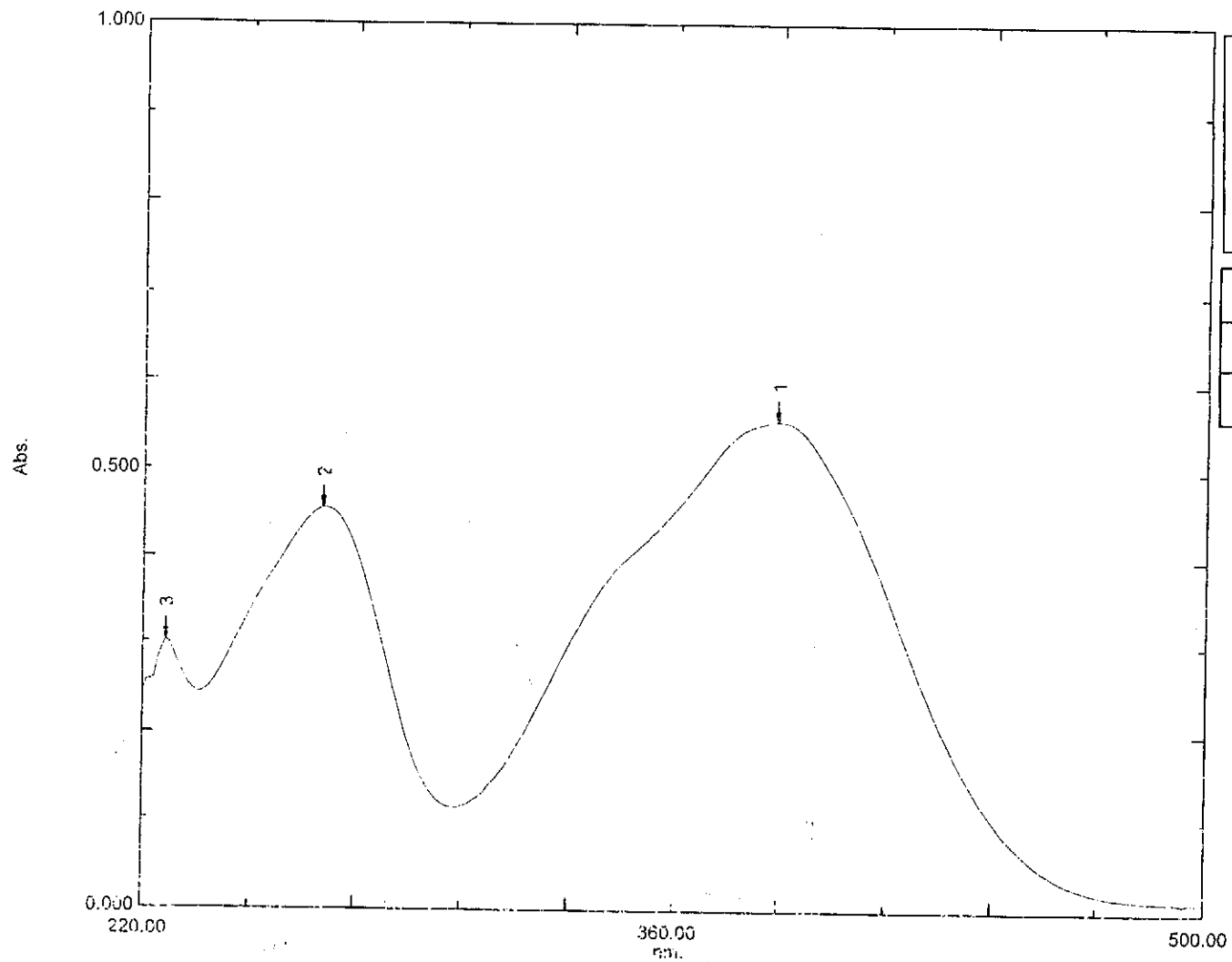
Nov15-2011-NK-Kaalin 14 1 /opt/topspin NK



NOESY spectrum of compound 12

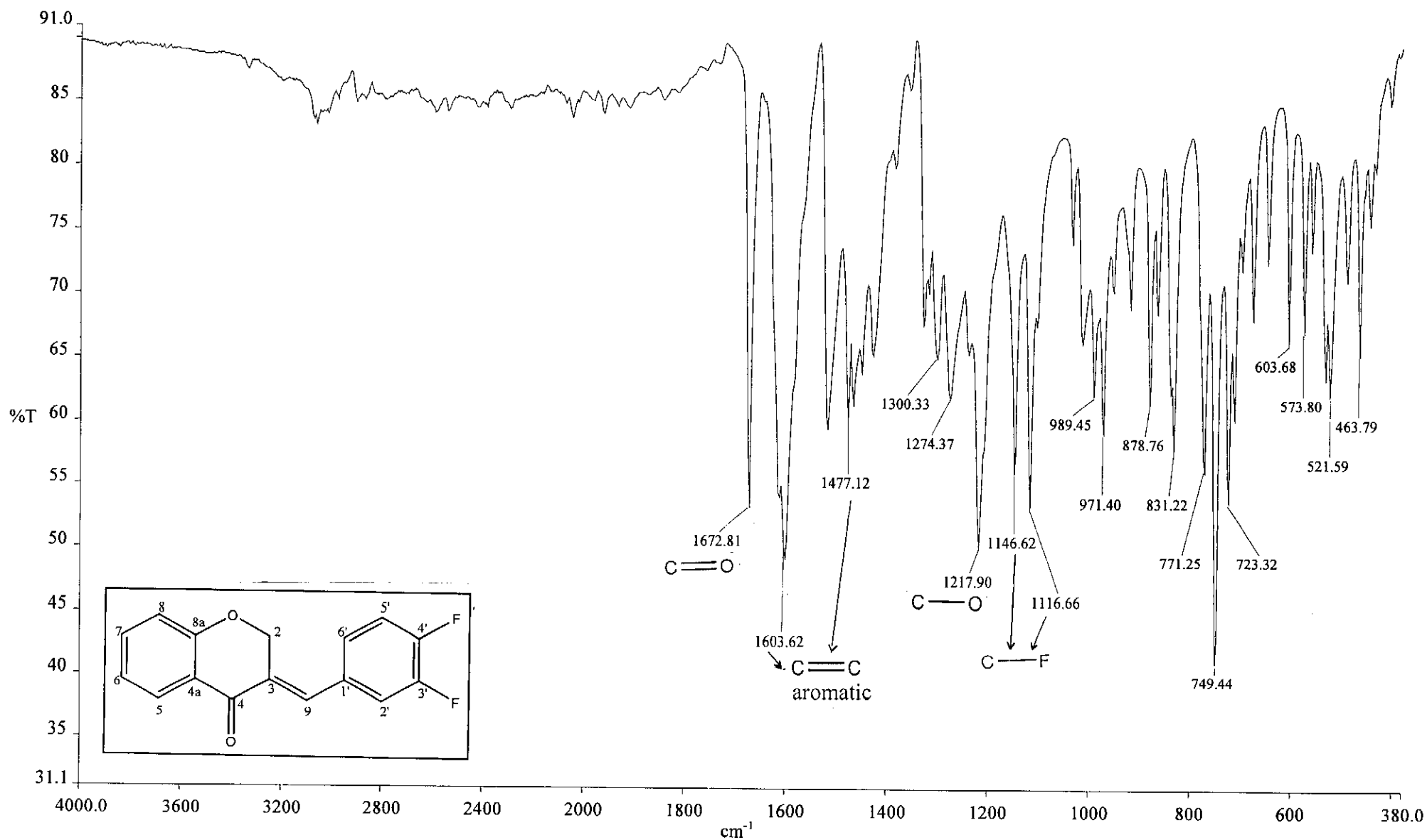
Overlay Spectrum Graph Report

15/05/2012 01:03:25 PM



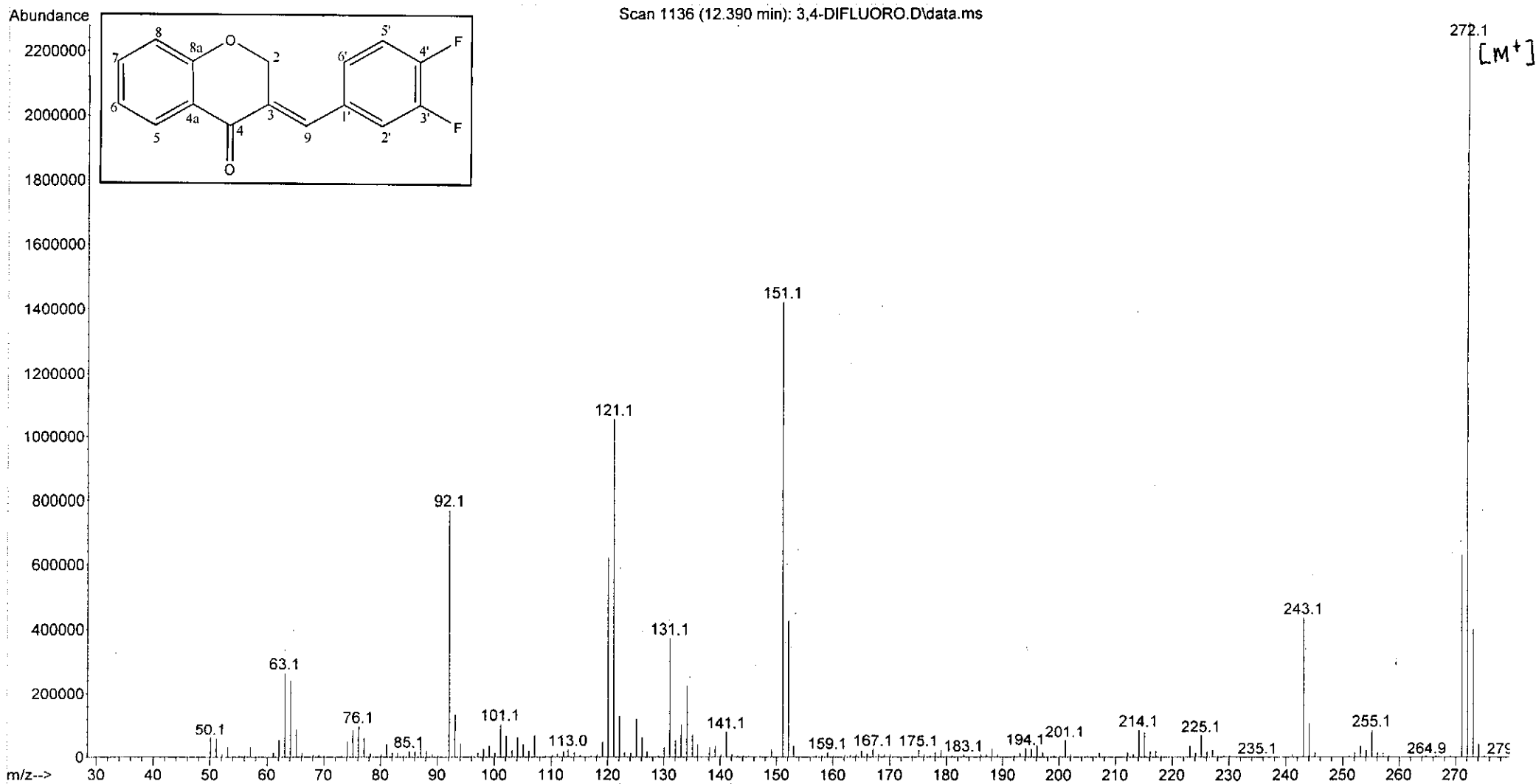
Wavelength/ nm	Absorbance	Log ϵ
267	0.455	3.96
387	0.557	4.05

UV-Vis spectrum of compound 12



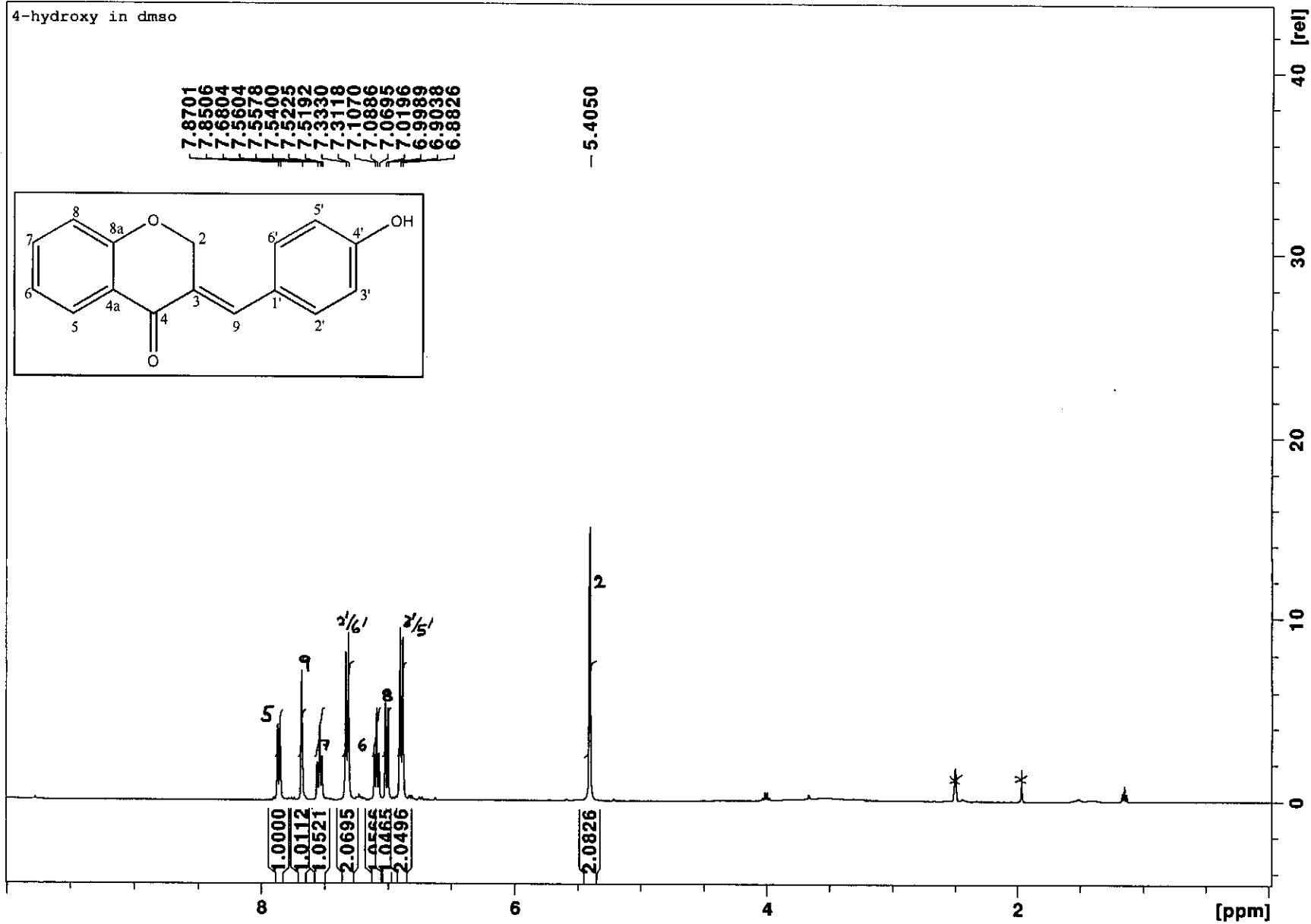
Infrared spectrum of compound 12

File :C:\msdchem\1\data\kaalin\3,4-DIFLUORO.D
Operator :
Acquired : 13 Jan 2012 10:52 using AcqMethod NATPRODUCTS MANUAL INJ.M
Instrument : 5973N
Sample Name:
Misc Info :
Vial Number: 1



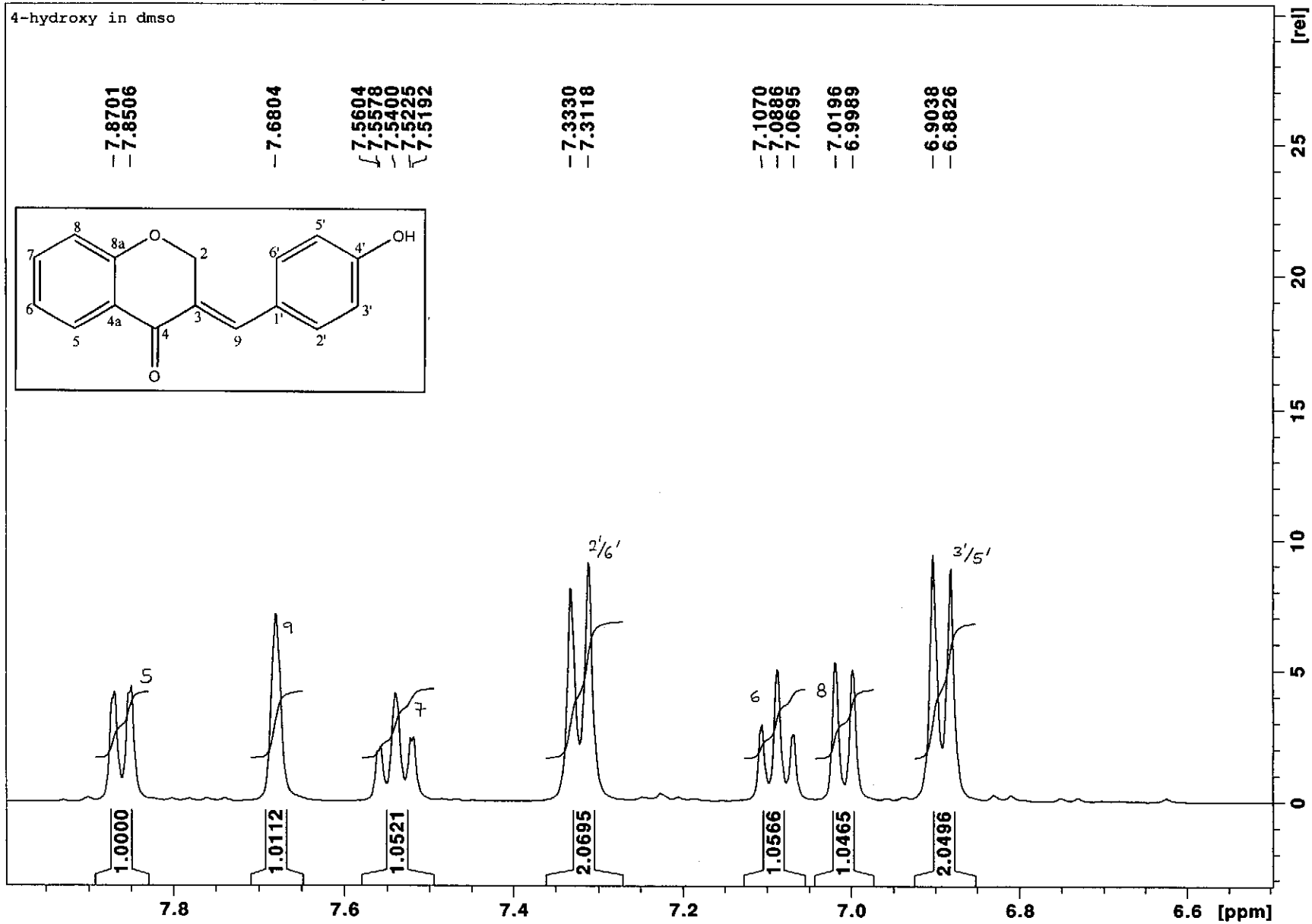
Mass spectrum of compound 12

Dec05-2011-NK-kaalin 10 1 /opt/topspin NK



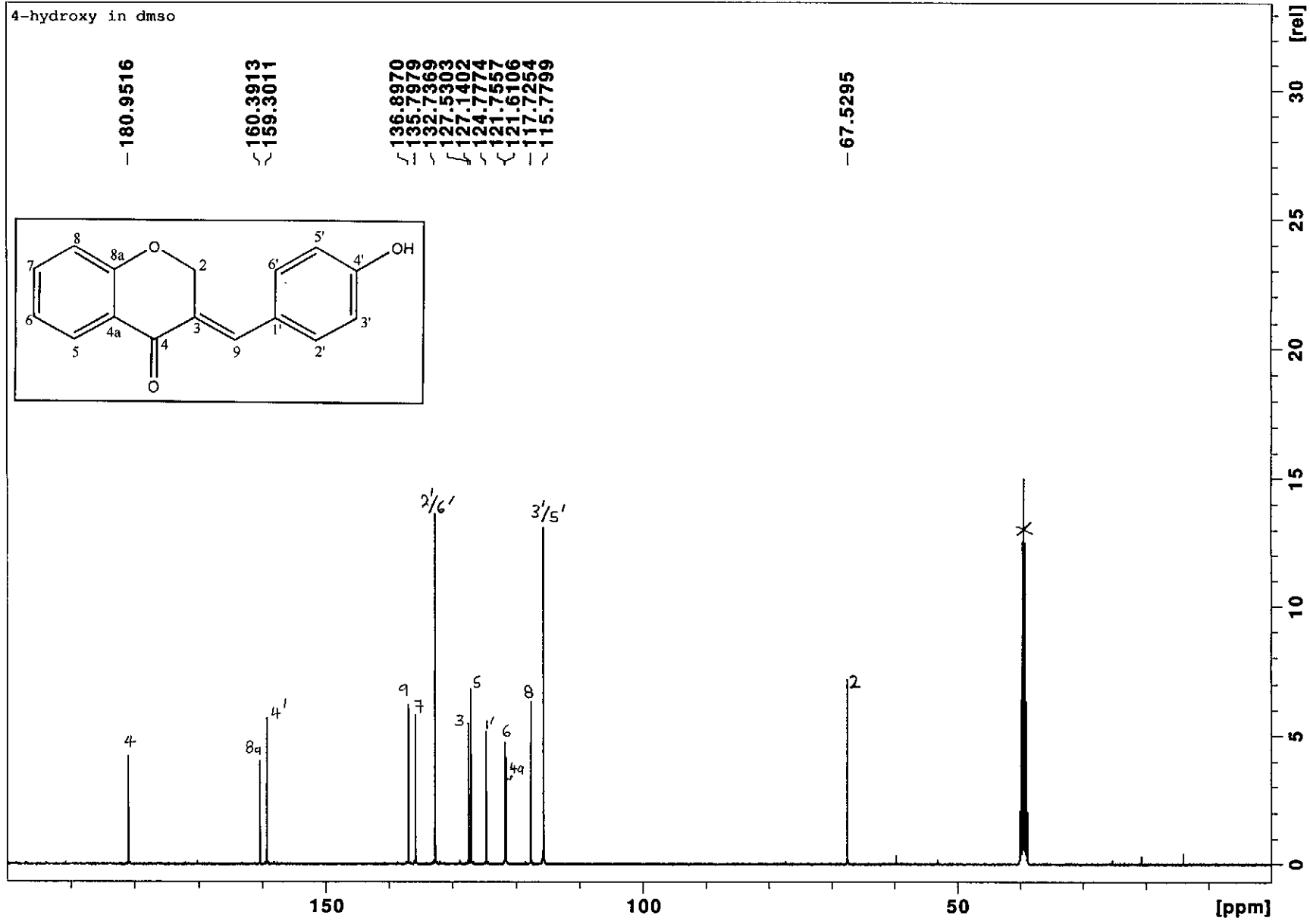
^1H NMR spectrum of compound 13

Dec05-2011-NK-kaalin 10 1 /opt/topspin NK



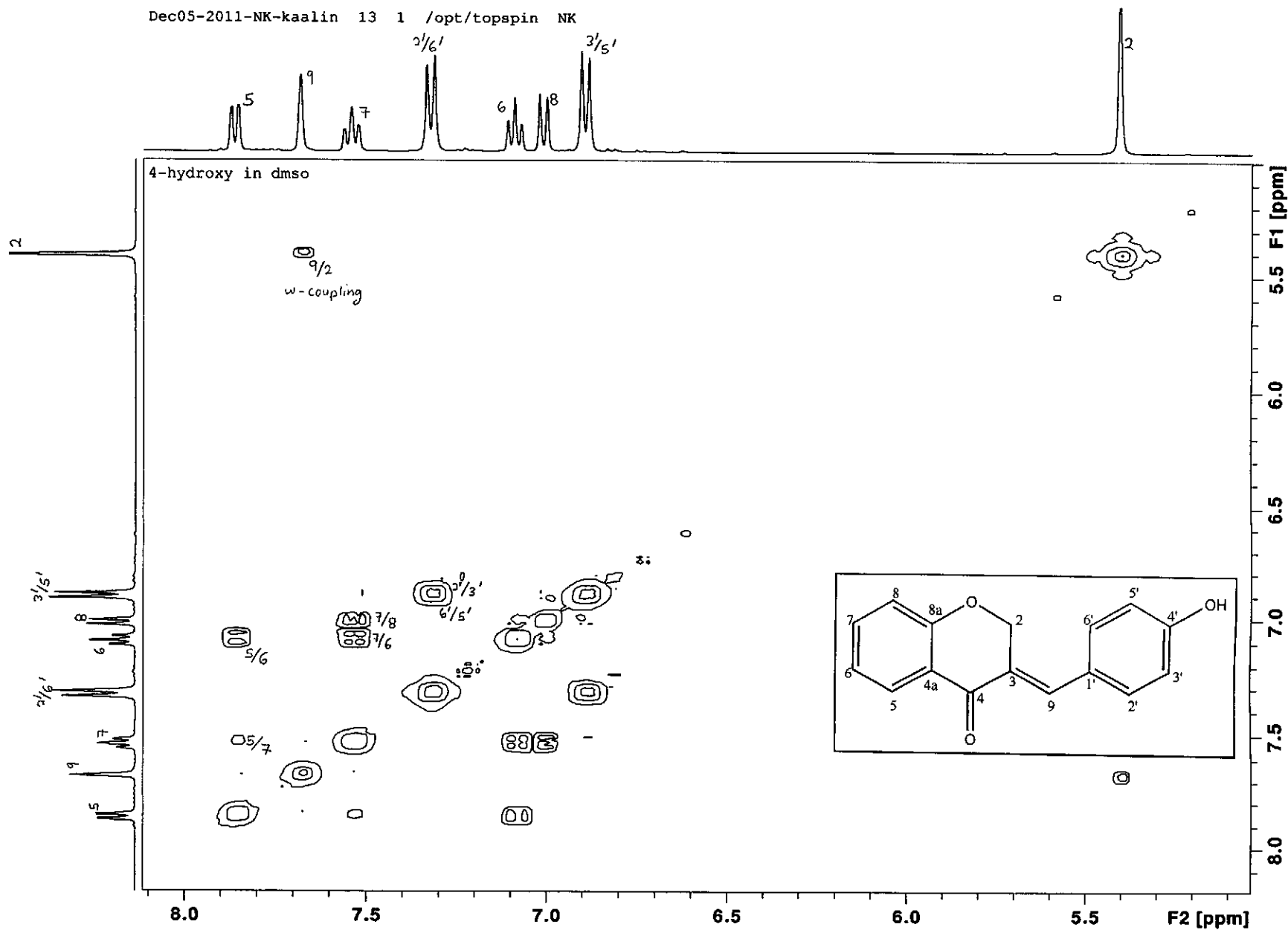
^1H NMR spectrum of compound 13 (expanded)

Dec05-2011-NK-kaalin 11 1 /opt/topspin NK

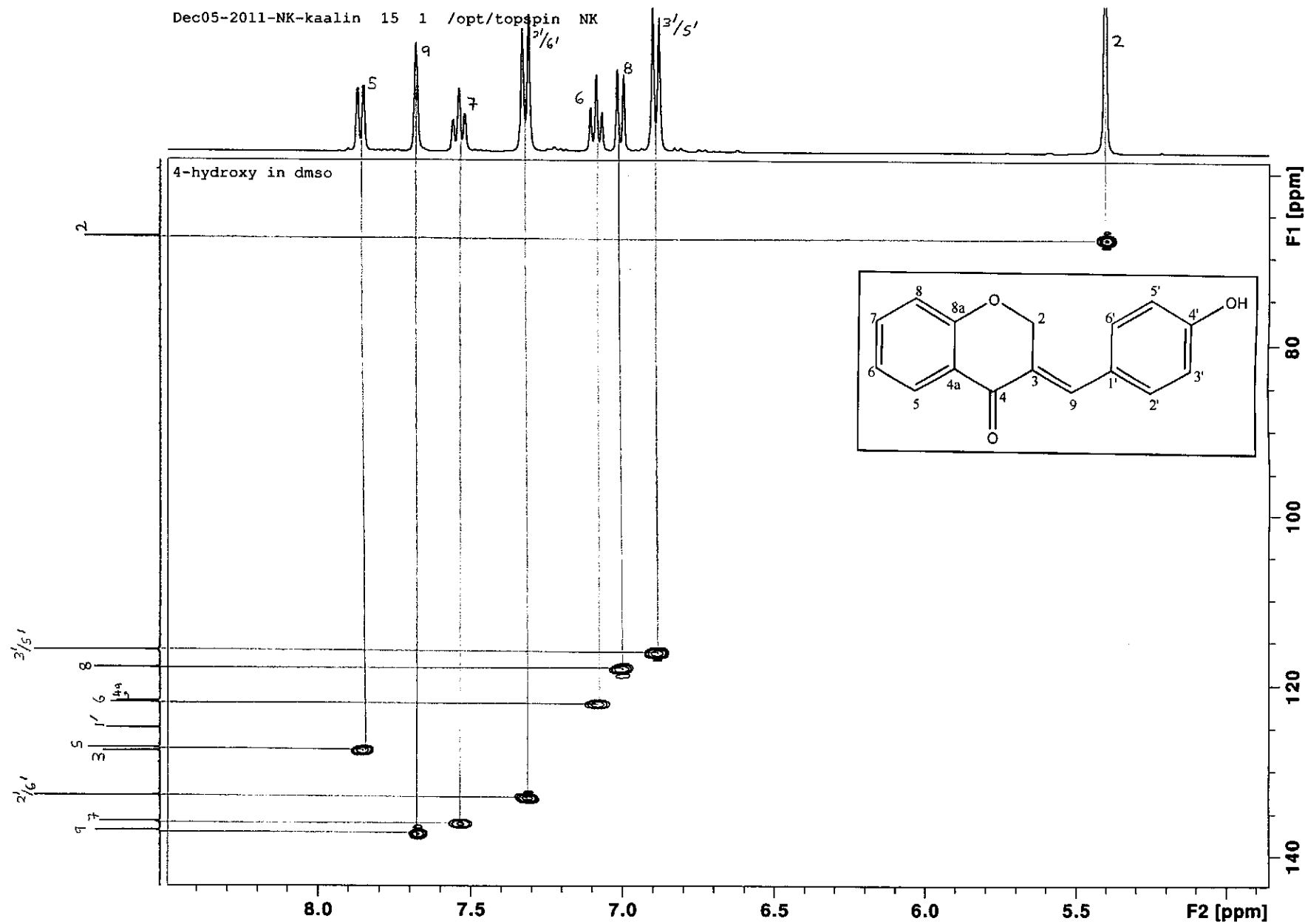


¹³C NMR spectrum of compound 13

Dec05-2011-NK-kaalin 13 1 /opt/topspin NK

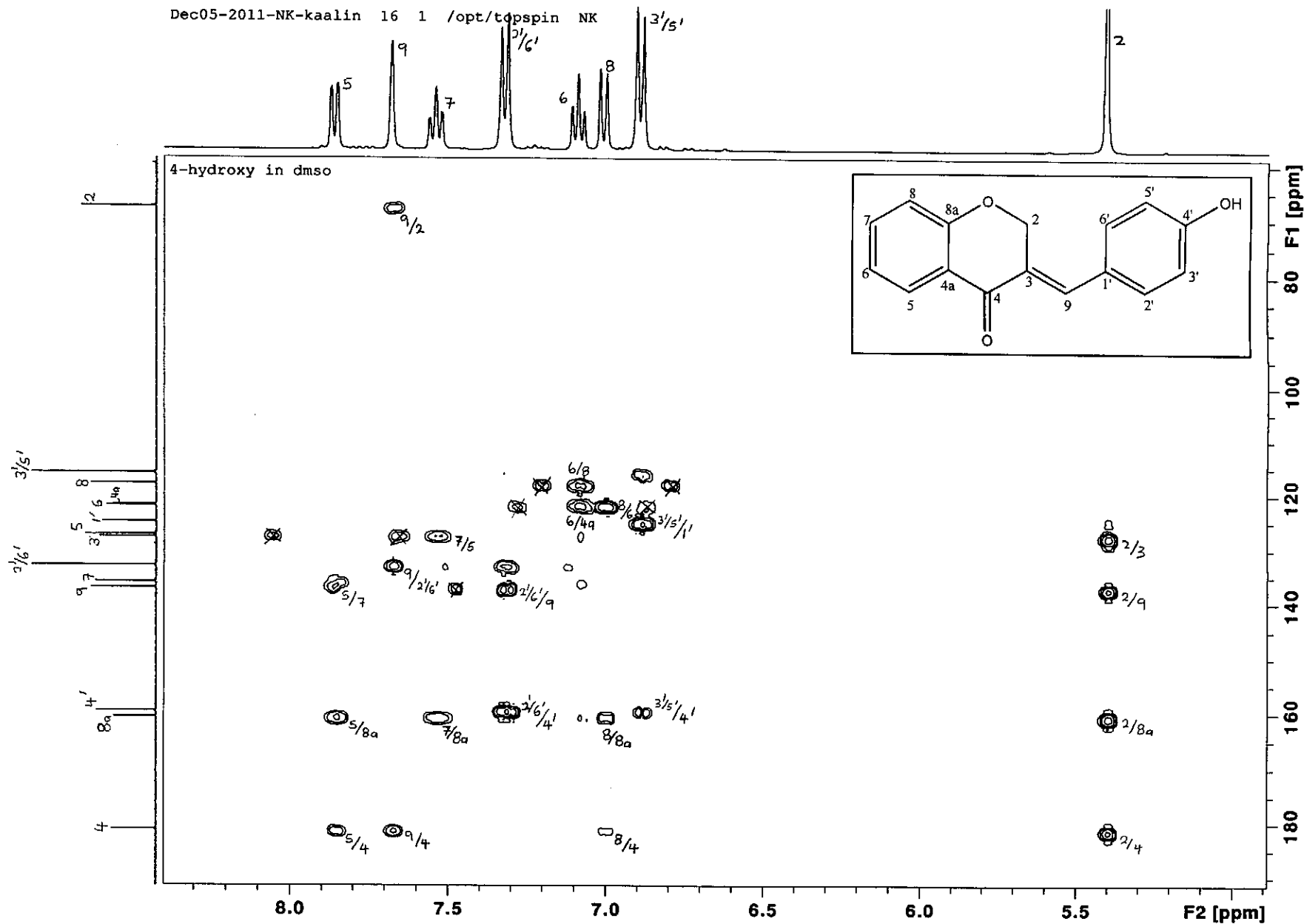


COSY spectrum of compound 13



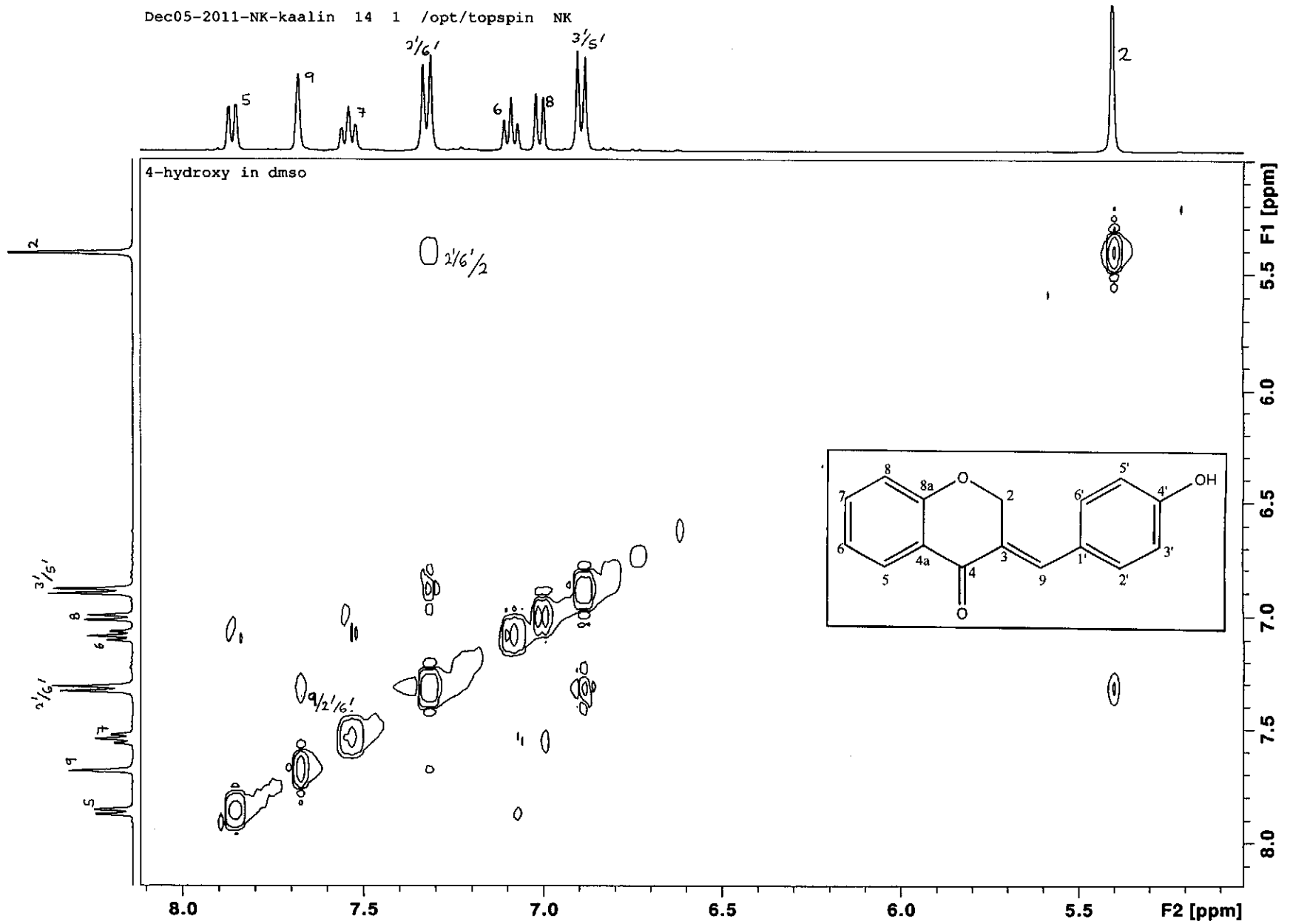
HSQC spectrum of compound 13

Dec05-2011-NK-kaalin 16 1 /opt/tdpspin NK



HMBC spectrum of compound 13

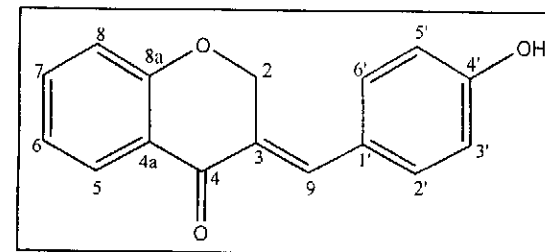
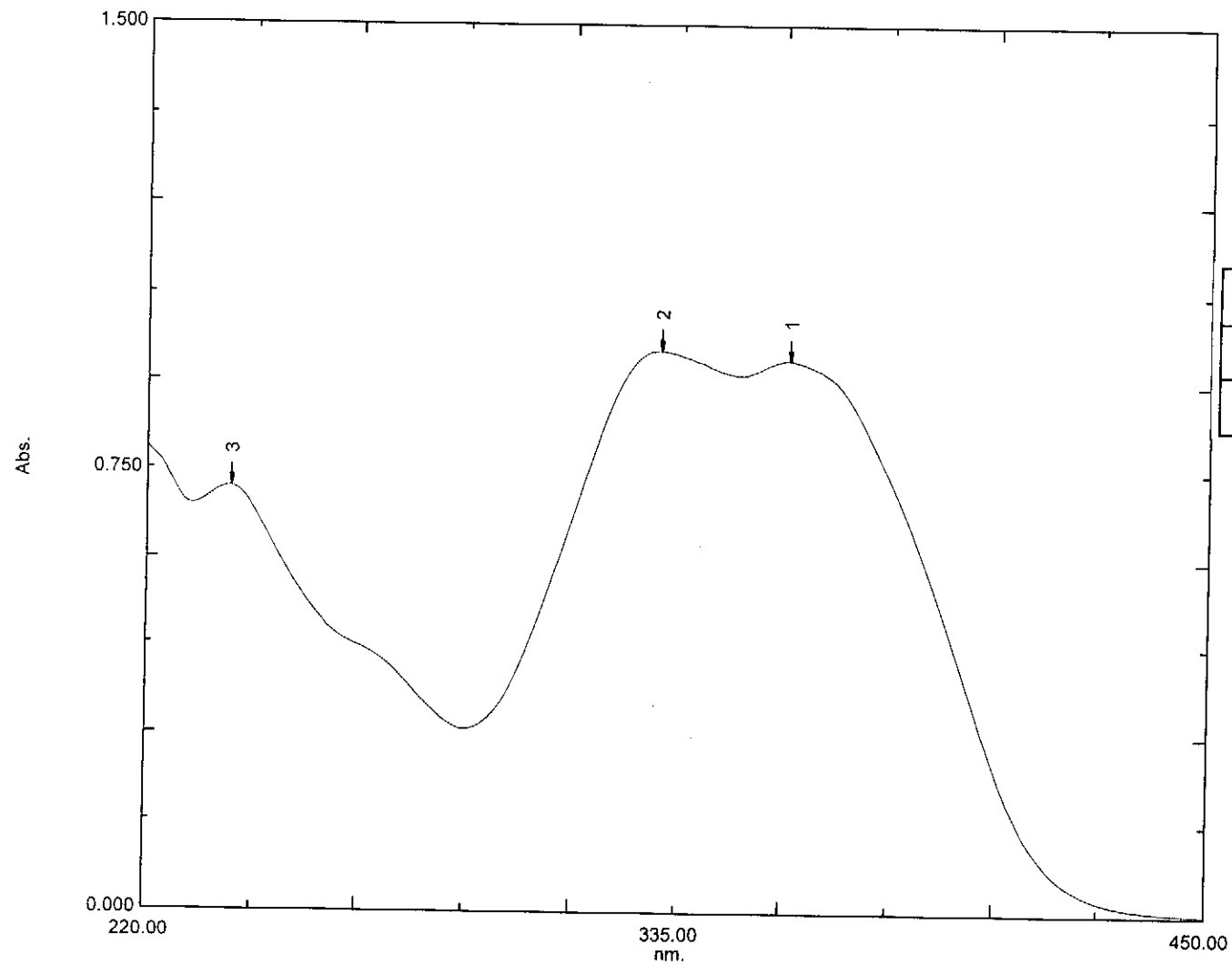
Dec05-2011-NK-kaalin 14 1 /opt/topspin NK



NOESY spectrum of compound 13

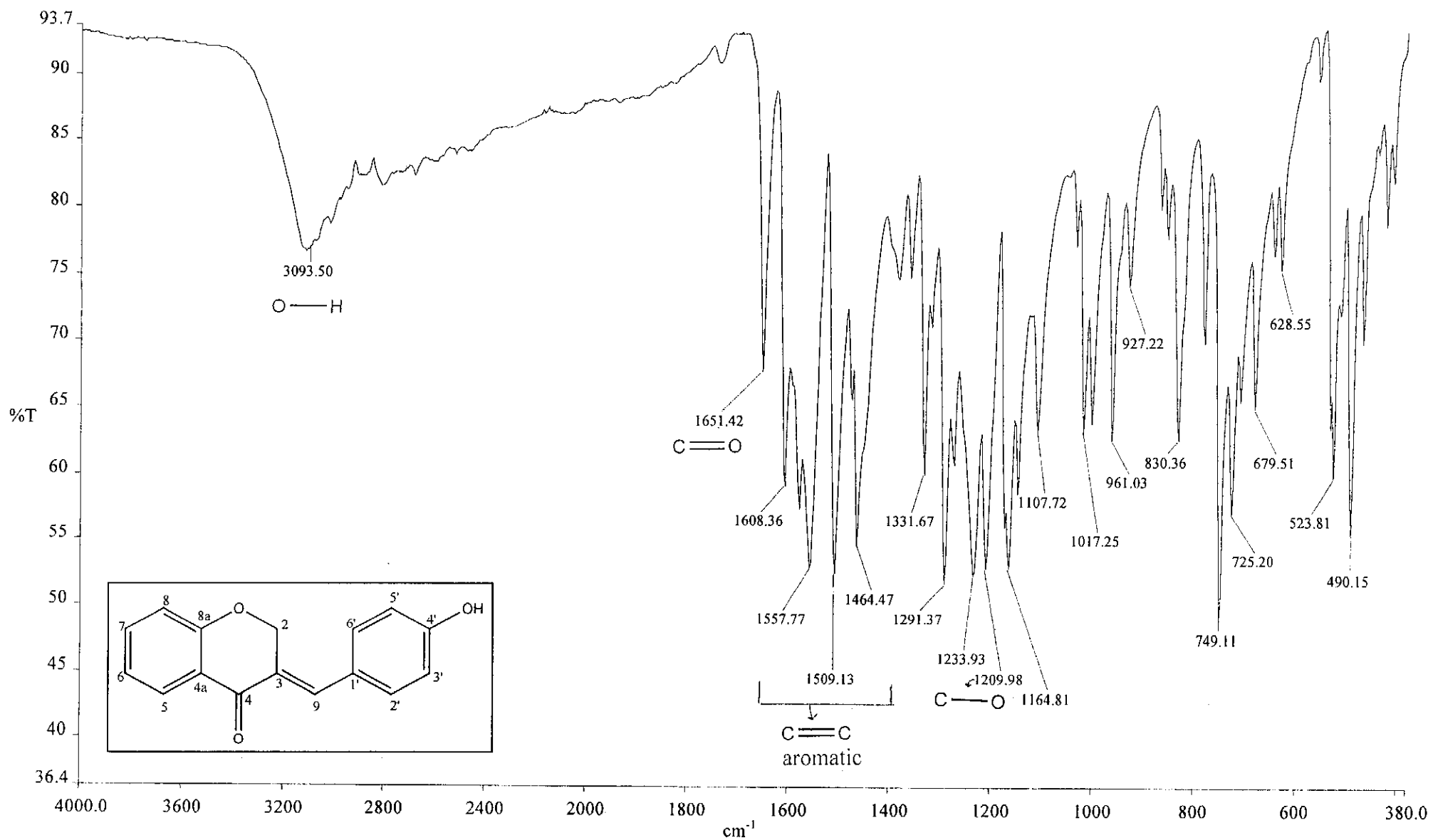
Overlay Spectrum Graph Report

15/05/2012 01:05:44 PM



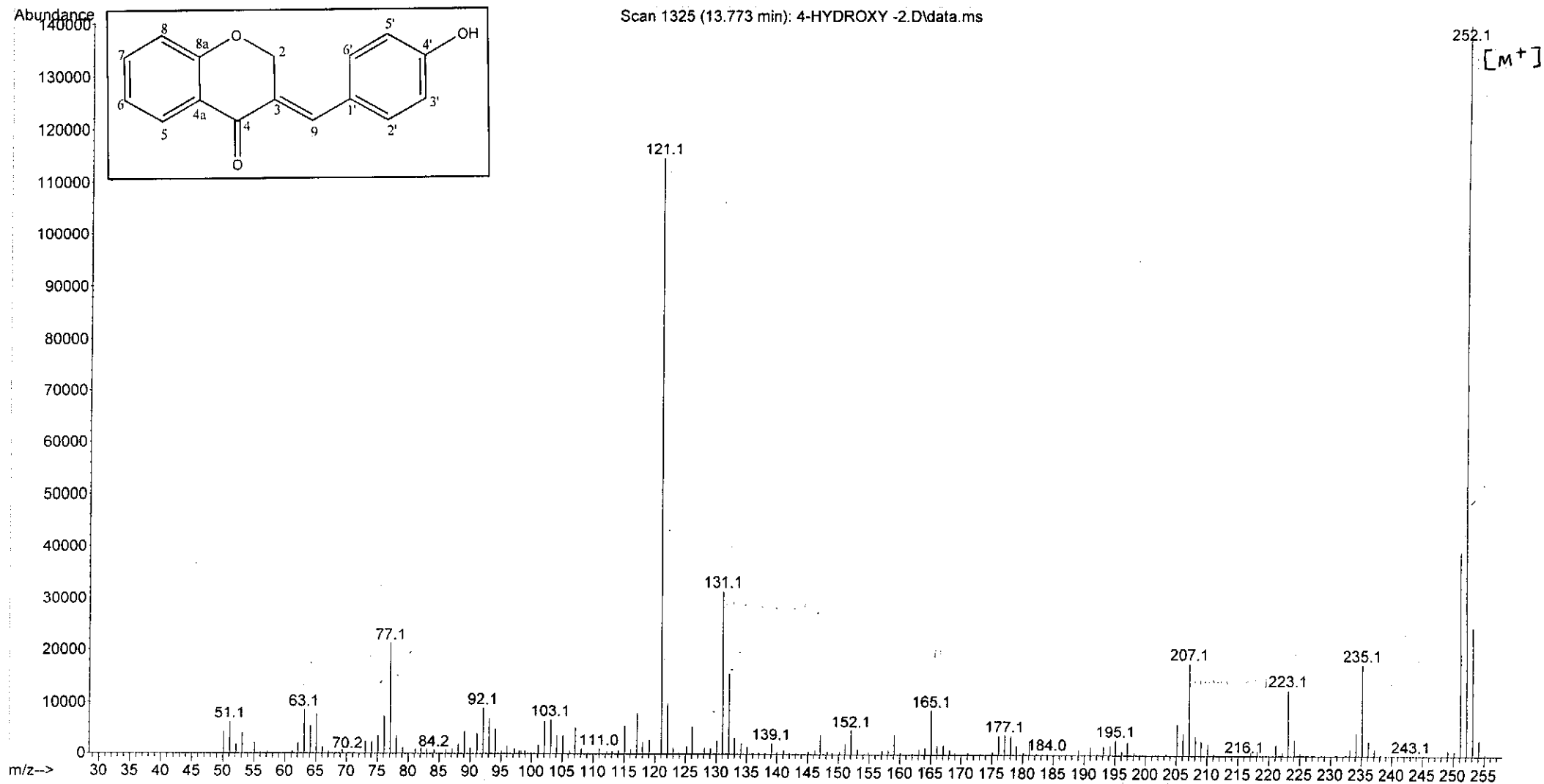
Wavelength/ nm	Absorbance	Log ϵ
331	0.956	3.98
359	0.941	3.97

UV-Vis spectrum of compound 13



Infrared spectrum of compound 13

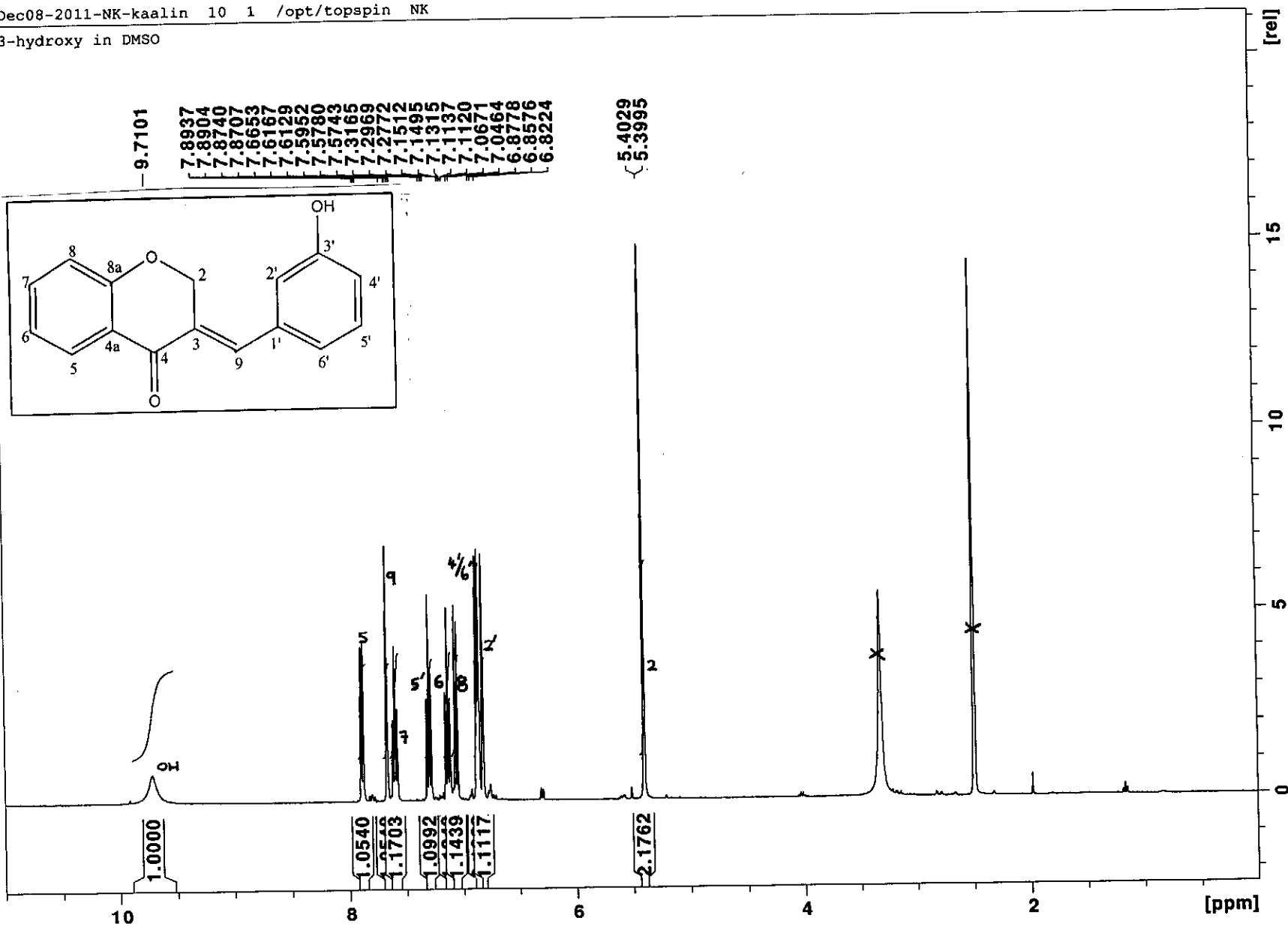
File :C:\msdchem\1\data\kaalin\4-HYDROXY -2.D
Operator :
Acquired : 13 Jan 2012 17:55 using AcqMethod NATPRODUCTS MANUAL INJ.M
Instrument : 5973N
Sample Name:
Misc Info :
Vial Number: 1



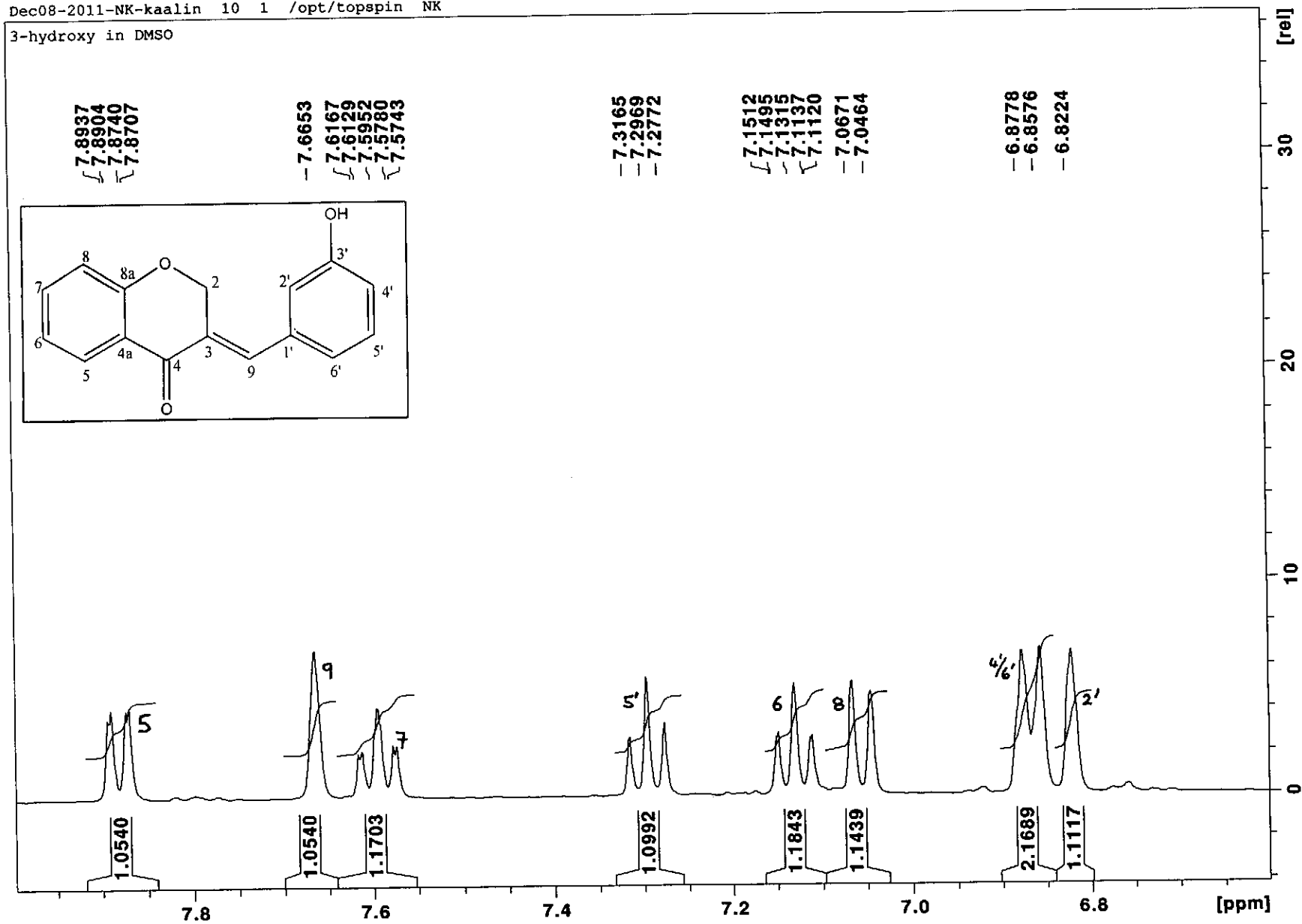
Mass spectrum of compound 13

Dec08-2011-NK-kaalin 10 1 /opt/topspin NK

3-hydroxy in DMSO



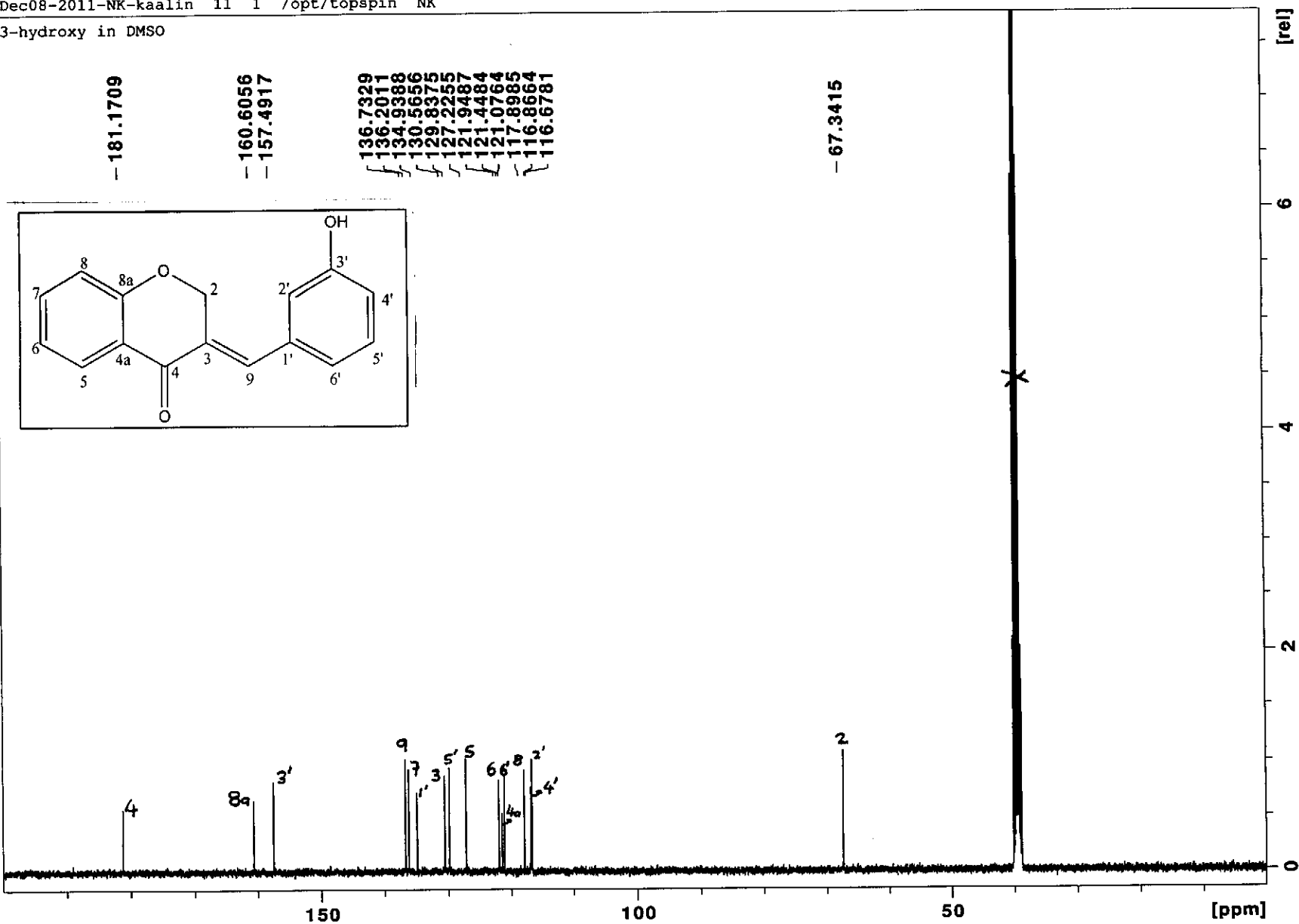
¹H NMR spectrum of compound 14



¹H NMR spectrum of compound 14 (expanded)

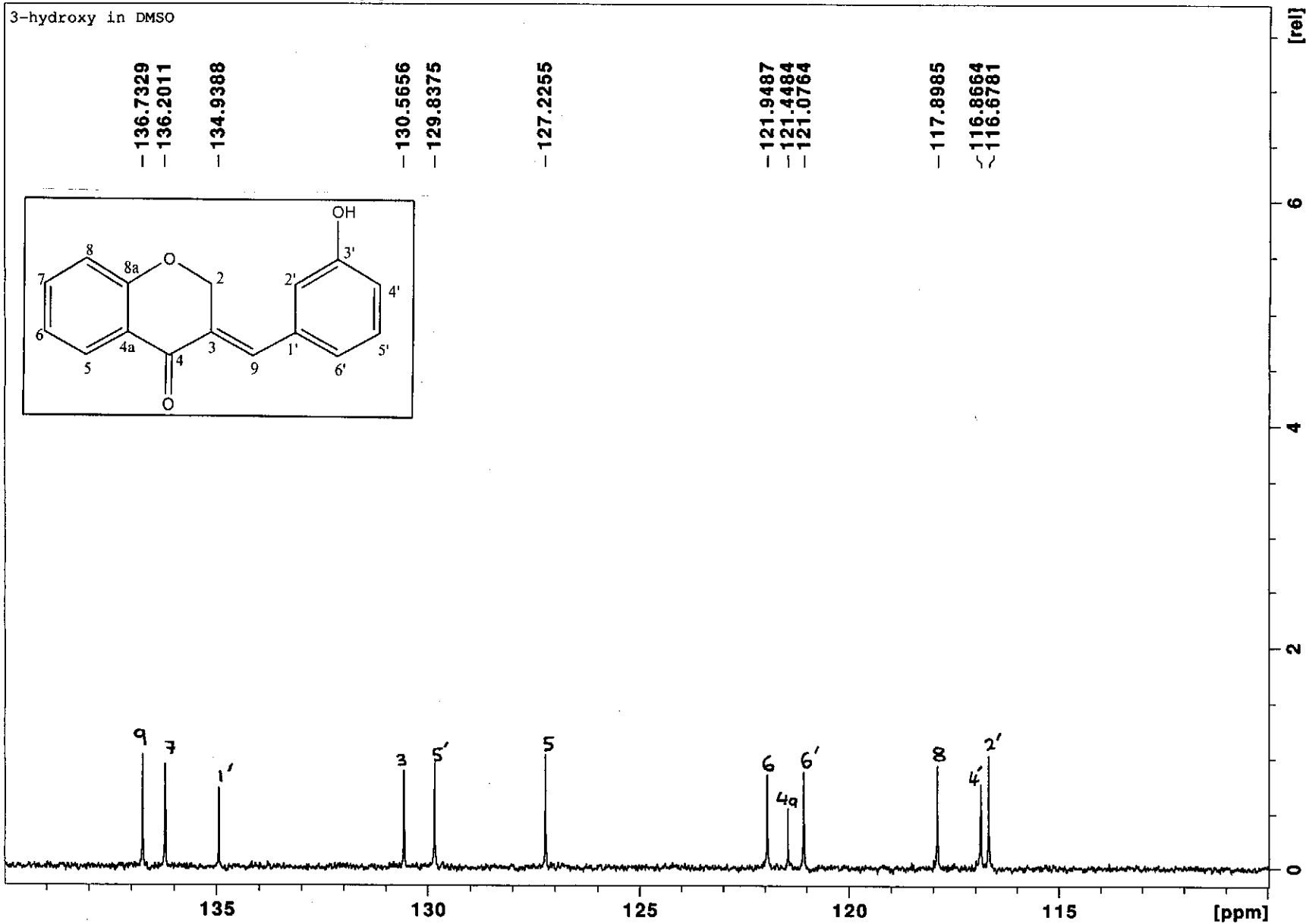
Dec08-2011-NK-kaalin 11 1 /opt/topspin NK

3-hydroxy in DMSO

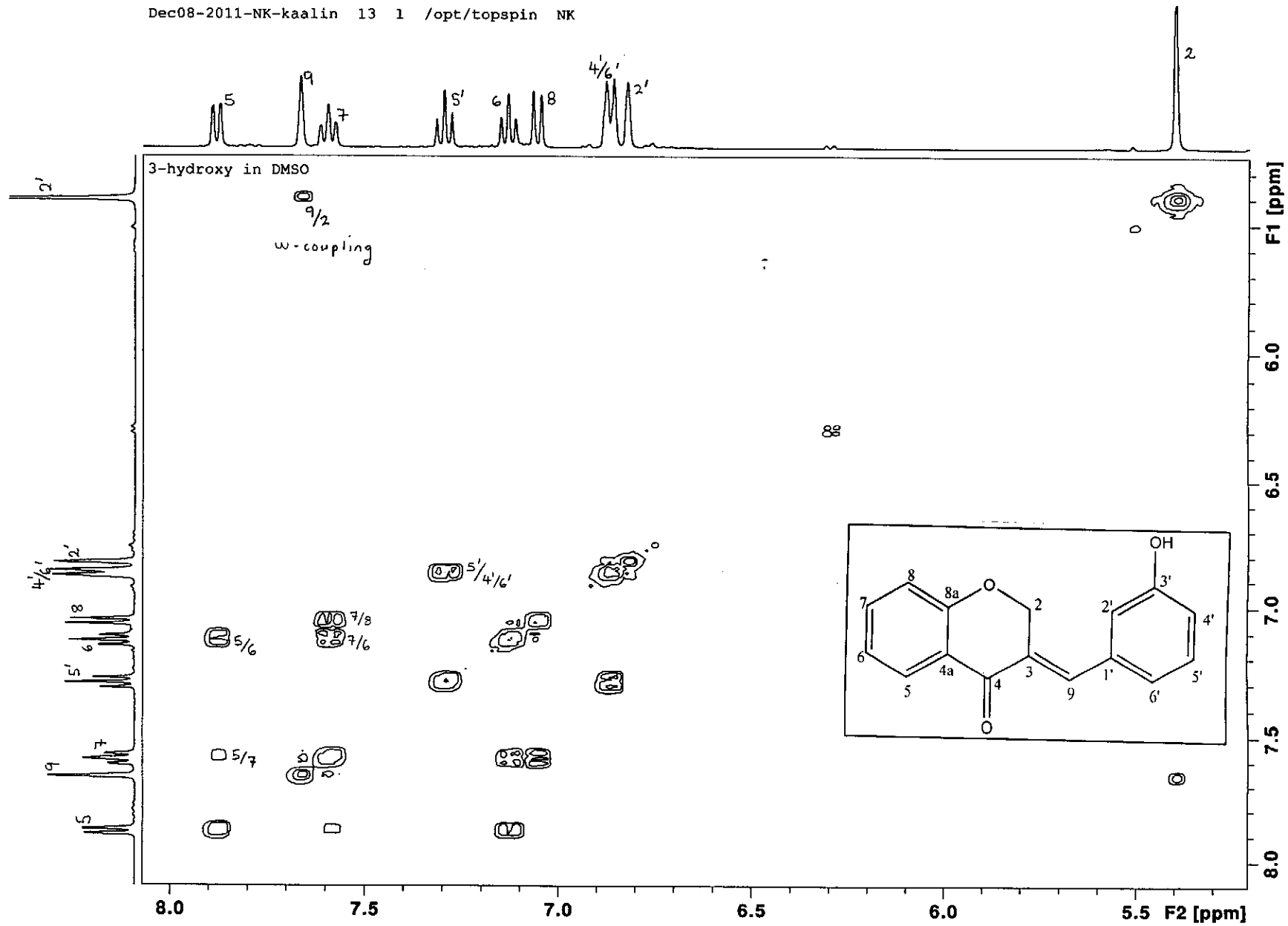


¹³C NMR spectrum of compound 14

Dec08-2011-NK-kaalin 11 1 /opt/topspin NK

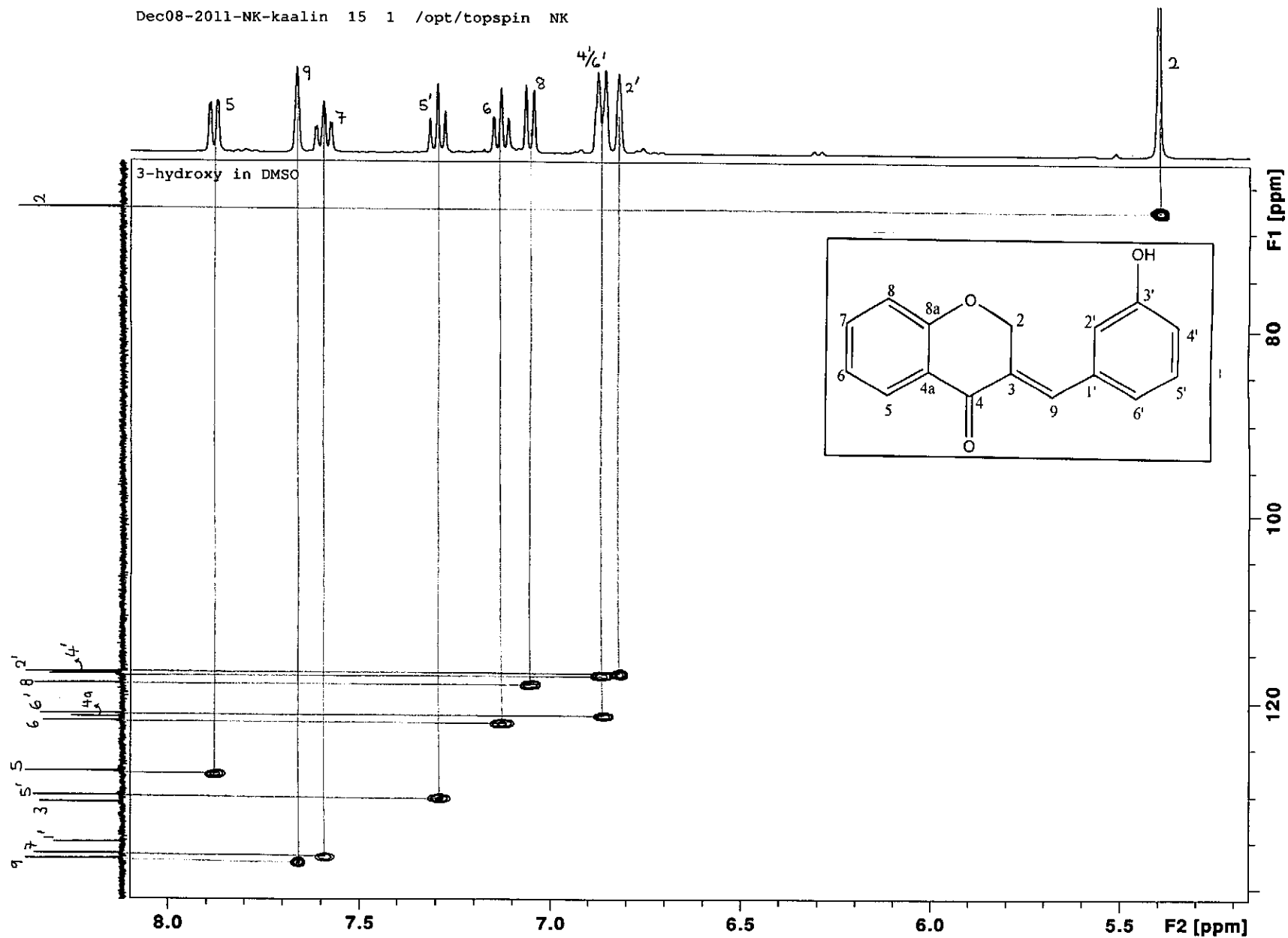


^{13}C NMR spectrum of compound 14 (expanded)

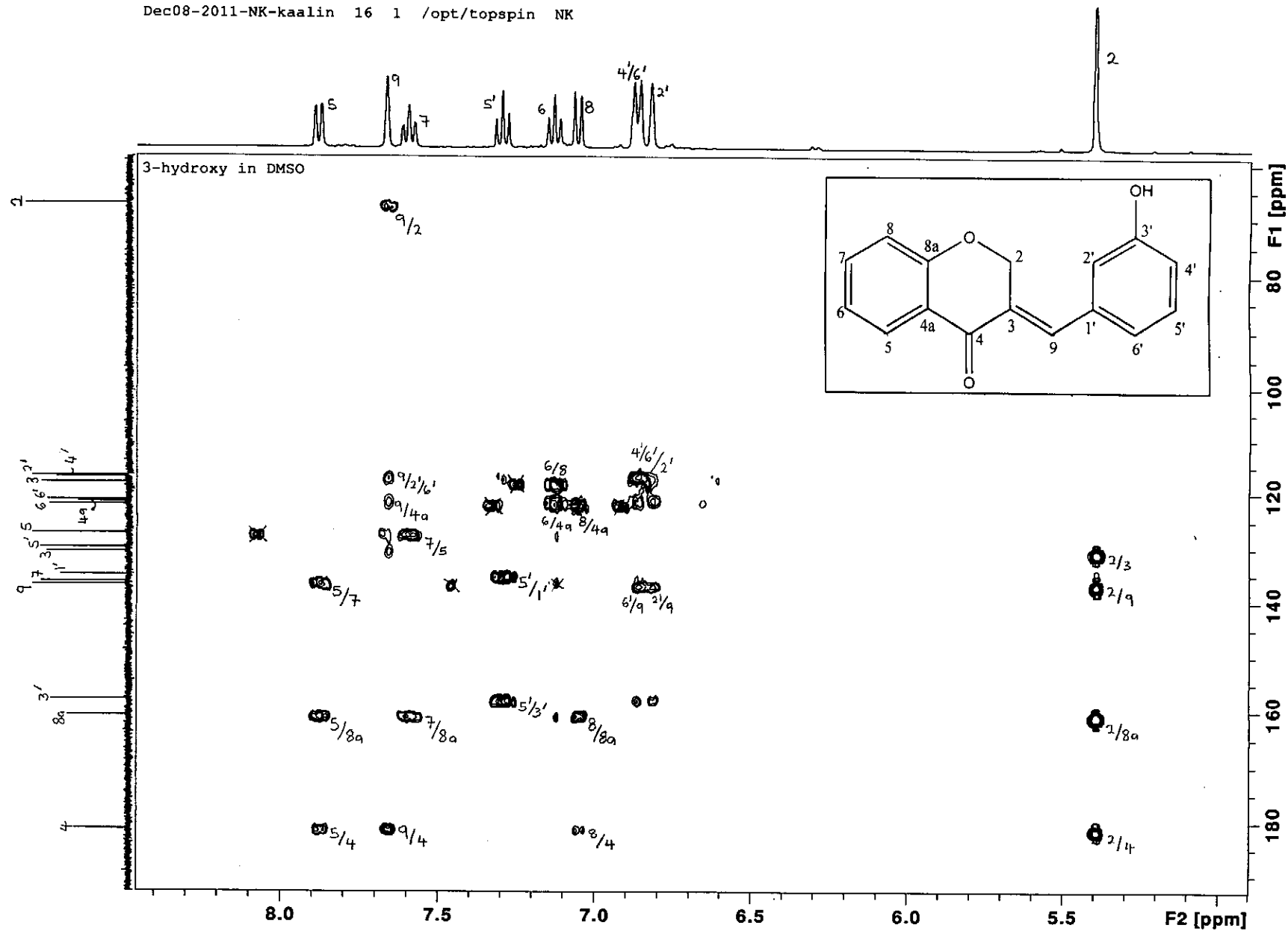


COSY spectrum of compound 14

Dec08-2011-NK-kaalin 15 1 /opt/topspin NK

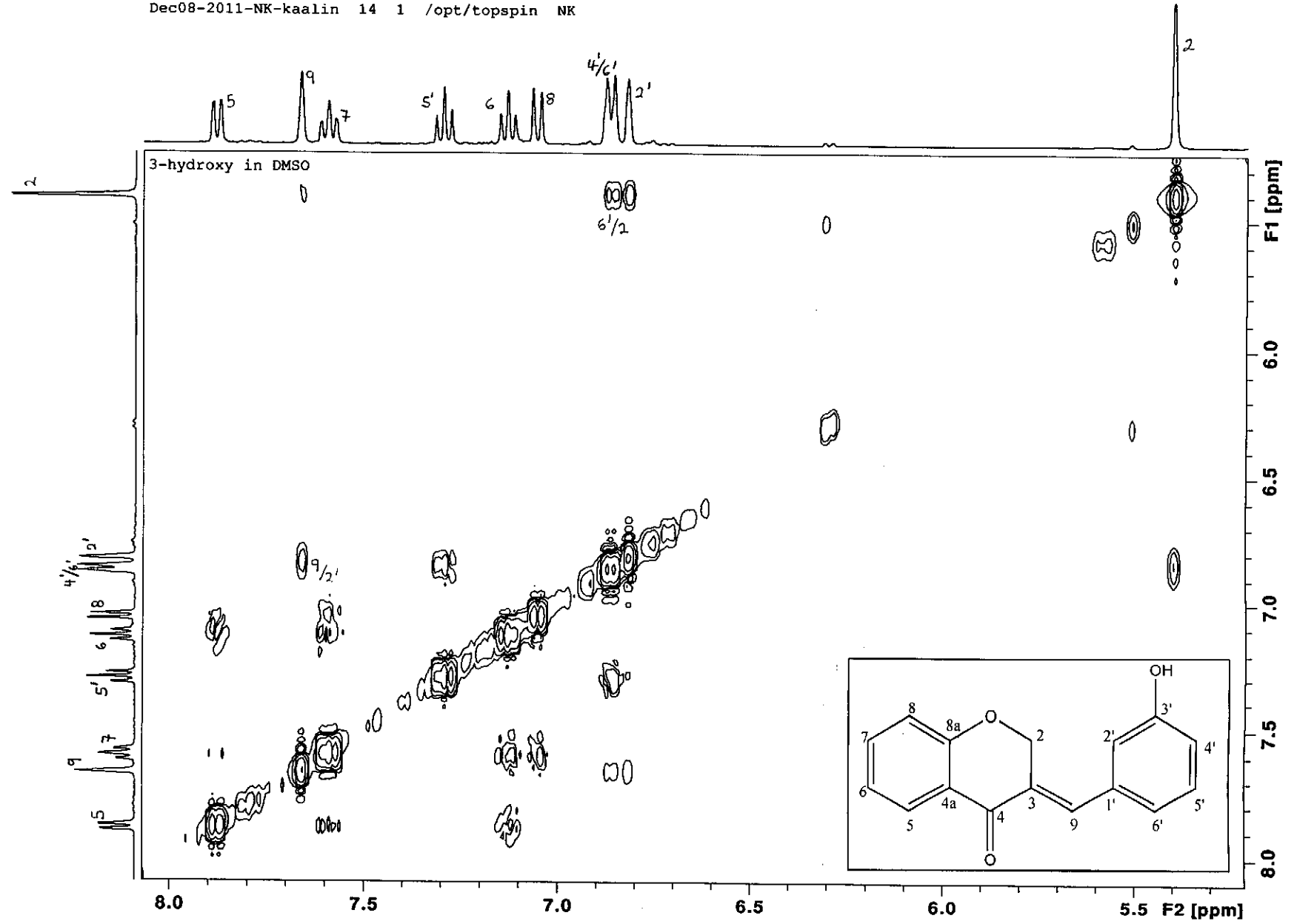


HSQC spectrum of compound 14



HMBC spectrum of compound 14

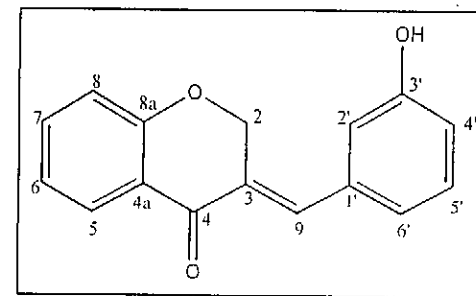
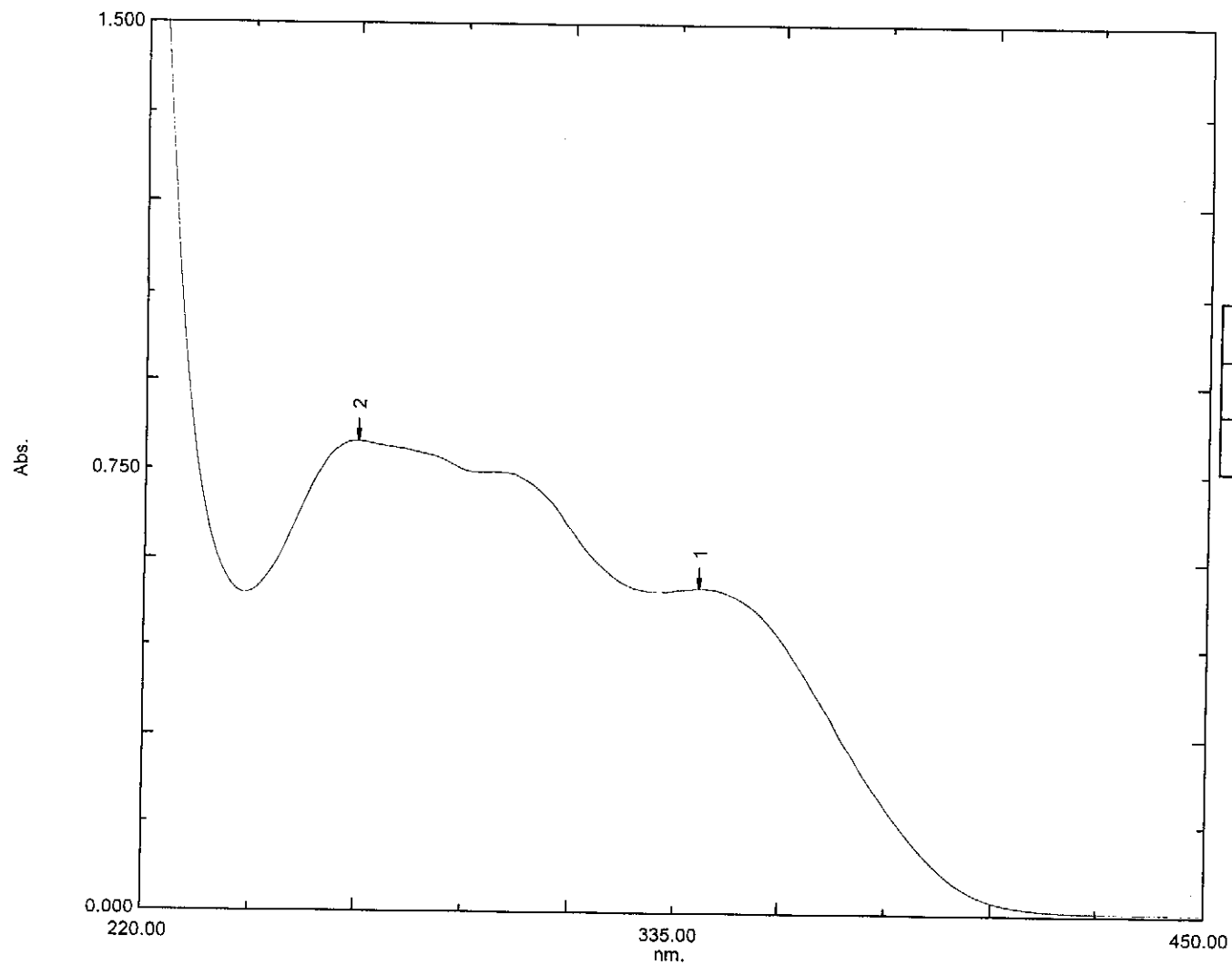
Dec08-2011-NK-kaalin 14 1 /opt/topspin NK



NOESY spectrum of compound 14

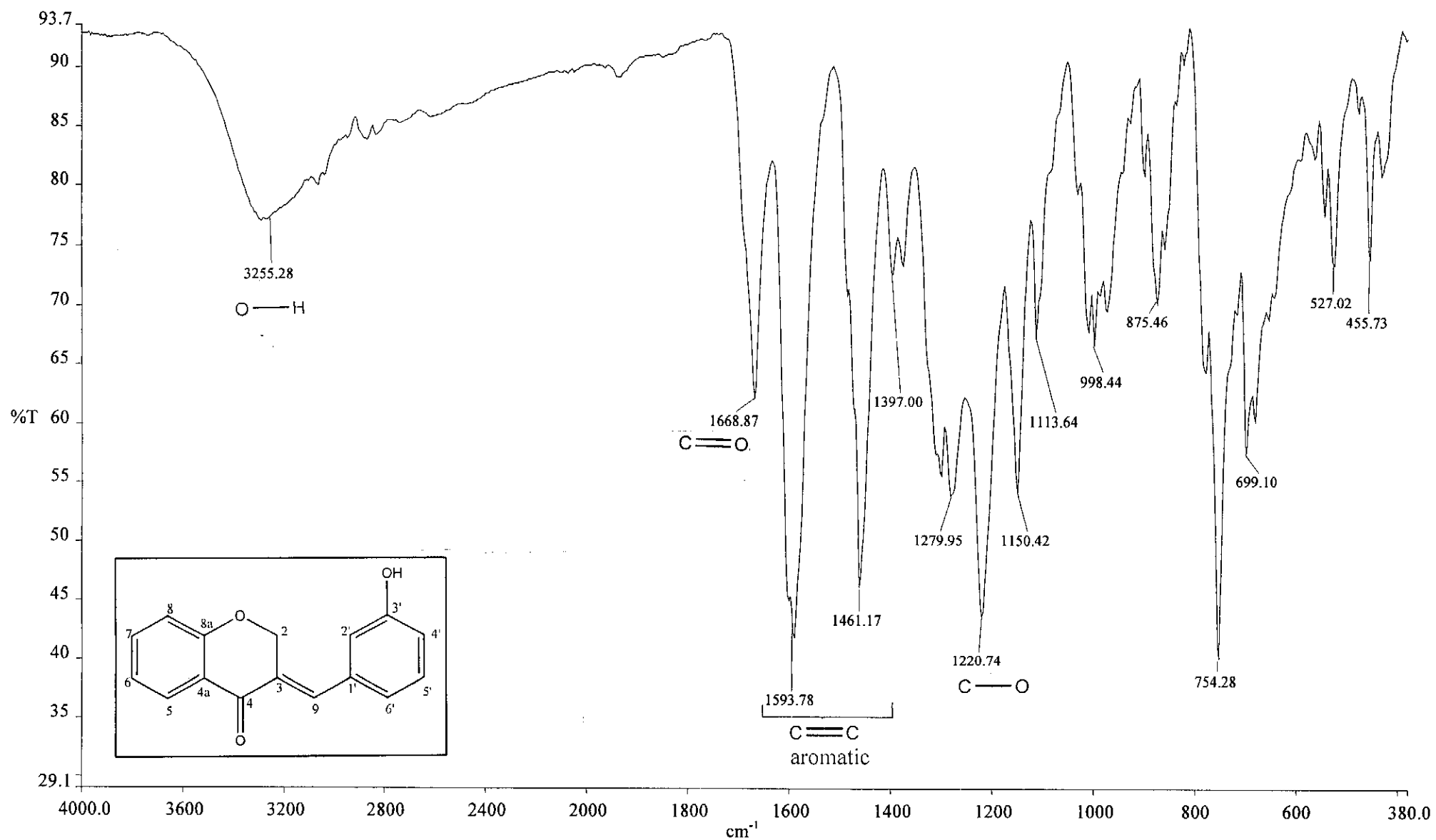
Overlay Spectrum Graph Report

15/05/2012 01:07:07 PM



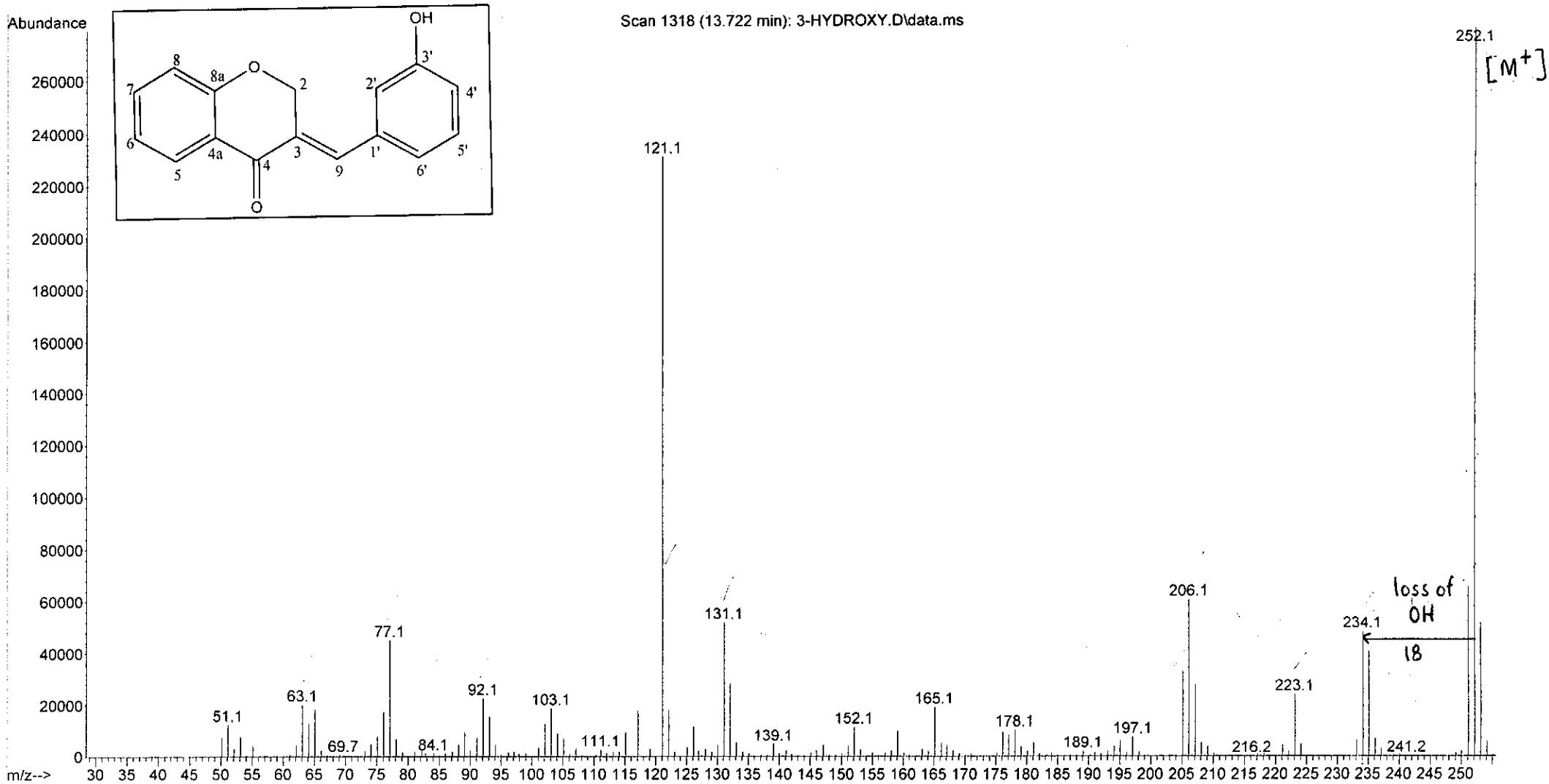
Wavelength/ nm	Absorbance	Log ϵ
267	0.799	4.20
340	0.551	4.04

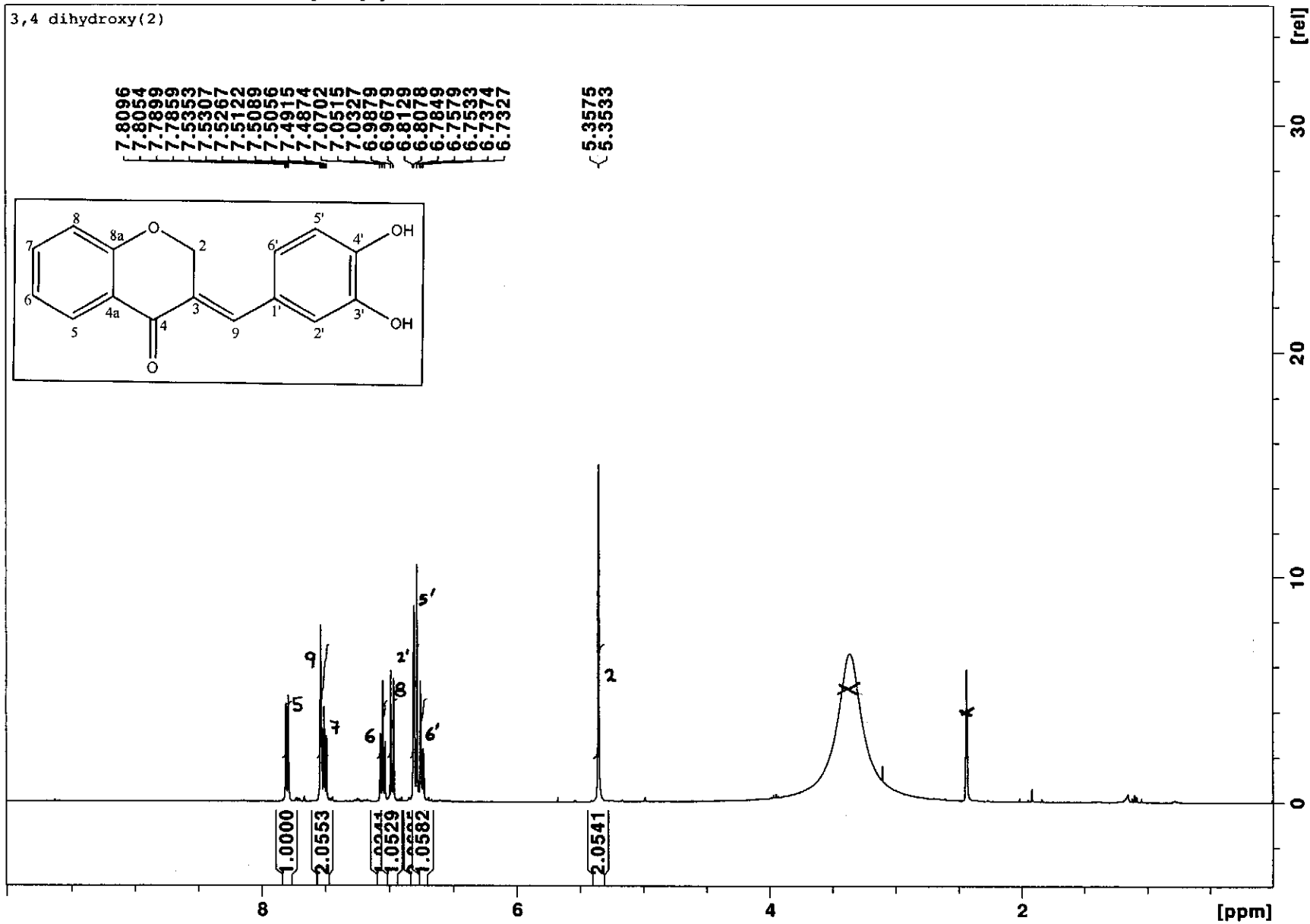
UV-Vis spectrum of compound 14



Infrared spectrum of compound 14

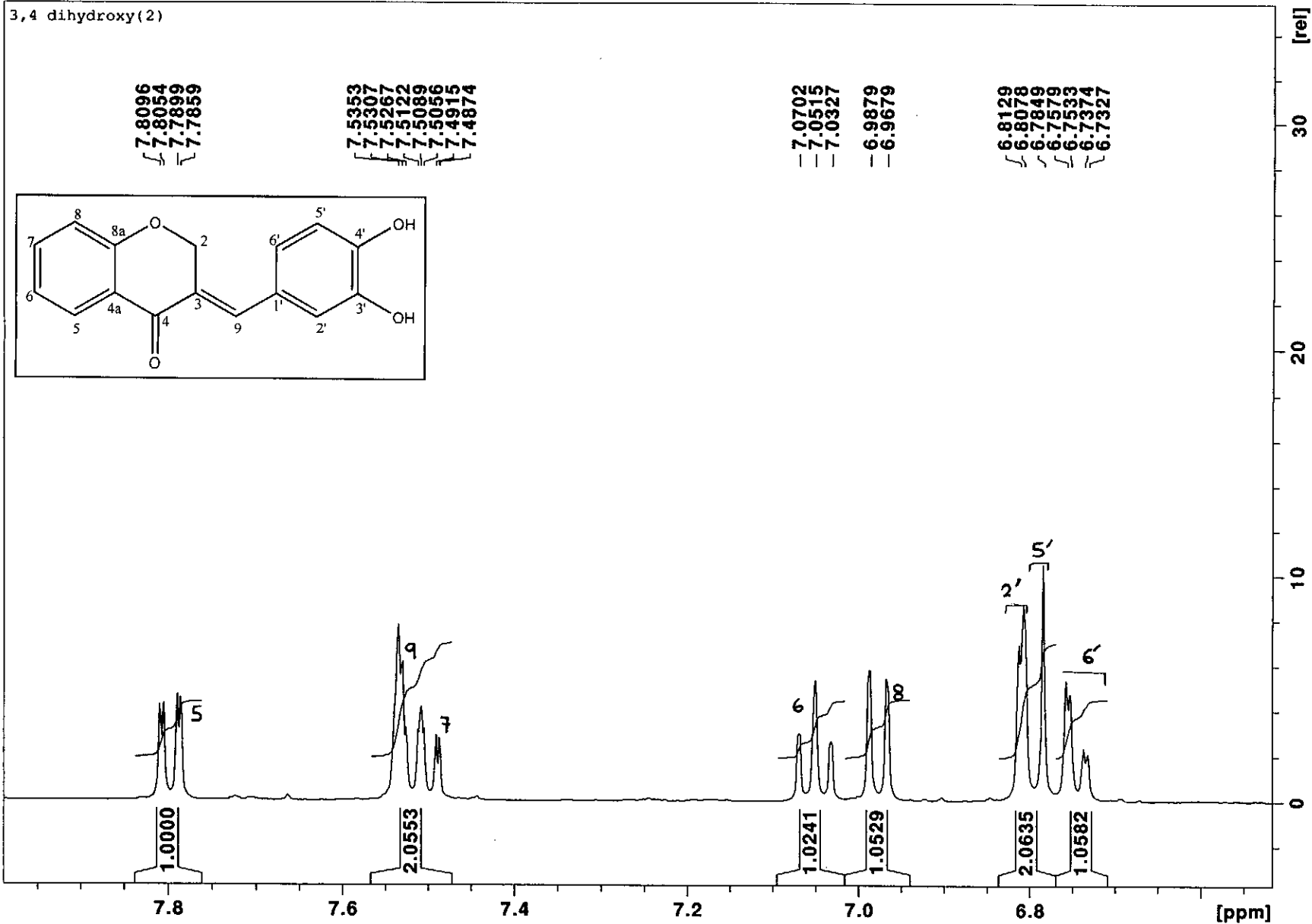
File : C:\msdchem\1\data\kaalin\3-HYDROXY.D
Operator :
Acquired : 13 Jan 2012 12:11 using AcqMethod NATPRODUCTS MANUAL INJ.M
Instrument : 5973N
Sample Name:
Misc Info :
Vial Number: 1





^1H NMR spectrum of compound 15

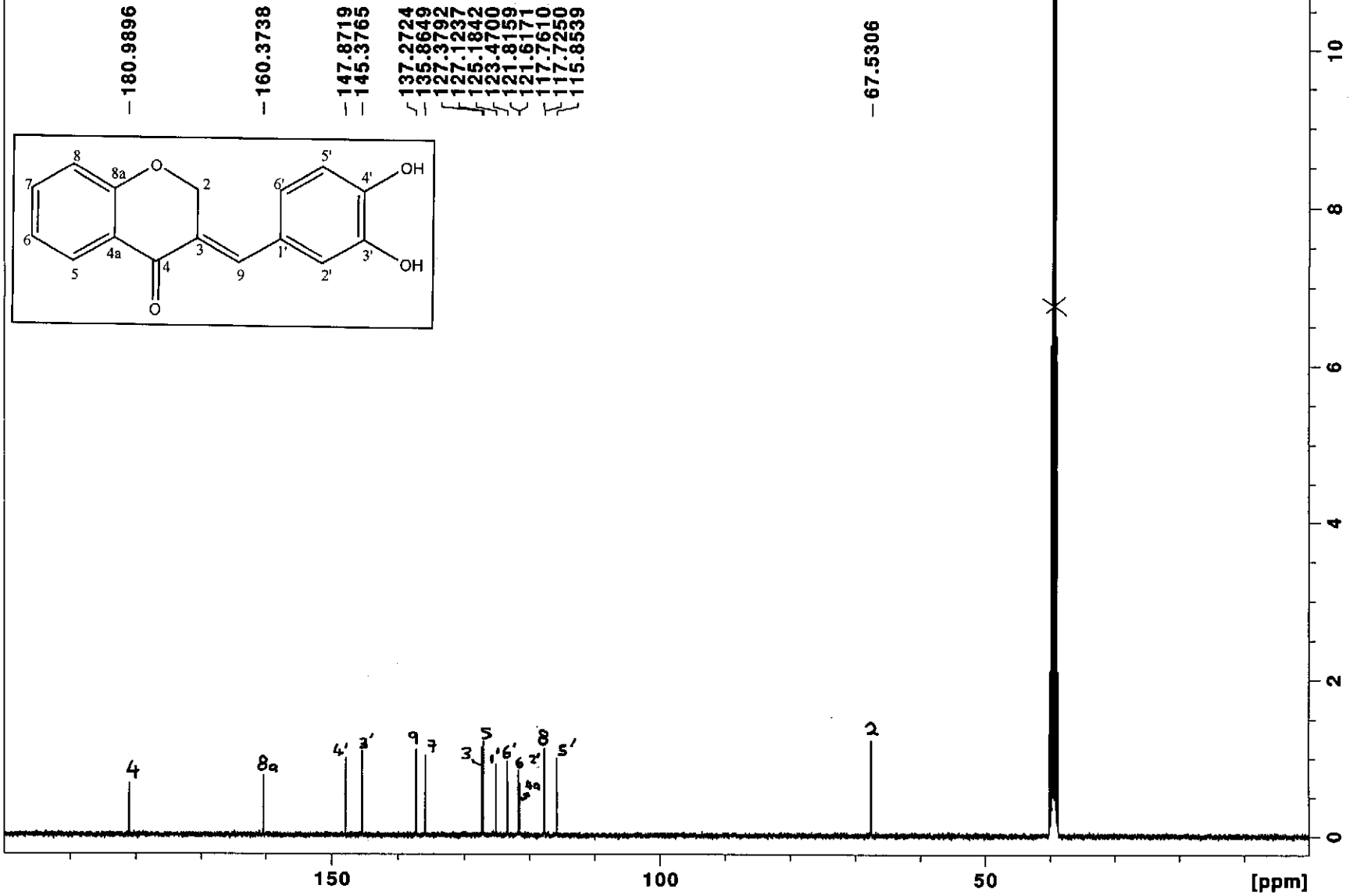
Nov16-2011-NK-kaalin 10 1 /opt/topspin NK



¹H NMR spectrum of compound 15 (expanded)

Nov16-2011-NK-kaalin 11 1 /opt/topspin NK

3,4 dihydroxy(2)



¹³C NMR spectrum of compound 15

3,4 dihydroxy(2)

— 127.3792
— 127.1237

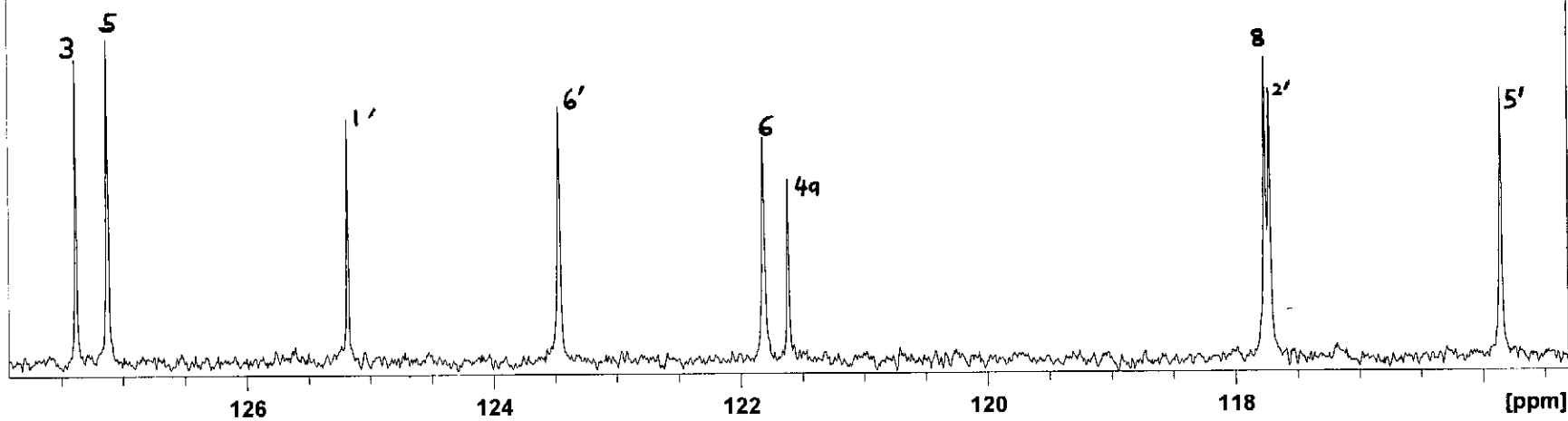
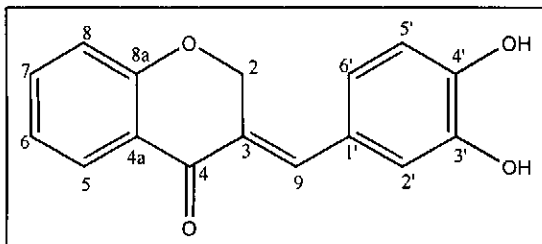
— 125.1842

— 123.4700

— 121.8159
— 121.6171

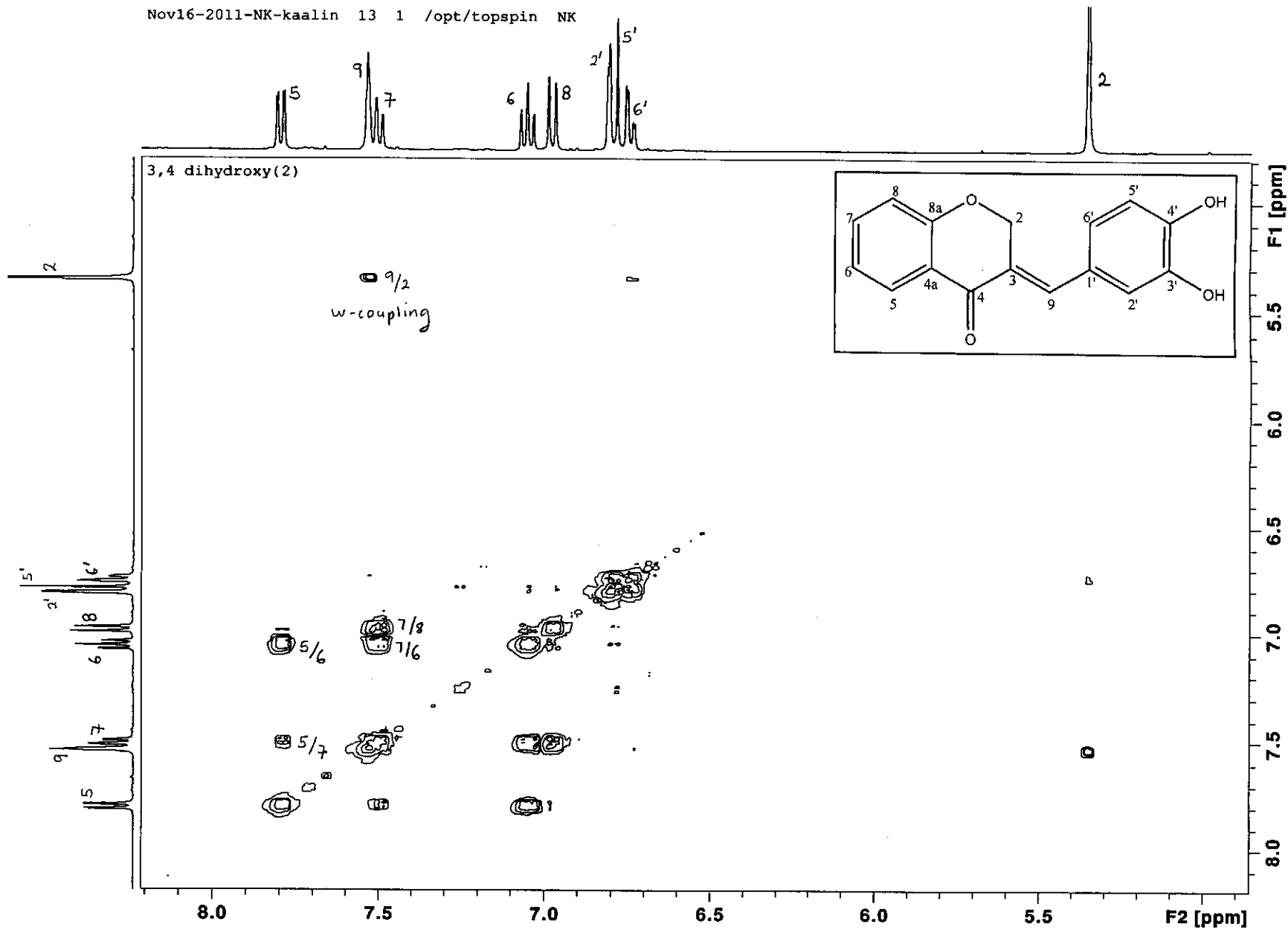
— 117.7610
— 117.7250

— 115.8539



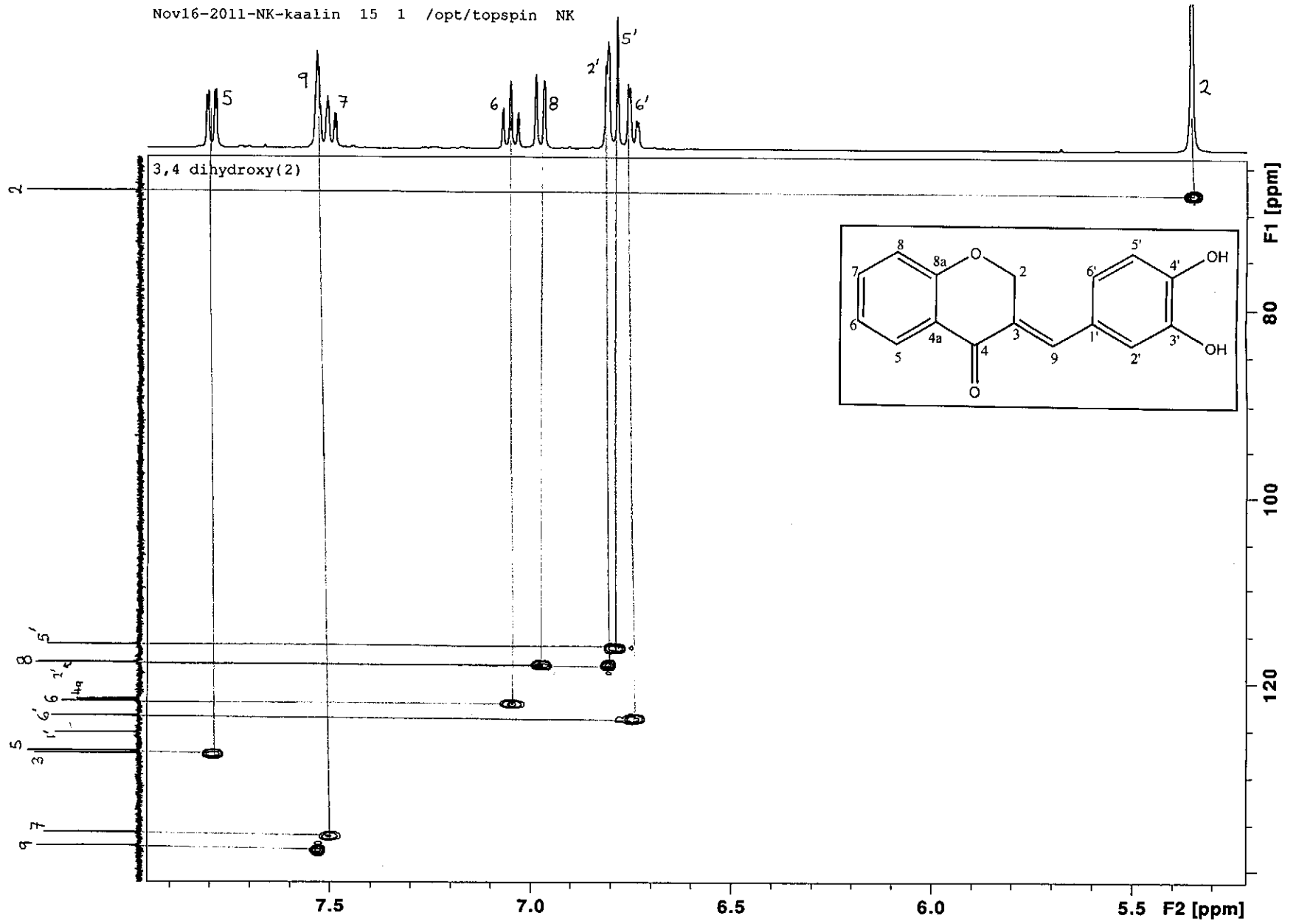
¹³C NMR spectrum of compound 15 (expanded)

Nov16-2011-NK-kaalin 13 1 /opt/topspin NK



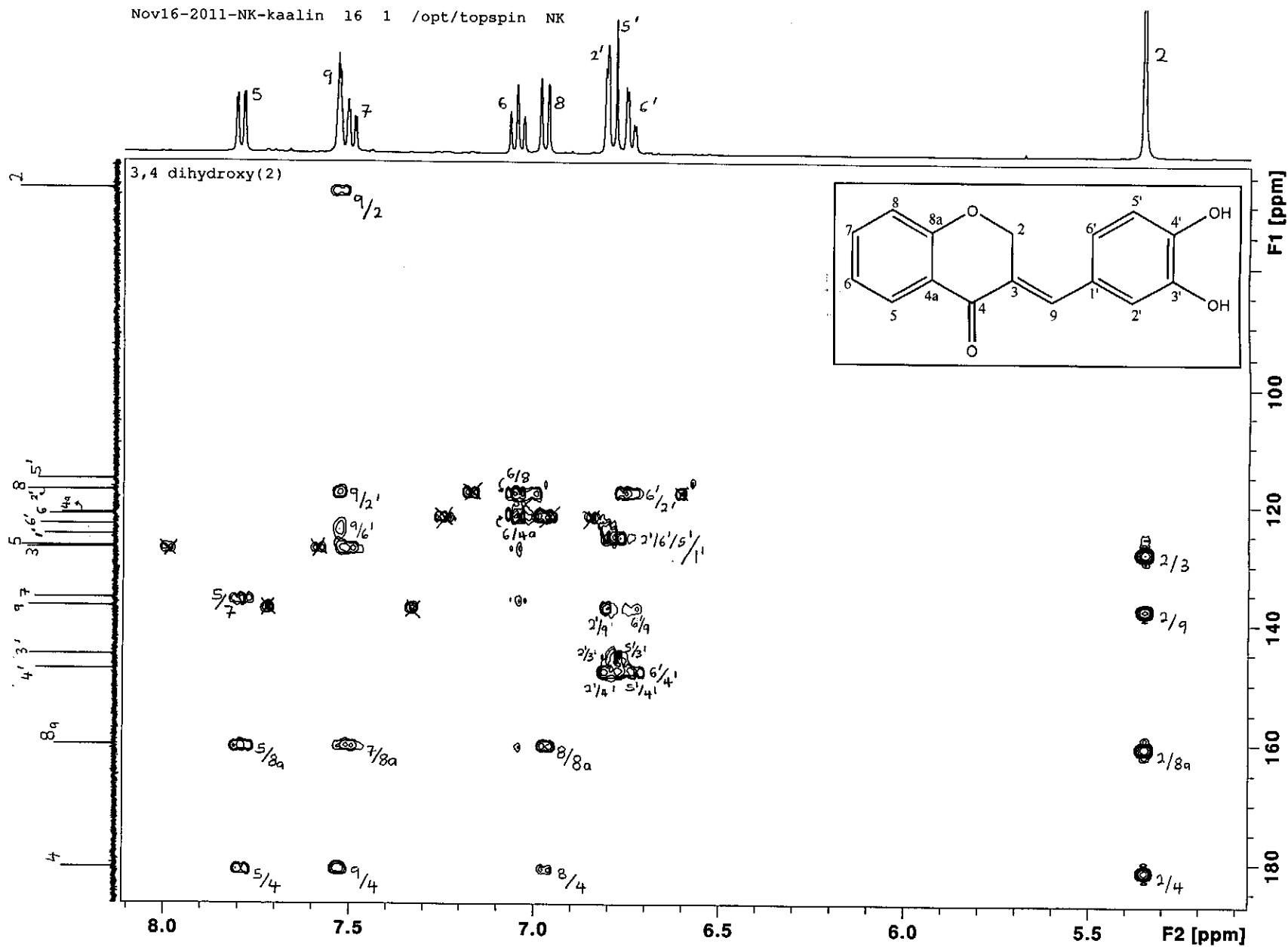
COSY spectrum of compound 15

Nov16-2011-NK-kaalin 15 1 /opt/topspin NK



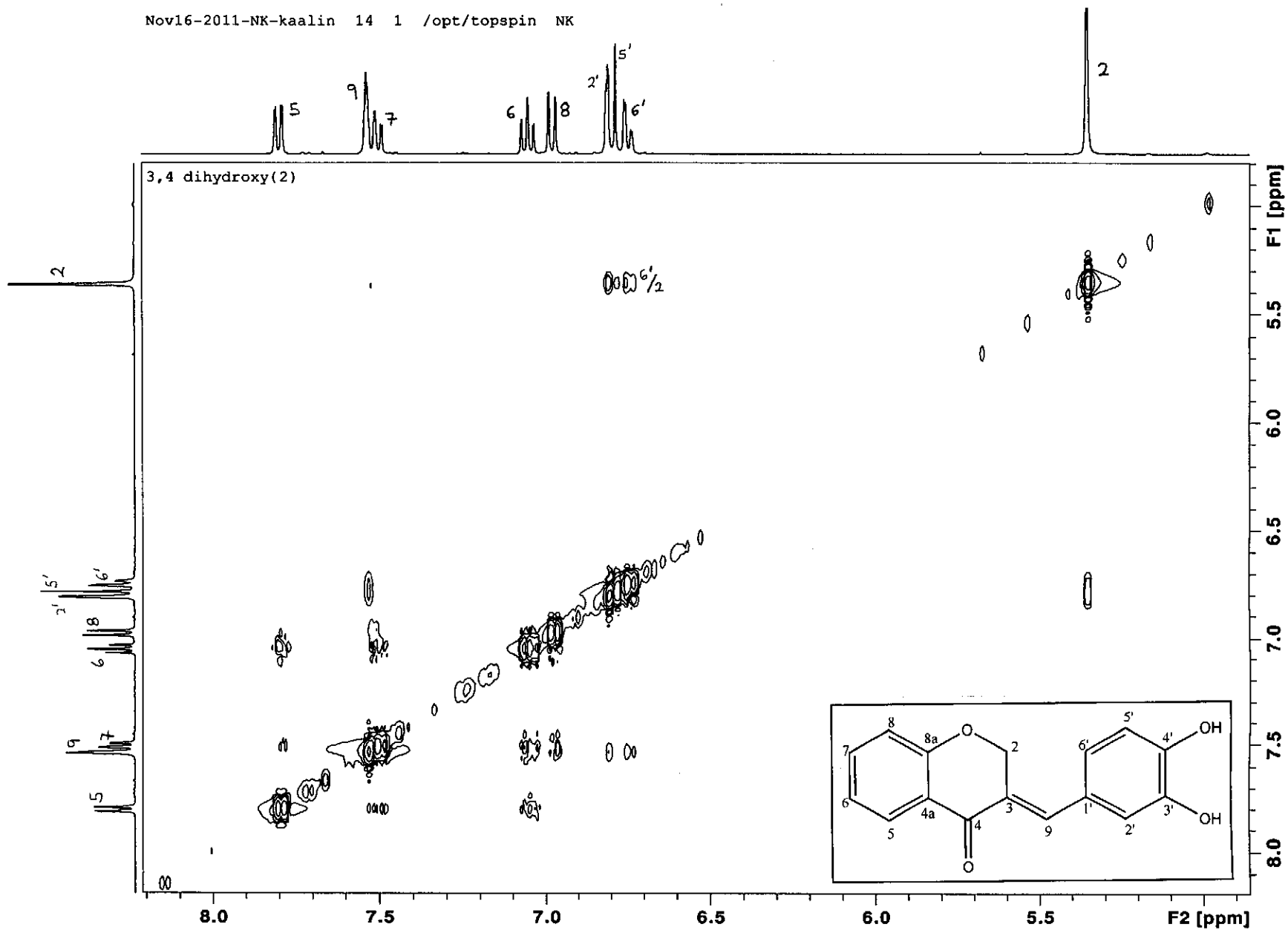
HSQC spectrum of compound 15

Nov16-2011-NK-kaalin 16 1 /opt/topspin NK



HMBC spectrum of compound 15

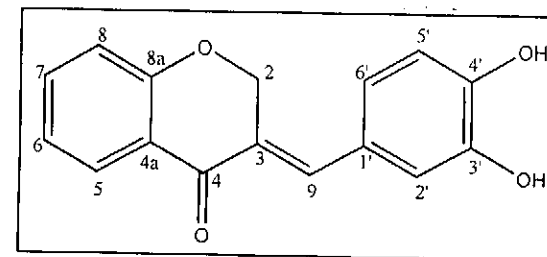
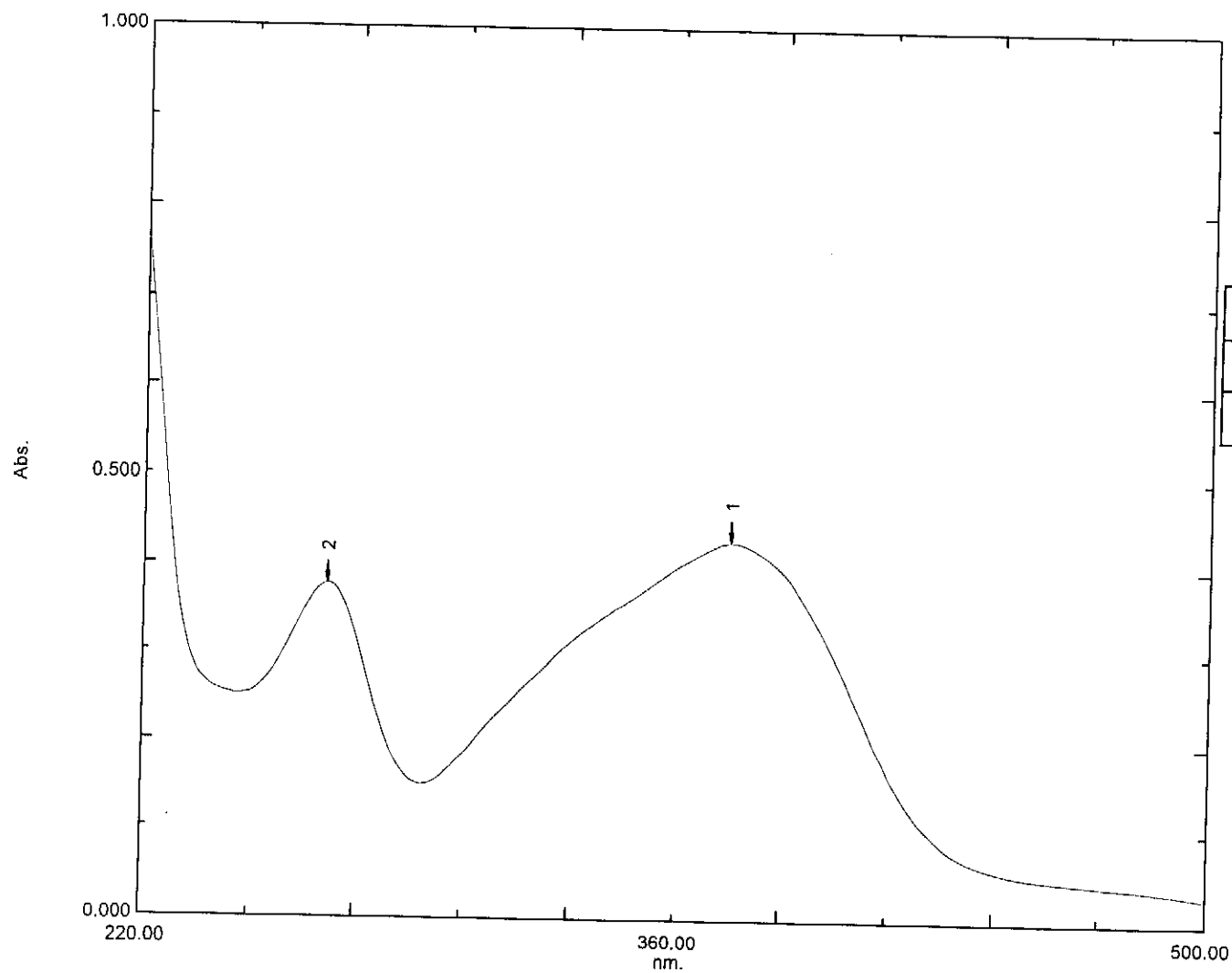
Nov16-2011-NK-kaalin 14 1 /opt/topspin NK



NOESY spectrum of compound 15

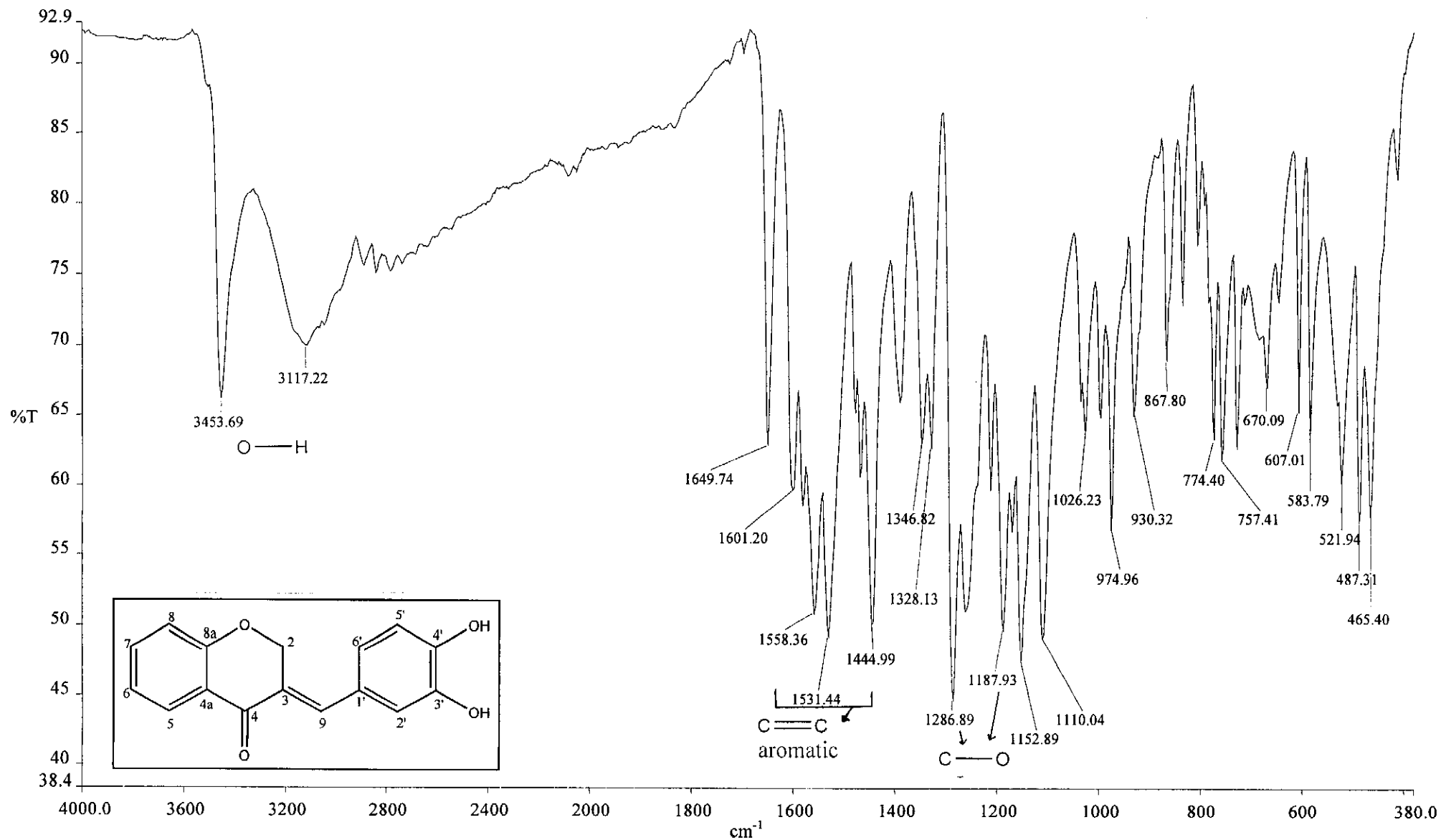
Overlay Spectrum Graph Report

15/05/2012 01:07:53 PM



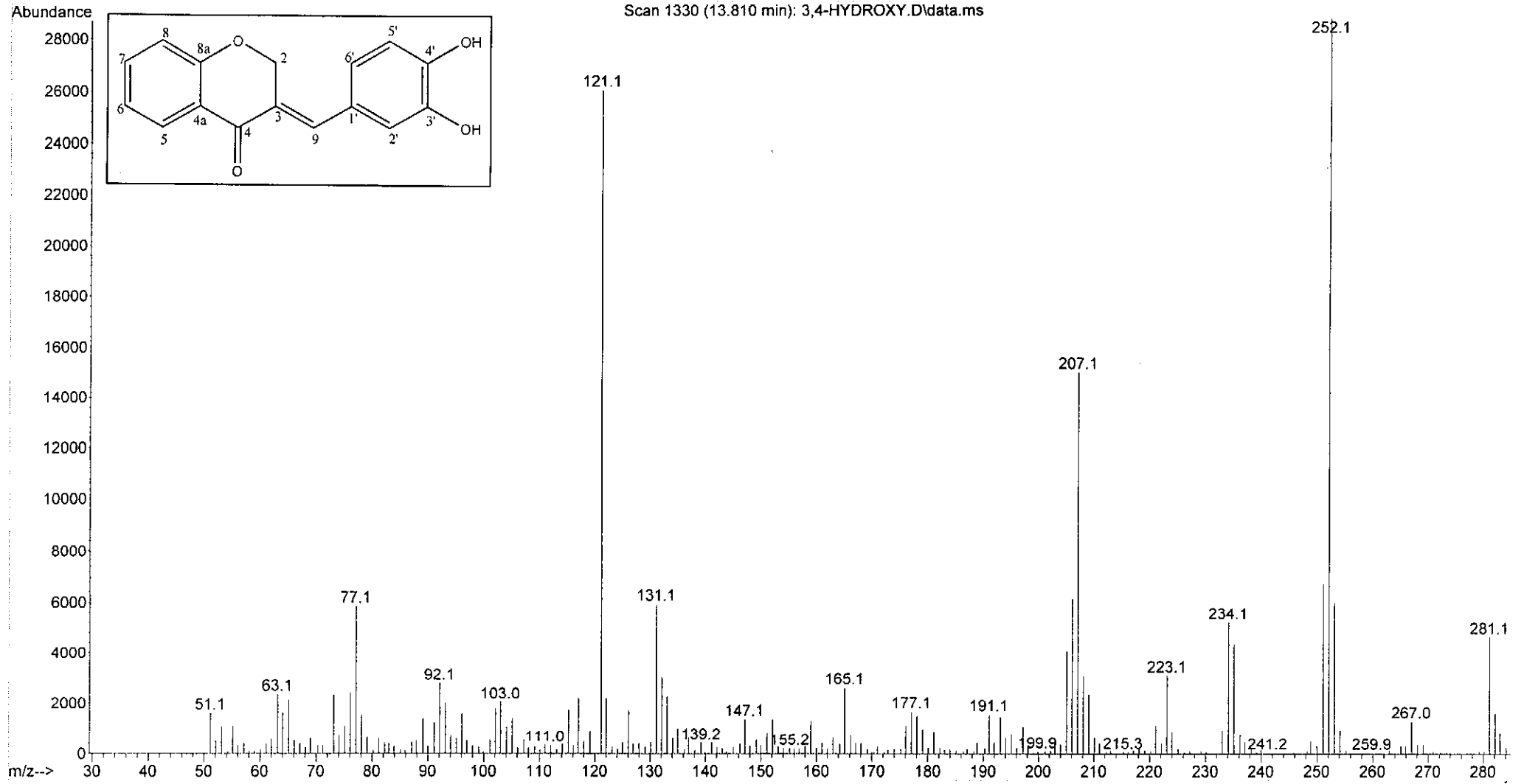
Wavelength/ nm	Absorbance	Log ϵ
268	0.377	3.62
374	0.428	3.68

UV-Vis spectrum of compound 15



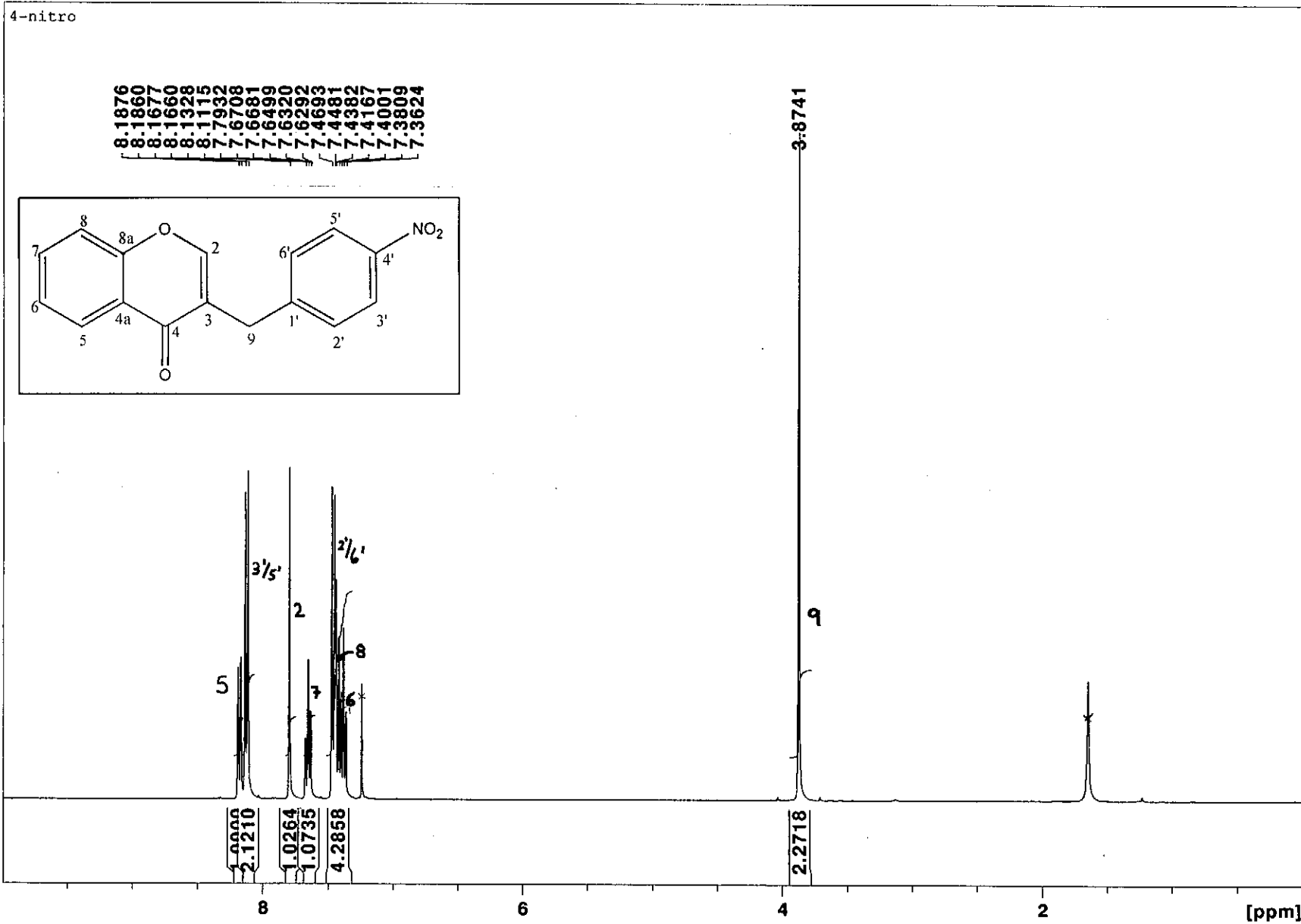
Infrared spectrum of compound 15

File : C:\msdchem\1\data\kaalin\3,4-HYDROXY.D
Operator :
Acquired : 13 Jan 2012 12:50 using AcqMethod NATPRODUCTS MANUAL INJ.M
Instrument : 5973N
Sample Name:
Misc Info :
Vial Number: 1

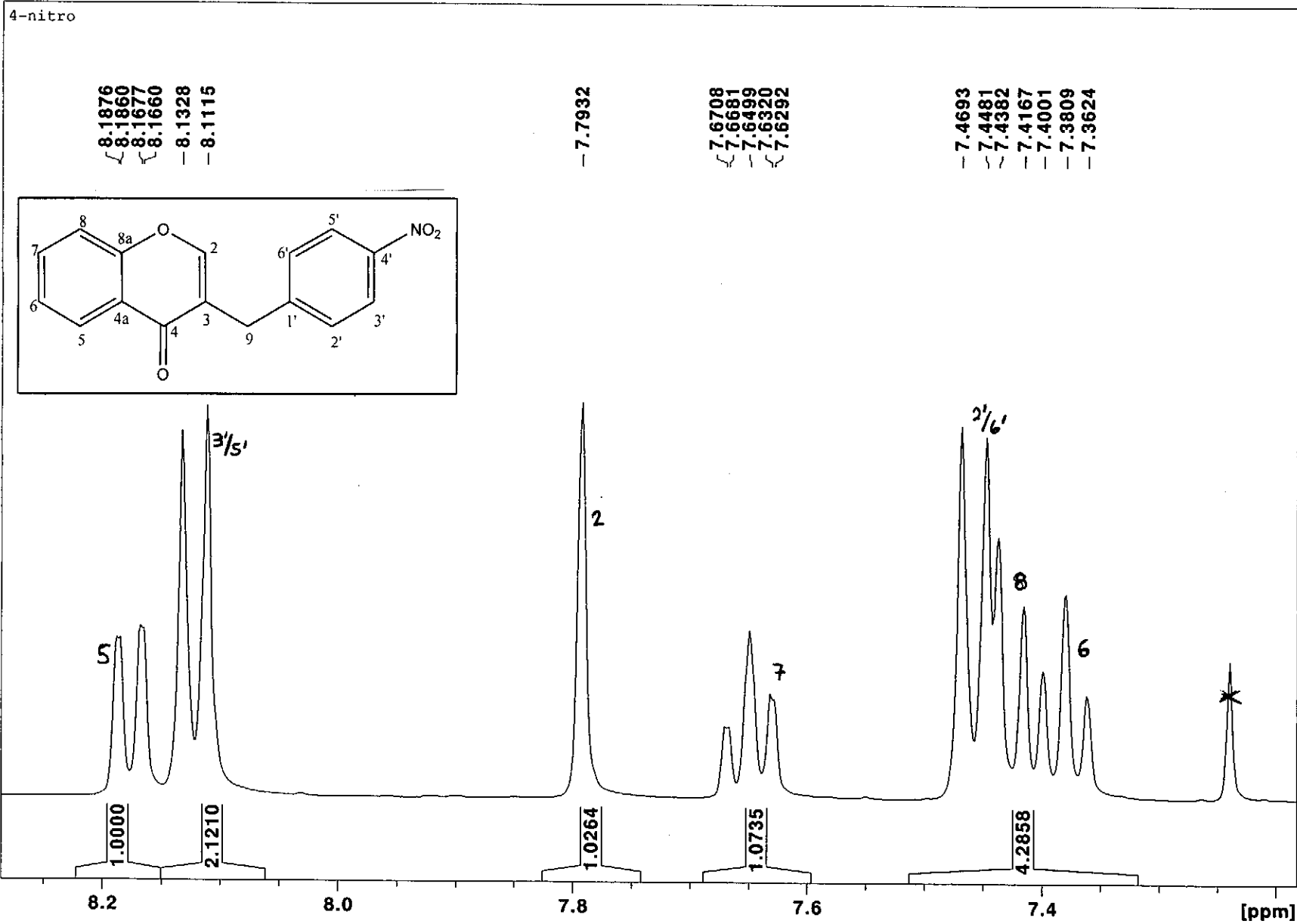


Mass spectrum of compound 15

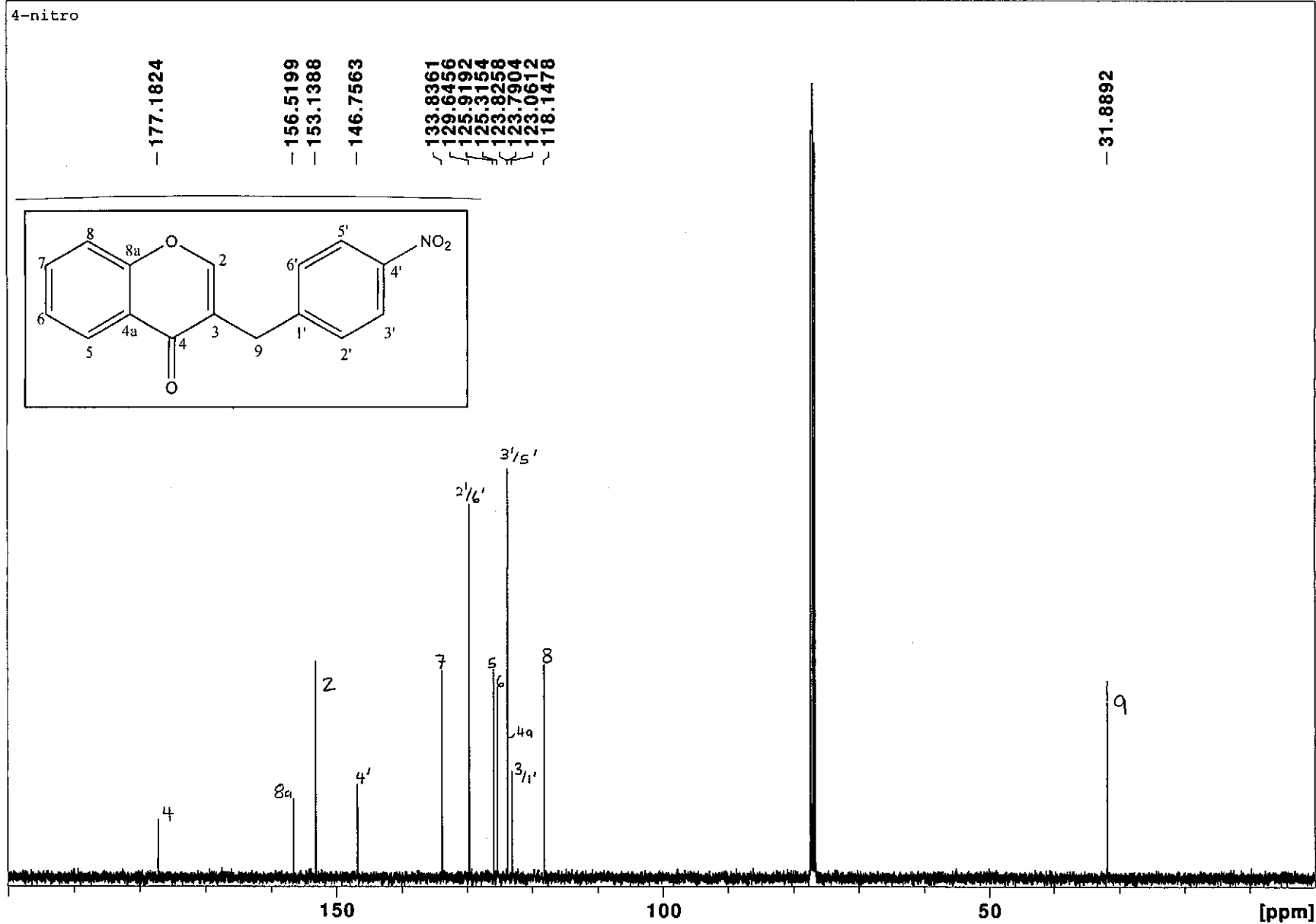
Mar20-2012-NK-kaalin 10 1 /opt/topspin NK



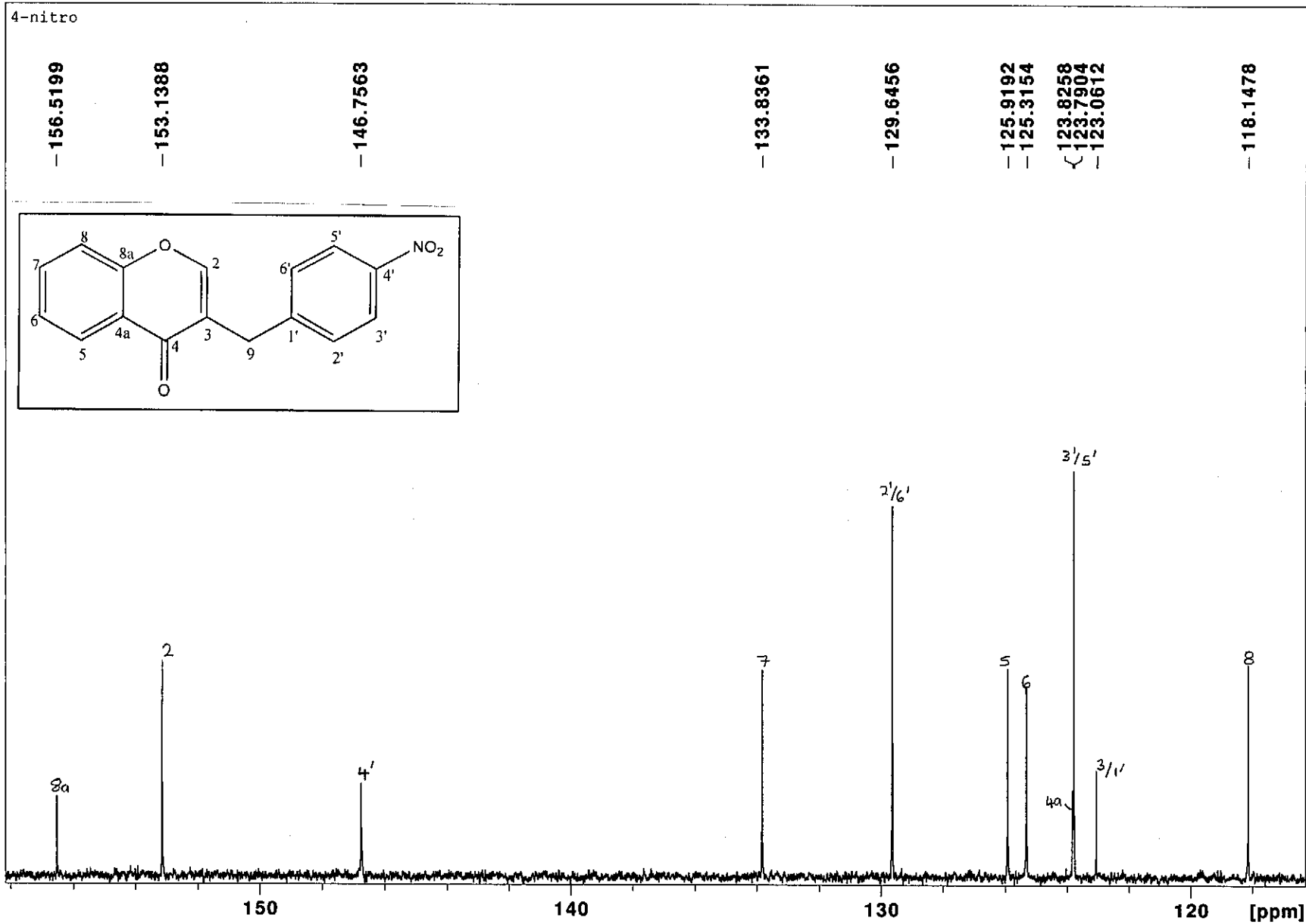
^1H NMR spectrum of compound 16



¹H NMR spectrum of compound 16 (expanded)

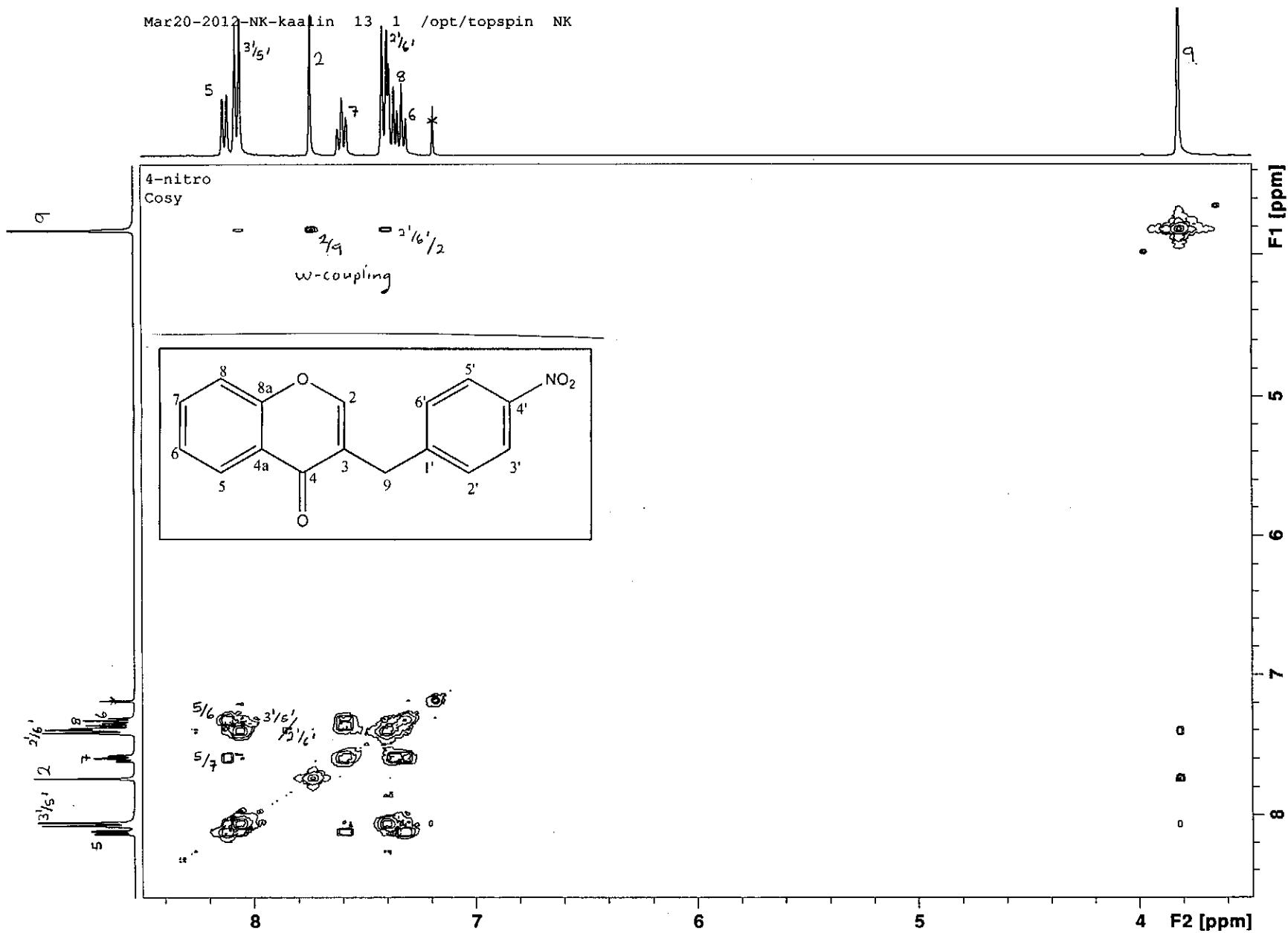


¹³C NMR spectrum of compound 16



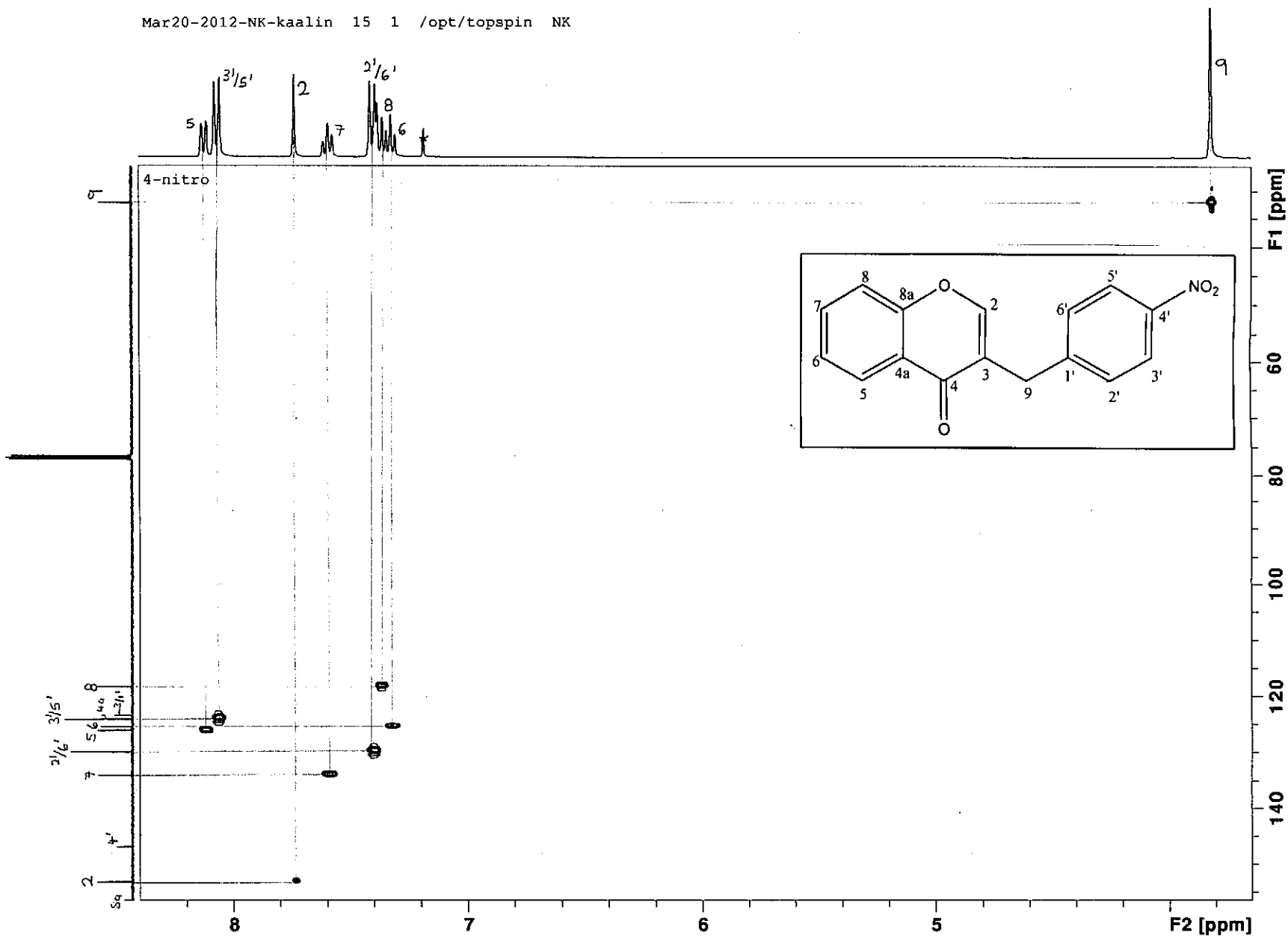
¹³C NMR spectrum of compound 16 (expanded)

Mar20-2012-NK-kaalin 13 1 /opt/topspin NK

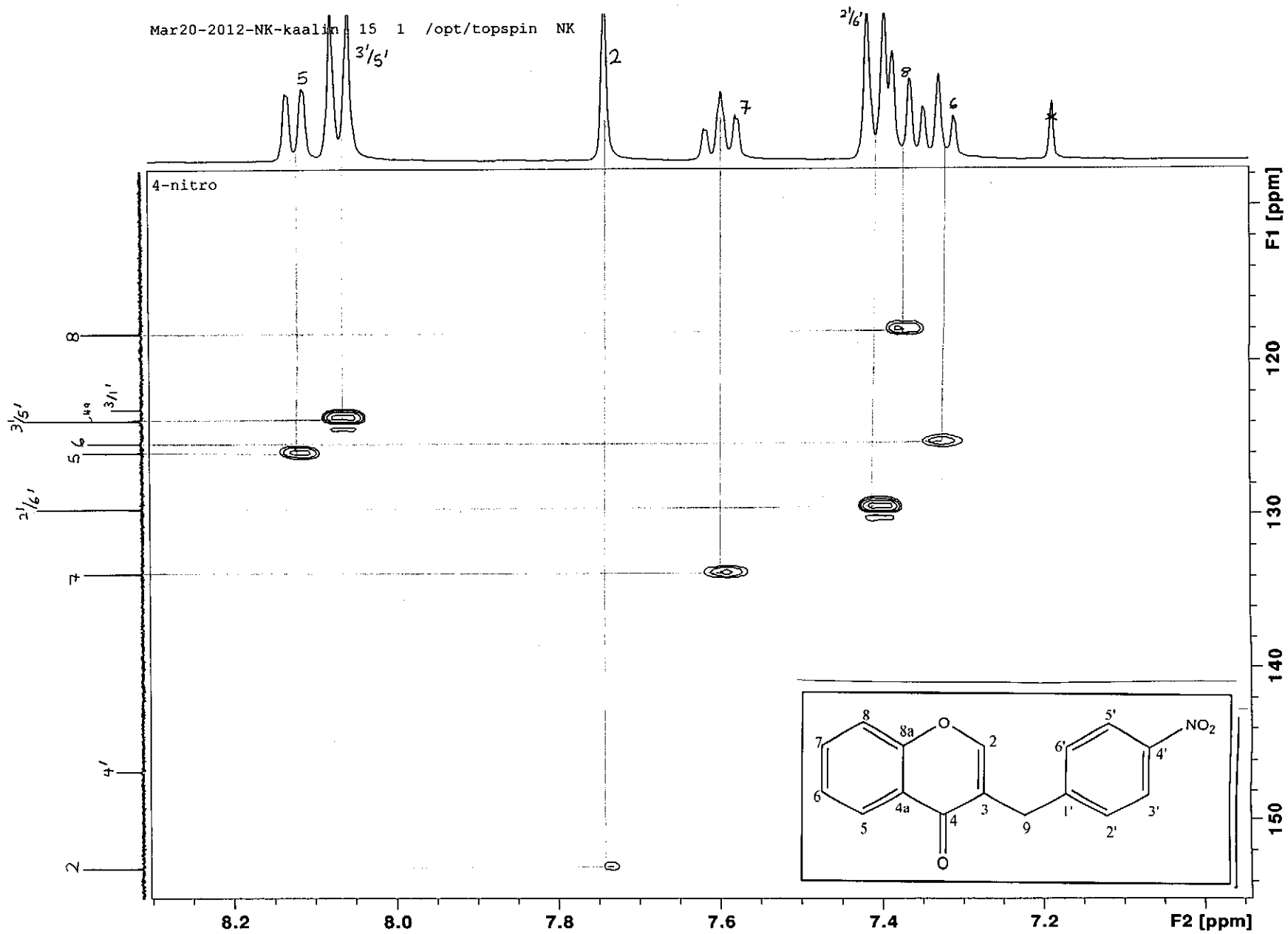


COSY spectrum of compound 16

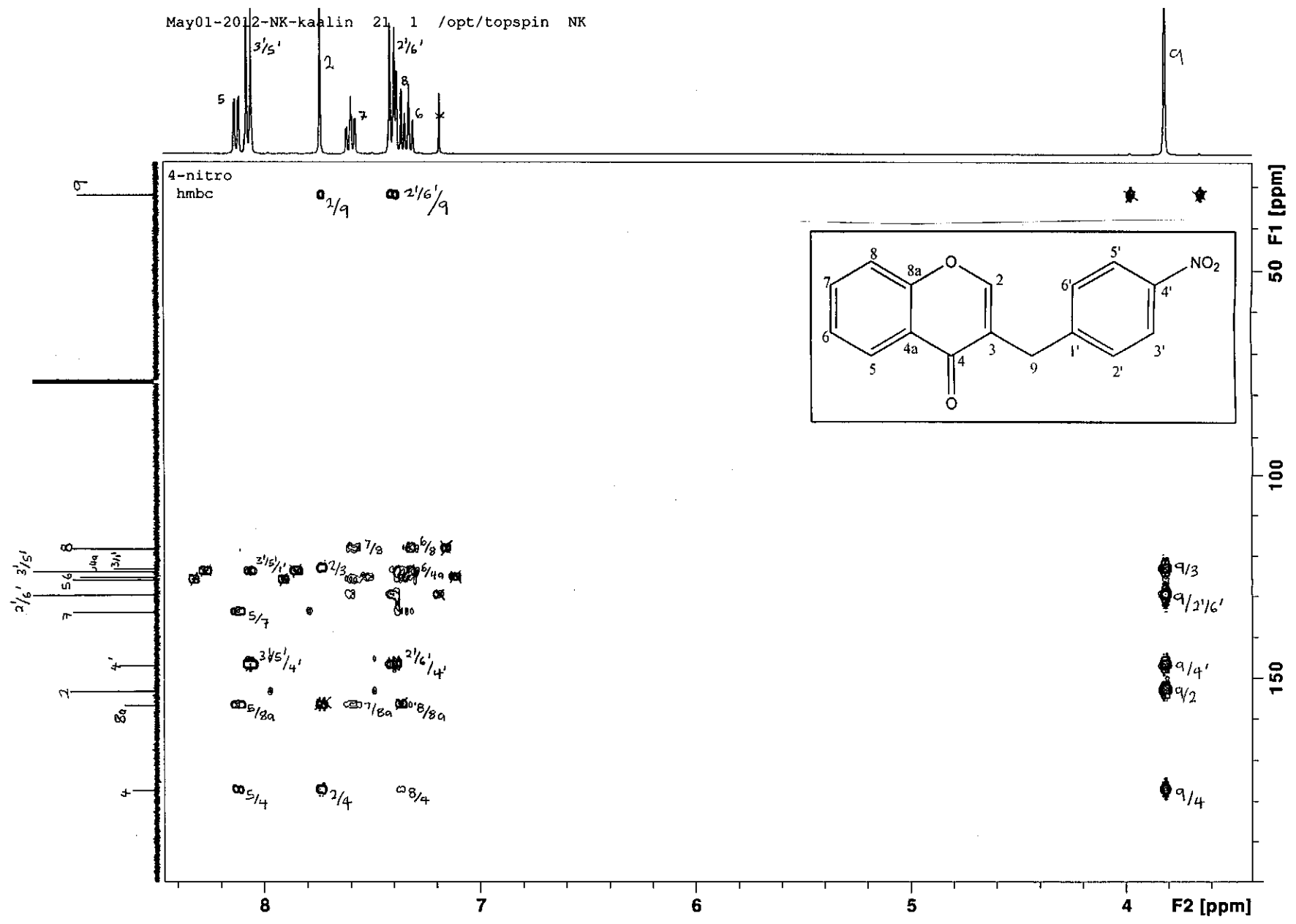
Mar20-2012-NK-kaalin 15 1 /opt/topspin NK



HSQC spectrum of compound 16

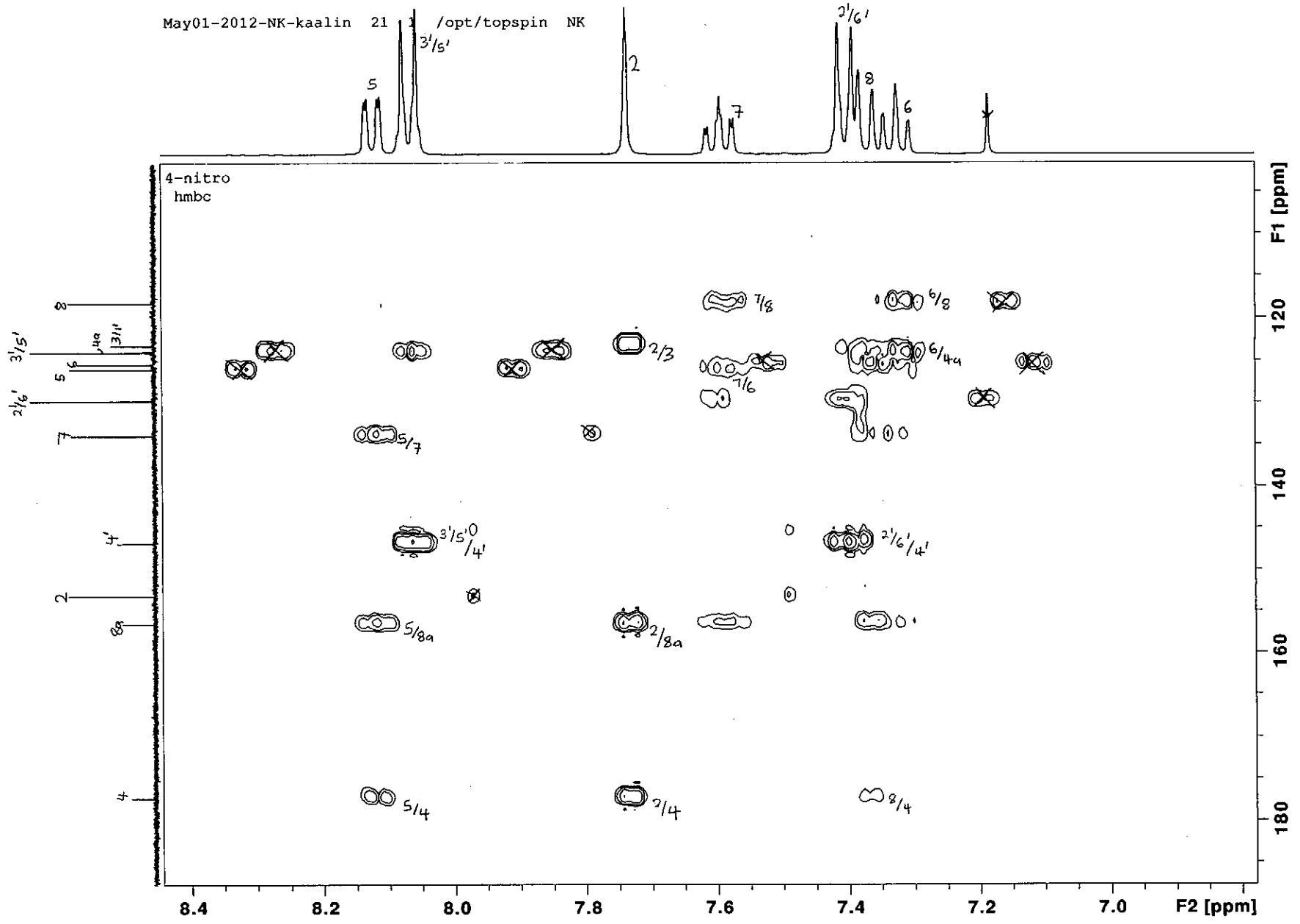


HSQC spectrum of compound 16 (expanded)



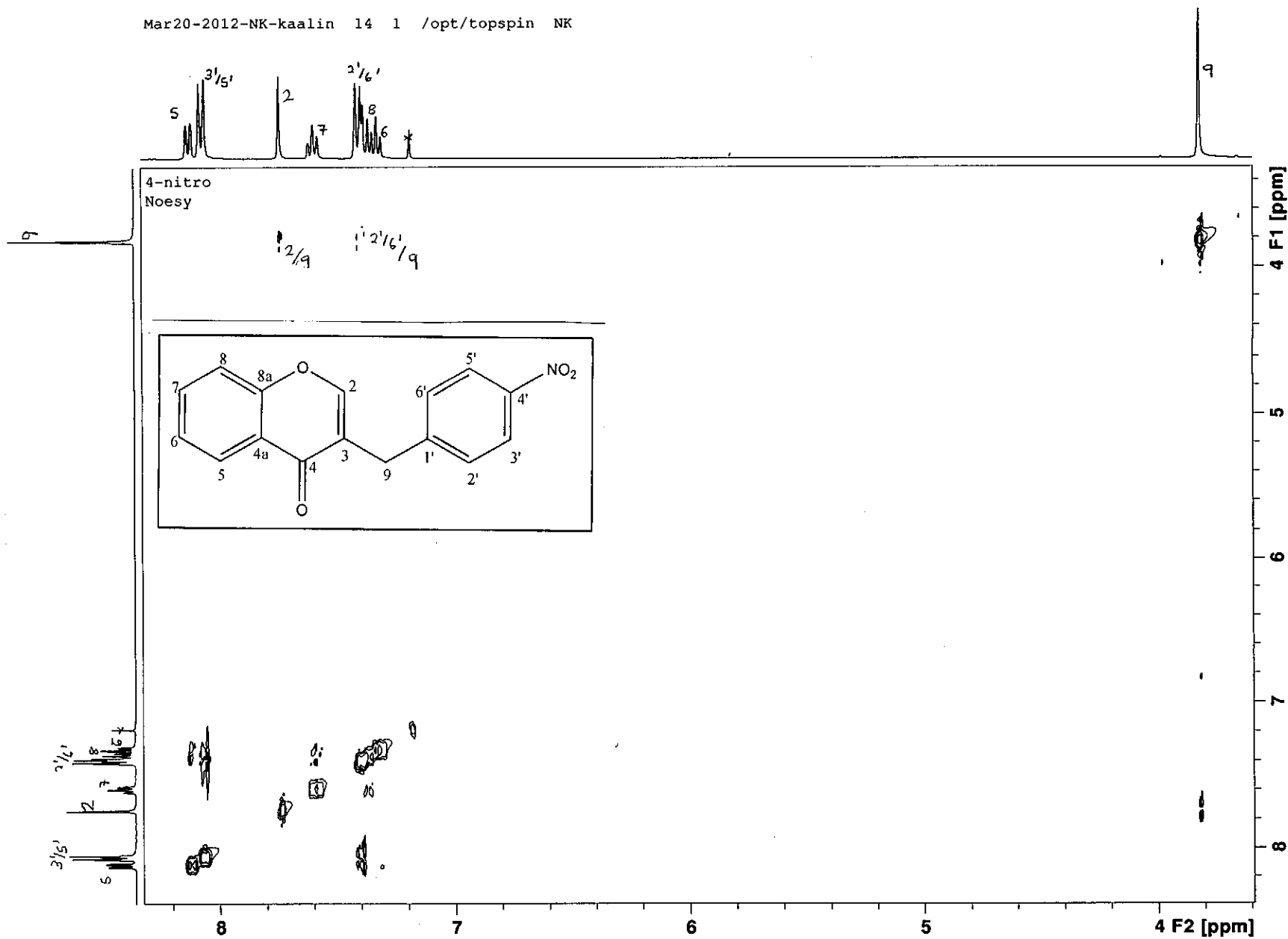
HMBC spectrum of compound 16

May01-2012-NK-kaalin 21 /opt/topspin NK



HMBC spectrum of compound 16 (expanded)

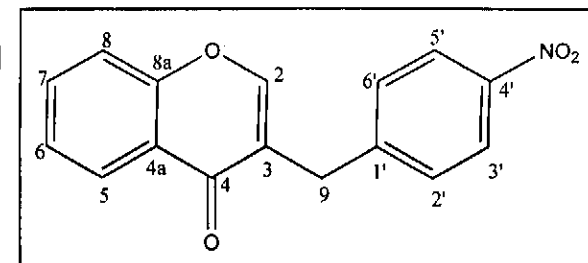
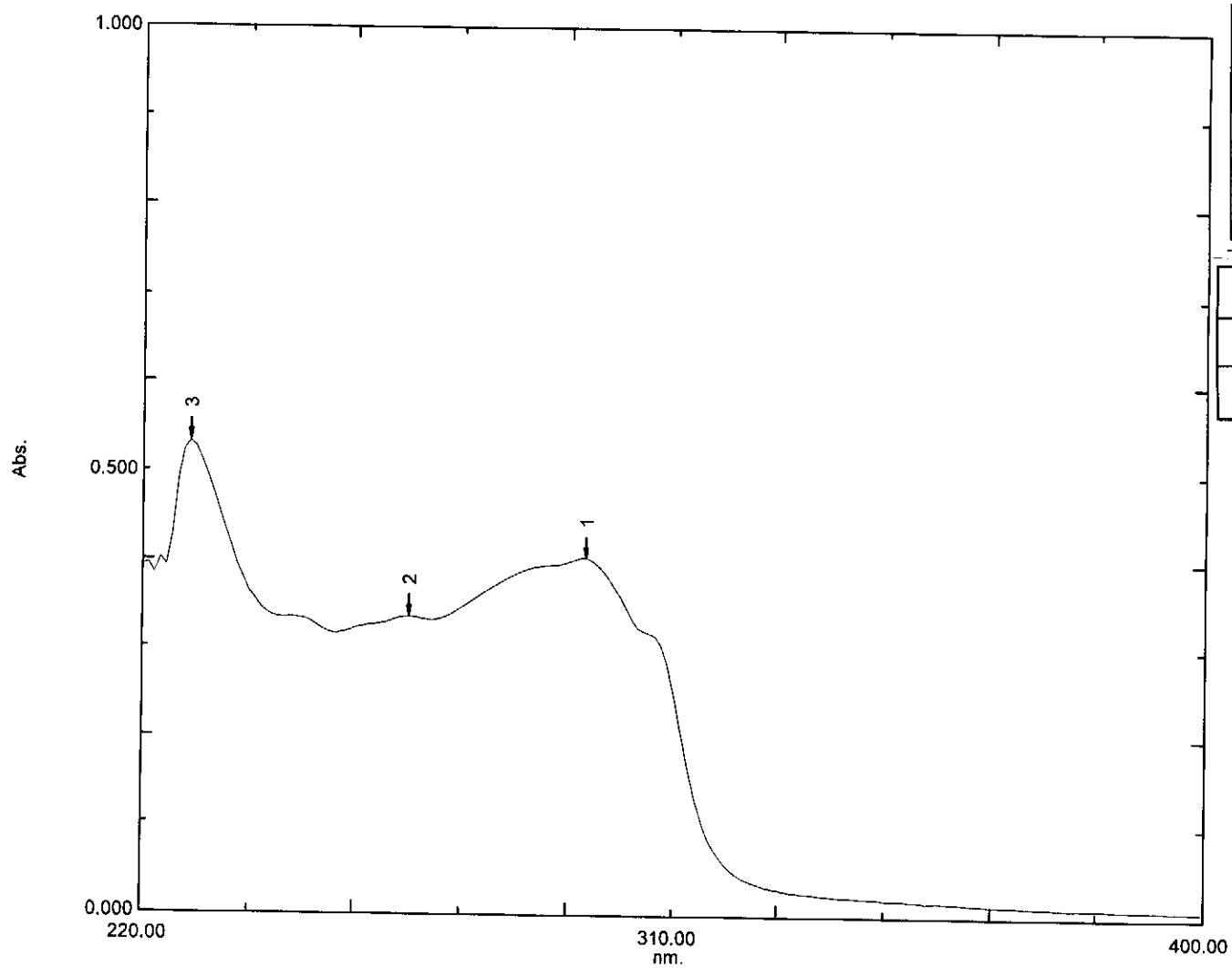
Mar20-2012-NK-kaalin 14 1 /opt/topspin NK



NOESY spectrum of compound 16

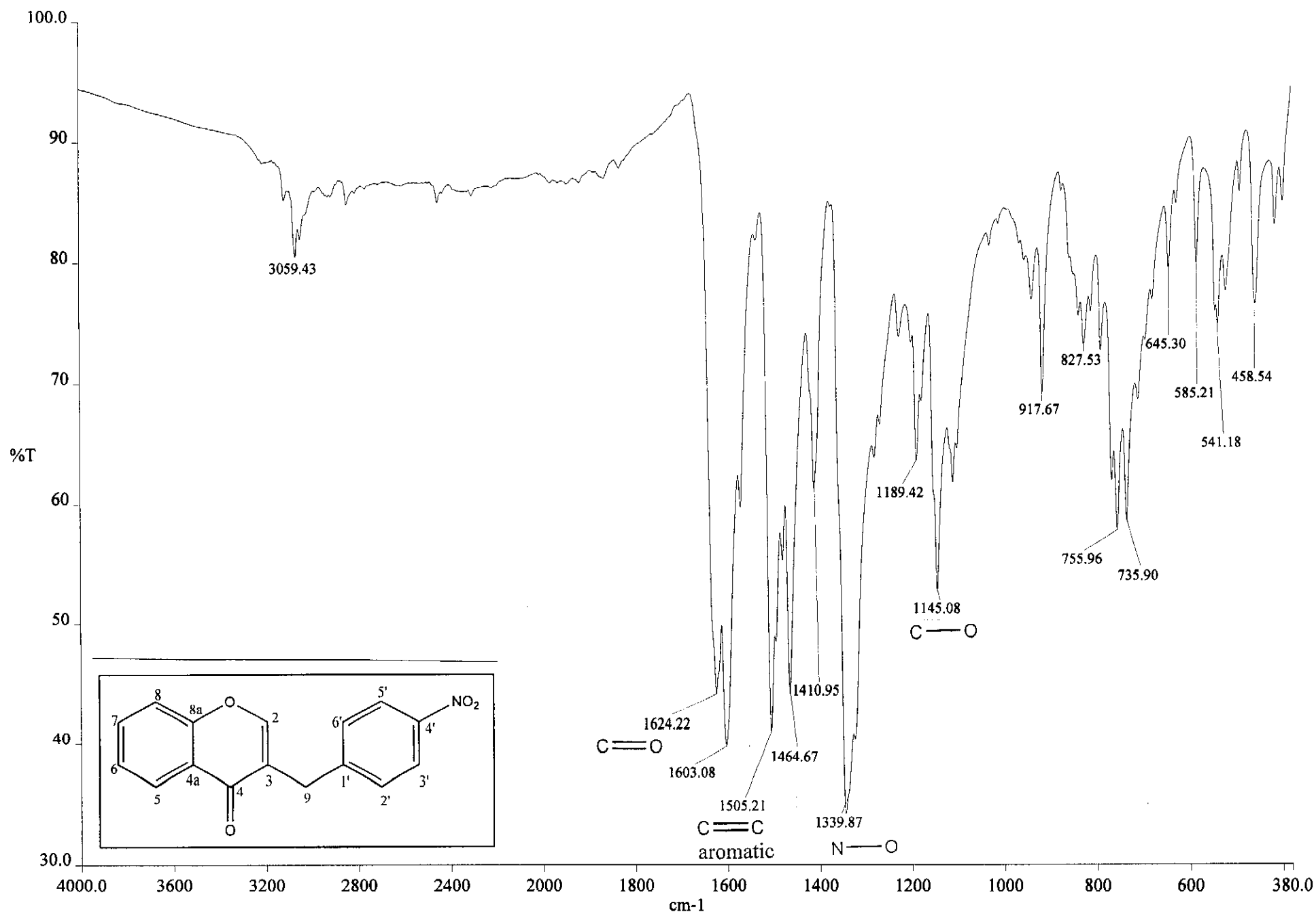
Overlay Spectrum Graph Report

15/05/2012 01:09:09 PM



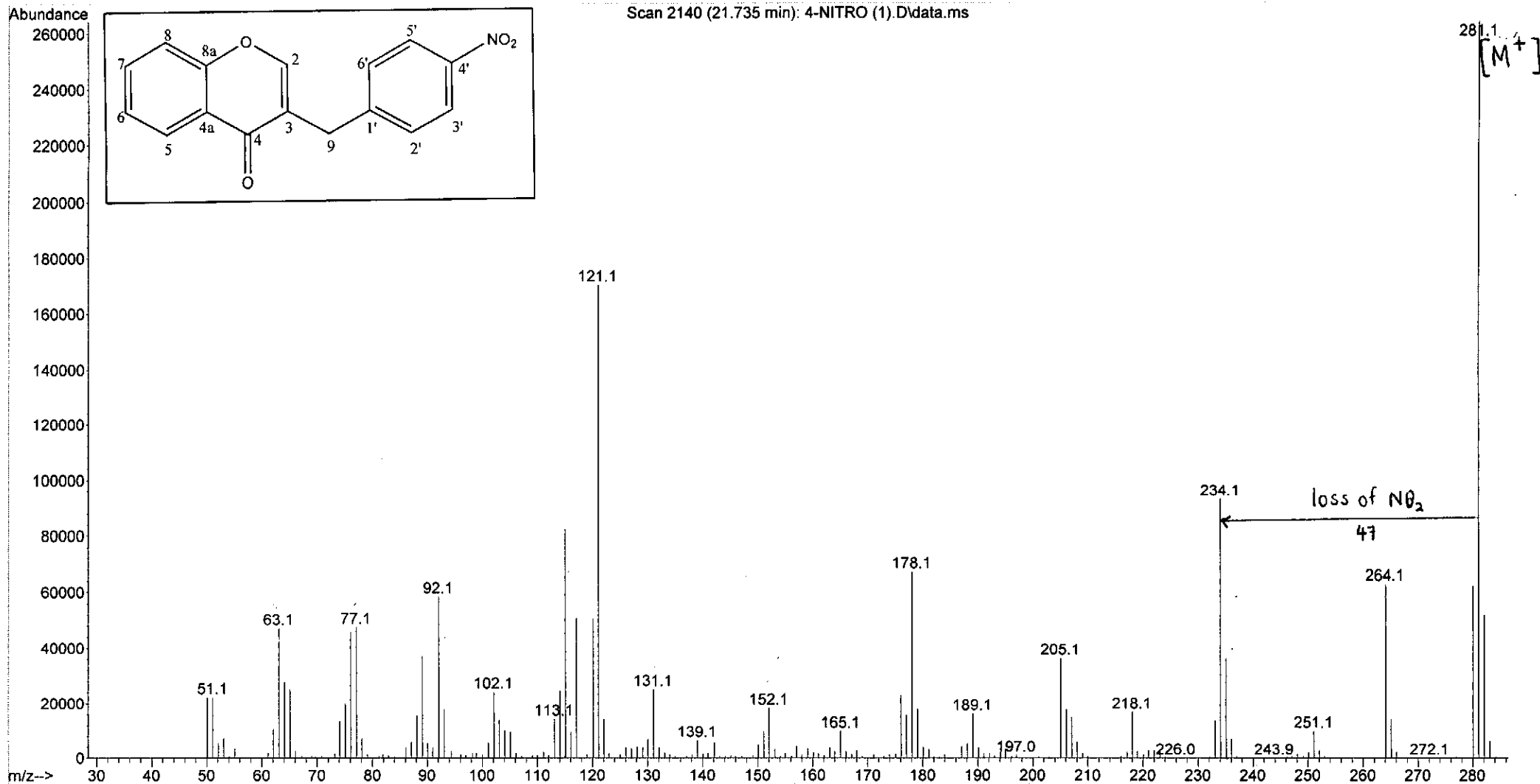
Wavelength/ nm	Absorbance	Log ϵ
265	0.336	4.07
295	0.404	4.15

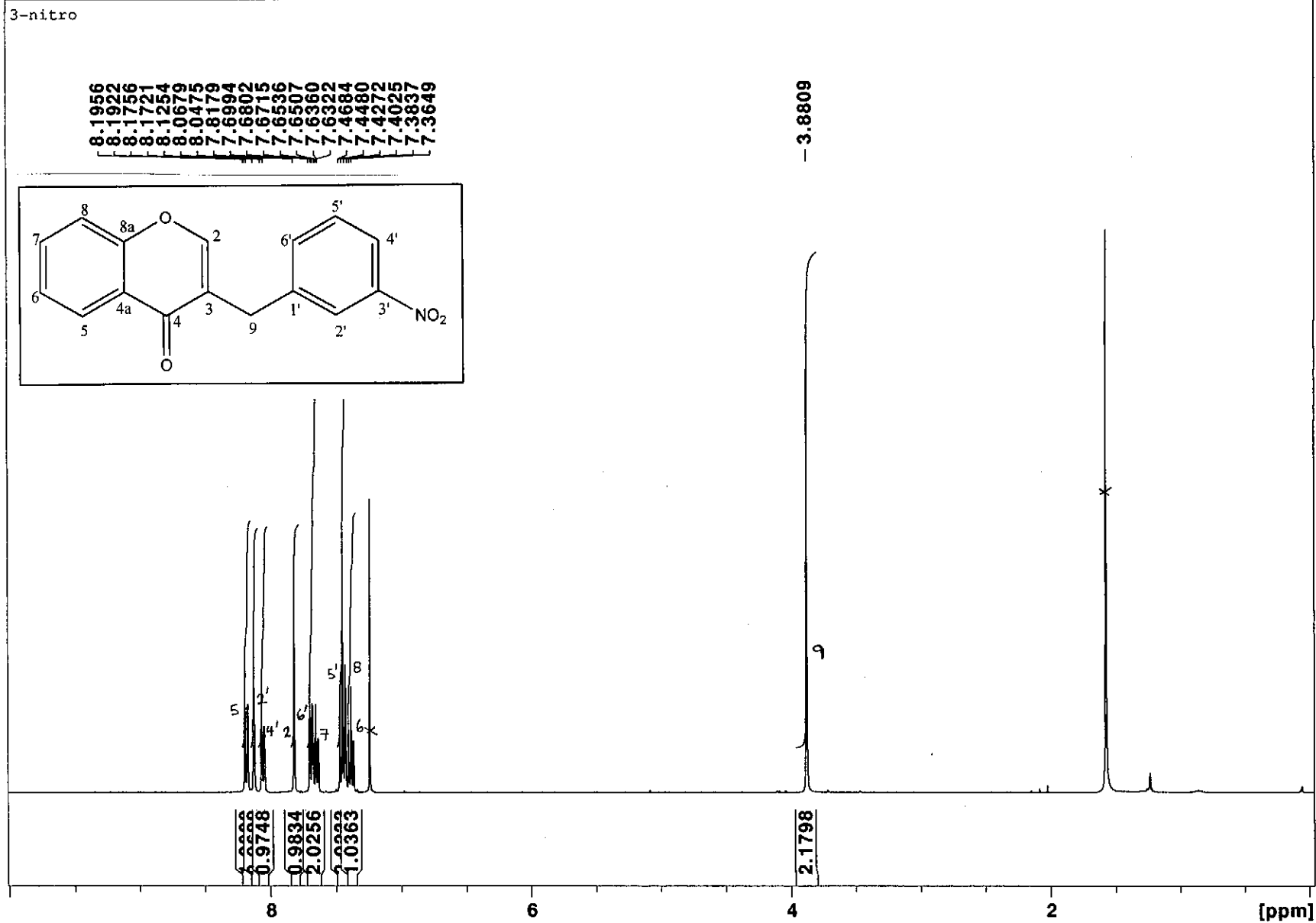
UV-Vis spectrum of compound 16



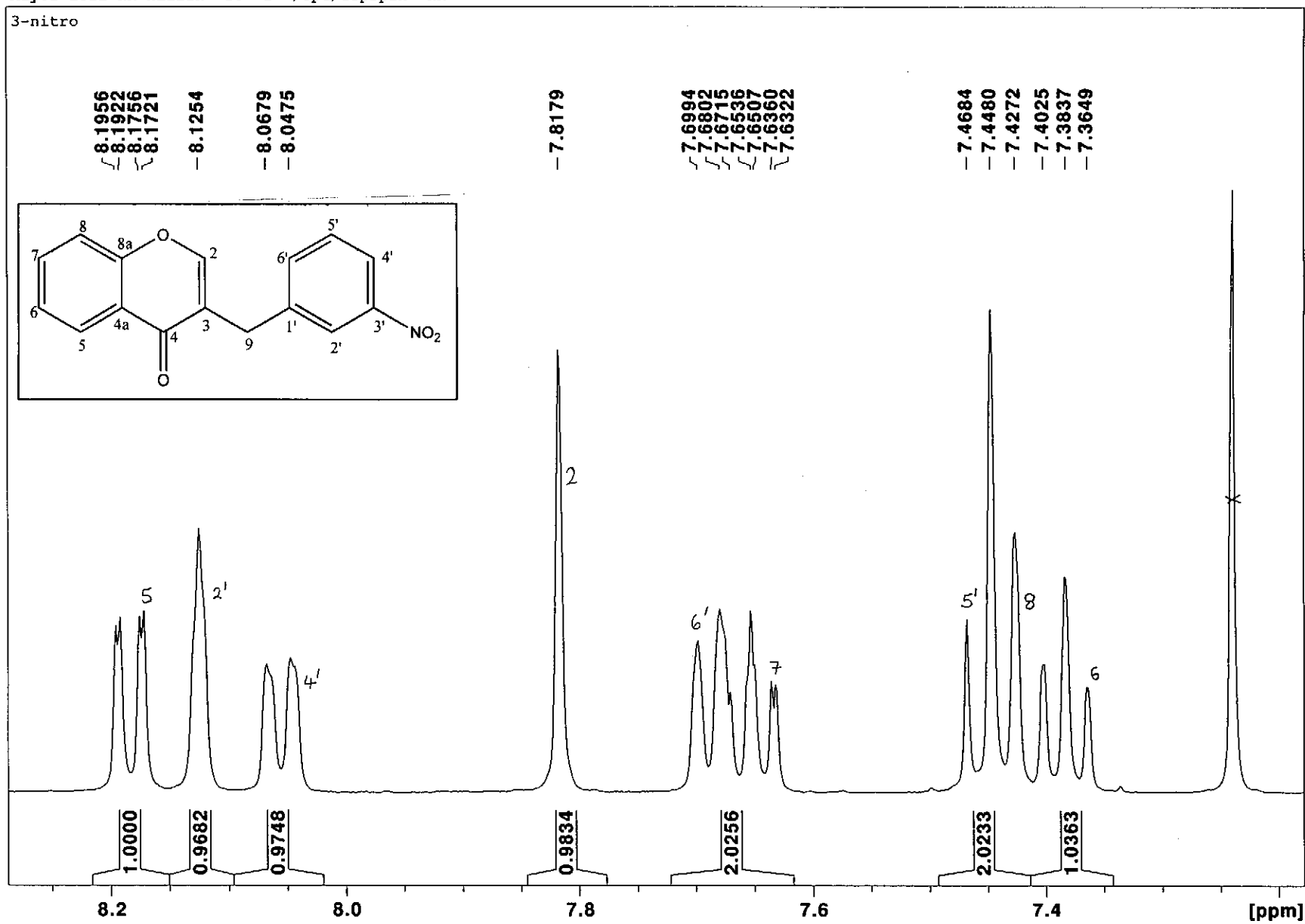
Infrared spectrum of compound 16

File :C:\msdchem\1\data\KAALIN 2\4-NITRO (1).D
Operator :
Acquired : 7 Jun 2012 12:34 using AcqMethod NATPRODUCTS MANUAL INJ SPLIT.M
Instrument : 5973N
Sample Name: 4-NITRO (1)
Misc Info :
Vial Number: 1

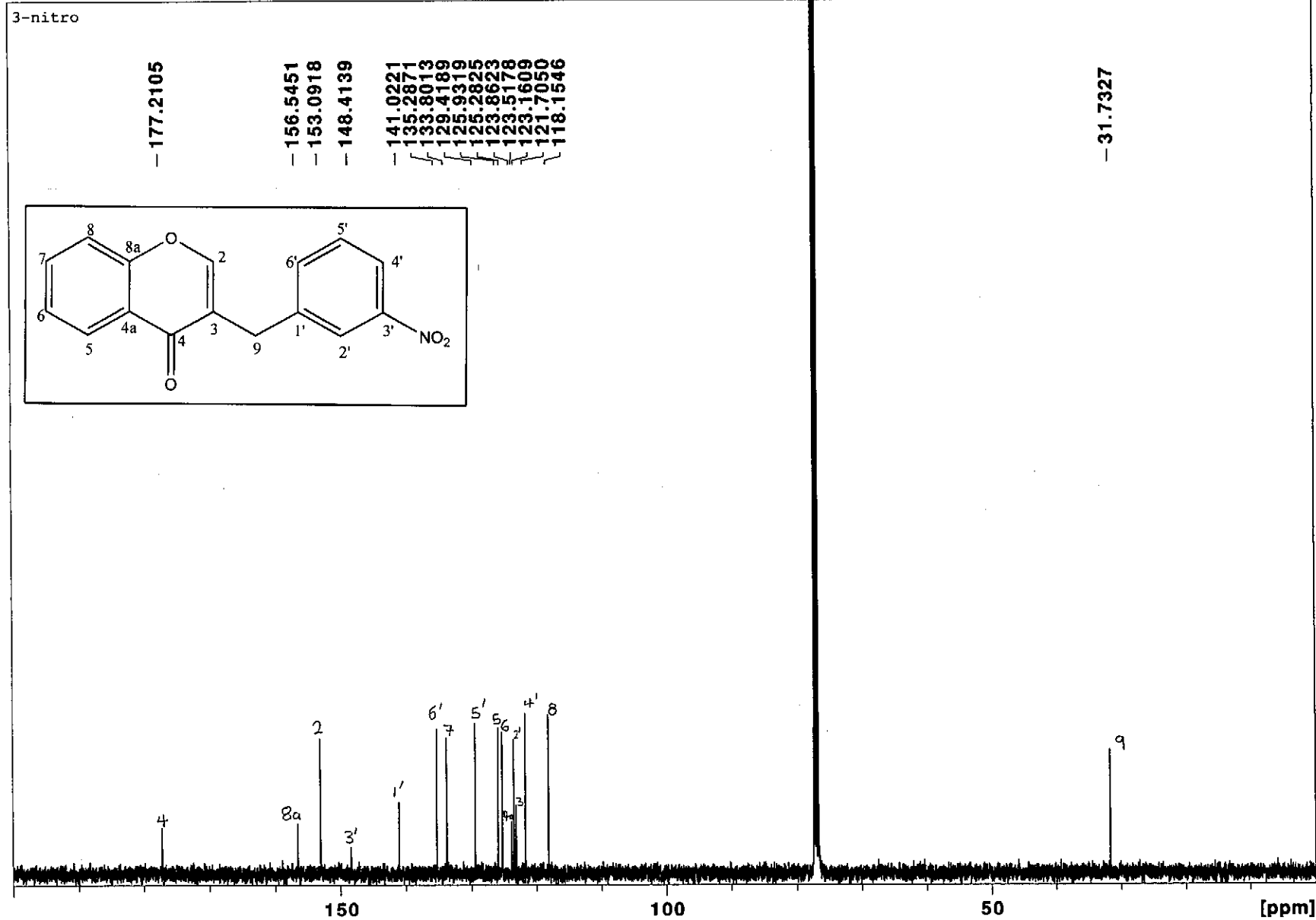




¹H NMR spectrum of compound 17



¹H NMR spectrum of compound 17 (expanded)



^{13}C NMR spectrum of compound 17

3-nitro

— 156.5451

— 153.0918

— 148.4139

— 141.0221

— 135.2871

— 133.8013

— 129.4189

— 125.9319

— 125.2825

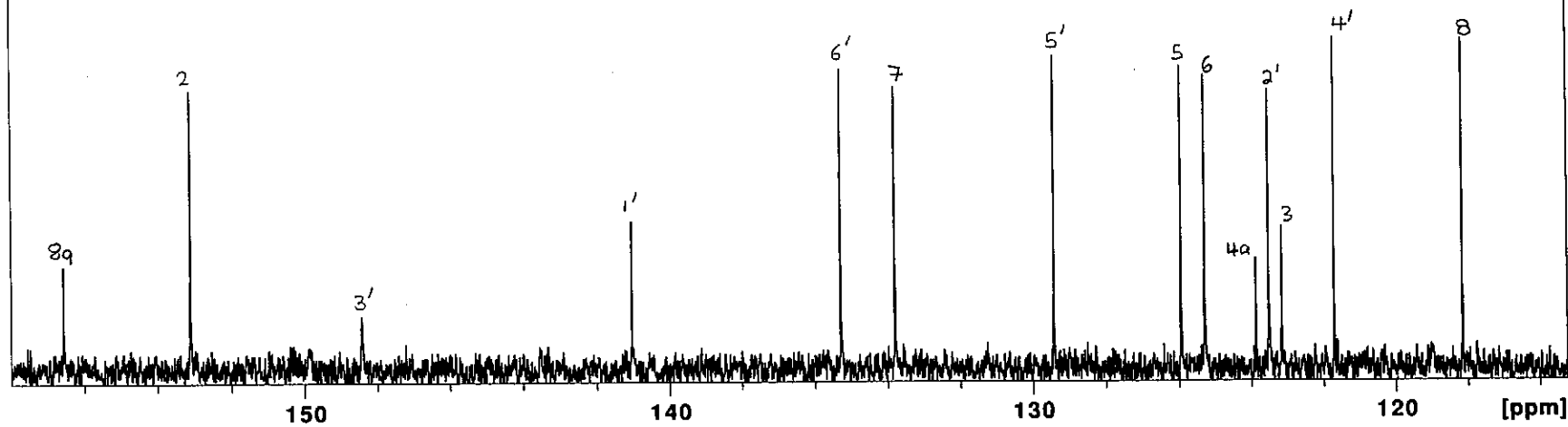
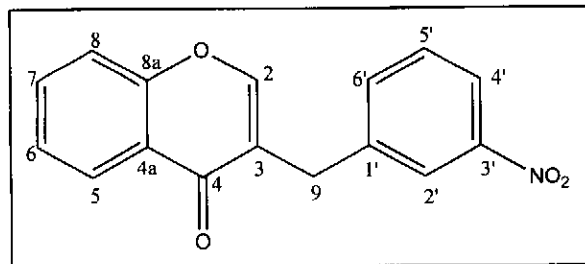
— 123.8623

— 123.5178

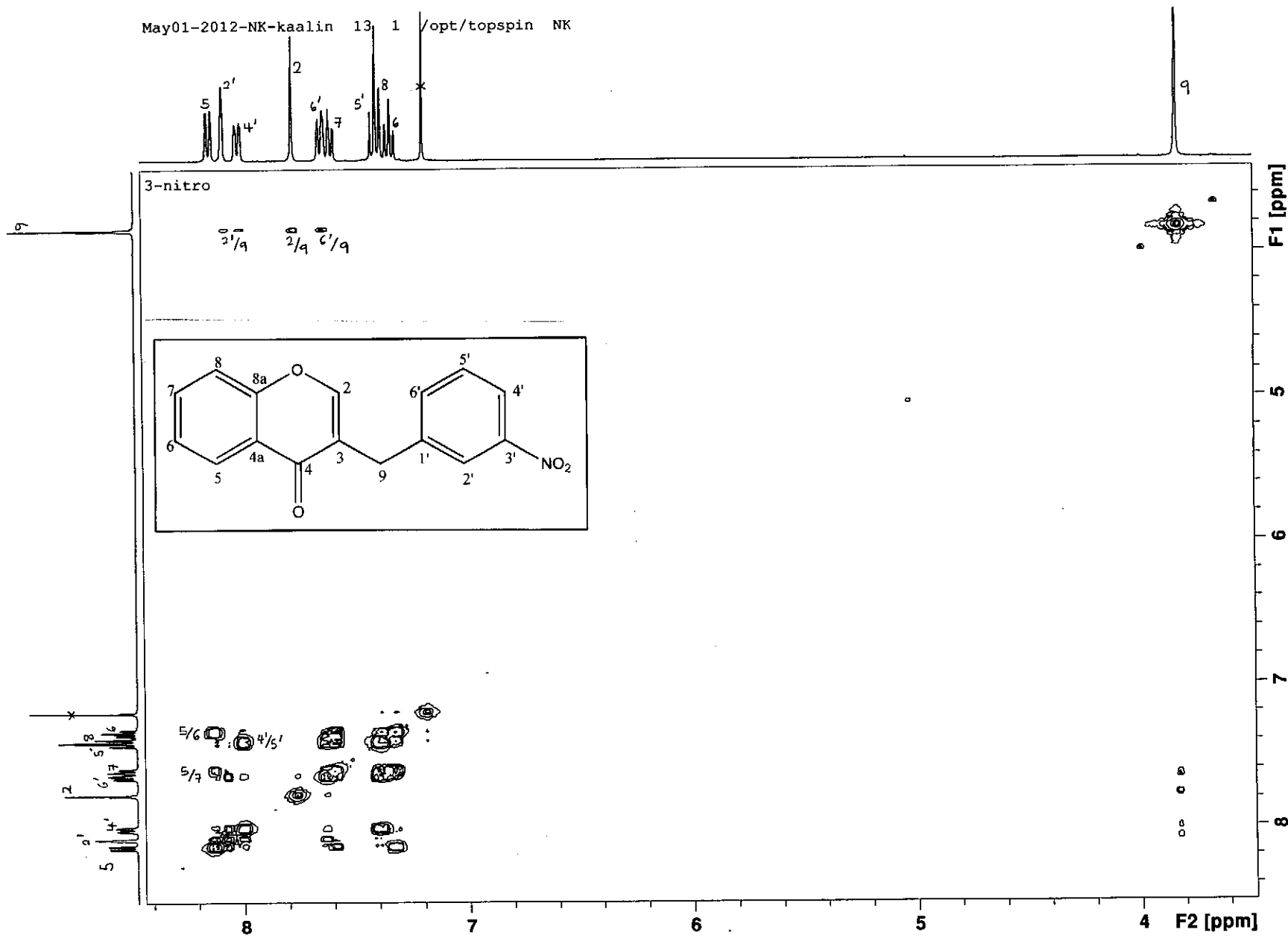
— 123.1609

— 121.7050

— 118.1546

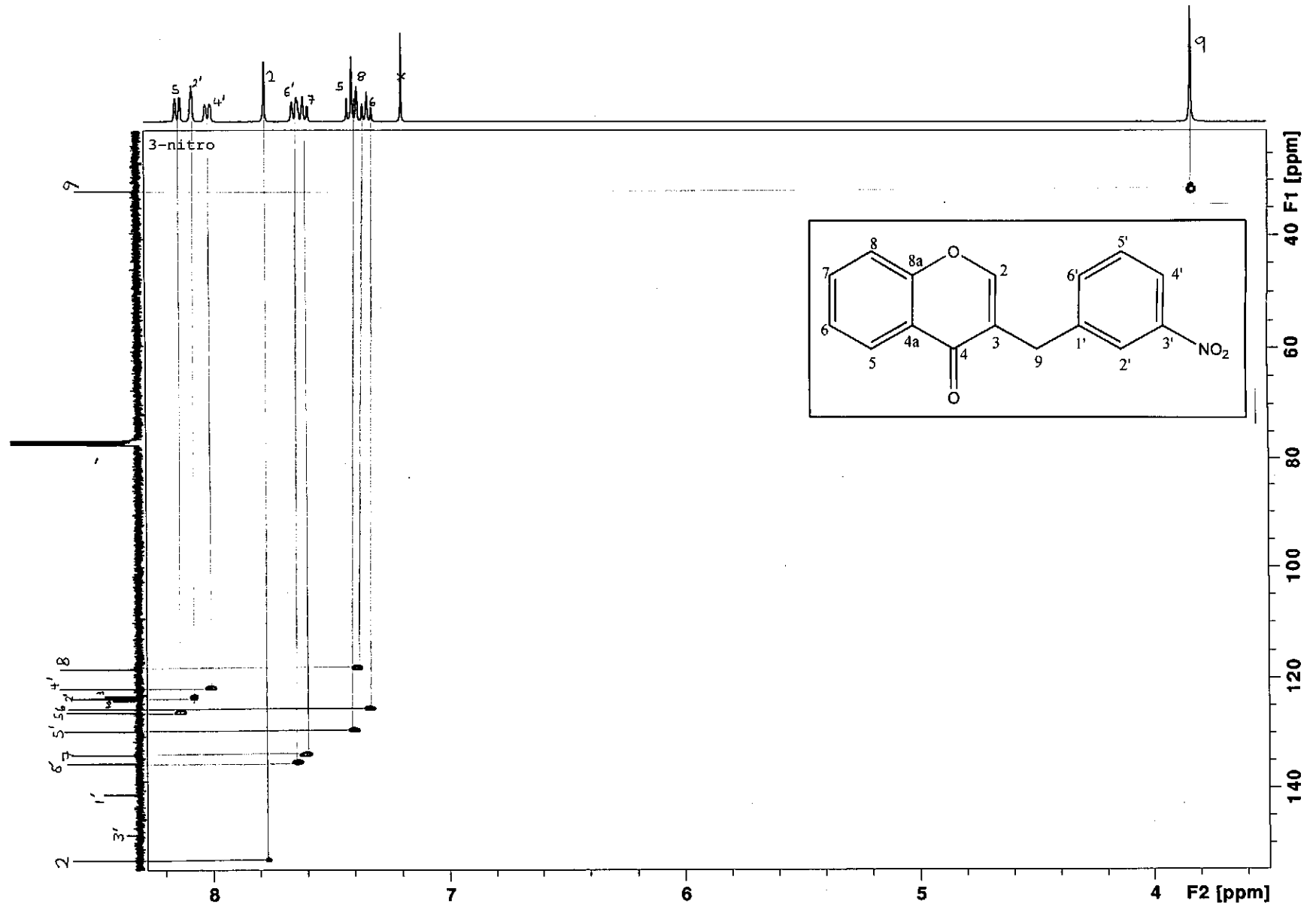


¹³C NMR spectrum of compound 17 (expanded)



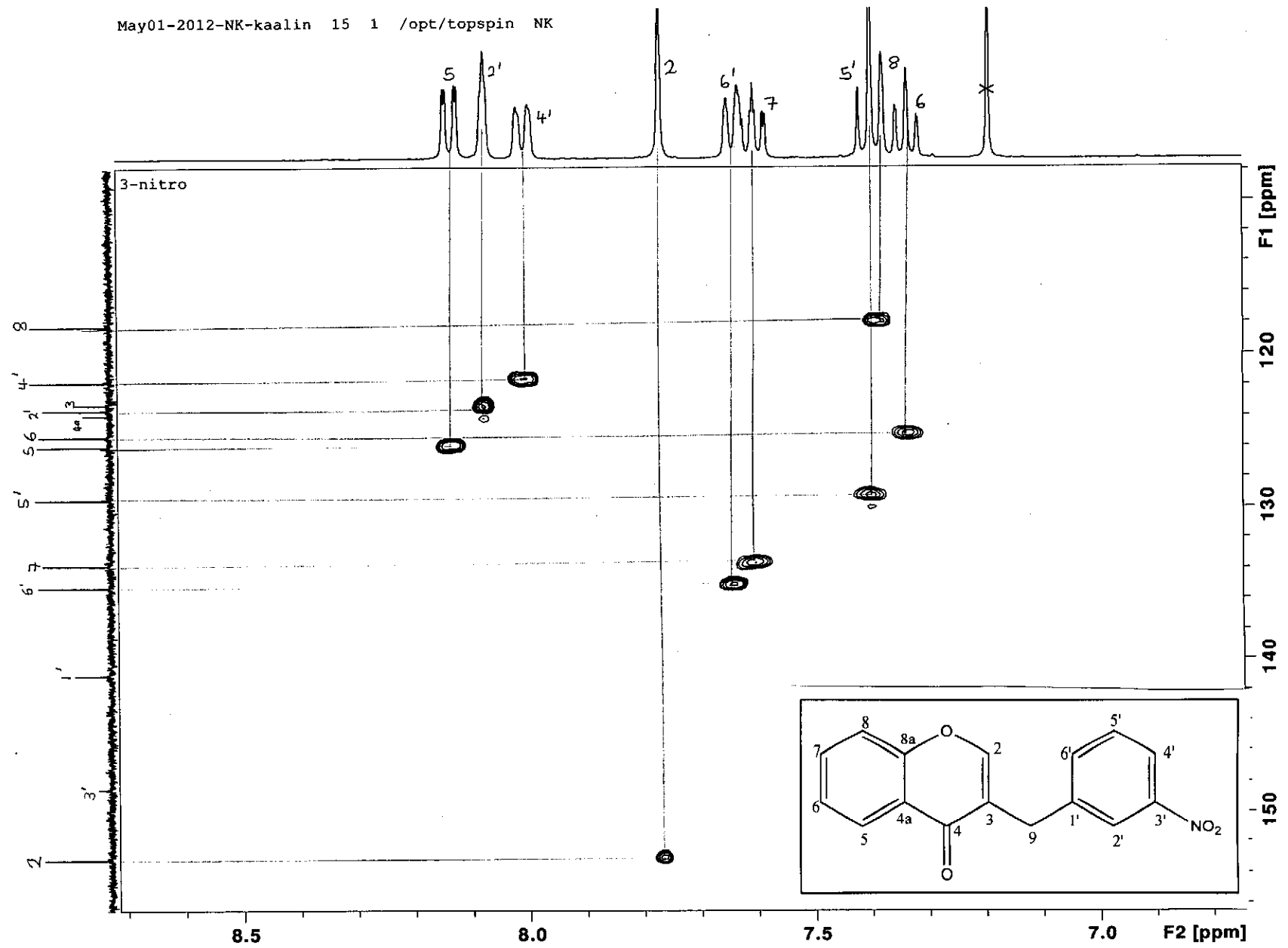
COSY spectrum of compound 17

May01-2012-NK-kaalin 15 1 /opt/topspin NK



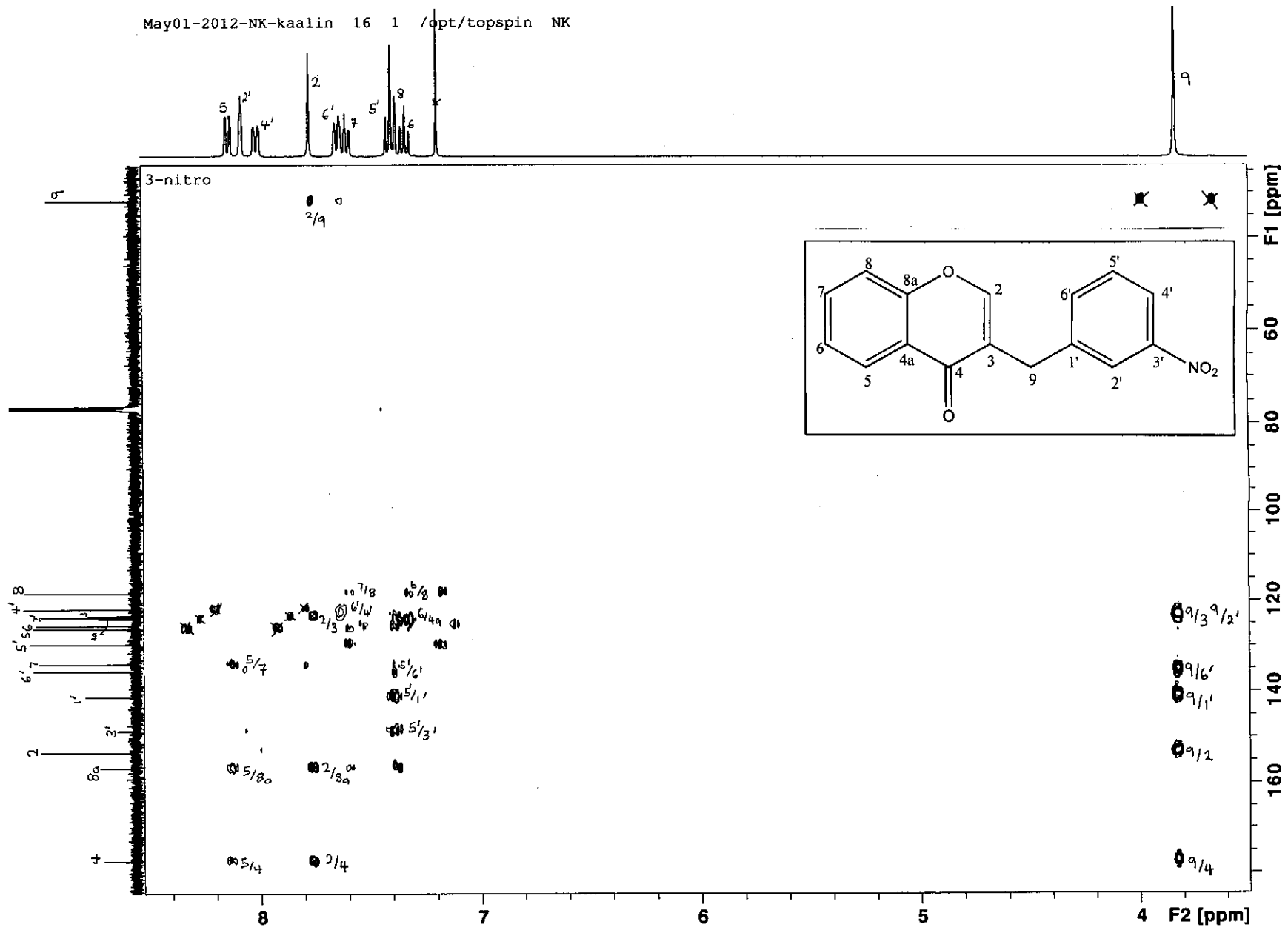
HSQC spectrum of compound 17

May01-2012-NK-kaalin 15 1 /opt/topspin NK



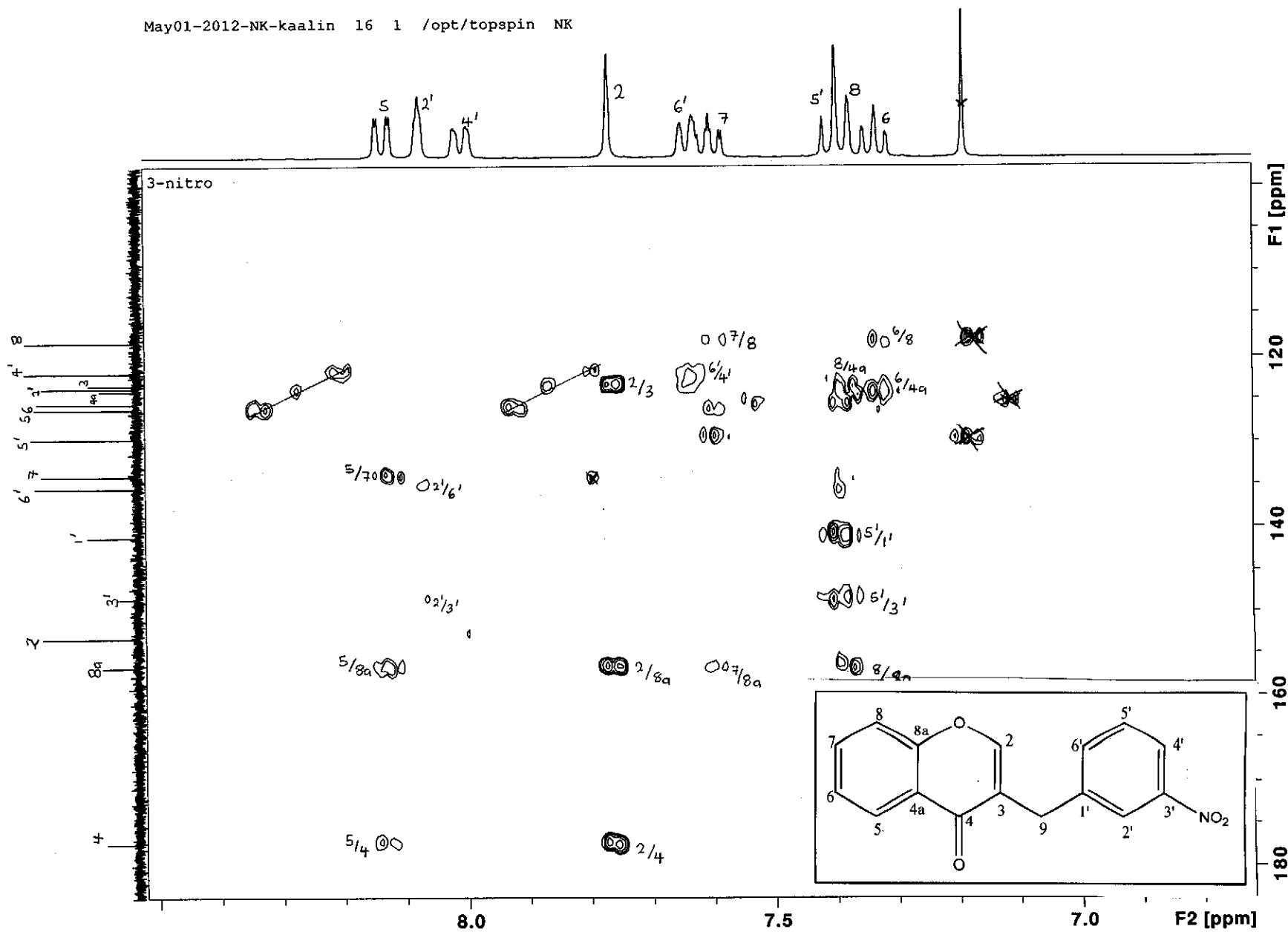
HSQC spectrum of compound 17 (expanded)

May01-2012-NK-kaalin 16 1 /opt/topspin NK

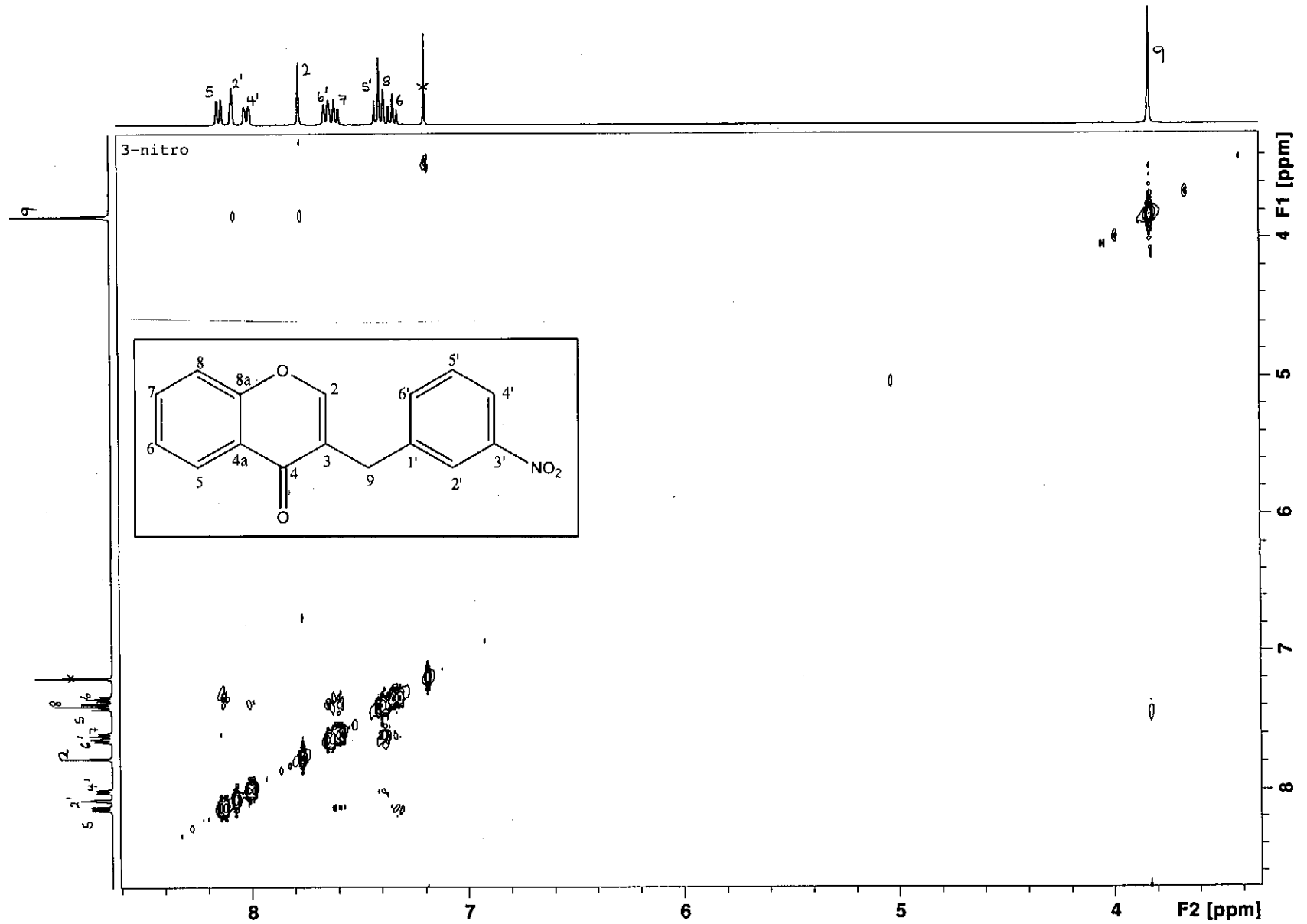


HMBC spectrum of compound 17

May01-2012-NK-kaalin 16 1 /opt/topspin NK

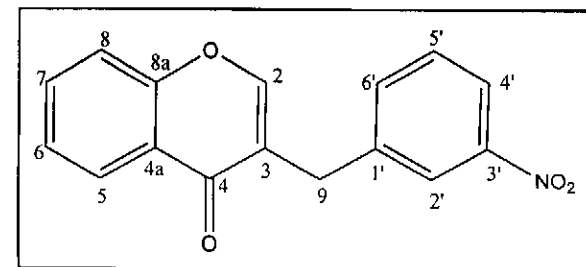
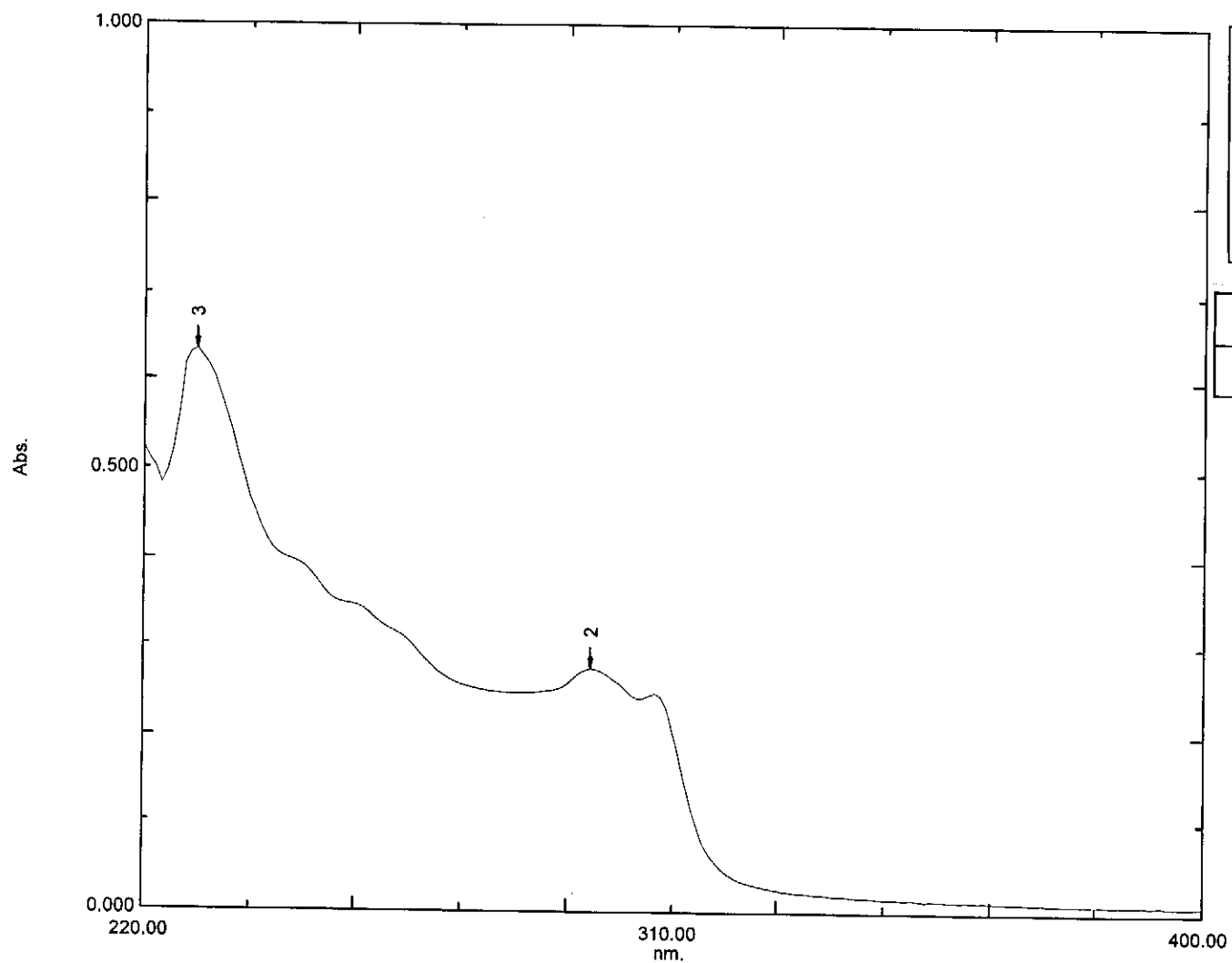


HMBC spectrum of compound 17 (expanded)



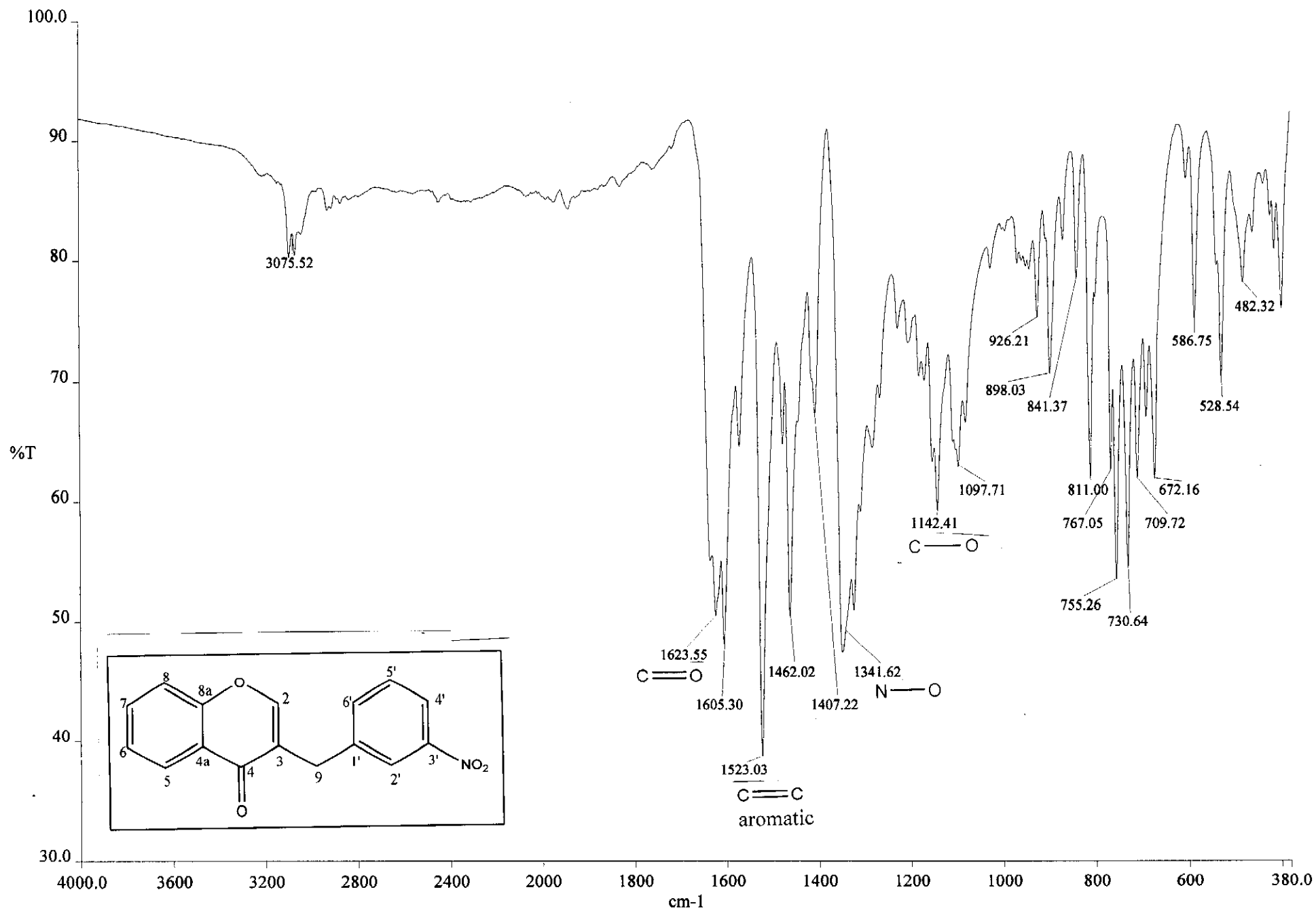
Overlay Spectrum Graph Report

15/05/2012 01:08:37 PM



Wavelength/ nm	Absorbance	Log ϵ
296	0.274	3.96

UV-Vis spectrum of compound 17



Infrared spectrum of compound 17

File :C:\msdchem\1\data\KAALIN 2\3-NITRO (1).D
Operator :
Acquired : 7 Jun 2012 13:14 using AcqMethod NATPRODUCTS MANUAL INJ SPLIT.M
Instrument : 5973N
Sample Name: 3-NITRO (1)
Misc Info :
Vial Number: 1

